PROCEEDINGS OF ICSF-1

FIRST INTERNATIONAL CONFERENCE ON SCOUR OF FOUNDATIONS

NOVEMBER 17-20, 2002
TEXAS A&M UNIVERSITY
COLLEGE STATION, TEXAS, USA

SPONSORED BY
Main Sponsors:
International Society for Soil Mechanics and Geotechnical Engineering
Texas Transportation Institute

Gold Level Sponsors:
Federal Highway Administration
National Science Foundation

Silver Level Sponsors:
ADSC, The International Association of Foundation Drilling
American Society of Civil Engineers (ASCE)
Coasts, Oceans, Ports, and Rivers Institute of ASCE
Environmental & Water Resources Institute of ASCE
Geo-Institute of ASCE
Structural Engineering Institute of ASCE
Texas A&M University Department of Civil Engineering
Transportation Research Board (TRB)

ADDITIONAL COPIES OF THIS BOOK CAN BE OBTAINED FROM

Texas Transportation Institute
Publications Dept.
Tel: (979) 845-4853
Fax: (979) 862-3703
Email: sales@ttimail.tamu.edu
Internet: http://tti.tamu.edu/product/

CONFERENCE COMMITTEES

Chairman of the Conference: Jean-Louis Briaud
Vice-Chairman of the Conference: Hamn-Ching Chen
Editors of the Proceedings: Hamn-Ching Chen and Jean-Louis Briaud

National Advisory Committee:

George Annandale, Larry Arneson, Jean-Louis Briaud, Hamn-Ching Chen, Tom Dahl, Stan Davis, Jerry DiMaggio, Dave Froelich, Daryl Greer, Larry Harrison, Robert Henthorne, Carlton Ho, Rollin Hotchkiss, Beatrice Hunt, Peggy Johnson, Sterling Jones, Ed Kent, Peter Lagasse, Melinda Luna, Shawn McClemore, William Moore, Jorge E. Pagan-Ortiz, Gary Parker, Art Parola, Richard Phillips, Everett Richardson, Max Sheppard, Peter Smith, Steve Smith, David Stolpa, Phil Thompson, Mehmet Tumay

International Advisory Committee:

Laila Abed, Marco Falcon Ascanio, A. (Tony) Bracegirdle, Jean-Louis Briaud, Yee-Meng Chiew, Michael Heibaum, Sangseom Jeong, Hellgi Johannesson, Sterling Jones, Soo-Sam Kim, Boleslaw A. Klosinski, Raul A. Lopardo, Bruce Melville, Zlatko Mihalinec, Yahia E-A. Mohamedzein, Gaton Laporte Molina, A.V.S.R. Murty, Jorge E. Pagan-Ortiz, L. Rakoczi, Everett V. Richardson, A.M.M. Saffiullah, Makoto Shimamura, Testsuro Tsujimoto, Dirceu de Alencar Velloso, Narimantas Zdankus

Organizing Committee:

Michelle Benoit, Jamie Blakeney, Jean-Louis Briaud, Hamn-Ching Chen, Billy Edge, Richard Gehle, Harlow Landphair, Ya Li, Kathy Montemayor, Prahoro Nurtjahyo, Tobey Nutt, Josh Reinbolt, Susan Robertson, Jun Wang

Technical Program Committee:

Jean-Louis Briaud, Hamn-Ching Chen, Michael Heibaum, Bruce Melville, Jorge Pagan, Art Parola, Everett Richardson, Stephen Wright

Prediction Event Committee:

Jean-Louis Briaud, Kuang-An Chang, Hamn-Ching Chen, Jerry DiMaggio, Al DiMillio, Sterling Jones, Ya Li, Dave Mueller, Jorge Pagan, Jun Wang

PREFACE

Texas A&M University
September 16, 2002

Many people have contributed to making this conference a success. The teamwork that led to this event and to the proceedings will remain a very bright moment in my career. I would like to single out one person however for his tremendous contribution to this conference. Thank you Professor Chen for being such a great teammate and for your very demanding role as the main person responsible for the proceedings. You are definitely the MVP of this conference. I would also like to thank the reviewers for taking the time to review a large number of manuscripts in a relatively short period of time: Brian Barkdoll, Liang Cheng, Yee-Meng Chiew, Chen Onn Chin, Sung-Uk Choi, Keith E. Dennett, Duowen Ding, Robert Ettema, Oktay Guven, Willi H. Hager, Faruque Mia, Michael H. Heibaum, Sangseom Jeong, Yafei Jia, Peggy A. Johnson, J. Sterling Jones, Paul Kirshen, Peter Lagasse, Ya Li, Siow-Yong Lim, Richard May, Bruce Melville, David S. Mueller, Tatsuaki Nakato, Prahoro Nurtjahyo, Kunihiro Ogihara, Michael W. O'Neill, James D. Schall, D. Max Sheppard, Makoto Shimamura, Nels J. Sultan, B.Mutlu Sumer, Jun Wang. Richard Gehle and Josh Reinbolt were very helpful in assembling the proceedings electronically and in the details of the conference organization.

Our sponsors were numerous and very helpful: The International Society for Soil Mechanics and Geotechnical Engineering (Kenji Ishihara, William Van Impe), The Texas Transportation Institute (Herbert Richardson, Dennis Christiansen), The Federal Highway Administration (Sterling Jones, Al DiMillio, Jorge Pagan, Jerry DiMaggio), The National Science Foundation (Cliff Astill, Rick Fragaszy), ADSC: The International Association of Foundation Drilling (Scot Litke), American Society of Civil Engineers (ASCE), The Geo-Institute of ASCE (Carol Bowers, Gail Sor), The Environmental & Water Resources Institute of ASCE (Bryan Parsons), The Coasts, Oceans, Ports, and Rivers Institute of ASCE (Patricia Brown), The Structural Engineering Institute of ASCE (Jim Rossberg), The Transportation Research Board: TRB (Jay Jayaprakash), Texas A&M University Department of Civil Engineering (John Niedzwecki).

And then there was all the help from the various committees: International Advisory Committee, National Advisory Committee, Technical Program Committee, Prediction Event Committee, Organizing Committee. You can find the complete list of committee members within the previous page.

The Prediction Event was also a major undertaking. The Federal Highway Administration and the Texas A&M University Department of Civil Engineering were the two main sponsors with help from the USGS and several DOTs: many thanks to Sterling Jones, Dave Mueller, K. Van Wilson, Paul H. Rydlund, Richard J. Huizinga. At Texas A&M University, the flume tests were performed by Ya Li and Jun Wang with the cooperation of John Reed and Bob Randall.

I also wish to thank my wife Janet who was such a great support during all the time spent on the preparation of this conference.

Jean-Louis Briaud

Chairman of ICSF-1

First International Conference on Scour of Foundations ICSF-1
Texas A&M University, November 17 –20, 2002

Final Program

SUNDAY, NOVEMBER 17, 2002

9:00 a.m.-12:00 Noon	**ISSMGE TC-33 – Geotechnics of Soil Erosion Committee Meeting**
12:00 Noon-1:30 p.m.	**Lunch** – on your own
1:30 p.m.-3:00 p.m.	**Short Course:** Scour of Foundations **Organizers:** *J. E. Pagan*, (USA); S. Jones (USA); *J-L. Briaud*, (USA)
3:00 p.m.-3:30 p.m.	**Break**
3:30 p.m.-5:00 p.m.	**Short Course:** Scour of Foundations **Organizers:** *J. E. Pagan*, (USA); S. Jones (USA); *J-L. Briaud*, (USA)
5:30 p.m.-8:00 p.m.	**Reception in the Exhibits Hall - Registration**

MONDAY, NOVEMBER 18, 2002

7:00 a.m.-8:00 a.m.	**Breakfast and Registration in Exhibits Hall**
8:00 a.m.-8:30 a.m.	**WELCOME – Grand Ballroom** H. H. Richardson, Director, Texas Transportation Institute J. M. Niedzwecki, Head, Department of Civil Engineering J-L. Briaud, Chairman, ICSF-1, Acknowledgements
8:30 a.m.-10:00 a.m.	**SESSION (1): PLENARY SESSION I – Grand ballroom** **Session Chairs:** M. Tumay, P. Smith. **Invited Lecture 1.1:** *Scour Protection and Repair by Filtering Geosynthetic Containers.* M. H. Heibaum (Germany). **Invited Lecture 1.2:** Numerical Simulation of Scour Around Complex Piers in Cohesive Soil. *H-C. Chen* (USA). **Invited Lecture 1.3:** Unconventional Interpretation of Local Scour Downstream a Large Dam Stilling Basin. R. A. Lopardo (Argentina), J. M. Casado, M. C. Lopardo.
10:00 a.m.-10:30 a.m.	**Break in the Exhibits Hall**
10:30 a.m.-12:00 Noon	**Concurrent Sessions**
	SESSION (2): SCOUR PREDICTIONS I – Ballroom 1 **Session Chairs:** J. Audibert, C. Weber. **Invited Lecture 2.1:** *Indirect Methods of Measuring Shear Stress in the Bottom of a Scour Hole*. J. S. Jones (USA). **Presentation 2.2:** Shear Stress Approach to Pier Scour Predictions. Y. Li (USA), J-L. Briaud, H-C. Chen, P. Nurtjahyo, J. Wang. **Presentation 2.3:** A Review of Predictive Methods for General Scour. R. Bettess (UK). **Presentation 2.4:** Prediction of Local Scour Below Offshore Pipelines – A Review. L. Cheng (Australia). **Presentation 2.5:** Comparison of General Scour Prediction Equations for River Crossings. C. Lauchlan (UK), R. May.

SESSION (3): SCOUR MEASUREMENTS I – Ballroom 2
Session Chairs: C. Monk, N. Jaynes.
Invited Lecture 3.1*:* Local Scour Around Structures in Tidal Flows. R. W. P. May (UK), M. Escarameia.
Presentation 3.2*:* Movement of Bridge Pier by Water Flow Under Flood Condition. K. Ogihara (Japan), H. Muraishi, S. Masahiko, D. Nakajima.
Presentation 3.3: 3-Dimensional Measured and Simulated Flow for Scour Near Spur Dikes. R. Kuhnle (USA), Y. Jia, C. Alonso.
Presentation 3.4: Scour Experiments on Dike Angle, Porosity, and Hook for a Thin Dike. E. Martinez (USA), R. Ettema, A. Lachhab.
Presentation 3.5: Shallow Water Effect on Pier Scour in Clays. Y. Li (USA), J-L. Briaud, H-C. Chen, P. Nurtjahyo, J. Wang.

12:00 Noon-1:30 p.m. **Lunch** – **Oakwood Ballroom** (provided)

1:30 p.m.-3:00 p.m. **Concurrent Sessions**

SESSION (4): SCOUR PREDICTIONS II – Ballroom 1
Session Chairs: P. D'Odorico, D. Stolpa.
Invited Lecture 4.1: *Effect of Suspended Fine Sediment on Local Scour.* M. Sheppard (USA).
Presentation 4.2: *Numerical Simulations of 3-D Flows Around Bridge Piers.* S-U. Choi (Korea), W. Yang.
Presentation 4.3: *3-D Numerical Model for Wave-Induced Dynamic Behavior of Sand Beds at Bridge Piers*. F. Mia (Japan), H. Nago, S. Maeno.
Presentation 4.4: *Pier Scour at Woodrow Wilson Bridge and SRICOS Method.* K. Kwak (Korea), J-L. Briaud, Y. Cao, M-K. Chung, B. Hunt, S. Davis.
Presentation 4.5: *Bed Shear Stress Around Rectangular Pier: Numerical Approach*. P. Nurtjahyo (USA) H-C. Chen, J-L. Briaud, Y. Li, J. Wang.

SESSION (5): SCOUR MEASUREMENTS II – Ballroom 2
Session Chairs: W. Edge, R. Melek.
Invited Lecture 5.1: *Flume Experiments on Abutment Scour: Confronting Complexities in Process and Similitude.* R. Ettema (USA).
Presentation 5.2: *Scouring Downstream of Sluice Gate*. S-Y. Lim (Singapore), G. Yu.
Presentation 5.3: *Development of the New Inspection Method on Scour Condition Around Existing Bridge Foundations.* J. Fukui (Japan), M. Otuka.
Presentation 5.4: *Experimental Study on Toe Scour of Seawall Covered with Armor Units Due to Waves*. T. Sakakiyama (Japan), R. Kajima.
Presentation 5.5: *Scour Around Rubble-Mound Breakwater Head of Cheju Outer Port*. H. Kim, (Korea), B. C. Oh, B-S. Jung, S-Z Youn.

3:00 p.m.-3:30 p.m. **Break in the Exhibits Hall**

3:30 p.m.-5:00 p.m. **Concurrent Sessions**

SESSION (6): SCOUR PREDICTIONS III – Ballroom 1
Session Chairs: K. A. Chang, P. Nurtjahyo
Invited Lecture 6.1: *Analysis of Pier Scour Predictions and Real-Time Field Measurements*. D. S. Mueller (USA), C. R. Wagner.
Presentation 6.2: *Future Hydrographs and Scour Risk Analysis.* J-L. Briaud (USA), P. D'Odorico, E. J. Jeon
Presentation 6.3: *Database Program for Highway Bridge-Scour Data.* K. Farrag (USA), M. Morvant.
Presentation 6.4: *Nondimensional Analysis of Clear-Water Scour at Bridge*

Contractions in Cohesive Soils. O. Guven (USA), J. G. Melville, J. E. Curry.
Presentation 6.5: *FE Analysis of Coastal Cliff Erosion due to Ocean Wave Assailing*. K. Yasuhara (Japan), S. Murakami, Y. Kanno, Z. Wu.

SESSION (7): GEOTECHNICAL ASPECTS I - Ballroom 2
Session Chairs: C. Aubeny, X. Long.
Invited Lecture 7.1: *Theoretical and Practice Aspects of Rock Scour Prediction*. G. W. Annandale (USA), E. Bollaert, A. Schleiss.
Presentation 7.2: *Erosion Function Apparatus Overview and Discussion of Influence Factors on Cohesive Soil Erosion Rate in EFA Test*. Y. Cao (USA), J. Wang, J-L. Briaud, H-C. Chen, Y. Li, P. Nurtjahyo.
Presentation 7.3: *Identification of Dispersive Clays in Gaza Strip Area*; *and Filter Effects on Dam Safety*. M. A. Awad (Palestine).
Presentation 7.4: *Effects of Cohesion on Bridge Scour*. A. Molinas (USA), S. J. Jones.
Presentation 7.5: *Scour Around Submarine Pipeline in Clayey Soil.* S. Neelamani (India), A. Vijaya kumar, S. Narasimha Rao.

5:30 p.m.-6:30 p.m. **2001 TERZAGHI LECTURE – Grand Ballroom**
Session Chairs: P. Jeanjean, A. Niederoda.
Geotechnical Solutions for the Offshore: Synergy of Research and Practice S. Lacasse, (Norway)

7:00 p.m.-9:00 p.m. **Reception in the new Texas A&M University Hydraulic Laboratory**
(Buses leave every 10 minutes starting at 6:45 p.m.)

7:00 p.m.-10:00 p.m. **Committee Meetings – Mockingbird rooms**

TUESDAY, NOVEMBER 19, 2002

7:00 a.m.-8:00 a.m. **Breakfast and Registration in Exhibits Hall**

8:30 a.m.-10:00 a.m. **SESSION (8): PLENARY SESSION II – Grand Ballroom**
Session Chairs: S. Wright, B. Hunt.
Invited Lecture 8.1: Survey of Bridge Damages Due to a Heavy Rain in Northern Part of Kanto Region, Japan. J. Fukui (Japan), M. Nishitani.
Invited Lecture 8.2: The SRICOS-EFA Method**.** J-L. Briaud (USA).
Invited Lecture 8.3: *Failure Mechanisms of Riprap Layer Around Bridge Piers.* Y-M. Chiew (Singapore).

10:00 a.m.-10:30 a.m. **Break in the Exhibits Hall**

10:30 a.m.-12:00 Noon **Concurrent Sessions**

SESSION (9): COUNTERMEASURES I – Ballroom 1
Session Chairs: H. Landphair, W. Wang.
Invited Lecture 9.1: *Scour Protection Around Gravity Based Structures Using Small Size Rock*. K. J. Bos (Netherlands), H. J. Verheij, G. Kant, A. C. H. Kruisbrink.
Presentation 9.2: *Riprap as Permanent Scour Protection Around Bridge Piers*. C. D. Anglin (Canada), F. Itamunoala, G. Millen.
Presentation 9.3: *Riprap at Rectangular Bridge Piers Under Oblique Incident Flow*. J. A. Sainz (Spain), R. Salgado.
Presentation 9.4: *Countermeasure Construction Using Jet Grouting Methods to Combat Foundation Scour.* D. W. Boehm (USA).

Presentation 9.5: *Field Evaluation and Countermeasure Selection for Scour Critical Bridges in the Commonwealth of Kentucky*. K. J. Schaefer (USA), R. W. Gardner.

SESSION (10): GEOTECHNICAL ASPECTS II – Ballroom 2
Session Chairs: G. Biscontin, H. Hu.
Invited Lecture: 10.1. *GIS-Based Bridge Scour Prioritization.* C. L. Ho (USA), J. M. Di Stasi, P. Rees.
Presentation 10.2: *Erodibility Tests of Shale-Rock Samples Taken from Bridge Pier Construction Site on the Mississippi River.* T. Nakato (USA).
Presentation 10.3: *The Driving Force on Soil Grains and Its Effect on Scouring the Channel of Foundation.* L. Zhang (USA), D. Ding, W. Zhou.
Presentation 10.4: *Depth of Mobile Layer Under Severe Wave Conditions: Liquefaction Effect.* S. Sassa. (Japan).
Presentation 10.5: *Essence of Silt Factor for Scour Calculation Around Bridge Foundation.* R.K. Dhiman,(India), D. K. Mohapatra.

12:00 Noon-1:30 p.m. **Lunch** – **Oakwood Ballroom** (provided)

1:30 p.m.-3:00 p.m. **Concurrent Sessions**

SESSION (11): COUNTERMEASURES II – Ballroom 1
Session Chairs: D. Laefer, J. B. Seo.
Invited Lecture 11.1: *Impact of the Federal Highway Administration's Scour Evaluation Program in the United States of North America's Highway Bridges.* J. E. Pagan-Ortiz (USA).
Presentation 11.2: *Evaluation of Strategies to Control Erosion along U.S. Highway 50 Between Carson City and Lake Tahoe.* K. Dennett (USA), P. Fricthel, R. Siddharthan, A. Soltani.
Presentation 11.3: *Optimisation of Scour Protection Measures.* G. B. H. Spaan (Netherlands), M. H. Lindo, G. Kant.
Presentation 11.4: *Design and Construction of Bridge Scour Countermeasures Along the Salt River, Phoenix, Arizona*. D. L. Richards (USA).
Presentation: 11.5.

SESSION (12): ABUTMENTS AND EMBANKMENTS – Ballroom 2
Session Chairs: T. Dahl, S. Hilbrich.
Invited Lecture 12.1: *Abutment Scour Countermeasures: A Review* .B. Barkdoll (USA), R. Ettema, R. Kuhnle, B. Melville, T. Parchure, A. Parola, C. Alonso.
Presentation 12.2: *Countermeasures for Scour at Spill-Through Bridge Abutments.* B. Melville (New Zealand), S. Coleman, D. Hoe.
Presentation 12.3: *Hugo Reservoir Embankment Depression Study.* J. B. Nevels, Jr. (USA).
Presentation 12.4: *Pier and Abutment Scour-New Laboratory Data.* W. H. Hager (Switzerland), J. Unger, G. Oliveto.
Presentation 12.5: *Flow and Scouring in Main Channel due to Abutments.* G. Yu (Singapore), S-Y. Lim, S-K. Tan.

3:00 p.m.-3:30 p.m. **Break in the Exhibits Hall**

3:30 p.m.-5:00 p.m. **Concurrent Sessions**

SESSION (13): COUNTERMEASURES III – Ballroom 1
Session Chairs: S. Dunlap, X. Zhang.

Invited Lecture 13.1: *Treating Channel Instability at Bridges*. P. A. Johnson (USA).
Presentation 13.2: *Scour Hazard Mitigation for Tick Canyon Wash Bridge.* M. S. Islam (USA), J. Zha, A. Abghari.
Presentation 13.3: *Final Stages of Butte City Bridge Erosion Control Project.* S. K. Mishra (USA), W. B. Lindsey.
Presentation 13.4: Riprap Protection Around Bridge Piers in a Degrading Channel. *Y- M. Chiew* (Singapore).
Presentation 13.5: *Scour at a Submerged Rock Dike, Willapa Bay, Washington.* N. Sultan (USA). R. Phillips, H. Bermudez.

SESSION (14): PIER SCOUR – Ballroom 2
Session Chairs: S. Davis, J. Wang.
Invited Lecture 14.1: *3-D Numerical Modeling of Flow and Scour Around a Pile.* A. Roulund (Denmark), B. M. Sumer, J. Fredsoe, J. Michelsen.
Presentation 14.2: *New Approach to Scour Evaluation of Complex Bridge Piers.* E. V. Richardson (USA), J. S. Jones, D. M. Sheppard.
Presentation 14.3: *Time Rate of Local Scour at a Circular Pile.* W. Miller, Jr. (USA), D. M. Sheppard.
Presentation 14.4: *A Case Study of the Possible Effects of Long-Term Climate Change on Bridge Scour.* P. Kirshen (USA), L. Edgers, J. Edelmann, M. Percher, B. Bettencourt, E. Lewandowski.
Presentation 14.5: *Analysis of Pile Groups Considering Riverbed Scouring.* S. Jeong (Korea), J. Won, J. Suh.

5:30 p.m.-6:30 p.m. — **2002 BUCHANAN LECTURE – Grand Ballroom**
Session Chair: J-L. Briaud.
"The World Trade Center: Construction, Destruction, Reconstruction. A. Aronowitz, (USA)

7:00 p.m.-9:00p.m. — **Reception at the George Bush Presidential Library and Museum**
(Buses leave every 10 minutes starting at 6:45 p.m.)

WEDNESDAY, November 20, 2002

7:00 a.m.-8:00 a.m. — **Breakfast and Registration in Exhibits Hall**

8:30 a.m.-10:00 a.m. — **SESSION (15): PLENARY SESSION III – Grand Ballroom**
Session Chairs: A. Kosicki, H. Johanesson.
Invited Lecture 15.1: On the Challenges of Scour Prediction. G. Hoffmans (Netherlands), H. Verheij.
Invited Lecture 15.2: A Geotechnical Perspective: Design and Construction of Highway Bridge Foundations for Scour. C. E. Dumas (USA), J. Krolack.
Invited Lecture 15.3: Local Scour Depths at Bridge Foundations: New Zealand Methodology. B. Melville (New Zealand).

10:00 a.m.-10:30 a.m. — **Break in the Exhibits Hall**

10:30 a.m.-12:00 Noon — **Concurrent Sessions**

SESSION (16): SCOUR PROBLEMS I – Ballroom 1
Session Chairs: M. Luna, E. McDonald.
Invited Lecture 16.1: *Study on the Disasters of Bridge and Bed Protection Works During the Passage of Typhoon Herb*. C. Lin (Taiwan), T-C. Ho, P-H. Chiu, K-A. Chang.

Presentation 16.2: *Damages of the Roads-Bridges by Erosion and Remedial Measures in Albania*. L. Bozo (Albania), Y. Muceku.
Presentation 16.3: *Bridge Pier Scour in Bouldery Bed – Indian Scenario.* R. Singh (India), K. K. Razdan, R. K. Dhiman.
Presentation 16.4: *Scour Monitoring of Railway Bridge Piers via Inclination Detection.* N. Kobayashi (Japan), S. Kitsunai, M. Shimamura.
Presentation 16.5: *Non-Destructive Testing to Determine Unknown Pile Lengths Under Existing Bridges*. F. Rausche (USA), M. Huessin, M. Bixler.

SESSION (17): SCOUR MONITORING – Ballroom 2
Session Chairs: S. Smith, K. Y. Rhee.
Invited Lecture 17.1: *Instruments to Measure and Monitor Bridge Scour.* E. V. Richardson (USA).
Presentation 17.2: *Development and Implementation of a Scour Monitoring Program for Selected Bridges Crossing the Trukee River.* K. E. Dennett (USA), P. Fritchel, R. Siddharthan, A. Soltani.
Presentation 17.3: *Seismic Methods to Identify Scour Depth Around Deep Bridge Foundations.* E. J. Mercado (USA), E. B. Davies, J. A. McDonald, M. W. O'Neill.
Presentation 17.4: *Portable Scour Monitoring Research.* J. D. Schall (USA), G. R. Price.
Presentation 17.5: *Active Scour Monitor Instrumentation in the California Transportation System*. S. Ng (USA).

12:00 Noon-1:30 p.m. **Lunch** – **Oakwood Ballroom** (provided)

1:30 p.m.-3:00 p.m. **Concurrent Sessions**

SESSION (18): SCOUR PROBLEMS II – Ballroom 1
Session Chairs: R. Whitehouse, H. Shi.
Invited Lecture 18.1: *Determination of Unknown Bridge Foundation Depths with NDE Methods*. L. D. Olson (USA).
Presentation 18.2: *Scour of Railway Embankment Foundation Located on Sea-Cliff in Japan***.** H. Suzuki (Japan), M. Shimamura.
Presentation 18.3: *Design and Construction of Scour Foundations for Electric Power Transmission Line Structures.* P. M. Kandaris (USA), R. E. Kondziolka, J. P. Adams.
Presentation 18.4: *Propeller Induced Scour.* C-O. Chin (Singapore), W. Li.
Presentation 18.5: *Confederation Bridge – New Scour Design Methodology for Complex Materials.* R. B. Nairn (Canada), C. D. Anglin.

SESSION (19): CASE HISTORIES – Ballroom 2
Session Chairs: L. Arneson, Z. Lu.
Invited Lecture 19.1: *A Methodology for Predicting Channel Migration NCHRP Project No. 24-16.* P. Lagasse (USA), W. Spitz, L. Zevenbergen.
Presentation 19.2: *Predicting Meander Migration: Evaluation of Some Existing Techniques*. J-L. Briaud (USA), H-C. Chen, S. Park.
Presentation 19.3: *Collapse and Erosion of Khon Kaen Loess with Treatment Option.* P. Punrattanasin (Thailand), A. Subjarassang, O. Kusakabe, T. Nishimura.
Presentation 19.4: *Analysis of Contraction and Abutment Scour at Two Sites in Minnesota.* C. R. Wagner (USA), D. S. Mueller.
Presentation 19.5: *Factors Affecting Stream and Foundation Stability at Existing Bridges in New Jersey.* S. M. Baig (USA), J. J. Zarriello, M. A. Khan.

3:00 p.m.-3:30 p.m.	**Break in the Exhibits Hall**
3:30 p.m.-4:00 p.m.	**SESSION (20): PREDICTION EVENT – Grand Ballroom** **Session Chairs:** J. Benn, Y. Li. **Presentation: 20.1.** *Results of the FHWA Prediction Event.* J-L. Briaud (USA)
4:00 p.m. – 5:00 p.m.	**SESSION (21): *FUTURE SCOUR NEEDS. PANEL DISCUSSION* – Grand Ballroom** **Moderator:** J-L. Briaud (USA). **Panelists:** B. Melville (New Zealand). S. Jones (USA). J. Fukui (Japan). R. Whitehouse (UK). G. Hoffmans (Netherlands). C. Dumas (USA).
5:00 p.m.-9:00 p.m.	**Closing Ceremony – Reception at Janet and Jean-Louis Briaud's House** (3013 Coronado Drive, College Station, T: 979-693-3969).

TABLE OF CONTENTS

Page

VOLUME I

PLENARY

"Scour Protection and Repair by Filtering Geosynthetic Containers."
M. H. Heibaum **(Invited Lecture)** 1

"Numerical Simulation of Scour Around Complex Piers in Cohesive Soil."
H-C. Chen **(Invited Lecture)** 14

"Unconventional Interpretation of Local Scour Downstream a Large Dam Stilling Basin."
R. A. Lopardo, J. M. Casado, M. C. Lopardo **(Invited Lecture)** 34

"Survey of Bridge Damages Due to a Heavy Rain in Northern Part of Kanto Region, Japan."
J. Fukui, M. Nishitani **(Invited Lecture)** 47

"The SRICOS-EFA Method."
J-L. Briaud **(Invited Lecture)** 57

"Failure Mechanisms of Riprap Layer Around Bridge Piers."
Y- M. Chiew **(Invited Lecture)** 70

"On the Challenges of Scour Prediction."
G. Hoffmans, H. J. Verheij **(Invited Lecture)** 92

"A Geotechnical Perspective: Design and Construction of Highway Bridge Foundations for Scour." C. E. Dumas, J. Krolack **(Invited Lecture)** 112

"Local Scour Depths at Bridge Foundations: New Zealand Methodology."
B. Melville **(Invited Lecture)** 120

SCOUR PREDICTION

"Indirect Methods of Measuring Shear Stress in the Bottom of a Scour Hole."
J. S. Jones **(Invited Lecture)** 140

"Shear Stress Approach to Pier Scour Predictions."
Y. Li, J-L. Briaud, H-C. Chen, P. Nurtjahyo, J. Wang 156

"A Review of Predictive Methods for General Scour."
R. Bettess 162

"Prediction of Local Scour Below Offshore Pipelines – A Review."
L. Cheng 175

"Comparison of General Scour Prediction Equations for River Crossings."
C. Lauchlan, R. W. P. May 184

"Effect of Suspended Fine Sediment on Local Scour."
D. M. Sheppard **(Invited Lecture)** 198

"Numerical Simulations of 3-D Flows Around Bridge Piers."
S-U. Choi, W. Yang 206

"3-D Numerical Model for Wave-Induced Dynamic Behavior of Sand Beds at Bridge Piers."
F. Mia, H. Nago, S. Maeno 218

"Pier Scour at Woodrow Wilson Bridge and SRICOS Method."
K. Kwak, J-L. Briaud, Y. Cao, M-K. Chung, B. Hunt, S. Davis 227

"Bed Shear Stress Around Rectangular Pier: Numerical Approach."
P. Nurtjahyo, H-C. Chen, J-L. Briaud, Y. Li, J. Wang 242

"Analysis of Pier Scour Predictions and Real-Time Field Measurements."
D. S. Mueller, C. R. Wagner **(Invited Lecture)** 257

"Future Hydrographs and Scour Risk Analysis."
J-L. Briaud, P. D'Odorico, E. J. Jeon 272

"Database Program for Highway Bridge-Scour Data."
K. Farrag, M. Morvant 283

"Nondimensional Analysis of Clear-Water Scour at Bridge Contractions in Cohesive Soils."
O. Guven, J. G. Melville, J. E. Curry 292

"FE Analysis of Coastal Cliff Erosion due to Ocean Wave Assailing."
K. Yasuhara, S. Murakami, Y. Kanno, Z. Wu 307

SCOUR MEASUREMENTS

"Local Scour Around Structures in Tidal Flows."
R. W. P. May, M. Escarameia **(Invited Lecture)** 320

"Movement of Bridge Pier by Water Flow Under Flood Condition."
K. Ogihara, H. Muraishi, S. Masahiko, D. Nakajima 337

"3-Dimensional Measured and Simulated Flow for Scour Near Spur Dikes."
R. Kuhnle, Y. Jia, C. Alonso 349

"Scour Experiments on Dike Angle, Porosity, and Hook for a Thin Dike."
E. Martinez, R. Ettema, A. Lachhab 364

"Shallow Water Effect on Pier Scour in Clays."
Y. Li, J-L. Briaud, H-C. Chen, P. Nurtjahyo, J. Wang 373

"Flume Experiments on Abutment Scour: Confronting Complexities in Process and Similitude."
R. Ettema **(Invited Lecture)** 383

"Scouring Downstream of Sluice Gate."
S-Y. Lim, G. Yu 395

"Development of the New Inspection Method on Scour Condition Around Existing Bridge Foundations." J. Fukui, M. Otuka 410

"Experimental Study on Toe Scour of Seawall Covered with Armor Units Due to Waves."
T. Sakakiyama, R. Kajima 421

"Scour Around Rubble-Mound Breakwater Head of Cheju Outer Port."
H. Kim, B. C. Oh, B-S. Jung, S-Z Youn 437

GEOTECHNICAL ASPECTS

"Theoretical and Practice Aspects of Rock Scour Prediction."
G. W. Annandale, E. Bollaert, A. Schleiss **(Invited Lecture)** 449

"Erosion Function Apparatus Overview and Discussion of Influence Factors on Cohesive Soil Erosion Rate in EFA Test."
Y. Cao, J. Wang J-L. Briaud, H-C. Chen, Y. Li, P. Nurtjahyo 459

"Identification of Dispersive Clays in Gaza Strip Area; and Filter Effects on Dam Safety."
M. A. Awad 471

"Effects of Cohesion on Bridge Scour."
A. Molinas, S. J. Jones 485

"Scour Around Submarine Pipeline in Clayey Soil."
S. Neelamani, A. Vijaya kumar, S. Narasimha Rao 500

"GIS-Based Bridge Scour Prioritization."
C. L. Ho, J. M. Di Stasi, P. Rees **(Invited Lecture)** 516

"Erodibility Tests of Shale-Rock Samples Taken from Bridge Pier Construction Site on the Mississippi River." T. Nakato 528

"The Driving Force on Soil Grains and Its Effect on Scouring the Channel of Foundation."
L. Zhang, D. Ding, W. Zhou 540

"Depth of Mobile Layer Under Severe Wave Conditions: Liquefaction Effect."
S. Sassa. 546

"Essence of Silt Factor for Scour Calculation Around Bridge Foundation."
R. K. Dhiman, D. K. Mohapatra 560

VOLUME II

COUNTERMEASURES

"Scour Protection Around Gravity Based Structures Using Small Size Rock."
K. J. Bos, H. J. Verheij, G. Kant, A. C. H. Kruisbrink **(Invited Lecture)** 567

"Riprap as Permanent Scour Protection Around Bridge Piers."
C. D. Anglin, F. Itamunoala, G. Millen 582

"Riprap at Rectangular Bridge Piers Under Oblique Incident Flow."
J. A. Sainz, R. Salgado 597

"Countermeasure Construction Using Jet Grouting Methods to Combat Foundation Scour."
D. W. Boehm 609

"Field Evaluation and Countermeasure Selection for Scour Critical Bridges in the Commonwealth of Kentucky."
K. J. Schaefer, R. W. Gardner 623

"Impact of the Federal Highway Administration's Scour Evaluation Program in the United States of North America's Highway Bridges."
J. E. Pagan-Ortiz **(Invited Lecture)** 636

"Evaluation of Strategies to Control Erosion along U.S. Highway 50 Between Carson City and Lake Tahoe."
K. E. Dennett, P. Fricthel, R. Siddharthan, A. Soltani 642

"Optimisation of Scour Protection Measures."
G. B. H. Spaan, M. H. Lindo, G. Kant 656

"Design and Construction of Bridge Scour Countermeasures Along the Salt River, Phoenix, Arizona." D. L. Richards 670

"Treating Channel Instability at Bridges."
P. A. Johnson **(Invited Lecture)** 678

"Scour Hazard Mitigation for Tick Canyon Wash Bridge."
M. S. Islam, J. Zha, A. Abghari 684

"Final Stages of Butte City Bridge Erosion Control Project."
S. K. Mishra, W. B. Lindsey 699

"Riprap Protection Around Bridge Piers in a Degrading Channel."
Y-M. Chiew 707

"Scour at a Submerged Rock Dike, Willapa Bay, Washington."
N. Sultan, R. Phillips, H. Bermudez 719

ABUTMENTS AND EMBANKMENTS

"Abutment Scour Countermeasures: A Review."
B. Barkdoll, R. Ettema, R. Kuhnle, B. Melville, T. Parchure, A. Parola, C. Alonso
(Invited Lecture) 734

"Countermeasures for Scour at Spill-Through Bridge Abutments."
B. Melville, S. Coleman, D. Hoe 749

"Hugo Reservoir Embankment Depression Study."
J. B. Nevels, Jr. 764

"Pier and Abutment Scour-New Laboratory Data."
W. H. Hager, J. Unger, G. Oliveto 774

"Flow and Scouring in Main Channel due to Abutments."
G. Yu, S-Y. Lim, S-K. Tan 785

PIER SCOUR

"3-D Numerical Modeling of Flow and Scour Around a Pile."
A. Roulund, B. M. Sumer, J. Fredsoe, J. Michelsen **(Invited Lecture)** 795

"New Approach to Scour Evaluation of Complex Bridge Piers."
E. V. Richardson, J. S. Jones, D. M. Sheppard 810

"Time Rate of Local Scour at a Circular Pile."
W. Miller, Jr., D. M. Sheppard 827

"A Case Study of the Possible Effects of Long-Term Climate Change on Bridge Scour."
P. Kirshen, L. Edgers, J. Edelmann, M. Percher, B. Bettencourt, E. Lewandowski 842

"Analysis of Pile Groups Considering Riverbed Scouring."
S. Jeong, J. Won, J. Suh 854

SCOUR PROBLEMS

"Study on the Disasters of Bridge and Bed Protection Works During the Passage of Typhoon Herb." C. Lin, T-C. Ho, P-H. Chiu, K-A. Chang **(Invited Lecture)** 869

"Damages of the Roads-Bridges by Erosion and Remedial Measures in Albania."
L. Bozo, Y. Muceku 884

"Bridge Pier Scour in Bouldery Bed – Indian Scenario."
R. Singh, K. K. Razdan, R. K. Dhiman 896

"Scour Monitoring of Bridge Piers via Inclination Detection."
N. Kobayashi, S. Kitsunai, M. Shimamura 910

"Non-Destructive Testing to Determine Unknown Pile Lengths Under Existing Bridges."
F. Rausche, M. Huessin, M. Bixler 918

"Determination of Unknown Bridge Foundation Depths with NDE Methods."
L. D. Olson **(Invited Lecture)** 929

"Scour of Railway Embankment Foundation Located on Sea-Cliff in Japan."
H. Suzuki, M. Shimamura 945

"Design and Construction of Scour Foundations for Electric Power Transmission Line Structures." P. M. Kandaris, R. E. Kondziolka, J. P. Adams 954

"Propeller Induced Scour."
C-O. Chin, W. Li 968

"Confederation Bridge – New Scour Design Methodology for Complex Materials."
R. B. Nairn, C. D. Anglin 978

SCOUR MONTORING

"Instruments to Measure and Monitor Bridge Scour."
E. V. Richardson **(Invited Lecture)** 993

"Development and Implementation of a Scour Monitoring Program for Selected Bridges Crossing the Trukee River."
K. E. Dennett, P. Fritchel, R. Siddharthan, A. Soltani 1008

"Seismic Methods to Identify Scour Depth Around Deep Bridge Foundations."
E. J. Mercado, E. B. Davies, J. A. McDonald, M. W. O'Neill 1019

"Portable Scour Monitoring Research."
J. D. Schall, G. R. Price 1032

"Active Scour Monitor Instrumentation in the California Transportation System."
S. Ng 1042

CASE HISTORIES

"A Methodology for Predicting Channel Migration NCHRP Project No. 24-16."
P. Lagasse, W. Spitz, L. Zevenbergen **(Invited Lecture)** 1051

"Predicting Meander Migration: Evaluation of Some Existing Techniques."
J-L. Briaud, H-C. Chen, S. Park 1061

"Collapse and Erosion of Khon Kaen Loess with Treatment Option."
P. Punrattanasi, A. Subjarassang, O. Kusakabe, T. Nishimura 1081

"Analysis of Contraction and Abutment Scour at Two Sites in Minnesota."
C. R. Wagner, D. S. Mueller 1096

"Factors Affecting Stream and Foundation Stability at Existing Bridges in New Jersey."
S. M. Baig, J. J. Zarriello, M. A. Khan 1111

VOLUME III
PREDICTION EVENT

PREDICTION REQUEST

"Prediction Request for ICSF-1"
Prediction Event Committee 1127

PREDICTION PAPERS

"Pier Scour Prediction for Mississippi River Bridge / Pier 11 for the 08-03-93 flood event / Bridge Case 7." Guillermo Ferrando, Carlos Cian 1152

"Pier Scour Prediction for Mississippi River Bridge / Pier 17L for the 05-01-91 flood event / Bridge Case 8" Guillermo Ferrando, Carlos Cian 1155

"On the Prediction of the Maximum Depth of a Scour Hole Around Cylindrical Bridge Piers in Non Cohesive Soils" Oscar Link, Ulrich Zanke 1160

"Contribution Prediction Van Oord ACZ" T. Piepers 1166

"Prediction of Local Scour of Non-Cohesive Sediments Around Bridge Piers Using FVM-Based CCHE2D Model" Weiming Wu, Sam S. Y. Wang 1176

"Numerical Simulation of Local Scouring Around a Cylindrical Pier" Yafei Jia, Yichun Xu, Sam S. Y. Wang 1181

FLUME TESTS RESULTS

"Flume Tests Results" Ya Li , Jun Wang, Wei Wang, Jean-Louis Briaud , Hamn-Ching Chen 1188

COMPARISON BETWEEN PREDICTIONS AND MEASUREMENTS

"Comparison Between Predictions and Measurements" Ya Li, Jun Wang, Wei Wang, Jean-Louis Briaud, Hamn-Ching Chen 1208

Scour Protection Around Gravity Based Structures Using Small Size Rock

By

Klaas Jan Bos[1], Henk J. Verheij[1], Gijsbert Kant[1], Arno C.H. Kruisbrink[1]

ABSTRACT

This paper presents results of research onto scour around large scale submerged offshore structures (Gravity Based Structures) subjected to the combined effect of loads related to wind waves and currents. The research comprises small-scale model tests with a GBS, numerical simulation of the flow field around the structure, and the derivation of a scour prediction equation for practical engineering purposes. The physical model tests were carried out with a GBS protected by thick layers of various rock sizes, different hydraulic conditions and structure configurations. The flow field around a GBS was computed in order to increase the insight into the observed scour phenomena. Finally, as prediction formulas for structures like a GBS loaded by combined wave and current action do not exist, the obtained test data have been used to develop a scour prediction formula enabling designers to determine the scour depth and required minimum thickness of the rock protection.

INTRODUCTION

Little is known about scouring due to combined wave and current action around a GBS with a structure height of less than 50% of the water depth as well as the required rock as scour counter measure. The combined wave and current influence induce scour of an unprotected seabed, in particular near the corners of a GBS. Under North Sea conditions scour holes of 5 to 10 m can easily develop depending on the loading conditions. Then, a proper bed protection to ensure the stability of the GBS will be required. One of the possibilities is a thick layer of small-sized rock which extents up to a certain distance out of the GBS side walls. The design philosophy of this 'dynamic scour protection' is that, in principle, scouring of the rock is allowed as long as the full thickness of the layer is not eroded. Dynamic scour protections are environmental-friendly and can easily be constructed and maintained by using proven fall pipe technology and, therefore, they provide a good alternative to other types of GBS scour protections such as mattresses. However, design rules about the required minimum rock size and layer thickness in relation to the expected scour are not available.

In addition to the above mentioned lack of design rules for a dynamic scour protection, no scour prediction equations are available about GBS scour due to the combined wave and current action. Even observed data in physical models or

[1] WL | Delft Hydraulics, PO Box 177, 2600 MH Delft, The Netherlands.

prototype conditions about this combined scour are very scarce. In design manuals (Hoffmans and Verheij, 1997, Whitehouse, 1998) only scour prediction equations are presented for current-induced scour or wave-induced scour. Examples are the well-known formulas for current-induced scour of Khalfin (1983) and Teramoto (1973), of which the latter is applicable, even for submerged structures. With respect to wave-induced scour the formulas of Sumer et al. (1993a, 2001b) are well known. The only data on combined wave and current induced scour at large scale structures mentioned are those presented by Rance (1980). Data on combined wave and current induced scour at slender structures are presented by Sumer and Fredsøe (2001a).

Based on the above mentioned lacunas in scour knowledge the underlying study was initiated and carried out. The aim of the research was to collect data and, if possible, to derive a scour prediction formula in order to enable in the future a proper conceptual design of the scour protection for a GBS subjected to the action of combined waves and currents. Therefore, data were collected by carrying out small-scale model tests. Combined with literature data, amongst others of scour surveys at a GBS located in the F3 field in the North Sea, it was possible to derive a scour prediction equation. The equation allows to determine the expected scour and the required scour protection for conceptual design purposes.

PHYSICAL MODEL EXPERIMENTS

Description of the model

Physical model tests were carried out at in a basin with a length of 35 m and a width of 7 m at WL | Delft Hydraulics. In the facility waves and flows can be generated simultaneous. In the basin a test section was constructed comprising a bed protection over the total width of the basin with a length of about 4.5 m and a thickness of 0.1 m. On top of the bed protection a GBS model was placed with dimensions of 1.0 x 1.0 m^2. The local water depth at the bed protection was 0.65 m. A total of 12 tests were carried out in four main test series.

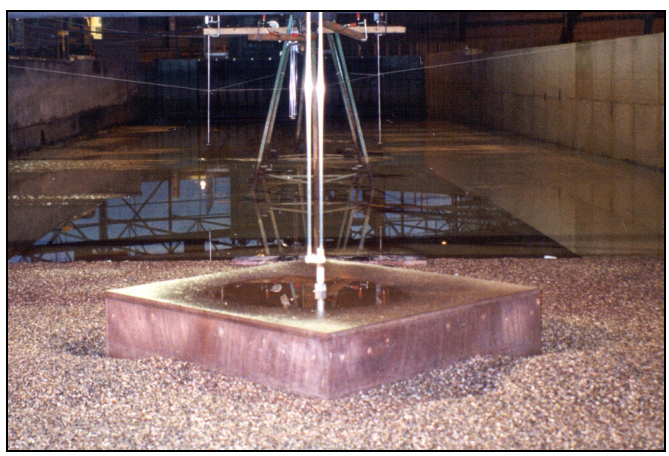

Figure 1: Physical model test on GBS scour

Test series

Four main test series were carried out, each focussing on a different parameter of the scour process. In Test series 1 the influence of the bed protection diameter was studied for a basic layout (square GBS with a height of 0.15 m, 45° orientation). The grain size was varied in three steps from d_{50} = 0.028 m to 0.085 m. In addition a test with increased wave load was carried out for the protection with the largest grain size.

For these tests the scour development in time was determined. In Test series 2 the hydraulic conditions were varied to study the influence of the hydraulics conditions on the scour. Tests were carried out for wave heights in the range H_s = 0.14 - 0.27 m and depth average flow velocities u_c varying from 0 - 0.25 m/s. These tests concentrated on the equilibrium scour depth. The development in time was not measured. In Test series 3 one test was carried out in which the height h_c of the GBS was varied from 0.15 m to 0.40 m. Test series 4 comprises two tests. One test was carried out with rounded corners of the GBS. In the second test the orientation of the GBS was changed from 45° to 90° relative to the wave and flow direction.

Test	d_{50} (cm)	h_c/h_0 (-)	H_s (m)	T_p (s)	$\hat{u}_\delta$ (m/s)	KC^* (-)	u_c (m/s)	u_{cw} (-)	u_*/u_{*cr} (-)	S_e (m)
1.1	2.8	0.23	0.22	2.0	0.33	1.02	0.21	0.38	1.05	0.064
1.2	3.7	0.23	0.22	2.0	0.33	1.02	0.20	0.38	0.99	0.065
1.3	8.5	0.23	0.22	2.0	0.33	1.02	0.21	0.38	0.78	0.048
1.4	8.5	0.23	0.27	2.3	0.44	1.56	0.19	0.30	0.87	0.062
2.1	3.7	0.23	0.27	2.3	0.44	1.56	0.20	0.31	1.12	0.081
2.2	3.7	0.23	0.22	2.0	0.33	1.02	0.00	0.00	0.95	0.091
2.3	3.7	0.23	0.23	2.0	0.34	1.05	0.09	0.21	0.99	0.062
2.4	3.7	0.23	0.16	1.6	0.20	0.49	0.00	0.00	0.76	0.033
2.5	3.7	0.23	0.14	1.6	0.18	0.44	0.25	0.59	0.77	0.024
3.1	3.7	0.62	0.14	1.6	0.18	0.44	0.25	0.59	0.77	0.071
4.1	3.7	0.23	0.22	2.0	0.33	1.02	0.24	0.42	1.00	0.036
4.2	3.7	0.23	0.22	2.0	0.33	1.02	0.25	0.43	1.00	0.046

d_{50} = median grain size, h_c = construction height GBS, h_0 = water depth, H_s = significant wave height, T_p = peak wave period, $\hat{u}_\delta$ = peak orbital velocity, KC* = modified Keulegan-Carpenter number (Eq. 2), u_c = depth average flow velocity, u_{cw} = nondimensional flow parameter (Eq. 1), u_* = bed shear velocity, u_{*cr} = critical bed shear velocity, S_e = equilibrium scour depth

Table 1: Overview of test parameters

Test conditions

From the measured hydraulic conditions various test parameters have been computed which are summarised in Table 1. Following Sumer and Fredsøe (2001a) a non-dimensional flow parameter has been used:

$$u_{cw} = \frac{u_c}{u_c + \hat{u}_\delta} \tag{1}$$

With u_c the depth average current speed and $\hat{u}_\delta$ the peak orbital velocity at the bed. Bed shear stresses and Shields values have been computed following well-known methods (see for instance van Rijn, 1993).

The Keulegan-Carpenter number, KC is defined by $KC = \hat{u}_\delta T_p / D$ in which D is the characteristic length of the structure and T_p the peak wave period. However, for large structures such as GBS it seems that not the dimensions of the structures are the

determining factor but the water depth (see also the next section about the new scour formula). Therefore, in the present study a slightly modified KC number has been used defined as:

$$KC^* = \frac{\hat{u}_\delta T_p}{h_0} \tag{2}$$

With h_0 the water depth. The test parameters for the tests are summarised in Table 1. In the final column of Table 1 the maximum observed scour depth S_e are included.

Physical model results

In Test series 1 the influence of the grain size has been studied as well as the scour development in time. Figure 2 shows the scour development in time. From the results it can be concluded that the scour develops relatively fast. In the first 50 minutes about 70% of the scour has already been developed. Hereafter the scour develops on a much smaller rate.

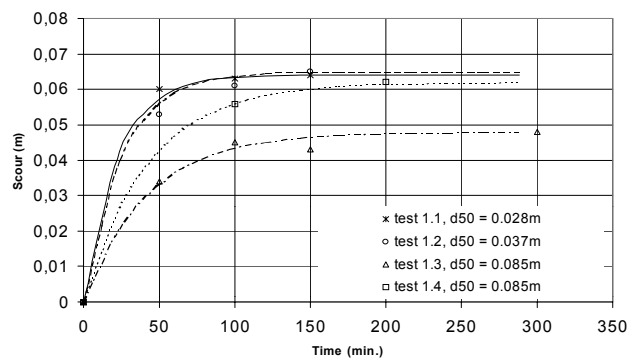

Figure 2: Scour development in time

Furthermore it can be concluded that the scour rate slows down with increasing grain size. However, after 150 minutes the scour was similar for the tests with d_{50} = 2.8 mm and 3.7 mm. A further increase of the grain size to d_{50} = 8.5mm results in a smaller scour depth even after an extension of the test series from 150 min. to 300 min. The smaller scour depth is explained by the flow velocities being less close to the critical flow velocities (see low ratio of u_* / u_{*cr} in Table 1). Test 1.3 has therefore been repeated with a higher wave height (Test 1.4). Although the ratio of u_* / u_{*cr} is still lower than those of Tests 1.1 and 1.2 the resulting erosion increased to similar values as measured for Tests 1.1 and 1.2.

Test series 2 focussed on the influence of the hydraulic conditions. Two typical examples of measured scour are shown in Figure 3. All tests clearly show that the scour is concentrated at the two side corners of the structure. The material from the scour holes has been deposited downstream, relatively close to the scour hole and the structure. The exception to this is Test 2.1 (see Figure 4) where probably due to the more severe hydraulic load the material is spread over a larger area outside the

measured area.

The most striking from these results are the larger scour depths for tests with waves only compared with tests with both waves and currents (see for example Test 2.2 versus 2.3 and Test 2.4 versus 2.5). The scour depth reduces with about 40% when a current is added to the hydraulic loads. A possible explanation for this phenomenon might be that eddy formation by the wave orbital motion is suppressed by the flow conditions imposed onto the wave action. This phenomenon is not yet fully understood and therefore further research is required to study the wave-current interaction and to explain the observed smaller scour for combined waves and currents.

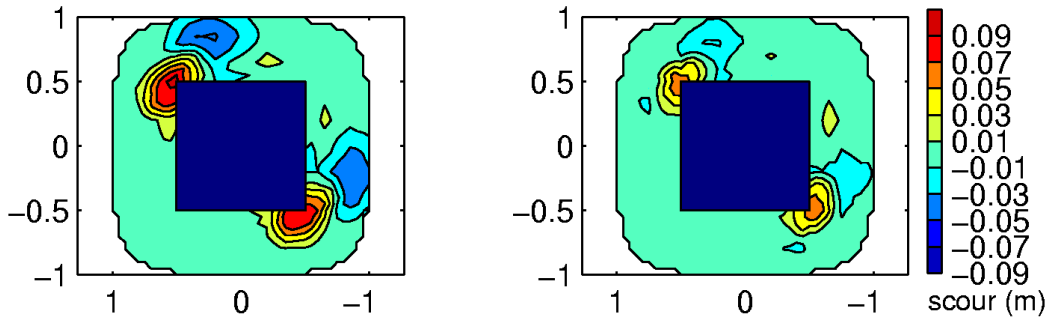

Figure 3: Scour results of Test 2.2 (left) and Test 2.3 (right), wave and flow direction is from lower left to upper right

Apart from the scour at the side corners the test results indicate secondary scour hole formation downstream of the primary scour holes at the GBS corners. This is the most pronounced in Test 2.1 (see Figure 4) but also visible in Tests 2.2 and 2.3.

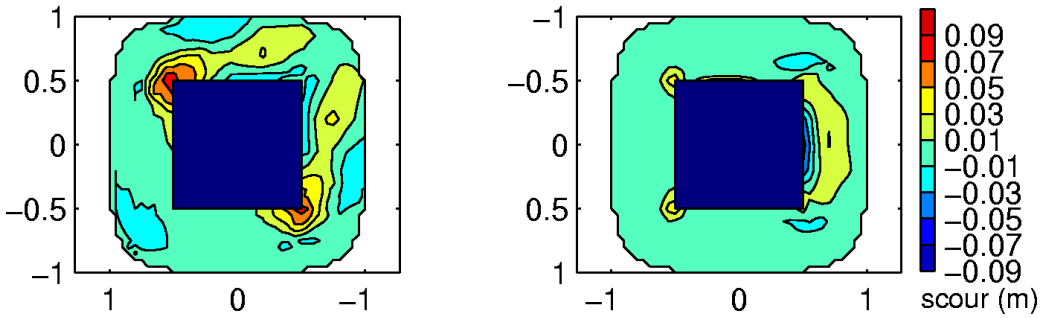

Figure 4: Scour results of Test 2.1 (left, wave and flow direction is from lower left to upper right) and Test 4.2 (right, wave and flow direction is from left to right).

In Test 3.1 the influence of the height of the structure has been studied by repeating Test 2.5 with increased structure height. The resulting scour clearly indicates the importance of the structure height. An increase of the structure height from 23% to 62% of the local water depth resulted into an increase of the scour depth with about 200%.

In Test 4.1 the shape of the structure has been modified by removing the sharp edges

of the square structure. A comparison with Test 1.2 with similar hydraulic conditions indicates a reduction of the scour with about 50%.

The results for a test situation with a 90° orientation of the structure relative to the wave and flow direction is shown in Figure 4 (Test 4.2). The test results indicated a reduction of the scour holes with 30% compared with Test 1.2 which was carried out with similar hydraulic conditions. The scour pattern for this test is different from the other tests. The largest scour is found at the front corners of the structure. Scour also occurred downstream of the structure. Scoured material has been deposited immediately at the back of the structure.

NUMERICAL FLOW MODELLING

From the observed scour in the physical model it was concluded that adding a flow velocity to the hydraulic load enforced secondary scour at the back of the structure (see Figure 4, Test 2.1). This secondary scour might be explained by eddy formation in the lee of the structure. Similar to the flow over a sill the current over the submerged GBS might generate an eddy with a horizontal axis at the back of the structure. The nearbed flow velocities in the eddy are directed opposite to the main flow direction. When the flow velocities are high enough, gradients in the transport capacity occur and hence erosion of the seabed. The maximum erosion occurs just downstream of the re-attachment point where the velocities diverge and the local horizontal velocity is zero. At the wall of the structure the bed velocities will be zero causing deposition of the bed material directly near the structure. These effects are visible in Figure 4.

In order to verify the above hypothesis, numerical flow simulations was carried out for the tested GBS geometry and a typical flow condition in the absence of waves. The simulations were carried out with the flow modelling software CFX, which enables the simulation of three-dimensional flows. Figure 5 shows the bed shear stress components in flow and lateral direction. The results illustrate that in the lee of the structure bed shear stresses are directed towards the structure. Furthermore, the bed shear stress pattern correlates well with the secondary scour pattern of Test 2.1.

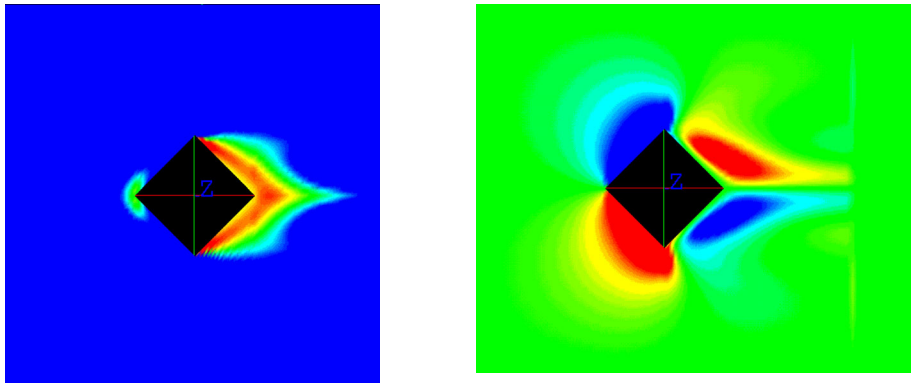

Figure 5: Bed shear stresses in flow direction (left) and in lateral direction (right), flow direction is from left to right.

From the above results it may be concluded that the flow simulations support the hypothesis of eddy formation and subsequent scour in the lee of the structure.

It should be noted that the presented results are representative for a situation with currents only (not tested in the physical model). The combined action of waves and currents will generate a much more complicated dynamic 3-dimensional flow field around the submerged structure. Further research is required to study the wave-current interaction around these type of structures.

SCOUR FORMULA

General shape

In order to develop a new formula for the prediction of the scour depth for large scale submerged structures the general concept presented by Breusers et al, (1977) has been applied, which describes the scour depth as the product of various influences:

$$S = S_e\, f(t) \quad \text{with} \quad S_e / L = \prod f_i \quad \text{and} \quad \prod_1^n f = f_1 \cdot f_2 \cdots\cdots\cdots\cdots f_n \qquad (3)$$

in which S = time-dependent scour, S_e = maximum scour, *f(t)* = function describing the time dependent scour, L = characteristic length, f_i = coefficients for various influences. These influences account for the wave characteristics, the ratio structure diameter - water depth, the influence of initiation of motion, the shape of the structure, the angle of wave and flow attack, sediment/rock diameter and gradation, etcetera.

This concept has been presented by Breusers et al, (1977) and has been adapted by various researchers (e.g. HEC-18, 1995; Escarameia & May, 1999; Melville & Coleman, 2000) to predict the scour around all types of structures. However, most of these formulas focus on one dominant process in particular situations, see for instance the formulas of Sumer et al. (1993, 2001b) for wave-induced scour only. In addition the time factor *f(t)* is not defined in many equilibrium scour formulas.

The underlying study was focused on large diameter structures, e.g. structures with a ratio diameter - water depth larger than 1.5. Scour around these type of structures depends less of the horizontal dimensions of the structure, but more of the water depth. Therefore, the characteristic length L has been replaced by the water depth h_0 and not by a characteristic or equivalent diameter of the structure D. Bridge piers may be considered as slender structures with $D/h_0 < 0.5$ and, subsequently, the characteristic length is the pier diameter. Breusers et al. (1977) presented a factor that takes this aspect into account automatically for slender and large structures, but also for intermediate range of $0.5<D/h_0<1.5$ (see also next section on influence of the ratio structure diameter-water depth).

The various parts of the total formula are discussed in the next section.

Influence of waves

The function f_1 describes the wave related scour. A linear relation between the modified Keulegan-Carpenter number KC* and the dimensionless scour depth S_e/h_0 could be derived from experimental data presented by Sumer and Fredsøe (2001b). If all other influences may be ignored the factor f_1 reads:

$$f_1 = 0.044KC^* \tag{4}$$

The water depth is the characteristic length in the modified KC^*-number and not the diameter.

Influence currents

The function f_2 describes the influence of a current on the scour depth. Recent work of Sumer and Fredsøe (2001a) resulted in the diagram given in Figure 6 showing the influence of a flow velocity on the scour depth for several KC numbers. The influence of the flow is the ratio between the scour depth at $u_{cw} = 0$ (waves only) and the scour depth for a given value of u_{cw}.

Sumer and Fredsøe (2001a) do not present a mathematical formulation and, therefore, an expression has been determined which approximates the given data points:

$$f_2 = \frac{A\tanh(3.5(u_{cw} - B)) + 1.9 - A}{A\tanh(-3.5B) + 1.9 - A} \tag{5}$$

$$\text{with } A = \frac{0.95}{1 + 0.005KC} \quad \text{and} \quad B = \frac{0.8}{1 + 0.005KC^2}$$

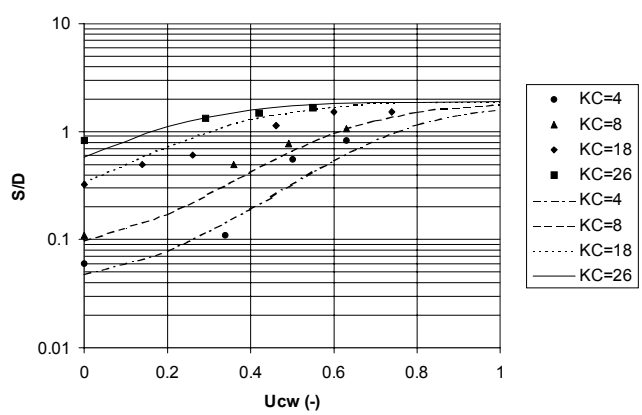

Figure 6: Influence of currents on scour depth (data points after Sumer and Fredsøe, 2001a).

Note that this formula has been derived from tests comprising slender structures, and as a consequence the formula is expressed in KC instead of KC^*. Future research

should be carried out to confirm the suitability of this relation for large diameter structures.

Influence initiation of motion

The factor f_3 describes the influence of the critical flow velocity. In the literature two types of formulations are found for this function: for clear water scour $f_3 = (2.u/u_{cr} - 1)$ for $0.5<u/u_{cr}<1.0$ (Breusers et al, 1977; Khalfin, 1983) or $f_3 = u/u_{cr}$ or $u_*/u_{*,cr}$ (Hoffmans and Verheij, 1997; Teramoto, 1973) and for live bed scour $f_3 = 1$ for $u/u_{cr} > 1$. Note that for $u/u_{cr} < 0.5$ no scour will occur. Escarameia and May (1999) presented similar influence factors, but made a difference between circular and square structures. As the tests carried out in this study were all clear water scour tests the formulation has been adapted with the bed shear velocities, because it is difficult to decide which value of u, e.g. depth-averaged value or the value at for instance 1 m above the bed, should be applied. So, f_3 reads:

$$f_3 = \frac{u_*}{u_{*,cr}} \tag{6}$$

The critical bed shear stress velocity was computed from the critical Shields parameter. The latter was computed following Soulsby and Whitehouse (1997).

Influence structure height

All other influence factors are derived for structures extending through the water surface (emerging structures). A GBS, however, is a submerged structure and this affects the scouring. The influence of the height is included in the f_4 function.

Theoretically the value of the factor should be equal to 1 for h_c/h_0 approaching 1. The structure then becomes emerged and the influence of the height will be negligible. From the measured data it appeared that the f_4 value depends on the value of u_{cw}. For the tests without a current a value for f_4 is required in the order of 1, while for tests with combined waves and currents a value smaller than 1 was required.

On the basis of the now available data the following relation could be determined to assess the influence of the structure height:

$$f_4 = 1 \quad \text{for} \quad u_{cw} = 0 \quad \text{or} \quad h_c/h_0 = 1 \tag{7}$$

$$\text{else } f_4 = \tanh\left[3.5U_{cw}\left(\frac{h_c}{h_0} - 1.4\right)\right] + 1$$

It should be noted that most tests were carried out with a GBS height of about 25% of the water depth and only one test has been conducted with a larger structure height of about 60%. Another possibility should have been to investigate whether the relationship is applicable presented by Khalfin (1983): $S_e/D \therefore (h_c/D)^{1.43}$. However,

this was not investigated because the parameter u_{cw} appeared to be relevant in our data set.

Influence structure shape

The function f_5 represents the influence of the shape of the construction. The other factors are all derived for circular piles, therefore the f_5 function is an influence factor for the shape relative to a circular shape. For slender structures various influence factors are presented in the literature (Melville & Coleman, 2000; Hoffmans and Verheij, 1997; HEC-18, 1995). However, for large structures these data are very limited, in fact only experimental results of large emerged objects presented by Rance (1980) are available. From the presented results the following values have been derived:

$$f_5 = 1.0 \text{ for circular structures} \tag{8}$$
$$f_5 = 2.0 \text{ for square structures } (90^0 \text{ orientation})$$
$$f_5 = 2.8 \text{ for square structures } (45^0 \text{ orientation})$$

Note: the influence of the angle of attack or alignment with respect to the flow direction is implicitly included in the f_5 value.

Influence ratio structure diameter-water depth

The function f_6 describes the effect of the length scale of the structure (usually the pier diameter) relative to the water depth. The function has been expressed by Breusers et al., (1977) as $f_6 = 1.5\tanh(D/h_0)$ (Note that the ratio D/h_0 has been reversed to account for the change of the characteristic length compared to the original Breusers formula), or in the HEC-18 formula as $f_6 = (D/h_0)^{0.65}$, while Escarameia and May (1999) presented a reverse function $f_6 = (h_0/D)^{0.6}$.

In principle, all those formulas could be applied, but having chosen the water depth as characteristic length (see previous section on general formula shape), a factor including the diameter of the structure is not longer important. Therefore, the value of the factor f_6 has been set at 1 for the present application of large scale offshore structures. However, in situations it is not clear whether D or h_0 is the decisive parameter, the function of Breusers is recommended, because it is valid for the whole range of h_0/D.

Influence time

In literature various equations are presented for the time-dependent development of the scour. Most of these formulations are of the form (Whitehouse, 1998; Sumer et al., 1993; Cardoso & Bettess, 1999; Melville & Coleman, 2000):

$$S = S_e\left[1 - \exp\left(-a\left(\frac{t}{T}\right)^b\right)\right] \tag{9}$$

with t the time in hours, T a characteristic time scale and a and b being coefficients.For simplicity a and b have been set at 1.0. Assuming the maximum measured scour depth for each test as the equilibrium scour depth only a value for T needs to be determined. In the literature various expressions for T are found. In most of these formulas T is expressed as a function of the grain size, relative density, structure diameter or water depth, KC number and flow velocity. As the data in the present study was limited a very simple relation for T was adopted which assumed a linear relationship between T and the sediment size d_{50}. The relation was derived from a fit through the data points and reads:

$$T = 0.2 + 60d_{50} \tag{10}$$

Resulting curves for the time variation of the scour for the various tests are presented in Figure 2. Further research is required to assessed a more generic formula expressing the time dependent scour.

Validation

For all test conditions the scour has been computed with the newly developed formula and compared with the measured scour depth in Figure 7b. From the results it can be concluded that for most tests the observed scour depths are within 80 - 120% of the predicted ones (computed value ±20%).

With respect to Test 4.1 with a square GBS with rounded corners a shape factor f_5 = 2.0 is required to match predicted and measured scour. As expected this value is between the value for a circular structure and square structure with a 45° orientation.

The developed formula to predict the scour depth has been verified with other relevant data sets available. They are summarised in Table 3.

GBS	origin data	h_0 (m)	h_c (m)	length x width (m^2)	H_s (m)	T_p (s)	u_c (m/s)
Case A*	model	41.8	12	63 x 56	12.4	15.6	1.3
F3	model	42.3	16	70 x 80	11.2	14.25	1.0
F3	field	42.3	16	70 x 80	9.5	13.25	0.64-0.82

* Data of tests carried out within framework of consultancy

Table 3 Validation data (all measures are prototype dimensions)

Data used for validation were from small-scale model tests for platforms in the North Sea and from a scour evaluation for an existing platform in the F3 field. The physical model tests for Case A were carried out on scale 55 for a 1/100 years storm event. The scour protection consisted of a thick layer of small size rocks at the corners of the GBS. For the two corners which face the most severe attack different grain sizes of respectively d_{50} =2.8 mm (model) and d_{50} = 3.7 mm (model) were used. Maximum measured scour depths and predicted values are summarised below and it may be concluded that the predicted scour is about 15 to 20% larger than the observed one.

rock size (mm)	Observed scour (mm)	predicted scour (mm)
2.8	85	97
3.7	78	91

Table 4: Comparison of measured and predicted scour, Case A

The tests for the F3 platform were carried out on scale 40 and also for a 1/100 years storm event. The bed consisted of sand with a characteristic grain size d_{50} = 0.210 mm. From the observed measurements the equilibrium scour depth was estimated at 100 mm, while the predicted scour is also 100 mm.

Yearly scour surveys were carried out at the GBS in the F3 field in the North Sea. Since the installation in 1992 the observed scour is about 3.0 m (sand diameter d_{50} = 0.150 mm). In Bos et al (2002) the environmental conditions which occurred after the installation of the GBS have been estimated on the basis of a hindcast and measured data. The wave conditions are used to determine the orbital flow velocities for 1/1 year and 1/10 year storm event. The comparison between observed and computed scour is presented below.

observed scour: 3.0 m
computed scour: 3.2 m

Note: In Bos et al (2002) a comparison has been made between the scour computed with a modified Khalfin formula (see Hoffmans and Verheij, 1997) for current-induced scour and the observed scour. The computed values predicted a scour of 3.6 m, which is an overestimation of the scour depth.

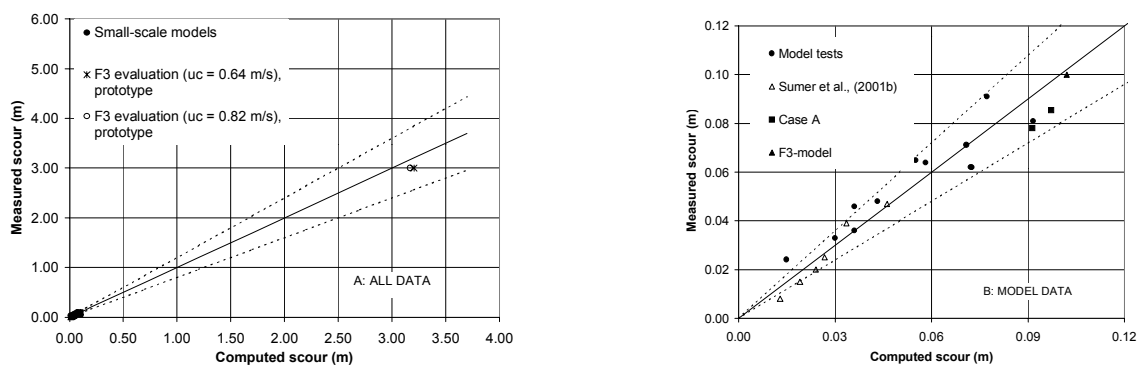

Figure 7: Comparison of measured and predicted scour depth

All scour data (computed and observed) are summarised in Figure 7. It can be concluded that for both model and prototype data most data points are within 20%. These results confirm the reliability of the developed formula. Although the amount of data is limited, obviously the formula predicts both prototype scour and model scour very well. The figure includes the data that has been used to develop the

formula, e.g. data in Table 1 and the Sumer data. It should be noted that, in principle, these data may not be used for verification as they have been used to develop the formula. However, with respect to the data of Sumer, the data show that the formula is also able to predict the scour for large emerged structures. Furthermore, it should be noted that all available cases are more or less similar e.g. GBS structures in North Sea conditions. More heterogeneous data are required for further verification and validation of the formula.

PRACTICAL APPLICATIONS

When using the present formula for practical applications the following is noted:

- Application of the formula in engineering practise should be restricted to conceptual design studies within the limits of the test conditions, as the available data were limited (North Sea conditions, little variation structure height). For final design purposes physical model testing is recommended to verify and optimise the design.
- The formula has been developed for a symmetrical GBS. Although we expect that the influence of an a-symmetrical structure is negligible, this has not been verified.
- The scour depth might be influenced by elements placed on the vertical walls of the GBS structure, especially when placed near the corners of the GBS. These effects are not included in the formula.

Finally, the new formula as described above has been summarised below:

$$S = S_e\, f(t) \text{ with } S_e / h_0 = \prod f_i$$

with:

$$f(t) = 1 - \exp(-t / T) \text{ with: } T = 0.2 + 60 d_{50} \text{ (Note: t in hours)}$$

$$f_1 = 0.044 KC^* \text{ with } KC^* = \frac{\hat{u}_\delta T_p}{h_0}$$

$$f_2 = \frac{A \tanh(3.5(u_{cw} - B)) + 1.9 - A}{A \tanh(-3.5B) + 1.9 - A}$$

$$\text{with: } A = \frac{0.95}{1 + 0.005KC} \text{ and } B = \frac{0.8}{1 + 0.005KC^2} \text{ with } KC = \frac{\hat{u}_\delta T_p}{D}$$

$f_3 = u_* / u_{*,cr}$ (clear bed scour) and $f_3 = 1$ (live bed scour)

$f_4 = 1$ *for* $u_{cw} = 0$ *or* $h_c/h_0 = 1$ *else* $f_4 = \tanh\left[3.5U_{cw}\left(\frac{h_c}{h_0} - 1.4\right)\right] + 1$

$f_5 = 1.0$ *for circular structures*
$f_5 = 2.0$ *for square structures* (90^0 *orientation*)
$f_5 = 2.8$ *for square structures* (45^0 *orientation*)

$f_6 = 1.5\tanh(D/h_0)$ (Note: 1.5 is a safety coefficient)

CONCLUSIONS

On the basis of the work presented in this report the following is concluded and recommended:

- A new design formula has been developed for large scale submerged offshore structures subjected to wave or combined wave and current attack. Using the formula the maximum and time dependent scour depth can be predicted. For the available model and prototype data sets the predicted scour depth has been shown to be within 20% of the observed scour.
- Maximum scour occurred during tests with waves only and a 45° orientation of the GBS. The main scour occurred at the corners of the GBS structure.
- The test results have shown a reduction of the scour depth when a flow is added to a situation with waves only. This observed phenomenon for submerged structures differs from results presented previously for emerging structures (see Figure 6) and is not yet fully understood. Furthermore it is noted that at the back of the GBS secondary scour formation is likely to be caused by enforced eddy formation in the lee of the structure due to the current flowing over the submerged GBS structure.
- It is recommended to improve and verify the formula on the basis of other data sets from either prototype measurements and results from new physical model testing programmes.
- Numerical model studies are recommended to increase our knowledge on the hydraulic and morphologic behaviour on submerged structures.

ACKNOWLEDGEMENT

This research was funded by the Dutch Ministry of Economic Affairs. The NAM is gratefully acknowledged for providing the scour surveys of the F3 GBS. We wish to thank J.W. Markvoort, student at Delft University of Technology, for his contribution to the physical model testing programme.

REFERENCES

Bos, K.J., Chen, Z., Verheij, H.J., Onderwater, M. and Visser,M. (2002): Local scour and protection of F3 offshore GBS plaform. Proc. 21st Intern. Conf. on Offshore Mechanics and Arctic Engineering, paper 28127, June 2002, Olso, Norway.

Breusers, H.N.C., Nicollet G. and Shen H.W., 1977. Local scour around cylindrical piers. Journal of Hydraulic Research 15 (1977) no. 3. pp 211 - 252.

Cardoso, A.H. and Bettess, R. (1999). Effects of time and channel geometry on scour at bridge abutments. ASCE, Journal of Hydraulic Engineering, Vol.125, No.4 April 1999.

Escarameia, M. and May, R.W.P., 1999. Scour around structures in tidal flows. HR Wallingford report SR 521, April 1999.

HEC-18 (1995). Evaluating Scour at Bridges. Federal Highway Administration, Hydraulics Engineering Circular No.18, Publication FHWA HI-96-031, Washington DC, U.S.A.

Hoffmans, G.J.C.M. and Verheij, H.J., 1997. Scour manual. A.A. Balkema /Rotterdam/Brookfield. ISBN 90 5410 673 5.

Khalfin, I.S.H., 1983. Local scour around ice-resistant structures caused by waves and current effect. P.O.A.C.-symposium 28, Helsinki, Vol. 2, pp. 992-1002.

Melville, B.W. and Coleman, S.E. (2000). Bridge Scour. Water Resources Publications, LLC. Colorado, U.S.A.

Rance, P.J., 1980. The potential for scour around large objects. Scour prevention techniques around offshore structures. Papers presented at a one-day seminar on 16 December 1980. Society for Underwater Technology. London. pp 41-53.

Rijn L.C. van, 1993. Principles of sediment transport in rivers, estuaries and coastal seas. Aqua publications. ISBN 90-800356-2-9

Soulsby, R.L. and Whitehouse, R.J.S.W., 1997. Threshold of sediment motion in coastal environments. Proc. Pacific Coasts and Ports '97 Conf., Christchurch, University of Canterbury, New Zealand.

Sumer, B.M., Christiansen, N. and Fredsøe, J., 1993. Influence of cross section on wave scour around piles. Journal of Waterway, Port, Coastal and Ocean Engineering ASCE, 119(5), pp 477-495.

Sumer, B.M. and Fredsøe, J., 2001a. Scour around a pile in combined waves and current. Journal of hydraulic engineering, May 2001. pp. 403 - 411.

Sumer, B.M. and Fredsøe, J., 2001b. Wave scour around Large Vertical Circular Cylinder. Journal of Waterway, Port, Coastal, and Ocean Engineering, May/June 2001. pp. 125-134.

Teramoto, S., 1973. Study on scouring of sit on bottom type offshore structures. Mitsubishi Heavy Industries Ltd., Japan.

Whitehouse, R.J.S., 1998. Scour at marine structures. Thomas Telford Publications. ISBN 0 7277 2655 2

Riprap as a Permanent Scour Protection Around Bridge Piers

D. Anglin[1], F. Itamunoala[2], G. Millen[3]

ABSTRACT

Scour design guidance in the United States (FWHA, 2001a, b, c) allows the use of riprap as a countermeasure to reduce the risk/implications of scour for existing bridges, but does not allow its use for new bridges. Rather, the foundation of new bridges must be placed "at such a depth that the structural stability will not be at risk with maximum scour". This approach may have significant implications with respect to the design and cost of the bridge structure. In contrast, riprap is generally accepted as a permanent countermeasure against scour for bridges in Europe (TRB, 1999) and in Canada (TAC, 2001). In addition, thousands of "rubblemound" structures have been designed and implemented in the field of coastal engineering over the past 150 years, including breakwaters (to protect harbour and other marine facilities), revetments, embankments and dams (to prevent erosion) and scour protection (for coastal structures, marine pipelines, etc.). Some of this experience can be applied to the design of scour protection for bridges.

Baird has recently undertaken scour assessments for two large bridges in Eastern Canada, including the St. John River Bridge on the Trans-Canada Highway in New Brunswick and the Confederation Bridge across the Northumberland Strait between New Brunswick and Prince Edward Island. Extensive analyses were undertaken for both projects in order to estimate potential scour depths, assess alternative scour countermeasures, and design effective scour protection systems. Physical modeling was undertaken in order to design riprap scour pads to prevent scour around the piers while also remaining stable under the extreme design conditions.

This paper provides an overview of these two projects and scour-related issues, focusing on the investigations undertaken to develop designs for riprap scour pads to provide permanent protection against scour. In particular, it is concluded that a carefully designed physical model investigation provides an accurate and cost-effective tool to assess/quantify the performance of riprap scour protection systems under extreme flow conditions, thereby allowing the design of permanent scour protection systems that may result in significant cost savings for many bridge projects.

THE ST. JOHN RIVER BRIDGE

Overview of Project

The Province of New Brunswick has recently upgraded the Trans-Canada Highway (TCH) between Fredericton and Moncton to a four lane freeway. This $585 million

[1] Baird & Associates, 500-1145 Hunt Club Road, Ottawa, ON, Canada, K1V 0Y3 (danglin@baird.com)
[2] Baird & Associates, 200-627 Lyons Lane, Oakville, ON, Canada, L6J 5Z7
[3] McCormick Rankin Corporation, 300-1145 Hunt Club Road, Ottawa, ON, Canada, K1V 0Y3

project includes 195 km of freeway, 58 interchanges and six river crossings, and opened in 2001 (see http://www.gnb.ca/dot/fred-mon.htm).

Baird, under contract to the Maritime Road Development Corporation (MRDC), was responsible for the scour assessment and design for the St. John River Bridge (refer to Anglin et al, 2001). This is a 1 km long high level structure supported by thirteen pile-supported piers (eleven standard piers and two larger main piers), with earth fill approach embankments and concrete abutments at either end of the structure (refer to Figure 1).

Figure 1 – The St. John River Bridge

The 100 year design conditions at the crossing location were defined by others using hydrodynamic model simulations. The peak water level was estimated to be +6.4 m GD, while the peak velocity was estimated to be 2.2 m/s in the navigation channel (near the main piers), with reduced velocities towards either riverbank.

Five of the piers are located on the flood plain (existing land elevation = +2 to +4 m GD), while eight are located within the main river channel (riverbed elevation = -3 to -5 m GD). The riverbed consists of loose, fine silty sand, with the potential for significant scour. Scour depth calculations undertaken using several methodologies, including those recommended in HEC-18 (FHWA, 2001a), suggested local scour depths of 6 to 12 m around the various piers and abutments. Contraction scour was estimated to be 1 m.

Preliminary Design of Scour Protection – Empirical Procedures

Given the potential for significant scour around the piers and abutments, preliminary designs were developed for riprap scour pads based on available published procedures. In general, these procedures are based on theoretical considerations and/or empirical

analyses of physical model test results. A list of the more common methodologies is provided below, along with the design manuals in which they are referenced:

- Canadian "compromise" curve (TAC, 1973; TAC, 2001);
- Isbash equation (ASCE, 1975; USACE, 1984; FHWA, 1989; FHWA, 2001c); and
- Maynord equation (USACE, 1994; TAC, 2001, USACE, 2001).

Numerous other scour protection design methodologies have been published in the technical literature, but have not yet received widespread application or been incorporated in design manuals. Each approach requires the definition of various input parameters, the most important of which are listed below:

- Density of riprap (ρ_r) and water (ρ_w);
- Ambient flow velocity (V) - including adjustments for pier location considering river alignment (i.e. straight or curved), cross-sectional variations, etc.;
- Velocity magnification factor (K) - to account for local influence of the bridge pier on flow conditions (the TAC, Isbash and Maynord approaches require specification of this parameter; the other methods inherently incorporate the local influence of the bridge pier on flow conditions, but require specification of a pier shape coefficient);
- Water depth (d);
- Factor of safety (FS); and
- Bed slope (θ)

Riprap design calculations were undertaken using various methods for the eleven standard piers and two main piers along the St. John River Bridge. The piers consist of a number of 0.7 m diameter vertical and battered piles (typically spaced at 1.7 m center to center) extending down from the pile cap into the riverbed. The overall width of the standard piers (based on the area encompassed by the pile caps and piles) ranges from 7.5 to 10 m between the water surface and the riverbed, with a "flow blockage ratio" in the order of 50 to 70% depending on the water level (debris blockage could increase this to 100%). The main piers are similar, but larger, with their overall width ranging from 12 to 15 m.

The riprap design calculations were undertaken for the 100 year design velocity of 2.2 m/s. A velocity magnification factor (K) of 1.7 was assumed for the TAC, Isbash and Maynord approaches in the absence of any relevant guidance for pile-supported piers. "Effective" pier widths of 7.5 and 12 m were assumed for the standard and main piers respectively. The results of the main pier calculations (design water depth = 10.4 m) are presented in Table 1.

Table 1
Empirical Estimates of Riprap Scour Protection Requirements
St. John River Bridge, Main Piers

Methodology/Reference	Stone Size D_{50} (m)	Min. No. of Layers	Min. Layer Thickness, t (m)
TAC (1973, 2001)[1]	0.45	2	0.9
Isbash/FHWA (1993)[1]	0.33	3	1.0
Maynord/USACE (1994)[1, 2]	0.23	1.5	0.5
Parola (1993)	0.41	n/a	n/a
Chiew (1995)[3]	0.10 to 0.37	n/a	n/a
Fotherby & Ruff (1996)	0.55	2	1.1
Lauchlan & Melville (2001)	0.50	2	1.0

Notes:
1. TAC, Isbash and Maynord calculations assume K = 1.7.
2. Maynord approach gives D_{30}; result has been converted to D_{50} assuming $D_{50} = 1.25*D_{30}$, based on assumed riprap gradation with $D_{85}/D_{15} = 2$.
3. Chiew results presented with and without "flow depth effect".

These results show considerable variation in the estimated size of riprap required to provide a stable scour pad. This variation may be due to numerous factors, including different testing facilities/methodologies, different observation/measurement procedures (such as damage criteria) and different test conditions (such as stone shape/gradation, flow depth, etc.). Further, this variation does not include the uncertainty associated with defining the velocity magnification factor for the pile-supported pier configuration.

Physical Modeling of Scour Protection

Given the variation in the empirical estimates of scour protection requirements, and the uncertainty in the selection of an appropriate velocity magnification factor for the pile-supported pier configuration, a site-specific physical model investigation was undertaken to refine and optimize the design of scour protection for the St. John River Bridge. The tests were undertaken in a 2 m wide tilting flume at the Canada Centre for Inland Waters (CCIW) in Burlington, ON at a geometric scale of 1:37.5. The focus of the model tests was the areal extent and thickness of the scour pads, and the requirement for a filter layer between the scour pad and river bed. Tests were undertaken with flow conditions up to and exceeding the 100 year flood event for two design concepts, as follows:

- a 1.0 m thick layer of riprap (D_{50} = 0.3 m) over a 0.3 m thick filter layer; and
- a 1.3 m thick layer of 0.45 m minus quarry run (D_{50} = 0.2 m).

The horizontal extent of both scour pads was 1.5 times the "effective" pier width, which represents the lower limit of published design guidance (1.5 to 2.0). Figure 2 presents a photograph of the model test setup for a standard pier.

Figure 2 – Standard Pier and Scour Pad in Test Flume

The test results showed acceptable performance of both designs under flow conditions up to and exceeding the 100 year design event, with no instability of either scour pad noted in the tests. Additional desktop analyses were undertaken in order to assess the quarry run design concept, specifically the potential to use smaller stone (D_{50}) with a greater layer thickness (t). The model test results were found to be generally consistent with empirical relationships for D_{50} versus t presented in USACE (1994) and Chiew (1995).

The physical model results led to a reduction in the areal extent of the scour pad relative to that recommended by HEC-23 (FHWA, 2001c), and confirmed the acceptable performance of a wide gradation quarry run material without a filter layer. Final designs were developed for both riprap and quarry run scour pads. The riprap design utilizes a relatively narrow stone gradation (D_{50} = 0.4 m) with a layer thickness of $2*D_{50}$ placed over a filter layer (granular or geotextile). The quarry run design, which does not require a filter layer, utilized a wider gradation of smaller stone (D_{50} approximately 60% of that of the riprap) and a layer thickness of $5*D_{50}$.

Construction

The project schedule evolved such that scour protection had to be placed after the piles and pile caps had been installed. As such, considerable difficulty was anticipated with respect to placing stone materials amongst the piles underneath the pile caps. This concern led to consideration of several alternative scour protection design concepts, including concrete filled Fabriform bags and tremie concrete. The tremie concrete option was selected by the successful contractor for the area under the pile caps, while the quarry run option was retained for the area outside the pile caps.

Construction of the St. John River Bridge, including its scour protection system, was completed in 2001. A scour monitoring program was developed by Baird and recommended to MRDC, including a visual/diver inspection of the scour protection around each pier and abutment following the spring flood each year, with the frequency of these inspections to be reduced in the future if appropriate. No scour monitoring data were available at the time this paper was prepared.

THE CONFEDERATION BRIDGE

Overview of Project

The 13 km long, $800 million Confederation Bridge crosses the Northumberland Strait and joins the provinces of New Brunswick and Prince Edward Island in Eastern Canada (refer to Figure 3). The bridge, developed under a finance-design-build-operate agreement between Strait Crossing Bridge Limited (SCBL) and the Canadian Government, was constructed in 1994-97, and opened to traffic on June 1, 1997.

Figure 3 – The Confederation Bridge (photo by Boily)

At the crossing location, the Strait is approximately 13 km wide, with water depths ranging up to 30 m, but typically in the order of 15 m. The seabed generally consists of weak, fractured bedrock (mudstone, siltstone and sandstone), with highly variable material characteristics. The bedrock is overlain by glacial till in some areas. Under extreme design conditions, this site may be exposed to 120 kph winds, 4.5 m/9 s waves (Hs/Tp) and 2.5 m/s currents (the latter generated by the combined effects of tides, surges and wave-driven longshore currents). In addition, the Strait has a very dynamic ice environment, with ice present two to three months per year, level ice thicknesses of up to 1.2 m, and first year pressure ridges with keel depths of up to 15 m.

The 65 bridge piers are large gravity structures with conical bases (16 to 22 m base diameter) and conical ice shields at the water level (refer to Figure 4). For the shallow water approach piers (21 piers in water depths less than 8 m), the pier base and ice shield are a single unit.

Figure 4 – Schematic of Main Bridge Pier with Conical Base and Ice Shield

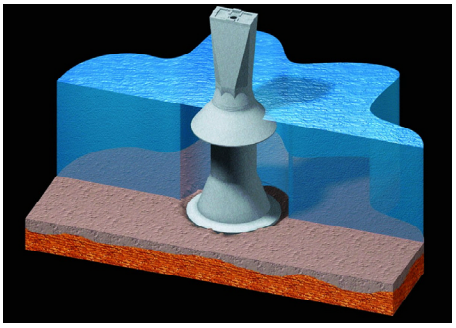

Overview of Scour Assessment and Design Investigations

Baird, under contract to SCBL, was responsible for the scour assessment and design for this project. This aspect of the project was complicated by several factors, including:

- Exposure to severe waves and currents;
- Conical pier bases, some founded in dredged pits;
- Complex and variable foundation conditions (weak, fractured bedrock).

These factors precluded the application of "standard" scour assessment and design methodologies (such as those in HEC-18, HEC-20 and HEC-23). Extensive investigations were undertaken to estimate the potential for scour around the pier bases, resulting in the development of a new methodology to assess scour potential in complex materials (based on the erodibility approach of Annandale, 1995), as discussed in a companion paper in these proceedings (Nairn and Anglin, 2002; refer also to Anglin et al, 1996).

There was considerable uncertainty in the scour assessment, principally due to the complex nature and highly variable characteristics of the foundation materials, but also due to the application of a new methodology to estimate scour potential. As such, a conservative approach was adopted in defining the requirement for scour protection, with scour protection recommended at any pier where the estimated factor of safety (FS) against scour during the 100 year design event was less than four. This approach led to the recommendation for scour protection around 14 of the 65 bridge piers, with the majority of these being shallow water approach piers (water depth less than 8 m), where wave action is the dominant mechanism with respect to scour and scour protection.

The design of scour protection was supported by the following investigations:

- numerical modeling to define long-term wave and current conditions at the site;
- literature review to identify the most relevant hydrodynamic parameter to define the combined effects of waves and currents ("stream power", P, was selected);
- extreme value analyses to define stream power as a function of return period at representative locations and depths along the crossing alignment;
- literature review and application of published procedures to estimate riprap scour pad design details (riprap size, horizontal extent, layer thickness and filter requirements);
- physical modeling of wave-current interaction with the bridge piers to establish pier magnification factors, and to optimize the design of the riprap scour pads;
- final designs, plans and specifications for bridge pier scour protection.

These investigations are discussed in more detail below.

Design of Scour Protection

Most scour assessment and design methodologies are applicable to river crossings, where the flow conditions are "unidirectional" and there is no significant wave action. Wave action results in "orbital motions" in the water column, and horizontal oscillating flow conditions at the seabed. A literature review undertaken for this project highlighted the absence of relevant scour design methodologies for bridge piers exposed to significant wave action. There is considerable information available on the design of toe/scour protection for coastal structures (such as revetments and breakwaters) exposed to wave action (for example, refer to USACE, 2001). However, these structures tend to be two-dimensional (2D) in nature (i.e. long and straight), and the associated toe/scour protection design methodologies cannot be applied with any confidence to the more complex three-dimensional (3D) flow conditions around bridge piers.

In the absence of more relevant procedures, preliminary scour protection designs for the shallow water approach piers were estimated using the toe/scour protection approaches of Tanimoto et al (1982) for "composite" breakwaters and CIRIA/CUR (1991) for "rubblemound" breakwaters. Figure 5 illustrates these breakwater design concepts, while Table 2 summarizes the results of the toe/scour protection calculations.

Figure 5 – Schematic Cross-Sections of Breakwater Design Concepts

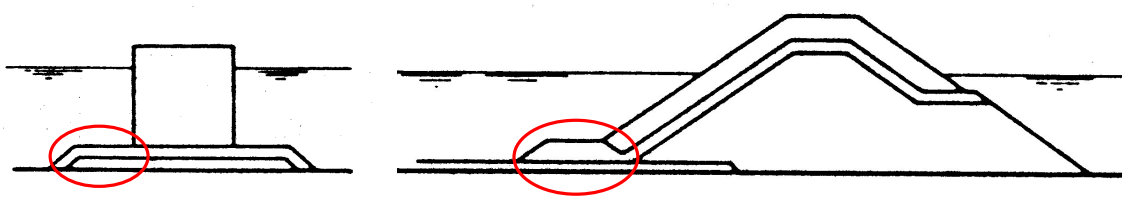

Vertical/Composite Sloping/Rubblemound

Table 2
Estimated Scour Protection Requirements for Approach Piers
Breakwater Toe/Scour Protection Design Methods

Breakwater Design Concept	Reference	D_{50} (m)
Vertical/Composite	Tanimoto et al (1982)	1.5
Sloping/Rubblemound	CIRIA/CUR (1991)	0.5

Clearly, there is a significant difference in these two estimates, and neither can be applied with any confidence to the complex, 3D flow conditions caused by the interaction of waves and currents with conical bridge piers. In addition, there is no relevant design guidance for the horizontal extent of scour pads around conical piers. "Conventional" design guidance suggests scour pad widths in the order of 1.5 to 2 times the pier diameter. Considering the variation in approach pier diameter from 10 m at the water line to 18 m at the base, this suggests scour pad widths in the order of 15 to 36 m.

Given these uncertainties, and the high cost of the preliminary scour protection designs, a physical model investigation was undertaken to assess scour protection alternatives and to refine and optimize the scour protection design. Two sets of model tests were undertaken in a 1.2 m wide wave-current flume at the Canadian Hydraulics Centre in Ottawa, ON. All tests were undertaken at a geometric scale of 1:70.

The first test series was completed to assess the influence of various pier shapes and dredged pit depths on flow conditions around the piers, specifically the characteristics and extent of accelerated flows and vortices. The flow patterns around the base of the model piers were defined with the aid of a laser doppler velocimeter, acoustic velocity meters, flow visualization and tracer materials. Pier magnification factors (PMF) were developed for the various water depths and pier geometries through a comparison of the flow conditions required to initiate the scour of a tracer material (coarse sand or fine gravel) placed on the model "seabed" with and without the pier in place (refer to Figure 6).

Figure 6 – Granular Tracer Mat around Model Pier Before and After Test

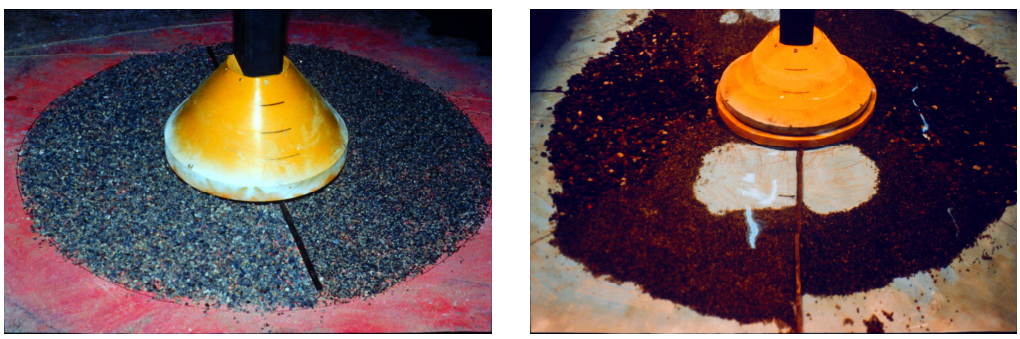

These tests were completed using various combinations of waves and currents, including each in the absence of the other. In general, the influence of the piers on flow conditions was limited to an area within 7 to 9 m from the toe of the conical pier bases (as noted earlier, the pier base diameters range from 16 to 22 m). The test flow conditions were quantified by the "stream power" parameter (P), which is the product of the nearbed shear stress (τ) and velocity (V). The stream power pier magnification factors (PMF's) varied from approximately 1.6 (deep water main pier placed in a deep pit) to 6.0 (moderate depth main piers and shallow water approach piers placed directly on the seabed). These PMF's correspond to velocity magnification factors of approximately 1.2 to 1.8 (stream power is proportional to the cube of velocity). The upper limit, for a conical pier base placed directly on the seabed, is somewhat larger than the values recommended in HEC-23 (FHWA, 2001c) for the application of the Isbash equation to design scour protection around round nose and rectangular piers (1.5 and 1.7 respectively). Additional information on the tracer tests and PMF's is provided in a companion paper in these proceedings (Nairn and Anglin, 2002).

The second test series was undertaken to investigate and optimize the design of scour protection around the pier bases. These tests were completed in the same wave flume as the tracer tests described above, again at a scale of 1:70. The horizontal extent of the

scour protection pads was defined based on the results of the tracer tests, which demonstrated that the "zone of influence" of the piers extended approximately 7 to 9 m out from the toe of the conical pier bases. Hence, 10 m wide scour pads were tested in the model. This width is similar to the pier diameter at the waterline, and approximately one-half of the pier diameter at the seabed. Scour protection tests were undertaken with one or two layers of armour stone placed around the model pier bases, in water depths ranging from 5 to 10 m. In general, the various designs were tested under progressively increasing combinations of waves and currents, with the onset of stone motion and progressive damage documented using visual observations and photographic records. Figure 7 shows photographs documenting the construction an armour stone scour pad around one of the model approach piers, while Figure 8 presents photographs of damage observed to a model armour stone scour pad following extreme flow conditions.

Figure 7
Construction of Model Scour Pad

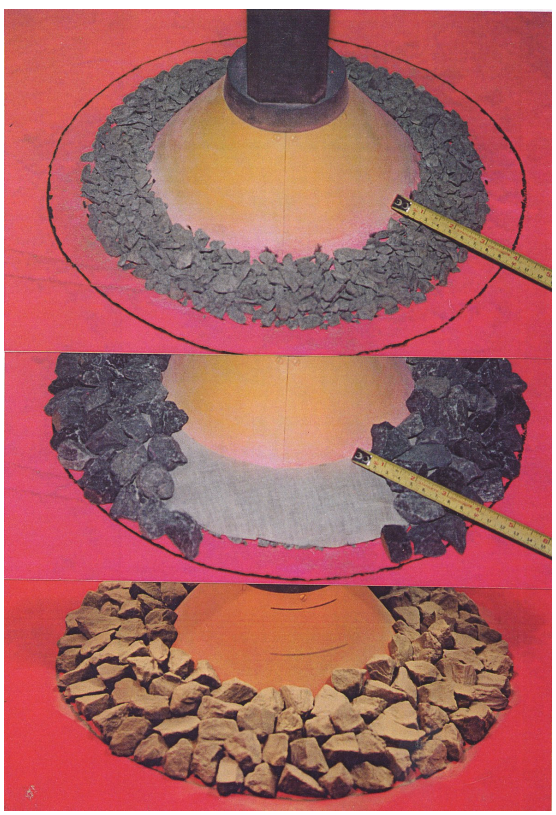

Figure 8
Damage to Model Scour Pad

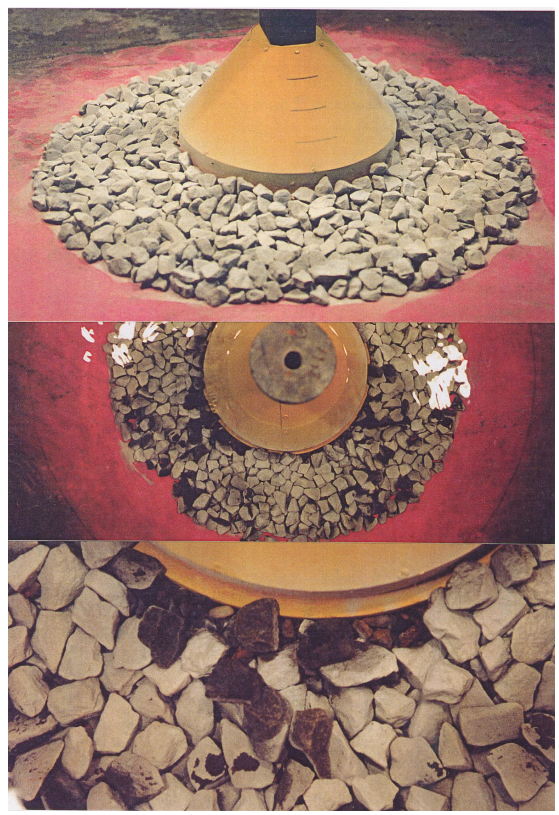

The recommended scour protection design consists of two layers of armour stone placed in a 10 m wide band around the base of the piers. The 10 m width is significantly less than the "conventional" estimate of 1.5 to 2 times the pier diameter. For the shallow water approach piers, the test results indicated that two layers of 2 to 4 tonne armour stone (D_{50} = 1.2 m, assuming angular stone) was required to provide a stable scour pad under the extreme design conditions. This result falls in between the stone sizes estimated for vertical/composite and sloping/rubblemound breakwater structures

presented earlier (refer to Table 2). An alternative design was also developed using a single layer of 5 to 7 tonne armour stone (D_{50} = 1.5 m, assuming angular stone). Smaller stone sizes were found to be stable for deeper piers, where the influence of wave action on the seabed (i.e. wave orbital velocities) is less.

For comparison purposes, additional calculations were undertaken using "conventional" riprap design equations for bridge pier scour protection by considering the combined design velocity associated with the wave orbital motion at the seabed and the unidirectional tidal/surge current. These calculations are summarized in Table 3.

Table 3
Estimated Scour Protection Requirements for Approach Piers
"Conventional" Riprap Design Equations with Combined Wave-Current Velocity

Methodology/Reference	D_{50} (m)
TAC (1973, 2001)[1]	1.3
Isbash/FHWA (1993)[1]	0.8
Maynord/USACE (1994)[1, 2]	1.1
Parola (1993)	0.9
Chiew (1995)[3]	0.2 to 2.8
Fotherby & Ruff (1996)	1.1
Lauchlan & Melville (2001)	0.7

Notes:
1. TAC, Isbash and Maynord calculations assume a velocity magnification factor (K) of 1.8 as per the physical model test results.
2. Maynord approach assumes $D_{50} = 1.2*D_{30}$ based on armour stone gradation with $D_{85}/D_{15} = 1.8$.
3. Chiew results presented with and without "flow depth effect"

These methods (excluding Chiew, 1995) suggest stone sizes (D_{50}) in the order of 0.7 to 1.3 m, as compared to the model study result of 1.2 m for the two layer design. The variation in the empirical estimates is significant, and none of the methods is considered to provide a reliable approach that can be applied with confidence to bridge piers exposed to wave action. Further, it is noted that the TAC, Isbash and Maynord calculations include a velocity magnification factor that was estimated from the model test results.

As such, the physical model was a critical component of the scour protection design. The model supported the development of designs that meet specific performance criteria (i.e. tolerable damage) under the extreme 100 year design flow conditions (waves and currents). In addition, the areal extent of the scour pads is significantly less than that suggested by "conventional" scour design guidance, with an associated reduction in cost.

Construction

SCBL chose to install scour protection at five of the 14 piers where Baird recommended protection. This decision was based on careful consideration of the cost of scour protection (approximately $0.5 million per pier) versus the risk of scour, recognizing the significant uncertainties and (likely) conservative approach to the assessment of scour potential. Armour stone scour pads were installed at three of these piers (see Figure 9), while construction logistics led to the development of a tremie concrete design concept at the other two piers. In the absence of a systematic design methodology, the tremie concrete design concept was based on experience and judgement. A minimum tremie thickness of 0.5 m was specified based on consideration of hydrodynamic lift forces, and "airlifting" of loose material from the seabed was required prior to tremie placement.

Figure 9 – Armour Stone Scour Pad at Shallow Water Approach Pier (photo by Boily)

Given SCBL's decision not to protect a number of "scour susceptible" piers, as well as the uncertainties in the overall assessment of scour potential, Baird recommended a detailed and systematic scour monitoring program. This recommendation was accepted by SCBL. The resulting monitoring program is discussed briefly below.

Scour Monitoring Program

As noted above, Baird assisted SCBL in the development and implementation of a systematic scour monitoring program for this project. This included dividing the piers into priority classes based on the estimated risk of scour, with the highest priority class (nine AA piers) being those at which scour protection was recommended by Baird (FS < 4) but not implemented by SCBL. In addition, Baird developed and installed a near real-time wave/current monitoring system for this project. This system quantifies the magnitude of storm events (considering the combined occurrence of waves and currents) to which the bridge is exposed and relates these to the design conditions, thereby providing a systematic method to define the requirement for monitoring of the seabed or scour protection around the base of each pier.

SCBL has followed this monitoring program since the bridge opened in 1997. Scour was detected around one of the AA piers in 1998; it was subsequently protected with an

armour stone scour pad. No scour of any significance has been observed around any of the other piers, despite the fact that the bridge has been exposed to several moderate storm events (the most severe of which had an estimated return period in the order of five years) for which the original scour assessment predicted scour at some of the AA piers. These results suggest that the original scour assessment may be conservative, as intended.

The archived wave/current information, along with the results of diver inspections undertaken between 1997 and 2002 and detailed multibeam sonar seabed surveys undertaken in 2001 and 2002, will be used to verify and improve the scour assessment and design methodologies, and, if appropriate, to reduce the scour monitoring requirements. Additional information on the monitoring program and the proposed scour reassessment study is provided in a companion paper in these proceedings (Nairn and Anglin, 2002).

DISCUSSION AND CONCLUSIONS

Extensive investigations undertaken for the St. John River Bridge and Confederation Bridge in Eastern Canada have highlighted limitations in existing scour protection design methodologies, and have clearly demonstrated the benefits of undertaking project specific physical model studies.

For example, riprap design calculations undertaken using published design methodologies give a wide range in stone sizes for unidirectional flow conditions. This variation, also reported by Lauchlan and Melville (2001), leaves the design engineer with the difficult task of selecting the most appropriate design methodology and/or specifying a design based on experience and judgement. Further, there is no methodology presently available to design scour protection for bridge piers exposed to significant wave action.

These uncertainties and limitations can be overcome by undertaking a site-specific physical model investigation. A physical model provides the best tool currently available to investigate the complex interaction of flows with structures, and can be used to develop, refine and optimize designs to meet specific performance objectives under extreme design conditions. For example, physical models have been used for decades in the field of coastal engineering to design cost-effective rubblemound breakwaters to provide permanent protection from extreme wave action for large, multi-million dollar marine/waterfront facilities (such as ports and harbours), and represent the accepted "standard of care" in the design of such structures (refer to USACE, 2001). In addition, physical models have been used extensively to assess the stability of riprap under unidirectional flow conditions, including the protection of stream beds/banks from flood flows (for example, Maynord, 1988; USACE, 1994), and the protection of embankments, dams etc. from overtopping flows (for example, CIRIA, 1987; Abt et al, 1998).

Similarly, a bridge scour design investigation can benefit significantly from a site-specific physical model study. The physical model investigation undertaken for the St. John River Bridge led to the development of a scour protection design using widely graded riprap

without a filter layer. The stone size was significantly smaller than that estimated using empirical design approaches. In addition, the model confirmed the acceptable performance of a scour pad with an areal extent at the lower limit of published design guidance. These features resulted in significant cost savings as compared to the preliminary designs developed using published design guidance.

For the Confederation Bridge, the physical model investigation was an essential step in the scour investigation due to the complex flow conditions (waves and currents), seabed characteristics (weak, fractured bedrock) and pier geometry (conical pier bases, some founded in dredged pits). These conditions precluded the application of "conventional" bridge scour methodologies. The physical model provided a wealth of information related to the complex flow conditions around the piers, and allowed the development and optimization of scour protection designs to resist the 100 year design flow conditions.

In general, and certainly for large, complex and/or unique bridge projects, experience indicates that the cost of a physical model investigation will be more than offset by the construction cost savings realized through design optimization of the scour protection. Further, a physical model allows demonstration/verification of the performance of the scour protection system under extreme flow conditions (design and "overload"), and can provide extremely useful information on damage/failure mechanisms and likely maintenance/repair requirements. This approach, in combination with a systematic monitoring program, allows the development of "permanent" scour protection designs that may result in significant cost savings for some bridges as compared to a foundation design that accommodates the maximum anticipated scour depth.

In addition, tracer tests allow accurate quantification of the "pier magnification factor". It is suggested this parameter should be quantified in any physical model investigation of bridge pier scour/scour protection in order to support the development of a comprehensive database for various pier geometries and flow conditions.

In closing, it must be emphasized that a physical model is only one aspect in a comprehensive bridge scour investigation. Clearly, the engineer must have a detailed and complete understanding of the site conditions (in particular, surface/subsurface conditions and bank and bed stability), extreme flow conditions, bridge foundation design, etc. prior to undertaking the physical model investigation. The interested reader is referred to HEC-18, 20 and 23 (FHWA, 2001a, b and c) for further information on these topics. In addition, the successful performance of any scour protection system is critically dependent on good quality materials and construction. Hence, an effective QA/QC program during construction is essential. Finally, a systematic post-construction monitoring program is strongly recommended for any bridge scour protection system.

ACKNOWLEDGEMENTS

The input and direction provided by MRDC and SCBL over the course of these projects is gratefully acknowledged, as is their permission to publish this paper.

REFERENCES

1. Abt, S.R., Johnson, T.L., Thornton, C.I. and Trabant, S.C. (1998), "Riprap Sizing at Toe of Embankment Slopes", Journal of Hydraulic Engineering, Vol. 124, No. 7, ASCE.
2. Anglin, C.D., Nairn, R.B., Cornett, A., Dunaszegi, L., Turnham, J. and Annandale, G. (1996), "Bridge Pier Scour Assessment for the Northumberland Strait Crossing", 25th International Conference on Coastal Engineering, ASCE, Orlando, FL.
3. Anglin, C.D., Itamunoala, F. and Millen, G. (2001), "Slope and Scour Protection, Trans-Canada Highway Project, NB", Canadian Coastal Conference, CCSEA, Laval, PQ.
4. Annandale, G.W. (1995), "Erodibility", Journal of Hydraulic Research, V.33, N.4.
5. Chiew (1995), "Mechanics of Riprap Failure at Bridge Piers", Journal of Hydraulic Engineering, Vol. 121, No. 9, ASCE.
6. CIRIA (1987), "Protection and Provision for Safe Overtopping of Dams and Flood Banks", Project Report 2.
7. Federal Highway Administration (FHWA, 1989), "Design of Riprap Revetment", Hydraulic Engineering Circular (HEC) No. 11, Second Edition.
8. Federal Highway Administration (FHWA, 2001a), "Evaluating Scour at Bridges", Hydraulic Engineering Circular (HEC) No. 18, Fourth Edition.
9. Federal Highway Administration (FHWA, 2001b), "Stream Stability at Highway Structures", Hydraulic Engineering Circular (HEC) No. 20, Third Edition.
10. Federal Highway Administration (FHWA, 2001c), "Bridge Scour and Stream Instability Countermeasures", Hydraulic Engineering Circular (HEC) No. 23, Second Edition.
11. Fotherby, L.M. & Ruff, J.F. (1996), "Riprap and Concrete Armor to Prevent Pier Scour", North American Water & Environment Congress and Destructive Water, ASCE, Anaheim, CA.
12. Maynord, S. (1988), "Stable Riprap Size for Open Channel Flows", U.S. Army Corps of Engineers, Hydraulics Laboratory, Technical Report HL-88-4.
13. Lauchlan, C.S. and Melville, B.W. (2001), "Riprap Protection at Bridge Piers", Journal of Hydraulic Engineering, Vol. 127, No. 5, ASCE.
14. Nairn, R.B. and Anglin, C.D. (2002), "Confederation Bridge – New Scour Design Methodology for Complex Materials", First International Conference on Scour of Foundations, Texas A&M University, College Station, Texas.
15. Parola, A.C. (1993), "Stability of Riprap at Bridge Piers", Journal of Hydraulic Engineering, Vol. 119, No. 10, ASCE.
16. Tanimoto, T., Yagyu, T. and Goda, Y. (1982), "Irregular Wave Tests for Composite Breakwater Foundations", 18th International Conference on Coastal Engineering, ASCE, Cape Town, South Africa.
17. Transportation Association of Canada (TAC, 1973), "Guide to Bridge Hydraulics", First Edition.
18. Transportation Association of Canada (TAC, 2001), "Guide to Bridge Hydraulics", Second Edition.
19. Transportation Research Board (TRB, 1999), "1998 Scanning Review of Europeon Practice for Bridge Scour and Stream Instability Countermeasures", National Cooperative Highway Research Program, Research Results Digest, No. 241, Washington, D.C.
20. U.S. Army Corps of Engineers (USACE, 1994), "Hydraulic Design of Flood Control Channels", Engineer Manual 1110-2-1601.
21. U.S. Army Corps of Engineers (USACE, 2001), "Coastal Engineering Manual", Engineer Manual 1110-2-1100.

Riprap at Rectangular Bridge Piers Under Oblique Incident Flow

By

José Angel Sáinz[1], Rodney Salgado[2]

ABSTRACT

The influence that protective riprap has on the scour holes that develop near bridge piers has been studied in clear water conditions with rectangular piers non-aligned with the flow. Non-dimensional graphs, relating the characteristic dimensions of the scour holes with the flow incident angle and with the riprap elevation above bed level and its width, are presented. Also, the necessary minimum width of riprap, deduced from tests, is compared to criteria proposed by various authors.

INTRODUCTION

In the last few decades the phenomenon of the localized scour holes around bridge piers has been investigated. Various authors (Breusers, 1977; Jain, 1981; Raudkivi, 1986; Melville, 1997) have analyzed experimentally, in clear water as well as live bed situations, the influence of the shape, size and situation of the pier, the size and gradation of the sediment, the flow depth, etc. on local scour magnitude.

The influence of the flow incident angle has been analyzed experimentally by various authors (Laursen et al., 1956; Chabert et al., 1956; Maza Alvarez, 1968; Témez 1988; Raudkivi et al., 1991; and Melville et al., 1988).

Countermeasures for local scour at bridge piers can be grouped in two categories: armouring devices and flow altering devices. Various authors have analyzed alternative armouring devices such as dolos, tetrapods (Fotherby, 1992), toskanes (Ruff et al., 1995), gabion mattresses (Simons et al., 1984) and cable-tied blocks (Bertoldi et al., 1994).

[1] Associate Professor, Departamento de Ciencias y Técnicas del Agua y del Medio Ambiente, Universidad de Cantabria, Avda. Los Castros s/n, 39005 Santander (España), (sainzja@unican.es)
[2] Civil Engineer, Consejo Nacional de Electricidad CONELEC, Avda.Amazonas N33-299 e Inglaterra, Quito (Ecuador), (rsalgado@conelec.gov.es)

In the case of protection by means of riprap, the size of the protective element as well as the riprap planform width must be defined.

The size of the riprap elements depends mainly on the flow velocity. Neill (1967) and Maynord (1989) studied the stability of the riprap elements in undisturbed flow. Various authors (Bonasoundas, 1973; Quazi et al., 1973; Breusers, 1977; Témez, 1988; Raudkivi et al., 1991; Parola, 1993; Chiew, 1995; and Lauchlan, 1999) have proposed equations for the specific case of protection of bridge piers. These formulations, applied to the same flow conditions, produce quite different results.

Concerning the necessary planform width of the riprap, various authors (Laursen et al., 1956; Maza-Alvarez, 1968; Bonasoundas, 1973; Témez, 1988; Chiew, 1995) have established criteria, that when applied to the same case, lead to very different solutions.

This work is an extension of Duarte et al. (1999) and its main purpose is to analyze the influence of the flow incident angle, the width of the riprap (w) and its placement level (d), on riprap stability as well as on the development of localized scour holes on rectangular bridge piers, in clear water situations under permanent subcritical flow.

EXPERIMENTAL PROGRAM

The tests were carried out in the Hydraulics Laboratory in the Civil Engineering School of the University of Cantabria (Spain) in a methacrylate horizontal channel, 9-m long, 0.90-m wide and 0.45-m high.

In the middle of the channel a 1.5-m long, 0.90-m wide and 0.18-m deep mobile bed zone was prepared and filled with sand of 2.65 t/m^3 specific weight and size between 0.84 mm and 1.19 mm (D_{50} = 1.0 mm).

In order to define the critical velocity of beginning sand motion, in conditions of undisturbed flow, several tests were carried out by gradually increasing the discharge. A value of 0.32 m/s was obtained for this velocity, with a discharge of 40 l/s and a water depth of 14 cm. In order to guarantee the flow in clear water conditions during the remaining tests, a discharge of 35 l/s was adopted with a corresponding velocity of 0.29 m/s (U/U_c = 0.9) and a water depth of 13.5 cm.

The characteristics of the channel have conditioned the dimensions of the piers and the flow incident angle to be tested. One type of pier was considered: a rectangular section with a 50-mm width (b) and 100-mm length. Four values of the flow incident angle (β) were considered: 0º, 10º, 20º and 30º.

Based on the results from Duarte (1996), a riprap element size in the range between 4,8 mm and 6,4 mm (D_{p50} = 5,5 mm) has been considered. This value is in accordance with the application of the criteria proposed by some of the aforementioned authors to test conditions.

Three types of cases have been considered, according to the elevation of the riprap:

- above the channel bed (d = -b/2 and -3b/4)
- at bed level (d = 0)
- below the channel bed (d = b/2 and b)

These cases attempt to represent the real situations in which the riprap can be found: above, at, or below bed level corresponding to the general scour during floods (Figure 1).

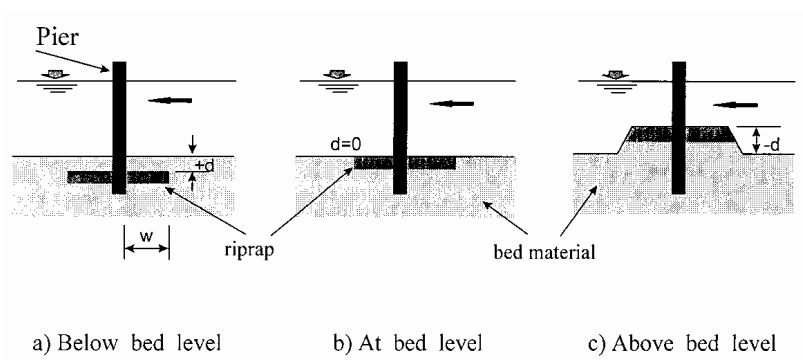

Fig. 1. Riprap arrangements with regard to the bed level.

Also, for every elevation of the riprap, different uniform widths (w = b, 3b/2 and 2b) around the pier were considered, using a rectangular format. A value of b/3 was adopted as protection thickness, which always constituted a minimum of two element layers.

Each of the 64 test cases was submitted for 10 hours to a practically uniform flow, of coincident direction with the alignment of the pier, with a flow depth y_0 =13.5 cm and a velocity U = 0.29 m/s.

EXPERIMENTAL OBSERVATIONS

Initially, the behaviour of unprotected rectangular piers was analyzed and used as a reference term. The maximum depth (d_s) observed was 63 mm, 76 mm, 84 mm and 95 mm for the flow incident angle values of 0º, 10º, 20º and 30º, respectively.

For all tests, qualitative and quantitative observations were made (Salgado, 1997). Qualitative observations include those related to the location of the scour hole.

In the case of an unprotected pier or when the riprap is located below bed level, the scour hole develops around the pier and the riprap is partially uncovered. When the riprap is located at or above bed level, the scour hole develops downstream the riprap.

From a quantitative point of view, a detailed analysis of the scour hole was carried out in each one of the tests. With the help of a device specially designed to move over the canal, the scour hole depth was determined on a grid. These data were processed by means of a computer program and a graphic representation was obtained in the form of elevation curves for each scour hole. Figures 2 and 3 show the scour holes corresponding to two specific tests.

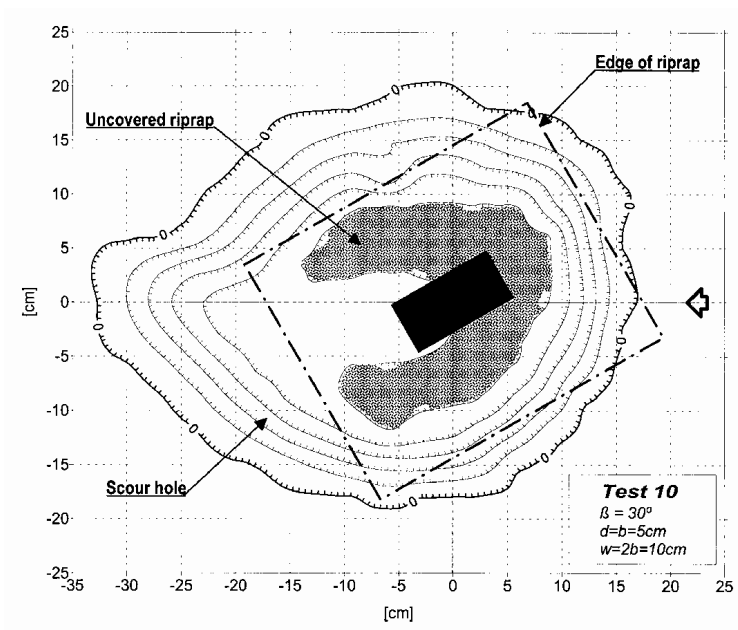

Fig. 2. Scour hole produced in test No. 10, with riprap below bed level.

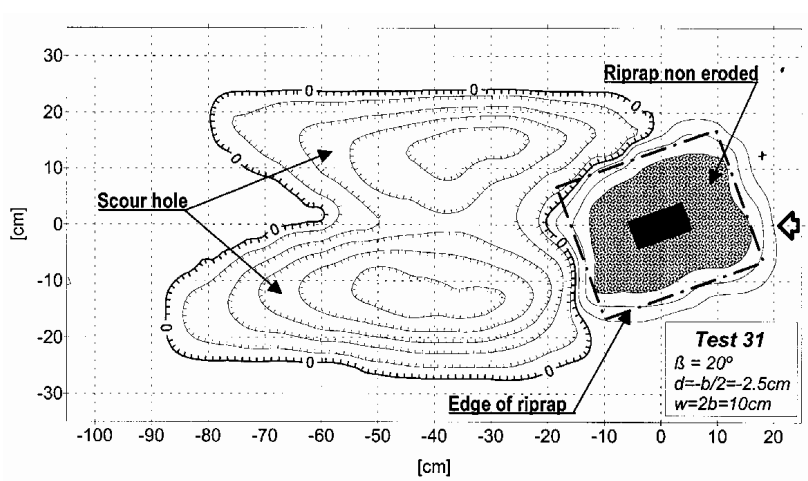

Fig. 3. Scour hole produced in test No.31, with riprap above bed level.

Figures 4 and 5 show the variables measured in the 64 scour holes drawn by means of the computer program: the frontal (L_1) and back (L_2) longitudinal extension of the scour hole, its maximum depth (d_{sm}) and the width of the uncovered riprap surface. This width is characterized by the maximum of the dimensions a_1, a_2, a_3 and a_4.

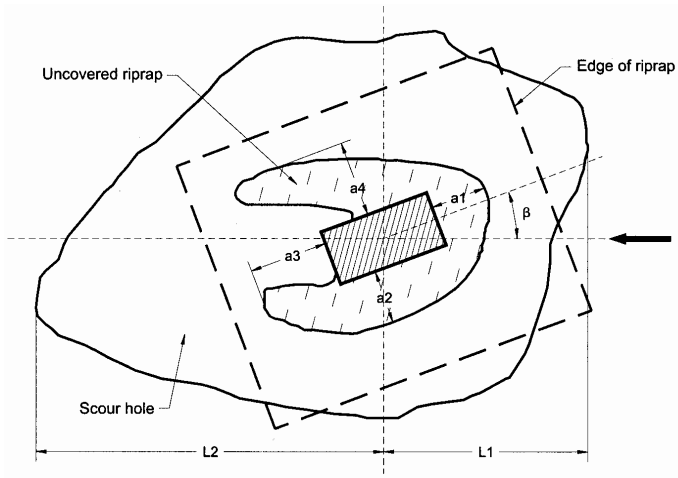

Fig. 4. Schematic definition of the variables with riprap below bed level.

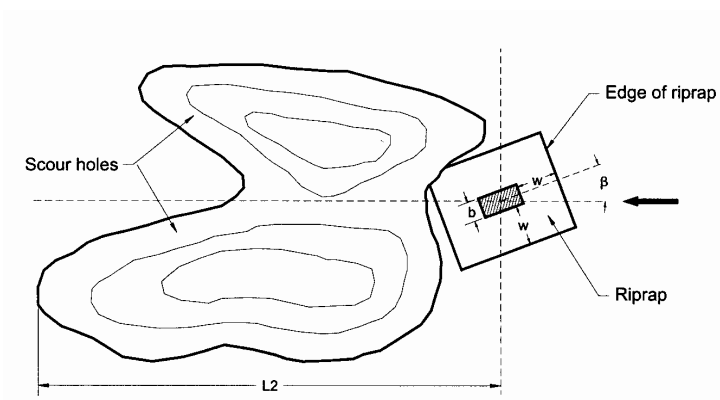

Fig. 5. Schematic definition of the variables with riprap above bed level.

ANALYSIS OF RESULTS

The values of the variables (L_1/b; L_2/b; d_{sm}/d_s; a/b) are presented in non-dimensional graphs. In said graphs, the points corresponding to each series of measurements, associated with the same symbol, have a straight line drawn through them, reflecting the result of a possible linear interpolation among them.

Longitudinal extension of the scour hole

The scour hole extends upstream mainly when the protection is located below bed level ($d > 0$). In which case, practically no variation of its length exists in function with d, nor does an influence of the parameters w and β exist ($L_1/b \cong 3.5$).

The downstream longitudinal extension is more important than the upstream longitudinal extension. Figure 6 illustrates the variations of the scour hole length downstream, as a function of *d*, *w*, and β. The greater values are produced for ripraps located above bed level, greatly increasing the length upon raising the placement level. The increase of downstream scour hole length is more sensitive to the raising of the placement level than to the increase of riprap width.

On the other hand, increasing β results in an increasing scour hole length. For every d/b value considered, the L_2/b variation is almost linear with β.

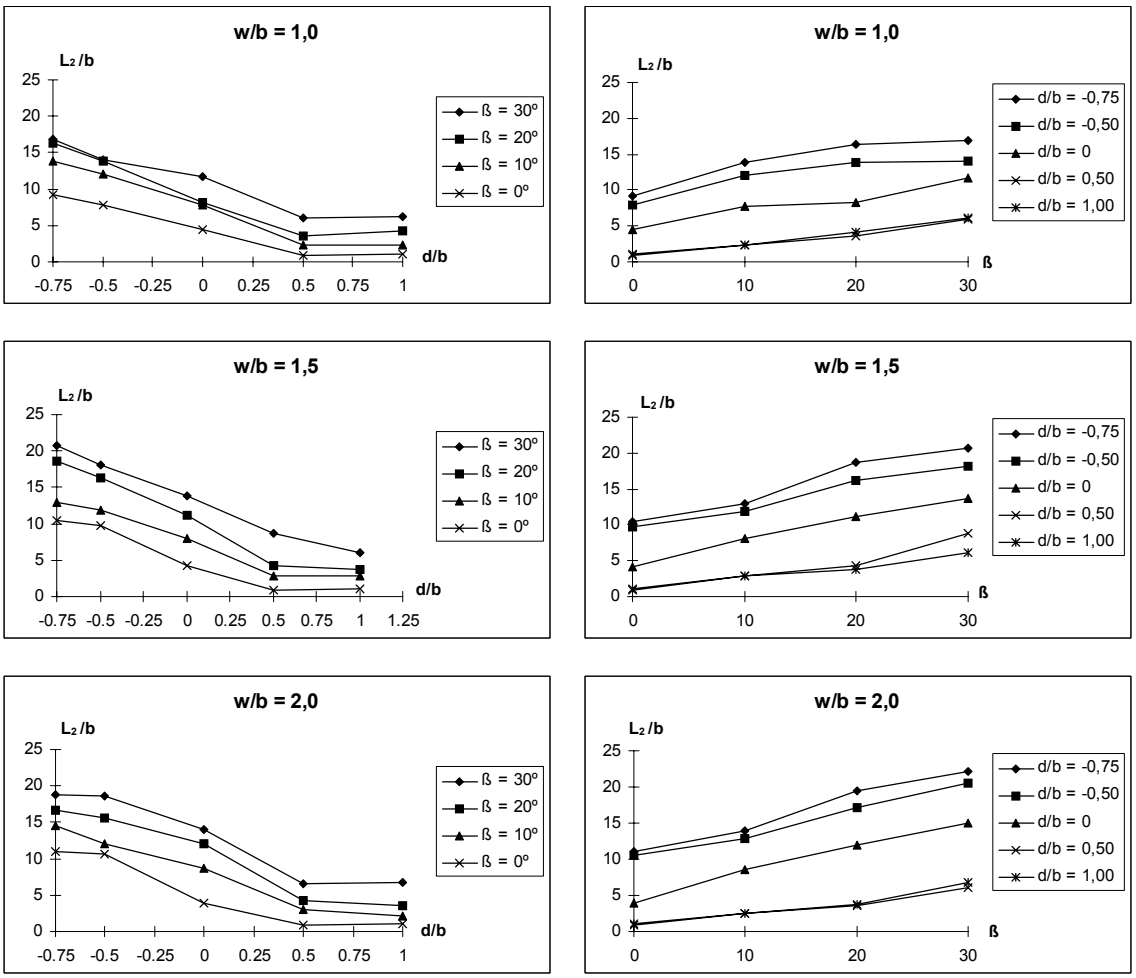

Fig. 6. Longitudinal extension of the scour hole downstream.

<u>Maximum scour hole depth</u>

In figure 7, the values of the maximum scour hole depth (d_{sm}) obtained from tests without protection are presented and compared with the values proposed by different authors, varying the flow incident angle. A very good agreement is observed.

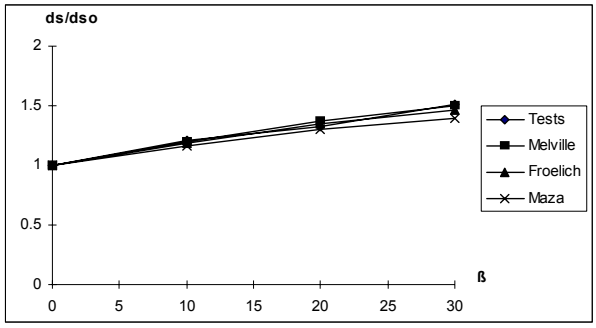

Fig. 7. Scour hole depth for unprotected piers. Comparative analysis

Obviously, when the riprap is located below bed level, the value of d_{sm} coincides with the riprap placement level. For $d = 0$ or $d < 0$, two almost parallel scour holes are developed downstream the riprap. Figure 8 illustrates the influence of d, w and β on the maximum scour hole depth (d_{sm}). The values obtained for w/b = 1.0 with β = 20º and β = 30º are anomalous due to the downstream edge of riprap failure.

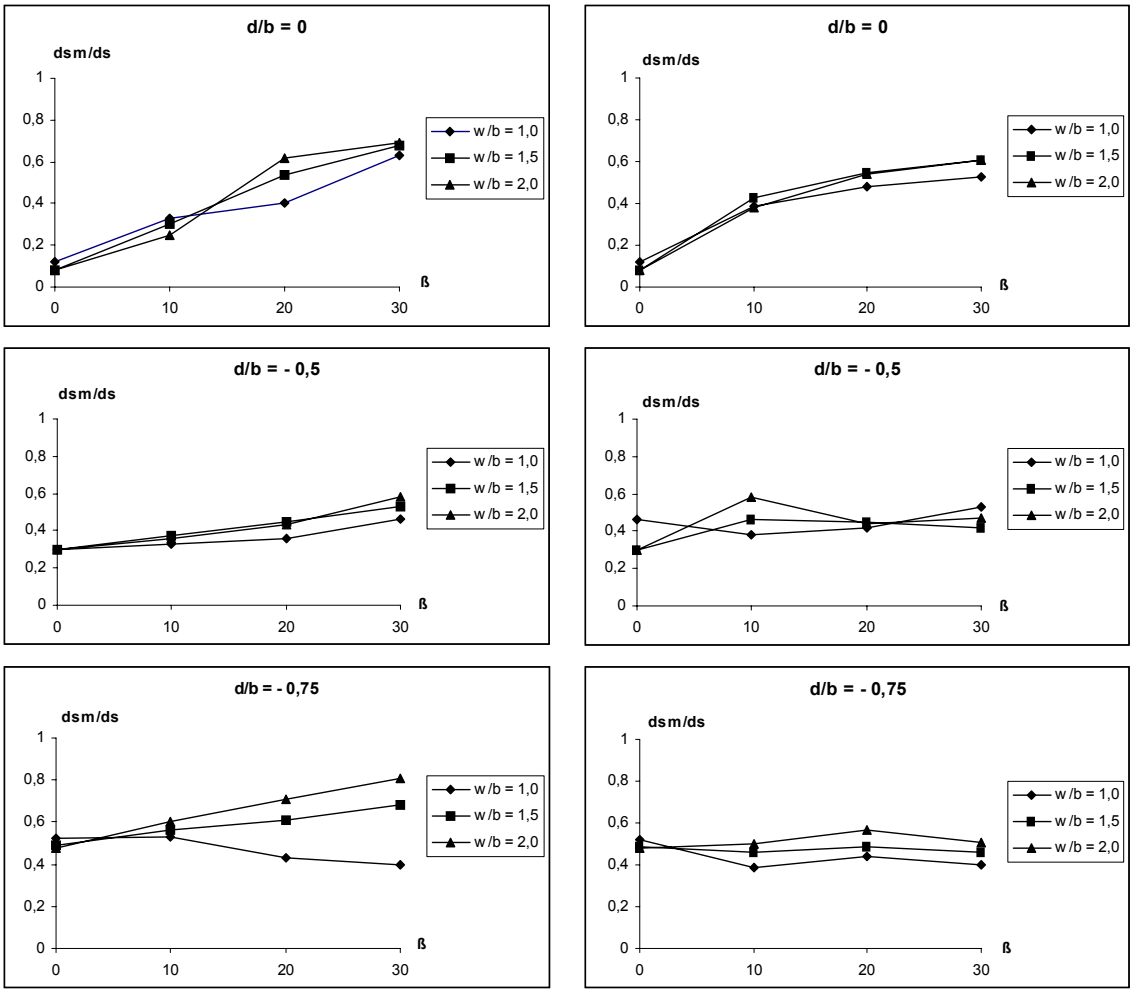

a) Left hole b) Right hole

Fig. 8. Maximum scour hole depth

Results for right and left scour holes differ slightly. For the left hole, the relation between d_{sm}/d_s and β is almost linear, with decreasing slope for increasing β values. For the right hole d_{sm}/d_s is almost independent of β for d/b < 0.

Minimum riprap width

When the riprap is located below bed level, the graphic representation of the different scour holes show than the extension of the uncovered protection from the right lateral side is the greatest of the four dimensions considered. This value is associated with the necessary minimum extension of the riprap protection.

Figure 9 represents the values of *a/b* deduced from the tests carried out with different flow incident angles. The values obtained for $d/d_s = 0.26$ and β = 30º are anomalous, due to the fact that the maximum width of the riprap protection considered has been insufficient.

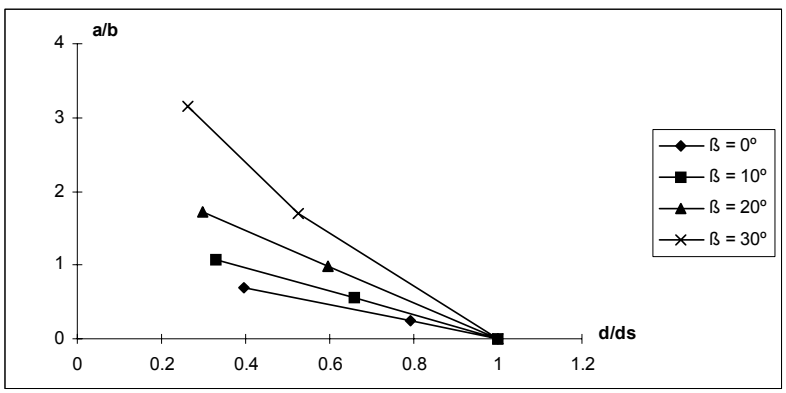

Fig. 9. Minimum width of the riprap. Test results.

The necessary minimum riprap width (*a/b*) decreases almost linearly upon increasing the depth of the protection below bed level (d/d_s), and grows upon increasing β.

On the other hand, the results obtained from tests and the values proposed by different authors have been compared. Neill (1967) and Lauchlan (1999) recommend a single value of *a* (*a* = 1.5 *b*), independent of *d*, while Témez (1988) and other authors relate such extension with the placement level (*d*) but also with the scour hole depth (d_s) of the unprotected pier.

Reorganizing the original equation proposed by Témez, in order to express it as a function of the non-dimensional variables *a/b* and d/d_s, results in:

$$\frac{a}{b} = \frac{ds}{b}\left(1 - \left(\frac{d}{ds}\right)\right) \qquad (1)$$

considering the value of d_s deduced by applying the equation of Laursen:

$$\frac{ds}{b_*} = 1.5 \left(\frac{y_0}{b_*} \right)^{1/3} \tag{2}$$

to the test conditions, with:

$$b_* = b \left(\cos\beta + 2 \sin\beta \right) \tag{3}$$

Figure 10 represents the values of *a/b* deduced from the tests and those resulting from applying equations (1), (2) and (3).

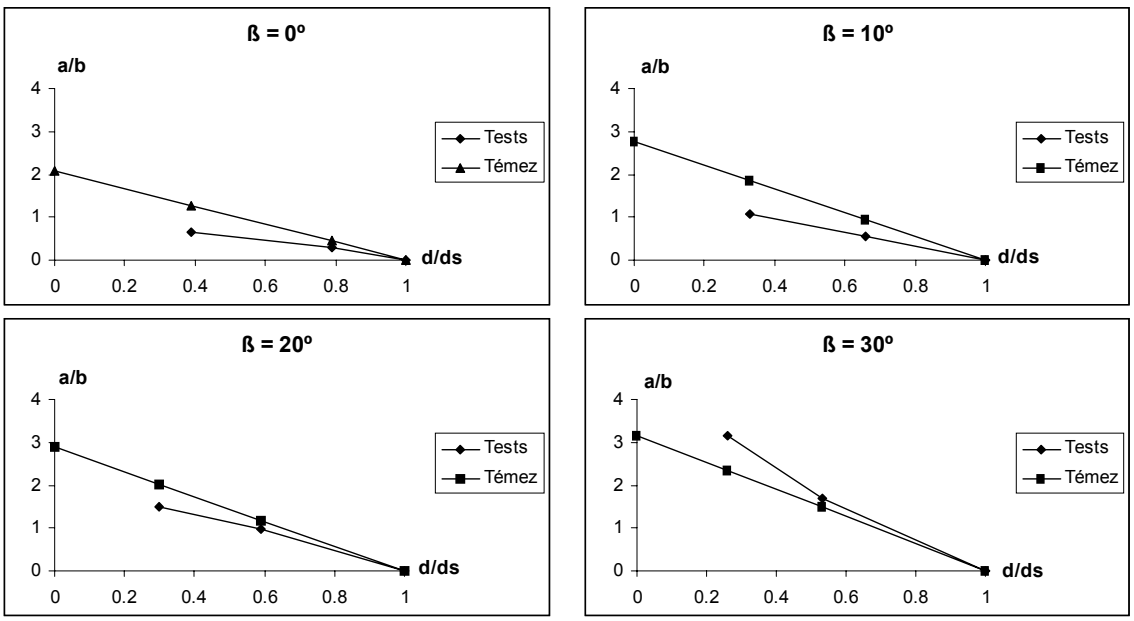

Fig. 10. Minimum width of the riprap. Comparative analysis.

By examining this figure, it is deduced that the measured values follow a similar trend to those calculated from the Témez equation; even though, the calculated numerical values are, on average, 80 %, 70 % and 25 % higher than measured test values in the cases of β = 0º, 10º and 20º, respectively, while they are 20 % lower in the case of β = 30º.

For β values equal to or greater than 20º, if the riprap protection is located at a small depth below bed level, the uncovered protection width is larger than the minimum width suggested by Neill and Lauchlan.

CONCLUSIONS

The qualitative and quantitative analyses of the results obtained in the experimental program from 64 laboratory tests lead to the following conclusions:

a) The maximum longitudinal extension of the scour hole is conditioned by the placement and width of the riprap and by the flow incident angle. For $d > 0$, the scour holes develop near the pier, with reduced extensions ($L_1/b \approx 3.5$ and $L_2/b \leq 7.5$) and without the influence of w/b. For $d \leq 0$, the scour holes develop downstream the riprap, with extensions that could become important ($L_2/b \cong 22.5$ for $d/b = -0.75$ and $\beta = 30^o$), and which grow slightly on increasing w/b and almost linearly on increasing β.

b) In relation to the scour hole depth, riprap functions best as a protection of bridge piers when placed at bed level ($d = 0$), since the scour hole is produced outside the protected zone and its depth is minimum for every value of β. When the riprap is located above bed level, even if the scour hole is developed downstream the protection, its depth could become important ($d_{sm}/d_s = 0.81$ or $d_{sm}/b = 3.2$ for $\beta = 30^o$).

c) The equation proposed by Témez is a good design tool to define the minimum riprap extension, as a function of placement level, for flow incident angles no greater than 25º. Its use is equivalent to adopting a safety factor, decreasing from 1.8 for β = 0º to an approximate value of 1.0 for β ≅25.

d) According to the trend of the experimental observations, the application of Lauchlan's criterion for β ≥ 20º results in unsatisfactory values of minimum width of riprap.

NOTATIONS

a	= Necessary minimum extension of the riprap protection.
a_1, a_2, a_3, a_4	= Extension of the uncovered protection in frontal, lateral and back sides, respectively (see figure 4).
b	= Width (or diameter) of the pier.
d	= Placement level of riprap with regard to the bed level (positive downward).
d_s	= Scour hole depth of the unprotected pier.
d_{so}	= Scour hole depth of unprotected and aligned-flow piers.
d_{sm}	= Maximum scour hole depth with riprap.
D_{50}	= Mean size of the bed material.
Dp_{50}	= Mean size of the riprap elements.
L_1, L_2	= Longitudinal and back extension of the scour hole, respectively (see figures 4 and 5).

U	= Flow velocity.
U_c	= Critical flow velocity.
y_0	= Water depth.
w	= Width of the riprap in all directions from the pier face.
β	= Flow incident angle.

REFERENCES

1. Bertoldi, D.A., Jones, J.S. (1994). “An experimental study of scour protection alternatives at bridge piers”. Report, Turner-Fairbank Laboratory, Federal Highway Administration, U.S. Department of Transportation, U.S.A.
2. Chabert, J., Engeldinger, P. (1956). “Etude des affouillements autour des piles des ponts”. Laboratoire d’Hydraulique, Chatou, France (in French).
3. Chiew, Y.M. (1995). "Mechanics or riprap failure at bridge piers". J. Hydraulic Engineering, ASCE, Vol. 121, no. 9, pp. 635-646.
4. Duarte, C.A. (1996). "Influencia de la extensión en planta y de la cota de colocación del manto de escollera en su estabilidad y en el desarrollo de la erosión local en pilas de puente". PhD. Thesis, Universidad de Cantabria, España. (in Spanish).
5. Duarte, C.A., Sainz, J.A. (1999). “Riprap at bridge piers”. J. Hydraulic Research, IAHR, Vol. 37, no. 3, pp. 291-302.
6. Fotherby, L.M. (1992). “Footings, mats, grout bags, and tetrapods: Protection methods against local scour at bridge piers”. M.S. Thesis, Colorado State University, Fort Collins, Colorado, USA.
7. Lauchlan, C.S. (1999). “Countermeasures for pier scour”. PhD. Thesis, The University of Auckland, Auckland, New Zealand.
8. Laursen, E.M., Toch, A. (1956). "Scour around bridge piers and abutments". Iowa Highway Research Board, Bulletin no. 4, Iowa, USA.
9. Maynord, S.T. (1989). "Riprap design". J. Hydraulic Engineering, ASCE, Vol. 115, no. 7, pp. 937-949.
10. Maza Alvarez, J.A. (1968). "Socavación en cauces naturales". Instituto de Ingeniería, U.N.A.M., Publ. no. 177, México. (in Spanish).
11. Melville, B.W., Sutherland, A.J. (1988). “Design method for local scour at bridge piers”. J. Hydraulic Engineering, ASCE, Vol 114, no. 10, pp 1210-1226.
12. Melville, B.W. (1997). "Pier and abutment scour: Integrated approach". J. Hydraulic Engineering, ASCE, Vol. 123, no. 2, pp. 125-136.
13. Neill, C.R. (1967). "Mean velocity criterion for scour of coarse uniform bed-material". Proc. 12th Congress AIRH, Fort Collins, paper C6, pp. C6.1-C6.9.
14. Parola, A.C. (1993). "Stability of riprap at bridge piers". J. Hydraulic Engineering, ASCE, Vol. 119, no. 10, pp. 1080-1093.
15. Quazi, M.E., Peterson, A.W. (1973). "A method for bridge pier riprap design". Proc., First Canadian Hydraulics Conf., University of Alberta, Edmonton, Canada, pp. 96-106.

16. Raudkivi, A. (1986). "Functional trends of scour at bridge piers". J. Hydraulic Engineering, ASCE, Vol. 112, no. 6, pp. 1-13.
17. Raudkivi, A., Breusers, H. N. (1991). "Scouring". Hydraulic Structures Design Manual, IAHR, Balkema Publishers, Rotterdam, The Netherlands.
18. Ruff, J.F., Fotherby, L.M. (1995). “Bridge scour protection systems using toskanes”. Final Report Project 91-02, Engineering Research Center, Colorado State University, Fort Collins, Colorado, USA.
19. Salgado, R. (1997). “Erosión local y estabilidad de mantos de escollera en pilas de puente no alineadas con el flujo”. Universidad de Cantabria, Spain. (in Spanish).
20. Simons, D.B., Chen, Y.H., Swenson, L.J. (1984). “Hydraulic test to develop design criteria for the use of Reno mattresses”. Report, Colorado State University, Fort Collins, Colorado, USA.
21. Temez, J.R. (1988). "Control de la erosión fluvial en puentes". Ministerio de Obras Públicas y Transportes. España. (in Spanish)

Countermeasure Construction Using Jet Grouting Methods to Combat Foundation Scour

Dennis W. Boehm, MSCE[1]

Abstract

There is substantial information on the prediction and performance of bridges and other coastal construction due to the damaging effects of scour. Currently, predictions are formulated by using numerical modeling software. In general this software is based upon historical data of stream flows or coastal storms and does not take into account unusual extremes in precipitation causing inaccuracies. When unpredicted extreme weather events do take place, calculated scour patterns can change resulting in serious foundation damage to structures. Countermeasure construction must be employed to repair damage and the compromise of crucial foundations. Jet grouting has been successfully used for many years to repair foundations damaged by scour as well as to construct scour protection in situ. Four projects are described in this paper, to demonstrate the value and acceptance of jet grouting as a countermeasure construction for combating scour for both bridge and coastal structures.

Introduction

Many structures adjacent to and across waterways have suffered the effects of scour on foundations. According to documented information, in the United States alone more than 500 bridges have suffered significant damage on their foundation elements in just the past 30 years (Shirole and Holt 1991). The number of coastal structure collapses directly caused by large coastal storms is not as well documented.

There is substantial information that indicates that maximum scour depth in coarse-grained soils usually occurs during the first major flood event. However in fine-grained soils the process may take years and is not as predictable.

The current practice for predicting scour is to use the numerical modeling technique provided in HEC-18 and HEC-20. The use of this water-flow modeling

[1] Senior Project Manager, Hayward Baker Inc., 2510 Decatur Avenue, Fort Worth, Texas 76106; phone 817-625-4241; dwboehm@haywardbaker.com

software usually makes it possible to design structures to proper depths to prevent the detrimental effects of scour. But the impact of unusual storm patterns cannot be predicted by using hydraulic models. As a result, in spite of the use of water-flow modeling, structures can be undermined or damaged. In such cases, jet grouting can be used to prevent further scour of the foundation soils and ultimately extend the life of the structure. With coastal structures, jet grouting can be used to decrease the susceptibility of the structure to the effects of scour.

Because jet grouting has been used successfully in many ground improvement projects, it has gained wide acceptance throughout the world. In the United States, this acceptance began during the late 1980's, and since then it has become more than just an underpinning tool. Jet grouting has been defined by the ASCE Geotechnical Engineering Division Committee on Grouting (1980) as a "technique utilizing a special drill bit with horizontal and vertical high speed water jets to excavate alluvial soils and produce hard impervious columns by pumping grouts through the horizontal nozzles that jets and mixes the foundation material as the drill bit is withdrawn." Figure 1 shows how the jet grouting process is carried out in sequence, while Figure 2 depicts the three methods of jet grouting currently practiced in the United States.

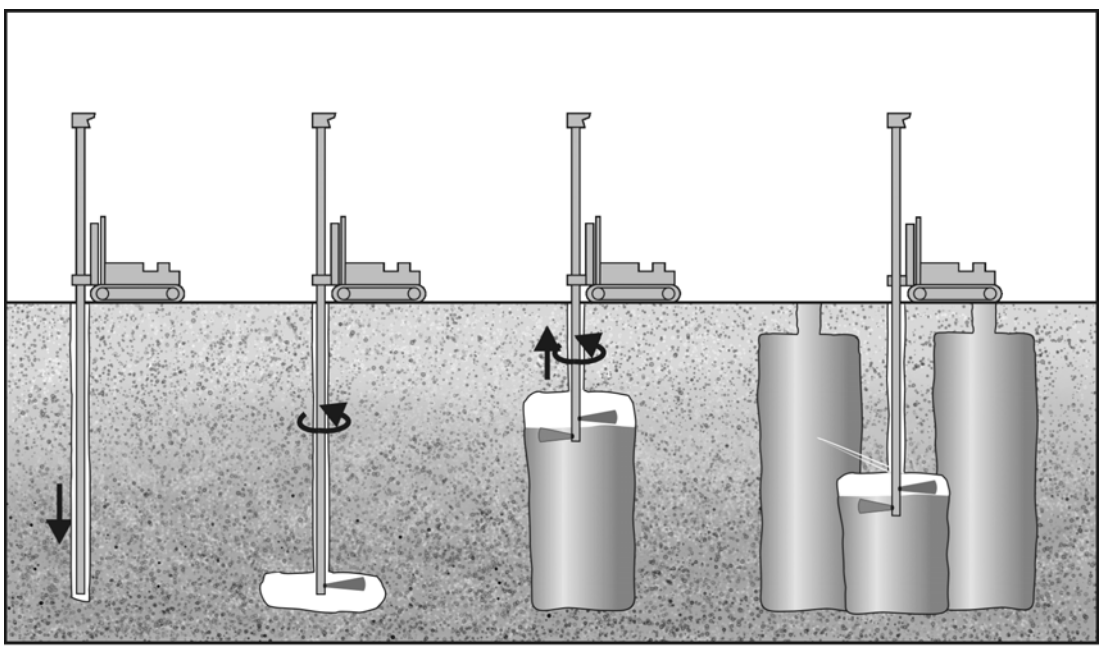

Figure 1. Jet grouting construction sequence, from Hayward Baker

Compared to any other grouting system, jet grouting is effective across the widest range of soil types, including silts and clays. Because it is a soil erosion-based system, geometry and quality can be predicted. The quality of the final jet grout product, often referred to as soilcrete (Burke and others 1992), is dependent on the soil types being jetted. Cohesionless soils typically erode more easily than cohesive soils as shown in Figure 3. Sands and gravels generally provide the highest strength, and clays provide the lowest (Figure 4). The result of higher strengths in granular

materials is due to sands and gravels providing a better aggregate within the soilcrete matrix as opposed to cohesive materials, which provide soft inclusions within the soilcrete matrix.

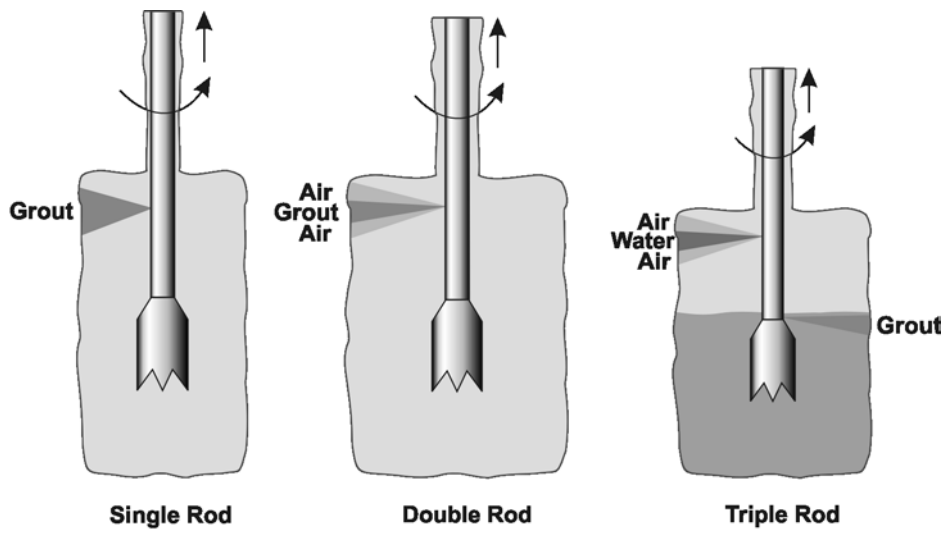

Figure 2. Jet grouting types, Single, Double and Triple fluid, from Hayward Baker

Figure 3. Erodibility scale for jet grouting systems, from Hayward Baker

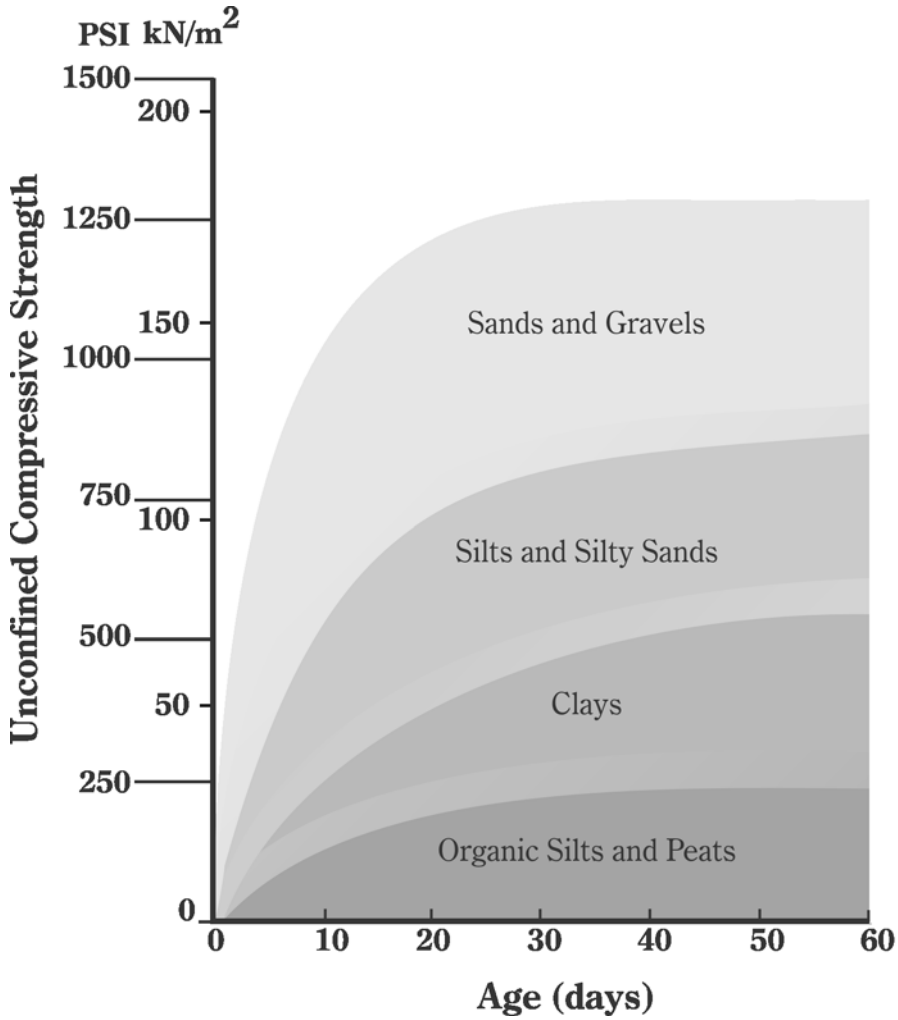

Figure 4. Typical strengths obtainable with jet grouting in various soil types, from Hayward Baker

To demonstrate the effective use of jet grouting as a scour countermeasure to repair or prevent the future impact of scour on structures, four projects are described in this paper. These projects are:

- **Old US-80 Highway Bridge at Gila River** in Maricopa County, Arizona, where jet grouting was used for scour repair and to arrest future scour of several affected bridge piers.
- **Highway 60 Bridge at Salt River** in Salt River Canyon, Arizona, where jet grouting was used to halt the further advancement of scour on an existing bridge footing.
- **CSX Railroad Bridge over the Conasauga River** in Conasauga, Tennessee, where jet grouting was used to halt the further advancement of scour on an existing bridge footing.

- **Bally's Park Place Hotel and Casino** in Atlantic City, New Jersey, where jet grouting was used to construct a barrier wall to minimize the future risk of coastal scour to the existing foundation.

Old US-80 Highway Bridge At Gila River

The Old US-80 Highway Bridge in Maricopa County, Arizona, over the Gila River is a nine span trestle type bridge constructed in the early 1900's. The bridge is situated approximately 91.44 meters (100 yds) downstream from Gillespie Dam, which controls downstream flows during heavy periods of upstream rains (Figure 5). The bridge's founding structure is composed of large concrete pedestal type piers founded upon caliche hardpan (Figure 6). During heavy desert monsoon rains in 1993, the dam failed, sending water in volumes of up to 4,248 cubic meters per second (150,000 cfs) downstream (Figure 7). The early 1900's bridge design did not allow for the structural endurance for such an event. As a result, the high velocity of water against the existing bridge created scour on the three eastern most piers. Pier numbers two, three and four suffered some minor cracking, which extended vertically down the center of the pedestal.

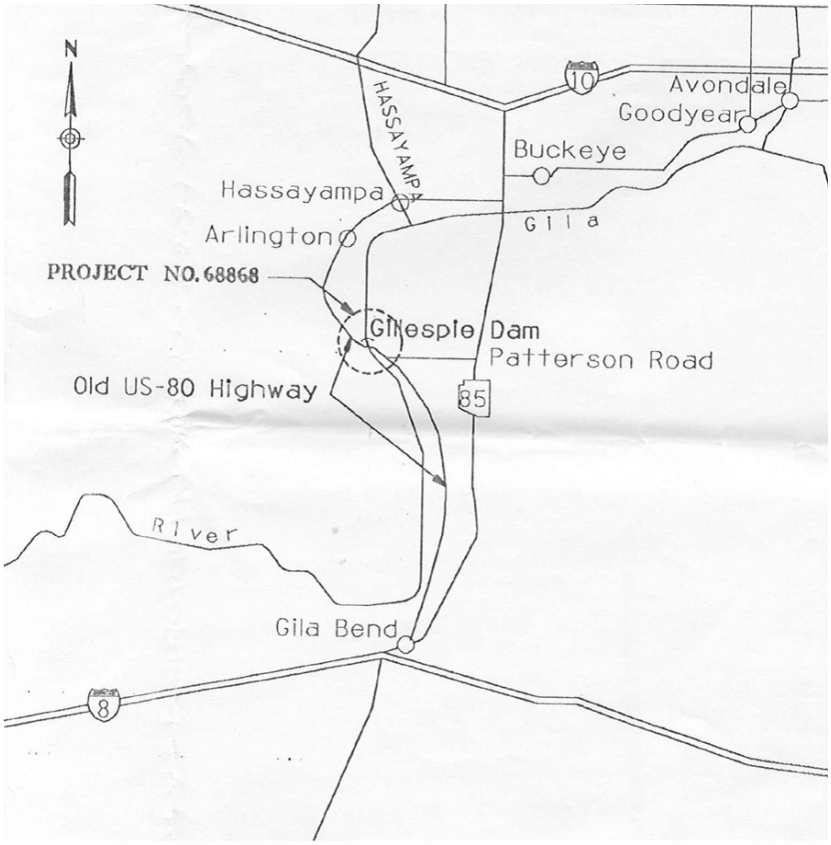

Figure 5. Site vicinity map from the Gillespie Dam project, from original contract documents

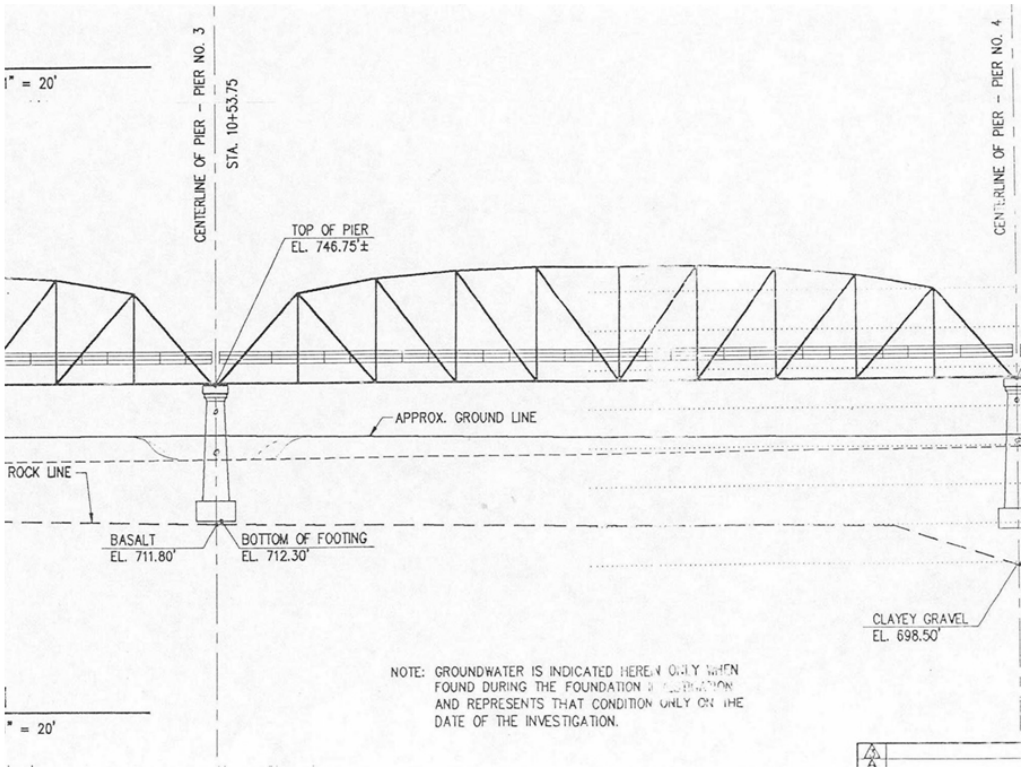

Figure 6. Elevation of typical span of the US-80 bridge over the Gila River, from construction documents

Figure 7. Failed portion of the Gillespie Dam just upstream from the US-80 Bridge

Once stream flows subsided, a geotechnical investigation of the foundation soils was performed near the affected piers of the bridge. All of the borings were performed from the existing streambed. The abutment and Pier number one was not damaged during the flood. Pier number two was constructed just below the rock line and Pier number three just above it. Pier number four was found to be constructed some six to ten feet above the existing rock line. The profile for the boring taken at Pier number four showed sands and gravels to a depth of 7.3 meters (24 ft) and then 1.8 meters (6 ft) of sandy clay overlying hard basalt (Figure 8).

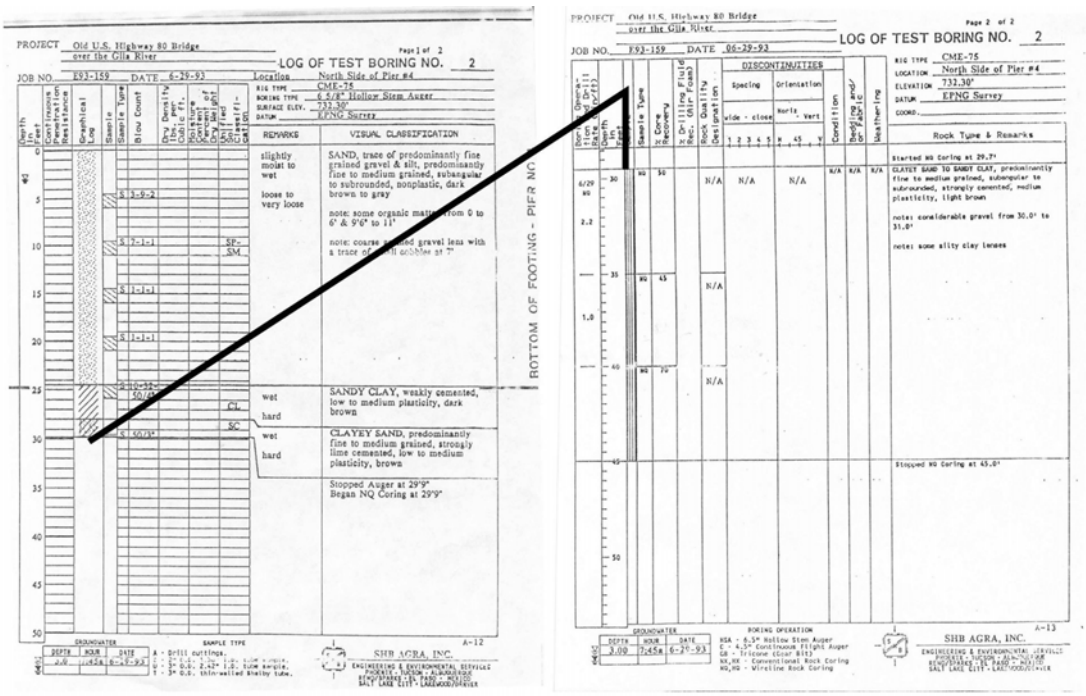

Figure 8. Log of test boring no. 2 taken at the site, from construction documents

During the review of repair options, jet grouting was determined to provide the most economical method to underpin and extend the life of the structure. Other underpinning options such as minipiles were found to be to time consuming to implement and not cost effective. Interconnected jet grout columns, 0.9 meters (3 ft) in diameter, were constructed along the upstream face of each of the three piers. The jet grout columns were installed from 0.9 meters (3 ft) above the foundation and socketed a minimum of 0.3 meters (1 ft) into the underlying basalt (Figure 9).

Prior to the start of production jet grouting, a section was tested to confirm that the minimum column diameter could be achieved in the foundation soils. The geometry of the jet grout columns was initially verified using feeler pipes, and was later visually inspected during excavation. In total some 81-jet grout columns were installed around each of the three piers using the triple system fluid of jet grouting. Soilcrete unconfined compressive strength from samples taken at the site ranged from 4.8 to 16.5 MPa (700 to 2,400 psi), depending upon the stratum being eroded during the sampling.

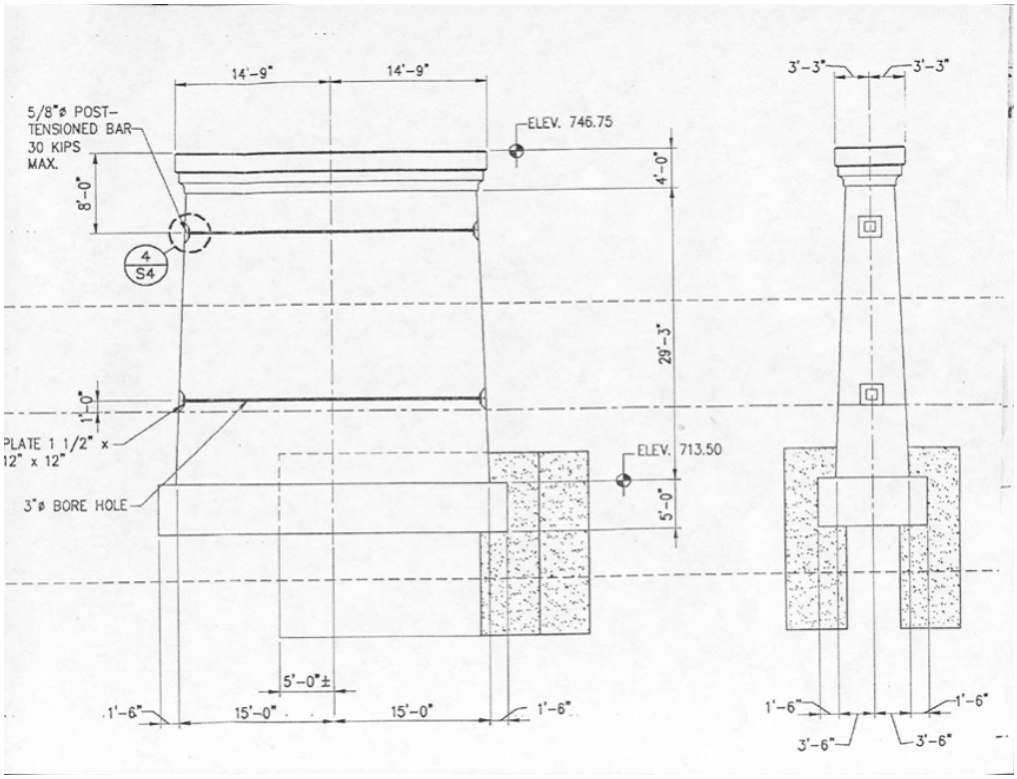

Figure 9. Jet grouting details for the repair of the scour damage, from US-80 construction documents

Highway 60 Bridge At Salt River

A new Highway 60 Bridge over the Salt River, located some 193 km (120 miles) east of Phoenix, Arizona, was constructed in 1993, some distance downstream from the original heavily traveled structure. During the construction period, excessive rains significantly increased the river flow to some 9.1 meters (30 ft) above normal, which was high enough to surround the new bridge abutment. Most of the canyon walls beneath the bridge are shear rock faces. Once the flow of the river subsided, an area immediately adjacent to the new abutment, which was thought to be rock face, was scoured out. This scour hole measured approximately 9.1 meters (30 ft) wide and 6.1 meters (20 ft) deep and threatened the newly constructed bridge abutment footing. The excessive volume and flow of water in the river also washed out the access road beneath the bridge.

The Arizona Department of Transportation (ADOT) quickly assessed the situation and determined that jet grouting of the soils beneath the water line, coupled with an above grade retaining wall constructed between the two sides of the scour hole, would provide a rapid solution to the scour problem. The existing soils at the site consisted of sands and gravel alluvium extending to a depth of some 3.1 to 6.1 meters (10 to 20 ft) below existing grade, with rock below this depth. The design called for three rows of interconnected jet grout columns to fill the scour hole below the normal river elevation (Figure 10).

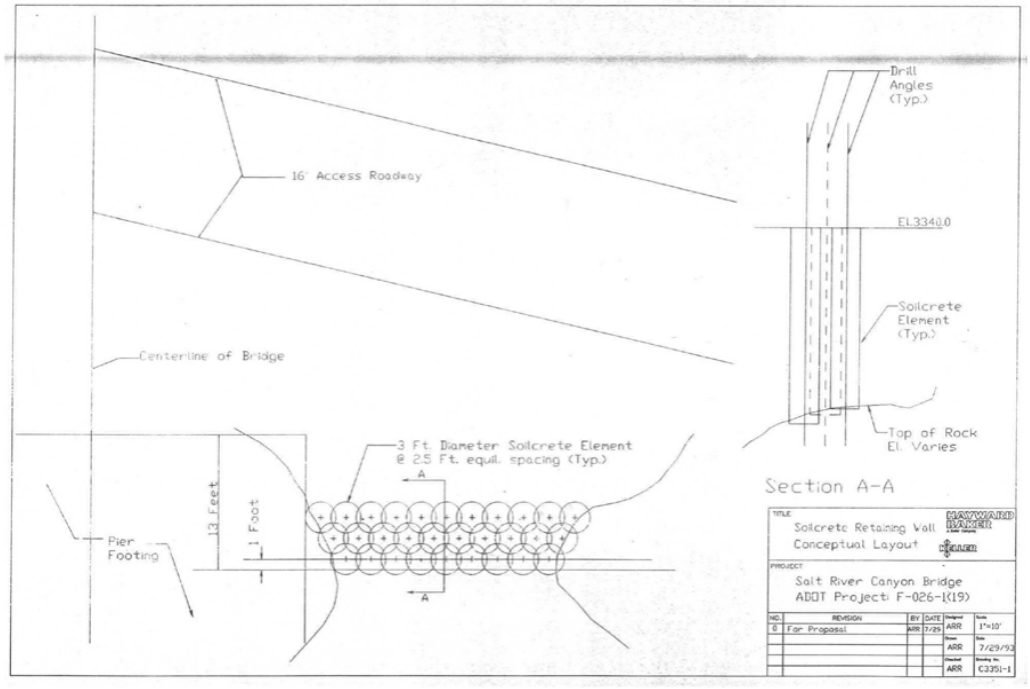

Figure 10. Layout of the jet grout columns surrounding the scour hole.

Figure 11. Completed repair of scour hole

Triple fluid system jet grouting was performed to construct 30, 0.9 meter (3 ft) diameter columns. Because of the tight working area and the loss of access roads,

heavy cranes were used to place the jet grouting equipment near the problem area. Special precautions were taken to ensure that none of the jet grout backflow entered into the river. Following construction of the jet grout wall, a new retaining wall was constructed to complete the repair (Figure 11).

CSX Railroad Bridge Over The Conasauga River

The CSX Bridge is a single-track railroad bridge composed of a steel main truss span, supported on each side of the river by a concrete pier. The piers are rectangular in shape, with a semi-oval upstream face, and are orientated with its long axis extending East-West. The track, originally constructed in 1905, runs in a general North-South direction. Approximately 30 to 40 trains cross the bridge per day. It was discovered that during a four-year period, the South pier was rotating towards the South and slightly towards the Southeast. This movement was measured at approximately three to four inches and was probably caused by scour during periods of high flow. In 1990, CSX hired consultants to provide a soils report on the existing ground conditions.

The investigation showed the subsurface conditions beneath the pier consisted of a zone of boulders in a matrix of loose sands ranging in thickness from 1.1 to 7.5 meters (3.5 to 24.5 ft), founded upon hard to moderately hard limestone bedrock (Figure 12). This matrix of soil between the boulders allowed scour to occur beneath the pier and was most likely accelerated during the heavy rains and flooding that occurred in 1989.

To protect the bridge pier against further scour, triple fluid system jet grouting was performed. The use of jet grouting would ensure transfer of all structural loads to the underlying limestone bedrock. Core drilling of the jet grout column was used to confirm the column strength and diameter of 1.1 meter (3.5 ft) (Figure 13). The core pieces as well as samples retrieved during production were tested for unconfined compressive strength to ensure that the 3.5 MPa (500-psi) design strength was met. The compressive strength testing performed on all samples averaged over 4.8 MPa (700 psi). In all, some 30 vertical and battered columns were installed to underpin the existing railroad bridge pier (Figure 14).

Bally's Park Place Hotel And Casino In Atlantic City, New Jersey

Atlantic City ordinance requires that any foundation system constructed above elevation – 10 be protected against the potential effects of scour caused by coastal storm events. Consulting engineers for Bally's Park Place Hotel and Casino accepted a jet grout solution to provide an in situ barrier to resist scour of the foundation, especially because the proximity of the Casino to historic structures precluded the use of driven or jetted sheetpile barriers. . There is sufficient documentation in the industry (Droof and others, 1995) to support the underpinning of historical structures with jet grouting. This new scour protection wall was constructed in beach sands and extended 76.2 meters (250 ft) along the Boardwalk and had a 34.5 meter (100 ft) long perpendicular return at one end.

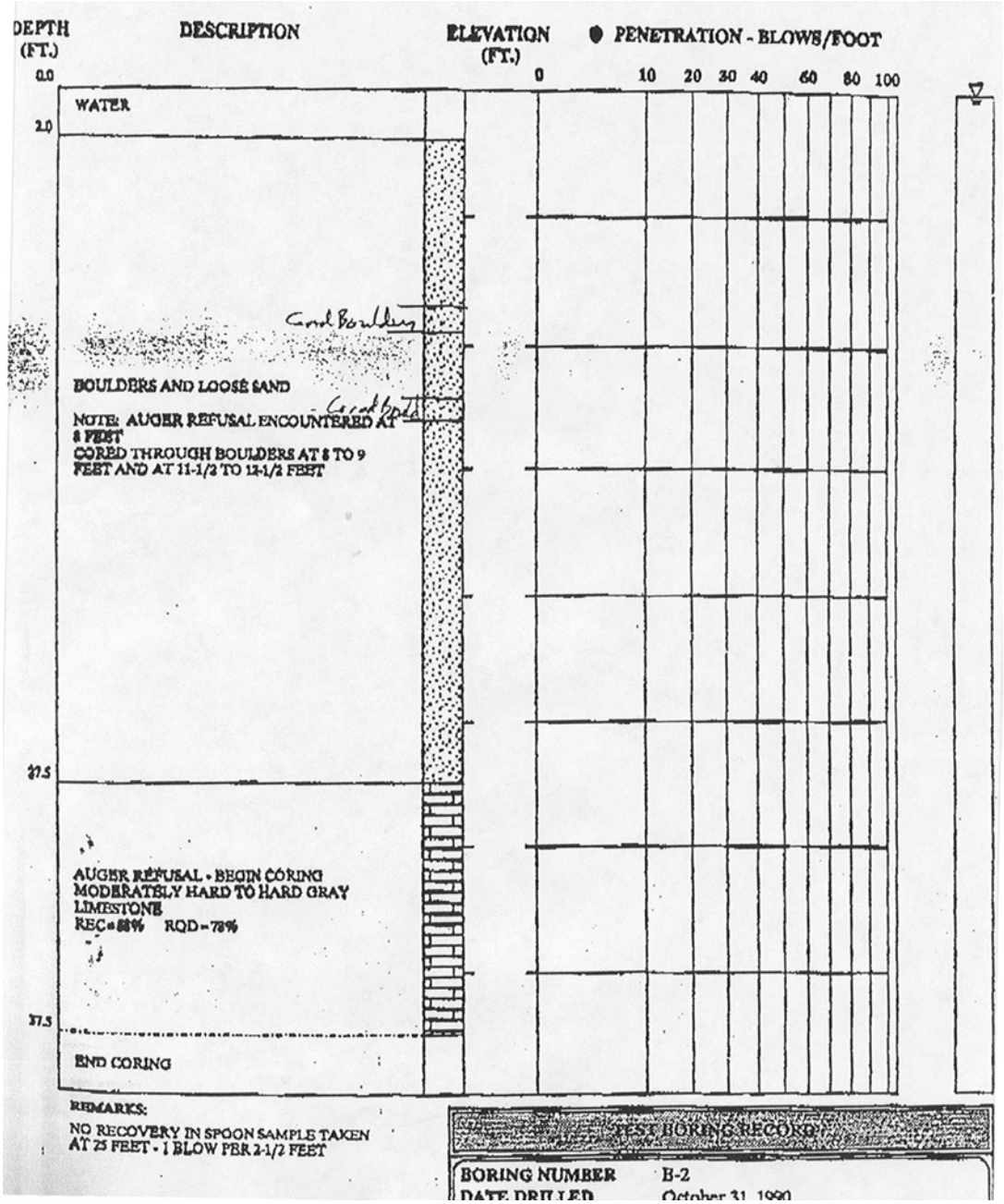

Figure 12. Boring taken from the site near the scoured Bridge Pier, from construction documents

HAYWARD BAKER
A Keller Company

Soilcrete Coring Log

Job No. J0510	Hole #1	Surf. Elev. --	Sheet No. of
Project CSX Conasauga Pier		Soilcrete Age 5 to 7 days	Date 7/16/91
			Driller Mark Gunter
			Inspector Allen Furth

A	B	C	D	E	F	G	H	
Run No.	Depth & Time From	Depth & Time To	Run Length	Recvd Length	E ÷ D Recovery %	Total Length of pieces ≥ Diameter	G ÷ E SQD	Description and Remarks*
1	0 / 11:05	4'2" / 12:35	50"	50"	100%	10"	0.2	Large cobbles: 30 - 40% gravels No Soilcrete
2	4'2" / 12:55	8'2" / 1:24	48"	48"	100%	43"	0.89	Top 9" concrete: Soilcrete with trace gravels, trace inclusions
3	8'2" / 1:45	12'2" / 2:10	48"	48"	100%	23"	0.48	Soilcrete: Trace boulders and cobbles Limestone rock at 8 feet.
4	12'2" / 2:30	16'0" / 3:30	46"	36"	75%	21"	0.58	Soilcrete: 10 - 20% gravels Large cobbles at 12 feet.
5	16'0" / 4:10	19'0" / 4:41	36"	34"	94%	21"	0.62	16 inch piece of limestone/ bedrock @ bottom of core 70 - 80% large gravels and cobbles.
EOC								
		Totals:	19'0"	18'0"	94.7%			

KELLER

* Indicate drilling fluid losses, down pressures, inclusions, cement odor, physical description and a degree of mixing.

Form #B961

Figure 13. Core recovery results from a production jet grout column

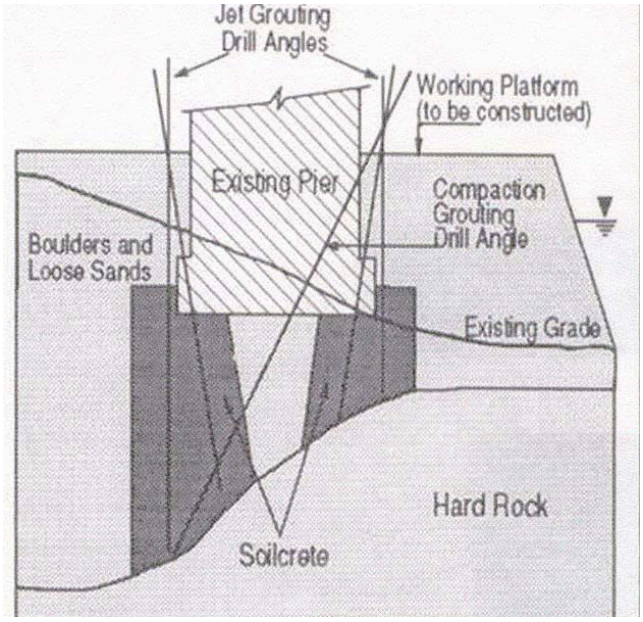

Figure 14. Cross section of jet grouting repair at the CSX Bridge

Jet grouting was performed using the double fluid system to construct five-foot diameter columns on 1.2 meter (4 ft) centers to the required depth of 4.6 meters (15 ft) below existing grade (Figure 15). The jet grout columns also supported loads from the structure where they coincided with each other. This would have been a difficult task using any other form of barrier wall. During the production work, jet grout wet samples taken exceeded the minimum required compressive strength of 5.5 MPa (800 psi). Jet grouting was also able to circumvent obstacles in the existing below grade soils. These obstacles, such as tie rods and dead man anchors, were once used to support an old bulkhead along the existing Boardwalk.

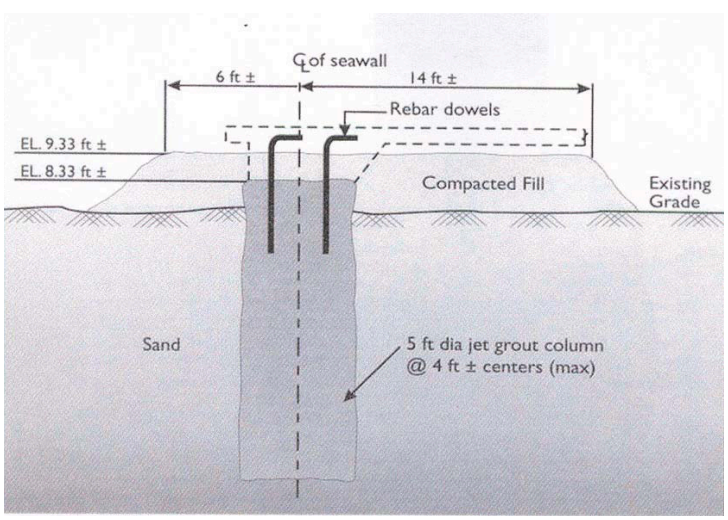

Figure 15. Cross section of jet grout scour barrier installed at Bally's Park Place Hotel and Casino

CONCLUSIONS

Jet grouting has gained a wide acceptance within the United States in the past decade and as a result, consulting engineers and other authorities have recommended it as a solution for a range of problems beyond conventional underpinning. The above case histories demonstrate how jet grouting can reduce the effects of scour, prevent scour or substantially extend the life of a structure subjected to the effects of scour. At the same time, jet grouting provides a solution that can be performed economically and quickly, insitu. These case histories also demonstrate how jet grouting can be done from above the effected structure without creating excavations or building structural connections to the existing structures. It is for these two reasons, that jet grouting provided the most economical approach in the repair of these structures. All of the repaired structures have been subjected to flooding, high stream flows and coastal storms since they have been repaired with jet grouting and have shown no signs of movement or additional scour.

REFERENCES

1. Shirole, A. M., and Holt, R. C. (1991). "Planning for a comprehensive bridge safety assurance program." Transp. Res. Rec. 1290, transportation Research Board, Washington, D. C., 137-142
2. Burke, George K. and Brill, Gary T. (1992) "Foundation stabilization system using jet grouting techniques." Proceedings of the Twenty-Third Ohio River Valley Soils Seminar
3. Droof, Furth, and Scarbrough (1995) "Jet grouting to Support Historic Buildings." Foundation upgrading and repair for Infrastructure Improvement, ASCE 50

Field Evaluation and Countermeasure Selection for Scour Critical Bridges in the Commonwealth of Kentucky

By

Kurt J. Schaefer, PE[1], and Ron W. Gardner, PE[2]

ABSTRACT

The Kentucky Transportation Cabinet (KYTC) implemented a scour countermeasures program in 2001 to aggressively target approximately 200 bridges deemed 'scour critical' throughout the twelve KYTC districts which comprise the commonwealth. The program was initiated in June and completed under a fast-track schedule, following applicable FHWA, KYTC and HEC –23 guidelines, and involving a two-phase approach. The first phase involved field evaluations of the bridges to: verify the scour critical designations, gather basic field data at the bridge site, formulate proposed countermeasures, and to create budgetary cost estimates of the proposed countermeasures for project funding purposes. The second phase of the project involved developing 'contract ready plans' for each bridge from the field evaluations. These plans consisted of a written description of the proposed countermeasures and basic construction plans, notes and specifications. The development of these contract ready plans allows for immediate letting of projects as funding becomes available.

This paper presents the procedures and thought processes used in developing and performing the field evaluations for the project, as well as selecting appropriate countermeasures. Discussions are offered regarding the rationale behind countermeasure selection in terms of: site suitability, site access, physiographic region, and availability of materials. Typical countermeasures to be discussed include riprap, gabions, concrete collars, A-Jacks (concrete armoring units), and natural stream design structures.

INTRODUCTION

Bridges sometimes fail due to scour processes around bridge substructure elements, resulting in a potential for loss of life, property, and interruption of transportation on the nation's roadways. The Kentucky Transportation Cabinet performed a study to identify bridges in the Commonwealth of Kentucky that might be at risk of failure due to scour. The study identified approximately 200 out of 8,600 KYTC maintained bridges as "scour critical", and in need of immediate attention. Subsequently, a scour countermeasures program was established with Fuller, Mossbarger, Scott and May Engineers, Inc. (FMSM) in the summer of 2001, and those 200 bridges were visited, evaluated in the field, and scour countermeasures were designed. The Bridge Scour Countermeasure Program was based on the principles set forth in the following Federal Highway Administration (FHWA) publications:

1. Project Manager, Fuller, Mossbarger, Scott and May Engineers, Inc., Lexington, Kentucky
2. Project Manager, Kentucky Transportation Cabinet, Division of Operations, Frankfort, Kentucky

- HEC-11, Design of Riprap Revetment, March 1989 - IP-89-016
- HEC-18, Evaluating Scour at Bridges, May 2001 - FHWA NHI 01-001
- HEC-20, Stream Stability at Highway Structures, March 2001 - FHWA NHI 01-002
- HEC-23, Bridge Scour and Stream Instability Countermeasures, March 2001 - FHWA NHI 01-003

Each publication can be obtained at the web address: http://wwwcf.fhwa.dot.gov/bridge/hydpubl.htm. Other applicable resources specific to installing countermeasures at bridges in Kentucky include KYTC's "Best Management Practices for Maintenance Activities in and Around Streams" published in 2000, the current edition of KYTC's Standard Specifications for Road and Bridge Construction (SSRBC), and KYTC's Division of Construction Guidance Manual.

The locations of the bridges evaluated during the contract are presented on the following map of Kentucky in Figure 1. The map is subdivided into 12 areas, which correspond to the 12 operational districts of the Kentucky Transportation Cabinet.

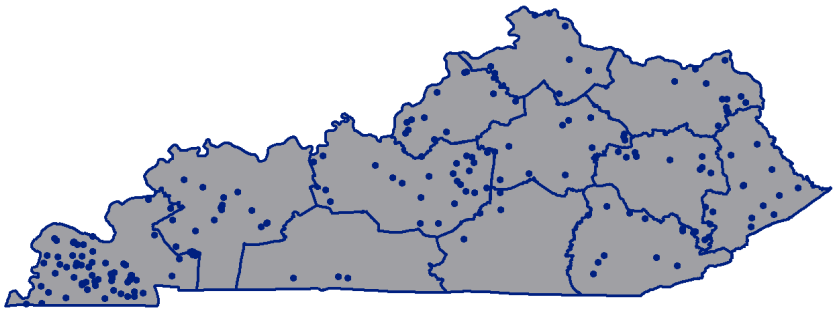

Figure 1. Locations of Countermeasure Bridges

This paper is the result of the knowledge base created during the field evaluations and designs of countermeasures across the Commonwealth of Kentucky.

SCOUR PROCESSES

Scour occurs at bridges when the oncoming stream flow is obstructed by piers, abutments, approach embankments, and/or debris, causing the channel bed to erode and expose the bridge substructure elements (piers, piles, footings and abutments) or undercut the streambank/roadway approaches. Scour failure can be defined as when the streambed erodes beyond the point at which the bridge foundation can support the superstructure, or the roadway approach is damaged, making the crossing dangerous or impassable. The amount of scour that occurs at any given bridge is related to the type of bed material, the force and direction of the oncoming flow, and the substructure geometry. Bed material type and stream gradient are naturally dictated by the physiography of the watershed, and it is vital to understand these components when evaluating a bridge for scour. The Commonwealth of Kentucky is relatively diverse in physiography, with five major regions identified. The eastern portion of Kentucky rests at the foothills of the Appalachian Mountains and is known as the Eastern Kentucky Coalfield physiographic region. This region is mountainous, supporting elevations in excess of 4,000 feet,

is highly dissected by v-shaped valleys, is mainly forested with cleared bottom lands, and is underlain by bedrock consisting of shale, coal, siltstone and sandstone. The north-central portion of the commonwealth is identified as the Bluegrass physiographic region, and is typically represented by rolling grassy hills of clay soils overlying limestone bedrock. The Western Kentucky Coal Field physiographic region occupies the western portion of the commonwealth and is characterized by rolling hills with some escarpments. The land varies from wooded to pasture and typically consists of clayey soils overlying shales, sandstones and limestones and coal. Surrounding the Western Kentucky Coalfield region is the region known as the Mississippian Plateaus. This area is hilly, wooded to grassy, and is characterized by the karstic activity of the limestone bedrock. This karstic nature of the bedrock leaves the area dotted with thousands of sinkholes, sinking creeks and caves. The Mississippi Embayment physiographic region occupies the southwestern tip of the state and is part of the Gulf Coastal Plain. This area is relatively flat, wooded to grassy to swampy, with topographic relief on the order of 100 feet, and the lowest ground surface elevation in the commonwealth, elevation 260 feet. Bedrock is exceptionally deep in this area and the overburden soils consist of highly erodible sediment deposits.

There are four primary components of scour that typically occur at bridge sites in Kentucky: long-term aggradation and degradation, local scour, contraction scour, and lateral channel migration. Aggradation and degradation represent the long-term raising or lowering of the stream reach. These processes are most prevalent in highly erodible soils or in stream reaches physically altered by man. Local scour results from the obstruction that any given bridge substructure element or debris rack presents to oncoming flow, and is site specific to that obstruction. Contraction scour is the erosion that occurs across most or the entire crossing in the immediate vicinity of the bridge. The flow is contracted due to the decreased area available at the bridge opening compared to the flow area available in the channel and floodplain upstream of the bridge. Lateral channel migration is a natural process in which the channel shifts laterally (meandering) over time to seek a balanced state. Lateral changes in stream location can threaten the stability of bridge abutments, approaches and overbank piers.

It is vital to the countermeasure program to understand and relate the scour components and physiographic regions. The region will typically dictate the type of scour by natural physics, unless the bridge itself modifies the process. Understanding these interactions will reveal whether the structure or the stream should be addressed by the countermeasure.

FIELD EVALUATION OF SCOUR CRITICAL BRIDGES

The scour countermeasure process begins by performing a field evaluation of the bridge. The purpose of a field evaluation was to determine the extent and cause of the scour (i.e. channel migration, debris blockage and subsequent flow redirection, etc.), and to collect the data necessary to determine the type(s) and extent(s) of scour countermeasures required to correct the problem. It is during this evaluation that a majority of the design issues were addressed. Before the evaluators left the site, they had a plan of action and sketches for implementing the appropriate countermeasure(s). For the KYTC scour countermeasure program, it was established that only shallow water bridges would be involved. If the water around substructure elements was too deep to be safely waded, the evaluation would be diverted to a separate contract to be performed by engineer divers. Another criteria of the scour program was that all work to

remediate the bridge had to be kept within 100 feet upstream and downstream of the structure when at all possible. Work outside these limits would necessitate permits and easements, delaying the contracting process.

While at the bridge, the evaluators performed the following procedures:

- Became familiar with any previous inspection reports and other data provided on the Kentucky Bridge Information System (KBIS) data forms for the bridge.
- Reviewed previous photos of each bridge for comparison purposes – noted if there were changes to: the streambed or streambank, scour conditions, structural conditions, and debris rack size and composition.
- Noted the type and composition of bed material, i.e. clay, sand, gravel, cobble. Noted the bedrock type and durability, if present, and noted if the foundations were rock bearing.
- Evaluated the structure site, noting evidence of scour, bank erosion, channel migration and aggradation/degradation. Scour holes at piers and abutments were carefully measured, and soft material in scour holes were probed to determine the location of a firm bottom. Also, noted were bars, islands, or vegetation constricting the flow at the bridge and concentrating it in one section of the bridge opening or causing it to attack piers and/or abutments.
- Maintained consistency with previous KYTC inspections and nomenclature by referencing all data collected during the field visit using left and right nomenclature (left and right looking *downstream).* All substructure elements were numbered increasing from left to right looking downstream.
- Noted the size, quantity, and composition of debris rack(s), if present. Noted the location of any high water mark(s) (debris line), and mentally established how the structure operates during a flood.
- Noted potential contractor access points to bridge for construction purposes (i.e., from bridge deck only, from left upstream floodplain, etc.) and any visible overhead/underground utility conflicts (location estimated from bridge face).
- Recorded pier/abutment geometry, bridge opening width and height. Obtained vertical measurements of bridge opening from along the upstream and/or downstream face of bridge, using a weighted tape. Several measurements were obtained along the face, and all measurements were referenced to the same bridge element (top of curb or bridge deck for vertical measurements, edge of left abutment for horizontal measurements) referenced in the KBIS data. All measurements needed for defining the bridge opening were obtained.
- Determined if a flow training structure (J-Hook, Cross Vane or W-Weir) was necessary or applicable, and established the appropriate bankfull width and elevation (referenced to the bridge structure). In addition: an estimate of the average particle size of the reach bed material was made, and the reach upstream and downstream of

the bridge was reviewed. The detailed data acquisition required for a natural stream design was typically beyond the scope of this countermeasure program, and was recommended to be performed under a separate contract.

- Noted the type and condition of existing countermeasures, if present. Recommendations regarding proposed countermeasure(s) to be used at the bridge were made and referenced to KYTC standards (type of geotextile, channel lining, etc.) as applicable.
- Noted special issues needing to be addressed during construction/installation of countermeasures. This included the presence of mature trees that would need to be worked around or incorporated into the design, farm fences which needed to be removed and replaced in-kind, and noting if sites have a particular aesthetic or cultural quality which the contractor should maintain when working in the area.
- Obtained photos of the following (as applicable): structure face(s), debris racks/drift, existing countermeasures, areas where countermeasures were proposed (piers, abutments), construction access point(s) and existing utilities, and overall channel and bank condition.
- Created an overall plan view of the site, showing bridge, roadway, and stream relationships, as well as existing countermeasures, scour areas, and special construction considerations (trees to preserve, etc.).
- Prepared neat, legible sketches of proposed countermeasure(s) and pier/abutment dimensions as needed (did not need to be to scale).

A field evaluation and data collection form was prepared by FMSM for use in this scour countermeasures program. A copy of the form is presented as an appendix. The evaluators were instructed to confirm that all applicable portions of the form have been addressed prior to leaving the bridge site.

COUNTERMEASURE DESCRIPTION AND APPLICATION

The FHWA identifies three primary groups of countermeasures: hydraulic countermeasures, structural countermeasures, and monitoring (HEC-23). In selecting a countermeasure it is necessary to evaluate how the stream may respond to the proposed countermeasure. It is also necessary to estimate or anticipate future activities by adjacent landowners and the resulting influence upon the countermeasure. For these reasons, it is recommended that countermeasures be inspected periodically to evaluate performance, to determine if modifications to the original design are necessary, or if any maintenance efforts are required.

1. Hydraulic Countermeasures. There are two classifications of hydraulic countermeasures; river training structures and armoring countermeasures. River training structures modify the flow path to mitigate the erosive forces that occur along the streambed, streambank or substructure elements of the bridge. Armoring countermeasures provide resistance to the erosive forces and provide protection of the streambed in the immediate vicinity of the armor protection. River training structures selected for use in Kentucky consist primarily of rock vane structures: J-Hooks, Cross-Vanes, and W-Weirs. These types of countermeasures are effective in controlling the scour location and directing the flow of water through the bridge

such that scour at substructure elements is eliminated, reduced, or managed. This form of countermeasure is applicable for mitigating local and contraction scour, and addressing both vertical and horizontal channel instability.

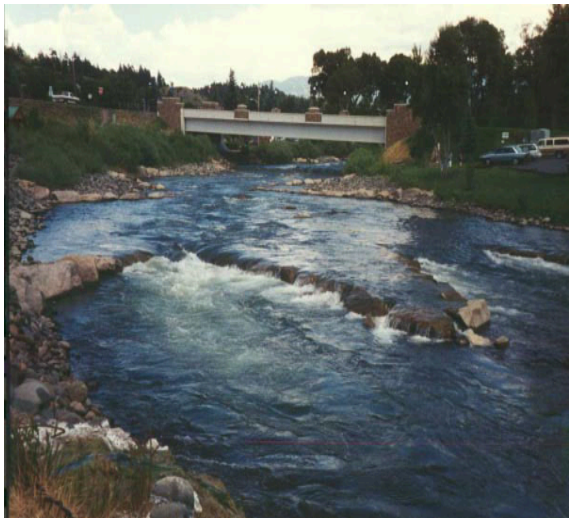

Example of a River Training Structure

The objective of armoring countermeasures is to protect the streambed or streambank from erosive forces induced by the hydraulic conditions created when stream flow is obstructed or modified by the bridge crossing. Armoring techniques are commonly aesthetically less desirable than river training countermeasures, and while they provide protection, the scour problem is addressed symptomatically rather than by addressing the source of the problem (flow velocity and direction). Nevertheless, armoring countermeasures are appropriate and necessary for use in certain circumstances such as work limit restrictions and/or funding constraints. The following types of armoring countermeasures have been implemented in Kentucky.

- Riprap/Channel Lining – Riprap consists of varying sizes of rock underlain with a non-woven geotextile fabric. Riprap can be used to protect against local scour at abutments, piers and embankments. The specific size of rock to be used must be calculated based on the flow velocity for the design event to ensure it will not be scoured away. The KYTC recommends the 100-year storm frequency be used as the design event for sizing riprap. Common methods of riprap placement are hand placing; machine placing, such as from a dragline, or some other form of bucket; and dumping from trucks and spreading by loader. Dumping from excessive heights is discouraged. Hand placement produces the best results, however, it is generally the most expensive method of placement. Non-woven geotextile fabric should underlie all channel lining applications other than rock or gravel bed streams to reduce the potential of piping of foundation soils from under the stone.

Riprap Protection at Pier

Gabions at Bridge Abutment

- Gabions – Gabions consist of durable rock enclosed in wire. Gabion baskets are bound together and stacked laterally

and vertically. Gabion mattresses consist of rock enclosed in wire, placed laterally in a series and fastened together. Gabions can be used to protect against local scour at abutments, piers, and embankments; contraction scour, and to address stream instability. They are generally used when large rock is not available, space is limited or tight, or the area to be protected is on a slope too steep for riprap to be placed.

- A-Jacks® – A-Jacks is the trademark name for a type of concrete armor unit countermeasure shaped like a child's toy jacks. The A-Jacks has six protrusions, two in each direction of three perpendicular axes. A-Jacks counter-measures consist of a system of interlocking concrete jacks placed in individual clusters bound by cables. A-Jacks are available in standard sizes of two, four, six, and eight feet, measured tip to tip. The two-foot A-Jacks can be assembled and installed by hand. Larger sizes require a crane and must be assembled and lowered into place. Each jack, regardless of size, is manufactured in two pieces that must be assembled and installed. The halves of jacks larger than two feet in size are cemented together with grout. A-Jacks can be used to protect against local scouring at piers and abutments, contraction scour and bank erosion. Non-woven geotextile fabric should be used underneath all A-Jacks installations (except those on exposed bedrock) to prevent the loss of fines and the migration of the A-Jacks into the foundation soils.

A-Jacks® Installation

- Articulated Concrete Block Systems (ACBS) – Articulated concrete block systems consist of interlocking concrete blocks connected laterally together with cable. The mats can be used to protect piers, abutments and embankments from scour, and to armor the streambed to mitigate contraction scour. Most of the bridges evaluated in Kentucky did not require extensive armoring which might justify the use of ACBS.

Articulated Concrete Block Installation

2. Structural Countermeasures. Structural countermeasures involve either strengthening the foundation of the bridge or modifying the geometry of the substructure element. Examples of structural countermeasures that strengthen the foundation include crutch bents, cross bracing, pumping grout or concrete under a footing, and lowering the foundation. Examples of pier geometry modifications include extended footings, pier shape modifications, debris deflectors and pile redundancy. A brief description of structural countermeasures typically used in Kentucky is as follows:

- Concrete Collars – Concrete collars are used to repair and/or prevent undermining of abutments and piers, particularly when the bridge is founded upon rock. The collars can also serve to protect the bridge substructure elements from impact damage due to drift and debris. Typically, each collar extends approximately 18 inches from the face of the abutment or pier for constructibility reasons, and is embedded into the streambed and/or doweled into bedrock. Construction of collars involves the use of Class A concrete and reinforcing steel consisting of dowels and longitudinal bars. In some situations, the collars may be required at a fully-submerged bridge element; in that case, a modified concrete mixture for submerged placement is used.

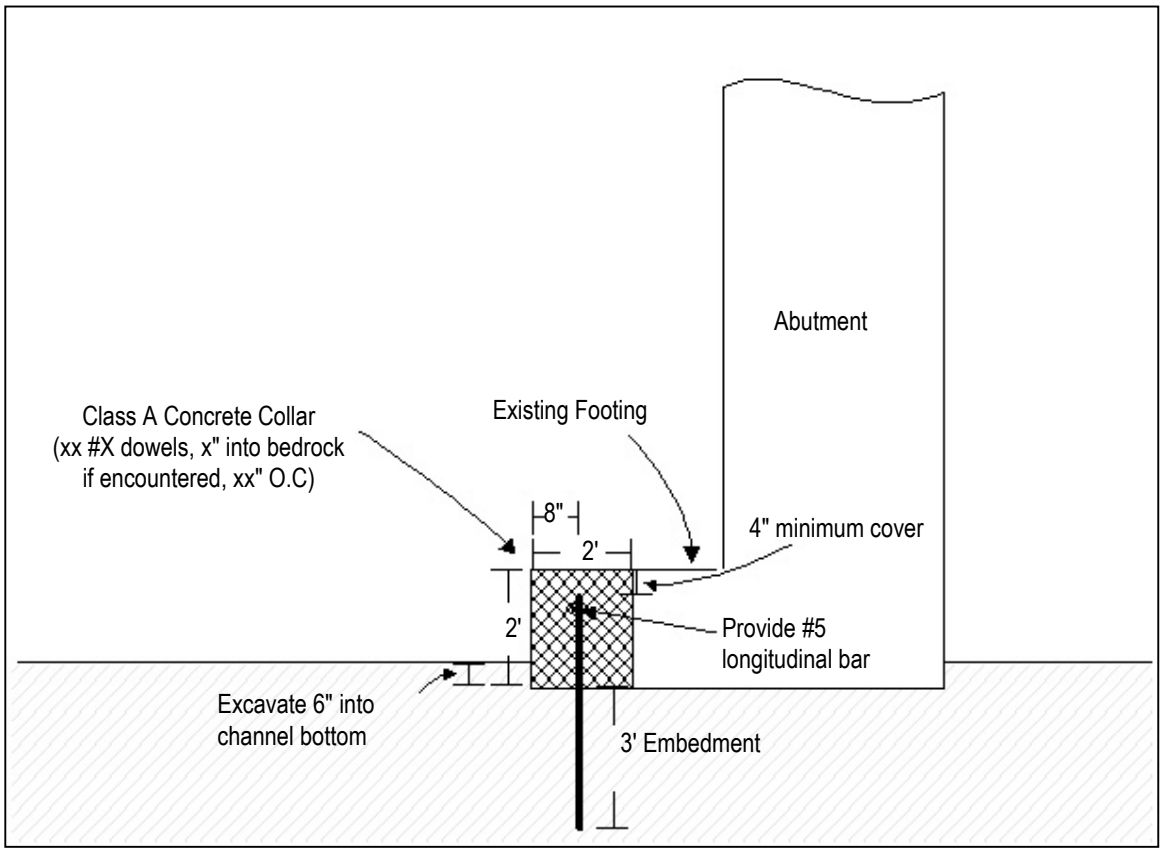

Figure 2. Concrete Collar

- Debris Deflectors – Debris is a primary cause of scour at bridges in Kentucky due to the constriction and redirection of flow into the abutments/embankments and increased flow vortices at piers. Debris deflectors called "Debris Free®" can be used for bridges that are prone to capture large amounts of debris, and are currently under consideration for installation at several pilot sites across Kentucky. Debris Free technology consists of a freely rotating deflector that floats up and down with the water level while sliding on a stainless steel rail system attached to the upstream face of the pier(s). The purpose of the unit is to divert the debris away from the pier and pass debris through the bridge.

Debris Free Technology

- Wingwall Extensions – In many cases, especially in laterally unstable channels, the embankment erodes behind abutment wingwall(s) of the bridge. The wingwall can be extended to a point beyond the existing flow path to better direct the flow through the bridge and armor the eroded bank.
- Retaining Walls – Retaining walls may be used in cases where the roadway embankment is threatened or the adjacent channel banks have experienced detrimental erosion and other forms of flow redirection are not suitable. Retaining walls are usually "stand-alone" structures, and are therefore not doweled into the bridge. The wall serves two purposes in that it will direct flow through the bridge and provide streambank protection. Two common types of retaining walls used in Kentucky include mass concrete gravity walls and reinforced concrete cantilever walls. The design of any wall should only be performed by a qualified professional engineer who has adequate site specific geotechnical and hydraulic information to make proper design recommendations.

3. Monitoring. The goal of monitoring as a countermeasure is to detect scour problems or progression early, through instrumentation or visual inspection. Instrumentation can be fixed or portable. Fixed instrumentation is typically attached to the bridge at a pier or abutment to measure scour at a particular location and may employ the use of a data storage device. Types of fixed instruments for monitoring include sonar devices which can provide a record of scour depths, and other instruments, such as a magnetic collar, which record only the maximum scour depth. Similar portable devices may be used, the difference being that the units are not attached to the bridge, are not automated, and only record depths at the time the physical monitoring occurs.

Monitoring by visual inspection requires that the bridge be inspected on a regular basis and possibly during or after high flow events. Monitoring does not eliminate the scour susceptibility of a bridge. The current KYTC BMP for Maintenance Activities in and around streams states that all bridges will be inspected after flood events.

COUNTERMEASURE SELECTION

In the course of evaluating a bridge site for scour remediation, the team had to determine the proper 'fix' for the bridge. Each team carried a field book containing typical countermeasure applications and standard drawings from which to reference ranges for dimensions and material quantities. The process of selecting the most appropriate countermeasure involved iterating between the four following questions:

1. Is the proposed countermeasure suitable for the site?
2. Will site access allow installation?
3. How will the countermeasure operate in that specific physiographic region?
4. Are materials available to construct the countermeasure?

1. Is the proposed countermeasure suitable for the site? An initial thought to fix a single span bridge suffering from scour at the vertical abutment faces might be to apply properly sized riprap to the abutments. This might be a mistake because the riprap could significantly reduce the opening size of the bridge and initiate or increase contraction scour. Likewise, in streams carrying acidic mine drainage, gabions would be a poor choice because of corrosion potential of the wire baskets.

2. Will site access allow installation? Looking at the surrounding terrain, can the countermeasure be installed from the bridge deck, or from within the stream? If the work area is extremely confined, can the countermeasure be constructed by hand?

3. How will the countermeasure operate in the physiographic region? Just because foundations are on bedrock does not necessarily mean they are scour proof! Several physiographic regions in Kentucky contain shale, siltstone and sandstone bedrock which are non-durable (scourable). Both the water forces and abrasion by bedload combine to eat away the rock under footings. Is the stream causing the scour 'flashy' or does it carry a large sediment load? Do a large number of trees or logs carry downstream in flood events? For example, the Mississippi Embayment physiographic region supports exceedingly thick sediment depositions, which are highly erodible. This translates typically into friction-bearing bridge foundations endangered by degrading stream bottoms. A suitable countermeasure cannot merely protect an element, but must protect the entire crossing in this case.

4. Are the required materials readily available to construct the countermeasure? A proposed countermeasure may be feasible by all other standards, but acquiring the traditional materials may be cost-prohibitive. For example, in the southwestern tip of Kentucky, a countermeasure may require large durable boulders for a cross-vane. There may not be local sources for quarry stone of this size, so the large boulders may need to be replaced by gabions to avoid high costs associated with transporting large boulders long distances.

Overall, the above questions are just part of a method of refining a common sense solution to the scour problem. Some issues are far more complex, and may require looking beyond the physical bridge to funding issues, replacement schedules for the bridges, or cost analysis. It may be estimated that a proper countermeasure to stop stream degradation for a bridge would cost $150,000, while the cost to replace the bridge may only be $120,000 and the bridge will now completely span the affected stream, negating the problem. For this example, the cost savings realized by replacing the bridge will free funding for other projects.

SUMMARY

In the summer and fall of 2001, Fuller, Mossbarger, Scott and May Engineers, Inc. evaluated approximately 200 scour critical bridges for the Kentucky Transportation Cabinet, and developed countermeasure designs for each bridge to be remediated. The procedures developed both before and during the bridge evaluations, and subsequent countermeasure selections are an efficient means of focusing on sensible solutions and can be readily adapted to any scour countermeasure program.

REFERENCES

Federal Highway Administration, "Evaluating Scour at Bridges", Hydraulic Engineering Circular No. 18, FHWA NHI 01-001, May 2001.

Federal Highway Administration, "Stream Stability at Highway Structures", Hydraulic Engineering Circular No. 20, FHWA NHI 01-002, March 2001.

Federal Highway Administration, "Bridge Scour and Stream Instability Countermeasures", Hydraulic Engineering Circular No. 23, FHWA NHI 01-003, March 2001.

Kentucky Transportation Cabinet, "Best Management Practices for Maintenance Activities in and Around Streams", 2000.

Rosgen, David L., "The Cross-Vane, W-Weir and J-Hook Vane Structures….Their Description, Design and Application for Stream Stabilization and River Restoration". Proceedings of ASCE Wetlands Engineering and River Restoration Conference.

Fuller Mossbarger Scott & May FMSM ENGINEERS

Field Evaluation Form
KYTC Countermeasures Program

1. Bridge Number: _____ 2. Date: _____

District No.: _____ Route: _____ 3. Time: Arrive _____ Depart _____

County: _____ 4. Crew: _____

Water Body: _____ 5. Weather Conditions: _____

Bridge Length: _____ Temperature: _____

Opening Width: _____ # of Spans: ____ 6. Stream Conditions (muddy, clear, etc.): _____

7. Construction Access Locations: _____

8. Utilities:

☐ Overhead Type: _____ Distance from Bridge: _____

☐ Underground Type: _____ Distance from Bridge: _____

9. Bed Material:

☐ Silt ☐ Gravel ☐ Boulders ☐ Clay ☐ Sand

☐ Cobbles ☐ Bedrock, Type _____

10. Channel Size (Width):

☐ Small (<100 ft.) ☐ Medium (100-500 ft.) ☐ Wide (>500 ft.) Approximate Width: _____

11. Channel Sinuosity:

☐ Straight ☐ Sinuous ☐ Meandering ☐ Highly Meandering

12. Channel Bank Condition (vegetated/nonvegetated, tree lined, erosion/instability, leaning trees, etc.)

Upstream _____

Downstream _____

13. Floodplains:

☐ Little or None (<2 x channel width) ☐ Narrow (2-10 x channel width) ☐ Wide (>10 x channel width)

Description (agricultural/wooded) _____

14. Debris Racks:

☐ Sticks ☐ Tree Limbs ☐ Trees ☐ Timbers ☐ Steel Beam

☐ Construction Debris ☐ Waste Concrete ☐ Other: _____

Percent Blockage of Bridge Opening _____ Location(s): _____ Approximate Quantity _____ cubic yd.

Location(s): _____ Approximate Quantity _____ cubic yd.

Bridge No. _____

Fuller Mossbarger Scott & May FMSM ENGINEERS

Field Evaluation Form
KYTC Countermeasures Program

15. Cross Section Data: (Identify beginning point of section horizontally and vertically – reference bridge top of curb, abutment face, etc.)

Upstream Face			Downstream Face		
Horizontal Distance (ft.)	Depth to Bed (ft)	Depth to Water Surface (ft.)	Horizontal Distance (ft.)	Depth to Bed (ft.)	Depth to Water Surface (ft.)

16. Substructure Data:

Substructure Element	Location US/DS Face	Dimensions (L x W x D)	Description

17. Scour:

Substructure Element	Location US/DS Face	Scour Dimensions (L x W x D)	Scour Type	Description

Bridge No. _____

Fuller Mossbarger Scott & May ENGINEERS

Field Evaluation Form
KYTC Countermeasures Program

18. Countermeasures:

Existing Countermeasures (Y/N) _____ Type and Location: _____

Condition: ☐ Good ☐ Fair ☐ Poor

Recommended Countermeasures:

☐ Rip Rap ☐ Gabion Mattresses ☐ Gabions ☐ "Debris-Free" Technology

☐ Art. Conc. Block ☐ Toskanes/A-Jacks ☐ Concrete/Grout Mattress ☐ Replace Cattle/Water Gate

☐ Channel Realignment ☐ Flow Directing Structure Type: _____
(i.e., rock "J" hook, crossvane, "w" weir)

☐ Debris Removal ☐ Monitoring ☐ Other: _____

Other Comments (location, extent of countermeasures; include explanatory sketches):

_____

19. Special Construction Issues (mature trees to avoid, fences replaced in-kind, aesthetics):

_____

20. Photos:

Photo No. (Camera)	Photo No. (Bridge)	Description
	1	
	2	
	3	
	4	
	5	
	6	
	7	
	8	
	9	
	10	

Bridge No. _____

Fuller Mossbarger Scott & May ENGINEERS

Field Evaluation Form
KYTC Countermeasures Program

22. Sketches:

Bridge No. _____

Impact of the Federal Highway Administration's Scour Evaluation Program in the United States of North America's Highway Bridges

By

Jorge E. Pagán-Ortiz[1]

ABSTRACT

Since the establishment of the scour evaluation program by the Federal Highway Administration (FHWA) in 1988, over 368,000 of the 484,264 bridges reported by State departments of transportation (DOTs) over riverine or tidal waterways have been evaluated for scour vulnerability as of April 2002. As a result of this program and the diligent work of professionals from the transportation community, including DOTs, Federal agencies, consultants and researchers, more than 26,100 bridges have been identified as scour critical.

This paper will highlight the accomplishments of this program and the partnership within the transportation community to ensure that bridges are designed, evaluated and protected, for the potential or observed scour condition, for the safety of the public users in the United States of North America.

[1] Senior Hydraulics Engineer, Federal Highway Administration, Office of Bridge Technology, HIBT-20, Washington, D.C. 20590, USA.

INTRODUCTION

The scour evaluation program was established by the FHWA of the United States Department of Transportation in September 1988 as the result of the catastrophic failure of the New York Thruway Authority bridge over Schoharie Creek in the State of New York in April 1987, caused by the effect of local scour around the foundation of Pier 3. Two years after this failure, another catastrophic failure occur as a result of the combination of lateral channel migration and local scour, the Northbound U.S. Route 51 Bridge over the Hatchie River in the State of Tennessee. These failures claimed the lives of 18 persons, and raised questions about the scour vulnerability of the Nation's highway bridge infrastructure. The FHWA was identified as the responsible agency, by the United States of North America's National Transportation Safety Board, to develop and disseminate guidance on scour for the State departments of transportation (DOTs) on the design of new bridges and the evaluation of existing bridges.

GUIDELINES

The FHWA conducted a survey in 1988 to establish a baseline of guidance used by the DOTs to design new bridges and evaluate existing bridges for scour. The survey showed that there was a need to develop design guidelines on stream stability and scour and guidelines for conducting evaluation of bridges susceptible to scour. In addition, the survey showed that there was a need to train engineers and inspectors on both stream stability and scour.

FHWA provided leadership by developing scour guidelines. Initially, guidance on scour was disseminated through technical advisory (TA) T 5140.20 titled "Scour at Bridges" dated September 1988. This TA focused on designing bridges for scour, prioritizing bridges for scour evaluations, and developing an plan of action for bridges, determined by the engineer, to be scour critical. The TA disseminated a document titled "Interim Procedures for Estimating Scour at Bridges." The Interim Procedures contained detailed guidance for designing new bridges and evaluating existing bridges for scour. Also, it contained guidance for bridge inspectors to aid them during their inspection of the channel condition in the vicinity of the bridge as well as indications of scour problems around the bridge foundations. As technology continued to evolve through research and experience gained by the transportation community on scour and stream stability, the TA was revised and issued as technical advisory T 5140.23 titled "Evaluating Scour at Bridges" dated October 1991. The interim procedures were updated to an FHWA Hydraulic Engineering Circular (HEC), No. 18 titled "Evaluating Scour at Bridges." The need to expand the knowledge on stream stability problems in the river environment and to address stream instability problems in the vicinity of bridges led FHWA to develop another publication, HEC-20 titled "Stream Stability at Highway Structures."

The guidance provided in the HECs has helped DOTs to structure their scour

evaluation programs. Another FHWA Publication, Hydraulics Design Series 6 titled "River Engineering for Highway Encroachments" (formerly know as "Highways in the River Environment," provided guidance on stream stability and scour. DOTs have now virtually completed the screening of all bridges over waterways for scour using the following scour categories, as recommended by FHWA: *Low Risk; Scour Susceptible; Unknown Foundations; Tidal; and Scour Critical.*

The *Low Risk* category identifies bridges with low risk of failure or low vulnerability to scour as determined by the engineer. *Scour Susceptible* identifies bridges susceptible to scour, which need an evaluation, by an engineer, to determine their scour vulnerability. *Unknown Foundation* identifies bridges whose foundation type is unknown and/or the pile tip elevation is unknown. *Tidal* identifies bridges over tidal waterways, which need to be evaluated by an engineer. The last category, *Scour Critical*, identifies bridges determined to be unstable, by an engineer or an inspector, for the calculated or observed scour condition. As State DOTs continued to make progress in this program, the population of bridges in the low risk and scour critical categories increased while the population of scour susceptible population decreased. FHWA developed HEC No. 23 titled "Bridge Scour and Stream Instability Countermeasures," to assist State DOTs develop a plan of action and to assist in the selection of countermeasures to protect bridges identified as scour critical. HEC-23 presents managerial and inspection strategies for developing a plan of action. Also, it presents state-of-the-practice guidance on a large variety of bridge scour and stream instability countermeasures.

TRAINING ON STREAM STABILITY AND SCOUR

DOTs have been reporting their progress on the scour evaluation program since1990. While reporting on their scour status and conducting scour evaluations, DOTs have identified the need to provide technical training to bridge inspectors and engineers who are responsible for bridge inspection and for the scour evaluation of existing bridges and the design of new bridges, respectively. To respond to the State DOT training needs in stream stability and scour, FHWA developed a training course through the FHWA's National Highway Institute (NHI) for engineers performing scour evaluation on existing bridges and/or new bridge design, "Stream Stability and Scour at Highway Bridges." Currently, several DOTs require that, in order for a private consultant to do bridge scour evaluations and/or new bridge design work for that DOT, the engineering staff must attend this NHI training course. Another NHI training course, "Stream Stability and Scour at Highway Bridges-Bridge Inspectors Module," is available for bridge inspectors responsible for reporting and coding the condition of bridges. These courses have been presented in 45 of the 52 DOTs in the United States of North America. A new NHI training course, "Countermeasure Design for Bridge Scour and Stream Instability" has been developed, which present guidelines for developing a plan of action for scour critical bridges, including managerial and inspection strategies, a countermeasure matrix with selection and design criteria, State DOTs installation experience and design references, and scour monitoring and instrumentation techniques.

STATUS OF THE SCOUR EVALUATION PROGRAM

Thanks to the partnership between the FHWA and DOTs in the scour evaluation program, most of the bridges over waterways have been evaluated and categorized following the guidelines provided by FHWA. The following status report, as of April 2002, serves to quantify the impact of this program on a nationwide basis:

- Most DOTs exceeded the FHWA major milestone of 90 percent of the bridge scour evaluations completed for bridges requiring an evaluation (42 DOTs with 90 percent or more).

- A detailed analysis of the April 2002 status report showed the following percentages by category:
  1) 70.6 percent of the reported 484,264 bridges over waterways -- *Low Risk*
  2) 18.3 percent, *Unknown Foundations*
  3) 5.5 percent, *Scour Susceptible*
  4) 5.4 percent, *Scour Critical*
  5) 0.2 percent, *Tidal*

Figure 1 presents the status of the scour evaluation program, reported by State DOTs, as of April 15, 2002.

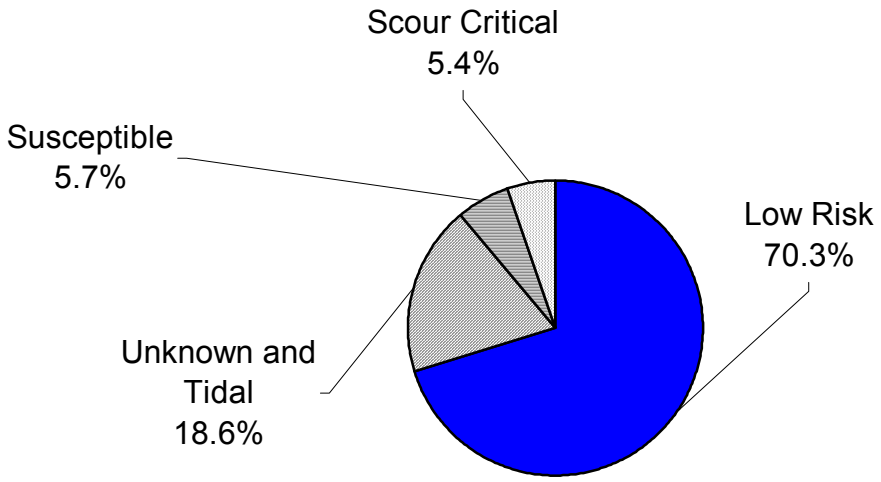

Figure 1. Status of Scour Evaluation Program (As of April 15, 2001)

CURRENT ACTIVITIES

The scour evaluation program has served to identify other areas where technology should be developed and/or enhanced in order to continue to provide state-of-the-art guidance to DOTs. Two major areas are how to evaluate and how to identify unknown foundations. Technology for identifying unknown foundations is now available for some foundation types, thanks to the results obtained from the National Cooperative Highway Research Program (NHCRP) Project 21-5(1). Another NCHRP project, 21-5(2), will investigate other devices for potential use in this area.

Technology on tidal hydrology and hydraulics has been enhanced through advancements made through a pooled-fund project on tidal hydraulics, led by the South Carolina DOT in partnership with several coastal States in the United States of North America and the FHWA. Currently, FHWA is developing a new Hydraulic Engineering Circular (HEC) publication, HEC-25, which would present guidance for estimating the hydrology and hydraulic parameters needed to estimate scour at bridges over of tidal waterways. A new training course on Tidal Hydraulics is under consideration by FHWA to disseminate the guidance contained in the new HEC-25.

The scour evaluation program has also served to identify needs to develop specifications for pier and abutment scour countermeasures, methods to assess channel migration, and portable devices for monitoring scour. Research activities, sponsored by NCHRP are currently underway to address these technology needs. In addition, the scour program has served to identify the need to update microcomputer software for scour modeling in a continuous basis. As such, FHWA has been actively enhancing microcomputer software for bridge hydraulics and scour calculations. The microcomputer software WSPRO, a one-dimensional bridge hydraulics, has been updated to include bridge scour modeling. This software is available through the Office of Bridge Technology website at www.fhwa.dot.gov/bridge. The microcomputer FESWMS, a two-dimensional bridge hydraulics, has been updated to include bridge scour and sediment transport modeling. A program interface, Surface-Water Modeling System, provides enhanced input/output data management and graphics for FESWMS.

SUMMARY

Since the initiation of the scour evaluation program, State and local DOTs have been able to identify and prioritize scour critical bridges in need of corrective actions due to the impact of stream instability and/or scour upon the bridge foundation. Some DOTs have developed plans of action that include specific instructions for bridge inspectors and other actions such as corrective measures to be designed and implemented on these bridges. FHWA developed a generic plan of action (GPOA) based on the guidance presented in HEC-23 to assist State DOTs. The GPOA has been distributed to all the State DOTs and is posted as part of a presentation titled "Approach to Developing a Plan of Action" in the Office of Bridge Technology Website at http://www.fhwa.dot.gov/bridge/sctrb.htm. FHWA plans to promote the implementation of the GPOA through its FHWA field offices.

REFERENCES

1. Technical Advisory T 5140.20, "Scour at Bridges," which includes the "Interim Procedures for Evaluating Scour at Bridges," September 1988, United States Department of Transportation, Federal Highway Administration.
2. Technical Advisory T 5140.23, "Evaluating Scour at Bridges," July 1992, United States Department of Transportation, Federal Highway Administration, Washington, D.C.
3. Federal Highway Administration, Hydraulic Engineering Circular No. 18, "Evaluating Scour at Bridges," Fourth Edition (Dual Units), May 2001.
4. Federal Highway Administration, Hydraulic Engineering Circular No. 20, "Stream Stability at Highway Structures," Third Edition (Dual Units), March 2001.
5. Federal Highway Administration, Hydraulic Engineering Circular No. 23, "Bridge Scour and Stream Instability Countermeasures," Second Edition (Dual Units), March 2001.
6. Federal Highway Administration, National Highway Institute Training Course No. 135046, "Stream Stability and Scour at Highway Bridges," December 1995.
7. Federal Highway Administration, National Highway Institute Training Course No. 135047, "Stream Stability and Scour at Highway Bridges-Bridge Inspectors Module," November 1995.
8. Pooled-Fund Project, "Development of Hydraulic Computer Models to Analyze Tidal and Coastal Stream Hydraulic Conditions at Highway Structures," South Carolina Department of Transportation, July 2000.
9. National Cooperative Highway Research Program Project 21-5 (1) and (2), "Determination of Unknown Subsurface Bridge Foundations," Transportation Research Board, Washington, D.C.

Evaluation of Strategies to Control Erosion along U.S. Highway 50 Between Carson City and Lake Tahoe

Keith Dennett[1], Pat Fritchel[2], Raj Siddharthan[3], and Amir Soltani[4]

PROJECT OVERVIEW

Severe erosion is occurring at several locations along U.S. Highway 50 in Nevada between Carson City and Lake Tahoe. Surface water runoff from seasonal snowmelt and infrequent high intensity rain events can cause erosion and transport substantial quantities of soil and sediment. Severe erosion can cause problems related to slope stability along the roadway, especially at the discharge of culverts. During significant runoff events, erosion negatively impacts water quality as evidenced by dramatic increases in turbidity and suspended solids entering surface streams. The erosion, transport, and deposition of soil and sediment also increases maintenance requirements for the Nevada Department of Transportation (NDOT). The deposition of suspended solids within drop inlets and culverts can substantially reduce the hydraulic capacity of these drainage structures. This may lead to overtopping of curbing along the roadway shoulders resulting in surface flow across unstable, easily erodible slopes.

Corrective action must be taken to limit the erosion of soil and transport of sediment during runoff events. NDOT has budgeted approximately $1 million per year over the next several years to implement erosion control strategies along this section of Highway 50. Numerous erosion control products are commercially available. However, the effectiveness and suitability of these products is often difficult to predict.

This ongoing research project is investigating a variety of erosion control strategies. A combination of laboratory tests and field studies are being conducted to assess the performance of potential erosion control products. This research project will help NDOT identify appropriate and cost effective strategies for mitigating erosion problems along this section of Highway 50.

BACKGROUND AND INTRODUCTION

Erosion can cause problems related to slope stability along roadways and generally increases maintenance requirements, especially those associated with drainage structures. During significant runoff events, erosion can also cause dramatic increases in turbidity and suspended solids entering surface streams. The subsequent deposition of suspended sediments in slower moving receiving waters can also negatively impact fish populations and may smother the

[1] Assistant Professor, Department of Civil Engineering, Mail Stop 258, University of Nevada, Reno, NV 89557,USA, E-mail: dennett@unr.nevada.edu
[2] Graduate Research Assistant, Department of Civil Engineering, Mail Stop 258, University of Nevada, Reno, NV 89557, USA
[3] Professor, Department of Civil Engineering, Mail Stop 258, University of Nevada, Reno, NV 89557, USA
[4] Chief Hydraulic Engineer, Nevada Department of Transportation, 1263 S. Stewart Street, Carson City, NV 89712, USA

benthic community (Dennison, 1996).

Erosion involves the processes of particle detachment, transport, and deposition. Any site where soils are exposed to water, wind, and ice is susceptible to erosion (Dennison, 1996). For erosion caused by water, the specific forces that initiate the detachment of particles include the impact of raindrops and the shear stresses exerted by surface runoff (Lal and Elliot, 1994; Dennett, 1995).

Three recognized types of soil erosion that may occur along hillsides and steep slopes include: (1) surface erosion; (2) gully erosion; and (3) mass soil movement (Ffolliott *et al.*, 1995). Surface erosion occurs as a result of the collective action of the impact of raindrops, thin film surface flows, and concentrated surface runoff flows. Surface erosion may also be further classified as either interrill erosion or rill erosion (Lal and Elliot, 1994; Elliot and Ward, 1995) because it promotes the formation of rills and small gullies on the land surface.

As overland flow becomes concentrated and moves downslope, the velocity of the flow generally increases which increases the kinetic energy of the flow (Ffolliott *et al.*, 1995). This subsequently increases the turbulence and ultimately the erosive potential of the flow, which varies with the square of the velocity (Goldman *et al.*, 1986). In general, surface flows with velocities as low as approximately 0.5 feet per second (160 mm/s) are capable of eroding soil particles that are 0.3 mm in diameter (Bell, 1999). In order to reduce the erosive potential of flowing water, the channel velocity can be reduced by lining the channel bottom with a roughened surface such as vegetation and rip rap or by increasing the width of the channel.

A gully is a relatively deep, recently formed eroding channel on hillslopes where no well-defined channels existed previously. Gullies usually result from uncontrolled, concentrated surface runoff down hillslopes that have very little vegetative cover and contain highly erodible soils (Ffolliott *et al.*, 1995). Gullies are likely to form whenever concentrated surface flow passes over a point where an abrupt change in elevation or gradient of the land surface occurs. After gully erosion is initiated, it is very difficult and costly to control (Ffolliott *et al.*, 1995).

The four principal factors that influence the erosion of soils are: (1) climate; (2) soil characteristics; (3) topography; and (4) groundcover (Goldman *et al.*, 1986; Roberts, 1995). Groundcover usually refers to vegetation but also includes other surface treatments such as mulches, wood chips, crushed rock, jute mesh or netting, and filter fabric (Goldman *et al.*, 1986). Most of these surface treatments are considered as temporary erosion control measures until natural vegetation is established. In regions with harsh climates, it is usually difficult to establish vegetative cover. Thus, more permanent surface treatments such as geotextile blankets and mats are commonly used in these regions in order to allow more time for vegetation to become established.

Four soil characteristics that are important in determining the erodibility of soils and sediments include texture, organic content, structure, and permeability (Goldman *et al.*, 1986). These characteristics largely determine the infiltration capacity of soils. The steepness and length of slopes are important considerations related to topography. Long, continuous slopes tend to increase the momentum of flowing water, thereby increasing the erosive potential of the water.

Erosion can be accelerated by any activities that: (1) change natural drainage patterns; (2) alter undisturbed soil conditions; and (3) decrease the amount of permeable area for infiltration of water (Dennison, 1996). All of these activities tend to increase the quantity and the velocity of surface runoff. Areas that are most highly susceptible to erosion due to the increased quantity and rate of surface runoff include areas with steep slopes and areas with little or no vegetative cover (Dennison, 1996).

Ffolliott *et al.* (1995) summarized a number of actions that can be taken to limit the progression of surface erosion. These include: (1) protecting the soil surface against the impact of raindrops; (2) increasing the roughness of the soil surface in order to reduce the velocity of the surface flow; (3) reducing the inclination of slopes; (4) increasing the infiltration capacity of soils in order to reduce the quantity of surface runoff; and (5) preventing the concentration of overland flow. In most cases, significant surface erosion can be prevented or minimized using appropriate vegetative management practices (Ffolliott *et al.*, 1995). Thus, the implementation of erosion control strategies that improve the infiltration of water into a soil will generally improve the opportunity for plant growth that can eventually lead to the development of a protective vegetative cover.

The selection of appropriate strategies to prevent and/or control erosion of soils and the transport of sediments must consider site-specific conditions such as land use, existing structures, hydrology, climate, soil type, and topography (Dennison, 1996). In locations where significant surface erosion has already occurred, structural and/or mechanical erosion control strategies must typically be employed in order to control additional surface erosion until protective vegetative cover can be established (Ffolliott *et al.*, 1995).

Structural and mechanical controls are typically designed to reduce the erosive energy of flowing water. Examples of structural erosion control strategies include the construction of pipe slope drains, energy dissipators, check dams, and terraces as well as the installation of gabions and channel linings such as rip rap. Examples of mechanical controls include contour furrows, contour trenches, pitting, and basins. The main disadvantage of structural and mechanical erosion control strategies is their relatively high cost.

As mentioned previously, the most effective long-term methods for controlling surface erosion are based on establishing and maintaining a cover of protective vegetation (Ffolliott *et al.*, 1995). A variety of erosion control strategies involve the application of temporary or permanent surface materials or treatments that are designed to promote the establishment of a protective vegetative cover over time. Examples of these surface treatments include topsoiling, mulching, chemical stabilization, and erosion control blankets (ECBs) and mats.

Topsoiling may be used when the existing soil is not suitable for establishing vegetation because of acidity, low nutrient content, poor texture, or other conditions (Roberts, 1995). In general, topsoiling is not recommended on slopes steeper than 2 horizontal to 1 vertical (Roberts, 1995).

Mulching is typically a temporary erosion control method that protects soil from the impact of rainfall and overland flow. Mulching also promotes retention of moisture within the soil horizon which encourages the growth of vegetation. The materials commonly used for mulching may be

organic or synthetic and include hay, straw, fiber mulch, and soil binders (Roberts, 1995).

Chemical stabilization techniques can also be used to stabilize and protect the soil surface (Roberts, 1995) or promote the aggregation of soil particles within the soil horizon (Haigh, 2000). Chemical stabilization involves the application of soil binders or tackifiers such as emulsified asphalt, nonasphaltic emulsions, polyvinyl acetate, and acrylic copolymers. These soil binders may be used alone or in conjunction with mulches. The application of soil binders is only a temporary method for controlling erosion since they typically decompose within 90 days (Roberts, 1995). In addition, commercially available soil binders are relatively expensive, are usually designed for agricultural use, and do not work reliably on all soils (Haigh, 2000).

ECBs and mats may be used to control erosion while providing time for vegetation to become established. ECBs can provide important protection against periodic, highly erosive overland flows that are common in dry climates and drought prone regions where vegetation is typically slow to develop (Bhandari *et al.*, 1998). Erosion control blankets may be organic or synthetic. Organic blankets may be composed of wood fibers (excelsior), jute net, or coconut coir fiber (Roberts, 1995; Bhandari *et al.*, 1998). Coconut coir blankets are relatively resistant to decay and may last for as long as five to ten years in arid regions.

Synthetic ECBs or mats (e.g., gabions, mattresses, geogrids, geomats, geocells, and geowebs) are typically constructed of non-biodegradable materials and will last for many years (Bhandari *et al.*, 1998; Rickson, 1995). The two main categories of synthetic blankets include turf reinforcement mats and erosion control and revegetation mats (Roberts, 1995). These mats are typically permanently installed and allow vegetation to grow through surface of the mats.

The most severe erosion along Highway 50 typically occurs at the discharge of culverts. In some locations, the free discharge of culverts onto unstable hillslopes has resulted in the formation of gullies as shown in Figures 1 and 2. In a number of other locations, there is evidence of additional surface erosion due to overtopping of the curb and gutter along the outer edge of the roadway shoulder.

Erosion along Highway 50 is exacerbated by steep slopes, shallow soil profiles with low permeability, a lack of nutrients and organic matter in the soils, and limited vegetative cover. Also, the cold and dry climate in the higher elevations of the Sierra Nevada mountains is not very favorable for growth of natural vegetation. Thus, the soils in this region are highly susceptible to erosion.

In order to prevent or effectively control the formation of gullies, the gradient of hillslopes must be stabilized and abrupt changes in elevation must be eliminated. Check dams are often an effective structural erosion control strategy for controlling gully erosion (Ffolliott *et al.*, 1995). Another alternative that has been used at some culverts along Highway 50, as shown in Figure 3, is a pipe slope drain that conveys water from the top to the bottom of the slope. Pipe slope drains are commonly used in conjunction with diversion dikes or swales constructed at the top of a slope (Goldman *et al.*, 1986). The installation of channel linings such as rip rap has also been effective at some locations along Highway 50 as shown in Figure 4. Each of these strategies for mitigating gully erosion is relatively expensive and difficult to construct and/or install.

This research project is evaluating the effectiveness and suitability of alternative, economical, long-term erosion control strategies designed to establish and maintain a cover of protective vegetation. Specific erosion control strategies that will be examined include surface treatments like chemical stabilization and the installation of ECBs and mats.

PRODUCT EVALUATION

A variety of erosion control products, namely chemical stabilization and ECBs and mats, are being evaluated using a combination of laboratory and field-testing. Representative soil and sediment samples from the watershed along U.S. Highway 50 have been characterized. Bulk quantities of soil and sediment have been obtained by NDOT and transported to the University of Nevada, Reno (UNR).

The performance of the erosion control products is being evaluated initially by monitoring the erosion of soil and the resuspension of sediment during laboratory flume studies. The studies are being conducted in a manner that simulates the field conditions of soils and sediments as closely as possible. The results of the laboratory studies will help expedite the selection of products that are suitable for further study during field testing.

Based on the results of the laboratory studies, the most effective erosion control products will be evaluated further during field testing. Test plots at the project site will be constructed and monitored for a period of 24 months. Recommendations for the most suitable erosion control strategies will be developed by considering the results from both the laboratory studies and the field testing

Collection and Characterization of Soil Samples

The locations within the project area where substantial erosion is occurring have been identified. Whenever possible, the type of erosion will be classified as surface erosion, gully erosion, or soil mass movement (Ffolliott *et al.*, 1995).

Samples of the soil and sediment at these locations have been characterized with respect to grain size distribution using sieve analyses. Typical results of the sieve analyses are shown in Figure 5 and a sample of the typical soil is shown in Figure 6. The brown colored soil particles range in size from approximately .25 to 7.5 mm, with a mean particle size (D_{50}) of 1.6 mm. This cohesionless soil consists mainly of decomposed granite and appears to be the dominant soil type that is subject to erosion. The properties of each soil sample are being classified initially according to the Unified Soil Classification System (USCS). In locations where eroded sediments have been redeposited, changes in particle size distribution with sediment depth will also be examined. Column settling tests will be performed to determine the settling velocities of the various size fractions within each sample.

Laboratory Flume Studies

Laboratory flume studies are being conducted in a rectangular, recirculating, tilting flume at UNR in order to evaluate the performance of various erosion control products. The flume is 24 meters long and 0.9 meters wide. Plan and profile views of the flume are shown in Figure 7. The

soil test section for the flume studies is 6 m long by 0.9 m wide by 15 cm deep. The test section has a 5 cm by 10 cm wooden perimeter for attaching and anchoring the erosion control products in place over the test section. The soil test section is shown in Figure 8.

Specific objectives of the laboratory studies are: (1) to determine the critical shear stresses required to initiate the erosion of soil and/or the resuspension of sediment; (2) to determine the erosion rates of soils and the rates of resuspension and/or deposition of sediments under varying flow conditions; and (3) to monitor the reduction in erosion due to various erosion control strategies.

The bed shear stress applied to the soil and sediment samples can be adjusted by varying the depth of the flow, the approach velocity of the flow, and the bed slope of the flume. The critical shear stress is the bed shear stress required to initiate the erosion and/or resuspension of particles. When the bed shear stress is below the critical shear stress, no erosion or resuspension will occur. When the critical shear stress is exceeded, particles will be eroded and transported (Dennett, 1995; Dennett *et al.*, 1998; and Ravisangar *et al.*, 2001).

The flume studies are being conducted in a manner that simulates the field conditions of the soils and sediments and the flow induced shear stresses as closely as possible. ASTM D 6460-99: Standard Test Method for Determination of Erosion Control Blanket (ECB) Performance in Protecting Earthen Channels from Stormwater-Induced Erosion provides some guidelines for conducting the flume studies. As recommended, the duration of each test is 30 minutes at the desired bed shear stress. The performance of each product is being evaluated by comparing the sediment yields with and without erosion protection over a range of bed shear stresses.

The performance of four ECBs and turf reinforcement mats (TRMs) manufactured by SI Geosolutions (Chattanooga, Tennessee, USA) has been evaluated during laboratory flume testing. These included Landloc 435, Landloc 450, Pyramat, and natural coir (coconut) fiber mat. Three of these products are shown in Figure 9. In order to compare the performance of products available from another manufacturer, three additional products manufactured by North American Green (Evansville, Indiana, USA) will be tested using identical test procedures. These ECBs and TRMs include SC250, C350, and P550. The properties of the various products being tested are summarized in Table 1. These products are anchored along the perimeter of the soil test section in the laboratory flume in accordance with the recommendations of the manufacturer.

The sediment yield for the unprotected, bare soil over a range of shear stresses is shown in Figure 10. For this cohesionless soil, the sediment yield varies linearly with bed shear stress. Figure 11 shows the substantial reduction in sediment yield that was observed when the soil test section was protected using the four different ECBs. For example, when the soil was protected with Pyramat, the mass of soil eroded was approximately 10.4 kg at a bed shear stress of 31.7 N/m^2. This was about one half of the mass of unprotected, bare soil that eroded at a bed shear stress of only 2.5 N/m^2. Thus, ECBs like Pyramat have the potential to significantly reduce the erosion of soils along Highway 50 within the project site.

Construction and Monitoring of Field Plots
Following the completion of laboratory flume studies, selected erosion control products will be evaluated further through the construction and monitoring of field plots along Highway 50. Field plots will be constructed and monitored using the methodologies developed by Mutchler *et al.* (1994). The performance of each field plot will be monitored for a period of 24 months.

It is anticipated that three to five field plots will be constructed. Various products will be evaluated for slope stabilization and channel protection. The exact location and size of the field plots will be determined in consultation with the Hydraulics Section and maintenance personnel at District II of NDOT.

CONCLUSIONS

This research will help design engineers in the Hydraulics Section at NDOT identify the most suitable and cost effective strategies for controlling erosion along U.S. Highway 50 between Carson City and Lake Tahoe. The combination of laboratory studies and field studies can expedite the selection of suitable commercially available erosion control products.

Preliminary results of the laboratory flume studies indicated that the use of erosion control blankets and mats will substantially reduce the erosion downstream from the outlets of culverts along Highway 50. Further evaluation during field-testing will help identify various products that are durable enough over time to withstand the rather harsh climate in the Sierra Nevada mountains. It is expected that the engineers in the Hydraulics Section will be able to incorporate some of the results of this research project into erosion control mitigation plans to be developed within the next 12 to 24 months.

REFERENCES

1. Bell, F.G. (1999) "Soil Erosion and Desertification", *Geological Hazards: Their Assessment, Avoidance, and Mitigation*, E and FN Spon, Routledge, New York, 390-451.
2. Bhandari, G., Sarkar, S.S., and Rao, G.V. (1998) "Erosion Control with Geosynthetics", *Geohorizon: State of the Art in Geosynthetics Technology*, edited by S.S. Sarkar, A.A. Balkema Publishers, Brookfield, Vermont, 151-169.
3. Dennett, K.E. (1995) *Flume Studies on the Erosion of Cohesive Sediments*, Ph.D. Dissertation, Georgia Institute of Technology, December 1995.
4. Dennett, K.E., Sturm, T.W., Amirtharajah, A., and Mahmood, T. (1998) "Effects of Adsorbed Natural Organic Matter on the Erosion of Kaolinite Sediments", *Water Environment Research*, Vol. 70, No. 3, May/June 1998, 268-275.
5. Dennison, M.S. (1996) *Storm Water Discharges: Regulatory Compliance and Best Management Practices*, CRC Lewis Publishers, Boca Raton, Florida.
6. Elliot, W.J., and Ward, A.D. (1995) "Soil Erosion and Control Practices", *Environmental Hydrology*, edited by A.D. Ward and W.J. Elliot, CRC Press, Boca Raton, Florida, 177-204.
7. Ffolliott, P.F., Brooks, K.N., Gregersen, H.M., and Lundgren, A.L. (1995) *Dryland Forestry: Planning and Management*, John Wiley and Sons, New York, 344-364.

8. Goldman, S.J., Jackson, K., and Bursztynsky, T.A. (1986) *Erosion and Sediment Control Handbook*, McGraw-Hill, New York.

9. Haigh, M.J. (2000) "Erosion Control: Principles and Some Technical Options", *Reclaimed Land: Erosion Control, Soils, and Ecology*, edited by M.J. Haigh, A.A. Balkema Publishers, Brookfield, Vermont, 75-110.

10. Lal, R., and Elliot, W. (1994) "Erodibility and Erosivity", *Soil Erosion Research Methods*, second edition, edited by R. Lal, Soil and Water Conservation Society and Saint Lucie Press, Delray Beach Florida, 181-208.

11. Mutchler, C.K., Murphree, C.E., and McGregor, K.C. (1994) "Laboratory and Field Plots for Erosion Research", *Soil Erosion Research Methods*, second edition, edited by R. Lal, Soil and Water Conservation Society and Saint Lucie Press, Delray Beach Florida, 11-37.

12. Ravisangar, V., Dennett, K.E., Sturm, T.W., and Amirtharajah, A., "Effect of Sediment pH Resuspension of Kaolinite Sediments", *Journal of Environmental Engineering*, American Society of Civil Engineers, Vol. 127, No. 6, June 2001, 531-538.

13. Rickson, R.J. (1995) "Simulated Vegetation and Geotextiles", *Slope Stabilization and Erosion Control: A Bioengineering Approach*, edited by R.P.C. Morgan and R.J. Rickson, E and FN Spon, London, 95-132.

14. Roberts, B.C. (1995) *Best Management Practices for Erosion and Sediment Control*, Report No. FHWA-FLP-94-005, Federal Highway Administration, Washington, D.C.

Figure 1. Culvert with free discharge at top of slope

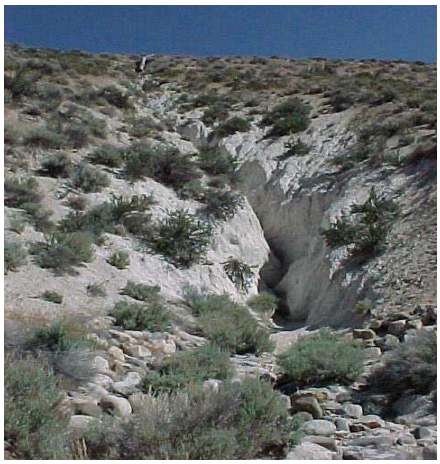

Figure 2. Gully erosion resulting from culvert with free discharge

Figure 3. Culvert with a pipe slope drain

Figure 4. Channel lined with rip rap

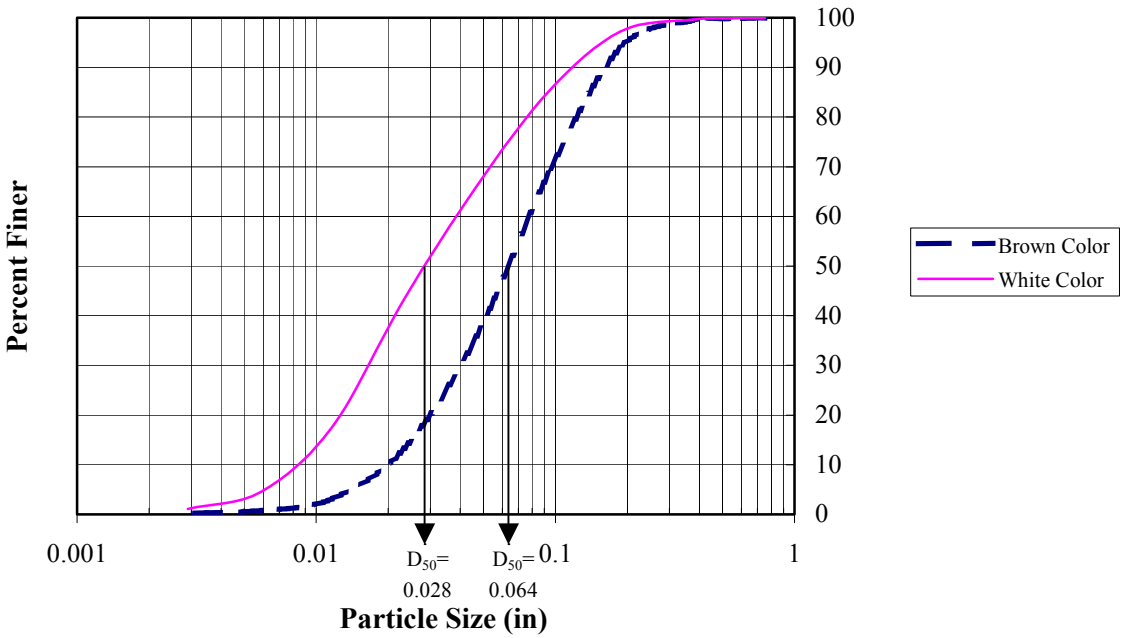

Figure 5. Gradation Curves for Test Soils

Figure 6. Typical Soil Sample

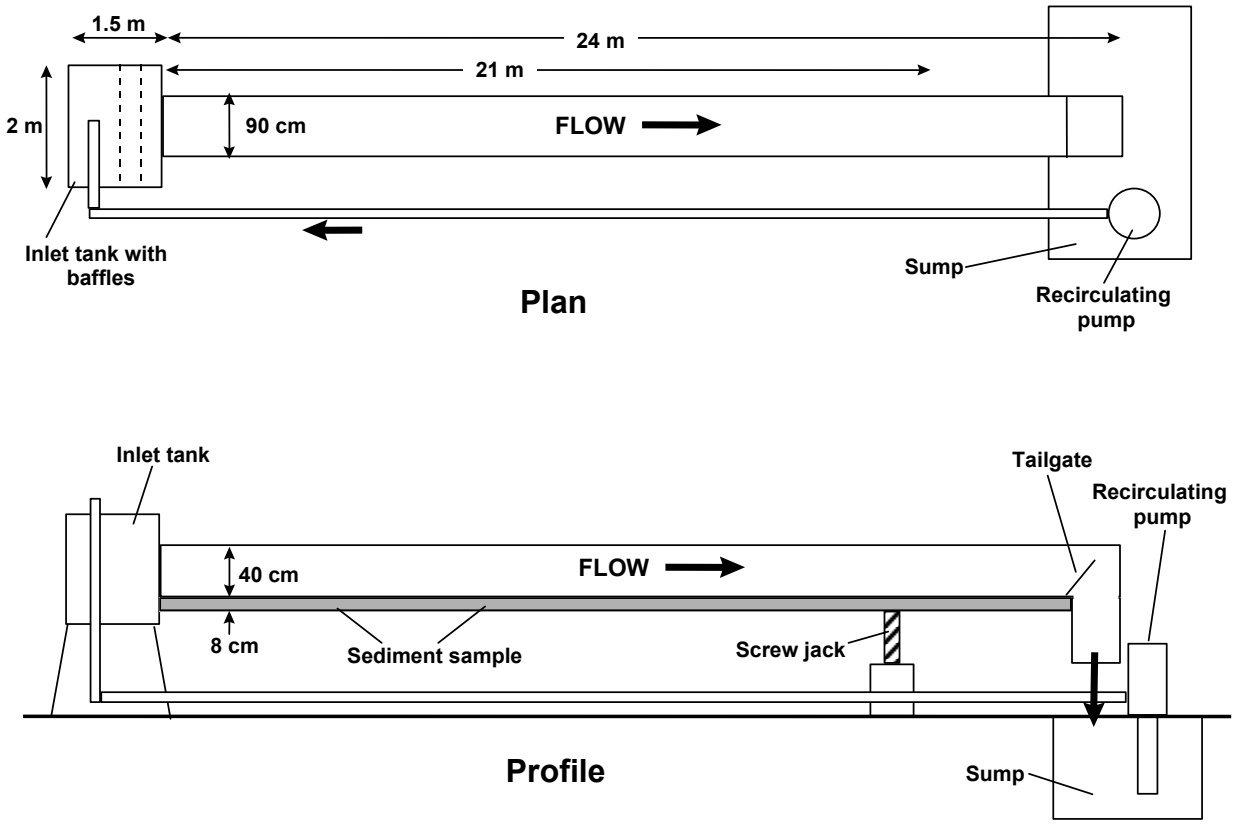

Figure 7. Plan and profile views of the laboratory flume

Figure 8. Soil Test Section within Flume

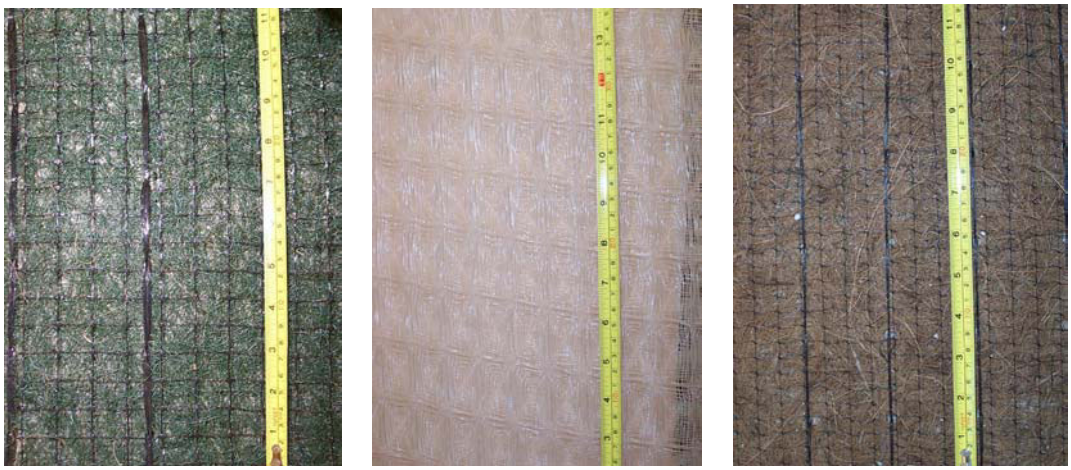

(a) **(b)** **(c)**

Figure 9. Photos of Erosion Control Blankets: (a) Landloc 435; (b) Pyramat; and (c) Coconut fiber

Table 1. Properties of Erosion Control Test Products

Product Name	Product Description	Thickness (inches)	Mass Per Unit Area (oz/yd^2)	Tensile Strength (lb/ft^2)	Velocity Rating (ft/s)	Shear Stress Rating (lb/ft^2)	Similar Product Example Company Name (Product Name)	Total Cost ($/yd^2)
SI Geosolutions, Inc., Chattanooga, Tennessee, USA								
C2	Erosion Control Blanket. For use as a channel liner with high velocity intermittent flows. Also used as an erosion control blanket on extreme slopes and very harsh sites. 100% natural coir (coconut) fiber, long lasting UV stabilized photodegradable netting on both sides.	0.30	10.5	150 x 150	6	2	North American Green (C125 & C350); PPS Packaging (XCEL Coconut CC4) American Excelsior (CURLEX III HV) Maccafer RI Gabions (BIOMAC C) Erosion Control Systems (High Impact Excelsior) Greenfix (CFO72 RR)	3.61
CS2	Erosion Control Blanket. Suitable for slopes with heavy runoff conditions where protection is needed for 2 to 4 years. Made from 70% wheat straw and 30% coir fiber. CS2 has a lightweight photodegradable netting on both sides, and long lasting UV stabilized, photodegradable netting on the topside.	0.40	8.7	100 x 100	6	2	North American Green (SC 150) PPS Packaging (XCEL Coconut/Straw C53) American Excelsior (CURLEX III) Maccafer RI Gabions (BIOMAC S/C) Greenfix (CFO72 R)	4.00
Landlok TRM 435	Turf Reinforcement Mat. For use on slopes and channels. Composed of a three dimensional web of green polyolefin fibers bonded between two nets. Considered non-biodegradable.	0.35	8	145 x 110	16	5	North American Green (C 350) PPS Packaging (PERMAMAT 200F) Mirafi (MIRAMAT TM8) AKZO Colbond (ENKAMAT 7020) TENAX (MULTIMAT 100) Greenfix (CFO72 RP)	6.70
Landmark TRM 450	Turf Reinforcement Mat. Thicker design than the LL 435. For use on slopes and channels. Composed of a three dimensional web of green polyolefin fibers bonded between two nets. Considered non-biodegradable.	0.50	10	170 x 130	18	7	North American Green 300) Mirafi (MIRAMAT 1800) AKZO Colbond (ENKAMAT 7220) Tensar (TB 1000) Contech (C-45)	7.60
PYRAMAT	For use on steep slopes, water containment structures and high flow channels. Composed of polypropylene monofilament yarns woven in a configuration of pyramid-like projections. Considered non-biodegradable.	0.50	14	3200 x 2200	20	8	AKZO Colbond (ENKAMAT S-20) Maccafer RI Gabions (MACMAT R-8)	13.50
North American Green, Inc., Evansville, Indiana, USA								
SC250	Composite turf reinforcement mat. Machine produced mat consisting of 70% straw and 30% coconut fiber matrix. Incorporated into a permanent three-dimensional netting structure. Designed for medium to high flow channels with slopes of 1:1 and greater.	0.73	16.21	700 x 500	9.5	3		5.65
P550	Composite turf reinforcement mat. Machine produced mat consisting of 100% UV stabilized polypropylene fiber matrix. Incorporated into a permanent three-dimensional netting structure. Designed for extremely high flow channels with a slope of 1:1 and greater.	0.76	20.28	1500 x 1300	12.5	3.5		8.65

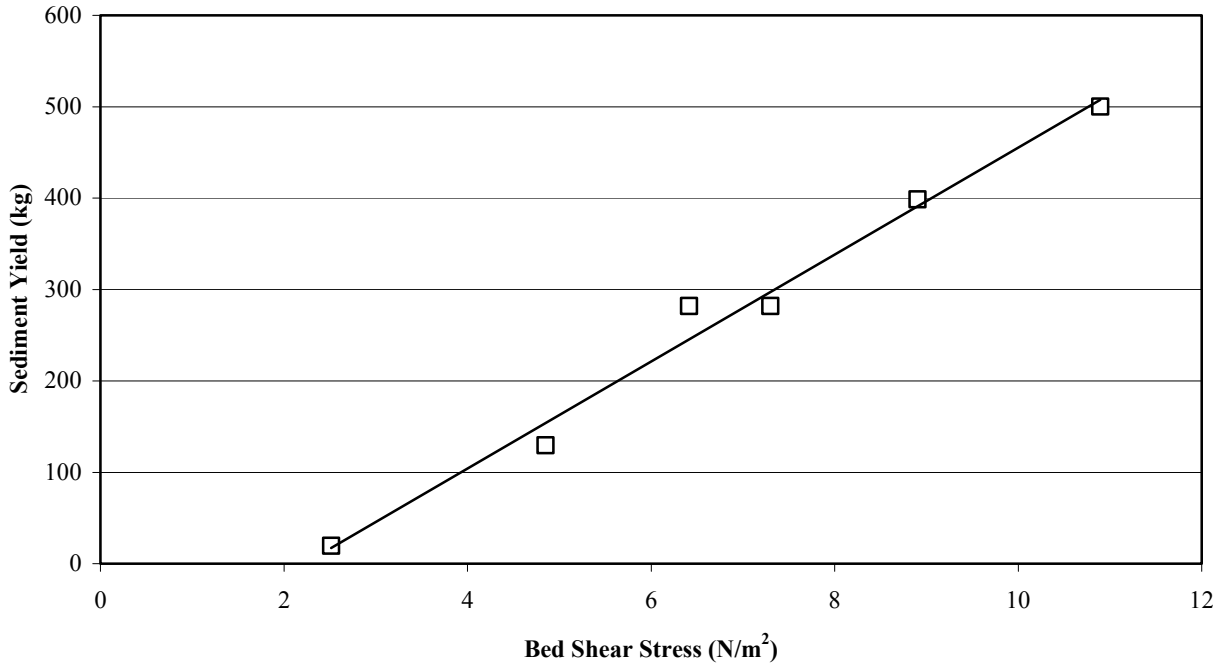

Figure 10. Variation in Mass of Bare Soil Eroded with Bed Shear Stress

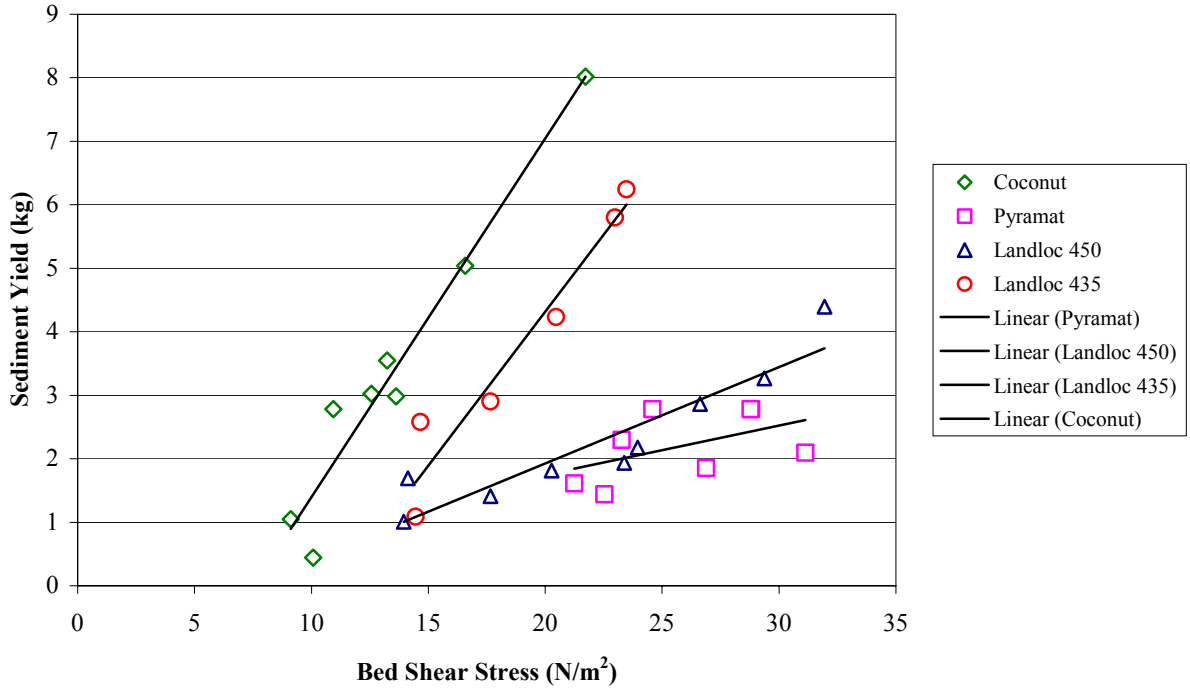

Figure 11. Variation of Mass of Soil Eroded with Bed Shear Stress for Four Erosion Control Blankets

Optimisation of Scour Protection Measures

By

G.B.H. Spaan[1], M.H. Lindo[2], G. Kant[3]

ABSTRACT

For most construction works, the final design of scour protection measures focuses on finding a balance between the extent and impact of possible damage (scour hole development and subsequent construction damage) and the costs of the required scour protection measures. In this paper the basic questions are discussed which all scour protection designers have to deal with: Which rock size and scour protection layer thickness is required to guarantee the stability of the main structure and what is the required horizontal extent of the scour protection? This extent of the scour protection determines the total protected area and is thus a significant part of the total cost calculations.

Several, principally different, solutions are discussed from a practical (installation contractors) perspective:

1. Conventional design approach: based on the provision of a hydraulic and geo-technical statically stable scour protection;
2. Falling apron principle: erosion is permitted to the extremities of the scour protection, resulting in a reduction of the area covered by the scour protection;
3. Dynamic design approach: scour hole development both in and behind the scour protection is permitted whilst the primary function of the scour protection, which is to guarantee the geo-technical stability of the structure, is still maintained.

Three examples from practice are given: two offshore gravity based structures and a storm surge barrier. Based on these examples some recommendations regarding design, execution and operational aspects are discussed.

INTRODUCTION

It is well-known that when a structure is placed in a marine environment, the very presence of the structure will change the existing wave and current induced flow patterns leading to the development of complex phenomenon such as flow contraction, horseshoe vortex formation, lee-wake vortices, generation of turbulence and adaptation of possible waves. These structure-induced changes will usually cause an increase in local sediment transport capacity. When the seabed consists of transportable sediment the flow

[1] Marine Engineer, Engineering Department, Van Oord ACZ Marine and Dredging Contractors, Gorinchem, The Netherlands (gspaan@voacz.com).
[2] Head Engineering Department, Van Oord ACZ Marine and Dredging Contractors, Gorinchem, The Netherlands.
[3] Senior Advisor Harbour and Offshore Technology, Marine, Coastal, and Industrial Infrastructure Department, WL | Delft Hydraulics, Delft, The Netherlands.

pattern changes may lead to scour which, in turn, might be a direct threat for the geo-technical stability of the structure and should therefore be prevented or controlled. Most structure designs take account of some limited scour, however the changes in flow patterns are usually such that specific scour protection measures around the structure are required.

Due to the complex three-dimensional situation the design of such a scour protection is usually not straightforward. In general the scour protection design can be divided into the following issues:

1. Required armour grading stable under survival (design) conditions;
2. Required filter grading (if necessary);
3. Layer thickness, derived from the grading requirements;
4. Horizontal extent of the scour protection.

Based on physical scale model experiments, various semi-empirical relations have been derived which describe the progression of the scouring process with time and estimate the ultimate equilibrium scour depth around a marine structure under the local environmental conditions. During the extensive research for the Dutch Delta Works, design criteria for the horizontal extent of the scour protection were also deduced (e.g. Delft University Press, 1987).

In the Scour Manual of Hoffmans and Verheij (1997) some practical scour relations are given that designers can use to calculate the dimensions of the scour holes and subsequently determine the required scour protection measures (see Figure 1):

- Equilibrium scour depth and horizontal scour extent;
- Slope stability;
- Critical velocity and amplification factor for the local velocity.

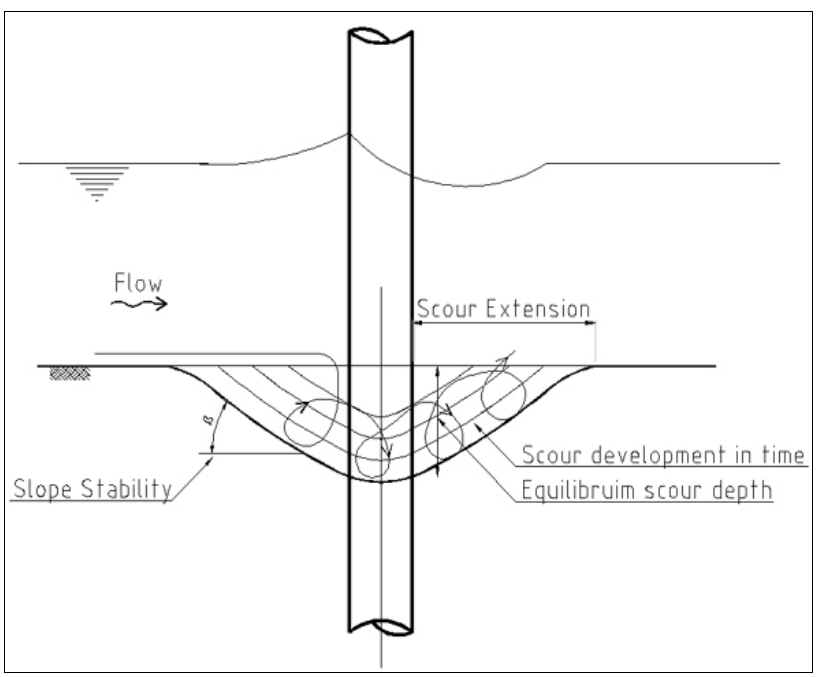

Fig. 1 – Scouring around marine structure

This paper, however, is not intended to describe these different relations. Here considerations are discussed on the incorporation of the design and ultimate construction of marine structures based on, in principle, different solutions: conventional design, falling apron and dynamically stable design.

SCOUR PROTECTION PRINCIPLES

Several in principle differing solutions have been applied in the past to prevent structure failure due to scour:

1. Conventional design;
2. Falling apron principle;
3. Dynamically stable principle.

The above scour protection solutions are described briefly in the following.

Conventional design

A conventional scour protection consists of a hydraulically and geo-technically stable scour protection of sufficient length, see Figure 2. The rock grading of the top layer must be stable under the extreme design conditions. This usually results in a heavy rock grading; depending on the environmental conditions e.g. 40-200 kg up to 6-10 tonne rock grading behind a storm surge barrier as in the Eastern Scheldt in the Netherlands. Beneath the armour layer either one or more filter layers or alternatively, and in order to reduce the number of layers, a sand tight geotextile must be applied to comply with the filter rules.

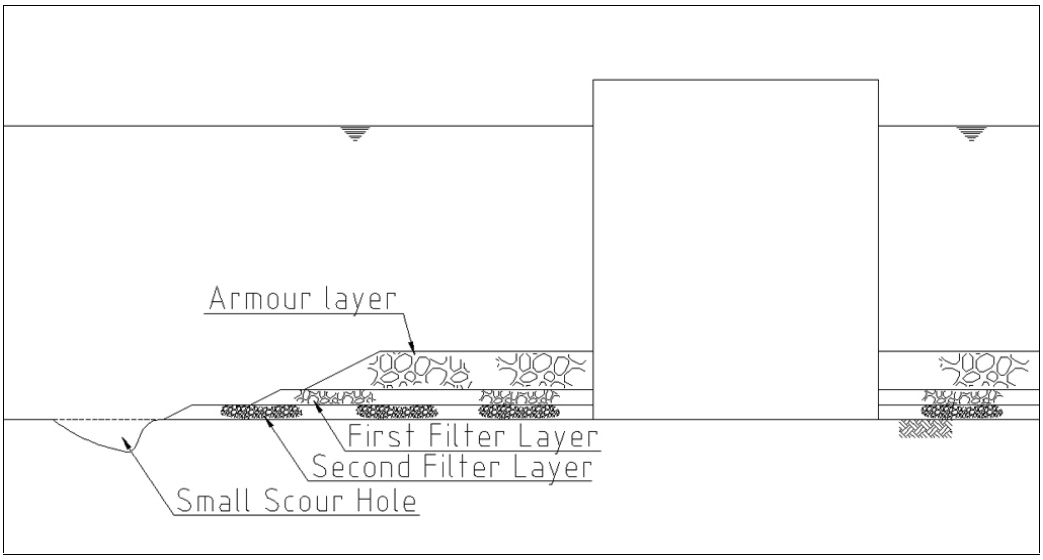

Fig. 2 – Scour protection based on conventional design

An increased turbulence occurs at the downstream side of the scour protection under the influence of the flow contraction due to the presence of the structure and because of the differences in roughness between the scour protection and the seabed. This increased turbulence subsequently introduces scouring of the seabed material at the edge of the scour protection. The resulting scour hole partly undermines the edge of the statically stable scour protection, especially when liquefaction is possible. Some of the rock will relocate thereby eventually stabilising the scour slope. The depth of the

scour hole that will form at the edge of the scour protection system as well as the resulting slope influences the partial or global geotechnical stability of the structure and must therefore stay within certain limits.

Falling apron principle

A falling apron is an amount of granular material at the toe of a revetment or around a structure. When scour starts to develop the material is redistributed onto the developing slope, see Figure 3. The loose rock material is assumed to cover the scour hole slope to a thickness large enough to retain the original bed material (Hoeven, 2002). The rock in the falling apron should be large enough to withstand the possible flow forces (Schiereck, 2001).

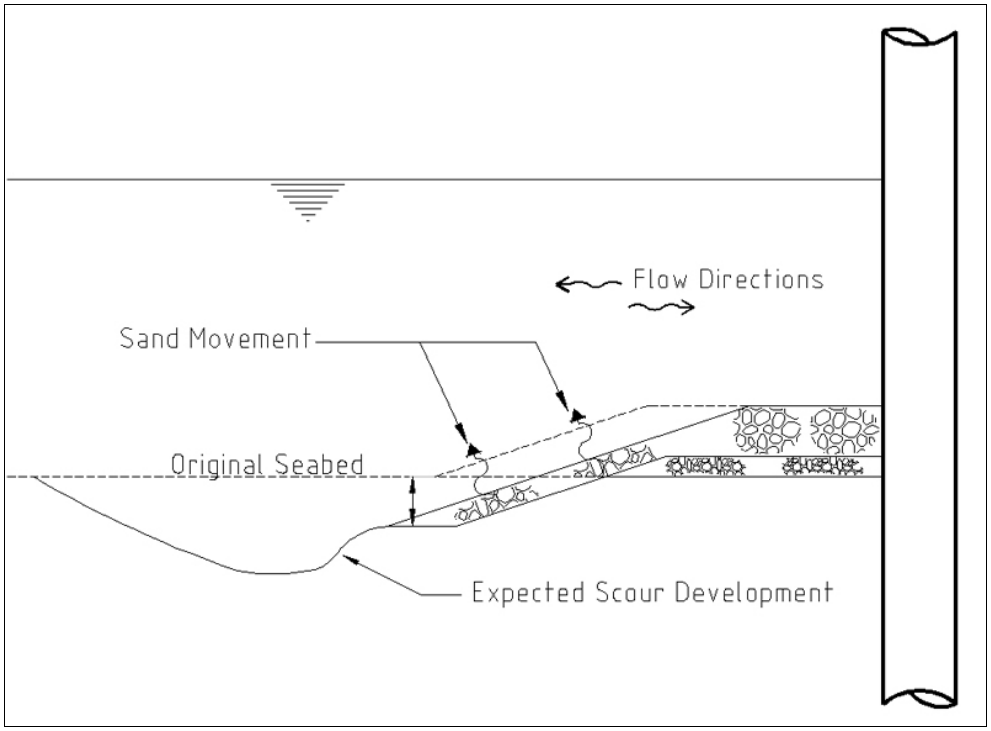

Fig. 3 – Scour protection based on falling apron principle (after several storms)

When applying the falling apron (or imperfect filter) principle the previous described scour hole development at the edge of the scour protection occurs and causes some of the scour protection to re-locate. The protective influence of the re-located rock leads to the formation of gentler scour hole slopes (WL | Delft Hydraulics, 1988). These slopes are taken into account in the geo-technical stability calculations. This will give a reduction in the required extent of the scour protection. Especially when liquefaction is a concern the falling apron will reduce the risk of undermining the structure due to the gentler slopes that will occur. Under the armour layer section one or more filter layers must still be applied satisfying the filter rules. However, under the falling apron section no filter is present. The thickness here should be around 2 to 3 times D_{50} in order to allow “controllable” migration of sand from underneath this part of the scour protection. Schiereck (2001) even recommends a layer thickness of about 5 times D_{50}. The required length of the falling apron is approximately 1.5 times the design scour depth (Hoeven, 2002). It is also possible to apply a mattress underneath the rock that provides an extra support for the rock. A

frequently applied rock grading for a falling apron is a 10-60kg grading. The rock of this grading is large enough to allow sand to pass, but is also sufficiently small to limit this process.

Dynamically stable principle

For a dynamically stable scour protection the development of limited scour (damage) in and/or behind the scour protection is permitted. The main principle is that a large amount of relatively small rock (e.g. 2-10″ rock grading) is placed around the marine structure. The scour protection is designed in such a way that the maximum expected scour hole in the rock protection is smaller than the total rock layer thickness, see Figure 4. “Dynamically” refers to the fact that scour holes will develop in the scour protection layer. “Stable” refers to the fact that eventually a practically stable situation will be reached. The advantages of this scour protection design are that (i) the construction is relatively simple, (ii) relatively small diameter rock is required and (iii) maintenance can easily be carried out by additional dumps of rock.

A dynamically stable scour protection requires regular monitoring and possible maintenance. It should be noted that for all types of scour protection regular monitoring is always recommended and in the offshore industry it is a compulsory activity.

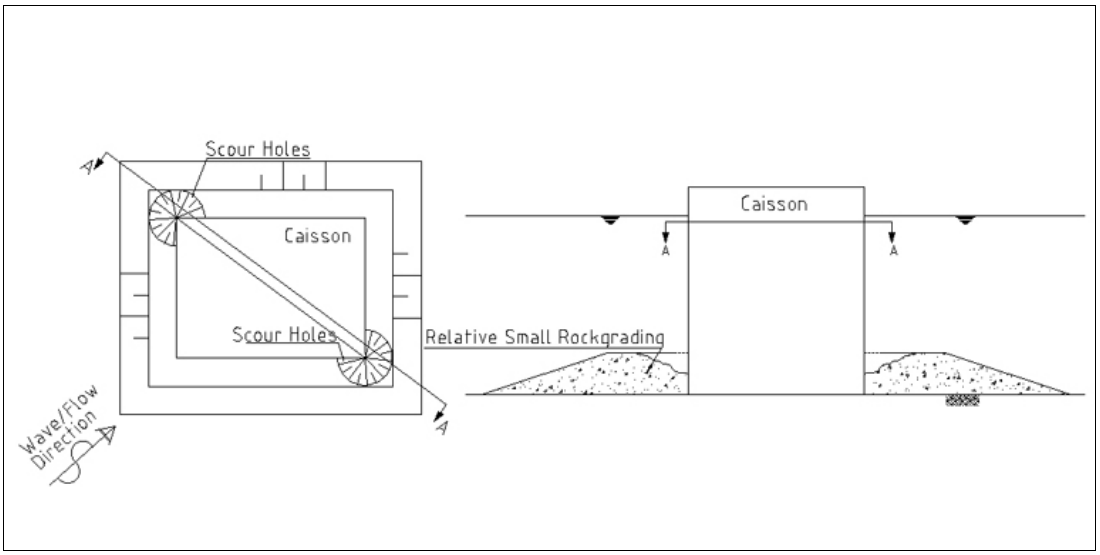

Fig. 4 – Dynamically stable scour protection

DESIGN AND CONSTRUCT PROJECT

There is a global move for large marine infrastructure works to the EPIC (Engineering, Procurement, Installation and Construction) or “Design and Build” tender approach. For this approach the Tenderer is required to perform the design activities and then to price for the construction and installation of this design. Contractors are therefore stimulated to optimise their design and generate innovative solutions taking into account their own construction tools and techniques in order to achieve a competitive price. This approach generally leads to a lower total construction cost, due to an optimal interaction

between design and practical construction possibilities, than the traditional approach whereby the Client performs the design.

OPTIMISATION EXAMPLES

In the following sections some scour protection measures are illustrated and discussed based on Van Oord ACZ and WL | Delft Hydraulics practical experience. For each example case only the items that are considered relevant for the present paper are described. The link between the examples is that, based on advanced engineering, the final design of the scour protection was more cost-effective and/or technically optimised when compared to a conventional designed scour protection due to the strong interaction between design and construction.

Offshore platform

Both Van Oord ACZ and WL | Delft Hydraulics have been involved in various projects concerning the design and installation of offshore platforms and the required scour protection around it. Two recent Van Oord ACZ projects are the installation of the Molikpaq Gravity Based Structure close to Sakhalin Island, Russia for the Sakhalin Energy Investment Company Ltd. (Marathon Oil, Mitsui, Shell and Mitsubishi) and the installation of the Malampaya Concrete Gravity Substructure in the Philippines for Shell.

The Sakhalin project comprised the towing and installation of the steel gravity structure Molikpaq (approximately 100m x 100m, height of 90m including topsides), preparation of the seabed and placement of the required scour protection. The initial scour protection design was developed by Sandwell Engineering Inc. for the Client based on standard model tests. Initiated by Van Oord ACZ the design was further optimised using model tests conducted by the Canadian Hydraulics Centre (Davies, 1999). These model tests involved positioning of a model of the platform on an erodable bed and applying the design current and storm conditions on the scaled situation.

Planning of the work was critical due to ice conditions occurring near Sakhalin Island. The towing and installation of the Molikpaq platform and scour protection was successfully carried out between August and October 1998.

The Malampaya project involved, amongst other things, the installation of a 112m x 70m and 16m high Concrete Gravity Substructure (CGS) and the required scour protection. Van Oord ACZ, together with Ove Arup and John Holland formed the Malampaya CGS Alliance. Within this alliance John Holland was responsible for the construction of the CGS, Ove Arup and Partners (1999) carried out the design of the CGS and subsequently of this scour protection while Van Oord ACZ was responsible for all offshore installation aspects, including the installation of the scour protection. The seabed preparation and installation works were carried out between March and July 2000.

Prior to the discussion of the Sakhalin and Malampaya project, a short description is given of the Flexible Fall Pipe System that was used for the scour protection construction of both projects.

Flexible Fall Pipe System

The Flexible Fall Pipe System guides the rock to a level several metres above the seabed and is therefore especially suitable for accurate dumping in deeper water (Lindo, 1991). Standard installation depths range from about 20 to 300 metres. However, this method has also been used to successfully install rock in depths of over 800 metres.

The system consists of a vessel from which a flexible pipe (strings of buckets) can be lowered until the bottom of the fall-pipe is a few meters above the sea bottom, see Figure 5. Major positioning is performed by the global positioning system of the vessel with the finer adjustment performed using the Remote Operating Vehicle (ROV) which is equipped with several thrusters. The ROV is also used as the platform for the survey equipment with which, in addition to the pre- and post-dump surveys, monitoring of the rock dump process is carried out.

The dump material is transported by means of a system of hoppers and conveyor belts into the fall pipe. While tracking along the structure of pipeline at a constant speed, the rock is placed at the required location. During dumping operations the vessel is kept in position by a dynamic positioning system. The vertical movement is controlled and restricted by a heave-compensating system.

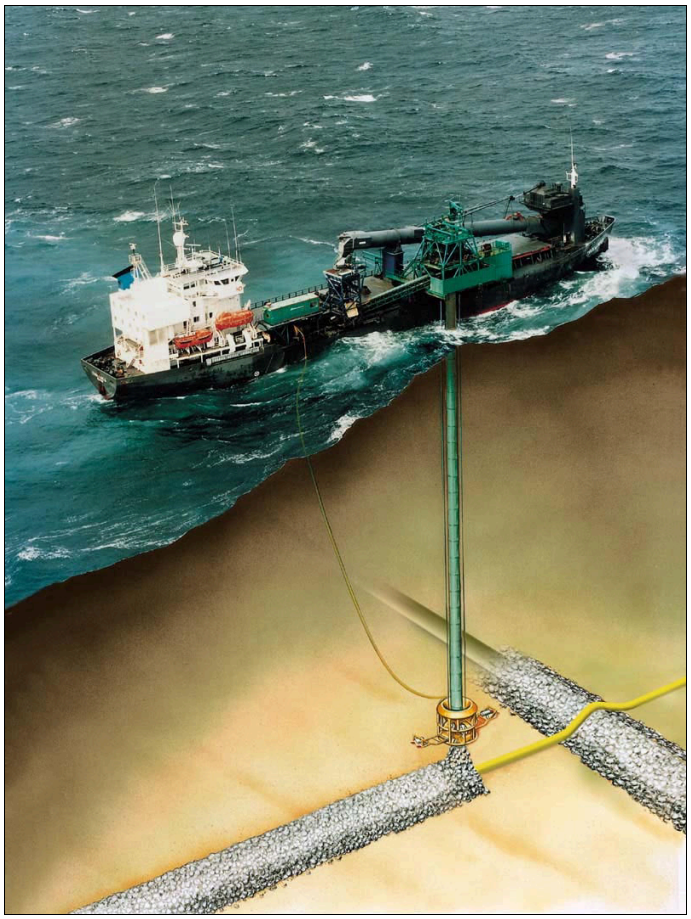

Fig. 5 – Flexible Fall Pipe Vessel "*Trollnes*"

Sakhalin

Boundary conditions

The water depth at the Sakhalin platform was approximately 30m. The scour protection for this platform had to be resistant with minimal damage to an extended duration annual storm with H_s=6m and a crosscurrent of 1.0m/s. The design conditions (return period of 100 years) were H_s=9.8m and a crosscurrent of 1.5m/s (Hollowell, 1999).

Armour layer

The scour protection for the Sakhalin Molikpaq platform was tested at the Canadian Hydraulics Centre at 1:70 scale. As installation was foreseen using Van Oord ACZ's flexible fall pipe system, the rock grading was pre-specified, resulting in a maximum grading of 60-400kg (with D_{100}<600mm). The model tests indicated that a 1.5m thick armour layer thick on top of a (closed) filter of 10-100mm would be adequate.

Horizontal extent

In front of the armour layer for the Sakhalin Molikpaq platform an 8m (4m along the sides) wide falling apron was designed to control erosion of the scour protection toe (open filter layer 60-200mm). The horizontal extent of the armour layer in the more exposed eastern corners was 9m, in the western corners this was only 6m. Along the sides of the platform the extent of the armour layer was limited to only 3m.

From the model tests it was found that the extent of the scour protection could be significantly reduced due to the shape of the Molikpaq platform, see Figure 6. The fact that the Molikpaq, being tapered over the upper 15m of the water column, created a 'wave-shadow' meant that the protection was required mostly to protect against current acceleration around the corners and sides. Protection was only required close to the structure.

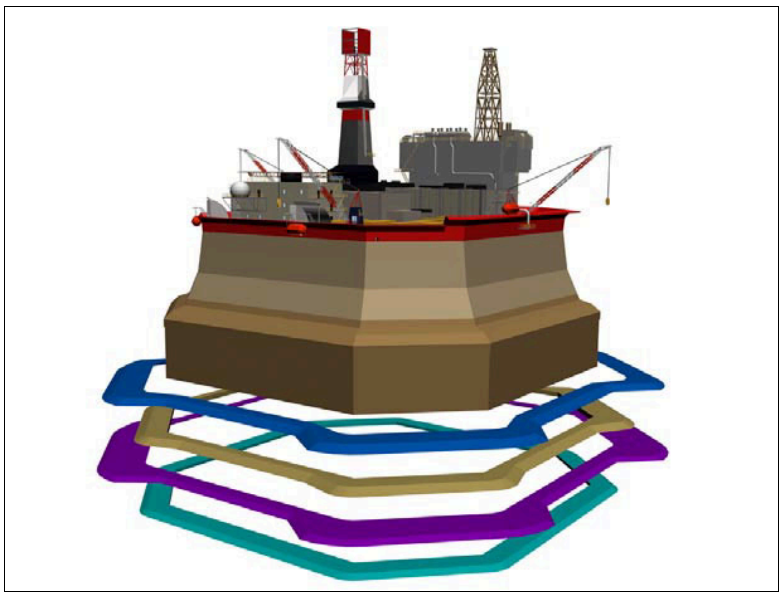

Fig. 6 – Sakhalin Molikpaq platform

The application of the 3-dimensional model tests including far-field scour effects resulted in a considerable reduction of required rock volumes of almost 40% from the conventional design volumes. The optimised scour protection design can be seen as a hybrid between the statically stable and falling apron principle.

Installation

The scour protection for the Sakhalin project was installed with the DP Flexible Fall Pipe Vessel *Rocky Giant*. Special care was taken when dumping the 60-400kg armour layer because of the ratio of fall pipe diameter versus rock size. In all, installation of the scour protection around the platform took just over 25 days.

Optimisation

The tests at the Canadian Hydraulics Centre that were undertaken for the Sakhalin project allowed the scour protection layout to be optimised with a 40% reduction in the volume of material required. The 3-dimensional model tests provided insight allowing for optimised placement of the material at those locations where scour was most severe. The adoption of a dynamically stable “sacrificial” protection layer proved to be a very cost-effective solution for a remote location such as offshore Sakhalin Island.

Malampaya

Boundary conditions

The Malampaya CGS was placed in approximately 43m water depth with a design wave height of 9.7m and an accompanying mean zero-up-crossing wave period of 8.9s (return period of 100 years). The maximum joint occurrence near-bed current velocity was estimated as 0.27m/s. On top of these a safety factor of 1.3 was applied.

Numerical computations indicated a maximum amplification at one of the corners of 2.5 times the ambient undisturbed current velocity and occurs within a narrow zone extending out-line to about 10m from the platform. The maximum amplification of the wave-induced flow is approximately 3 times the ambient and occurs approximately 2m from the corner.

Armour layer

The design of the Malampaya scour protection consisted of a light rock grading that can be considered as a dynamically stable scour protection. It was decided to install a 1m thick layer of small rock with a 2-10″ grading (maximum rock size of approximately 250mm) and with an outer slope of 1:3.

Horizontal extent

The horizontal extent of a dynamically stable scour protection and thus the total amount of rock must be large enough to ensure that the rock at the edge of the sill is stable. A structure introduces local turbulence due to the obstruction of the flow. The obstruction of the Malampaya CGS, however, is relative small because of the small height of 16m compared to the total water

depth of 43m. Based on the numerical studies, a required scour protection extent was determined of 6m (perpendicular to the walls) of the CGS within 15m of the corners (parallel to the walls).

Installation

With Van Oord ACZ DP Flexible Fall Pipe Vessel *Rocky Giant* approximately 24,000 tonnes of rock was dumped to level the Malampaya seabed (D_{50}=18mm, average height of 1.4m). Directly after complete installation of the CGS the *Rocky Giant* placed the 3,000 tonnes crushed rock scour protection (2-10″ grading) around the structure, see Figure 7.

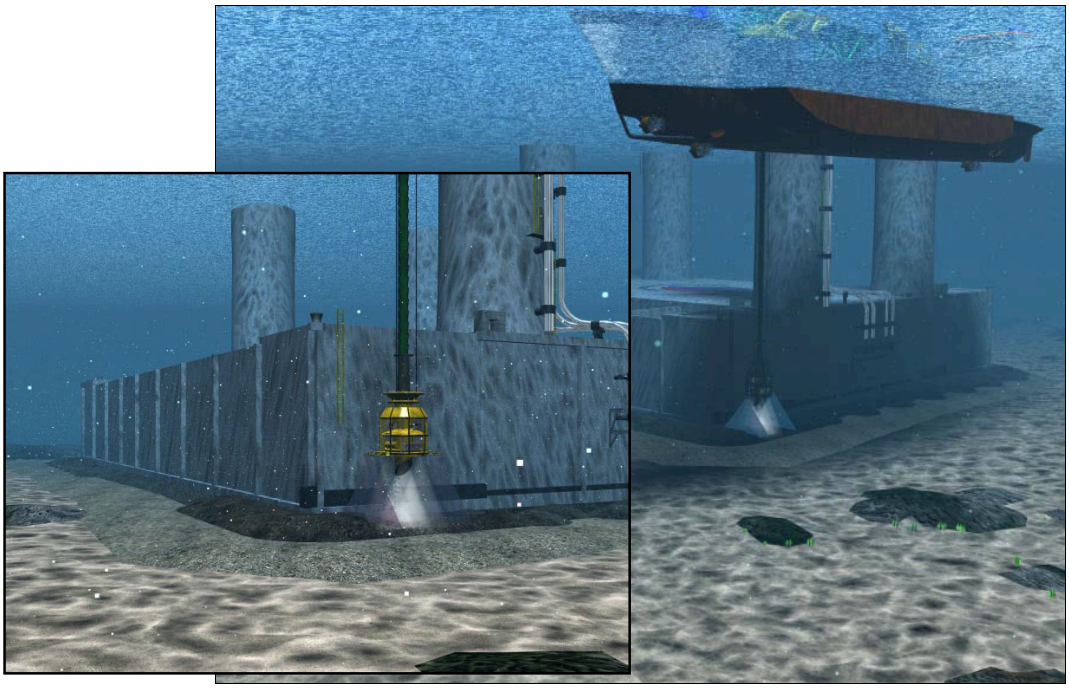

Fig. 7 – Flexible Fall Pipe Vessel dumping crushed rock around Malampaya CGS

Optimisation

The application of a dynamically stable scour protection instead of a conventional statically stable protection causes a significant reduction in installation costs. Application of heavy rock grading in marine conditions and very close to the structure is time-consuming and thus expensive. Small rock gradings can be placed accurately by means of flexible fall pipe vessels.

Storm surge barrier

In a detailed study for the design and construct project for the storm surge barrier in the "*Nieuwe Waterweg*", the entrance to the Port of Rotterdam, The Netherlands, Van Oord ACZ (as part of the so-called NIWAS combination of contractors) developed a new methodology for the design of the bottom protection. WL | Delft Hydraulics carried out various physical model test studies (1989) on, among other things, the stability of the NIWAS storm surge barrier bottom protection and the scouring behind it.

Although another concept than the one put forward by NIWAS for the barrier (and thus a different bottom protection) was finally selected, a similar

(probabilistic) methodology was used for the final design of the ultimate bottom protection.

Boundary conditions

The "*Nieuwe Waterweg*" is a 17m deep shipping channel under tidal influence as well as one of the river Rhine delta outflows, see Figure 8. The stability of the scour protection must be guaranteed for an open barrier during extreme tide flow of 2.2 to 2.6m/s. The design condition, however, occurs when closing the sector doors: the rapid acceleration in the current can be considered as a concentrated jet leading to high turbulences. In the model tests measured maximum flow velocities during closing were in the order of 5 to 6m/s (when the gap between the doors is approximately 40m, during flood conditions). This extreme flow velocity reduces only from approximately 50m behind the barrier.

Fig. 8 – "*Nieuwe Waterweg*", entrance to the Port of Rotterdam

Design philosophy armour layer

Based on the two and three dimensional model tests (WL | Delft Hydraulics, 1989) a damage method was established that determined the amount of armour rock that was removed from its original section. The derived formulae contained the exposure time, the nominal rock diameter, the rock density, the head difference and certain location and geometry dependent coefficients. The main advantage of the derived damage method was that in this way the damage development of the armour rock in time could be estimated. It was also possible to carry out probabilistic computations. In addition a Shields based method was used for situations without an unambiguous damage pattern. With this procedure of probabilistic and deterministic computations the effects on the bottom protection of various different scenarios and strategies could be simulated, without having to carry out additional model tests.

Horizontal extent and falling apron

Based on the model tests, flow influenced factors for scour hole development were determined at various locations. Based on these the required horizontal extent of scour protection in the centre of the "*Nieuwe Waterweg*" was estimated for the riverside extent as 110m.

The model tests on scouring indicated furthermore that the application of a falling apron (or imperfect filter) at the edge of the scour protection parallel to the flow direction, had a significant reducing effect on the start slope and the eventual maximum scour depth (about 20 to 40%). Furthermore the deepest point of the scour hole was located further from the scour protection at approximately 25m from the edge. This principle was therefore applied along the caissons on both river-shores with a width of approximately 25m.

Filter layer

Due to the foundation construction works it was not possible to apply a geotextile or other mattresses in the vicinity of the barrier. Here a geometric closed filter (granular filter) was designed.

Optimisation

Due to the physical model tests and the derived damage method various different scenarios and strategies could be taken into account to design an optimal scour protection. The application of a falling apron in the areas with parallel flow gave a further reduction is required armour rock.

Figure 9 gives an overview of the NIWAS designed scour protection of the storm surge barrier in the "*Nieuwe Waterweg*".

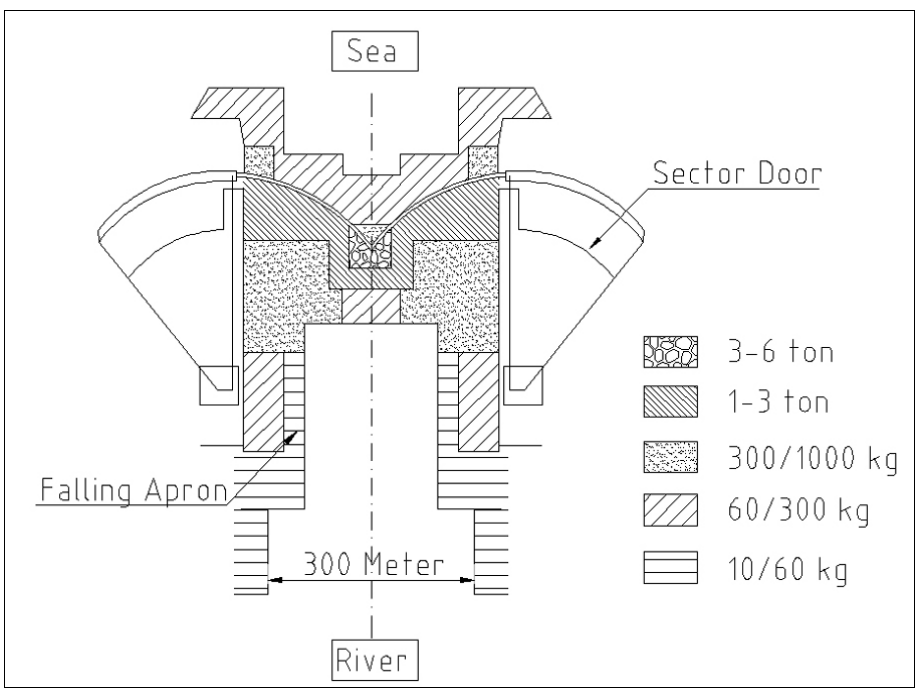

Fig. 9 – NIWAS scour protection

SUMMARY AND CONCLUSIONS

The global tendency that tenders for large marine infrastructure works must comprise both the final design as well as the ultimate construction and installation of the structures usually results in a decrease of the total construction costs, due to an optimal interaction between design and practical construction possibilities. In this paper practical examples have been described and discussed in support of this central idea.

Based on the given examples it is clear that the design of scour protection systems is not straightforward. Important factors are of course the local soil and hydraulic conditions and the structural dimensions. However, in order to achieve a competitive price the Installation Contractor must propose innovative design solutions. Although, in principle, innovative solutions can not be generalised, the following can be concluded from the given examples:

- A conventional design with a statically stable armour layer and normally designed filter layers is usually expensive;
- By applying the falling apron principle the required extent of the scour protection can be reduced significantly, especially when the soil is sensitive to liquefaction;
- A dynamically stable scour protection, combined with an adequate monitoring program can result in a cost-effective and feasible solution;
- Physical model tests are essential in the design of the scour protection: from these tests critical unexpected aspects can be identified but also cost-reducing elements might come out. Also, based on the model tests relations can be derived to study the effects of various scenarios and strategies.

REFERENCES

1. Davies, M.H., Canadian Hydraulics Centre, J.S. Readshaw, Sandwell Engineering Inc., M.A. Sullivan, Institute for Marine Dynamics, and H.C. Wells, 1999, Marathon Upstream Sakhalin Services, Model Testing in Support of Molikpaq Deployment at Sakhalin, OTC 10817, Offshore Technology Conference, Houston, U.S.A.
2. Delft University Press, 1987, The Closure of Tidal Basins, Closing of Estuaries, Tidal Inlets and Dike breaches, Delft, The Netherlands.
3. Hoeven, M.A. van der, 2002, Behaviour of a falling apron, Final Report, Thesis study Delft University of Technology, Delft, The Netherlands.
4. Hoffmans G.J.C.M., Verheij H.J., 1997, Scour Manual, A.A. Balkema, Rotterdam, Netherlands;
5. Hollowell, J.A., Sakhalin Energy Investment Company Ltd. And T. Gijzel, W. op den Velde, Van Oord ACZ, Installation of the Vityaz Production Complex, OTC 10820, Offshore Technology Conference, Houston, U.S.A., 1999.
6. Kok, M.B.A.M., 1989a, Evaluation of the bottom protection for the storm surge barrier in the New Waterway (in Dutch), MSc thesis, Delft, The Netherlands;

7. Kok, M.B.A.M., 1989b, Evaluation of model tests NIWAS damage method (in Dutch), MSc thesis, Delft, The Netherlands;
8. NIWAS, 1989, Design storm surge barrier in the New Waterway (in Dutch), Utrecht, The Netherlands;
9. Ove Arup and Partners, 1999, Malampaya Concrete Gravity Substructure, Scour Protection Design Report, London, United Kingdom;
10. Lindo, M.H., Van Oord ACZ, 1991, Design and Construction of Rock Protection Works for Submarine Pipelines and Offshore Structures, Paper of regional seminar on coastal and offshore engineering, Kuala Terengganu, Malaysia;
11. Schiereck, G.J., 2001, Introduction to bed, bank and shore protection, Delft University Press, Delft, The Netherlands.
12. WL | Delft Hydraulics, 1988, Behaviour of a bottom protection outline under the influence of parallel and perpendicular flow (in Dutch), Delft, The Netherlands;
13. WL | Delft Hydraulics, 1989a, Storm surge barrier New Waterway, Part II, Flow pattern and stability of the bottom protection (in Dutch), Report on model tests, Carried out for NIWAS, Delft, Netherlands;
14. WL | Delft Hydraulics, 1989b, Storm surge barrier New Waterway, Part III, Scouring behind bottom protection (in Dutch), Report on model tests, Carried out for NIWAS, Delft, Netherlands.

Design and Construction of Bridge Scour Countermeasures on the Salt River, Phoenix, Arizona

By

Dennis L. Richards[1]

ABSTRACT

The U.S. Army Corps of Engineers, the City of Phoenix, Arizona, and the Maricopa County Flood Control District are working together on a habitat restoration project for a reach of the Salt River within the City of Phoenix. The project includes construction of a low-flow channel that follows the historic alignment of flows of the Salt River channel. The constructed low-flow channel is as much as 61 meters (200 feet) wide and up to 3.66 meters (12 feet) below the pre-project channel invert. There are five highway bridges that span this reach of the Salt River. One of these bridges is founded on spread footings with the top of the footings 4.6 to 6.1 meters (15 to 20 feet) below the pre-project channel invert. Another bridge is founded on steel pile footings, approximately 12.2 meters (40 feet) below the pre-project channel invert.

Both hydraulic and structural countermeasures were evaluated for the two bridges. Hydraulic countermeasures included a bed armoring alternative and two local scour armoring alternatives. The recommended alternative at both bridges was a roller compacted concrete (RCC) apron located within the low-flow channel with a RCC grade-control structure at the downstream end of the apron. The RCC apron provided a higher level of protection than either of the local armoring alternatives. The paper discusses the alternatives evaluated, factors considered in selecting the RCC apron alternative, and the cost of the selected alternative.

INTRODUCTION

The Los Angeles District of the Corps of Engineers, the City of Phoenix, Arizona, and the Flood Control District of Maricopa County are partners in a habitat restoration project known as the Phoenix Rio Salado Habitat Restoration Project. The Rio Salado Project is located within the banks of the Salt River plus a 15.25 meter (50 ft) wide area at the top of each bank. The project begins immediately downstream of Interstate 10 (I-10) and extends west to 19th Avenue, a distance of approximately 8.85 kilometers (5.5 miles).

[1] Vice President, WEST Consultants, Tempe, Arizona 85282, (drichards@westconsultants.com)

The Rio Salado project will include a low flow channel constructed in the bottom of the present river; habitat elements including riparian tree species, volunteer riparian grasses and shrubs, open water ponds, and a small flowing stream; wells and a water delivery system to bring water to the trees and other vegetation, wetlands, ponds, and the stream; and recreation and interpretive trail system. A key feature of the project is the low flow channel which was designed and constructed with "soft" sides and bottom while conveying a design discharge of 345.5 cms (12,200 cfs) without significant scour or deposition. The 100-year event for this reach of the Salt River is 4,700 cms (166,000 cfs).

The low flow channel adds to the flood carrying capacity of the river through the project and balances the loss of capacity resulting from the introduction of plants and trees in the channel. This channel has a minimal footprint, thereby maximizing the area available for overbank park and recreation and habitat development. The invert of the low flow channel is 2.44 (8 ft) to 3.66 meters (12 ft) below the existing channel invert and the bottom width of the low flow channel ranges from 62.5 meters (205 ft) in the lower reach of the project to 48.8 meters (160 ft) in the upper reach (WEST, 2000). Grade control structures are included along the channel to help maintain channel stability.

BRIDGE CROSSINGS

Several major bridges cross the Salt River within the Rio Salado project reach. These bridges are located at 24th Street, 16th Street, 7th Street, Central Avenue, and 7th Avenue. In addition, there were two sand and gravel mining operation conveyor bridges located near the 11th Avenue and 19th Street alignments.

A multi-disciplinary team of hydraulic, structural, and geotechnical engineers evaluated the structures to determine if the bridges were stable for proposed project conditions. The analyses were conducted for both existing and proposed conditions using the 100-year discharge of 4,700 cms (166,000 cfs). Bridge scour was evaluated per Federal Highway Administration guidelines (FHWA, 1995). The evaluation determined that the Central Avenue Bridge and the 24th Street Bridge as well as both conveyor bridges were vulnerable to scour under proposed design conditions.

Central Avenue Bridge

The Central Avenue Bridge was constructed in 1975. It is a nine-span structure approximately 275.2 meters (903 ft) long and 24.7 meters (81 ft) wide. The structure is supported by tapered, 0.76 meter (2.5 ft) round-nose piers and spill-through abutments. Both the piers and abutments are founded on spread footings with the spread footings at elevation 307.8 meters (1010.0 ft). The channel invert elevation at the Central Avenue Bridge, prior to the construction of the Rio Salado low flow channel, was 317.3 meters (1041.1 ft).

With the Rio Salado low flow channel, the channel invert elevation at the Central Avenue bridge is 313.3 meters (1027.8 ft). The total pier scour depth for the 100-year event was estimated to be 6.95 meters (22.8 ft) resulting in a total scour elevation of 306.3 meters (1005.0 ft) or 1.5 meters (5 ft) below the bottom of the spread footings.

24th Street Bridge

The 24th Street Bridge was constructed in 1980 and is a twelve-span structure approximately 263.4 meters (864 ft) long and 24.4 meters (80 ft) wide. The structure is supported on 0.76 meter (2.5 ft) wide and 15.25 meters (50 ft) long round-nose piers with 0.91 meter (3 ft) wide and 26.2 meters (86 ft) long pier caps. Both the piers and the abutments are founded on footings with steel piles extending to elevation 313.3 meters (1028.0 ft). The channel invert at the 24th Street Bridge, prior to the construction of the Rio Salado low flow channel, was 325.8 (1069.0 ft).

For proposed conditions, the low flow channel invert is at an elevation of 323.5 meters (1061.3 ft). The total scour depth was estimated to be 7.13 meters (23.4 ft) resulting in a total scour elevation of 316.35 meters (1037.9 ft). The bottom of the 24th Street footings are at elevation 320.45 meters (1051.3 ft) resulting in scour of 4.1 meters (13.4 ft) below the footings for the 100-year event.

Conveyor Bridges

The conveyor bridge along the 11th Avenue alignment was on piles with a pile tip elevation of 313.85 meters (1029.7 ft). The total scour elevation for proposed conditions was estimated to be 311.4 meters (1021.7 ft). Although this bridge was no longer being used for sand and gravel mining operations, it was being considered as a pedestrian walkway. However, due to the cost of providing countermeasures, it was decided to dismantle the structure
.
The conveyor bridge along the 19th Street alignment was on spread footings with a bottom of footing elevation of 310.5 meters (1018.7 ft). The total scour elevation for proposed conditions was estimated to be 306.1 meters (1004.2 ft). This structure had been retrofitted following previous flood events.

Since neither of the conveyor bridges were being utilized for sand and gravel mining operations and the cost of providing countermeasures was large, the decision was to remove both structures.

COUNTERMEASURES

Both hydraulic countermeasures and structural countermeasures were evaluated for the Central Avenue Bridge and the 24th Street Bridge. Hydraulic countermeasures included a bed armoring alternative and two local scour armoring alternatives. The following paragraphs provide additional information on the countermeasures evaluated.

Bed Armoring Alternative

The bed armoring alternative evaluated was a RCC apron located within the low flow channel and extending both upstream and downstream of the bridge. The apron ties into an RCC grade-control structure located downstream of the bridge. The RCC grade-control structure extends the full width of the Salt River channel. The apron provides protection for each of the two piers located with the low flow channel as well as the first pier on each side of the low flow channel. The apron has a 3.05 meters (10 ft) toe-down on the upstream end and along both sides.

Local Armoring Alternatives

Local armoring alternatives evaluated for the Rio Salado project were an articulated concrete block (ACB's) system, and A-Jacks® concrete armor units. The ACB system consisted of preformed concrete units held together by cables to form a continuous blanket or mat with filter fabric placed beneath the mat. The ACB's were to be placed in the immediate vicinity of the piers to armor the bed and thereby prevent or minimize local pier scour. The dimensions for the armor mat were based on guidelines provided in the Federal Highway Administration's Hydraulic Engineering Circular No. 23, "Bridge Scour and Stream Instability Countermeasures." (FHWA, 1997)

The second local armoring alternative evaluated was the A-Jacks concrete armor units system. These units consisted of an interlocking system around the piers to provide protection against high-velocity flows and thereby minimize local scour. The system was to be constructed onsite in the dry and banded together in clusters around the pier, after suitable bedding layers had been placed.

Structural Alternative

At the Central Avenue Bridge, the structural countermeasure evaluated was concrete jacketing around the spread footing with additional drilled shafts located outside the existing footing. For the 24th Street Bridge, placement of concrete around the piles was evaluated. Both of these structural alternatives required extensive excavation at the footing and would have been expensive to complete due to the extensive construction requirements beneath the existing structures.

SELECTED ALTERNATIVE

The selected alternative for both the Central Avenue Bridge and the 24th Street Bridge was a RCC apron constructed within and immediately adjacent to the low flow channel. This alternative provides a higher level of protection than either of the local armoring alternatives. Factors considered in selecting this alternative included the durability of the system in a river system such as the Salt River where there are large quantities of gravels and cobbles transported, depth and quantity of excavation, and the ease of construction.

The RCC aprons were constructed with the top of the apron at the invert elevation of the low flow channel. The depth (thickness) of the aprons is 1.22 meters (4 ft). This depth provides a structure that exceeds the 1.5 factor of safety against uplift while allowing for some erosion of the surface of the apron. The upstream end and both sides of the apron have 3.05 meters (10 ft) deep by 2.74 meters (9 ft) wide RCC toe-downs. Figure 1 is a section view of the Central Avenue apron. The RCC mix design specified a seven day compressive strength of 13.8 Mpa (2,000 psi).

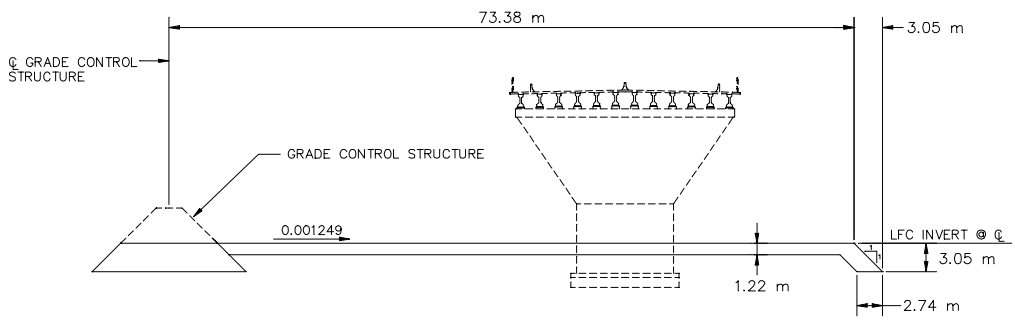

Figure 1. Section of RCC Apron along Low Flow Channel Centerline

For both the Central Avenue Bridge and the 24th Street Bridge, the apron provides protection of the two piers located within the bottom of the low flow channel as well as the first pier on each side of the low flow channel. Figure 2 shows a typical section of the Central Avenue apron. At the interface of the RCC apron with the bridge piers, a 0.10 meter (4 inches) expanded polystyrene jacket was placed around the piers. Figure 3 shows the polystyrene jacket.

At Central Avenue, the bottom width of the low flow channel is 62.5 meters (205 ft). The width of the RCC apron is 109.7 meters (360 ft) and the length is 73.5 meters (200.75 ft). Site constraints required the grade-control structure to be located a distance downstream of the bridge resulting in a longer RCC apron than originally planned. At 24th Street, the bottom width of the low flow channel is 48.8 meters (160 ft). The width of the RCC apron is 80.5 meters (264 ft) and the length is 61 meters (200 ft).

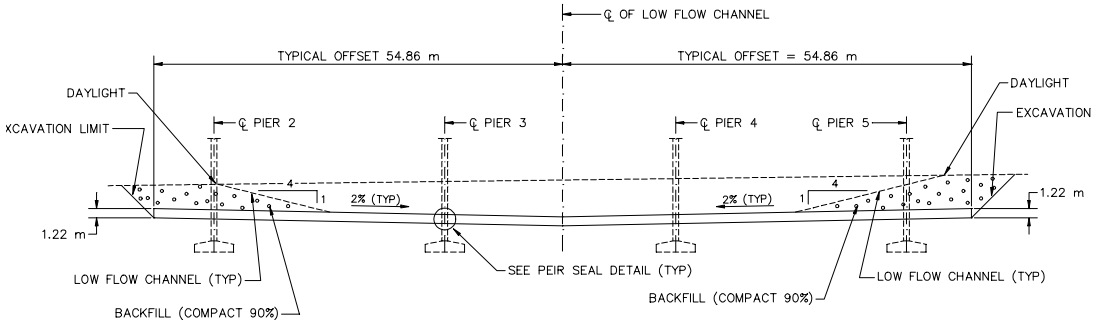

Figure 2. Typical Section of RCC Apron and Bridge Piers

Figure 3. Jacket at RCC Apron / Pier Interface

The Rio Salado Low Flow Channel was constructed in two phases. The Central Avenue structure was included in Phase I and the 24th Street structure in Phase II. The unit price of RCC was about $64.10 per cubic meter ($49 per cubic yard) for the Central Avenue structure and $75.90 per cubic meter ($58 per cubic yard) for the 24th Street structure. This unit price includes the cost for furnishing all equipment, labor, and materials (including cement and fly ash) necessary to complete the RCC structure, including dewatering, trench excavation and toe backfilling, watering, mixing, placing, and compacting.

The Central Avenue RCC grade-control structure and apron required nearly 26,760 cubic meters (35,000 cubic yards) for a total construction cost of about $1,700,000. Construction of the Central Avenue countermeasure was completed in November 2000. Figure 4 is looking downstream during construction of the RCC grade-control structure and apron.

Figure 4. Central Avenue – RCC Grade-Control Structure and Apron

The 24th Street grade-control and apron required nearly 19,880 cubic meters (26,000 cubic yards) for a total construction cost of approximately $1,500,000. Construction of the 24th Street countermeasure was completed in December 2001. Figure 5 is looking upstream at the 24th Street grade-control structure and apron.

Figure 5. 24th Street – RCC Grade-Control Structure and Apron

REFERENCES

Federal Highway Administration, 1995, "Evaluating Scour at Bridges," 3rd Edition, Hydraulic Engineering Circular No. 18, Report No. FHWA HI-96-031, November 1995.

Federal Highway Administration, 1997, "Bridge Scour and Stream Instability Countermeasures," Hydraulic Engineering Circular No. 23, Report No. FHWA HI-97-030, July 1997.

U.S. Army Corps of Engineers, Los Angles District, South Pacific Division, 1998, "Rio Salado Salt River, Arizona Feasibility Report and Environmental Impact Statement," April 1998.

WEST Consultants, Inc., 2000, "Low Flow Channel Design Analysis for Rio Salado (Salt River), Arizona," January 2000.

Treating Channel Instability at Bridges

By

Peggy A. Johnson[1]

ABSTRACT

The design of stream stabilization and naturalization projects often includes stream reaches with one or more highway crossings. A transition is needed at the intersection of the project and the bridge to pass water and sediment through the bridge opening without increasing scour or aggradation. There are a number of structures that have been used in stabilizing and naturalizing streams that can be used for this purpose. Each of the structures have a variety of applications and limitations as well as numerous sources of uncertainties.

INTRODUCTION

Projects to stabilize and naturalize streams disturbed by highway construction, urban development, and channel modifications, such as straightening and dredging, are being implemented in many areas across the country. It is common for streams to intersect one or more roadways in a given project reach, particularly in urban settings. Therefore, it is critical to the success of the stabilization project as well as the safety of the bridge, that the intersection of the roadway and stream be appropriately incorporated into the design.

At the intersection of road crossings and stream projects, the design of the channel project must often be disrupted so that all or part of the flow returns to the channel or near channel, depending on the configuration of the bridge approaches and abutments. Thus, a transition is needed that: (1) conveys flood flows up to the design flood for the bridge, (2) conveys sediment flow without causing additional scour at the bridge piers and abutments, and (3) does not produce aggradation beneath the bridge. Ideally, the transition should provide a more effective conveyance channel that actually promotes water and sediment flow through the bridge opening. Several methods for achieving such transitions are described in this paper.

FLOW ALIGNMENT MEASURES

Flow alignment devices were originally developed to divert high shear stresses away from channel banks to prevent channel migration and bank widening. More recently, some of these measures have been tested or used to alleviate problems at bridges due to local and contraction scour. These measures include submerged (Iowa) vanes, bendway weirs, guidebanks, rock vanes, cross vanes, and w-weirs.

Small isolated submerged vanes, known as Iowa vanes, have been used for many years to deflect flows and sediment to control spiral flow in bends and erosion at banks. The ability of

---

[1]Associate Prof., Dept. of Civil and Environmental Engrg., Pennsylvania State University, University Park, PA 16803. Phone: 814-867-4844; E-mail: paj6@psu.edu

submerged (Iowa) vanes to reduce scour at bridge piers was recently tested at the University of Auckland (Lauchlan, 1999). They found that the vanes could reduce scour at the pier by up to 50 percent. A variety of experimental studies (Odgaard and Kennedy, 1983; Odgaard and Lee, 1984; Odgaard and Mosconi, 1987) have yielded the following guidance in the design of these types of vanes.

- Submerged vanes are effective over a wide range of flow depths from two to eight times the vane height.
- The ratio of the vane height to flow depth should be between 0.2 and 0.5 at the erosion-causing or design flow rates.
- The length should be about three to four times the vane height with an optimum angle of about 20° from the primary direction of flow.
- Lateral spacing of the vanes should be less than about twice the flow depth.
- Vanes are typically constructed from sheet pile or reinforced concrete founded on adequately deep pilings, but could also be made of large rocks or wood with footers of adequate depth to resist erosional forces.

Bendway weirs are low elevation stone sills, very similar to vanes, used to improve lateral stream stability and flow alignment problems (Lagasse et al., 1997). Bendway weirs are typically not visible at bankfull flow. They redirect flow by causing the flow to pass perpendicularly over the weir. They are made from stone, tree trunks, or grout filled bags. Based on HEC-23 (Lagasse et al., 1997), a brief summary of design guidelines is given.

- The weir height should be 30 to 50 percent of the flow depth at the mean annual high water level.
- The angle from the upstream bank tangent line to the centerline of the weir should be about 50 to 85 degrees (this high angle is due to the placement of the weirs at channel bends).
- The length should not exceed one-third the mean channel width, with typical values between one-tenth and one-fourth of the channel width.
- Spacing of the weirs is dependent on the channel radius of curvature, weir length, and channel width.
- The top width of the weir should be two to three times the diameter of the largest of the rocks used to construct the weir.
- At least three weirs are used to direct flow around a bend.

Guidebanks can be used when embankments encroach on wide flood plains. They provide a smooth transition of flow though bridge openings, and thus, reduce turbulence and move scour away from the abutments (Lagasse et al., 1997). Guidebanks are constructed from earthen materials, then covered with riprap to resist erosion. The height and length of a guidebank is a function of the design discharge. The top of the guidebank must be at least at the elevation of the flow depth associated with the design discharge (i.e., the bridge capacity). Overtopping of the guidebanks should be avoided to reduce the possibility of high shear stresses in undesirable locations behind the guidebanks.

Rock vanes, cross vanes, and w-weirs are stream restoration structures promoted by Rosgen (1996) to improve lateral stability and flow alignment and, in the cases of cross vanes and w-weirs, provide some grade control on degrading beds. Like bendway weirs, these structures tend to be very effective in flow depths up to about five times their height. They were recently tested in a laboratory flume to assess their ability to move scour away from pier and abutment

foundations, thereby reducing scour at bridges (Johnson et al., 2001a; Johnson et al., 2001b). Both a single span and a double span bridge were modeled for testing vanes and cross vanes at an abutment of a single span bridge and w-weirs at a bridge pier. The results showed that scour at the pier or abutment was generally reduced on the order of 65 to 90 percent, depending on flow conditions and the structure configuration. The scour was moved away from the abutment or pier into the center of the channel. These structures have not yet been systematically tested in the field and were tested in the laboratory for only two types of bridges; however, preliminary design criteria for these structures are given in Johnson et al. (2001a; 2001b) and are summarized below:

- Vanes should be orientated upstream at 30° to the bank.
- The vane should extend no more than about 1/3 of the bankfull channel width into the channel from the bank.
- At the bank, the height of the vane should be at the bankfull elevation, pitching down to the channel invert at its tip. This pitch from the horizontal should not exceed about 7.5% on low to moderate slopes less than about 0.02. On higher slopes, 0.02 up to about 0.045, a higher pitch can be used, on the order of 12-14%.
- The channel must have a width to depth ratio of at least 10.
- The vane should be placed upstream from the abutment such that $1.5W \leq d \leq 2W$, where W = channel width and d = the projected distance along the bank from the upstream corner of the abutment to the upstream tip of the vane (with $d \geq 0$).
- If a second vane is used, the spacing between the vanes should be based on the same calculation as the spacing between the bridge and the vane except that the distance will be measured from the upstream tip of the first (downstream) vane to the upstream tip of the second (upstream) vane.
- Cross vanes are designed similarly to vanes except that the connecting central portion (the center 1/3 of the channel) is placed at the channel invert.
- W-weirs are placed upstream of bridge piers such that the flow is diverted around the pier.
- At the banks, the w-weir height is at the bankfull elevation to maintain the proper horizontal pitch from the bank to the channel bed, the same as for vanes.
- At the central apex, the w-weir height is about 3/4 bankfull elevation and the two upstream apexes are at the channel invert.
- The angle at the bank should be 25° for a w-weir while the angle in the central apex should be about 40°.
- The w-weir should be placed 0.3W upstream from the pier, where W is the bankfull channel width.

APPLICABILITY AND UNCERTAINTY OF FLOW ALIGNMENT STRUCTURES

All mitigation structures have limitations and appropriate applications. Lagasse et al. (1997) provide a table summarizing the appropriate physical conditions for many of these structures. In Table 1, the applicability of each of the structures discussed in this paper for providing a transition from the stream channel through the bridge opening is given. The information in Table 1 is based on Johnson (2002), Johnson et al. (2001a), Johnson et al. (2001b), and Brown and Johnson (1999). In addition, each structure has advantages and disadvantages. For example, rock vanes, cross vanes, and w-weirs are relatively simple to design and construct and are typically constructed from inexpensive materials. However, the bank must be appropriately aligned and possibly modified to accept the vane configuration. In addition, excavation of the

channel is required for placement of a footer. Cross vanes and w-weirs can be used to control both degradation and bank erosion. The main advantage of submerged vanes over rock vanes is that the bank can be in poor alignment with the bridge abutment; the vane will gradually cause the channel to realign itself. Thus, the submerged vanes require less excavation. Also, since they are submerged, they have a minimal effect on the aesthetics of the channel. In some cases, they may even become gradually buried and vegetated as the channel realigns. Given the flexibility in the design of submerged vanes, there are few limitations in the size of the stream. Bendway weirs are also submerged much of the time and so have a minimal effect on the stream aesthetics. However, the angle of bendway weirs to the bank may be too high to provide an effective transition in some cases. Guidebanks can protect outflanking from occurring at the bridge embankments. The main disadvantage of these structures is that they are relatively large structures that may not fit into the aesthetics of the stream.

In addition to limitations, advantages, and disadvantages of each of the structures, there are several sources of uncertainty that should be considered in using any of these diversion structures at bridges. The primary sources of uncertainty, listed in order of their relative importance, are given below.

- *Lack of systematic field testing and documentation.* Most of these structures have not been systematically tested. Although some have been used widely in stabilizing streams, documentation on their effectiveness over a range of flows is minimal. Some have been tested for selected conditions in laboratory settings, but systematic field testing is mostly lacking. Thus, known successes at bridges during high flows, such as the 100-year flood, is nonexistent for most of these structures.

- *Construction experience and implementation.* The availability of skilled or experienced contractors may greatly influence the level of uncertainty. The ease of access to the site as well as the level of difficulty in working with bed and bank materials will also contribute to uncertainty in the structure's ability to provide an adequate transition and to protect the bridge against scour.

- *Design*. The level of uncertainty in design is a function of the availability of detailed design procedures, the appropriateness of the design for specific flow and channel conditions, and the experience of the designer. Although some design guidelines exist for the measures discussed here, they cannot account for all applications and conditions.

- *Detection of failure*. The ability to detect failure or impending failure of these structures ranges in difficulty in the methods that are required, such as visual observations, surveys, or real-time monitoring. Thus, uncertainty arises when the engineer or inspector is unaware of the condition of the structure during high flows and whether it is continuing to be effective in providing an adequate transition and preventing or controlling instabilities or scour at the bridge.

- *Maintenance*. The uncertainties listed above necessitate monitoring and maintenance for most of these structures. Lagasse et al. (1997) describe the maintenance of vanes as high to medium, guidebanks as medium to low, and bendway weirs as low. However, it is unclear how often and over what period monitoring and maintenance are required. For example, they

could be examined annually, following every flood, or during bridge inspections. The frequency of monitoring and a maintenance schedule that would be suitable given all of these uncertainties are unknown.

- *Estimation of hydraulic parameters.* For any of these designs, a design discharge, velocity, and flow depth must be determined. Although models exist to estimate velocity and depth given a discharge, uncertainty exists in making those estimates (Johnson, 1996).

CONCLUSIONS

Rock or submerged vanes, cross vanes, w-weirs, bendway weirs, and guidebanks can be used to create a smoother transition during high flows from the stream channel through a bridge opening. The smoother transition and the creation of depositional zones along the banks and, in the case of w-weirs, in mid-channel, can prevent undesirable scour from occurring at the bridge abutments and piers. Uncertainty in the design, implementation, maintenance, detection of failure, parameter estimation, and the lack of systematic testing leads to uncertainty in the effectiveness of these structures. These uncertainties should be carefully considered prior to design. The uncertainties can be lessened through experience and testing.

REFERENCES

Johnson, P.A. (1996). Uncertainty of hydraulic parameters. Journal of Hydraulic Engineering, ASCE, 122(2), 112-115.

Johnson, P.A. (2002). Incorporating road crossings in stream restoration projects. Ecosystem Restoration (in press).

Brown, E.R., and Johnson, P.A. (1999). Maryland's Guidelines to Waterway Construction. Maryland Department of the Environment, Baltimore, Maryland.

Johnson, P.A., Tessier, M. Hey, R.D., and Rosgen, D.L. (2001a). The use of vanes for local abutment scour reduction. Journal of Hydraulic Engineering, ASCE, 127(9), 772-779.

Johnson, P.A., Hey, R.D., Brown, E.R., and, Rosgen, D.L. (2001b). Stream restoration in the vicinity of bridges. Journal of the American Water Resources Association. (Accepted).

Lagasse, P.F., Byars, M.S., Zevenbergen, L.W., and Clopper, P.E. (1997). Bridge Scour and Stream Instability Countermeasures. FHWA Report HI-97-030, HEC-23, Federal Highway Administration, Arlington, Virginia.

Lauchlan, C.S. (1999). Pier Scour Countermeasures. University of Auckland, School of Engineering, Report No. 590, Auckland, New Zealand.

Odgaard, A.J., and Kennedy, J.F. (1983). River-bend bank protection by submerged vanes. Journal of Hydraulic Engineering, ASCE, 109(8), 1161-1173.

Odgaard, A.J., and Lee, H.Y.E. (1984). Submerged vanes for flow control and bank protection in stream. IIHR Report No. 279, Iowa Institute of Hydraulic Research, Univ. of Iowa, Iowa City, Iowa.

Odgaard, A.J., and Mosconi, C.E. (1987). Streambank protection by submerged vanes. Journal of Hydraulic Engineering, ASCE, 113(4), 520-536.

Rosgen, D.L. (1996). Applied River Morphology. Wildland Hydrology, Pagosa Spring, Colorado.

Table 1. Applicability of structures for providing transitions at road crossings (W = well suited , M = moderately well suited, N = not suitable).

Structure	Abutment Scour Protection	Pier Scour Protection	Grade Control	Contraction Scour Protection	Improve Alignment
Rock vanes	W	N	N	M	M
Submerged vanes	W	W	N	M	W
Guidebanks	M	N	N	W	N
Cross vanes	W	N	W	M	M
W-weirs	W	W	W	M	M
Bendway weirs	M	N	N	M	M

Scour Hazard Mitigation for Tick Canyon Wash Bridge

Mohammed S. Islam[1], Jinxing Zha[2], and Abbas Abghari[3]

Abstract

This paper presents the case history, with particular emphasis on the geotechnical aspects, of a bridge scour countermeasure design project in California. In addition to local, contraction and long-term degradation scour, this bridge site is susceptible to a potential head-cut of about 10 meters due to downstream aggregate mining operations. After considering a range of options, a 46-m long tieback check dam retaining wall system consisting of cast-in-place concrete panels, and supported by Cast-in-Shell-Steel soldier and anchor piles, was proposed to mitigate scour hazard at this site. Design of the proposed check dam retaining wall system was controlled mainly by geotechnical considerations including soil piping potential due to seepage forces, lateral soil and water pressures, and pile lateral capacity. Results of the analyses performed to determine the various design parameters including the minimum panel embedment depth, pile embedment depth, and lateral pile capacity by considering pile-soil-pile interaction are presented in this paper. It is shown that a simple numerical analysis method utilizing p-y soil spring model can more accurately predict the complete response of a pile supported tieback retaining wall than the conventional empirical or semi-empirical methods.

Introduction

Loss of foundation support due to scour has been the most common cause of bridge failure in the United States (Kattell and Eriksson 1998, Briaud et. al 1999). In California, about 4,700 State owned bridges crossing active rivers, streams, creeks or washes could be subjected to catastrophic failures due to scour. In response to Federal requirements, California Department of Transportation has initiated a comprehensive program to identify, evaluate and mitigate scour hazards for all the State owned bridges. More than one half of these bridges have been evaluated so far, and approximately three percent will require mitigation. Mitigation work began in 1998-99, and was to be completed in 10 years.

This paper summarizes the results of a site-specific geotechnical investigation conducted for a scour evaluation and hazard mitigation project in California. The project involved design and construction of a scour countermeasure for the Tick Canyon Bridge on Route 14 in Ventura County. An elevation view of the bridge is shown in Figure 1. This is a three-span continuous bridge supported on two end diaphragm abutments and two bents, all founded on pile foundations. The structure was built in 1963, and widened and seismically retrofitted in 1997 utilizing 610-mm diameter cast-in-place concrete piles. A detailed scour analysis (Avila, 1998) confirmed the categorization of this bridge as scour critical. Both the abutments and piers are

[1] Senior Transportation Engineer, [2]Transportation Engineer, and [3]Supervising Transportation Engineer, Office of Geotechnical Earthquake Engineering, California Department of Transportation, 5900 Folsom Boulevard, Sacramento, CA 95819, U.S.A.

supported on scour susceptible sandy alluvial soils. Aggravating the local scour hazard is the general degradation and scour of the wash bottom that has resulted from aggregate mining operations at its confluence to the Santa Clara River approximately 0.8 km downstream of the bridge. Field review indicated that the two separate grouted riprap check dams, previously constructed on the downstream side of the bridge as scour countermeasures, were severely undermined by continued erosion. A total head cut depth of about 10 m was estimated for this natural trapezoidal channel in the event of a 100-year design flood. The bridge structure was determined to be unstable for the calculated scour depth and in need of a scour countermeasure. After considering various scour mitigation measures, a tieback retaining wall consisting of cast-in-place concrete panels and supported by Cast-In-Steel-Shell (CISS) soldier and anchor piles was selected for design.

Significant geotechnical issues related to the design of the proposed check dam included lateral load capacity of the soldier and anchor piles by considering soil-structure interaction, and the effects of differential water levels on the opposite sides of the wall including seepage forces and soil piping potential. As in the cases of most California bridge sites, the geotechnical issues also included seismic hazards including fault rupture potential, ground motion, soil liquefaction and lateral spreading. Geotechnical issues during construction include excavation stability and pile driveability.

Scour Evaluation

The Tick Canyon Wash is a natural trapezoidal canal with a bottom width of about 15 m and side slope of 2:1 (H:V). The channel bottom slope at the site is about 0.012. The streambed consists of mostly sand with some gravel and cobbles, and is therefore highly susceptible to scour. The streambed remains mainly dry during most of the year with the exception of very little water within the pilot ditch in the center of the stream.

The bridge has a history of scour problems with short piles, steep streambed slope, high flow velocity and downstream gravel mining operations. It was noted in late 1970, that the channel had degraded by about 1.2m, probably due to the partial failure of a downstream check dam, and that the bridge was threatened by a mining operation in Santa Clara River about 0.8 km downstream of the bridge. To protect the bridge from scour resulting from this mining operation, two check dams were constructed about 15 m and 30 m, respectively, downstream from the bridge site. These check dams were considered essential to the stability of the channel bed. An existing earthen construction access road adjacent to the Santa Clara River also provided some protection.

The Wash drains approximately 14.8 km^2 mountainous areas with steep rocky ridges above the bridge site. A discharge of $Q_{100} = 67\ m^3/s$ was estimated for a 100-year flood by using the USGS Regional Regression equation with urbanization only in the lower basin and a mean annual precipitation of 457 mm. Water surface profiles and flow velocities were calculated by using the computer program HEC-2 (U.S. Army Corps of Engineers 1991). These profiles were extended approximately 60 m upstream and downstream of the bridge. The values of the Manning roughness coefficient "n" of 0.045 and 0.03 were chosen for the channel bank and the streambed, respectively. A water depth of 2 m at the upstream side of the bridge was calculated based on an additional 915 mm width added to each of the two bents in the waterway, and the streambed

elevation at 501.7m. The corresponding stream velocity was estimated to be 4.5 m/sec. Potential total scour (local, contraction and long term degradation) was estimated to be about 3.1 m.

Currently, the bent piles are protected by gabions. Scour hazard at abutment is not of concern since the abutments are not reachable by the 100-year flood. Recent field observations indicated that the two existing check dams were severely deteriorated. In the event of a failure of these dams, the channel would degrade rapidly and pose a significant threat to the bridge. Because of the close proximity to the Santa Clara River, the mining effect would be felt at the bridge site in the form of a head cutting (dropping of the channel bottom), and the earthen road and the deteriorated check dams could be washed out with a vertical elevation change of 10 m at the bridge. Removal of streambed material at the bridge site would reset the channel bottom elevation to about 491.9 m, essentially to pile tip elevation at the supports.

Scour Countermeasure

Potential scour countermeasures and their drawbacks are summarized in Table 1 below:

Table 1. Potential Scour Countermeasures

Countermeasure	Drawbacks
1. Install a series of engineered check dams that could accommodate the potential head-cut and scour.	A) This will necessitate going out of the State Right-of Way (ROW). B) An existing sanitary sewer between the structure and the existing first check dam will be an issue. C) Check dams will need to be inspected after significant events to ensure their structural integrity. D) Will require passive monitoring system such as "float outs"
2. Install one large check dam within or outside the ROW.	A) Check dam will be greater than 14 m in height, and would, therefore, need to be a concrete dam. The free-fall of water would be substantial. B) The existing sanitary sewer will be an issue. C) The check dam will need to be inspected after significant events to ensure their structural integrity D) Will require passive monitoring system such as "float outs"
3. Replace the bridge structure and install new piles to much greater depth to accommodate the anticipated scour and head-cut.	A) Costly. B) Both structures were just widened and seismically retrofitted in 1997.
4. Super bents with foundations deep to accommodate the projected scour and head-cut.	A) Costly. B) Placement of the bents will reduce the width of the waterway possibly causing a water way adequacy problem. C) Will not protect the abutments if potential head-cut migrates upstream.

5. Footing strengthening for both abutments and piers. This will entail installing cast-in-drilled hole piles to a depth low enough to mitigate both scour and head-cut hazards.	A) Costly. B) Construction will necessitate drilling through deck. C) Traffic control and detour will be an issue. D) Will result in long unsupported pile length.
6. Monitor the bents, the existing check dams and the earthen construction road with electronic devices (float outs).	A) This is a passive scour-monitoring alternative, and will not eliminate the potential of scour or head cutting reaching the structure.

After discussion in an inter-disciplinary meeting, a 50-m long check dam–retaining wall system shown in Figures 2 and 3, which eliminates many of the above drawbacks, was selected. The proposed check dam consisting of two rows of 914-mm diameter CISS piles and concrete panels is to be constructed on the down-stream side of the bridge. As shown in Figure 3, the front row of piles are designed as soldier piles, with a single tieback per pile, for a retaining height of 10 meters in the event of the anticipated head-cut. The back row of piles will act as anchor piles to provide additional lateral resistance to the front piles through high strength rods. Site specific-geotechnical issues related to the design and construction of the check dam-retaining wall are summarized in the following sections.

Subsurface Conditions

A subsurface exploration comprising two rotary wash borings was conducted at the site of the proposed check dam. Four exploratory borings drilled in 1994 for the bridge widening and seismic retrofit project were also reviewed as part of this investigation. These borings included measurement of the Standard Penetration Test (SPT) blow count as per ASTM Standard D1586 at a depth interval of 1.5 m. Soils were continuously logged and classified in the field during drilling in accordance with the Unified Soil Classification system. Based on this information, the subsurface profile at the site consists of a 5 to 10 m thick layer of loose to low medium dense silty sand underlain by 15 to 20 m of fine to medium-grained, dense to very dense sand with some gravel and small to large cobbles. Gravel and cobble conglomerate formation underlies the above units to the maximum explored depth of about 30 m below existing ground surface. Two interbedded thin layers of stiff sandy clay were encountered at 15 m and 24.5 m below the existing the ground surface. Groundwater was measured during the field exploration at a depth of about 25 m below the existing channel bottom. Though deep groundwater was observed at this site, seasonal surface water may form a temporary groundwater mound around the channel's watercourse and saturate the sand layers.

Seismic Hazards

The project site is located within a seismically active region of Southern California. The primary seismic hazards include ground shaking and ground rupture during earthquakes. Based on the Department's current design practice, the San Gabriel fault zone located about 8 km southwest from site is the controlling seismic source. The San Andreas Faults is located about 24 km northeast from the bridge site. Based on California Department of Mines and Geology (CDMG,

1994), this northeast-southwest trending fault is of reverse oblique type and has experienced displacements during the Holocene period. This fault is capable of generating a Maximum Credible Earthquake (MCE) of moment magnitude, M_w=7.25, and the corresponding Peak Bedrock Acceleration (PBA) at the site is estimated to be about 0.5g (Maulchin, 1996). The corresponding Peak Ground Acceleration (PGA) is estimated to be the same as the PBA since the soil profile can be classified as the NEHRP (BSSC, 1994) Type D. The project site is not considered susceptible to ground rupture since no known fault crosses or extends toward the site.

Based on the depth of the permanent groundwater table, the site is not considered susceptible to soil liquefaction during seismic events. However, as mentioned above, temporary water mounds can form around the watercourse and saturate the near surface soils. In that case, localized zones of loose to medium dense sand within the upper 5.0 to 10 m are considered susceptible to liquefaction during strong seismic events. The potential for lateral spreading at the site is considered to be low due to localized zones of liquefiable soils.

Seismic design for retaining structures includes consideration of the seismically induced active lateral earth and water pressures, in addition to the static lateral pressures, due to ground motion. The potential effects of soil liquefaction include increased seismically induced active lateral pressures, and loss of passive soil resistance and bearing capacity. In the absence of any significant differential scour or head-cut, the retaining wall will not be subjected to any significant unbalanced static or seismic lateral pressures. A 100-year flood resulting in 10 m of head-cut and a MCE resulting in significant ground shaking and liquefaction are two extreme events that are very unlikely to occur simultaneously at the site. Therefore, the design of the proposed check dam is based only on the static lateral loading due to the anticipated 10 m head-cut. It is recognized that any head-cut will be repaired immediately following storm events.

Minimum Panel Embedment below Potential Head-cut Elevation

In the event of a 10-m head-cut, the total hydraulic head difference between the upstream and downstream sides of the wall creates an unbalanced hydrostatic pressure on soil particles. This unbalanced hydrostatic pressure may lead to “boiling” or “piping” in the soil on the down-stream side, a phenomenon in which soil particles float or flow due to reduction in the submerged unit weight from the upward unbalanced seepage pressure. Therefore, the concrete panels are need to be placed deep enough so that the unbalanced hydrostatic pressure becomes insignificant to cause any “boiling” or “piping” in the soil on the down-stream side.

The reduction in the submerged effective unit weight due to the upward unbalanced pressure may be estimated by the following expression (Terzaghi 1954 and United States Steel 1975) since the soil on the down-stream side of the wall has fairly uniform permeability.

$$\Delta\gamma' = 20H_u/D \qquad (1)$$

Where $\Delta\gamma'$ = reduction in effective unit weight of soil (pcf) on the down-stream side; H_u = the total hydraulic head difference between the up- and down-stream side of the wall; and D = embedment depth as shown in Figure 4.

Given that the total hydraulic head difference H_u = 10 m, the required minimum embedment depth below potential head-cut elevation can be estimated from the Terzaghi's formula to be D = 4.5m (with a safety factor of 1.5). This minimum embedment depth should maintain a downward effective unit weight of soil particles at the down-stream side of the wall. A sheet pile cutoff wall or a grouted/injected cutoff wall may substitute the portion of the concrete panel below the head-cut elevation.

Minimum Tieback Force and Embedment Depth for Soldier Piles

Preliminary calculation indicated that the 914mm (36-inch) diameter CISS soldier piles were inadequate to support a 10 m high cantilever wall in the event of the maximum potential head-cut. Thus, a single tieback per pile supported by an anchor pile was designed to provide additional lateral support to the wall. The minimum tensile force on the tieback rod was estimated according to the Department's Trenching and Shoring Manual, Section 10 – Soldier Piles (Caltrans, 1995), as presented in Table 2 below for different tieback anchor depths and soil parameters. The corresponding minimum embedment depths for the soldier piles for static equilibrium are also presented in the table.

The minimum tieback force and the minimum pile embedment depth are functions of water level elevation and soil parameters. The soil parameters were estimated from correlations with SPT blow counts. This design was based on the maximum anticipated hydrostatic pressure due to a running water depth of 2 m on both sides of the wall corresponding to Q_{100} = 67 m^3/s.

Table 2. Minimum Tieback Force and Minimum Embedment Depth for Soldier Piles

Case	Tieback/Anchor Depth, m	Soil 1 ϕ_1 (^{o})	Soil 2 ϕ_2 (^{o})	Tieback Force	Pile Embedment
				kN (kips)	M (ft)
1	1.0	30	33	1517 (341)	9.6 (31.5)
2	1.5	30	33	1557 (350)	9.5 (31.1)
3	2.5	30	33	1655 (372)	9.2 (30.1)

ϕ_i – angle of internal friction of soil

Soil 1 and Soil 2 in Table 2 refer to the soil above and below the potential head-cut line. It is recommended that the minimum pile embedment depth be multiplied by a safety factor of two (2) to obtain the design pile embedment depth. From the Table 2, it can be seen that the ultimate tieback force for Case 1 – with a buried depth of one meter is approximately 9% less than that for Case 3 – with a buried depth of 2.5 meters. A shallower buried depth of tieback rods may be used if a lower ultimate tieback force is desirable for structural design.

Lateral Load – Deflection Curves

The minimum tieback force and soldier pile embedment depths presented above are based on a semi-empirical method in which pile deflection shape, and full mobilization of the ultimate soil passive resistance and active pressure are assumed. This approach may be appropriate for rigid

short piles, but cannot predict the lateral response of long flexible piles. A long flexible pile subjected to lateral loading interacts with its surrounding soil depending on its relative stiffness. Response of a laterally loaded long flexible pile should be determined based on methods that can more accurately determine its flexural deformation shape. Such methods include numerical analyses in which soil resistance is represented by a series of soil springs such as p-y curves. With the p-y soil spring model, the pile-soil interaction can be realistically taken into consideration and more accurate embedment depth, pile moment and shear can be obtained for pile structural design. In addition, analysis of the pile-soil-pile interaction involving the tieback rod can be performed based on the uncoupled lateral load – deflection curves for piles at the check dam and the anchor wall.

Uncoupled lateral load - deflection curves for 914mm (36-inch) diameter (PP914x19mm or PP36x3/4") CISS piles at the check dam and the anchor wall were determined using the computer program LPILE 4 (Ensoft, 2000). Two representative subsurface soil profiles used for the analyses of the soldier pile and the anchor pile are presented in Figures 6 and 7, respectively. The concrete modulus of elasticity for pile material was assumed to be E_c = 23.4GPa (3400 ksi) which corresponds to a concrete compressive strength, f'_c = 25 MPa (3600 psi). The reduction in the submerged effective unit weight of the soil due to upward unbalanced hydrostatic pressure was considered in these analyses. Lateral load - deflection curves for the soldier piles and the anchor piles are plotted in Figures 8 and 9, respectively. In Figure 9, the tieback force on the soldier pile is presented as negative values since it is in the opposite direction to the tieback force on the anchor pile. Representative plots of pile lateral displacement, moment and shear distributions with depth for a range of tieback load are shown in Figures 10 and 11 for the Case 1 in Table 2.

Utilizing the results presented in Figures 8 and 9, it can be shown, by trial and error, that at equilibrium a tieback force, F= 1180 kN (265 kips) is developed between the soldier pile and the anchor pile at a lateral displacement of 105 mm (4.1 inches) for the Case 1. The force is much smaller than that (F = 341 kips) obtained based on the semi-empirical method. Based on results presented in Figure 10, a length of 15 m (50 feet) is adequate for the anchor piles. From Figure 11, a minimum pile length of 24.5 m (80 feet) below which the pile response is insignificant may be used for the soldier pile. The corresponding embedment depth is comparable to that given in Table 2 with a factor of safety of 2.

Construction Considerations

Construction issues related to the proposed check dam include pile driveability and stability of excavation to install the cast-in concrete panel. Hard driving conditions should be anticipated since cobbles and occasional boulders will be encountered during pile driving. Steel cutting shoes may be required to facilitate pile driving and to prevent pile damage. Predrilling can results in significant reduction in the pile lateral load capacity, and is not recommended.

It is anticipated that running surface water and/or shallow groundwater will be encountered, especially in the middle of the stream, during most of the year. Subsurface soils within the depth of the proposed excavation are predominantly granular, loose and highly permeable. Excavations in such soils are susceptible to instability when saturated and subjected to seepage forces. Thus, some seepage control, the extent of which will depend on the season and the excavation details,

should be anticipated. Efforts should be made to schedule construction during the dry season when minor seepage may be expected in the excavations.

Summary

Human activities such as aggregate mining can result in significant scour head-cut and undermine the stability of highway bridges. Designing deep bridge foundations or other common scour countermeasures may not be suitable for mitigating hazard from such deep scour. In this case, a tieback retaining wall type check dam supported by piles is considered to be a more appropriate scour countermeasure system.

Currently, pile foundations for tieback walls are designed based on empirical or semi-empirical methods such as those included in the Department's Trenching and Shoring Manual. These methods are based on an assumed pile deflection shape, uniform soil conditions and the full mobilization of the ultimate soil passive/active pressures. Such methods are usually more appropriate for short rigid piles, and may overestimate the tieback force and underestimate the minimum pile embedment depth.

Pile supported tieback walls can be more realistically analyzed by simple numerical methods using the p-y soil spring model. There are several computer programs commercially available for such analysis. A complete uncoupled pile response including lateral displacement, moment, and shear distribution with depth can be obtained to determine the required pile embedment depth and the cross section. The p-y method is very convenient for layered soils and piles with varying cross section. Furthermore, analysis can be performed to determine the complete system response including the tieback force by considering the soldier pile-soil-anchor pile interaction.

References

1 Avila, C. (1998), "*Scour Evaluation and Preliminary Hydraulic Parameters for Advanced Planning Study (APS*)", Tick Canyon Wash, Br. No. 53-1547, File No. 07-LA-14-35.34, California Department of Transportation, Sacramento, California.

2 Briaud, J., Ting. F., Chen, H., Gudavalli, R. Perugu, S, and Wei, G. (1999), "*SRICOS: Prediction of Scour Rate in Cohesive Soils at Bridge Piers*", Journal of Geotechnical Engineering and Environmental Engineering, Vol. 25, No. 4, April.

3 BSSC (1994), *NEHRP Provisions*, 1994 Edition, Building Seismic Safety Council, Washington D.C.

4 California Division of Mines and Geology (1994), *The Fault Activity Map of California and Adjacent Areas*, Scale 1:750,000.

5 Caltrans (1995), *Trenching and Shoring Manual, Section 10 – Soldier Piles (Revised 06/95)*, California Department of Transportation, Sacramento, California.

6 Maulchin, L. (1996), *Caltrans California Seismic Hazard Map*, California Department of Transportation, Sacramento, California.

7 Ensoft, Inc., (2000), *Technical Manual of LPILE Plus 4.0 for Windows – A Program for Analysis of Piles and Drilled Shafts under Lateral Loading*, Austin, Texas.

8 Kattell, J and Ericksson, M (1998), "*Bridge Scour Evaluation: Screening, Analysis & Countermeasures*", Forest Service, U.S. Department of Agriculture.

9 Terzaghi, K. (1954), *Anchored Bulkheads*, Transactions, ASCE, Vol. 119.

10 U. S. Army Corps of Engineers (119), "*Water Surface Profile User' Manual*", HEC-2, Hydrologic Engineering Center, Davis, California.

11 United States Steel (1975), *Steel Sheet Piling Design Manual*, Updated and Reprinted by US Department of Transportation/FHWA with permission.

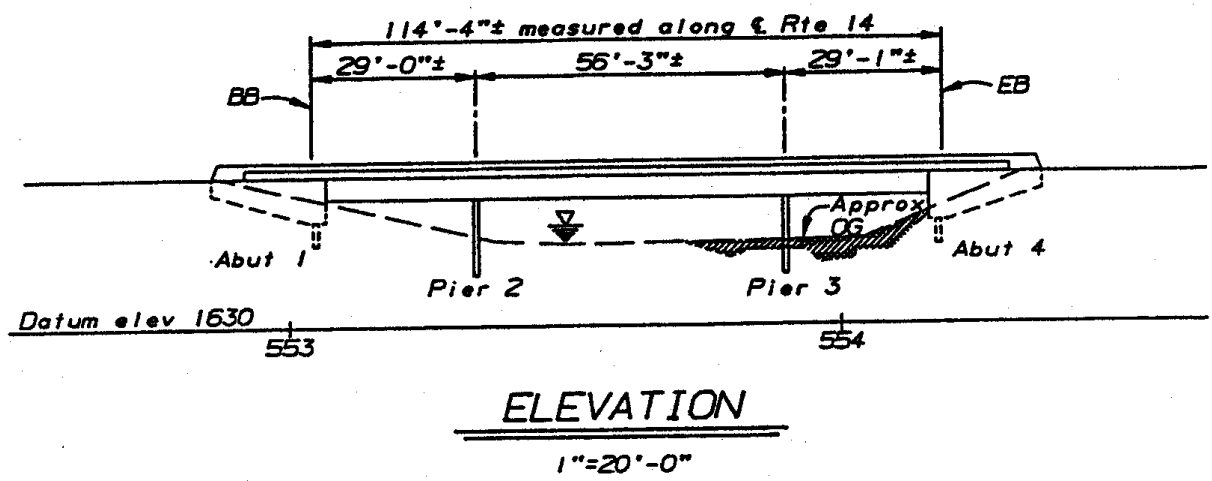

Figure 1. Elevation View of the Tick Canyon Bridge

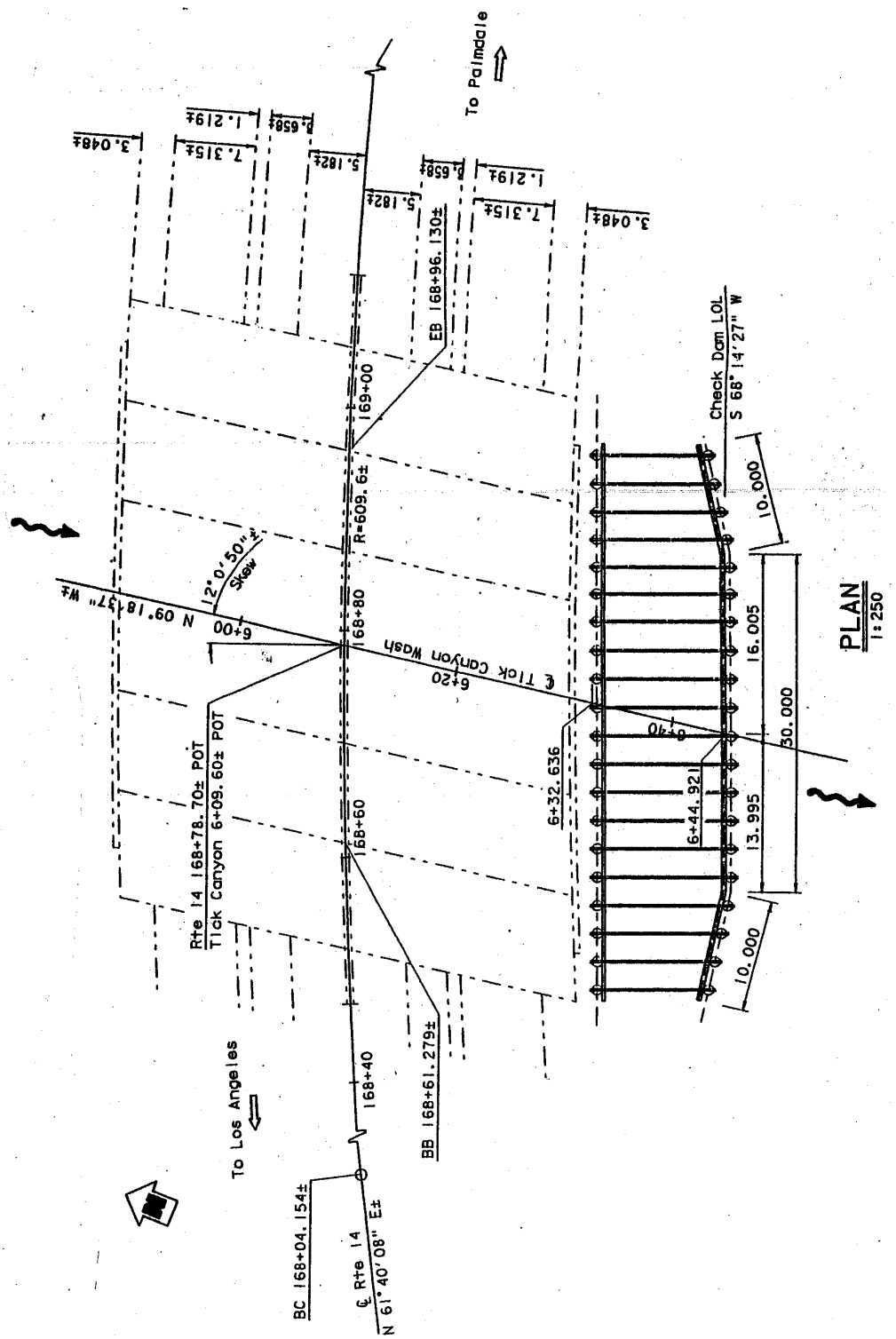

Figure 2. Plan View of the Check Dam-Retaining Wall System

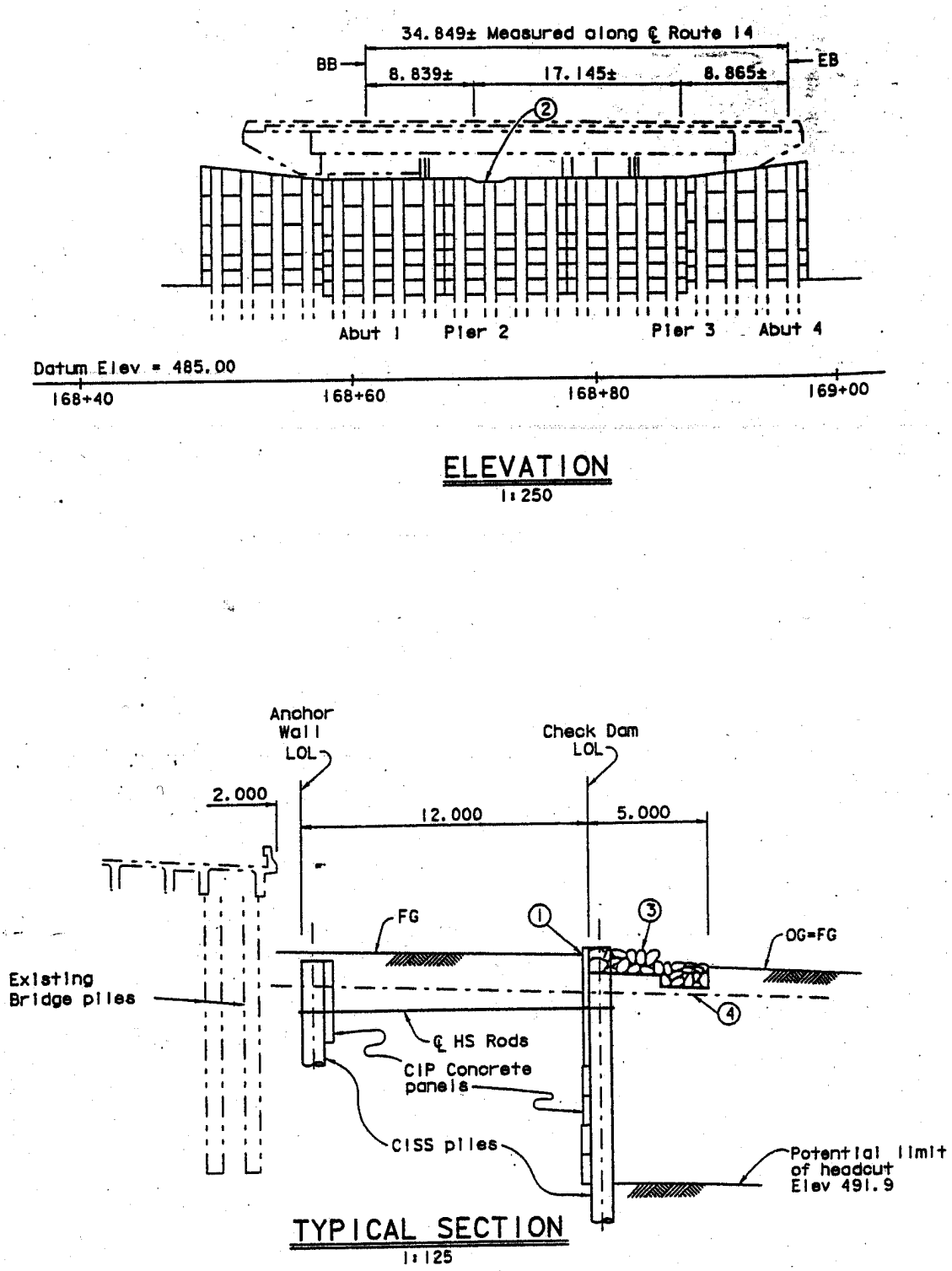

Figure 3. Typical Section and Elevation View of the Check Dam-Retaining Wall System

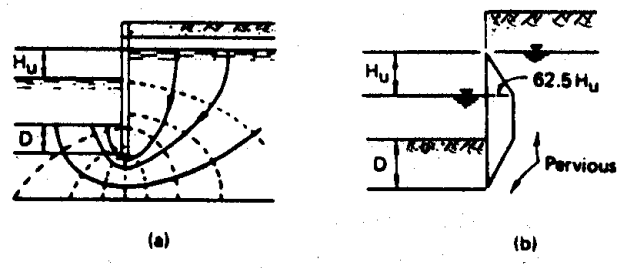

Figure 4. Hydrostatic and Seepage Pressures (after Terzaghi , 1954)

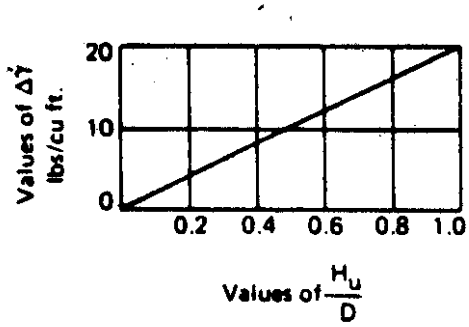

Figure 5. Average Reduction in Effective Unit Weight of Passive Wedge due to Seepage Pressure Exerted by the Upward Flow of Water (after Terzaghi, 1954)

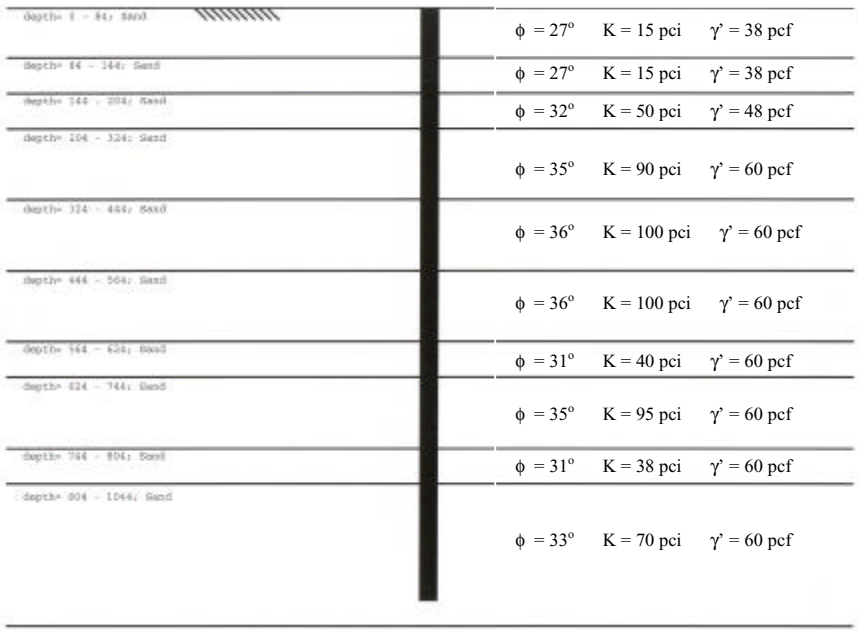

Figure 6. Soil Profile A for Analysis of Anchor Piles

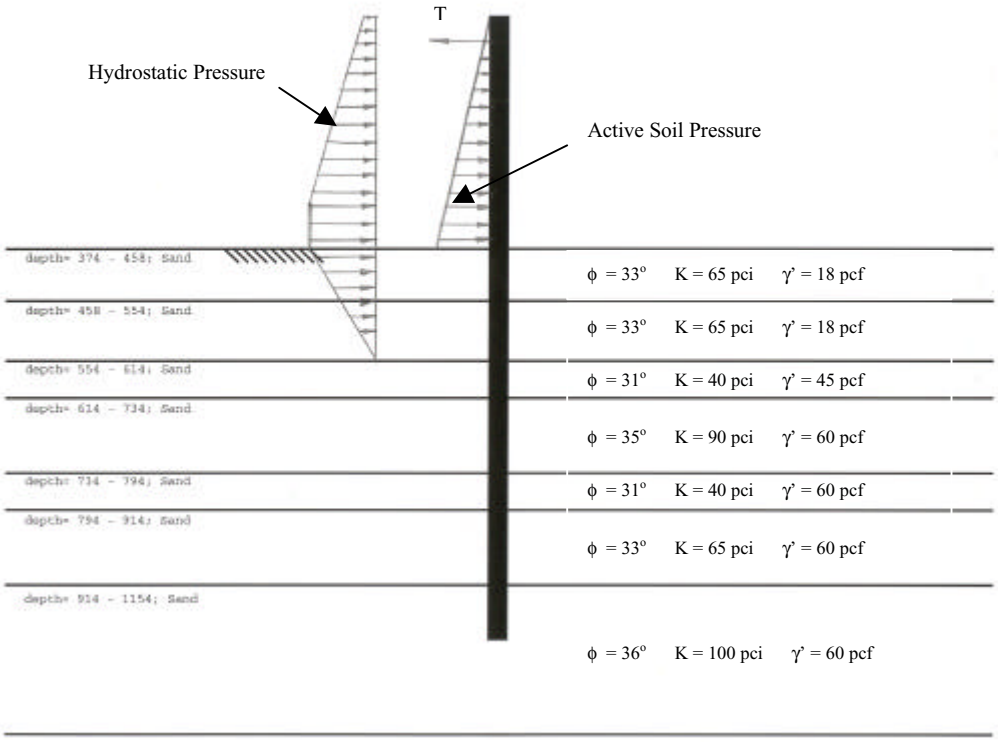

Figure 7. Soil Profile B for Analysis of Soldier Piles

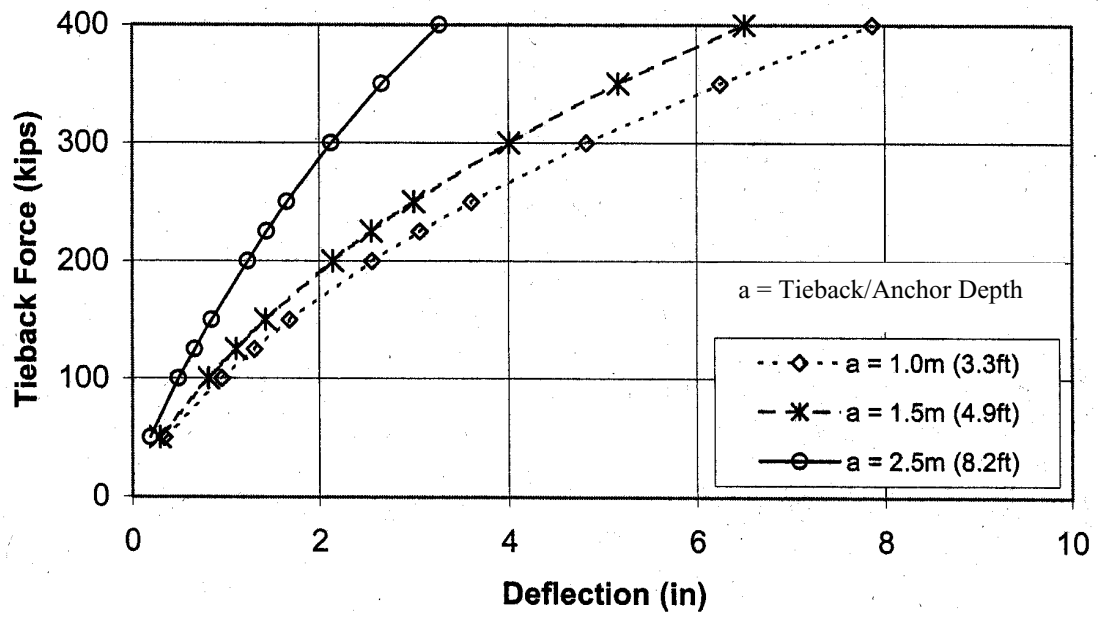

Figure 8. Lateral Load – Deflection Curve for Anchor Pile

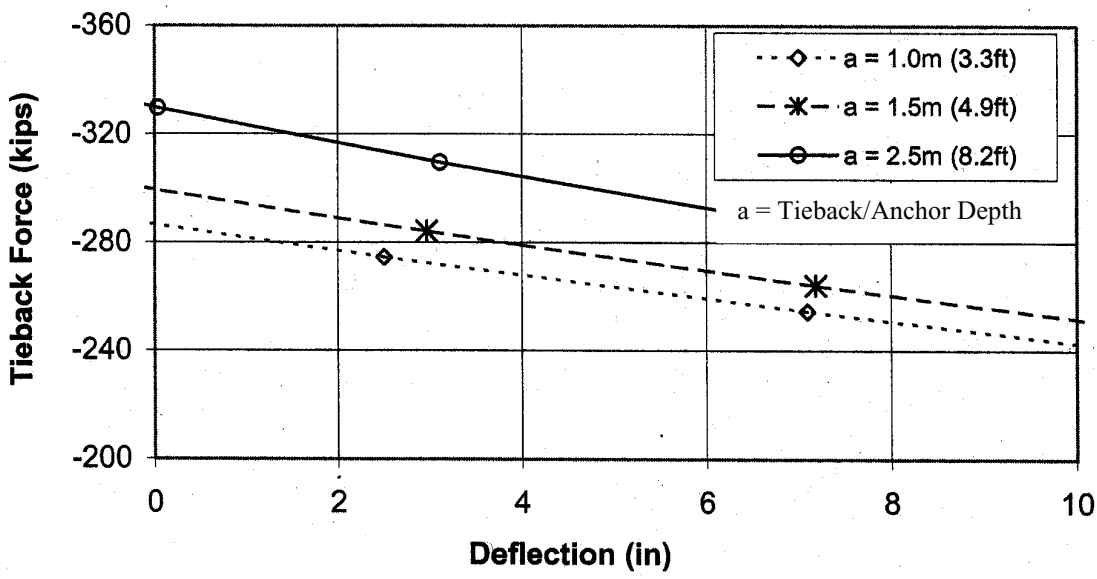

Figure 9. Lateral Load – Deflection Curve for Soldier Pile

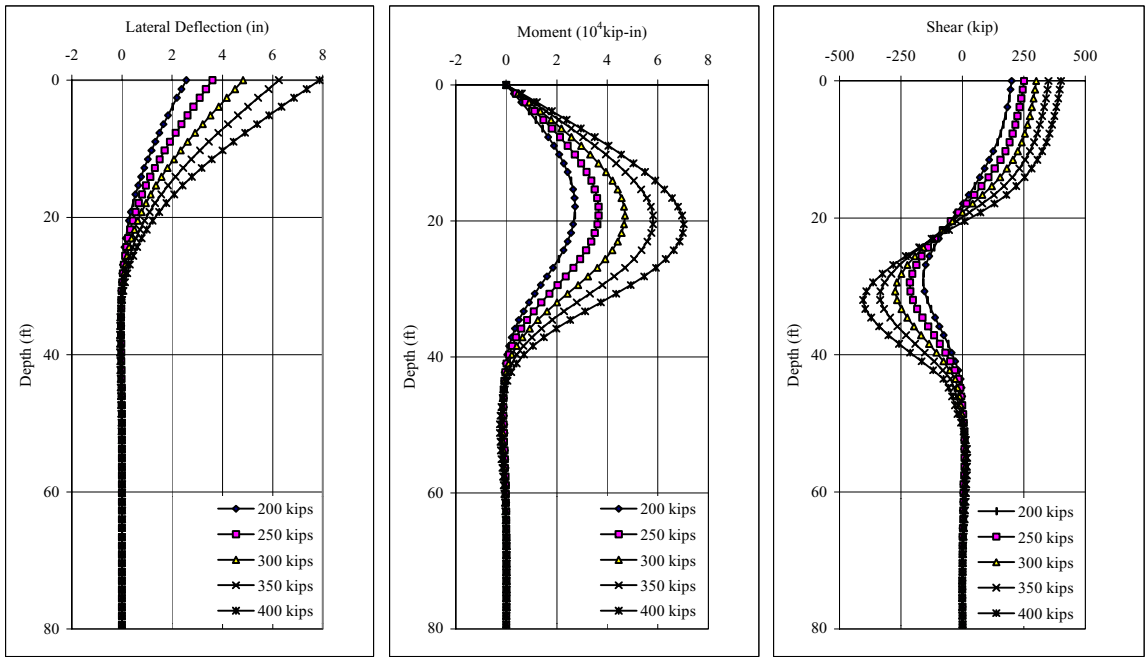

Figure 10. Displacement, Moment, and Shear for Anchor Pile

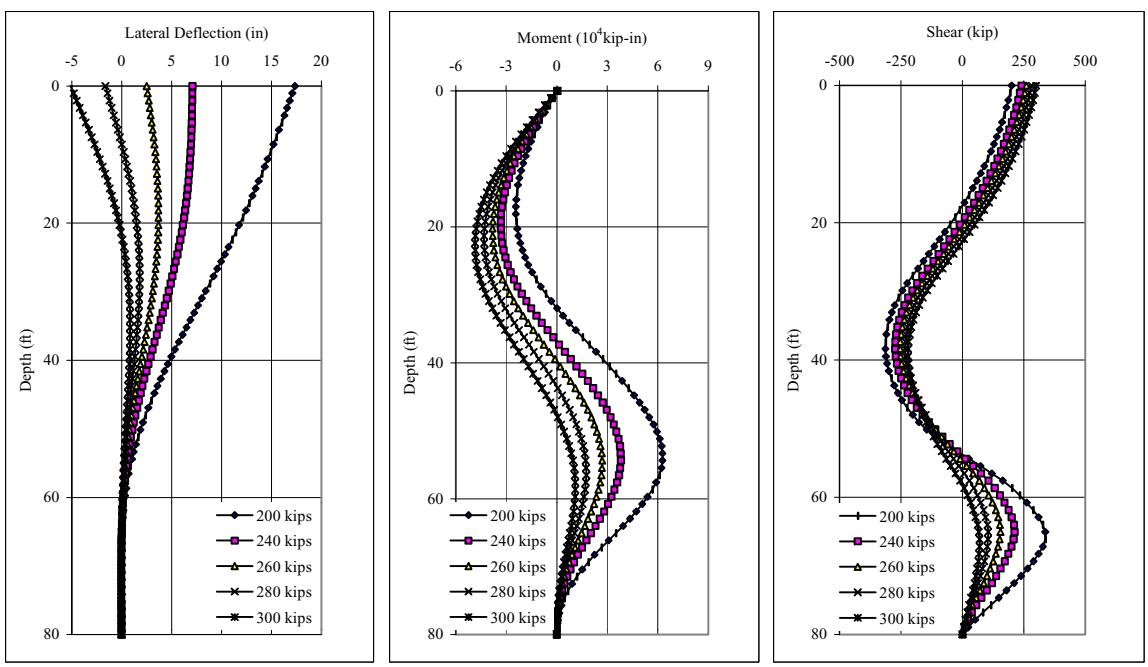

Figure 11. Displacement, Moment, and Shear for Soldier Pile

Final Stages of Butte City Bridge Erosion Control Project

Subhendu K. Mishra (1) and William B. Lindsey (2)

(1) PhD, P.E., Hydraulics Branch, Department of Transportation, State of California, 1891 Alhambra Blvd., Sacramento, CA; email: Subhendu_Mishra@dot.ca.gov
(2) P.E., Office Chief, Hydraulics Branch, Department of Transportation, State of California, 1891 AlhambraBlvd., Sacramento, CA; email: Bill_Lindsey@dot.ca.gov

Abstract

The bridge scour evaluation and mitigation program undertaken by the California Department of Transportation is in full swing and outstanding progress has been made in the last three and half years (1999, 2000, 2001, and 2002). The scour critical bridges are continuously screened out and countermeasures for these bridges against scour are studied and implemented. Some of the scour mitigation projects by Caltrans have been extremely challenging due to their complexities. This paper presents a very complex scour mitigation project undertaken by the Capital Outlay Support Team of the Hydraulics Branch of Caltrans.

The Butte City Bridge is located on Route 162 in Glenn County, California over Sacramento River. The bridge was originally constructed in 1948 as a replacement structure. Riverbank erosion was first noted at the bridge site in 1953, and has been continuing till present. The proposed project is to construct a series of rock spurs with sheet piles along the westerly bank of the Sacramento River in an effort to protect the Butte City Bridge from continued erosion of the upstream bank. The construction of the designed structures is currently scheduled for the summer of 2003. The Department of Transportation of the State of California is also taking active roles in pursuing a model study with collaboration with the University of California, Davis to determine the possible effects of the project on the surrounding area, the environment, and the river itself. The project has indeed reached a challenging position not only from the point of management but also technicality.

Introduction

A bird's eye view of the bridge location is illustrated in the Figure 1. The length of the Butte City bridge is 1337.8 meters and it is supported by 111 piers and 2 abutments. The estimated flood with a return period of 100 years at this location of Sacramento River is about 6575 cubic meters per second. Pile exposure was noticed on the piers on the west side of the river after the 1992/1993 winter season. Figure 2 presents a view of the river just upstream of the bridge before the major floods of 1996/1997. The floods of 1996/1997 eroded about 6 meters of the riverbank rendering the piers 107, 106, and 105 scour critical (piers identified in Figure 1). Figures 3 and 4 illustrate the bank erosion caused by the floods of 1996 and 1997. Emergency repair work was conducted to prevent any additional damage to the affected piers which might have resulted in closure of the bridge. The repair work consisted of installing 18-meter-deep sheet piles with tie backs. The sheet piles were constructed to enclose and protect the bridge piers. In addition, rock slope protection was

placed both upstream and downstream of the bridge to stabilize the embankments. Figure 5 shows the repair work done in 1997.

Figure 1: A bird's eye view of the bridge location

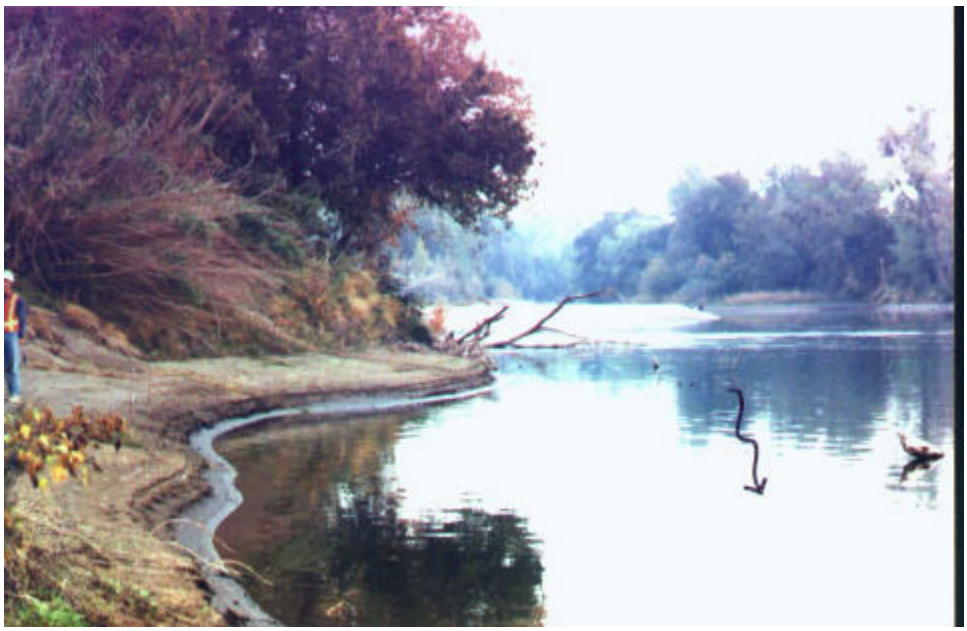

Figure 2: Upstream of the Butte City Bridge prior to the 1996/97 floods

Figure 3: Erosion caused by the 1996/97 floods on the west bank

Figure 4: Scour caused by the floods of 1996/97 at pier no. 107

River Reaction

While the emergency the emergency repair work was focussed at the bridge site due to right of way constraints, riverbank erosion extends both upstream and downstream of the bridge. Of significance to the bridge structure a natural bend has been observed upstream of the bridge. Historical data suggest that the river will continue to migrate westward. The current alignment of the river at the project site has a significant potential of scour and erosion of the west bank of the river. Continued migration of the river will have a severe impact on the bridge relatively shallow piers

located on the west flood plain of the river. This will render the bridge unsafe for the travelling public, and thus force closure of the bridge.

Figure 5: Repair work at pier 107 done in 1997

Stream Instability and Bridge Failure

A great many number of bridge failures have been caused by abutment failures. The stream becomes misaligned with the bridge developing massive erosional forces on the banks around the bridge abutment leading to its failure. Several types of countermeasures against stream instability have been listed in Federal Highway Administration (1997).

Alternatives

Three alternatives were mainly considered. These are 1) Bendway weirs, 2) Rock slope protection for extended lengths upstream and downstream of the bridge, and 3) Rock spurs.

Bendway weirs are not normally visible for stages above low water. They are intended to redirect flow by utilizing weir hydraulics over the structure. Flow passing over bendway weirs is redirected towards the downstream channel centerline. These structures reduce velocities and concentrations of currents near the outer banks resulting in a better alignment of the channel.

Federal Highway Administration (1997) also lists that the bendway weirs do not perform well in degrading or sediment deficient reaches

Rock slope protection (riprap) for extended lengths upstream and downstream of the bridge was an obvious alternative to consider. This alternative was not accepted because of the steep natural slopes of the riverbanks at the project site and due to the lack of success of this method in various scour mitigation projects undertaken by Caltrans.

Rock spurs are similar in appearance to the bendway weirs, but have significant functional differences. Spurs are typically visible above the flow line. These are designed so that flow is either diverted around the structure, or flow along the bank line is reduced as it passes through the structure. The spur design concept is listed in Federal Highway Administration (1995).

A spur is a pervious or impervious structure projecting from the stream bank into the channel. Spurs are used to deflect flowing water away from, or to reduce flow velocities in critical zones near stream bank, to prevent erosion of the bank, and to establish a more desirable channel alignment or width. The main function of the spurs is to reduce flow velocities near the bank, which in turn, sediment deposition due to these reduced velocities. By moving the location of any scour away from the bank, partial failure of the spur can often be repaired.

Project Proposal

After considering the above alternatives the Hydraulic and Hydrology branch of California Department of Transportation has proposed to construct a series of rock groins which used the rock spur idea listed in Federal Highway Administration (1995) with some modifications in the design. The proposed rock groins combine sheet piles driven into the bed and bank of the river with rocks piled on both sides of the sheet piles. Each groin will be placed at a different angle with the bank in order to stream line the flow of water. Figure 6 and 7 show schematic diagrams of the groins to be constructed. The alignments and the lengths of the groins are presented in Table 1. The total escalated cost of the project is estimated to be 5.6 million dollars.

Table 1: Alignment and lengths of Groins

Groin No.	Length	Angle between groin and the D/S side of the bank	Distance from the bridge
1.	6 m (20 ft.)	60 degrees	290 m (950 ft.)
2.	12 m (40 ft.)	75 degrees	244 m (800 ft.)
3.	20 m (65 ft.)	95 degrees	183 m (600 ft.)
4.	12 m (40 ft.)	110 degrees	122 m (400 ft.)
5.	6 m (20 ft.)	120 degrees	76 m (250 ft.)

Environmental Issues

The permitting process for the project will be extensive. The project is located in what would be considered environmentally sensitive habitat. The Sacramento River is habitat for several species of migrating salmon including the winter chinook salmon which is considered an endangered species. A National Wildlife Refuge (NWR) exists both upstream and downstream of the Butte City Bridge (Sul Norte and Cordora Units of the Sacramento River NWR). As proposed, a portion of the project limits will encroach on NWR property. Part of the conceptual 'charter' of the U.S. Fish and Wildlife Service for this refuge area is to allow the river to meander as a means of habitat restoration and rehabilitation. Consultations and approval will be needed from the U.S. Fish and Wildlife Service.

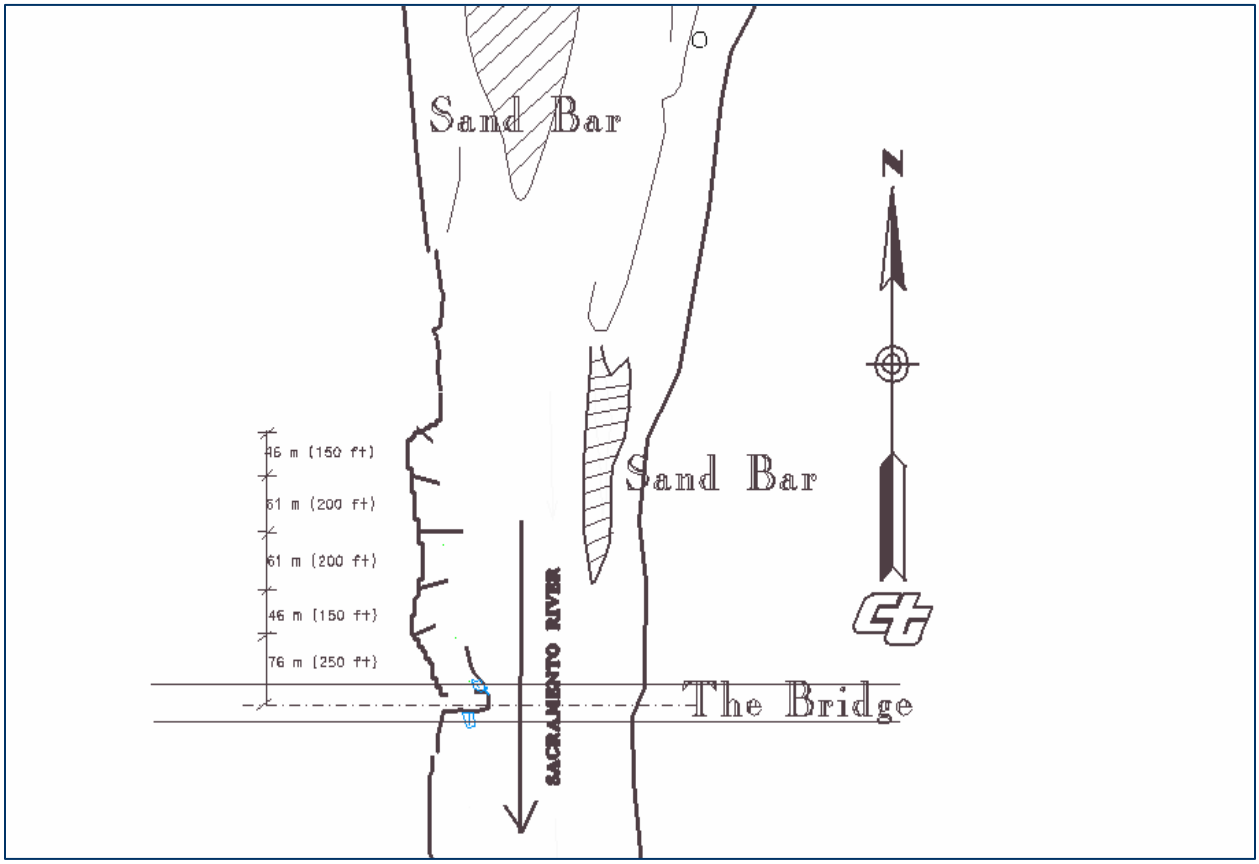

Figure 6: Alignment and placement of the proposed rock groins

An individual permit application is required from the Army Corps of Engineers, which regulates many projects which may impact national waterways through the Nationwide Permit process. A Water Quality Certification will be required from the State Regional Water Quality Control Board. This will set requirements with regard to erosion control, siltation, and water quality control parameters.

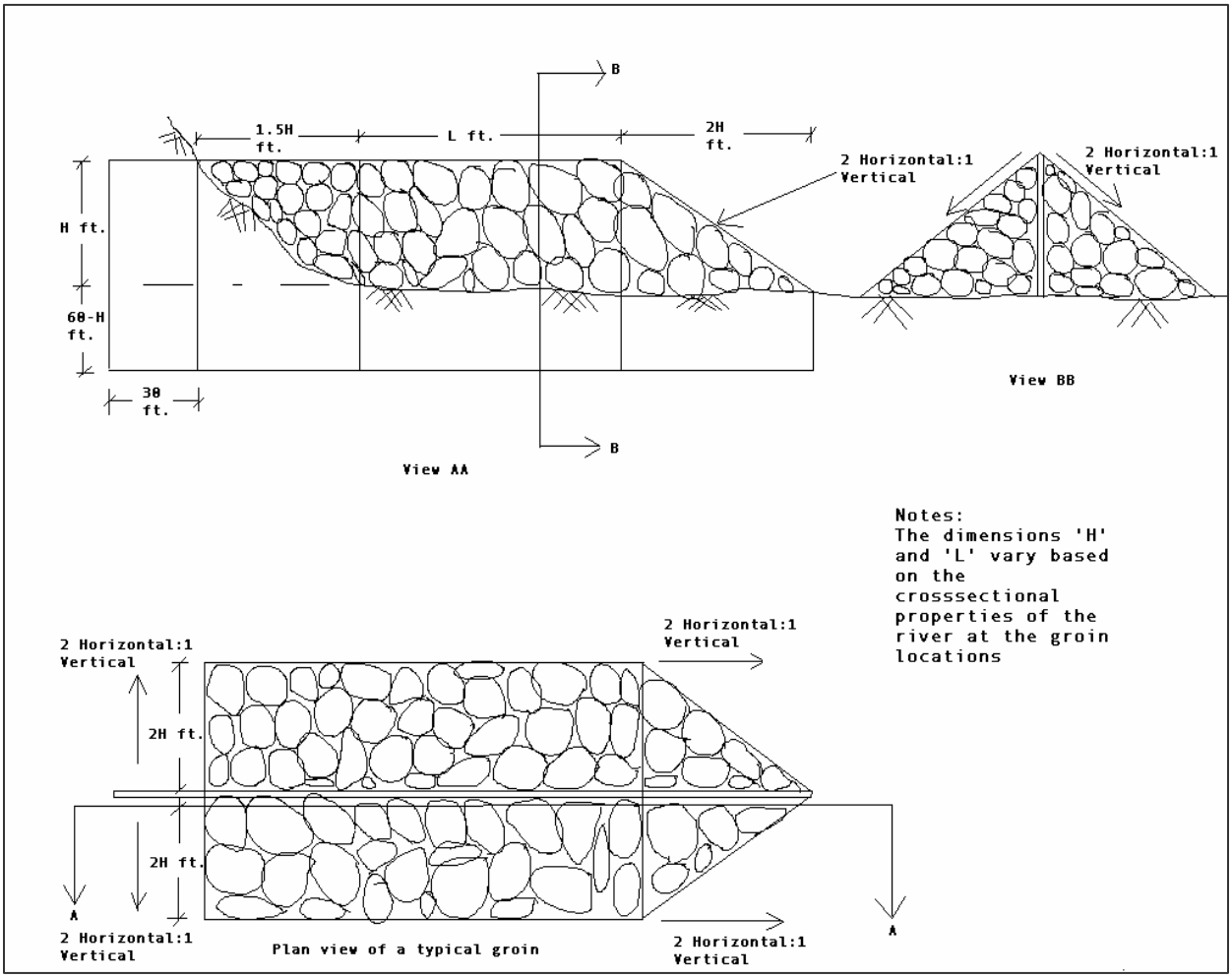

Figure 7: Detailed view of a typical groin

An agreement will have to be made with the Department of Fish and Game. Erosion control methods, habitat protection, and revegetation requirements will be set in this agreement. An approval will be needed from the California Department of Boating and Waterways. Encroachment into the floodplains of the river will also require review and approval from the State Reclamation Board.

Model Studies

A physical model study in collaboration with University of California, Davis (UCD) has been proposed to assess the functionality of the proposed solution as well as the effects of the project on the surrounding areas, environment, and the river itself. Details of the model study are being worked out with the UCD staff. It is expected that the results of the model studied will be obtained in Fall, 2002. These results will be utilized to produce an optimum design of the structures to produce the most desired results.

Conclusions

Sacramento River has historically shown a westward migration. The continued erosion of the west bank at the upstream side of the Butte City Bridge has been threatening the safety of the bridge. Several countermeasures were considered to protect the bridge from failing. The proposed project is to construct a series of rock groins with sheet piles along the westerly bank of the Sacramento River. The design of the rock groins is a modified form of the spur concept listed in the Federal Highway Administration (1995). The final detailed design of groins may be modified or changed after the final analysis.

References

Federal Highway Administration (1995). "Stream stability at highway structures." *Publication No. FHWA HI-96-032.*

Federal Highway Administration (1997). "Bridge Scour and Stream Instability Countermeasures." *Publication No. FHWA HI 97-030.*

Riprap Protection Around Bridge Piers in a Degrading Channel

By

Yee-Meng Chiew[1]

ABSTRACT

This study shows the behavior of a riprap layer around bridge piers in a degrading channel. The major failure modes found in riprap layers in a stable channel, such as shear failure, edge failure, winnowing failure and bed feature destabilization, are also present here. An additional feature that is unique to riprap layers around bridge piers in a degrading channel is the net degradation of the bed level that consists of finer sediment particles, while the larger riprap stones remain intact. This causes the formation of a riprap mound around the pier. Although this mound appears to serve its function in protecting the pier against erosion, the study shows that additional floods with large dunes translating past the pier can have dire consequences on the integrity of the riprap mound. Observations showed that the riprap layer had disintegrated significantly when two floods of similar magnitude were allowed on the riprap layer cum bridge pier. This result suggests that recurrent maintenance is necessary to ensure the effectiveness of the riprap layer in protecting the pier against scour in a degrading channel.

INTRODUCTION

Bridge failure due to pier scouring can often be attributed to the combination of general and local scour. The former is defined as the degradation of the riverbed in the absence of a pier, whereas the latter is defined as scour due to the 3-dimensional boundary layer separation around the structure. Much research and investigation on local scour at bridge piers has been conducted worldwide over the last half century and the information gained has been comprehensive. However, there is comparatively little information on the relationship between general scour and bridge pier failure. The present experimental study aims to provide an improved understanding of the effect of general scour on pier protection when riprap material is used. To date, the study of riprap protection around bridge piers has been conducted under the condition where the bed level remains unchanged under both clear-water and live-bed conditions, i.e., without general scour. While this condition may be applicable

[1] Associate Professor, School of Civil & Environmental Engineering, Nanyang Technological University, Nanyang Avenue, Singapore 639798 (cymchiew@ntu.edu.sg)

in certain rivers, it is clearly not universal. The failure of Koaping Bridge in southern Taiwan is an excellent example of the important correlation between riverbed degradation and bridge pier stability. Figure 1 reveals how bed degradation has exposed the pile foundation, while Figures 2(a) and 2(b) show the eventual demise of the bridge on August 28, 2000. The cause of failure of Kaoping Bridge is complex but it would not be erroneous to state that it is closely related to the combined effect of general and local scouring.

The main objective of this experimental study is to examine how bed degradation affects the effectiveness of a riprap layer in protecting bridge pier against scouring.

EXPERIMENTAL SETUP AND PROCEDURE

The experiments were conducted in a flume that was 18 m long, 0.6 m wide and 0.6 m deep. The longitudinal bed slope of the flume is adjustable. Water in the flume was re-circulated using an axial flow pump driven by an AC motor. A variable speed electronic unit was used to control the speed of the motor. An adjustable weir at the downstream end of the flume controlled the depth of flow in each test. Figure 3 shows the schematic layout of the flume used in the study.

The circular model pier had a diameter, D = 50 mm and was constructed from clear perspex tube. The bed sediment consisted of cohesionless coarse sand with a median grain size, d_{50} = 0.91 mm and a specific gravity, Ss = 2.65. The particle size distribution of the bed sediment is uniformly distributed with a geometric standard deviation, $\sigma_g = \sqrt{d_{84.1} / d_{15.9}}$ = 1.24. The sediment used to simulate the riprap stones is medium gravel with a median grain size, d_{50R} = 10.4 mm, σ_g = 1.10 and Ss = 2.65. The choice of the riprap material is based on the design recommended by the U.S. Federal Highway Administration (Richardson et al. 1995). The riprap material is designed for an undisturbed approach velocity U = 1.4 times the critical mean velocity for bed sediment entrainment, U_c. For the bed sediment used in the present study, this corresponds to a mean velocity of 0.48 m/s. The critical velocity, U_c is computed from the critical shear velocity (determined from the Shields Curve) using the mean velocity equation, with the undisturbed approach flow depth, y_o = 150 mm. Using the U.S. FHWA guideline stated in Richardson et al. (1995), the minimum riprap size is 11 mm and the cover and thickness of the riprap layer is 5D and 3 d_{50R}, respectively. Figure 4 shows the layout of the model pier and the riprap layer.

Three types of test were conducted for each series of run for a given flow condition. They are (1) run without pier or riprap layer; (2) run with pier only; and (3) run with both pier and riprap layer. In all the test runs, the sand bed was first leveled before commencement of the experiment. In the Type 2 and 3

tests, the pier and riprap layer is placed at the location approximately 12 m downstream from the entrance to the flume. Three different velocity ratios, at U/U_c = 1.2, 1.4 and 1.7 were tested in this study. However, the present paper only describes the observations and results for test conducted with U/U_c = 1.4, i.e., the condition whereby the riprap layer is designed for.

RESULTS AND DISCUSSION

Since the velocity ratio, U/U_c used in the test was 1.4, the bed sediment will move. Because there is no sediment re-circulation in the test, the bed will undergo degradation. The objective of the Type 1 test was to determine how much degradation the bed will undergo when it is subjected to the given flow condition. At the beginning of the test, transport of sediment particles occurred with the formation of dunes on the bed. With time, the sediment particles moved away from the test section, causing bed degradation and a corresponding reduction in flow velocity. As this took place, the sediment transport rate decreased with an eventually disappearance of the sand dunes on the approaching bed as sediment transport eventually ceased when the mean flow velocity approached the critical velocity for sediment entrainment. Figure 5 shows the equilibrium bed profile of both the Types 1 and 2 tests measured after duration of 216 and 192 hours, respectively. The data show that the extent of bed degradation or general scour is similar, confirming that the pier, whose center is located at X = 8.24 m, has little influence on general scour. The equilibrium bed degradation is approximately equal to 70 mm. It must be pointed out that the large scour hole that forms at $X \approx 3$m is due to the rigid bed (false floor) upstream of X = 0. This phenomenon is common in laboratory studies that consist of a rigid-loose bed boundary.

In the Type 2 test, the measured equilibrium depth of pier scour (local + general scour depth) was found to be 169 mm below the original bed level. For tests conducted in a stable channel, Chiew and Melville (1987) found that the dimensionless time-average depth of pier scour, d_{av}/D was 1.95 for a similar flow condition. For a circular pier with diameter = 50 mm, this yields an equilibrium pier scour depth of 97.5 mm. The results show that the depth of scour associated with a degrading channel is 1.73 times higher than that when bed degradation is not present at U/U_c = 1.4. An interesting point to note from the above data is that the sum of general scour depth (70 mm) and the expected depth of pier scour (97.5 mm) observed by Chiew and Melville (1987) is 167.5 mm. This value is almost identical to the total scour depth of 169 mm measured in the present study. This feature is most likely to be coincidental.

In the Type 3 test, a riprap layer is placed around the bridge pier and its geometrical layout shown in Figure 4. When the pier cum riprap layer is subjected to a flow at U/U_c = 1.4 and y_o = 150mm, the first sign of weakness occurs on the finer bed sediment at the edge of the riprap layer. As the bed

sediment was eroded, a small indentation forms, causing the riprap stone to drop into it. This observation is consistent with those described in the literature, for example, Chiew (1995). With time, bed feature destabilization, caused by the propagation of dunes past the pier and the riprap layer, sets in resulting in damages to the riprap layer. This phenomenon was described in detail in Chiew and Lim (2000) and Lim and Chiew (2001). In this test, an additional dimension, which was not observed in these previous studies, is present in that the sediment bed is also subject to degradation. Although the entire bed degrades, the riprap layer did not because it is designed to withstand the flow at $U = 1.4\ U_c$, i.e., shear failure of the riprap stones did not occur. As a result of this, a mound consisting of the riprap stones forms around the pier. This phenomenon is often observed in the field. The photographs in Figure 6 show the formation of the riprap mound around the pier. Figure 6(a) shows the layout of the riprap layer around the cylindrical bridge pier before commencement of the test. The second figure (Figure 6b) shows a close-up view of the riprap mound after general degradation of the bed level, while the large stones making up the riprap layer remain intact. Figure 6(c) shows the side view of the riprap mound with a dune approaching it. At this stage the riprap mound is generally stable because general scour has rendered a lower velocity excess for the given steady flow condition in the study. Moreover, the rate of sediment transport has also decreased markedly.

The riprap mound that formed around the pier shown in the present study is not uncommon in many field conditions. It forms because the entire bed degrades due to general scour while the riprap stones remain intact. This is because the latter is designed to resist the flood flow. At this juncture, the riprap layer appears to be able to function as it was intended. In this study, a second flood with a similar U/U_c-value as the first was simulated after the formation of the riprap mound to examine whether it can protect the pier against further erosion. Besides this, because much of the sand has already been eroded from the flume, additional sand was placed in the flume at a location upstream of the pier and riprap mound. When the flow was initiated, dunes were formed and they propagate past the riprap mound. When the dune approached the mound, water flowed over the dune crest and reattached onto the riprap layer. Observations show that this reattached flow is very important in destabilizing the riprap stones, as was also observed in the study by Chiew and Lim (2000). When this takes place, the exposed riprap stones were eroded and transported downstream exposing the layer to winnowing failure, where the underlying fine sediment was lifted through the voids formed by the interstices of the larger stones. This causes the stones to self-embed, leading to its eventual failure. Figure 7 shows the riprap mound after it was subjected to a second flood of a similar magnitude. The first photograph shows the riprap mound just before the dune arrives at the pier. At this point in time, the riprap layer is subjected to high erosion, due partly to the reattachment of flow over the dune crest. This flow is very efficient in eroding the large riprap stones, especially for those that are

exposed. Many stones were eroded by the reattached flow over the dune crest. The second photograph shows that the riprap layer was completely embedded by the propagating sand dune. At this juncture, it is surmised that little erosion was taking place, but some form of position readjustment was probably unavoidable. The last photograph shows the remains of the riprap mound after subsidence of the second flood. Clearly the riprap mound is significantly different from that shown in Figure 6. Many of the stones making up the riprap layer were entrained and transported downstream. A large degradation, which resembles the lee-wake scour associated with erosion around a submarine pipeline (Chiew, 1990; Sumer et. al, 1988), can be seen downstream of the pier. A comparison of the riprap mound in Figure 7(c) and those in Figures 6(b) and 6(c) reveals significant differences between them. It is not unreasonable for one to infer from this study that further floods will eventually cause the complete demise of the riprap layer.

An important deduction from this result is that a riprap layer may appear to function adequately at first glance after the passage of a designed flood, it, nevertheless, may be found wanting when subjected to subsequent floods. The study calls for regular maintenance of the riprap layer in order to ensure the effectiveness of the riprap layer in protecting the bridge pier against scouring.

CONCLUSIONS

The experimental study shows how a riprap layer around a bridge pier would respond to the flow in a degrading channel. The main difference between such riprap layers and those found in a stable channel is the net degradation of the bed level; while the riprap layer, when subject to the designed flow, would remain intact. This phenomenon results in the formation of a riprap mound around the bridge pier. The study shows that a second flood accompanied by dunes translating past the bridge pier can cause further erosion to the riprap mound. It is surmised that further floods may cause the eventual failure of the riprap layer.

For the case where there is no riprap layer around the bridge pier, the test conducted with a velocity ratio, $U/U_c = 1.4$ in a degrading channel shows that the total depth of pier scour below the original bed level is 1.7 times that encountered in a stable channel with the same flow condition.

REFERENCES

1. Chiew, Y. M., 1990, “Mechanics of Local Scour around Submarine Pipelines”, Journal of Hydraulic Engineering, ASCE, Vol. 116, No. 4, pp. 515-529.
2. Chiew, Y. M., 1995, "Mechanics of Riprap Failure at Bridge Piers", Journal of Hydraulic Engineering, ASCE, Vol. 121, No. 9, pp. 635-643.

3. Chiew, Y. M., and Lim, F. H., 2000, "Failure Behavior of Riprap Layer at Bridge Piers under Live-Bed Conditions", Journal of Hydraulic Engineering, ASCE, Vol. 126, No. 1, pp. 43-55.
4. Chiew, Y. M., and Melville, B. W., 1987, ""Local Scour around Bridge Piers", Journal of Hydraulic Research, IAHR, Vol. 25, No. 1, pp. 15-26.
5. Lim, F. H. and Chiew, Y. M., 2001, "Parametric Study of Riprap Failure around Bridge Piers", Journal of Hydraulic Research, IAHR, Vol. 39, No. 1, pp. 61-72.
6. Richardson, E. V., and Davies, S. R., 1995, "Evaluating Scour ar Bridges", 3rd Edition, HEC 18, U. S. Department of Transportation, Federal Highway Administration.
7. Sumer, B. M., Jensen, H. R., Mao, Y., and Fredsoe, J., 1988, "Effect of Lee-Wake on Scour Below Pipelines in Current", Journal of Waterway, Port, Coastal and Ocean Engineering, ASCE, Vol. 114, No. 5, pp. 599-614.

Figure 1. Bed Degradation at Kaoping Bridge, Taiwan causing exposure of pile foundation

(a) Looking downstream

(b) Looking upstream

Figure 2. Failure of Kaoping Bridge, Taiwan due to a combination of general and local scour (Courtesy of Professor C. Lin)

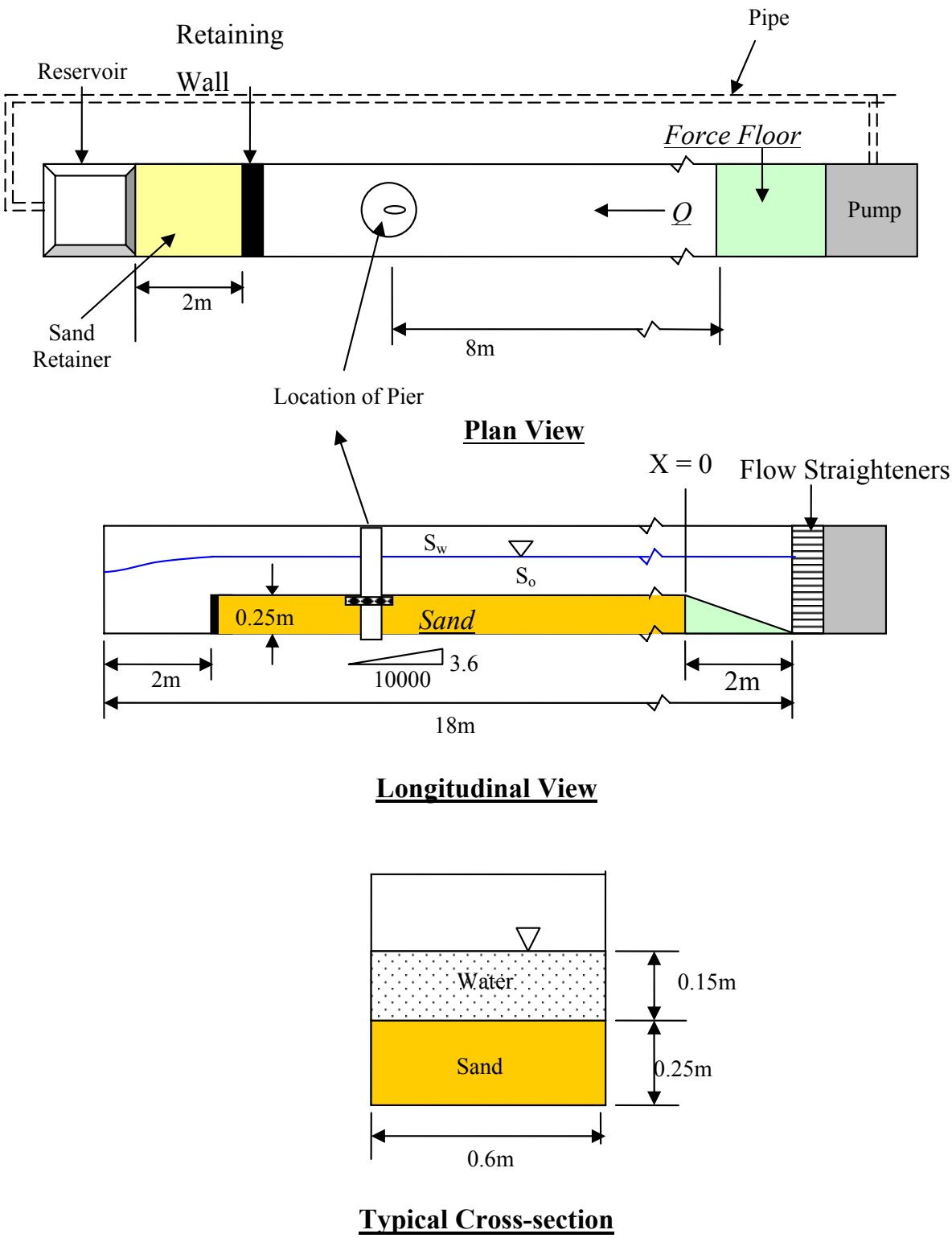

Figure 3 : Schematic Layout of Flume Used in Study

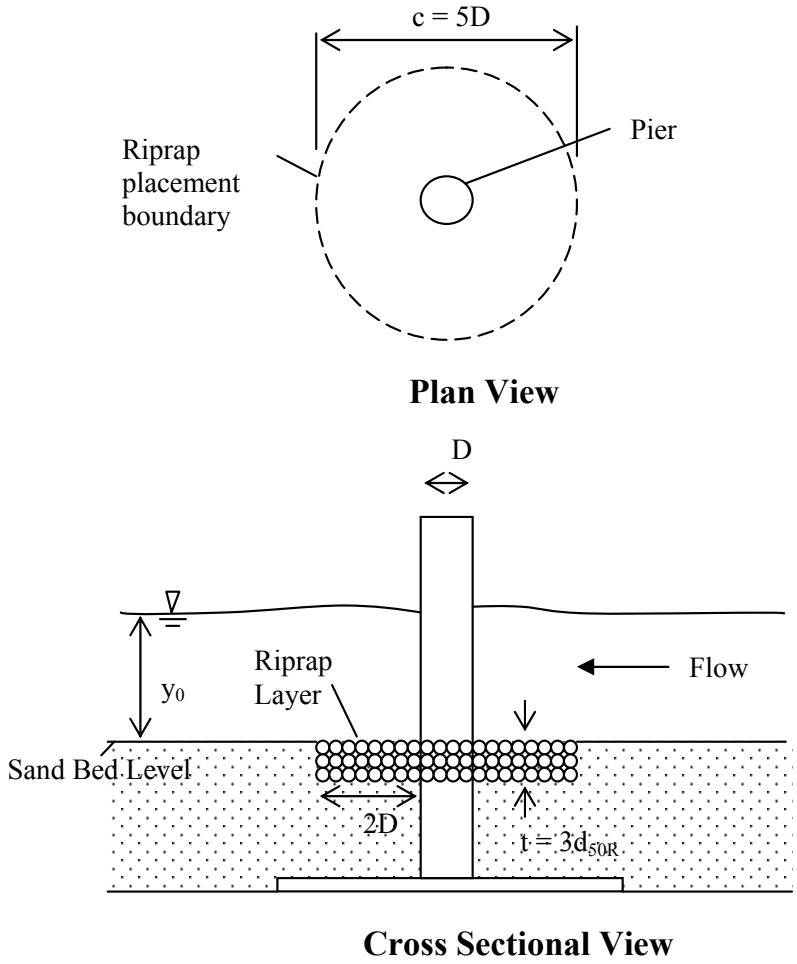

Figure 4. Layout of model pier and riprap layer

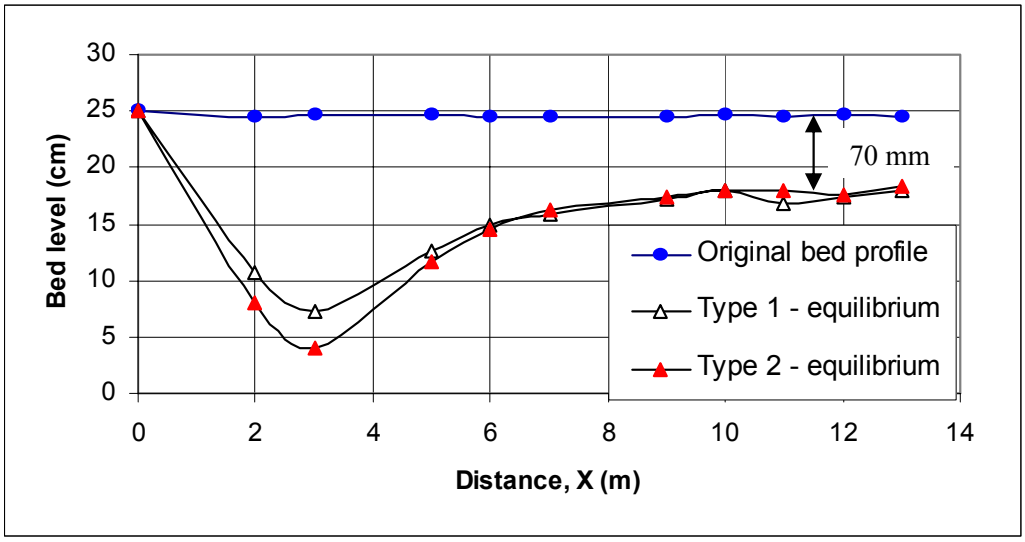

Figure 5. Equilibrium bed profile of Type 1 and 2 Tests ($U/U_c = 1.4$)

(a) Riprap layer at the commencement of test

(b) Formation of riprap mound around pier (flow from right to left)

(c) Dune approaching the riprap mound which is generally stable
(flow from right to left)

Figure 6. Formation of riprap mound around bridge pier in a degrading bed

(a) Dune from second flood approaching the riprap mound
(flow from left to right)

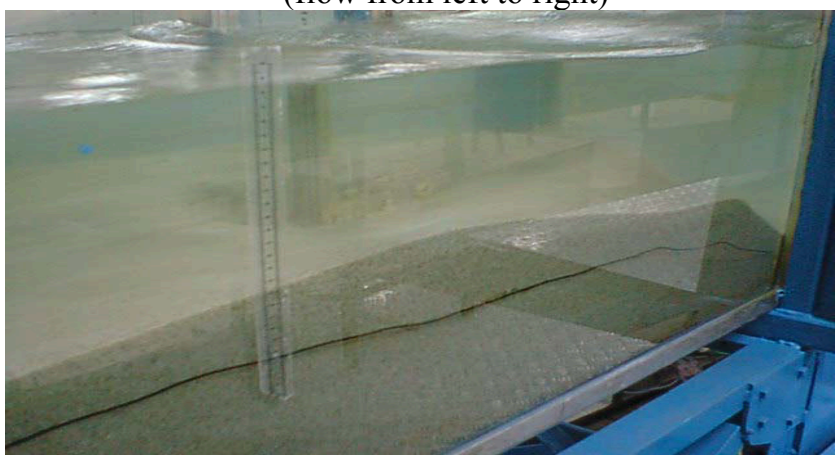

(b) Dune completely bury the riprap mound
(flow from left to right)

(c) Remains of the riprap mound after subsidence of the second flood
(flow from right to left)

Figure 7. Effect of second flood on riprap mound

Scour at a Submerged Rock Dike, Willapa Bay, Washington

N. Sultan[1], R. Phillips[2], H. Bermudez[3]

Abstract: This paper describes scour at a submerged rock structure on the coast of Washington. The SR-105 Emergency Stabilization Project was constructed in the summer of 1998 to protect a stretch of state highway from destruction because of shore erosion. The structure consists of a rubble-mound groin and dike. The rock groin extends approximately 1,600 feet from the shore. A submerged rock dike at the end of the groin functions in part as toe protection. The dike structure is 500 feet long at the crest and is built from 157,000 cubic yards of rock placed by bottom dump barge. The rock structure has induced relocation of a deep tidal channel 500 to 2000 feet further from the shore. The project performs as expected and reduces erosion along an extremely erosive shoreline northwest of the project site. Scour has developed in the vicinity of the toe of the structure. This scour was expected and the design incorporates a "launched-toe" feature to accommodate the predicted scour. Monitoring since construction shows that the structure has maintained its integrity. However, maintenance may be necessary should the scour continue and a maintenance concept design has been developed.

INTRODUCTION

The SR-105 Emergency Stabilization Project was built in the summer of 1998 to protect a state highway from destruction by a rapidly eroding shoreline. Figure 1 shows the project location. The project includes a rubble-mound dike and groin structure. The shoreline along the northern tidal channel at the inlet to Willapa Bay, Washington, has been one of the most rapidly eroding shorelines in the United States. The major causes of erosion at North Cove are northward migration of the

1) Coastal Engineer, Pacific International Engineering, P.O. Box 1599, Edmonds, Washington
2) Civil Engineer, Pacific International Engineering, P.O. Box 1599, Edmonds, Washington
3) Coastal Engineer, Pacific International Engineering, 3415 Greystone Drive, Austin, Texas

deep north tidal channel and wave action. The majority of the tidal current flows through the north channel, immediately adjacent to the shoreline. The shoreline erosion rate recently has been up to 150 feet per year. The historical rate has been observed to be greater than 250 feet per year (Figure 2). Recently, erosion threatened a 2,000-foot stretch of State Highway 105 (SR-105) near the town of North Cove, Washington. Relocation of the highway (for the second time this century) was not economically feasible.

ENVIRONMENTAL CONDITIONS

The project site is immediately north of the north entrance channel to Willapa Bay. The major causes of erosion at North Cove are northward migration of this deep north tidal channel and wave action. The entrance channel is constantly changing alignment and position and is a region of massive sediment movement. The sediment is non-cohesive fine sand. Hands and Shepsis (1999) describe cyclic behavior of the entrance channel location and associated bar. Waves offshore of Willapa Bay are regularly measured in excess of 30 feet, but are reduced as they pass through the entrance channel. The majority of the tidal current flows through the north channel, immediately adjacent to the shoreline. The depth averaged tidal current speeds in this channel frequently exceed 6 feet/second. The mean depth averaged current speeds are typically 3 feet/second for ebb tides and 2 feet/second for flood tides. The total tidal flows at the entrance to Willapa Bay are estimated to be 500,000-800,000 cfs, which exceed the discharge rate of the Mississippi River.

Figure 1. Location Map

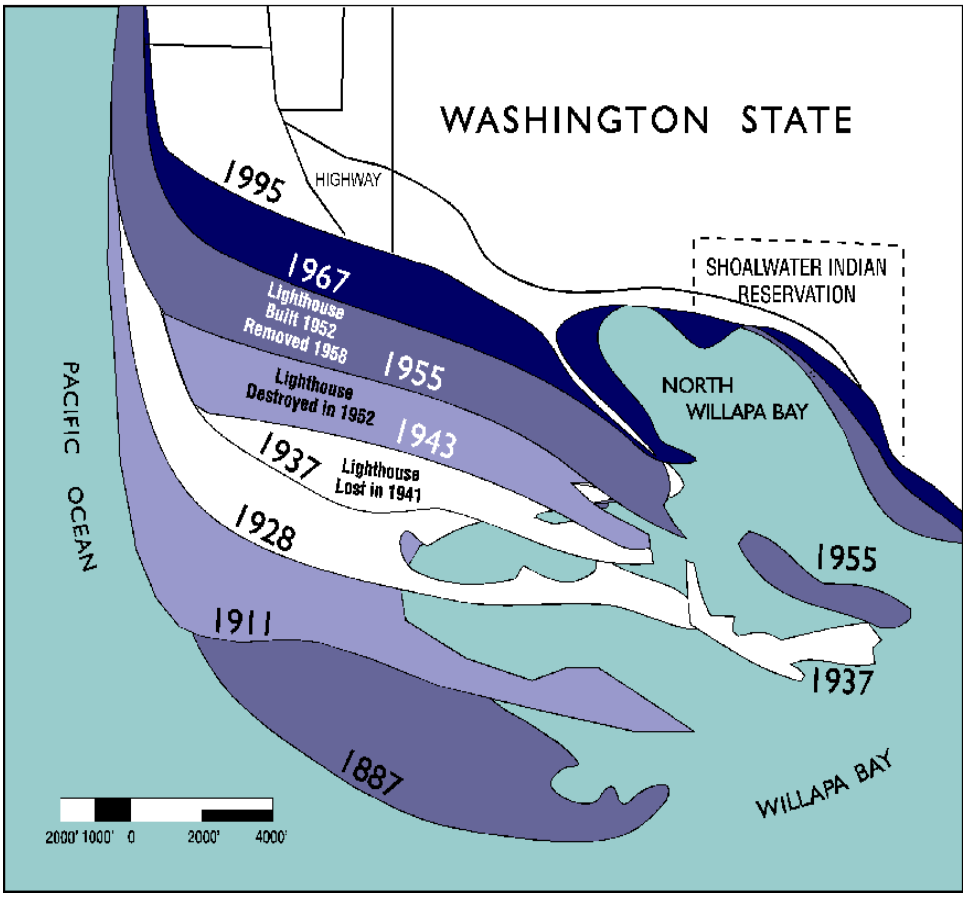

Figure 2. Erosion History at Project Area, 1887-1995

Figure 3. Aerial Photo

PROJECT DESCRIPTION

The project design consists of a rubble-mound underwater dike, a rubble-mound groin and beach nourishment. The project is shown superimposed on an aerial photo in Figure 3. Figure 4 shows in plan view the project elements. The rock groin structure extends seaward from the shoreline out to the northern edge of the North Channel. The underwater dike extends from the end of the groin across a portion of the North Channel. The beach nourishment is placed behind the dike to protect the shoreline adjacent to the highway. The project was built in the summer of 1998.

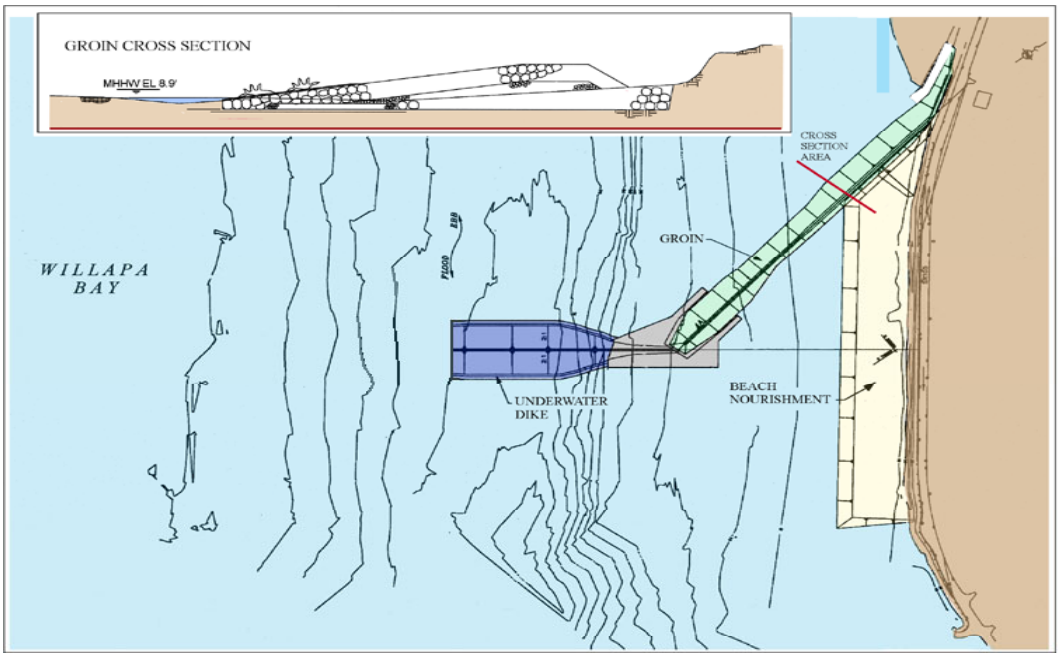

Figure 4. Project Design Features

The rock groin structure extends approximately 1,600 feet from the shoreline. The groin is aligned perpendicular to the predominant wave direction at an angle of 40 degrees to the shoreline. The seaward exposed portion of the groin was designed and built with a 7H:1V slope. The leeward side of the groin was constructed at a 7H:1V slope at locations not covered by beach nourishment material. The outermost 150 feet of the groin has a top elevation of -2.5 feet, Mean Lower Low Water (MLLW) and 3H:1V side slopes. The top of the groin varies from a maximum design elevation of +18 feet, MLLW at the groin's leeward end, to a minimum design elevation of -2.5 feet, MLLW at the offshore end (northern edge of the North Channel). The minimum height of the groin above existing ground is approximately 13.5 feet.

Different rock sizes were used to construct the groin. 8 inch minus was used as bedding material. An 8 inch to 24 inch rock gradation was used for the core. The

armor stone was a 2 to 4 ton gradation. At the outer end of the groin 10 ton armor stone was used.

Approximately 350,000 cubic yards of beach fill was placed between the groin and the shoreline using a cutter-suction head dredge. The beach nourishment was constructed to a top elevation of +25.0 feet, MLLW.

The function of the dike is to deflect the tidal current away from the shoreline and reduce local current speeds, thereby protecting the steep bank adjacent to the highway from further erosion. The dike also acts as scour protection for the groin. The design and construction of the dike are described below.

UNDERWATER DIKE DESIGN

The underwater dike was designed to extend from the end of the groin seaward to the south side of the North Channel, a distance of approximately 2,500 feet. However, the length of dike approved by resource agencies was only 1,520 feet. Because of site conditions, the as-built length of dike was further reduced to a length of 500 feet along the top edge. The constructed dike extends approximately 930 feet overall from the intersection with the groin to the seaward toe of the dike. The top elevation (crest) of the dike is -18 feet (MLLW). The bottom of the dike is constructed to a depth of –80 feet, MLLW.

The dike is a rubble-mound type of structure constructed from rock with different gradations. The underwater dike cross section was constructed with a bedding layer and inner core consisting of 18 inch minus rock material. The outer armor layer of the dike was constructed using 30 inch minus rock. A cross section through the dike is included in Figure 6. The stone sizes, slope of the dike surface and overall dike configuration were designed based on consideration of a number of factors, including cost, constructibility, availability of different rock sizes, and stone stability.

The dike functions as both a tidal current deflector, and as scour protection for the toe of groin. One design issue is the stability of the outer armor stone under the influence of waves and currents. A similar design issue is the scour that can be expected in the native, granular material near the dike.

Methods for predicting the dike armor stone stability under currents can be found in the Shore Protection Manual (1984) as well as in a number of references pertaining to the design of river training structures. Formulas based on calculating a local boundary shear stress were applied. For a current velocity of 6 feet/second a stone size of 4 inches is predicted to be stable. A larger stone size was used to account for uncertainties in the methodology and the increased stress from wave action.

Analysis of scour in the adjacent granular native material is more uncertain. Scour can clearly be expected at a structure of this nature. One analysis concept that may

be applicable is to treat the dike as a projection into a river. Scour at river structures has been well studied and a large number of references and design guides are available. A useful summary of a number of studies is contained in Przedwojski, et al (1995).

However, scour at the dike will also be influenced by wave action, in combination with tidal currents, and the resulting hydrodynamic regime clearly differs significantly from that of a river with a steady current. The literature concerning scour under combined waves and currents is considerably thinner than that for rivers. Recent research results on this topic are included in Sumer, et al (2001) and Whitehouse, (1998).

After review of a number of empirical equations, theory and project experience the dimensions and extent of future scour could not be predicted with an adequate level of confidence. Partly as a result, a "launched toe" feature was included in the dike design to allow for expected scour. As scour develops around the dike the rock material in the launched toe will eventually fill any scour hole that develops before it can threaten the integrity of the main structure. Also, post-construction project monitoring was included as part of the project partly in order to monitor scour and the integrity of the structure. As scour develops it would be detected and appropriate remedial/maintenance activity undertaken if necessary. With this "adaptive management" concept, scour prediction before project construction is less critical. Also, total project cost should be minimized by avoiding over-design of the scour protection before construction.

UNDERWATER DIKE CONSTRUCTION

The project was bid in April 1998 as two separate contracts, a first contract for the beach nourishment and groin/breakwater features and a second contract for the underwater dike feature. Two contracts were let to ensure the project was completed prior to the 1998 winter season and completion within the in-water work windows specified by natural resource agency permits. In May 1998, a unit price contract was awarded to Quigg Brothers Construction Inc. of Aberdeen, Washington for a low total bid of $8,260,000. Miller Contracting of Vancouver, British Columbia provided the rock source, transport barges and ocean tugs as a subcontractor. Figure 5 shows rock placement during project construction.

Construction of the underwater dike began on July 6, 1998 and was completed September 15, 1998. Approximately 299,000 tons of rock (175,000 CY) was placed to construct the underwater dike. Rock for the underwater dike was supplied by Miller Contracting from a source on the west coast of Vancouver Island, Canada. Rock from this source was primarily limestone and metamorphic. Rock was loaded onto flat deck and split hull barges and transported from Vancouver Island to the project site, a 20-hour one-way trip. Delivery of rock to the project site was scheduled to coincide with "slack" high tide to ensure navigation across the shallow, un-maintained Willapa Bay entrance bar and to time placement of rock

when tidal currents were a minimum.

Prior to the start of construction, the contractor requested a change to the specifications to provide additional armor stone and bedding stone in lieu of the core stone material at no additional cost to the owner. The contractor proposed to construct the bedding stone per plan at the outer edges of the dike and twice the specified thickness at the center of the dike. Additionally, they proposed to construct the remainder of the dike with armor stone instead of core stone. The request was granted with the requirement that the minimum bedding and armor stone thickness be maintained at all locations.

Equipment used to construct the dike consisted of a floating crane with clamshell and skiff buckets, four ocean tugs, one harbor tug, four split hull barges, two flat deck barges and a survey boat. The contract documents specified daily pre and post placement surveys be conducted by the contractor and submitted to the owner for review. The contractor provided a dedicated survey crew consisting of two survey boats fitted with differential GPS and echo-sounder equipment for quality control. Surveying was conducted daily before and after each individual placement of stone. Periodically, the owner's representative conducted independent hydrographic check surveys using single and multi-beam echo-sounder and side-scan sonar.

Three methods of rock installation were used to construct the dike, and are illustrated in Figure 6:

- Direct placement by side dumping off flat deck barges and by a floating crane with skiff bucket,
- fixed location split hull barge placement, and
- split hull barge "fly" spreading.

The first method (direct placement) was used to construct the dike in the shallows in and around the end of the breakwater/groin, between existing bottom elevation -12 and –20 feet, MLLW. The floating crane and flat deck barges were used for this construction method. The contractor developed a placement grid based on the contract drawings to determine the quantity of material to be installed within each cell of the grid. Flat deck barges were then tied to the crane barge and positioned over placement grid cells. A front-end loader located on the flat deck barge was used to place a pre-determined quantity of rock within each grid cell. Current velocities within this area were measured and did not have a significant impact on installation procedures. Daily quality control surveys were conducted to determine the adequacy of the installed rock. Areas outside the placement limits were "trimmed" using the floating crane with clamshell bucket.

The second method of placement used split hull barges tied to the floating crane. This method was primarily used for the installation of the interior dike material. The floating crane was anchored with four lines and then positioned using GPS to the appropriate location within the placement grid. The floating crane was then

used as a tie-up for the spilt hull barges while unloading. Current velocity magnitude and direction was measured to predict the trajectory of the rock being dumped. Current velocities within the middle portions of the channel were measured as high as 8 feet/sec during mid ebb/flood tides. Each barge load of rock was dumped at a predetermined location within the established grid cells at slack high tide. Hydrographic surveys were conducted to determine the location of each load of dumped rock. Areas determined to be out of tolerance were identified and delineated within the defined placement grids for trimming work. Final trimming to the specified lines and grades was conducted with the floating crane clamshell. GPS was installed on the floating crane boom to provide the operator control over the location of each bucket load of material removed and reinstalled within each grid cell.

The third method of placement used split hull barges to "fly" spread rock at specific dike locations. This method was primarily used for installing armor stone in the interior and at the top of the dike and for installing bedding stone. Using GPS, the incoming loads of rock were positioned over the desired placement cell, either unassisted or adjacent to the crane barge. The split hull barge was then opened at a slow rate and moved over the placement cells to spread the rock over a large area rather than an entire load dropped instantly at one location. This method was used to minimize trimming work by spreading each barge load over a greater area rather than installing large individual piles. Current velocity magnitude and direction was measured to predict the trajectory of the rock being spread. Rock was placed at slack high tide in order to work around the extremely high velocities encountered at the site during mid ebb and flood tides. The floating crane was positioned with GPS and securely anchored for use as a tie-up barge for each incoming bottom dump barge load of rock.

For both the "fly" spreading and moored barge placement methods, the initial barge dumps onto existing sand resulted in the material fanning out along the footprint to a 4H:1V to 5H:1V side slope. Once a foundation of rock existed, the dike began to rise up a 1.5H:1V to 1.25H:1V side slope; slightly steeper than the 2H:1V specified slope. Rock continued to be placed with split hull barges up to the specified side slope and top elevation tolerances.

Figure 5. Project During Construction

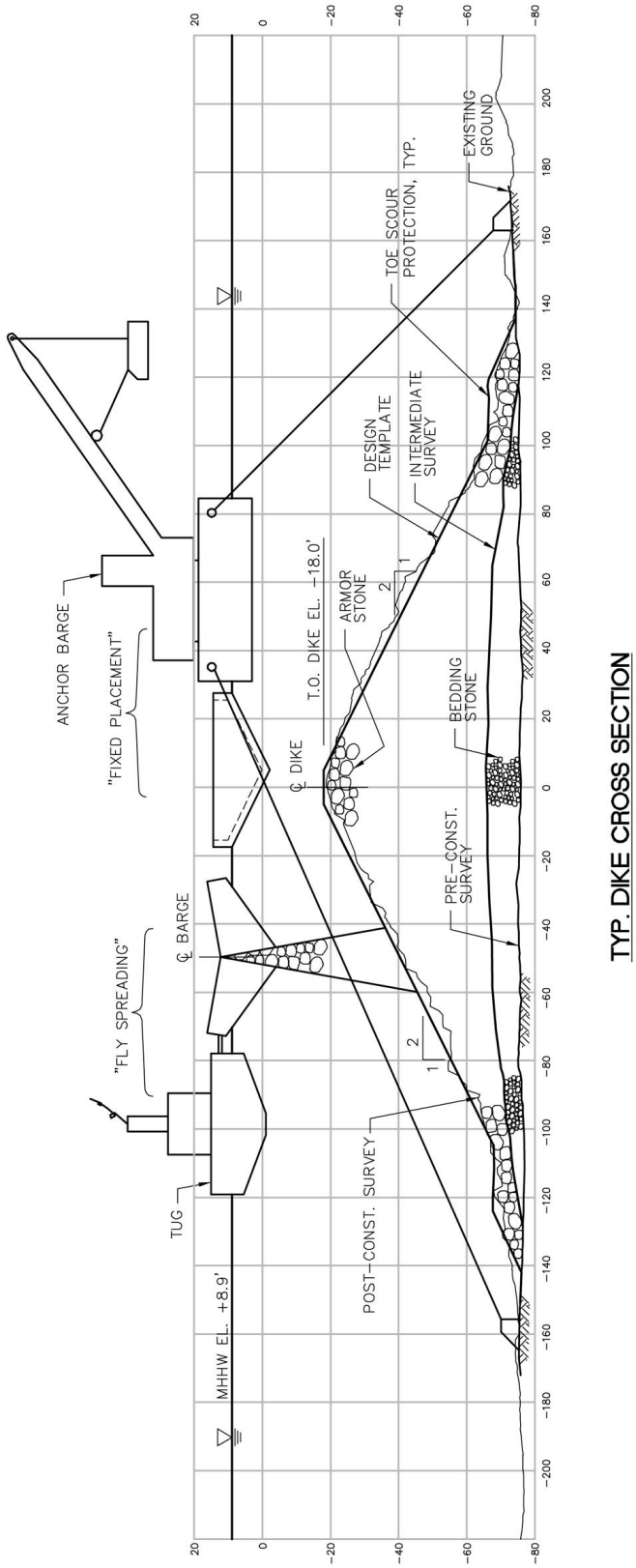

Figure 6. Underwater Dike Rock Placement

PROJECT MONITORING AND SCOUR HOLE ANALYSIS

Project monitoring included aerial photography, hydrographic and topographic surveys, water surface elevation (wave height) measurement and current velocity measurements. Currents and wave heights were measured from a tripod deployed on the seafloor and serviced at monthly intervals. Currents were also measured using Acoustic Doppler Current Profilers (ADCP) on a survey vessel moving along transects across the north tidal channel. In this manner, current velocities along a "slice" of the channel were measured. The monitoring program is described in Sultan (2002).

Hydrographic survey results show that the North Channel has moved south, 500 to 2000 feet, in response to project construction. The dike and groin have acted as a tidal current deflector and prevented further northward migration of the channel. North bank slopes in the vicinity of the project have generally accreted and moved southward. Figure 7 shows before and after hydrographic surveys taken across the north tidal channel.

Local scour in the vicinity of the structure is shown in Figure 7-Transect C. Also, the scour is shown in plan view in Figure 8, and in a section through the dike in Figure 9. The local scour induced by the groin appears overlapped, or superimposed, on a larger channel migration. The channel movement away from the north slope is caused by deflection of the tidal current by the groin. Some of the scour is likely due to a general channel migration away from the north bank. Figure 7-Transect C shows that the cross sectional area of the channel has increased more than the cross-sectional area of the dike and groin extending into the channel. The overall cross-sectional area of the north channel in the vicinity of the project has increased, as shown in Figure 7. This is consistent with velocity measurements showing a decrease in tidal current speeds near the shoreline along the north channel.

The scour hole immediately adjacent to the dike is approximately 40 feet deeper compared to pre-construction bathymetry. The scour hole forms a classic kidney shaped depression around the toe of the rock dike. The scour on the seaward side of the structure is deeper than the landward side. This may reflect the fact that ebb tide currents are stronger than the flood current. It may also be a consequence of the seaward side of the dike being generally more exposed to wave action than the landward side.

Comparisons have been made been the measured scour dimensions and predictions based on methodologies in Przedwojsk et al. (1995). The predicted scour hole dimensions are larger than that predicted from analysis based on sediment size and a steady current speed. One possible reason is the influence of waves combined

with a steady current. Another possible reason is that the scour hole is reacting in part to the overall migration of the tidal channel away from the dike and groin. It is probable that the scour hole is caused in part by large eddies generated in the vicinity of the dike, including eddies about a horizontal axis formed over the top of the dike. However, the current meters deployed in the field do not have sufficient temporal or spatial resolution to measure macro-turbulent eddies.

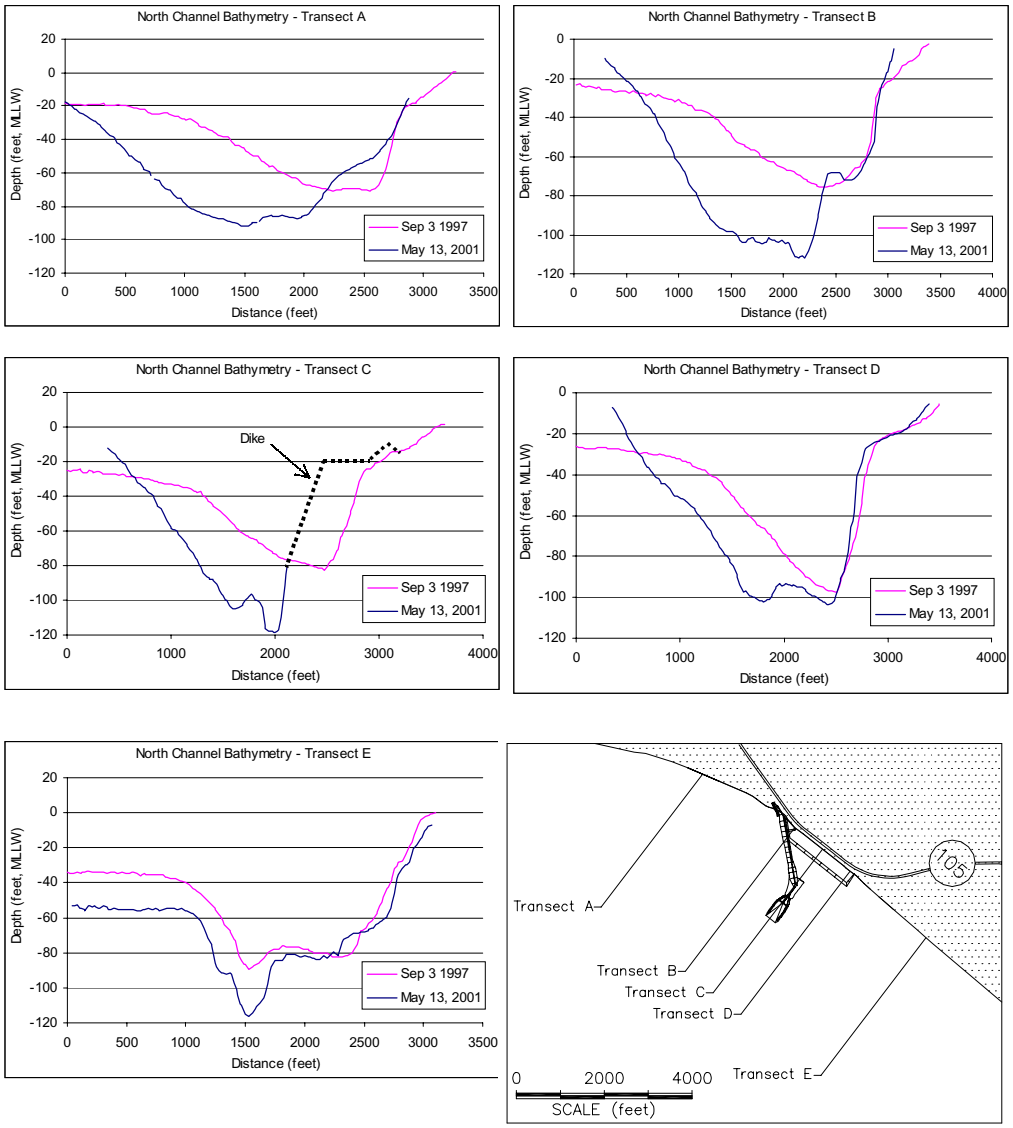

Figure 7. Hydrographic Survey Data

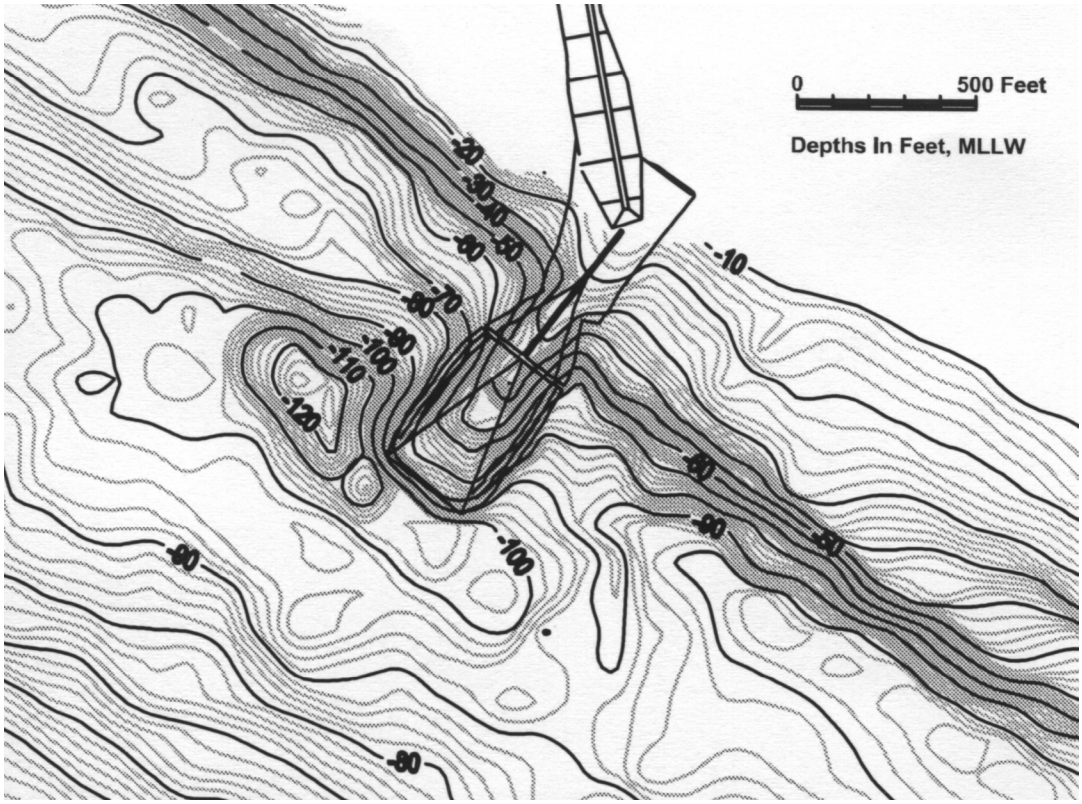

Figure 8. Scour Hole Bathymetry, April 2000

DIKE MAINTENANCE CONCEPT DESIGN

Figure 9 shows a maintenance concept design to address scour at the dike. If the deepening continues, scour may endanger the stability of this part of the structure and performance of the project. The design includes placement of rock at the toe of dike to protect from further scour. The rock is placed in the scour hole to form a "blanket".

The Coastal Engineering Manual (2001) provides design guidance for scour protection blankets. Application of a Shield's parameter type equation predicts that a stone size of 2 inches will be able to resist a depth averaged current speed of 6 feet/second at the scour hole. However, considering the additional influence of wave action and to account for other uncertainties, a larger stone size is recommended.

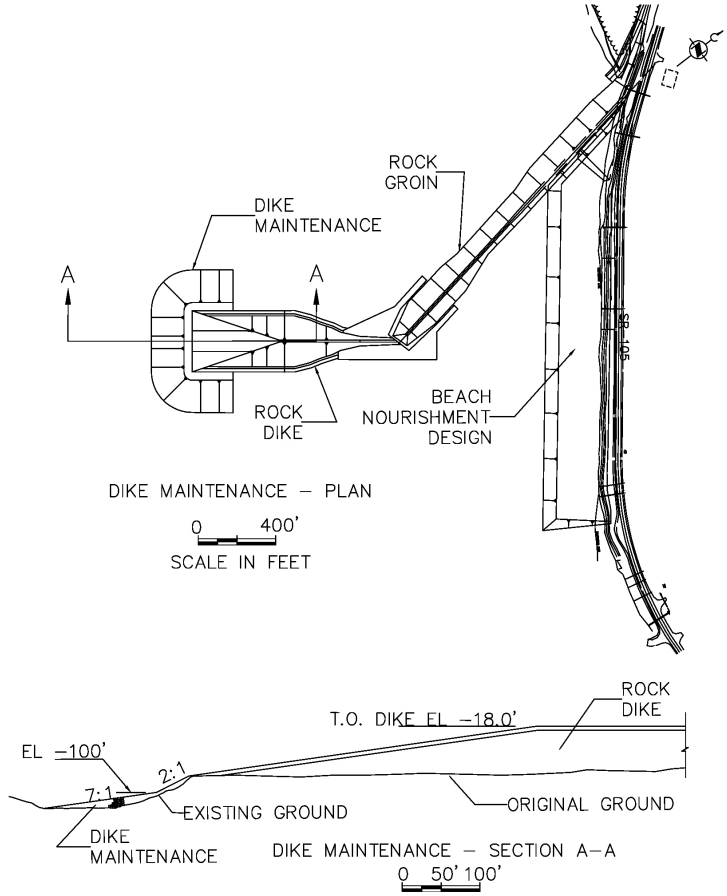

Figure 9. Dike Maintenance Concept Design

CONCLUSIONS

A rubble-mound rock groin and dike and beach nourishment was constructed to protect a highway from erosion. Monitoring since construction shows the project was constructed as designed and has performed as expected. Measurements of the groin and dike showed no signs of structural deterioration. Erosion has been greatly reduced and the shoreline has stabilized.

Scouring has occurred near the end of the underwater dike. If the scour continues this may endanger the stability of the dike part of the structure. A concept design involving the placement of rock scour protection has been developed.

A number of scour prediction methods have been applied and compared to the measured scour hole. The scour hole is deeper than predictions based on a steady current, such as occurs at river training structures. This may be a result of the combined effect of waves and currents.

REFERENCES

Coastal Engineering Manual, Part VI, Draft Edition (2001). US Army Corps of Engineers, Waterways Experiment Station, Vicksburg, Mississippi, EM 1110-2-1100.

Hands, E.B. and Shepsis, V. (1999). "Cyclic Channel Movement at the Entrance to Willapa Bay, Washington, USA", Proceedings of the Coastal Sediments Conference '99. American Society of Civil Engineers, pp. 1522-1537.

Przedwojski, B., Blazejewski, R. and Pilarczyk, K.W. (1995). River Training Techniques: Fundamentals, Design and Applications. A.A. Balkema, Rotterdam, Netherlands.

Shore Protection Manual (1984). US Army Corps of Engineers, Waterways Experiment Station, Vicksburg, Mississippi.

Sumer, B.M., Whitehouse, R.J.S. and Tørum, A. (2001). "Scour Around Coastal Structures: A Summary of Recent Research", Coastal Engineering 44, pp. 153-190.

Sultan, N.J. (2002). "Monitoring Results for a Shoreline Stabilization Project, Willapa Bay, Washington", Proceedings of the Solutions to Coastal Disasters Conference, American Society of Civil Engineers, 708-719.

Whitehouse, R. (1998). Scour at Marine Structures: A Manual for Practical Applications. Thomas Telford, London, UK.

Abutment Scour Countermeasures: A Review

By

Brian Barkdoll[1], Robert Ettema[2], Roger Kuhnle[3], Bruce Melville[4], Trimbak Parchure[5], Art Parola[6], and Carlos Alonso[7]

ABSTRACT

Scour of riverbeds at bridge abutments has been a problem for many years. Excessive scour can cause abutment damage and potential loss of life due to bridge collapse. Various countermeasures have been investigated and used with varying degrees of success. Countermeasures can be described in two categories: "bank and bed-hardening" and "flow-altering". Among bank- and bed-hardening countermeasures are rip-rap, cable-tied blocks, Toskanes and similar interlocking devices, and soil cement. Flow-altering countermeasures include vanes, guide banks, and spur dikes of various configurations. These countermeasures either reduce local scour at the abutment or attempt to maintain the channel alignment so that the channel does not outflank the bridge. However, several practical considerations limit the viability of most countermeasures. The considerations include washout of bank-hardening elements, winnowing of the fines between bank-hardening elements, and scour outside the lateral domain of the bank-hardening elements. Flow-altering devices can be outflanked, can be ineffective when flow direction is altered, may wash out themselves, and can snag debris or ice. A three-year research project is underway by the authors and sponsored by the National Cooperative Highway Research Program of the Transportation Research Board to define which countermeasures merit further study and to develop design guidelines for those countermeasures.

INTRODUCTION

The problem of scour around bridge abutments has been identified as one with potentially catastrophic results. Bridge failure can lead to the loss of life. In addition, the costs associated with repairs can be very expensive. Although extensive research has been performed on abutment scour, several questions remain. These substantial issues require further investigation. One issue concerns establishing effective countermeasures for

[1] Asst. Prof., Civil Eng. Dept., Univ. of Mississippi, University, MS 38677-1848, cvbark@olemiss.edu
[2] Prof., IIHR Hydroscience and Engineering, University of Iowa, Iowa City, IA 52242, Robert-Ettema@uiowa.edu
[3] Research Hydraulic Engineer, USDA-ARS National Sedimentation Lab., PO Box 1157, Oxford, MS, 38655, RKuhnle@ars.usda.gov
[4] Professor, Department of Civil and Env. Eng., Univ. of Auckland, Auckland, New Zealand, b.melville@auckland.ac.nz
[5] Research Hydraulic Engineer, US Army ERDC, 3909 Halls Ferry Road, Vicksburg, MS 39180-6199, Trimbak.M.Parchure@erdc.usace.army.mil
[6] Professor, Dept. of Civil Eng., Univ. of Louisville, Louisville, KY 40292, a.c.parola@louisville.edu
[7] Research Leader-CHWP, USDA-ARS National Sedimentation Lab., PO Box 1157, Oxford, MS, 38655, CAlonso@ars.usda.gov

protecting abutments against scour. The present paper was written to introduce a study aimed broadly at determining the range of effective scour countermeasures for abutments. It is hoped that presentation of the paper will stimulate useful discussion that may help the writers in conducting the study.

Unresolved Issues

There has been voluminous work done on pier and abutment scour over the years dating back at least to the 1700's. Much of the previous work on abutment scour is illuminated here, but there are several main issues remaining. The main ones are highlighted here.

Riprap is the most common countermeasure used by state bridge engineers, yet what should the size, lateral extent, and thickness of the riprap be? Is filter fabric necessary to prevent the fines under the riprap from winnowing out? Can the riprap stones at the edge of the riprap blanket be the same size as the rest of the stones or should the size gradually decrease to provide a smoother transition to the parent material? Does bedform migration across riprap cause failure? Is tying the riprap together necessary and under what conditions should this be done?

Another common method of protecting bridge abutments is to provide a foundation depth significantly deeper that the scour depth. This approach assumes that our predictions of scour depth are accurate. Should abutments be designed to act as piers, thereby allowing for the case when the river changes course and flows around both sides of an abutment?

In addition, can we use our experience on bridge piers to bear on abutment scour? Obviously piers and abutments differ in shape and location, but perhaps there are ideas and countermeasures that will work on both.

In reference to river migration, can we, or perhaps more philosophically, should we keep the river from migrating? In view of river restoration efforts, where the stream is seeking to re-establish equilibrium, is there a way we can still maintain transportation and yet allow the river to meander where it likes? Which river training structures are most appropriate and what is the most efficient design?

These are but just a few of the many queries left to wrestle with in the very rich topic of bridge abutment scour countermeasures.

Background and Problem Statement

Countermeasures for Pier Scour

The present study parallels an earlier study on countermeasures for bridge piers. The flow pattern around a pier and abutment have similar flow patterns in that both cause contraction scour, have a downward roller, side vortices, and vertical wake vortices. The countermeasures attempted for piers may also have applications for abutments. There have been studies on pier countermeasures by Lauchlan and Melville, 2001; Melville and Hadfield, 1999; Toro-Escobar et al., 1998; Melville et al., 1998; Richardson and Roberts, 1998; Shea and Ports, 1997; Burns et al., 1996; Bertoldi and Kilgore, 1993; Lewis, 1993; Richardson and Abed, 1993; Richardson and Wacker, 1991; Jones et al., 1995; Katsuya et al., 1989; and Richardson and York, 1989.

Fig. 1. Abutment scour at Muda River in Jediang, Malaysia (Photo courtesy of Shanker Kumar Sinnakaundan, River Engineering and Urban Drainage Research Center, Malaysia)

Flow around Abutments and Failure Mechanisms

In order to understand the mechanisms for abutment scour, it is first necessary to investigate the flow patterns as flow goes around an abutment. Most bridge abutments are in compound channels which are comprised of a main channel, in which flow would occur under non-flooding conditions, and a flood channel which is the over-bank area on either side of the main channel, in which flow occurs under flooding conditions.

The flow in compound open channels is an area of current research, but the present understanding is that the flow in the main channel is non-uniform, with a logarithmically-varying vertical velocity profile. This means slower velocities near the bed than near the water surface. In addition, the over-bank flow tends to be slower than the main channel velocities due to the higher roughness and lower flow depths.

When an abutment is introduced into this already-complicated flow field, vortices are formed that scour around the toe of the abutment and on the backside. Abutments come in various shapes and locations in the channel. Regardless of their extent into the channel, however, a vortex forms on the upstream side that has both a downward velocity and some lateral component. This is termed the downward flow/front vortex and can be associated with significant scour. As the flow turns the corner around the toe of the abutment a toe vortex forms that creates extensive scour. This is further exacerbated by the vertical wake vortex. Flow that is not involved in any of these vortices is returned from the over-bank areas into the main channel. This can lead to a contraction of the flow and subsequent flow acceleration. This acceleration can lead to what is termed "contraction scour" in the bed of the main channel (Richardson and Richardson, 1993a; Richardson and Richardson, 1993b).

If any of these scour events extend vertically below the abutment foundation, then collapse can result (Fig. 1).

Parola et al. (1998) document many observed abutment failures from which many of the above conclusions are based. Fischer has identified excessive contraction scour at several bridges in Iowa (Fischer, 1993, 1994, 1995, 1998).

There have been several studies to predict scour at bridge abutments. Principal among them are Melville (1992, 1997), Chang and Davis (1998), Kouchakzadeh and Townsend (1997, 1998), Melville (1995), Melville and Ettema (1993), Sturm (1998), Richardson and Richardson (1998), Hagerty and Parola (1992), Shen et al. (1993), Young et al. (1993, 1998), Sturm and Janjua (1993), Kheiraldin (1995), Sturm and Sadiq (1996), Dou et al. (1996), Sturm and Chrisochoides (1997, 1998a), Kohli and Hager (1997), and Molinas et al., (1998). While each of these studies has added some light to the subject, detailed design criteria need to be developed for existing and new countermeasures.

Armoring Countermeasures

One commonly-used scour countermeasure is the enhancement of the bed's ability to resist erosion. This method is referred to as armoring, since the top layer of the sediment is hardened like a suit of armor. Methods included in this category are riprap, dolos or tetrapods, tied mats (including gabions), and soil cement.

The placement of riprap at the base and side of abutments has been used extensively in river and coastal engineering (Gales, 1938; Quazi and Peterson, 1972; Neill, 1973; Posey, 1974; Hjorth, 1975; Breusers et al., 1977, Parola and Jones, 1991; Richardson et al., 1991; Parola, 1993; Chiew, 1992, 1994; Eve and Melville, 2000). Rip rap placed exclusively for abutment scour mitigation has been studied by Atayee et al. (1993), who give some guidelines for riprap at abutments, and Smith (1984) who gives details of a case history of riprap used to protect a bridge in Canada. Sela and Oliger (1993) note the over-prediction of scour by equations based on laboratory studies and give riprap placement guidelines. Atayee (1993) gives guidelines for riprap at spill-through abutments that allow some passage of water and, thereby, relieve the return flow and contraction scour. Failure mechanisms at riprap-protected abutments include (1) shear failure of armor units, (2) winnowing of parent material, (3) seepage erosion of parent material, and (4) edge failure. Shear failure occurs when the hydrodynamic forces of flow around the abutment are able to transport the riprap material. Winnowing and seepage forces occur when seepage and turbulence remove fine particles below the riprap. With the underlying material gone, the riprap settles. The use of a filter, for example a geotextile material, can reduce winnowing. Some riprap installations function well without a filter, however. The exact use of filters in riprap is one of the goals of the present study. Edge failure occurs when the edge pieces of riprap are eroded away due to a sudden change in roughness of the bed material. With the edge pieces gone, other pieces of riprap are susceptible to erosion as well. Edge erosion occurs when the lateral extent of the riprap is insufficient and the edge pieces are, therefore, in a region of high shear stress. Each of these failure mechanisms will be extensively studied in the present work and detailed design guidelines prepared to avoid failure by these and other failure mechanisms. See Figs. 2 and 3 for laboratory applications of riprap and cable-tied blocks.

Fig. 2. Failure of riprap on an abutment in a laboratory experiment (Eve, 2000).

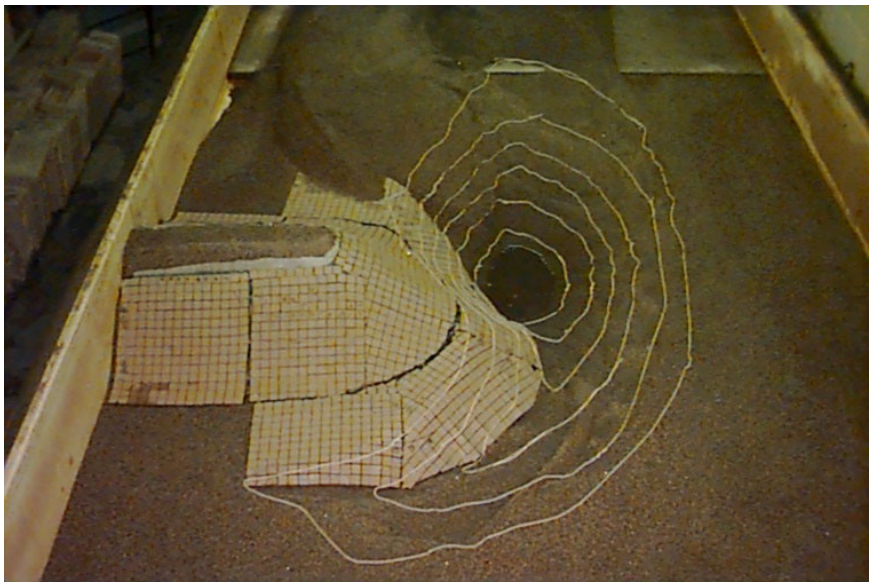

Figure 3: Laboratory test of spill-through abutment protection using cable-tied blocks, Hoe (2001)

Other methods that have been attempted for abutment scour mitigation are Toskanes, Tetrapods, reinforced soil, and tied mats. Burns et al. (1996) developed Toskanes as an alternative scour countermeasure where riprap is not feasible. Results of model studies and design guidelines are presented. Ruff et al. (1995) used Toskanes to protect bridge piers. Reinforced soil was used by Adams et al. (1999) for bridge abutments but they conclude that reinforced soil is not suitable for permanent bridges in scour zones.

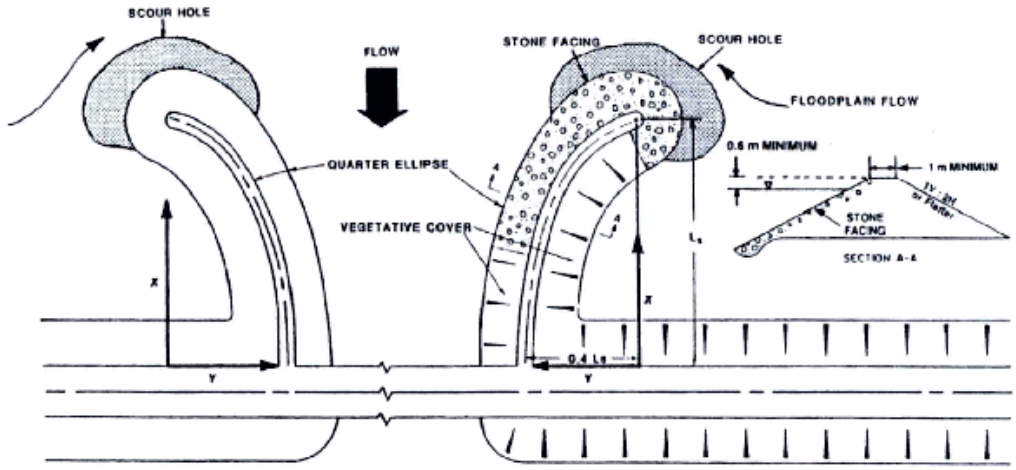

Fig. 4. Example of typical guide banks (from Lagasse et al., 2001).

Flow-altering Countermeasures

In contrast to countermeasures that armor the sediment surface, flow-altering countermeasures reduce the ability of the flow to scour sediment. Flow-altering countermeasures include guidebanks (Fig. 4), dikes or spurs (Fig. 5), to train the upstream river and in-channel devices such as vanes and bendway weirs. Although there have been many studies on spur dikes for river training (Kuhnle et al.,1997, 1998, and 1999; Farsirotou et al., 1998; Molinas et al., 1998; Zhang and Du, 1997; Soliman et al., 1997; Tominaga et al., 1997; Wu and Lin, 1993; Khan and Chaudry, 1992; Shields et al., 1991, 1995, and 1998; Molis et al., 1995; Mayerle et al., 1995; Muneta and Shimizu, 1994), the use of spur dikes specifically for use upstream of abutments was studied by Herbich (1967) using fixed-bed and movable-bed laboratory models and Richardson and Simons (1984) give design recommendations based on the literature. Lagasse et al., (1995) and Richardson et al. (1990) give design guidelines for impermeable and permeable spurs, guide banks, and riprap stability factor design. Richardson and Davis (1995) give guidelines for sizing rock riprap at abutments. Vanes have been used for erosion reduction on river bends (Ettema, 1990 and 1992; Odgaard and Kennedy, 1982; Odgaard and Kennedy, 1983; Odgaard and Lee, 1984; Odgaard and Mosconi, 1987; Odgaard and Spoljaric, 1986; Odgaard, Spoljaric, and Mosconi, 1988; Odgaard and Wang, 1990; Odgaard and Wang, 1990; Odgaard and Wang, 1991) and for reducing sediment ingestion in intakes (Barkdoll, Ettema, and Odgaard, 1999). They are small foils placed in the riverbed at an angle of attack to the flow, which creates a vortex downstream that can be used to manage sediment and alter flow.

Fig. 5. Spur dike on Goodwin Creek Experimental Watershed, Mississippi. Flow direction is from right to left.

Scale Effects

There is a widely held concern that laboratory studies on scour find greater scour depths than occur in full-scale situations. Sturm and Chrisochoides (1997) investigated scale effects for bridge abutments, but they used only two different scales. Ettema, Melville, and Barkdoll (1996), who focused on pier scour, also noted scale effects. They concluded that scale effects are significant and can be difficult to predict due to scale-related differences in strength of large-scale turbulence at piers and abutments. A set of experiments, entailing experiments over a wide range of scales, is needed to confirm the suspected scale effects.

Debris and Ice

Potential problems with debris and ice can plague hydraulic structures in general and may have implications for selection and design of abutment scour countermeasures in forested and/or cold regions.

Debris can collect on bridge piers and abutments and, if not cleared, can alter the flow characteristics considerably. Debris can also cause a type of contraction scour in which the flow area is constricted and, therefore, raises the flow velocity and correspondingly increases the scour of the bed. Studies addressing debris flow include Mueller and Parola, 1998; Parola et al., 1998; and Hagarty, Parola, and Fenske, 1995.

Ice runs and jams are the principal ice concern for bridges. Bridge abutments often serve as flow constrictions leading to ice jams. In this regard, ice and debris likely have similar effects on scour at bridge crossings. Ice may also freeze to and modify the performance of scour-protection systems, such as vanes, riprap (e.g., by plucking riprap stones), and fender structures. These actions of ice need careful consideration when

designing abutments for ice-prone rivers. In overall terms, little work has been done to determine on ice effects on scour at bridge abutments. The few prior studies concerning ice and local scour (e.g., Yankielun and Zabilansky (2000), Zabilansky 2000) have focused essentially on developing field instrumentation and on obtaining field measurements from a single bridge site. There is scope for considerable fundamental investigation into ice effects on scour at abutments.

The principle studies in the area of ice interaction with hydraulic structures are: Ettema, 1999; Ettema et al., 1999;Tan, Sinha, and Ettema, 1999; Streitz and Ettema, 1998; Ettema et al., 1998;Ettema et al., 1997a and b; Smith and Ettema, 1997a and b; Braileanu, Ettema, and Muste, 1997; Urroz and Ettema, 1994a, b, c, and d; Urroz, Schaefer, and Ettema, 1994; Teal, Ettema, and Walker, 1994a and b; Yoon and Ettema, 1993; Nixon, Ettema, Matsuishi, and Johnson, 1993; Braileanu, Ettema, and Wuebben, 1996; Chung, Howard, and Ettema, 1992; Yoon, Patel, and Ettema, 1992 and 1996; Tsai and Ettema et al., 1990; Ettema et al., 1991; Crissman, Ettema et. al., 1995; Ettema and Urroz-Aguirre, 1991; Jain and Ettema, 1989; Ettema et al., 1989; Schaefer, Ettema, and Nixon, 1989; Stern, Ettema, and Lazaro, 1989; Nixon and Ettema et al., 1989; Teal and Ettema, 1994; Ettema et al., 2000.

ABUTMENT SCOUR COUNTERMEASURE STUDY

This review of existing countermeasures is part of an ongoing study funded by the National Cooperative Highway Research Program of the Transportation Research Board. At the writing of this paper, Project NCHRP 24-18 is finishing Phase I in which all existing information was gathered, each state Department of Transportation was surveyed as to their abutment scour countermeasure experiences, and countermeasures worthy of further laboratory study were identified. Phase II will include laboratory experiments to guide in the formation of design guidelines for selected abutment scour countermeasures.

REFERENCES

1. Adams, M., Ketchart, K., Ruckman, A., DiMillio, A.F., Wu, J., and Satyanarayana, R. (1999). "Reinforced soil for bridge support applications on low-volume roads." Transportation Research Record, *Proc. 7th Int. Conf. On Low-Volume Roads*, p. 150.
2. Atayee, A.T., Pagan-Ortiz, J.E., Jones, J.S., and Kilgore, R.T. (1993). "Study of riprap as scour protection for bridge abutments." *Proc. Conf. Hydraulic Engrg*, Part 1, ASCE, p.973.
3. Austroads (1994) "Waterway design - A guide to the hydraulic design of bridges, culverts and floodways," Austroads, Sydney, Australia, 139pp.
4. Barkdoll, B.D., Ettema, R., and Odgaard, A.J. (1999). "Sediment control at lateral diversion: limits and enhancements to vane use." *J. Hydraulic Engrg*, Vol. 125, No. 8, Aug 1999, ASCE, p. 862.
5. Bertoldi, D. and Kilgore, R. (1993). "Tatrapods as a scour countermeasure." *Proc. Nat. Conf. Hydraulic Engrg*, ASCE, p.1385.
6. Biglari, B. and Sturm, T.W. (1998). "Numerical modeling of flow around bridge abutments in compound channel." *J. Hydraulic Engrg*, v 124 n 2 Feb 1998, ASCE, p. 156.
7. Blodgett, J.C. and McConaughy, C.E. (1985) "Evaluation of rock riprap design practices for protection of channels near highway structures - Phase I," Preliminary Report subject to revision, prepared by the U.S. Geological Survey in cooperation with Federal Highway Administration.
8. Braileanu, F., Ettema, R., and Muste, Marian (1997). "Laboratory study of suspended-sediment transport in ice-cover flow." *Congr. Int. Assoc. of Hydraulic Research, IAHR*. Part B-2 v B pt 2 ASCE p 1239

9. Braileanu, F., Ettema, R., and Wuebben, (1996). "Evaluation of flow resistance in ice-covered channels." *Proc. 1996 8th Int. Conf. Cold Regions Engrg* Aug 12-16 1996 ASCE p 606
10. Breusers, H.N.C. and Raudkivi, A.J. (1991). "Scouring." *IAHR Hydraulic Structures Design Manuel 2*, IAHR.
11. Breusers, H.N.C., Nicollet, G., and Shen, H.W. (1977). "Local scour around cylindrical piers*." J. Hydraulic Resrch.*, 15(3), p.211.
12. Brown, S.A. and Clyde, E.S. (1989) "Design of riprap revetment," Hydraulic Engineering Circular 11 (HEC-11), Report No. FHWA-IP-89-016, Federal Highway Administration, U.S. Department of Transportation, Washington, D.C., U.S.A.
13. Burns, R.S., Fotherby, L.M., Ruff, J.F., and Carey, J.M. (1996) "Design example for bridge pier scour measures using Toskanes." *Transportation Research Record* n 1523 Nov 1996 p 173
14. Central Board of Irrigation and Power (1989) "River behaviour management and training," edited by C.V.J. Sharma, K.R. Saxema and M.K. Rao, Publication No. 204, Vol. 1, Central Board of Irrigation and Power, New Delhi, India, 469pp.
15. Chang, F. and Davis, S. (1998). "Maryland SHA procedure for estimating scour at bridge abutment; Part 1 and 2." *Conf. Proc. Hydraulic Engrg*, 1998, ASCE p. 169.
16. Chiew,Y.M.(1992)."Scour protection at bridge piers." *J.Hydr. Engrg*., ASCE, 118(9), p. 1260.
17. Chiew, Y.M. (1995) "Mechanics of riprap failure at bridge piers," Journal of Hydraulic Engineering, A.S.C.E., 121(9), 635-643.
18. Chiew, Y.M. (1994). "Riprap protection around a bridge pier*." Proc. 9th Congr. APD of IAHR*, 24-26 August, Singapore, Vol.2 p.11.
19. Chung, P.Y., Howard, W.S., Ettema, R. (1992). "Innovative intake design for Raritan river." 1992 *Nat. Conf. Environmental Engrg* - Water Forum '92 Aug 2-6 1992 ASCE p 220
20. Crissman, R.D., Ettema, R., Andres, D., and Carson, R. (1995). "Ice jamming in upper Niagara River: processes and plan of study." J. *Cold Regions Engrg* v9 n2 Jun 1995 ASCE p 89
21. Croad, R.N. (1989) "Investigation of the pre-excavation of the abutment scour hole at bridge abutments," Report 89-A9303, Central Laboratories, Works and Development Services Corporation (NZ) Ltd., Lower Hutt, New Zealand, 38pp.
22. Dou, X, Jia, Y., and Wang, S.Y. (1996). "Numerical simulation of bridge abutment scour development." *Conf. Proc. Hydraulic Engrg*, 1996, Session BS-18.
23. Dou, X., Jones, J.S., Young, G.K., and Stein, S.M. (1998) "Using a 3-D model to predict local scour." *Proc. Int. Water Resources Engrg Conf*. Part 1 (of 2), ASCE p. 198.
24. Escarameia, M. (1995) "Channel protection – Gabion mattresses and concrete blocks," Report SR 427, HR Wallingford, Oxfordshire, U.K.
25. Escarameia, M. and May, R.W.P. (1982) "Channel protection – Turbulence downstream of structures," Report SR 313, HR Wallingford, Oxfordshire, U.K.
26. Ettema, R. (1990). Hydraulic model studies of circulating-water and essential-service-water pump-intake structures, Korea Electric Power Corporation Yonggwang Station, Units 3 and 4. IIHR Limited Distribution Report No. 173
27. Ettema, R. (1992). Enhanced performance and reliability of water intakes for generating stations. Proposal of Iowa Institute of Hydraulic Research to Electric Power Research Institute
28. Ettema, R. (1999). "Loose-bed issues in river-ice hydraulics." *Proc. Int. Conf. on Cold Regions Engrg 'Putting Research Into Practice'* ASCE, p 588
29. Ettema, R., Braileanu, F., and Muste, M. (2000). "Method for estimating sediment transport in ice-covered channels." *J. Cold Regions Engrg* v14 n3 Sep 2000 ASCE p 130
30. Ettema, R., Fujita, I., Muste, M., and Kruger, A. (1997a). "Particle-image velocimetry for ice-field velocities."*Proc. 1997 27th Congr. Int. Assoc. Hydr. Resrch*, IAHR. Part B-1 vB pt 1 ASCE p 137
31. Ettema,R., Fujita, I., Muste, M., Kruger, A. (1997b). "Particle-image velocimetry for whole-field measurement of ice velocities." *Cold Regions Science and Technology* v 26 n 2 Oct 1997 p 97
32. Ettema, R., Melville, B.W., and Barkdoll, B.D. (1998). "Scale effect in pier-scour experiments*." J. Hydraulic Engrg*., Vol. 124, No. 6, ASCE, p. 639.
33. Ettema, R., Muste, M, and Kruger, A. (1999). "Ice jams in river confluences." *CRREL Report n99-6* May 1999 p 70.
34. Ettema, R.; Schaefer, J.A.; Huang, H.P (1998). "Ice-tank data on brash-ice loads against barges." *J. Cold Regions Engrg* v 12 n 3 ASCE p 153.

35. Ettema, R., Sharifi, M.B., Georgakakos, K.P., and Stern, F. (1991). "Chaos in continuous-mode icebreaking." *Cold Regions Science and Technology* v 19 n 2 May 1991 p 131
36. Ettema, R., Stern, F., and Lazaro, J. (1989). "Dynamics of continuous-mode icebreaking by a polar-class hull. part 1. mean response." *J. Ship Research* v 33 n 2 Jun 1989 p 115
37. Ettema, R., Urroz-Aguirre, G.E. (1991). "Friction and cohesion in ice rubble reviewed." *Cold Regions Engrg Sixth Int. Cold Regions Engrg Conf.* ASCE, p 316
38. Ettema, R. Zabilansky, L. and Bledsoe, B., (2000). "Ice-induced thalweg oscillations along the Fort Peck Reach of the Missouri River." ASCE Water Resources Conference, Minneapolis, MN.
39. Eve, N. (2000) "Riprap protection at bridge abutments," Thesis submitted in partial fulfilment of the requirements for the degree of Master of Engineering, The University of Auckland, Auckland, New Zealand, 163 pp.
40. Eve, N.J. and Melville, B.W. (2000). "Riprap protection of bridge abutments under clear water conditions," ASCE, *Proc. Conf. Water Resources Engrg and Water Resources Planning and Management*, Minneapolis.
41. Farabee, G.B. (1986)"Fish species associated with revetted and main channel border habitats in Pool 24 of the Upper Mississippi River," N. American J. of Fisheries Management 6, 504-508.
42. Farraday, R.V. and Charlton, F.G. (1983) "Hydraulic factors in bridge design," Hydraulics Research Station, Wallingford, England, 102pp.
43. Farsirotou, E.D., Soulis, J.V., and Dermissis, V.D. (1998). "Two-dimensional, multi-grid, viscous, free-surface flow calculation." *Proc. 1998 7th Int. Conf. Hydraulic Engrg. Software*, HYDROSOFT, p 13.
44. Fischer, E.E. (1993). "Scour at a bridge over the Weldon River, Iowa." *Conf. Proc., Hydraulic Engrg '93*, Vol. 2, ASCE, Reston, VA, pp. 1854-9.
45. Fischer, E.E. (1994). "Contraction Scour at a Bridge over the Iowa River." *Conf. Proc., Hydraulic Engrg '94*, Vol. 1, ASCE, Reston, VA, pp. 31-5.
46. Fischer, E.E. (1995). "Contraction Scour at a Bridge over Wolf Creek, Iowa." *Conf. Proc., Hydraulic Engrg '95*, Vol. 1, ASCE, Reston, VA, pp. 430-4.
47. Forchheimer, P. (1914) "Hydraulik," Teubner, Leipzig/Berlin.
48. Gales,R.R. (1938). "The principles of river training for railway bridges, and their application to the case of the Harding Bridge over the Lower Ganges at Sara." *J. Inst. of Civil Engrgs* (UK), 10(2), p.136.
49. Gregorius, B.H. (1985) "Waterway design procedures - Guidelines," Civil Division Publication, Ministry of Works and Development, Hamilton, New Zealand, 57pp.
50. Hagerty, D.J. and Parola, A.C. (1992). "Seepage influence on stability of bridge abutments." *Conf. Proc. Hydraulic Engnrg*, 1992, ASCE, p. 900
51. Hagerty, D.J., Parola, A.C., and Fenske, T.E. (1995). "Impacts of the 1993 Upper Mississippi River Basin floods on highway systems," *Proc. 74th Ann.Mtg*., TRB.
52. Herbich, J.B. (1967). "Prevention of scour at bridge abutments." *Proc. 12th Congr. Int. Assoc. Hydraulic Resrch*., p.74.
53. Harris, J.D. (1988) "Hydraulic design of bridges," Chapter I, MTC Drainage Manual, Drainage and Hydrology Section, Ontario Ministry of Transportation, Downsview, Ontario, Canada.
54. Hjorth,P. (1975). "Studies of the nature of local scour." *Bulletin Series A,* No. 46, Dept. of Water Resources Engineering, Univ. of Lund, Sweden.
55. Hoe, D. (2001) "Cable-tied block protection of bridge abutments," Fourth Year project in Resource Engineering, Department of Civil and Resource Engineering, The University of Auckland, Auckland, New Zealand.
56. Hudson, K. and East, G.R.W. (1991) "Geo-textiles," Transit New Zealand Research Report, Wellington, New Zealand.
57. Isbash, S.V. (1935) "Construction of dams by dumping stones in flowing water," A. Dovjikov, translator, War Department, U.S. Engineer Office, Engineering Division, Eastport, Me.
58. Isbash, S.V. (1936) "Construction of Dams by Depositing Rock on Running Water" Trans. 2nd Congress on Large Dams, Vol. 5, Washington, D.C. 1936, pp. 123-135.
59. Jain, S.C. and Ettema, R. (1989). "Minimization of frazil-ice production by river-flow regulation." *J. of Hydraulic Engrg* v 115 n 9 Sep 1989 p 1256
60. Jones, J. S., Bertoldi, D., Stein, S. (1995). "Alternative scour countermeasures." *Proc. 1st Int. Conf. Water Resources*. Part 2 (of 2) Aug 14-18 1995 v2 1995 ASCE p 1819

61. Khan, K.W.; Chaudhry, M.H. (1992) "Numerical modelling of flow around spur dikes." *Proc.4 Int Conf Hydraul Eng Software HYDROSOFT/92 p 223*.
62. Kheiraldin, K.A. (1995). "Scour at bridge abutments." *Conf. Proc. Water Resources Engrg*, 1995, ASCE, p.1829.
63. Kohli, A. and Hager, W.H. (1997). "Building scour in floodplains." *Conf. Proc. Hydraulic Engrg*, 19937 ASCE p. 214.
64. Kouchakzadeh, S. and Townsend, R.D. (1997). "Influence of lateral momentum transfer on bridge abutment scour." *Conf. Proc. Hydraulic Engrg.*, 1997, ASCE, p.190.
65. Kouchakzadeh, S. and Townsend, R.D. (1998). "Bridge abutment scour in compound-shaped river channels." *Stream Stability and Scour at Highway Bridges*, ASCE Reston, VA pp. 417.
66. Kuhnle, R.A., Alonso, C.V., Shields,F.D. (1997). "Volume of scour holes associated with spur dikes." *Proc. 1997 27th Cong. Int. Assoc. Hydraulic Research*. Part B-1, v B pt, p.418.
67. Kuhnle, R. A.; Alonso, C.V., Shields, F.D. (1998). "Volume of scour holes for angled spur dikes." *Proc. 1998 Int. Water Resources Engrg Conf*. Part 2 (of 2) v 2 1998, ASCE, p .1613.
68. Kuhnle, R. A.; Alonso, C.V., Shields, F.D. (1999). "Geometry of scour holes associated with 90-degree spur dikes." *J. Hydraulic Engrg* v 125 n 9 Sep, 1999, ASCE, p.972.
69. Lagasse, P.F, Schall, J.D., Johnson, F., Richardson E.V., and Chang, F. (1995) "Stream Stability at Highway Structures." *Report No. FHWA IP-90-014, HEC-20, FHWA*.
70. Lagasse, P.F., Byars, M.S., Zevenbergen, L.W., and Clopper, P.E. (1997). "Bridge scour and stream instability countermeasures*." FHWA HI-97-030 HEC-23, FHWA.*
71. Lauchlan, C.S. (1999) "Pier Scour Countermeasures" Ph.D. thesis, The University of Auckland, Auckland, New Zealand.
72. Lauchlan, C.S. and Melville, B.W. (2001) "Riprap protection at bridge piers," Journal of Hydraulic Engineering, ASCE, 127(5), 412-418.
73. Lewis, G.L. (1993). "Shale scour at BNRR Yellowstone River Bridge, MT." *Proc. Nat. Conf. on Hydraulic Engrg* Jul 25-30 1993 npt 2 1993 ASCE p 2255
74. Lim, F.H. and Chiew, Y.M. (1997) "Stability of riprap layer under live-bed conditions," Conference on Management of Landscapes disturbed by Channel Incision, Oxford, Mississippi, U.S.A., May.
75. Mayerle, R.; Toro, F.M.; Wang, S.S.Y.(1995)."Verification of a three-dimensional numerical model simulation of the flow in the vicinity of spur dikes." *J. Hyd.r Research* v33 n2 1995 p 243.
76. McCorquodale, J.A., Moawad, A. and McCorquodale, A.C. (1993)"Cable tied block erosion protection," Hydraulic Eng. 93, ASCE conference, San Francisco, California, pp.1367-1373.
77. Macky, G.H. (1986) "Model testing of bridge abutment scour protection," Report 3-86/12, Central Laboratories, Ministry of Works and Development, Lower Hutt, New Zealand, pp62.
78. Maynord, S.T. (1987) "Stable riprap size for open channel flows," Ph.D. thesis, Department of Civil Engineering, Colorado State University.
79. Maynord, S.T. (1988) "Stable riprap size for open channel flows," Technical Report HL-88-4, U.S. Army Engineer Waterways Experiment Station, Vicksburg, Miss.
80. Maynord, S.T. (1993) "Flow impingement, Snake River, Wyoming," Technical Report HL-93-9, U.S. Army Engineer Waterways Experiment Station, Vicksburg, Miss.
81. Maynord, S.T., Ruff, J.F. and Abt, S.R. (1989) "Riprap design," Journal of Hydraulic Engineering, ASCE, 115(7), 937-949.
82. Melville, B.W. (1992). "Local scour at bridge abutments." *J. Hydr, Engrg*., ASCE, 118(4), p. 615.
83. Melville, B.W. (1995). "Bridge abutment scour in compound channels." *J. Hydr, Engrg*., ASCE, 121(12), p. 863.
84. Melville, B.W. (1997) "Pier and Abutment Scour: An Integrated Approach", Journal of Hydraulic Engineering, ASCE, 123(2), 125-136, February 1997.
85. Melville, B.W. and Coleman, S.E. (2000). *Bridge Scour*, Water Resources Publications.
86. Melville, B.W. and Ettema, R. (1993). "Bridge abutment scour in compound channels." *Conf. Proc. Hydraulic Engnrng*, 1993, ASCE p. 767.
87. Melville, B.W. and Hadfield, A.C.; (1999). "Use of sacrificial piles as pier scour countermeasures*." J. Hydraulic Engrg* v125 n11 1999 ASCE p 1221
88. Melville, B.W., Hadfield, A.C., and Lauchlan, C.S.; *Proc. 1998 Int. Water Resources Engrg Conf*. Part 1 (of 2) Aug 3-7 v 1 1998 Memphis, TN, USA, Sponsored by : ASCE p 39

89. Melville, B.W. and Parola, A.C. (1995). "The need for additional abutment scour research." *Proc. 1st Int. Conf. Water Resources Engrg*, ASCE, San Antonio, Texas, p. 1239.
90. Ministry of Works and Development (1979) "Code of practice for the design of bridge waterways," Civil Division Publication CDP 705/C, Ministry of Works and Development, Wellington, New Zealand, 57pp.
91. Molinas, A., Kheireldin, K., Wu, and Baosheng (1998). "Shear stress around vertical wall abutments*." J. Hydraulic Engrg*, v 124 n 8 Aug 1998 ASCE, p.822.
92. Molinas, A., Reiad, N.G.Y., and Jones, S. (1998). "Effect of cohesion on abutment scour." *Conf. Proc. Water Resources Engrg*, 1998, ASCE p. 252.
93. Molis, I.; Chaudhry, M. Hanif; Khan, K. Wasey (1995) "Numerical simulation of two-dimensional flow near a spur-dike." *Advances in Water Resources* v18 n4 1995 p. 227.
94. Mueller, D.S. and Parola, A.C. (1998). "Detailed scour measurements around a debris accumulation." *Proc. 1998 Int. Water Resources Engrg Conf*. Part 1 (of 2) Aug 3-7 1998 v 1, ASCE p 234
95. Muneta and Shimizu, 1994 "Numerical analysis model with spur-dike considering the vertical flow velocity distribution "*Proc. Japan Soc. of Civil Engrg* n 497 pt 2-2 1994 p. 31.
96. Neill, C.R. (1967) "Mean velocity criterion for scour of coarse uniform bed material", 12th IAHR Congress, Fort Collins, Colorado, Proc. Vol. 3, C6.1 - C6.9.
97. Neill, C.R. (1973). "*Guide to bridge hydraulics*." Roads and Transportation Assoc. of Canada, Univ. of Toronto Press, Toronto, Canada.
98. Nixon, W.A., Ettema, R., Matsuishi, M., and Johnson, R.C. (1993). "Model study of cable-moored conical platform." *J. Cold Regions Engrg* v 7 n 1 Mar 1993 p 12
99. Nixon, W.A., Ettema, R., Matsuichi, M., and Johnson, R.C. (1989). "Model study of a cable-moored platform in sheet ice." *Proc. Eighth Int. Conf. Offshore Mechanics and Arctic Engrg* - 1989 Mar 19-23 v 4 n 8 1989 ASME, p 459
100. Odgaard, A.J. and Kennedy, J.F. (1982). Analysis of Sacramento River bend flows, and development of a new method for bank protection. IIHR Report No. 328, Iowa Institute of Hydraulic Research,
101. Odgaard, A.J. and Kennedy, J.F. (1983). "River-bend bank protection by submerged vanes." J. Hydraulic Engrg, A.S.C.E., 109(8), 1161-1173.
102. Odgaard, A.J. and Lee, H.Y.E. (1984). Submerged vanes for flow control and bank protection in streams. IIHR Report No. 279, Iowa Institute of Hydraulic Research
103. Odgaard, A.J. and Mosconi, C.E. (1987) "Streambank protection by submerged vanes." J. Hydraulic Engrg, A.S.C.E., 113(4), 520-536.
104. Odgaard, A.J. and Spoljaric, A. (1986). "Sediment control by submerged vanes." J. Hydraulic Engrg, ASCE, 112(12), 1164-1181.
105. Odgaard, A.J., Spoljaric, A., and Mosconi, C.E. (1988). A new marketable structure for streambank protection. IIHR Report No. 145, Iowa Institute of Hydraulic Research
106. Odgaard, A.J. and Wang, Y. (1990). Sediment control in bridge waterways. IIHR Report No. 336, Iowa Institute of Hydraulic Research
107. Odgaard, A.J. and Wang, Y. (1990). Hydraulic-laboratory model study of river intake at Duane Arnold Energy Center. IIHR Limited Distribution Report No. 177, Iowa Inst. of Hydraulic Resrch
108. Odgaard, A.J. and Wang, Y. (1991). "Sediment management with submerged vanes. I: theory." J. Hydraulic Engrg, ASCE, 117(3), 267-283.
109. Okada, K., Muraishi, H., and Kunihiro, T. (1989). "Statistical judgement about stability of protection against scour around pier." Proc. *Japan Soc. Civil Engnr* n 403 pt 6-10 Mar 1989 p 65
110. Pagan-Ortiz, J.E. (1991) "Stability of rock riprap for protection at the toe of abutments located at the flood plain," Report No. FHWA-RD-91-057, Federal Highway Administration, U.S. Department of Transportation, Washington, D.C., U.S.A.,125 pp.
111. Parker, G., Parola, A.C., Chiew, M., and Melville, B.W. (1989). "Countermeasures to protect bridge piers from scour." *NCHRP Report*, Transportation Research Board.
112. Parker, G., Toro-Escobar, C. and Voigt, R.L., Jr. (1998) "Countermeasures to protect bridge piers from scour," Final Report (Project NCHRP 24-7) prepared for National Co-operative Highway Research Program, University of Minnesota, Minneapolis, Minnesota, U.S.A., 402pp.
113. Parola, A.C. (1993)."Stability of riprap at bridge piers."*J. Hydr.c Engrg*, ASCE,119(10)p. 1080.

114. Parola, A. C., Hagerty, D. J., and Kamojjala, S. (1998). "NCHRP 12-39: Highway Infrastructure Damage Caused by the 1993 Upper Mississippi River Basin Flooding." *National Research Council, Transportation Research Board 1483,* Washington, DC.
115. Parola, A.C., Hagarty, D.J., and Fenske, T.E. (1994). "Damage to highway infrastructure—1993 Mississippi River basin flooding." *Proc. ASCE Nat. Conf. on Hydraulic Engrg*, p.26.
116. Parola, A.C., Kamojjala, S., Richardson, J.E., and Kirby, M.W. (1998). "Numerical simulation of flow patterns at a bridge with debris." *Proc. Int. Water Resources Engrg Conf.* Part 1 (orf 2), ASCE, p.240.
117. Pilarczyk, K.W. (1990) "Coastal protection," Short Course on Coastal Protection, Delft University of Technology, Balkema, Rotterdam, The Netherlands.
118. Posey, C.J. (1974). "Test of scour protection at bridge piers." *J. Hydraulic Engrg*., ASCE, 110(12), p.1773.
119. Pzedwojski, B., Blazejewski, R. And Pilarczyk, K.W. (1995) "River training techniques," A.A. Balkema, Rotterdam, The Netherlands.
120. Quazi, M.E. and Peterson, A.W. (1972). "A method of bridge pier riprap design." *Proc. First Canadian Hydraulics Conf.*, Univ. of Alberta, Edmonton, Canada, p.96.
121. Richardson, E.V. and Abed, L. (1993). "Top width of pier scour holes in free and pressure flow." *Proc. 1993 Nat. Conf. Hydraulic Engrg*. Part 1 (of 2) Jul 25-30 1993 npt 1 1993 ASCE p 911
122. Richardson, E.V. and Davis, S.R. (1995). "Evaluating Scour at Bridges." *Publication No. FHWA HI-96-031, HEC 18, FHWA.*
123. Richardson, E.V. and Davis, S.R. (1995) "Evaluating scour at bridges," Report No. FHWA-IP-90-017, Hydraulic Engineering Circular No. 18 (HEC-18), Third Edition, Office of Technology Applications, HTA-22, Federal Highway Administration, U.S. Department of Transportation, Washington, D.C., U.S.A., November, 204pp.
124. Richardson, E.V., Simons, D.B. and Julien, P.Y. (1988) "Highways in the river environment," Federal Highway Administration, U.S. Department of Transportation, Washington, D.C., U.S.A.
125. Richardson, E.V., Harrison, L.J., and Davis, S.R. (1991). "Evaluating scour at bridges." *Report No. FHWA-IP-90-017 HEC 18*, Federal Highway Administration (FHWA), Washington, D.C.
126. Richardson, J.R. and Richardson, E.V. (1993a) Discussion of "Local scour at bridge abutments," by B.W. Melville, *J. Hydr. Engrg*., ASCE, 119(9), 1069-71.
127. Richardson and Richardson (1993a), "The fallacy of local abutment scour equations." *Conf. Proc. Hydraulic Engng*, 1993, ASCE, p. 749.
128. Richardson, J.R. and Richardson, E.V. (1993b) "Determining contraction scour." *Stream Stability and Scour at Highway Bridges*, ASCE Reston, VA pp. 483-91.
129. Richardson, J.R. and Roberts, D.L. (1998). "Non-structural method to reduce local pier scour." *Proc. 1998 Int. Water Resources Engrg Conf.* Part 1 (of 2) Aug 3-7 1998 v 1 1998 Memphis, TN ASCE p 768
130. Richardson, E.V. and Simons, D.B. (1984). "Use of spurs and guidebanks for highway crossing.: *Proc. Transportation Research Record 2nd Bridge Engrg. Conf.* v2 p.184.
131. Richardson, J.R. and Wacker, A.M. (1991). "Bridge scour and stream instability countermeasures." *Proc. 1991 Nat. Conf. Hydraulic Engrg* Jul 29-Aug 2 1991 1991 Nashville, TN, ASCE p 317
132. Richardson, J.R. and York, K. (1999). "Hydrodynamic countermeasures for local pier scour." *Transportation Research Record* n1690 1999 p 186
133. Ruff, J.F., Fotherby, L.M., and Burns, R.S. (1995). "Bridge pier scour protection using Toskanes." *Proc. 1st Int. Conf. Water Resources*. Part 2 (of 2), ASCE p 1167.
134. Schaefer, J.A., Ettema, R., Nixon, W.A. (1989). "Measurements of icing hardness." *Cold Regions Science and Technology* v 17 n 1 Sep 1989 p 89
135. Sela, E. and Oligar, G.R. (1993). "In-depth scour evaluations for bridges in Pennsylvania." *Proc. 1993 Nat. Conf. on Hydraulic Engrg*. Part 1 (of 2), ASCE, p. 525.
136. Shea, C. and Ports, M. (1997). "Physical and computational modeling of bridge scour at Oregon inlet, North Carolina." *Proc. 1997 27th Congr. Int. Asso. Hydraulic Research, IAHR*. Part A Aug 10-15 1997 v A 1997 San Francisco, CA, ASCE p 220
137. Shen, H.W., Chan, C.T., Lai, J.S., and Zhao, D. (1993). "Flow and scour near an abutment." *Conf. Proc. Hydraulic Engnrng*, 1993, ASCE p. 743.

138. Shields, F.D., Cooper, C.M., and Testa, Samuel, III. (1995) "Towards greener riprap: Environmental considerations from microscale to macroscale," River, coastal and shoreline protection, erosion control using riprap and armourstone, C. R. Thorne, S. R. Abt, F. B. J. Barends, S. T. Maynord, and K. W. Pilarczyk, eds., John Wiley, New York, 557-574.
139. Shields, F.D. Jr.; Knight, S.S.; Cooper, C.M.; "Rehabilitation of watersheds with incising channels." *Water Resources Bulletin* v31 n6 Dec 1995 p 971.
140. Simons, D.B. and Lewis, G.L. (1971) "Report - flood protection at bridge crossings," prepared for the Wyoming State Highway Department in conjunction with the U.S. Department of Transportation, C.S.U. Civil Engineering Report No. CER71-72DBS-GL10.
141. Smart, G.M. (1990) "Riprap scour protection: Practices for New Zealand roads," DSIR, Hydrology Centre, Christchurch.
142. Smith, C.D. (1984). "Scour control at Outlook Bridge – a case study." *Canadian J. Civil Engrg*, v 11 n 4 Dec 1984 p. 709.
143. Smith, B.T.; Ettema, R. (1997a). "Ice-cover influence on flow structure over dunes." *J. Hydraulic Resrch* v 35 n 5 1997 p 707
144. Smith, B.T.; Ettema, R. (1997b). "Flow resistance in ice-covered alluvial channels." *J. Hydraulic Engrg* v 123 n 7 July 1997 ASCE p 592
145. Soliman, M.M., Attia, K.M., Kotb, Talaat, A.M., and Ahmed, A.F. "Spur dike effects on the river Nile morphology after high Aswan dam." *Proc., Cong. Int. Assoc.Hydraulic Research*, Part v A 1997 p 805.
146. Sousa Pinto, N.L. de (1959) "Riprap protection against scour around bridge piers," Masters thesis, University of Iowa, Iowa City, Iowa, U.S.A.
147. Spring, F.J.E. (1903) "River training and control of the guide bank system," Technical Paper No. 153, Railway Board, Government of India, New Delhi.
148. Stevens, M.A. and Simons, D.B. (1971) "Stability analysis for coarse granular material on slopes," Chapter 17 in Shen, H.W. (ed.), 1971, River Mechanics Water Resources Publications, Fort Collins, Colorado.
149. Stevens, M.A., Simons, D.B. and Lewis, G.L. (1976) "Safety factors for riprap protection," Journal of the Hydraulics Division, ASCE, 102(HY5), 637-655.
150. Streitz, J. and Ettema, R. (1998). "Tiltable windtunnel for investigating icing of planar surfaces." *Proc. 1998 9th Int. Conf. on Cold Regions Engrg*, ASCE, p 447.
151. Stern, F., Ettema, R., and Lazaro, J. (1989). "Dynamics of continuous-mode icebreaking by a polar-class hull. part 2. Spectral analysis." *J. Ship Research* v 33 n 3 Sep 1989 p 236
152. Sturm, T.W. (1998). "Abutment scour in compound channels." *Stream Stability and Scour at Highway Bridges*, ASCE Reston, VA, pp. 443.
153. Sturm, T.W. and Chrisochoides, A. (1997). "Local scaling of bridge abutment scour in compound channels." *Conf. Proc. Hydraulic Engnrng*, 1997, ASCE p. 196.
154. Sturm, T.W. and Chrisochoides, A. (1998a). "Abutment scour in compound channels for variable setbacks." *Conf. Proc. Water Resources Engnrng*, 1998, ASCE p. 174.
155. Sturm, T.W. and Chrisochoides, A. (1998b). "One-dimensional and two-dimensional estimates of abutment scour prediction variables." *Transportation Research Record* n 1647 Nov 1998 p. 18.
156. Sturm, T.W. and Janjua, N.S. (1993). "Bridge abutment scour in a floodplain." *Conf. Proc. Hydraulic Engnrng*, 1993, ASCE p. 761.
157. Sturm, T.W. and Sadiq, A. (1996). "Bridge abutment scour in floodplain with backwater." *Conf. Proc. Hydraulic Engnrng*, 1996, ASCE, Session BS-5.
158. Tan, C.A., Sinha, S.K., and Ettema, R. (1999). "Ice-cover influence on near-field mixing in dune-bed channel: numerical simulation." *J.Cold Regions Engrg* v 13 n 1 Mar 1999 ASCE p 1.
159. Teal, M.J.; Ettema, R. (1994)."Estimation of mean velocity for flow under ice cover." *Proc. Symp. Fundamentals and Advancements in Hydraulic Measurements Experimentation* ASCE p 242
160. Teal, M.J.; Ettema, R., and Walker, J.F (1994a). "Estimation of mean flow velocity in ice-covered channels.; *J. Hydraulic Engrg* v120 n12 Dec 1994 ASCE p 1385
161. Teal, M.J.; Ettema, R., and Walker, J.F (1994b) "Estimation of mean flow velocity in ice-covered channels." *J. Hydraulic Engrg* v120 n12 Dec 1994 ASCE p 1385
162. Thorne, C.R., Abt, S.R. and Maynord, S.T. (1995) "Prediction of near-bank velocity and scour depth in meander bends for design of riprap revetments," River, coastal and shoreline protection:

Erosion control using riprap and armourstone, C. R. Thorne, S. R. Abt, F. B. J. Barends, S. T. Maynord, and K. W. Pilarczyk, eds., Wiley, New York, 115-133.

163. Tominaga, A., Nagao, M., and Nezu, I (1997). "Flow structures and mixing processes around porous and submerged spur dikes." *Proc. 27th Congress of the Int. Assoc. of Hydraulic Resrch*., IAHR. Part B-1 v B pt 1 p 251.

164. Toro-Escobar, C., Voigt, R., and Parker, G. (1998). "Cable-tied blocks as an alternative for protecting bridge piers against scour under mobile-bed conditions." *Proc. 1998 Int. Water Resources Engrg Conf.* Part 1 (of 2) Aug 3-7 1998 v 1 1998 Memphis, TN ASCE p 15

165. Tsai, Whey-Fone; Ettema, R., Wang, S.L., Shih, L.Y., Hsiung, G.C., Hazell, C.R., Wortley, C. A. (1990) "Mathematical modelling of icebreaking pattern based on the elastic wave theory." *IAHR – Symp. Ice 1990* Aug 20-24 1990 Helsinki Univ of Technology p 811

166. Urroz, G.E. and Ettema, R. (1994a). "Ice accumulation rate and the geometry of ice jams in river bends." *Proc. 1994 ASCE Nat. Conf. Hydraulic Engrg*, p 386

167. Urroz, G.E. and Ettema, R. (1994b). "Application of two-layer hypothesis to fully developed flow in ice-covered curved channels." *Canadian J. Civil Engineering* v 21 n 1 Feb 1994 p 101

168. Urroz, G.E.;Ettema, R. (1994c). "Small-scale experiments on ice-jam initiation in a curved channel." *Canadian J. Civil Engrg* v21 n5 Oct 1994 p 719

169. Urroz, G.E. and Ettema, R. (1994d). Small-scale experiments on ice-jam initiation in a curved channel" Canadian J. Civil Engrg v21 n5 Oct 1994 p 719

170. Urroz, G.E.; Schaefer, J., and Ettema, R. (1994). Bridge-pier location and ice conveyance in curved channels; *J. Cold Regions Engnrg* v 8 n 2 Jun 1994 ASCE p 66

171. Wu, X.; Lim, S.Y (1993). "Prediction of maximum scour depth at spur dikes with adaptive neural networks." *Civil-Comp93*, Part 3: Neural Networks and Combinatorial Optimization in Civil and Structural Engineering Civil-Comp93, p 61.

172. Yankielun, N.E. and Zabilansky, L.J., (2000). "Laboratory investigation of a time domain reflectometery system for real-time bridge scour detection and monitoring." J. Civil Engrg, Can. Soc. of Civil Engrg.

173. Yoon, B.; Ettema, R. (1993). "Droplet trajectories and icing-collision efficiencies for cylinders determined using LDV." *Cold Regions Science and Technology* v 21 n 4 Jul 1993 p 381

174. Yoon, J.Y., Patel, V.C., and Ettema, R. (1992). Computation of flow in ice-covered dune-bed channels." *Proc. 9th Conf. Engrg Mechanics* ASCE p 385

175. Yoon, J.Y., Patel, V.C., Ettema, R. (1996). "Numerical model of flow in ice-covered channel*." J. Hydraulic Engrg* v122 n1 Jan 1996 ASCE p 19

176. Young, G.K., Dou, X., Saffarinia, K., and Jones, J.S. (1998). "Testing abutment scour model." *Conf. Proc. Water Resources Engnrng*, 1993, ASCE p. 180.

177. Young, G.K., Palaviccini, M., and Kilgore, R.T. (1993). "Scour prediction model at bridge abutments." *Conf. Proc. Hydraulic Engnrng*, 1993, ASCE p. 755.

178. Zabilansky, L., Ettema, R., Wuebben J. L., and Yankielun, N. E., (2000). Survey of River-Ice Influences on Channel Bathymetry along the Fort Peck Reach of the Missouri River, Winter 1998-1999. CRREL Report (to appear Nov 2000). U.S. Army Corps of Engineers, Cold Regions Research and Engineering

179. Zabilansky, L.J., (2000)."Ice force and scour instrumentation for the White River, Vermont." U.S. Army Cold Regions Research and Engineering Laboratory,Hanover, NH,Special Report 96-6.

180. Zhang, Y. and Du, X., (1997). "Limited scour around spur dike and the evaluation of its depth." *J. Xi'an Highway Transportation* University v17 n4 97 p 56.

181. Zufelt, J.E.; Ettema, R. (1996). "Model ice properties." *CRREL Report* n1 Feb 1996 p19

Countermeasures for Scour at Spill-Through Bridge Abutments

By

Bruce Melville[1], Stephen Coleman[2], David Hoe[3]

ABSTRACT

Experimental data for the use of riprap and cable-tied blocks to protect the fill material at spill-through bridge abutments are presented, including data by Eve (1999) for riprap, and by Hoe (2001) for cable-tied blocks. The experiments were undertaken under clear-water conditions, which are relevant to bridge abutments situated in the floodplain.

Eve (1999) studied the use of riprap at spill-through bridge abutments under clear-water scour conditions. She determined that riprap is an effective protection for spill-through abutment fill material. A particular focus of the project was the use of an apron of riprap to protect the toe of the spill-through slopes. Based on her observations of progressive failure of the abutment embankments, she developed a relation for determining the extent of protection.

Hoe (2001) undertook similar investigations to those of Eve, using cable-tied blocks in place of riprap. The same experimental flume and abutment and flow configurations were used in both studies. Hoe determined that, although cable-tied blocks can offer protection to spill-through abutment fill material, the technique is probably inferior to the use of riprap.

INTRODUCTION

Protection of bridge abutments from scour includes countermeasures that alter flow and scour patterns and those that armour the bed, bank, floodplain and embankment slopes, such as riprap and cable-tied blocks. Armour protection frequently includes the coverage of susceptible portions of embankment slopes. Many design guidance documents recommend that an apron be constructed around the toe of the embankment slope. Armour aprons can protect vertical-wall abutments founded on spread footings. Filters have been recommended below the protection to prevent piping of soils through the armour layers. The filters also may be beneficial to prevent winnowing of soils from beneath aprons especially where the armour layer is used to protect embankments under live-bed conditions.

[1] Professor of Civil Engineering, The University of Auckland, Auckland, New Zealand
[2] Senior Lecturer in Civil Engineering, The University of Auckland, Auckland, New Zealand
[3] Design Engineer, Riley Consultants, Auckland, New Zealand

Riprap as a Scour Countermeasure

Riprap is a commonly used technique to protect bridge abutments and bridge approach embankments from scour. The increased weight of the riprap stones enables them to resist the increased turbulence caused by the presence of the abutment and approach embankment structures in the flow, and thereby provide an armour layer protection to the underlying sediments. Interlocking forces between adjacent stones also act to stabilise the riprap layer. Typically, the riprap is placed on the embankment slopes to protect the embankment material from scour. Riprap can also be placed in an apron, sometimes referred to as a launching apron, to fall onto the sides of a developing scour hole. This riprap acts to reduce the scour depth, and protect the abutment foundation from undermining.

Riprap is subject to certain failure mechanisms, dependent on where it is placed in respect to the bridge abutment. Riprap placed in the apron is subject to similar failure mechanisms as riprap placed about a bridge pier, whereas riprap placed on the embankment slopes is subject to not only dislodgement by the flow, but also slump and slide failures where the riprap moves down the embankment slope.

Parola (1993), Chiew (1995) and Lauchlan (1999) identify four failure mechanisms for riprap placed in an apron, viz. shear failure, winnowing failure, edge failure, and bed-form undermining. Similarly, Blodgett and McConaughy (1985) identify the principal failure modes for riprap placed on sloping embankments. These are particle erosion failure, translational slide failure, and slump failure.

Equations for selecting the size of riprap for bridge abutment protection have been proposed by Simons and Lewis (1971), Croad (1989), Brown and Clyde (1989), Pagan-Ortiz (1991), Austroads (1994), Atayee et al. (1993) and Richardson and Davis (1995), among others. Many of these equations can be arranged into the form

$$\frac{D_{50}}{y} = \frac{C}{(S_r - 1)} Fr^2 \tag{1}$$

where D_{50} is median stone size, y is flow depth, S_r is specific gravity of the riprap stones, Fr is Froude Number of the approach flow and C is a coefficient.

A graphical comparison of the various equations for S_r = 2.65 is shown in Figure 1. It can be seen that the various equations give a wide range of recommended riprap sizes for a given flow. The equations given by Croad (1989) and Richardson and Davis (1995) give larger riprap sizes in comparison with the other equations, whereas the equations given by Brown and Clyde (1989) and Pagan-Ortiz (1991) give relatively smaller riprap sizes.

Cable-Tied Blocks as a Scour Countermeasure

Cable-tied blocks consist of concrete blocks or slabs interconnected with metal or non-metallic cables. The cables used can be fabricated from steel, copper or synthetic materials, such as polypropylene (Przedwojski et al, 1995). An example of cable-tied blocks is given in Figure 2.

A key feature of cable-tied blocks is the interconnecting of small units, which may be unstable as individual blocks, into a framework capable of withstanding much higher flow velocities. The term "cable-tied blocks" typically refers to relatively small units. Articulated concrete mattresses, which rely on the same principles, are larger units commonly used for bank protection.

Previous studies and experiments on the use of cable-tied blocks for scour protection of bridge foundations are limited and are focussed on bridge piers (McCorquodale et al., 1993; Bertoldi et al., 1996; Jones et al., 1995; Parker et al., 1998).

Parker et al. (1998) identify three possible failure mechanisms:

- Overturning and rolling-up of the leading edge, which is exacerbated if the edge is not anchored
- Uplift of the centre of the mat, which can occur where the mat edge is inadequately anchored
- Winnowing of sediment between the mat and the bridge pier, if the mat is not sealed tightly to the pier.

EXPERIMENTS

The experimental studies were conducted to investigate the use of riprap and cable-tied blocks to protect spill-through abutments against scour under clear-water conditions. In particular, the use of an apron to extend the protection beyond the toe of the spill-through abutment slope (as shown in Figure 3 for riprap experiments) was investigated. The experiments were conducted in a 2.4 m wide, 0.30 m deep and 16.5 m long wooden-sided recirculating flume. A sediment recess section, 0.45 m deep, is located 7.2 m from the upstream end of the channel. A uniform-bed sediment, with median size, d_{50} = 0.85 mm, was used in all experiments.

Full details of the experimental technique are given in Eve (1999) and Hoe (2001) for riprap and cable-tied block experiments, respectively. The spill-through embankment shape was constructed from the bed sediment using a mould of sheet metal. The sand was packed inside the mould, which was then removed. Two approach embankment mould lengths of 975 mm and 1175 mm were used for the riprap experiments, while only the shorter length was used for the cable-tied block experiments. The spill-through slopes had a rounded frontal section of 375 mm radius, were 250 mm tall, and featured side slopes of 1:1.5 (H:V).

The median sizes, D_{50}, of the three uniform riprap sizes used in the riprap experiments were 16.3, 21.5, and 27.8 mm. The riprap was placed on the embankment slopes to a thickness of $2D_{50}$. An apron of the dimensions required was placed on the bed around the embankment. Commercially-manufactured ceramic bathroom tiles, of dimensions 25 mm x 25 mm and 5 mm high, were used to represent the cable-tied blocks. A synthetic filter fabric was used in most of the cable-tied-block tests, Figure 4. All tests were conducted at the same flow depth (y = 150 mm), under clear-water conditions on the

approach flow bed, with $V/V_c < 1.0$ (where V is mean velocity of flow and V_c is the mean velocity of flow at the threshold condition for sediment movement on the approach flow bed). For the riprap experiments, V/V_c was set at 0.73, while for the cable-tied block experiments, V/V_c varied from 0.66 to 0.98. The experiments were run for a maximum of 24 hours, if the abutment did not fail before this. Once a test was completed, the scour hole was profiled with string, laid at 50 mm intervals of depth, for photographic purposes.

Assessment of failure – riprap tests

The abutment and fill slopes were assessed for failure at the end of each riprap test. Criteria were developed to assess the failure, based on the ability of the abutment to continue to support a bridge foundation. The abutment was adjudged to have failed if the side slopes of the embankment fill material had shifted in any way. The three types of failure for riprap protection were:

- Total failure, where large-scale movement of sediment and riprap had occurred on the slopes of the fill material, the slope of the embankment having slumped, and large areas of embankment material having been exposed with no riprap protection.
- Partial failure, where riprap and sediment movement had been initiated in one part of the embankment, but a change in the embankment slope as a whole had not resulted. Typically partial failure was observed at the water level, with small numbers of riprap stones displaced a small distance down the embankment slope, and at the base of the embankment, if undermining of the toe had occurred.
- No failure, where no change could be seen in the embankment slope, and the sediment and riprap on the embankment slope had maintained their original position.

EXPERIMENTAL RESULTS

The configurations for the experiments, as well as the assessment of failure for each test, are summarised in Tables 1 and 2, for cable-tied block and riprap tests, respectively.

Riprap tests

For each riprap size, initial tests were carried out with an apron width of 300 mm, equal to $2y$, as recommended by most guidelines. The guidelines inherently assumed θ and ϕ values of zero, where θ and ϕ represent apron extent reductions on the downstream and upstream sides respectively, as shown in Figure 3. The apron width, W, was then reduced until a failure was observed. For the minimum apron size for which a failure did not occur, the apron coverage, in terms of θ and ϕ, was reduced until a full or partial failure was observed.

All riprap-protected abutments that failed exhibited the same failure mechanism. Undermining of the embankment toe lead to translational slide failure, where a mass of riprap stones moved down the embankment slopes. This resulted in a gentler slope, which eventually became stable. Tests conducted using the two smaller riprap materials also exhibited particle erosion failure, where the flow was able to entrain single stones from the riprap layer. Riprap stones displaced into the scour hole would be temporarily

entrained by the strong turbulence in the scour hole region and moved small distances downstream. In this manner riprap stones were displaced to positions nearer to the position of maximum depth, thus slowing the development of the scour hole.

Reductions in scour depth of 38% to 63% were achieved by protecting the abutment with riprap, compared to the expected scour depth at an unprotected abutment, as estimated using the method of Melville and Coleman (2000). The scour depth decreased with increasing apron width and increasing riprap size. The greater the width of the apron, the greater the decrease in scour depth for an increase in riprap size. The position of the point of maximum scour depth also moved progressively away from the abutment with increasing apron size and riprap size.

For a riprap apron of W = 0.3 m, no abutments failed. A typical test result is shown in Figure 5. This would indicate that an apron width of twice the flow depth ($2y$) is adequate for abutment protection under clear-water conditions, and within the limits of these tests. However, the results show that this is a conservative solution. The apron width can be reduced, and the extent of the apron in terms of θ and ϕ can be reduced also. The results suggest that there is a relationship between the total area of apron and degree of protection. The suggested form of this relationship is shown in Figure 6, which shows a clear zone of partial failure. Note that the values for the tests using a 0.3-m apron have been omitted, to allow the remainder of the data points to be seen more clearly.

The variable on the y-axis of Figure 6 is $\left(\frac{A_u + A_d}{A_*}\right)\left(\frac{b-L}{b}\right)$, where A_u is the area of riprap protection of the apron on the upstream side of the abutment, and A_d is the equivalent area on the downstream side. A_* is the area of riprap protection as recommended by current guidelines ($W = 2y$), with θ and ϕ equal to zero. These areas exclude the riprap area on the embankment slope. The first term in this expression can be expressed in terms of the parameters W, y, θ, ϕ, and an additional parameter r, which is defined as the radius of the toe of the spill-through abutment. The second term is the contraction ratio (β) for the channel. The line shown in Figure 6, defining the failure limit, can then be expressed as

$$\frac{W}{y}\left(\frac{0.5W + r}{y + r}\right) = \left(0.5 - 1.82\frac{D_{50}}{y}\right)\frac{1}{\beta}\left(\frac{180}{180 - (\theta + \phi)}\right) \tag{2}$$

which reduces to the following expression for $\theta = \phi = 0$

$$\frac{W}{y}\left(\frac{0.5W + r}{y + r}\right) = \left(0.5 - 1.82\frac{D_{50}}{y}\right)\frac{1}{\beta} \tag{3}$$

Expressions (2) and (3) are presently limited to $0.1 < D_{50}/y < 0.2$.

Cable-tied block tests

For the cable-tied block experiments, the standard layout used in all experiments is shown in Figure 7. This layout did not provide adequate protection for flow conditions approaching $V/V_c = 1.0$. In an attempt to improve the protection, additional cable-tied blocks were added for the final three experiments of $V/V_c \rightarrow 1.0$, as shown in Figure 8.

The additional cable-tied block mat areas are defined in Table 1 in terms of their radial extent measured from the bridge axis, namely α_u (upstream extent) and α_d (downstream extent). These additional apron areas did improve the level of protection afforded by the cable-tied block mats.

The failure mechanisms that were observed for cable-tied block experiments involved one or more of the following types:

- Undermining of the outer edge of the apron as scour developed, leading to slumping of the fill material (translational slide failure) and potential failure (settlement) of the abutment. This was the predominant failure mechanism.
- Lateral movement of the cable-tied mat protecting the embankment slopes on the upstream side, exposing the fill material to surface erosion. Attaching the edge of the cable-tied block mat to the flume wall prevented this movement from occurring.
- Undermining of the upstream edges of the cable-tied block apron, leading to overturning (role-up) of the upstream edge and accelerated erosion of the underlying sand bed material.
- Winnowing of fill material through the gaps between blocks in the mat. The presence of the filter layer significantly reduced this loss of fill material.

The scour depth reductions achieved with the cable-tied blocks were significantly less than those achieved with riprap protection. In some cases, as shown in Table 1, the maximum scour depth increased in relation to that for an unprotected abutment. In all cases, however, the position of the point of maximum scour was deflected away from the abutment by the presence of the cable-tied block mats. The reason for the increases in scour depth is that the cable-tied block mats settled into the developing scour holes, rendering them larger flow obstructions than the equivalent unprotected embankments (Figure 11). In doing so, the cable-tied block mats maintained their overall shape. Conversely, the ability of riprap stones to settle and change their relative positions allowed the riprap protection to armour the developing scour holes and thus limit the overall scour development. This inability of cable-tied block mats to adjust, in the manner of riprap, as scour develops is perceived to be a significant limitation to their potential use. The possibility of employing cable-tied block protection to all or part of the fill slope, together with a protective apron of riprap, is worthy of further consideration.

The relative performance of riprap and cable-tied blocks is highlighted by comparing the results for riprap-Test 17 and cable-tied block-Test 4. For these tests, the experimental conditions were similar, the velocity ratios being 0.73 and 0.66, respectively. The scour depth reductions for these two tests were 42% and –11%, respectively. The scour developed in each of these tests is shown in Figures 9 and 10.

The level of protection required using cable-tied blocks increased with increasing flow velocity. The effect of increasing flow velocity is seen by comparing Tests 5 and 6, for which V/V_c = 0.80 and 0.86, respectively. Test 5 (Figure 11) was adjudged to be a success, because the fill material did not slump near the top of the fill slope and an

abutment structure would not have failed. Conversely, Test 6 (Figure 12) was a failure because the fill material slumped near the crest.

CONCLUSIONS

The following conclusions are drawn from this study:

1. Riprap is an effective protection for spill-through abutment fill material under moderate clear-water scour conditions, pertinent to abutments situated on the floodplain. The ability of a riprap layer to settle into a developing scour hole and armour the base of the scour hole, is an important factor in the protection afforded.
2. Cable-tied blocks can offer protection to spill-through abutment fill material. This study has shown, however, that the technique is probably inferior to the use of riprap. The design of a protection system involving a combination of cable-tied blocks and riprap may lessen the disadvantages of the former technique.
3. Armour protection of bridge abutments and approach embankments, using either of these techniques, should extend around the end of the embankment and include an apron placed on the floodplain to protect the toe of the fill material.

REFERENCES

Atayee, A.T. (1993) "Study of riprap as scour protection for spill-through abutments", unpublished TRB paper No. 931021, presented at the 72nd Annual TRB meeting, Washington DC.

Austroads (1994) "Waterway design - A guide to the hydraulic design of bridges, culverts and floodways," Austroads, Sydney, Australia, 139pp.

Bertoldi, D.A., Jones, J.S., Stein, S.M., Kilgore, R.T., and Atayee, A.T. (1996) "An experimental study of scour protection alternatives at bridge piers," Report No. FHWA-RD-95-187, Turner-Fairbank Highway Research Center, Federal Highway Administration, U.S. Department of Transportation, U.S.A.

Blodgett, J.C. and McConaughy, C.E. (1985) "Evaluation of rock riprap design practices for protection of channels near highway structures - Phase I," Preliminary Report subject to revision, prepared by the U.S. Geological Survey in cooperation with Federal Highway Administration.

Brown, S.A. and Clyde, E.S. (1989) "Design of riprap revetment," Federal Highway Admin., U.S. Department of Transportation, Washington, D.C., Report FHWA-IP-89-016, HEC-11.

Chiew, Y.M. (1995) "Mechanics of riprap failure at bridge piers," Journal of Hydraulic Engineering, A.S.C.E., 121(9), 635-643.

Croad, R.N. (1989) "Investigation of the pre-excavation of the abutment scour hole at bridge abutments," Report 89-A9303, Central Laboratories, Ministry of Works and Development, Lower Hutt, NZ, 38pp.

Eve, N.J. (1999) "Riprap protection of bridge abutments", M.E. Thesis, Civil and Resource Engineering Department, The University of Auckland, Auckland, New Zealand, 163pp.

Hoe, D.A. (2001) "Cable-tied block protection of bridge abutments," Project Report No. PCRE 01:18, Department of Civil and Resource Engineering, The University of Auckland, Auckland, New Zealand, 75pp.

Jones, J.S., Bertoldi, D.A. and Stein, S. (1995) "Alternative scour countermeasures," Proc., Hydr. Engineering '95, San Antonio, Texas, U.S.A. 1819-1823.

Lauchlan, C.S. (1999) "Countermeasures for pier scour," PhD thesis, The University of Auckland, Auckland, New Zealand.

McCorquodale, J.A., Moawad, A. and McQorquodale, A.C. (1993) "Guide for Design and Placement of Cable-Tied Block Erosion Protection," Proceedings Hydraulic Engineering, San Francisco, 1367-1372.

Melville, B.W. and Coleman, S.E. (2000) "Bridge scour", Water Resources Publications, Highlands Ranch, Colorado 80163-0026, 550pp.

Pagan-Ortiz, J.E. (1991) "Stability of rock riprap for protection of the toe of abutments located at the flood plain," Federal Highway Administration, FHWA-RD-91-057, 125pp.

Parker, G., Toro-Escobar, C. and Voigt, R.L., Jr. (1998) "Countermeasures to protect bridge piers from scour," Draft Final Report (Project NCHRP 24-7) prepared for National Co-operative Highway Research Program, University of Minnesota, Minneapolis, Minnesota, U.S.A., 402pp.

Parola, A.C. (1993) "Stability of riprap at bridge piers," Journal of Hydraulic Engineering, A.S.C.E., 119(10), 1080-1093.

Richardson , E.V. and Davis, S.R. (1995) "Evaluating scour at bridges." Federal Highway Admin. Report No FHWA-IP-90-017, Hydraulic Engineering Circular No 18, 3rd. Edition, Office of Technology Applications, HTA-22, Washington, D.C., 204pp.

Przedwojski, B., Blazejeski, R. and Pilarczyk, K.W. (1995) "River Training Techniques," A.A. Balkema, Rotterdam, Netherlands.

Simons, D.B. and Lewis, G.L. (1971) "Report - flood protection at bridge crossings," prepared for the Wyoming State Highway Department in conjunction with the U.S. Dept. of Transportation, C.S.U. Civil Engrg. Report No. CER71-72DBS-GL10.

Table 1 - Experimental set-up and assessed failure for cable-tied block experiments

Test ID	V/V_c (-)	L (mm)	**Filter**[1]	α_u (°)	α_d (°)	**Failed**[1]	**Scour reduction (%)**
1	0.80	863	N	0	0	Y	-10
2	0.80	863	Y	0	0	Y	NA
3	0.66	863	N	0	0	N	-15
4	0.66	863	Y	0	0	N	-11
5	0.80	863	Y	0	0	N	27
6	0.86	863	Y	0	0	Y	22
7	0.86	863	Y	10	55	N	13
8	0.98	863	Y	10	55	Y	2
9	0.98	863	Y	55	55	Y	12

[1]Y = yes, N = no.

Table 2 - Experimental set-up and assessed failure for riprap experiments

Test ID	V/V_c (-)	L (mm)	D_{50} (mm)	W (m)	θ (°)	ϕ (°)	Failed[1]	Scour reduction (%)
16	0.73	863	16	0	0	0	Y	38
19	0.73	863	16	100	0	0	P	48
24	0.73	863	16	200	90	45	Y	49
22	0.73	863	16	200	90	0	N	52
23	0.73	863	16	200	45	45	N	55
21	0.73	863	16	200	60	0	N	41
20	0.73	863	16	200	45	0	N	42
18	0.73	863	16	200	0	0	N	42
17	0.73	863	16	300	0	0	N	42
10	0.73	863	22	0	0	0	Y	38
26	0.73	863	22	100	45	45	Y	41
25	0.73	863	22	100	45	0	P	55
14	0.73	863	22	100	0	0	N	49
15	0.73	863	22	200	0	0	N	55
13	0.73	863	22	300	0	0	N	49
1	0.73	863	28	0	0	0	Y	52
34	0.73	863	28	100	45	45	P	55
33	0.73	863	28	100	0	0	N	54
8	0.73	863	28	300	0	0	N	63
30	0.73	1063	16	100	45	0	Y	57
29	0.73	1063	16	100	0	0	P	56
28	0.73	1063	22	100	45	0	P	55
27	0.73	1063	22	100	0	0	N	55
32	0.73	1063	28	100	45	0	N	60
31	0.73	1063	28	100	0	0	N	60

[1] Y = yes, P = partial, N = no.

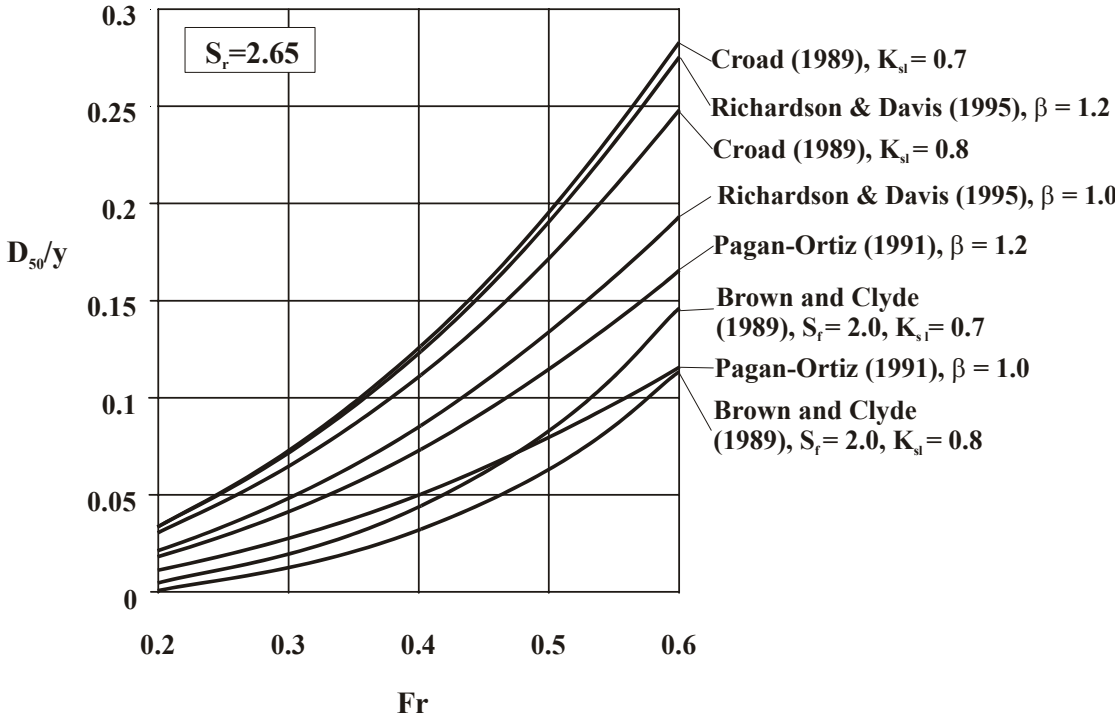

Figure 1 - Comparison of equations for riprap sizing at bridge abutments

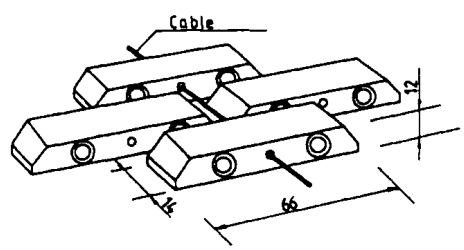

Figure 2 - Cable-tied blocks used as bank protection (Przedwojski et al, 1995)

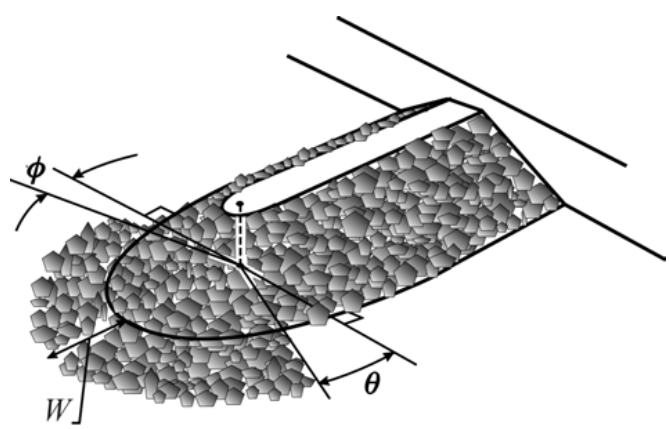

Figure 3 – Variables defining the geometry of a spill-through abutment and riprap layer

Figure 4 – The filter fabric placed over the sand embankment ready for placement of cable-tied blocks

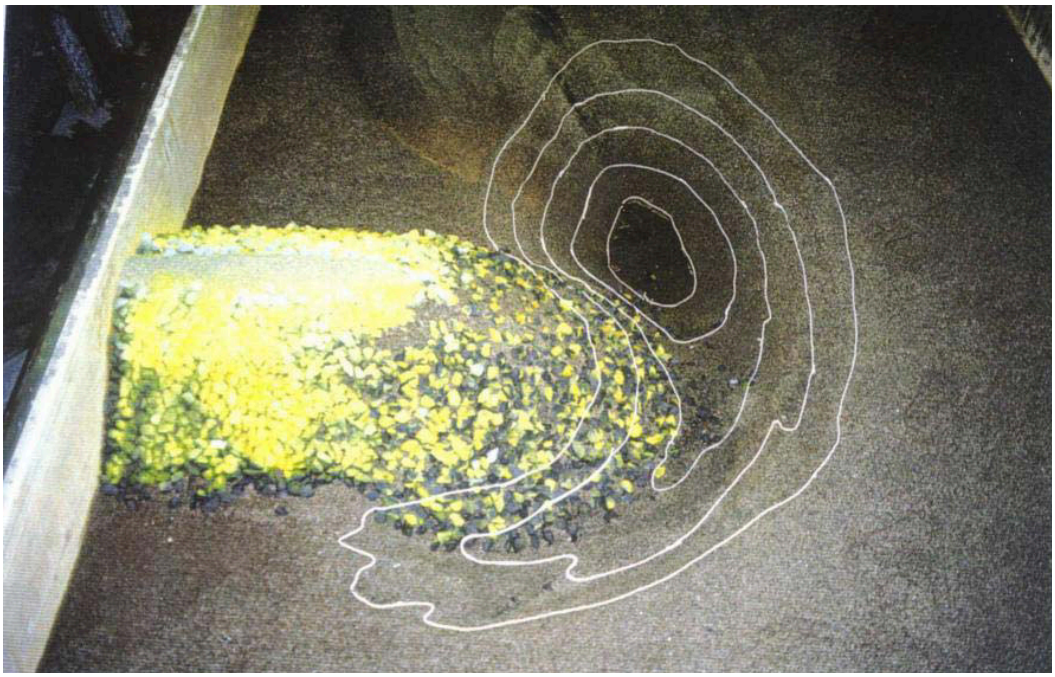

Figure 5 – Typical scour hole developed at an abutment (of no failure) with riprap protection, viewed from downstream

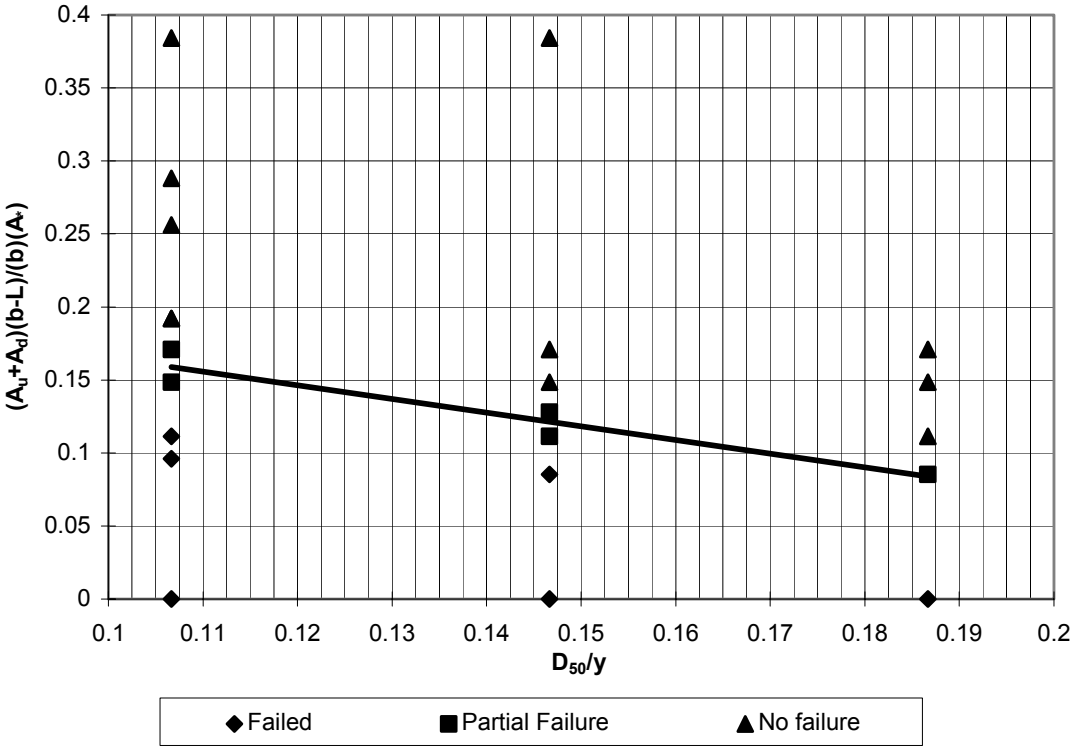

Figure 6 - Relationship between apron extent and riprap size.

Figure 7 – The standard apron used in all cable-tied block tests

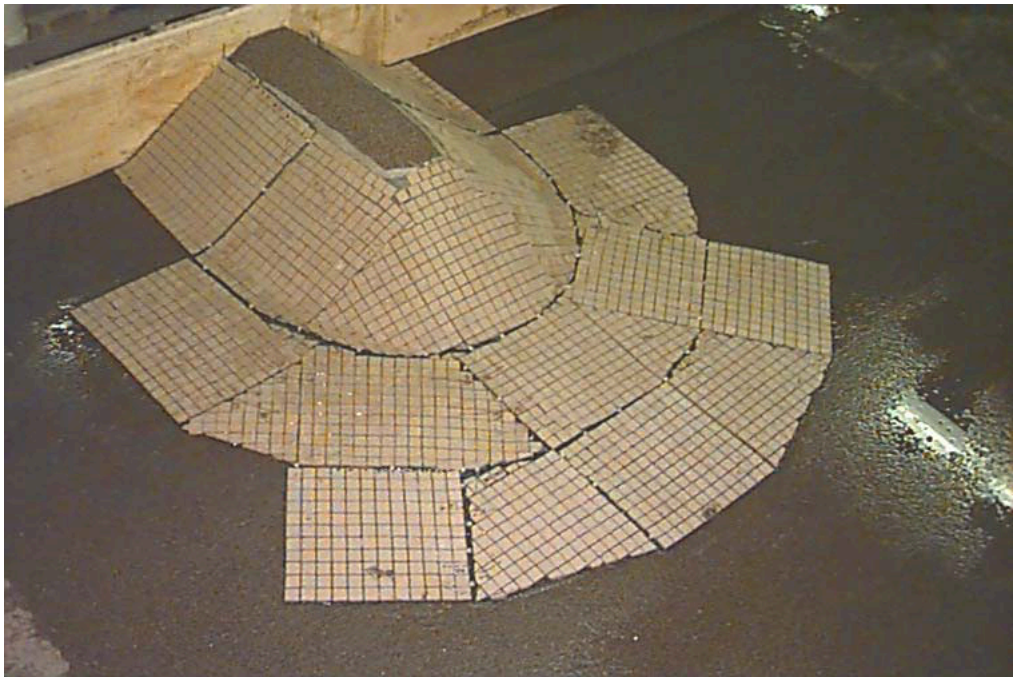

Figure 8 – Additional cable-tied block apron protection, for $V/V_c \rightarrow 1.0$

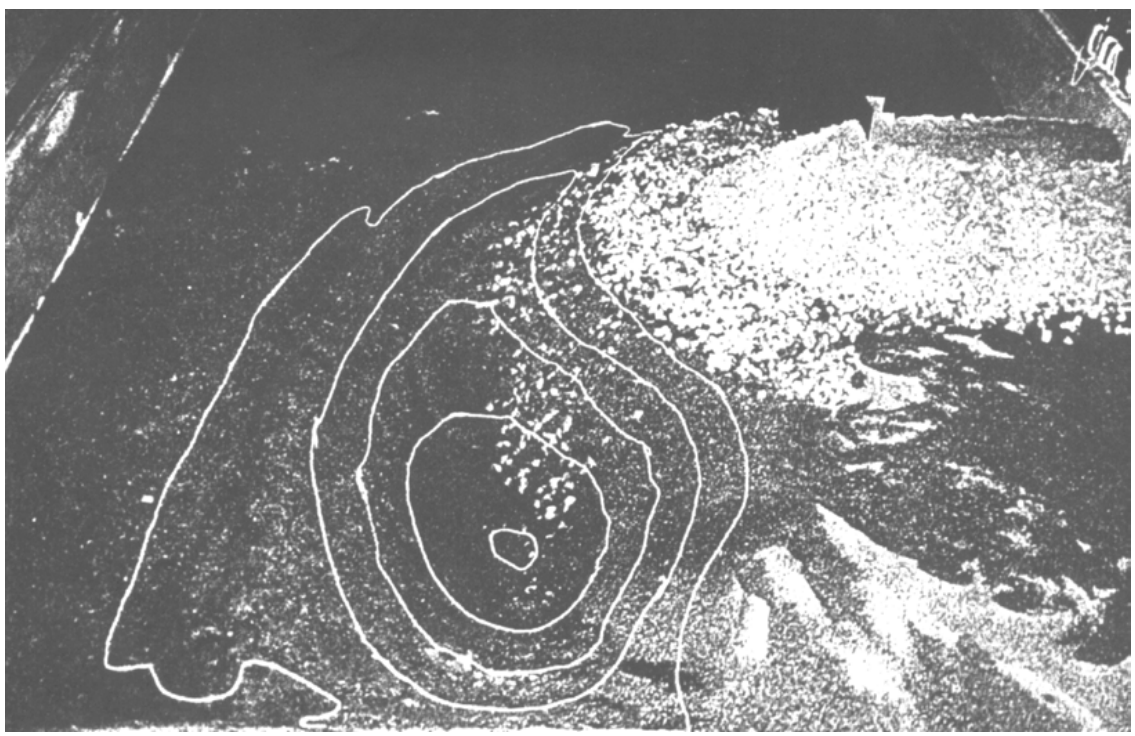

Figure 9 – Scour hole development for Test 17, with 16 mm riprap and $V/V_c = 0.73$, viewed from downstream

Figure 10 – Scour hole development for Test 4 using cable-tied blocks, with $V/V_c = 0.66$, viewed from downstream

Figure 11 – Typical scour hole development for cable-tied block protection (Test 5), viewed from downstream. In this test, the protection was deemed not to have failed

Figure 12 - Typical scour hole development for failed cable-tied block protection (Test 6), viewed from downstream. The failure was due to slumping of the fill material near the top of the embankment

Hugo Reservoir Embankment Depression Study

By

James B. Nevels, Jr.[1]

ABSTRACT

The cause of unusual depressions in the embankment slopes is examined of the causeway crossing over Lake Hugo in Southeastern Oklahoma. The design of the embankment slope consisted of a rip rap armor underlain by a filter fabric and 1.22m thick sand. The failure patterns observed from the lake were oblong depressions in the riprap varying in distance from the lake pool elevation up to and near the highway shoulder. The average depression dimensions (length, width, and depth) were 7.5, 2.1, and 1.5 m respectively clay plate. The embankment interior was constructed from an unclassified borrow source consisting of predominantly silty clay but lensed with layers of clayey silt, clayey sand, and silty sand. Twelve borings originally were made to evaluate the engineering properties of the clay plate and underlying embankment material. Extensive laboratory testing in supplementary investigations, documented through the crumb, double hydrometer, pinhole, soil chemistry, and x-ray diffraction tests, confirm that the A-6 clay plate material used was highly dispersive. The original design had specified an A-7 material for the clay plating, but a value engineering proposal was accepted using the A-6 soil. The repair of the depressions consisted of cutting off water infiltration into the clay plate along the shoulder and filling in the depressions. Results were not totally successful. Additional testing and monitoring of the road performance continued into the mid-nineties.

INTRODUCTION

The purpose of this report was to investigate the cause of 126 recorded depressions in the embankment slopes of a highway embankment causeway crossing Lake Hugo on state highway 93 in Choctaw County, Oklahoma. The causeway embankment was constructed in 1971-72, with the lake level in the Hugo reservoir filling up by the end of 1974. The earthwork was constructed under plans and special provisions of Project No. SAP 12(14). The extent of the depressions covered both right and left embankment slopes between stations 425+00 and 560+00; however, the preponderance of the depressions, 78.1 percent, were located on the lakeside embankment slope. Details of the slope design are presented in Figure 1. In 1979 fishermen began informing the Division 2 engineers in Antlers, Oklahoma of the depressions observed near the lake pool elevation extending up the slope to near the shoulder. Subsequently in September 1980, a geotechnical

[1] Soils and Foundations Engineer, Oklahoma Department of Transportation, Materials Division, Oklahoma City, Oklahoma.

investigation was conducted and preliminary findings reported. The primary dispersion test used in the 1980 investigation was the double hydrometer test, and results were generally indicative of dispersive soils. Four samples were also sent during this time to the USDA, Soil Conservation Service, and Technical Service Center in Ft. Worth, Texas. Their analysis indicated that all four samples were dispersive based on the pinhole and double hydrometer tests. Two samples were selected at random to be analyzed by x-ray diffraction by Dr. Lester Reed, at Oklahoma State University School of Agronomy (personal communication). The results were inconclusive with regard to identifying the presence of montmorillonite. Additional tests for dispersion were completed in a review of the project in 1993 to further explain the mechanisms involved. Monitoring of the roadway performance was done periodically from 1980 until the end of 1995. This paper presents the overall findings of these investigations.

The clay plate material was specified on the original plans to be an A-7 soil. The contractor submitted a value engineering proposal to change the soil classification from an A-7 to an A-6, since there was no significant difference in the compacted soil permeability between an A-6 and A-7 soil. The A-6 material was argued to be more economical being readily available along the state highway 93 corridor. The contractor was successful in his argument, and the clay plate was changed to an A-6 material and constructed.

FIELD INVESTIGATION

A detailed survey was first made of the 126 depressions by a field party in which the location of the depression in reference to the centerline of survey, length, width, and depth were recorded. Riprap was removed from slope in order to measure the depressions in the clay plate. The failure patterns observed from the lake as well as by physical measurement had the appearance of oblong depressions. The mean depression length, width, and depth measured were 7.5, 2.1, and 1.5 m respectively. Figure 2 presents a two dimensional view of the typical depression shape. It was observed that once the riprap and filter fabric had been removed, several depressions showed erosion tunnels and rills running up the slope. The clay plate material was observed to highly fissured. An unusual feature found in the clay plate construction was an approximately 0.5 m thick sand with gravel layer found in both cross sections slightly above the lake pool elevation, see Figure 3. No explanation was ever given by the Division 2 construction engineer.

A total of twelve borings were made in two cross-sections, stations 500+00 and 512+00 during the 1980 investigation. Borings 7 and 8 were continuous Standard Penetration Test borings at 0.304 m interval spacing according to ASTM D1586 standard, and the remaining ten were continuously sampled hand auger borings according to ASTM D1452 standard. The results of these borings indicated that the embankment was constructed from unclassified borrow sources within distances of 150 m from the toe of the embankment. The embankment consisted of mostly of silty clay lensed with clayey sands or silty sands. Borings at both cross-sections confirmed the presence of a 0.5m layer of coarse material near the lake pool elevation. In a 1993 supplemental investigation, the

hand auger borings 1 through 4 at station 500+30 were duplicated, see Figure 3. These borings were sampled at 100-mm intervals to a depth of 1.22 m.

The distinguishing characteristics of the A-6 clay plate material were the gray and strong brown mottled color and the fissured structure with iron concretions. A comparison of the clay plate description with bottomland soils mapped along the causeway corridor identifies it as coming from the Guyton soil series (Choctaw County Soil Survey, 1979, recorrelated). The soil taxonomy of the Guyton series indicates that it has predominantly argillic B-horizons but there is the potential for natric B-horizon inclusions. These alluvial clays are known for high perched watertables and occur in a hot, humid climate.

LABORATORY TESTS

Visual observation of the depressions and associated erosion and the potential of natric B horizon borrow being used from the surrounding Guyton soil series landscape suggest that the A-6 clay plate material was a dispersive clay. A testing regiment was set up in 1993 to provide additional data to reinforce the original conclusions of the 1980 report and explain mechanisms in more detail. The laboratory testing was divided into three phases: a) index property and compaction tests, b) mechanical soil dispersion tests, and c) chemical analysis tests, see Tables 1, 2, and 3 respectively. Appropriate test procedures are indicated in the respective tables (ASTM 04.08).

Two samples were selected at random to be analyzed for x-ray diffraction by Dr. Lester Reed at Oklahoma State University, School of Agronomy (Personal Communication) during the 1980 investigation. These samples were at the depths as sample numbers 3892 and 3910 from the 1993 investigation and were so labeled. The results of x-ray diffraction test ran on sample 3892 saturated with sodium showed that there was little indication of montmorillonite but the predominate clay mineral found was illite. When the sample was saturated with sodium, it went into permanent suspension. The results of x-ray diffraction on sample number 3910 after saturation with sodium indicates that the principle clay mineral is an interlayered vermiculite-montmorillonite-chlorite.

ANALYSIS

The sources of water that promote the formation of the depressions are presented graphically in Figure 4. It appears that the significant source of water was the sand and gravel layer discovered near the midpoint of the clay plate slope, providing an avenue for lake water to enter into the embankment. Other sources of water are rainfall on the slope and parallel internal seepage. The latter two sources of water would be dependent upon cracks and fissures in the clay plate soil, which were documented in the field investigation.

The depression shapes and associated tunnels and rills observed are consistent with dispersed soil features in our experience in Division 2. Case histories of tunnel formation and associated erosion on the lakeside slopes of earth dams near the lake waterline similar to this problem are reported by (Cole et al.1977) and by (Phillips, 1977).

It was determined in the 1993 sampling of borings 1 through 4 that one sample was classified as an A-4 soil, nine samples were an A-7 soil, and twenty-three samples as an A-6 soil, see Table 1 for summary statistics. The percentage of samples that met the revised specification was 69.7.

From the quantitative analysis in Table 2, the pinhole test data indicates that predominantly the samples tested were dispersive with 87.5 percent having a D2 classification and 12.5 percent having a probable dispersion classification of ND4. Based on the hydrometer test results from Table 2, 30.3 percent of the samples are probably dispersive with 66.7 percent where other tests are needed to establish whether the sample is significantly dispersive. And the crumb test results show that 53.1 percent of the samples are dispersive. The samples indicating a 3 or 4 reaction rating in the crumb test were positively dispersive in the pinhole test thus pointing to its value as a good positive indicator. The criterion used for these quantitative tests was (Soil Mechanics Note No. 13 1991).

In the chemical analysis test results from Table 3, a sample of the pore water is extracted from saturated slurry and analyzed for cations. A total of 55.2 percent of the samples was found to have more than 60 percent of their total salts being sodium, which indicates dispersive soils. A review of the relationship between dispersive soil classes and total dissolved pore water salts (Sherard et al., 1976) can be seen in Figure 5. Results indicate only 17.2 percent of the samples can be classified into Zone A for dispersive soils with the vast majority, 72.4 percent ranked in the nondispersive Zone B and the remainder in transition Zone C. The estimate for this result is at very low total salt concentrations, higher percentages of sodium may occur in samples and the samples still not have dispersive field behavior. Because so few salts occur in these soils, the influence on the soil behavior is minimal. Also from Table 3, the SAR and ESP provide a good indication of the stability of clay soil structure to breakdown and particle dispersion. A SAR between 4 and 12 (Carter et al., 2000) provides a good indication of soil dispersion and results show that 67.9 percent of the samples tested are potentially dispersive. Soils with an ESP greater than 2 percent may be susceptible to spontaneous dispersion (Mitchell, 1993). Results from Table 3 indicate that 84.4 percent of the samples are dispersive.

The results of the x-ray diffraction on the two samples tested are inclusive with regard to identifying the presence of montmorillonite clay mineral. However, both samples went into permanent suspension upon saturation with sodium.

CONCLUSION

It can generally be concluded from the battery of tests performed that the depressions are the result of dispersive soil behavior. Also there is the likelihood that an unexplained construction deviation from the plans in the form of a sand and gravel layer near mid height of the clay plate layer facilitated the formation of some of the depressions.

Results of the dispersion tests from Table 2 shows that the pinhole tests, a direct and performance test as opposed to double hydrometer and crumb tests, indirect and index tests, is far superior in identifying soil dispersive behavior. Similarly, in the chemical tests, SAR and ESP show indication of dispersive clay potential.

An explanation of the randomness of occurrences of the depressions can be found in the study of soil genesis of sodic (dispersive) soil development of the Guyton soil series. The soil taxonomy for the Guyton series points to the presence of a natric B-horizon inclusions found in the borrow source found along the causeway corridor. Classical soil science theory views natric (also known as solonetz) soils as one stage in evolution of the sodic (dispersive) soil (Carter et al., 2000). The natric soil has a relatively high amount of exchangeable sodium and a low amount of soluble salt references Figure 5. If there is a slow rate of lowering of the watertable, the ground water will add more sodium salts by capillary rise through the soil horizons, followed by evaporation during the hot season. During the rainy season, the soluble salts are leached. The amount of exchangeable sodium gradually increases. This soil natric soil genesis will have occurred as random inclusions.

ACKNOWLEDGEMENTS

The Oklahoma Department of Transportation's Materials Division, Soils and Foundations Branch conducted and preformed the 1980 and 1993 laboratory and field investigations as well as the long-term performance monitoring.

REFERENCES

1. ASTM D4.08, 1993
2. Personal Communication, Dr. Lester Reed, 1980
3. Cole, B.A., Ratanasen, Chalaw, Mariklad, Pramote, Liggins T.B., and Chirapuntu, Suphon, "Dispersive Clay in Irrigation Dams in Thailand", Dispersive clays, Related Piping, Erosion in Geotechnical Projects, ASTM STP 623, J.L. Sherard and R.S. Decker, Eds, 1977, pp.25-41.
4. Phillips, J.T., " Case Histories of Repairs and Designs for Dams Built with Dispersive Clays", Dispersive clays, Related Piping, Erosion in Geotechnical Projects, ASTM STP 623, J.L. Sherard and R.S. Decker, Eds, 1977, pp.330-340.
5. Soil Mechanics Note No. 13, Dispersive Clays, U.S Department of Agriculture, Soil Conservation Service Engineering Division, February 1991.
6. Carter, B.J., Ward III, P.A., Alemayehu, D., Jigoulina, E., and Ponte, K., "Identification of Dispersive Soils in Oklahoma by Physiochemical and Clay Properties, Oklahoma Department of Research and Development Division, Item 2140, May 25, 2000.
7. Mitchell, J.K., 1993, "Fundamentals of Soil Behavior", John Wiley & Sons, Inc., New York, New York, USA, pp. 437.

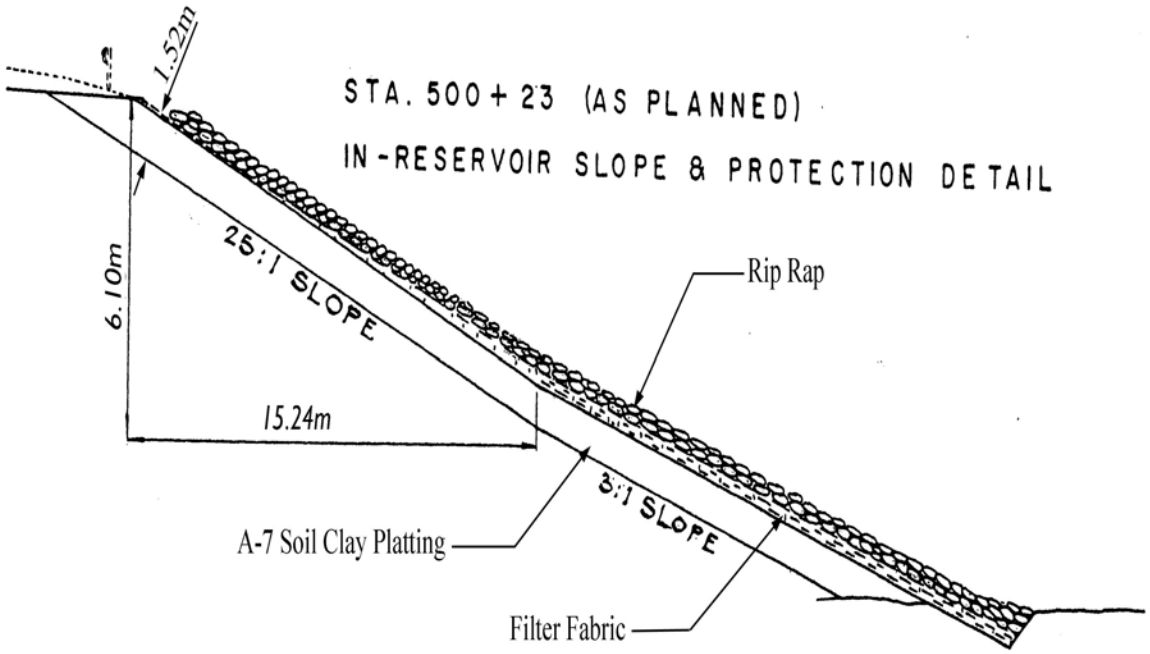

Figure 1 - Slope Design Detail

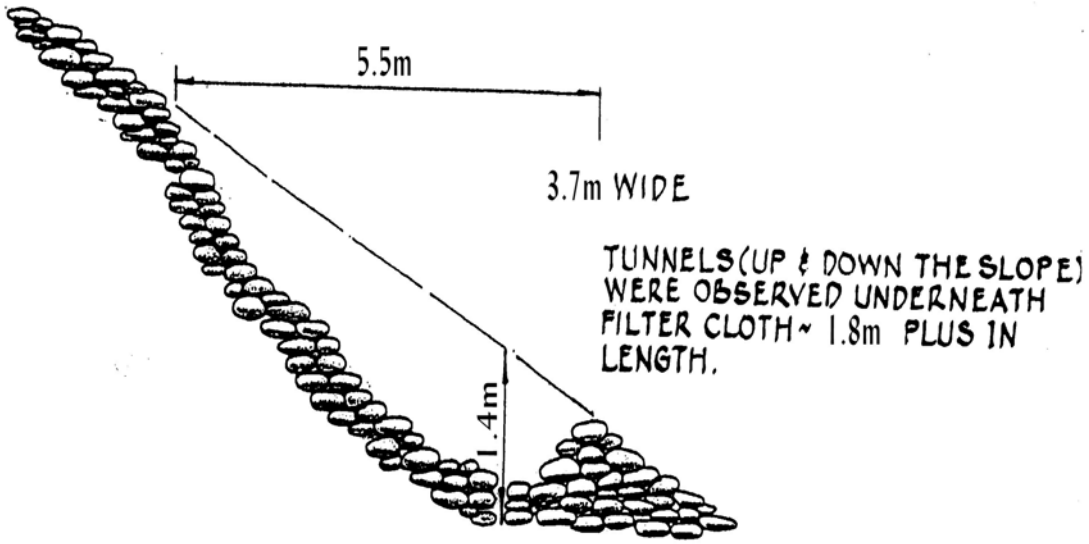

Figure 2 - Two Dimensional View of Typical Depressions

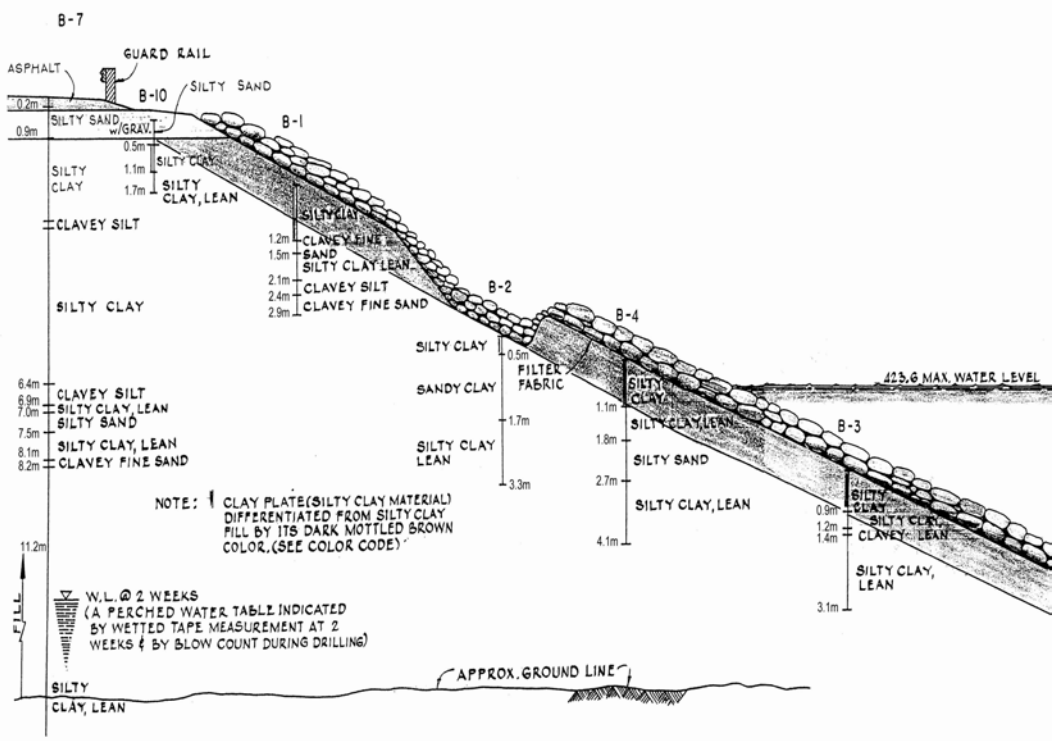

Figure 3 - Hand Auger Boring Location

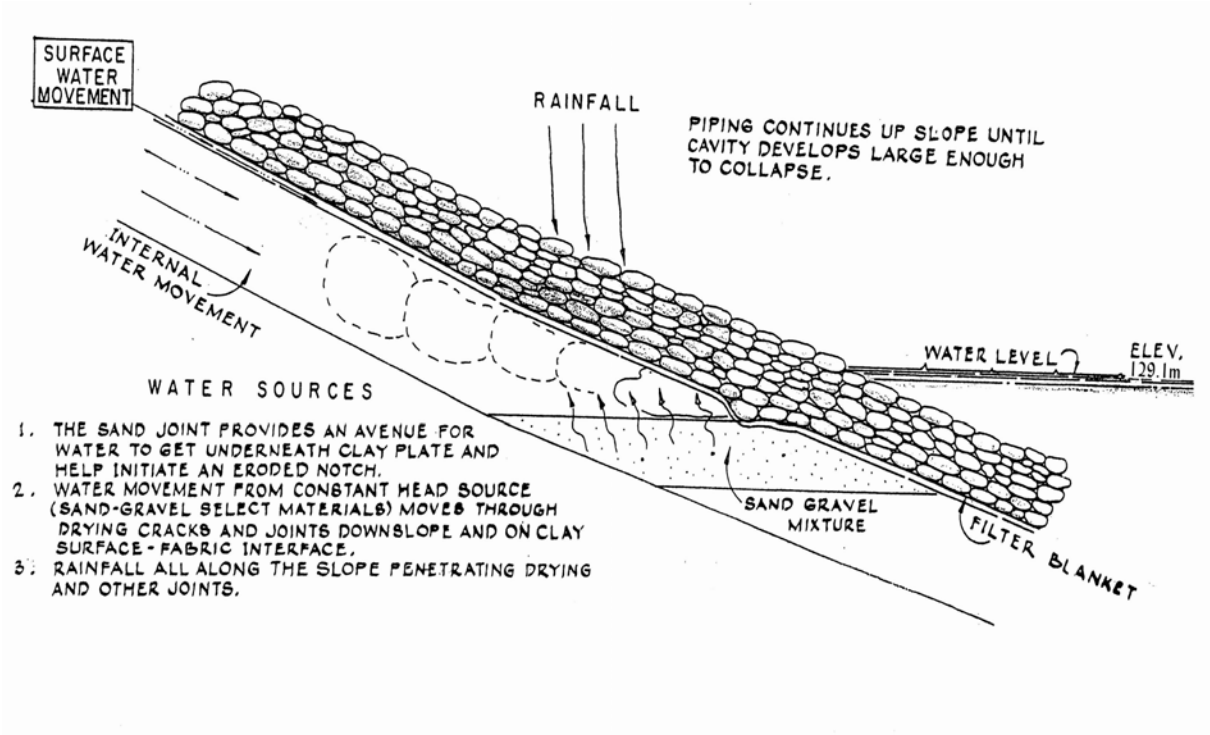

Figure 4 - Sources of Water

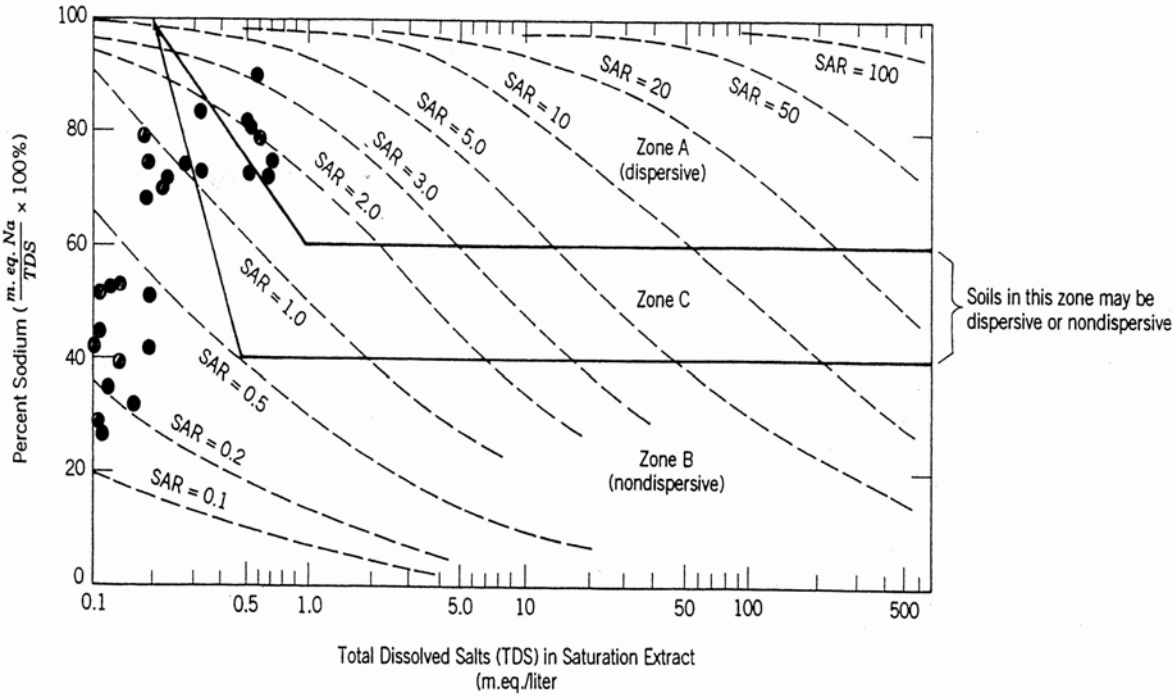

Figure 5 - Relationship Between Dispersive Soil Classes and Total Dissolved Salts

Pier and Abutment Scour-New Laboratory Data

by

Willi H. Hager[1], Jens Unger[2] ,Giuseppe Oliveto[3]

ABSTRACT

The purpose of this paper is threefold: (1) Presentation of a scour installation used over the past 6 years, (2) Summary of results pertaining to the Shields entrainment criterion that was expanded for bridge pier and bridge abutment; and (3) Discussion of new results. Based on a long term investigation of scour, the experimental method was improved to result presently in an installation that might be of general interest. Accordingly, details of the set-up are highlighted that allowed the analysis of both the entrainment criterion and the temporal development of bridge scour. Based on a wide range of pier and abutment geometries, various uniform and non-uniform sediments, and densimetric particle Froude numbers up to the threshold condition, both a generalized Shields formulation, and an equation for temporal scour progress were derived. These results are readily applicable for design, given the selection of basic parameters in the novel approach. They are highlighted with an example that illustrates also the accuracy of the present approach.

KEY WORDS: Abutment scour, Bridge hydraulics, Inception of transport, Movable bed, Pier scour, Scour inception, Shields'criterion.

INTRODUCTION

Scour has received significant attention in the past decades (Raudkivi 1998). Until recently, engineers employed scour equations that would mainly give some indication on the so-called end scour depth. Due to various difficulties in observing scour progress it was proposed that something like an end scour occurs after 2, maybe 6 or even more hours, mainly because observations could not be continued because of the progressively poorer hydraulic conditions in the scour channel. A comparison with prototype scour demonstrated at once significant differences with those scour equations, and research started to care for temporal scour development as one of the significant effects. Recently, the present authors presented a novel scour equation that satisfies the similarity criterion according to Froude. Using a large data basis collected at Versuchsanstalt für Wasserbau, Hydrologie und Glaziologie VAW, ETH Zurich, a scour equation was presented to demonstrate the significant effect of the densimetric Froude number. A time scale was derived using also the Froude law. The equation proposed and also presented in this paper was verified with all existing laboratory data accessible to the authors (Oliveto and Hager 2002), and a reasonable agreement was observed.

The purposes of the present paper are: (1) Presenting the VAW scour installation and procedure for obtaining long-time scour series, (2) Review of previous results relative to a generalized entrainment condition for scour inception, that simplifies to the Shields approach for a pier of infinitesimally small diameter. Also, the relation for temporal scour progress is reviewed, and (3) Application of the present results to an example to compare the present predictions.

[1] Professor, VAW, ETH-Zentrum, CH-8092 Zurich, Switzerland, (hager@vaw.baug.ethz.ch)
[2] Research student, VAW, ETH-Zentrum, CH-8092 Zurich, Switzerland, (unger@vaw.baug.ethz.ch)
[3] Dr., DIFA, Università della Basilicata, I-85100 Potenza, Italy, (oliveto@unibas.it)

EXPERIMENTS

Experimental Setup

VAW initiated scour research in 1995 by focusing so-called building scour. The scour channel set up satisfied special demands in this field of hydraulics. The experiments were conducted in a rectangular channel of width B = 1.00 m, depth of 0.70 m to the sediment surface, and length of 13 m, with a working section of about 5 m (Fig.1). The sediment surface was always inserted horizontal because of the *local* scour phenomenon. The channel was finished in smoothened steel, except for the left channel side made of a 43 mm thick glass wall to allow for observation. A pump with a maximum discharge capacity of 130 l/s was installed at the upstream channel side and connected to a stainless steel pipe with an internal diameter of 250 mm. A flow straightener made of geotextile mattresses was inserted at the transition between rigid and loose bed upstream of the test reach. Its purposes were: (1) Horizontal upstream water surface, (2) Elimination of macro-vortices due to asymmetric water supply, (3) Uniform velocity and discharge distributions in the upstream test reach, (4) Flow free of surface waves, (5) Elimination of macro-turbulence in loose bed intake reach originating from the sides of the intake, and (6) Overall excellent flow appearance to generate long-time scour observations (Fig.1a).

A fully submerged weir type structure at the downstream end of the test reach avoids sediment transport out of the scour area. A flap gate allowed external control of the water surface elevation to the nearest millimeter (Fig. 1b). A vertical filter wall prevented air bubbles to enter the return pipe. Further details are described by Hager et al. (2002). The present VAW installation allows to conduct scour tests of easily 1 week, with periods of up to 12 weeks having also been investigated.

Instrumentation

Piers and abutments were fabricated of plexiglass to the next millimeter to enable visual observation across these elements. Light sheets were mounted into a pier or an abutment, to study the velocity field. Piers of diameters D = 0.022, 0.050, 0.064, 0.110, 0.257, 0.400, and 0.500 m were used, and abutments had widths b = 0.05, 0.10, 0.20, 0.40, and 0.60 m measured from the channel side towards the channel axis. Maximum setting accuracy of an element was 1 to 2 mm.

Scour experiments were directed to observe both sediment and water surfaces. These characteristics were determined with conventional gauges. Axial and transverse water surface profiles were taken, in addition to particular points such as the stagnation flow depth upstream of the elements. The reading accuracy was within 1 mm, except for locations with a pronounced surface turbulence or standing surface waves. The sediment surface was observed with a shoe gauge, given its similarity with a shoe of 5 mm length to 2 mm width. Sediment surface readings were then much simpler than with a conventional point gauge with an accuracy of about 0.5 sediment diameter, or 1 mm.

Sediment readings involved the original bed elevation, the upstream beginning of scour, the transverse extent of scour at the element upstream and downstream sides, the maximum scour depths at these two locations, the location of maximum aggradation downstream of the elements besides particular points for each test. Test readings were made in short intervals close to the beginning, and at longer intervals after the initial scour phase. Normally, the main observations were conducted at 1, 3, 6, 10, and 20 minutes from scour initiation, and then followed in hours, half days, 1 day, and so on until additional readings were considered no more interesting.

Three sediments of almost uniform average size of 0.55, 3.3 and 4.8 mm, and three mixtures, with d_{50} = 5.3, 1.2, 3.1 mm, and $\sigma = (d_{84}/d_{16})^{1/2}$ = 1.43, 1.80 and 2.15, respectively, were used. These sediments allowed to specify the effects of average grain size and sediment non-uniformity on scour initiation and scour progress. An additional plastic sediment with a density ρ_s = 1.42 t/m^3 was employed to check for the density effect.

Experimental procedure

To obtain a horizontal sediment surface for scour initiation, a grading mechanism was employed, resembling a snow plough with a rectangular vertical plate at its downstream side. Sediment grading was always made under water of several centimeters height, because of ease in sediment movement (Hager et al. 2002).

To initiate an experiment, the flap gate was lifted to a position that would submerge the working section beyond sediment entrainment. The pump was started and discharge increased to the selected value, thereby carefully inhibiting sediment movement especially around the sides of the pier. Using the flap gate, the water surface elevation was carefully lowered, until inception of sediment transport around the element started. Once first particles moved (Hager and Oliveto 2002), the time origin was set to zero, and the water surface lowered to test conditions. Surface drawdown was completed within some seconds, to allow for the first reading of the sediment surface after 1 minute. In total almost 400 experiments were completed within the past 3 years, with a typical experimental duration of 2.5 days. The effects of upstream velocity, sediment size, sediment density, flow depth, pier diameter and abutment width were investigated resulting in two main papers. The first paper relates to the extended Shields entrainment criterion with piers or abutments present in a loose boundary flow, whereas the second predicts pier and abutment scour depth as a function of time, by accounting for all of the previously mentioned parameters (Hager and Oliveto 2002, Oliveto and Hager, 2002). In the following some observations during scour progress will be described.

Scour Initiation

Scour initiated once the upstream velocity $V_o = Q/Bh_o$ was equal to the entrainment (inception subscript i) velocity V_i with Q as discharge, B channel width and h_o upstream flow depth. In a flow without any elements the entrainment criterion for the viscous ($D_* \leq 10$), the transition ($10 < D_* < 150$) and the fully rough turbulent ($D_* \geq 150$) regimes, where $D_* = (g'/\nu^2)^{1/3} d_{50}$ with $g' = [(\rho_s - \rho)/\rho]g$ as the relative gravitational acceleration and ν as kinematic viscosity is (Hager and Oliveto 2002)

$$\mathrm{F}_{di} = 2.33 D_*^{-0.25} \left(R_h / d_{50}\right)^{1/6}, \qquad D_* \leq 10 \tag{1}$$

$$\mathrm{F}_{di} = 1.08 D_*^{1/12} \left(R_h / d_{50}\right)^{1/6}, \qquad 10 < D_* < 150 \tag{2}$$

$$\mathrm{F}_{di} = 1.65 \left(R_h / d_{50}\right)^{1/6}, \qquad D_* < 150 \tag{3}$$

Here, $\mathrm{F}_{di} = V_i/(g' d_{50})^{1/2}$ is the densimetric particle inception Froude number, R_h=hydraulic radius and d_{50} = average grain size. For the first two cases, F_{di} is proportional to a power of dimensionless grain size D_*, and increases with the relative hydraulic radius. For constant densities of sediment and fluid, the inception Froude number thus increases with the relative flow depth.

For a plane sediment bed containing a pier an additional effect may thus be observed that tends to zero for an extremely small pier diameter D. All effects originating from fluid flow and sedimentology are confined in (1) to (3), and the addition of relative pier diameter causes a purely geometrical effect. The effect of pier contraction $\beta = D/B < 0.65$ may be accounted for by the ratio $\Phi_\beta = \mathrm{F}_d/\mathrm{F}_{di}$ between the cases when the pier is present F_d, and the pier is absent as (Hager and Oliveto 2002)

$$\Phi_\beta = 1 - 1.10(2/3)\beta^{1/4} \tag{4}$$

Accordingly, sediment entrainment results in larger velocities for small relative pier diameters, and smaller velocities for large piers. Equation (4) states that no sediment transport occurs for a velocity V_o smaller than the entrainment velocity V_i of a pier. This lower limit of sediment entrainment has so far not been specified.

Scour progress

Most of the observations currently available refer exclusively to the scour depth, while other details of scour progress remain obscure. For pier scour, scour initiation is always at the upstream lateral side of the cylinder, roughly at 70° when 0 is the upstream axial direction from the center of pier. Depending on F_d, one may refer to small, medium or fast scour progress. For $F_{di} < F_d < 2$, scour is weak with a tendency for slightly asymmetric scour on the two pier sides. Typical clear water scour may be expected for $2 < F_d < F_{dt}$, with a significant effect of pier diameter on the scour extension. For $F_d > F_{dt}$, i.e. over the threshold (subscript *t*) condition of the upstream bed, scour does not really advance after a sufficient time because of an equilibrium between sediment transports into and out of the scour hole (Graf and Altinakar 1997, Hoffmans and Verheij 1997). This latter regime was not investigated in the present work because inaccuracies complicate data analysis.

Scour progress in the typical domain of densimetric particle Froude numbers between 2 and 3 can be described as follows (Fig. 2). Scour initiates at the sides of the cylinder, at an angle of approximately 70°, where the bottom shear stresses are expected to be a maximum due to acceleration of flow across the contraction by the pier. Material is washed downstream into the zone where velocity decreases, and thus aggradation starts at the end of the cylinder, close to the shear layer between the forward main flow and the recirculating wake flow of the cylinder. Progress of scour at the first stage is very strong, both in terms of scour and aggradation heights. Note that there is absolutely no scour at the upstream side of the cylinder, because of stagnation flow.

Figure 3 relates to lateral observation of scour progress, in which again scour initiation may be observed slightly upstream from the pier axis, then advancing to the upstream pier side at phase 3. Simultaneously, the aggradation of sediment reaches a maximum at about that stage, and then progressively is shifted downstream from the cylinder. It can also be seen that the scour maximum stays on the side of the pier until phase 5 and then migrates upstream to the leading face of the pier. This temporal progress of scour is typical for piers (and also abutments), with a maximum scour depth at the upstream face only at an advanced scour stage. An exception may occur for flow conditions with a densimetric Froude number very close to the entrainment condition. Then, this shift of scour maximum from the pier side to upstream of the pier does not occur because of too small forces involved after the initial scour phase.

At the end of the first stage, scour surface has extended both against and in the flow direction, with the scour maximum shifted upstream towards the pier axis. The second scour stage then starts. Most of the past descriptions of pier scour did not specify the migration of scour maximum against flow direction, and measurements were confined exclusively to the growth in the pier axis. Oliveto and Hager (2002) proposed an equation for scour progress both for pier and abutment. These two geometries differ only by a shape factor equal to N=1 for the pier, and N=1.25 for the abutment. For otherwise identical conditions, abutment scour is thus by 25% larger than pier scour.

The relative pier scour depth $Z = z/(D^{2/3}h_o^{1/3})$ depends essentially on: (1) Densimetric Froude number $F_d = (\sigma^{-1/3}V_o)/(g'd_{50})^{1/2}$ where $\sigma = (d_{84}/d_{16})^{1/2}$ is the standard deviation of sediment mixture, equal to 1 for a uniform sediment, and (2) Time scale $T = [\sigma^{1/3}(g'd_{50})^{1/2}/D^{2/3}h_o^{1/3}]t$ with t as time relative to scour initiation, as previously mentioned. The relation

$$Z = 0.068\, N\, F_d^{1.5} \log(T), \qquad F_{di} < F_d < F_{dt} \tag{5}$$

was established with the VAW data set and verified with the available literature data. In total some 600 scour progress series were employed to establish (5), resulting in a maximum standard deviation of some 10%. Details for the application of (5) were also provided by Oliveto and Hager (2002).To check the previous approach with a typical experiment, consider the following problem: Q = 0.107 l/s, h_o = 0.197 m, V_o = 0.54 m/s, D = 0.257 m, g' = 16.19 m/s^2, d_{50} = 0.0055 mm, σ = 2.26, thus F_d =1.38. The non-dimensional time T can be expressed as $T = t/t_R$ with the reference time $t_R = [\sigma^{1/3}(g'd_{50})^{1/2}/D^{2/3}h_o^{1/3}]^{-1}$ = 0.60 s. Figure 4 compares that particular experiment with the prediction according to (5), and a reasonable agreement between the two is noted.

VELOCITY DISTRIBUTION

To further knowledge for pier scour, velocity fields around a pier were observed, with a typical case being presented below. The test conditions were as for the example previously introduced, with a relatively small approach intensity. The velocity distribution was measured with a standard propeller meter to compare results with a more involved experimental technique to be described. The local angles of streamlines relative to the channel axis were measured first with an angle meter and the propeller was then positioned into the previously determined direction. Figure 5 shows plane velocity distributions (a) close to the free surface, (b) at 50% flow depth, (c) close to the original sediment surface, and (d) 50% below that elevation. At the free surface, the velocities may be described as one would expect for a two-dimensional flow around a cylinder. However, at a lower elevation, there appears to be an increase of velocity close to the cylinder, with a forward direction downstream of it. In the scour hole velocities are in about the same direction, yet with an absolute value somewhat smaller as the sediment bed is reached. From present experimental possibilities, such observations are of course crude, but they serve as a calibration for more sophisticated approaches, such as particle image velocimetry PIV or particle tracking. At present, that system is set up, and results will be presented later. Figure 5 (e) is a plot of the water surface with a maximum surface elevation at the stagnation point upstream from the cylinder, and a minimum laterally from the cylinder where scour started. Figure 5 relates to conditions where scour advance is small with a dimensionless time of approximately $T = 10^5$.

CONCLUSIONS

Bridge hydraulics has become a significant issue in the past years. The present work would like to add to two particular points: (1) Presentation of a hydraulic installation developed at VAW during the past years, with particular attention to the needs of scour investigation, and (2) Extension of Shields entrainment condition with an approach involving basic hydraulic parameters such that it can readily be determined if a pier or an abutment undergoes scour, or not. These results may also be applied to investigate the stability of a natural riverbed. Further, the temporal progress of scour is discussed in terms of a novel proposal taking into account the most significant parameters of pier scour. This relation resulted from extensive model observations and was tested with the available literature scour tests. As a third point, details of scour advance are described in terms of photographs taken from various locations. It is clearly stated that the maximum scour depth occurs only at an advanced stage upstream from the pier. Velocity distributions taken with a propeller may be used for calibration purposes but do not allow sufficient insight into the complex flow field around a pier. The need for advanced experimental instrumentation is outlined.

REFERENCES

1. Graf, W.H., Altinakar, M.S. (1996) *Hydraulique fluviale*. Presses Polytechniques et Universitaires Romandes: Lausanne (in French).
2. Hager, W.H., Oliveto, G. (2002) Shields entrainment condition in bridge hydraulics. *Journal of Hydraulic Engineering* accepted.
3. Hager, W.H., Unger, J., Oliveto, G. (2002) Entrainment criterion for bridge piers and abutments. Intl. Conf. Fluvial Hydraulics *River Flow 2002* Louvain-la-Neuve submitted.
4. Hoffmans, G.J.C.M., Verheij, H.J. (1997) *Scour manual*. Balkema: Rotterdam.
5. Oliveto, G., Hager, W.H. (2002) Temporal evolution of clear-water pier and abutment scour. *Journal of Hydraulic Engineering* tentatively accepted.
6. Raudkivi, A.J. (1998) *Loose boundary hydraulics*. Balkema: Rotterdam.

NOTATION

B	channel width
D	pier diameter
D_*	$=(g'/\nu^2)^{1/3}d_{50}$ dimensionless sediment size
d_{50}	mean grain size
F_d	$=V/(g'd_{50})^{1/2}$ densimetric particle Froude number
F_{di}	inception densimetric particle Froude number
g	gravitational acceleration
g'	$=((\rho_s-\rho)/\rho)g$ reduced gravitational acceleration
h	flow depth
R_*	$=u_*d_s/\nu$ grain Reynolds number
u_*	shear velocity
V	cross-sectional velocity
β	$=b/B$ or D/B contraction ratio
ν	kinematic viscosity
ρ	fluid density
ρ_s	sediment density
σ	$=(d_{84}/d_{16})^{1/2}$ sediment non-uniformity

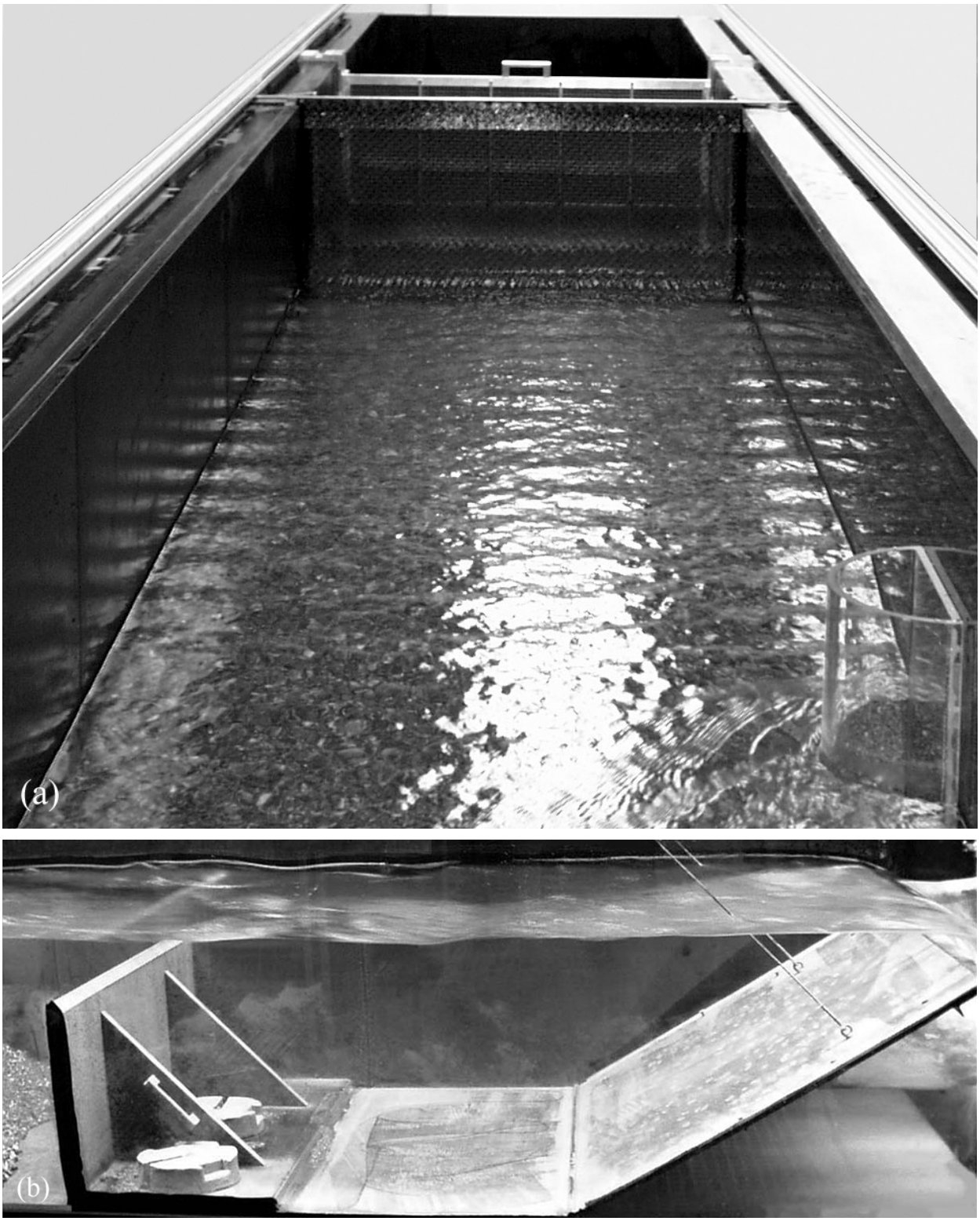

Fig. 1 - VAW scour channel (a) Upstream view with half-cylinder at glass wall, (b) Downstream view with submerged weir and flap gate.

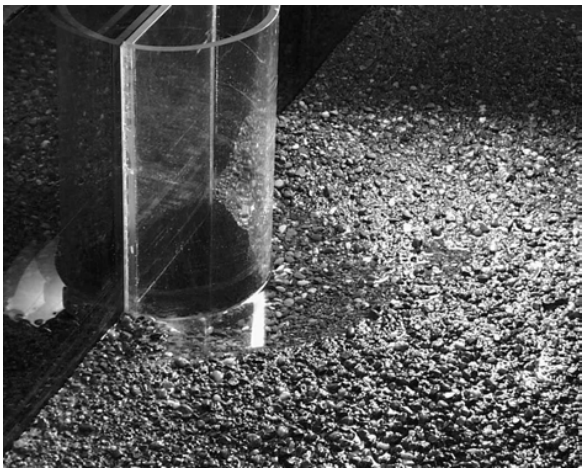
60 s

180 s

360 s

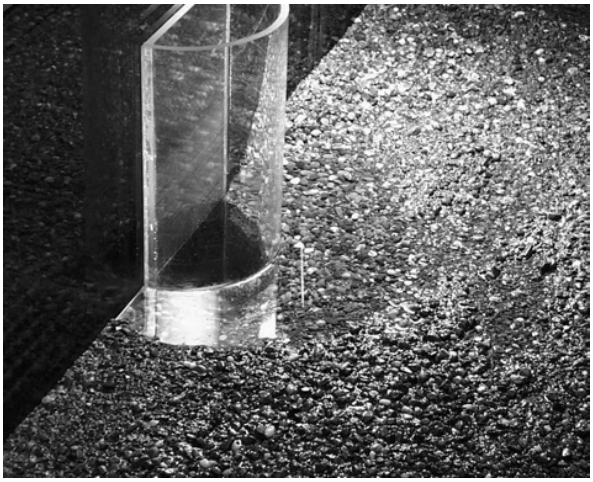
1200 s

52200 s

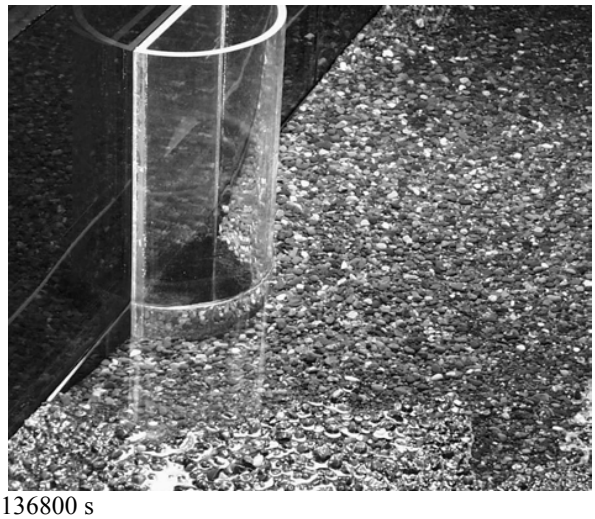
136800 s

Fig. 2 - Side view on half-cylinder to visualize scour progress at various times t, for h_o=0.15 m, d_{50}=0.045 m, σ=2.2 and F_d=2.5. Flow direction from bottom to top.

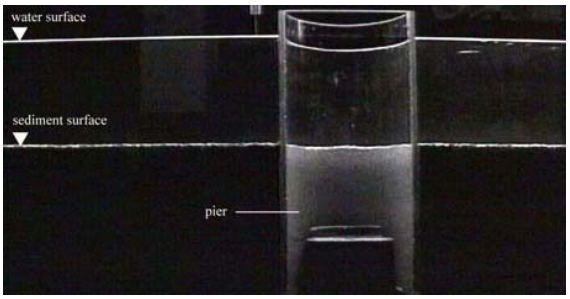

start

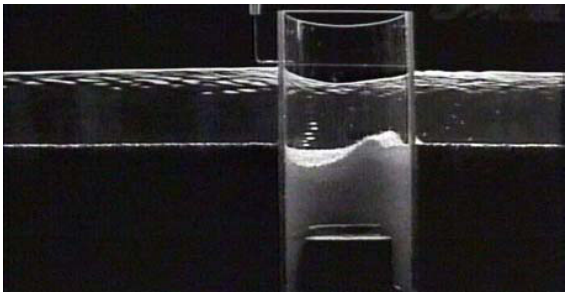
Phase 1

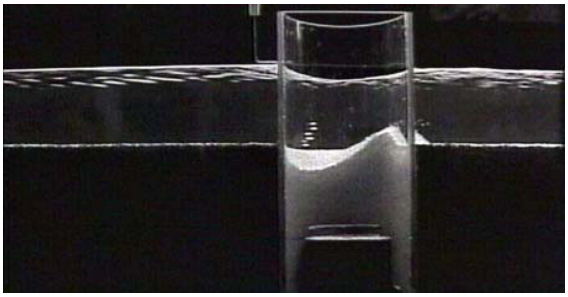
Phase 2

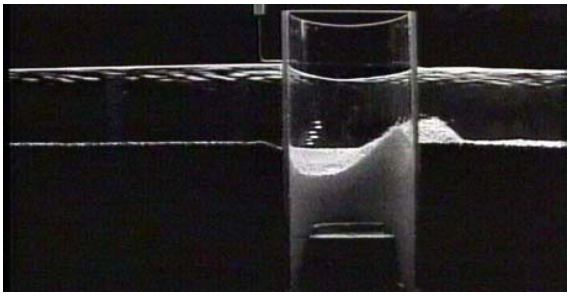
Phase 3

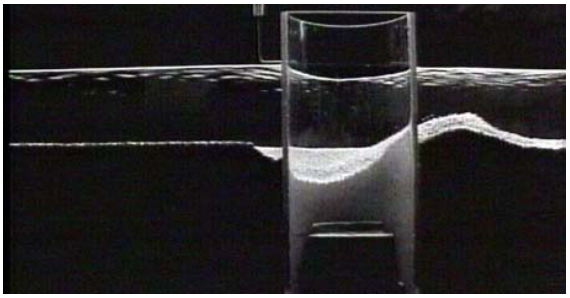
Phase 4

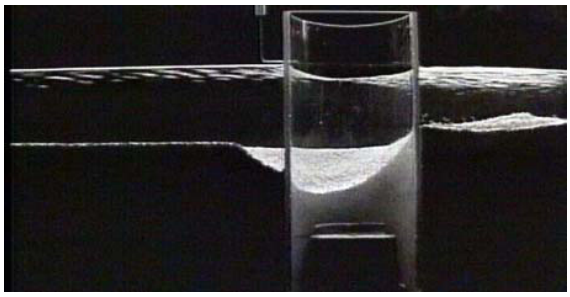
Phase 5

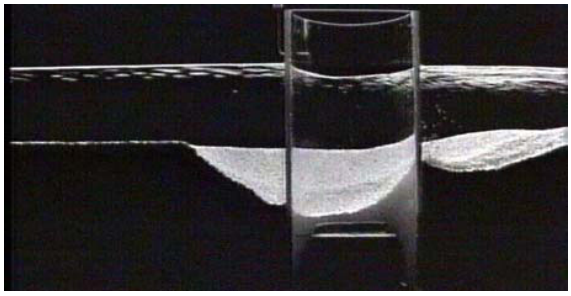
Phase 6

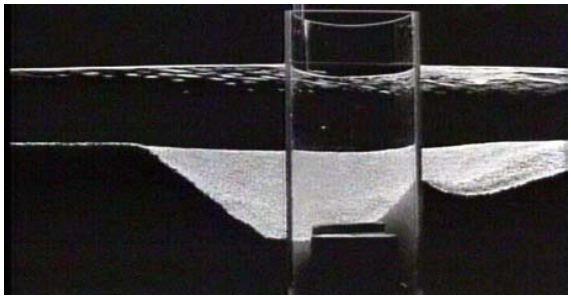
Phase 7

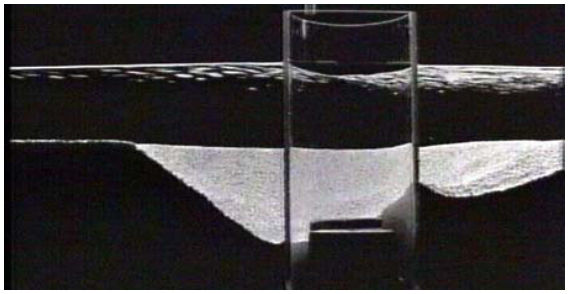
Phase 8

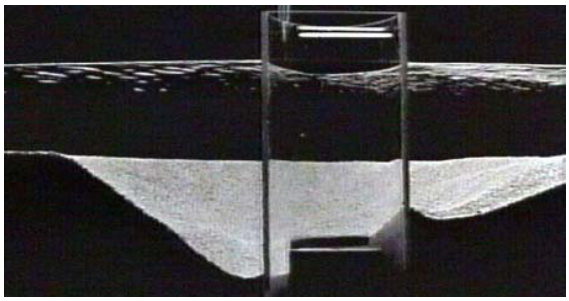
Phase 9

Fig. 3 - Lateral view of scour advance for a half-cylinder with ρ_s=1.41 t/m^3, h_o=0.15 m, D=0.257 m, d_{50}=0.0033 m and F_d=2.50

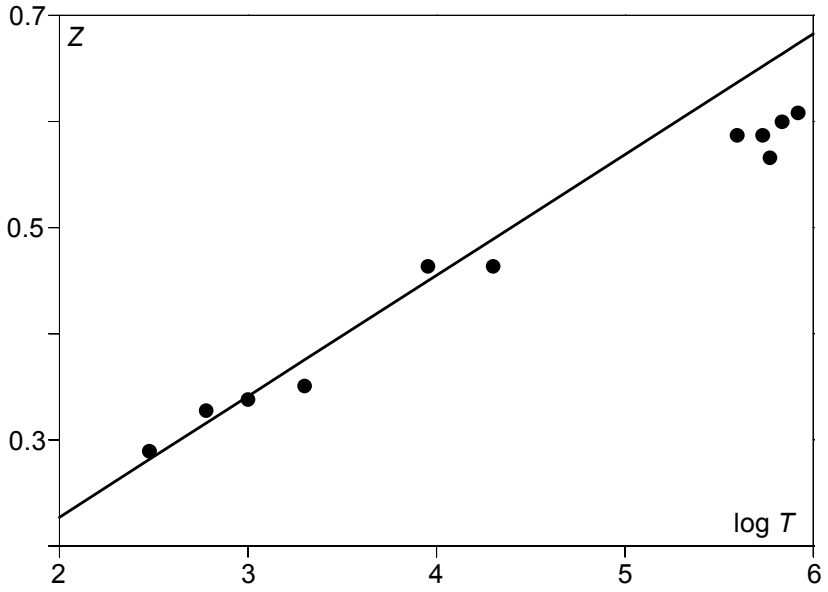

Fig. 4 - Comparison of (●) experimental test data with (—) prediction (5)

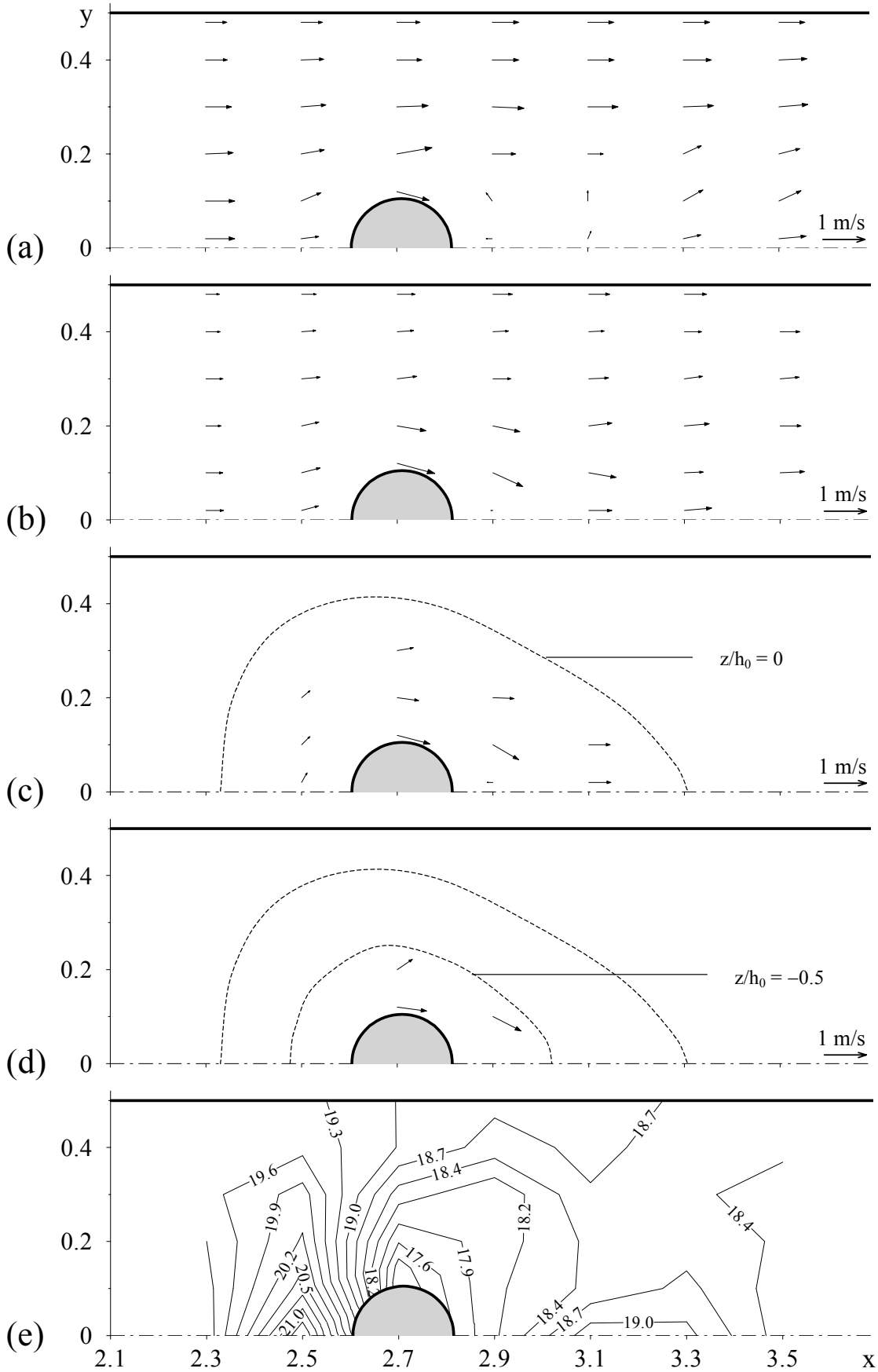

Fig. 5 - Velocity distributions in horizontal layers around a circular pier (a) close to the free surface, (b) at half flow depth, (c) close to sediment bed, (d) half flow depth below sediment bed, and (e) free surface geometry

Flow and Scouring in Main Channel due to Abutments

By

Guoliang Yu[1] Siow-Yong Lim[2] and Soon-Keat Tan[2]

ABSTRACT

This paper presents the flow and scouring characteristics around a vertical-wall abutment spanning across the floodplain and terminates at the edge of the submerged floodplain of a two-stage channel. The vertical velocity profiles around the abutment in the main channel were measured using an ADV. It was found that the flow pattern consists of complex interactions of spiral vortices around the abutment, downflows towards the bed, and upflow eddies behind the abutment nose. The velocity profiles around the abutment follow the logarithmic law near the bed, but the boundary layer thickness increases as the scouring process progresses. The increase of the bed shear stress around the abutment depends on the approach discharge. For the flat bed condition, equivalent to the beginning of scouring, the maximum value of the bed shear stress measured around the abutment nose was 3.8 times compared to that at the upstream approach section. At equilibrium scouring conditions, the bed shear stress at the deepest scour region was found to be approximately equal to the critical Shields value for sediment motion on a flat bed. At other sloping regions in the scour hole, the bed shear stress was smaller than the Shields value.

INTRODUCTION

A large number of bridge failures due to abutment scour during flood events have been recorded and this is of great concern to engineers and scientists (Melville, 1992, Richardson and Richardson, 1993). Basically abutment scour is caused by the flow impinging on the abutment, thereby changing the flow direction and resulting in bed shear stress increase near the abutment nose. This causes the erosion of the streambed material and formation of a scour hole at the abutment. For abutment scour in two-stage channels, the problem is more complicated. The abutment may be located on the floodplain or extends into the main channel, and in either case, it blocks and diverts the floodplain flow towards the main channel resulting in a complex flow pattern and an increase in velocity which cause the scouring at the abutment.

Current abutment scour prediction techniques are not applicable to a wide range of field conditions, and the scour depth is often over-predicted. Over-predicting abutment scour may result in construction of unnecessary countermeasures or excessively deep foundations, adding significant costs to bridge construction and maintenance (Niehus, 1996). Most experimental studies of scour around abutments have been conducted in rectangular laboratory flumes in which the distributions of flow velocity and bed shear stress were considered uniform in the transverse direction (Laursen 1963, Gill 1972, Melville 1992, Lim 1997). Idealized experiments in

1 Research Fellow, Maritime Research Centre, School of Civil and Environmental Engineering, Nanyang Technological University, Nanyang Avenue, Singapore 639798, cglyu@ntu.edu.sg

2 Assoc. Prof., Maritime Research Centre, School of Civil and Environmental Engineering, Nanyang Technological University, Nanyang Avenue, Singapore 639798, csylim@ntu.edu.sg, ctansk@ntu.edu.sg

rectangular flumes are representative of flow around abutments in well-defined incised channels or abutments in wide braided rivers. However, real river channels are different from these idealized laboratory conditions, and often have compound cross-sections. Due to the presence of the abutment and the redistributions of flow and bed shear stress between the floodplain and the main channel, the downflows, turbulence, and vortices near the nose of the abutment are quite different compared to that in a rectangular channel.

A few studies have been conducted on abutment scour in two-stage channels, but only a limited number of experiments have been done on abutments that terminate at the end of the floodplain (Sturm and Janjua 1994, Dongol 1994, Melville 1995, Kouchakzadeh and Townsend 1997, Cardoso and Bettess 1999, Lim and Yu 2001). This paper presents results on the flow conditions and bed scouring vis-à-vis bed shear stress around an abutment terminating at the interface between the floodplain and the main channel (Case III (b) of Melville's classification, 1995).

EXPERIMENTAL SET-UP

The experiments were conducted in a large two-stage channel as shown in Figs. 1 and 2. The two-stage channel is 19 m long, 1.6 m wide and 0.75 m high, in which there is one floodplain situated on one side of the channel. The floodplain is 1 m wide, 0.6 m deep and is at 0.15 m above the main channel bed. Both the floodplain and the main channel have a bed slope of 1/1000. A honey comb was placed at the inlet of the flume in order to obtain a uniform inflow velocity. The velocity was measured using a three-dimensional Acoustic Doppler Velocimeter (ADV) and the bathymetry of scoured bed was measured using a point gauge. Both the ADV and the point gauge were attached to a carriage installed on top of the flume.

Fig. 1 View of two-stage flume

Two sediment recess tanks 3 m long each were installed on the floodplain and the main channel, respectively, at a distance 11 m from the flume inlet. The tank was filled with the test sediment. The one on the floodplain is 0.40 m deep and the other in the main channel is 0.25 m deep. A vertical-wall abutment model of 1 m length and 0.05 m wide was installed perpendicular to the channel wall in the floodplain and

placed at the center of the sediment tank, as shown in Fig.3. Other than the sediment recess tank, the floodplain and main channel beds were made of steel. Sediment particles with diameters of 5-10 mm were sprinkled uniformly on the approach section in order to simulate bed roughness.

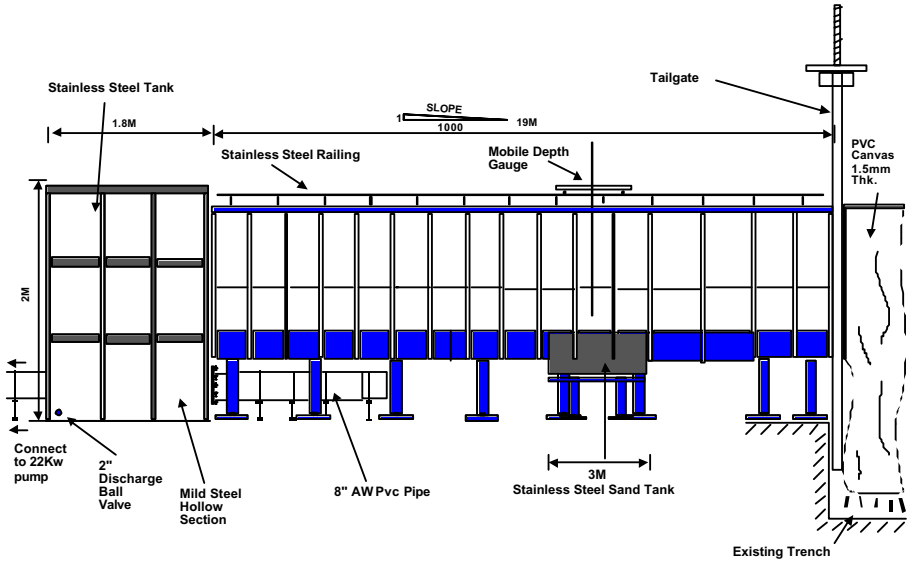

Fig. 2 Schematic sketch of flume

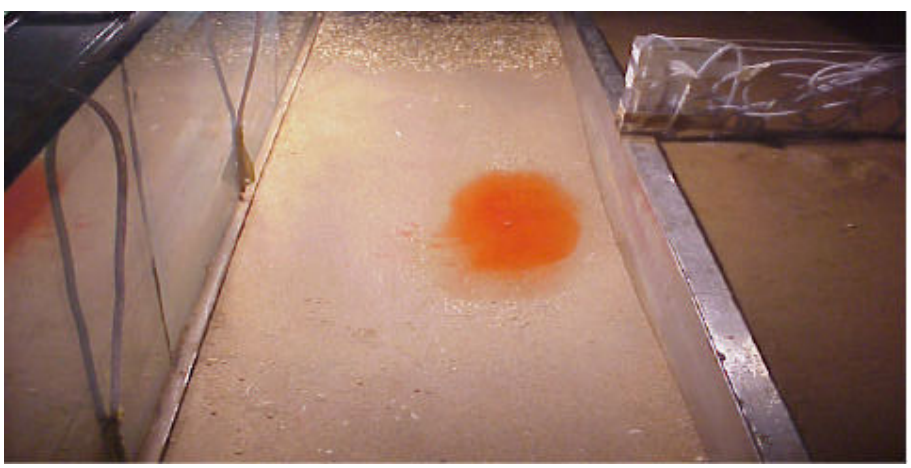

Fig. 3 View of abutment model

The sediment tanks were filled with uniform quartz sediment particles with a median diameter of 0.93 mm and a geometric sediment gradation of 1.17. The sediment beds were leveled to the same elevations as the floodplain and the main channel beds.

Each experiment was run for between one to three weeks, depending on the discharge, until the scouring process reached a static equilibrium state. Then, the pump was gently turned off and the water in the flume and the scour hole was slowly drained. When the scour hole was dry, the bathymetry of the scour hole was measured.

FLOW AROUND ABUTMENT

After the bathymetry measurement, the velocity field near the abutment was measured in the main channel using the ADV. The flow structure is shown in Fig. 4, based on extensive spatial velocity measurements around the abutment. The flow on the floodplain is diverted towards the main channel due to the abutment and converges with the main flow in the main channel. Spiral vortices can be seen generated at the upstream edge of the abutment nose. Viewing from the top, these spiral vortices rotate in an anticlockwise direction. Looking downstream, they roll in a clockwise direction. These vortices interfered and "blocked" the approach flow in the main channel. The blockage forced the approach flow to dive towards the bed with the formation of downflows on the right side of the spiral vortices. When the downflows pass under the vortices and then rise towards the water surface, large upflows (like an unsteady fountain) are generated on the left side of the spiral vortices (see Fig. 4). These upflow eddies in the main channel formed downstream of the abutment nose. The water surface elevation at the centers of the upflow eddies are generally higher than other places. The scales of the upflow eddies may be as large as the local flow depth. The upflow eddies eventually dispersed towards the floodplain. Fig. 4 also shows the formation of a large-scale flow circulation with a vertical axis at the corner behind the abutment.

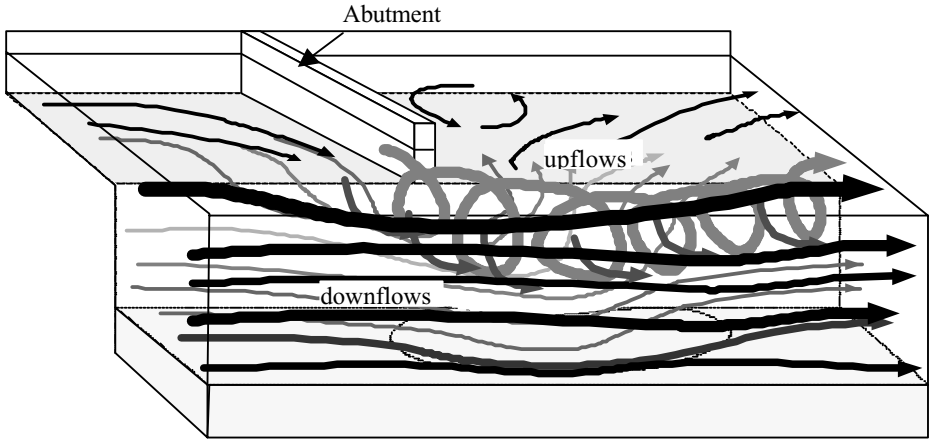

Fig. 4 Flow structure near abutment

The flow interactions and turbulence generated by the spiral vortices and upflow eddies are very strong, and these flow disturbances may be dangerous to navigation. At the core of the large-scale spiral vortices, the flow pattern is complex. At the edges of the spiral vortices boats may be sucked into the bottom by the diving downflows or turned over by the upflow eddies and spiral vortices. In order to investigate the path of the spiral vortices, floating objects were deliberately released upstream. The paths of the floating objects around and downstream of the abutment were recorded to obtain the centerlines of the spiral vortices. Fig. 5 shows the paths of the vortices as they spiraled from the abutment nose and their intrusion into the main channel. The 'intrusion' into the main channel is more severe as the flow discharge increases. The paths of the spiral vortices are similar to the trajectory of a projectile. The vortices generated at the upper edge of the abutment nose spiraled continuously into the main

channel and the maximum distance reached is approximately equal to the flow depth. The path then curves towards the floodplain region as the spiral proceed further downstream.

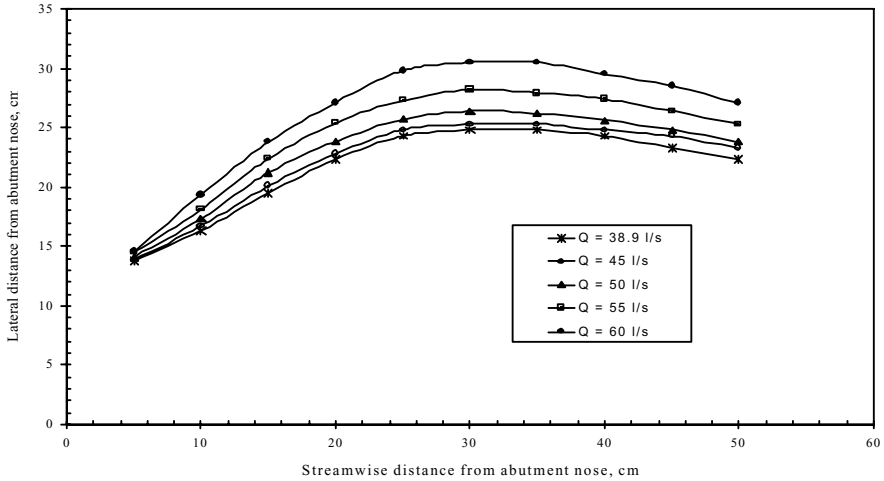

Fig. 5 Centerline location of large-scale vortices

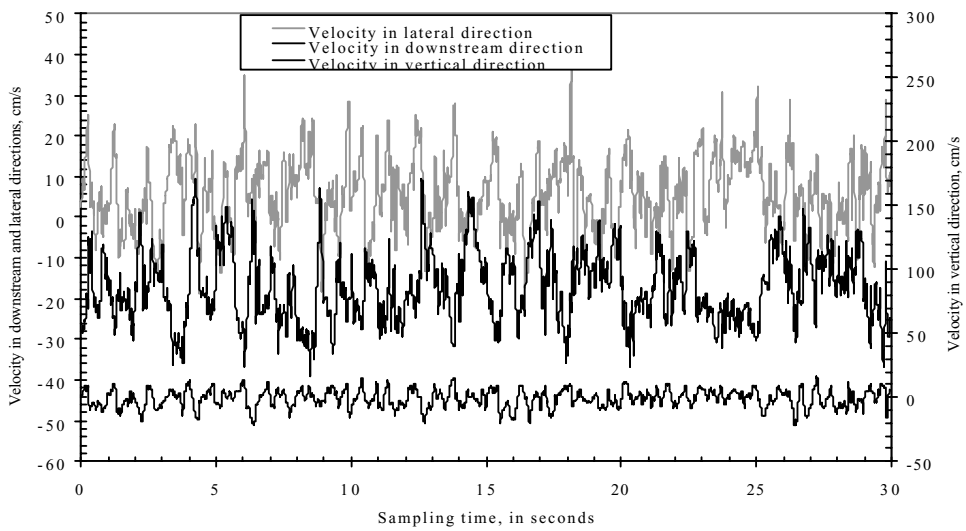

Fig. 6 Turbulence intensity in center of large-scale vortices

An example of the velocity fluctuation of the large scale vortex is shown in Fig. 6. The measurement was taken at a position 6.5 cm below the water surface in the main channel, 10 cm downstream of the abutment nose and 14 cm off the floodplain bank. The discharge was 60 l/s and flow depth in the main channel was 22.81 cm. The relative values of the average velocities in the lateral and vertical directions to the average velocity in the approach flow direction, $\bar{v}/\bar{u}$ and $\bar{w}/\bar{u}$, were about 0.31 and 0.06, respectively. However, the deviations of velocities in the three directions to the average velocity in the approach flow direction, $\sqrt{\overline{(u-\bar{u})^2}}/\bar{u}$, $\sqrt{\overline{(v-\bar{v})^2}}/\bar{u}$ and $\sqrt{\overline{(w-\bar{w})^2}}/\bar{u}$ were as high as 0.49, 0.52 and 0.41, respectively. The velocity measurements at other locations inside the large-scale vortices also show that the turbulence intensities are

high. This implies that the path of the large-scale vortices is a dangerous zone for navigation.

BED SHEAR STRESS DISTRIBUTION AROUND ABUTMENT

After the scour hole reached the equilibrium state, the velocity profiles near the bed at different locations within the scour hole were measured using the ADV. It was found that the velocity profiles complied with the logarithmic distribution. This is consistent with the findings of Ahmad and Rajaratnam (2000). Fig. 7 shows the velocity profiles at two locations with a discharge of 55 l/s. Fig. 7a shows a velocity dip near the water surface mainly because of the existence of the spiral vortices. The bed shear stress was obtained using a curve-fitting technique to the measured velocity profiles. The results indicated that the bed shear stress at the deepest location of the scour hole was very close to the critical shear stress for sediment motion on a flat bed, while at other places on the sloping part of the scour hole, the bed shear stresses were smaller than the critical shear stress on a flat bed. This may be due to the effect of the sloping bed on sediment motion. Figs. 8a to 8d show the bed shear stress distributions and scoured bed profiles for four different lateral sections in Run 9. The four locations in Figs. 8a to 8d are 24, 4, 12 and 32cm downstream of the abutment, respectively.

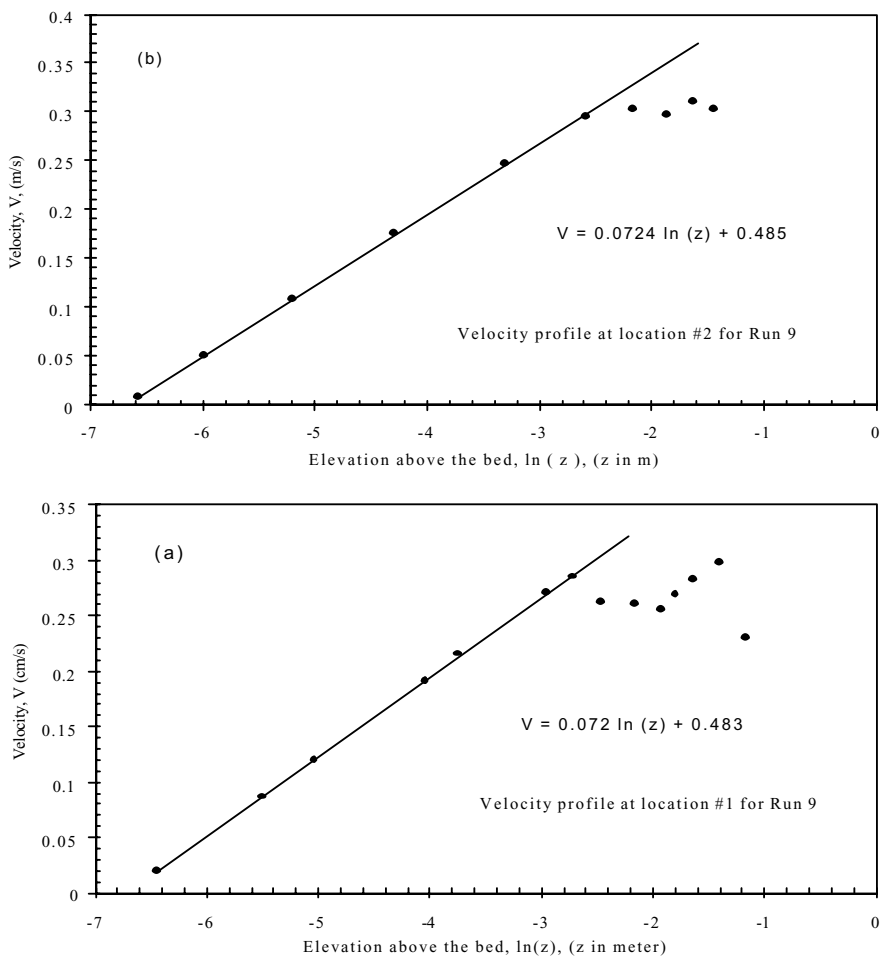

Fig. 7 Velocity profiles in scour hole for equilibrium scour

It was difficult to obtain the maximum bed shear stress near the abutment at the beginning of scouring because the rate of scouring was fast. However, it may be possible to obtain an estimate of the initial (time = 0) maximum bed shear stress near the abutment nose, t_{max} by interpolating the results of the shear measurements obtained at different scouring durations. The velocities at the planar location where the deepest scour hole occurred were measured every 30 minutes to obtain the bed shear stresses at different time interval. Fig. 9 shows the velocity profile for Run 9 after 85 minutes of scouring action. This maximum bed shear stress, t_{max}, was compared with the approach flat-bed shear stress, τ_{mc}, in the main channel (without abutment). As shown in Fig. 10, the interpolated ratios of t_{max}/τ_{mc} at time t = 0 were 3.8 and 3.6 for Runs 8 and 9, respectively.

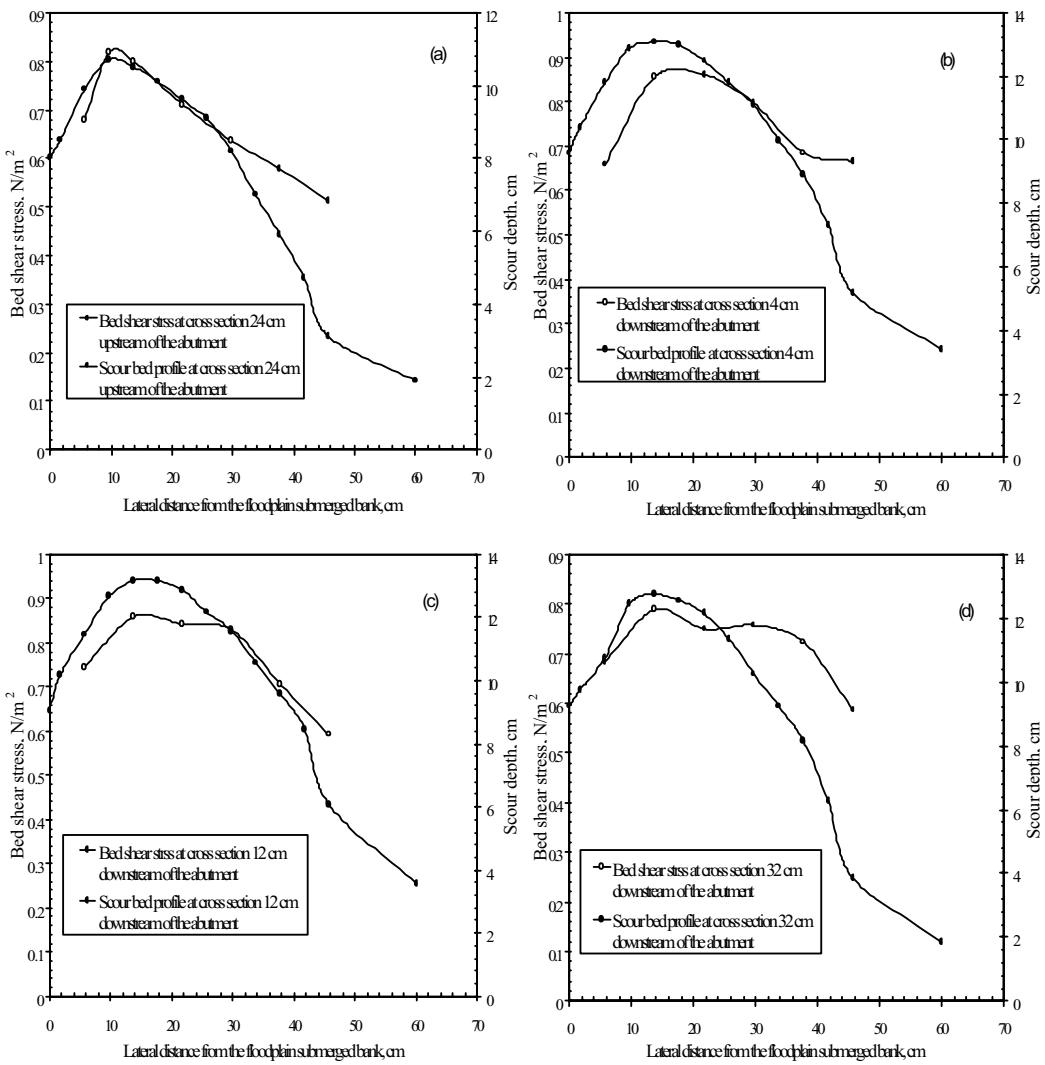

Fig. 8 Bed shear stress profiles in scour hole at equilibrium state for Run 9

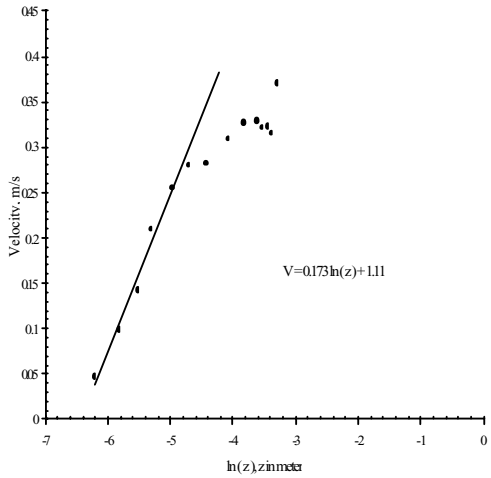

Fig. 9 Velocity profile after 85 minutes scouring

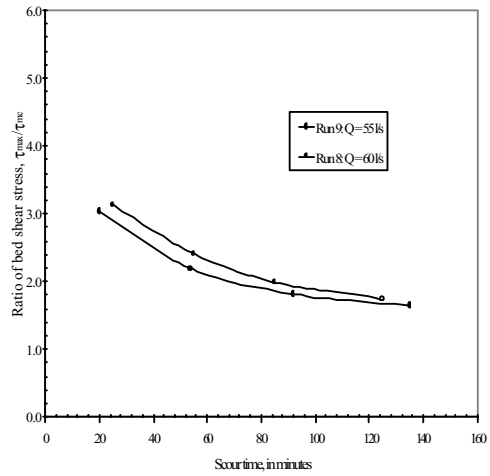

Fig. 10 Maximum bed shear stress decays with time

Fig. 11 shows the variation of t_{max}/τ_{mc} with approach discharge. The figure implies that t_{max}/τ_{mc} is dependent on the approach flow depth ratio and width ratio of the main channel and the floodplain. Fig. 11 shows that the maximum t_{max}/τ_{mc} = 3.8 was recorded for the maximum discharge, Q = 60 l/s used in this study. This value is comparable to that found by Ahmad and Rajaratnam (2000) on flow around abutments in rectangular channels. Their results show a maximum bed shear stress ratio amplification of about 3.63 times near the nose of the abutment. For circular bridge piers, the maximum bed shear stress ratio amplification was about 4.0 times at the nose of pier (Ettema 1980, Kothyari et al.; 1992). For flow around thin groynes, Rajaratnam and Nwachukwu (1983) found a fourfold increase in the bed shear stress near the tip of the groyne.

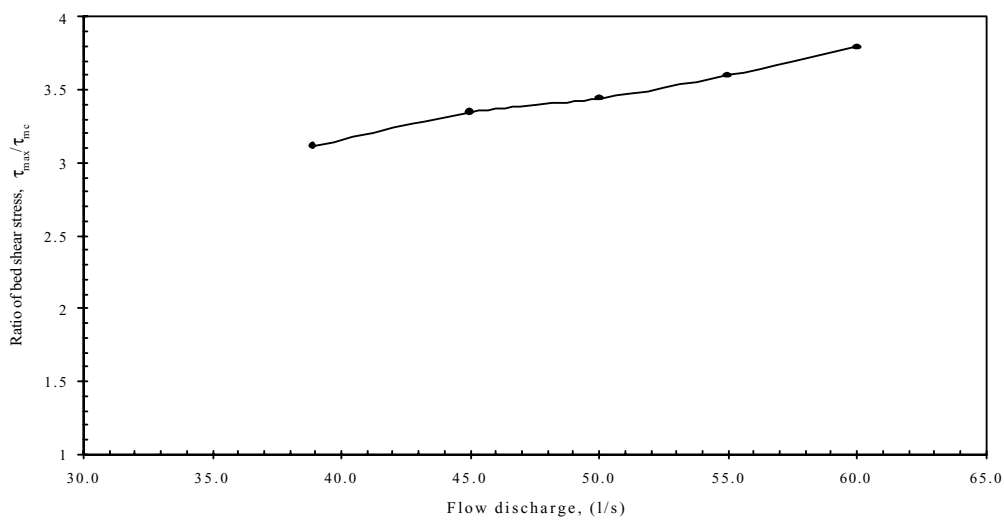

Fig. 11 Maximum bed shear stress in main channel against approach discharge

CONCLUSIONS

Experimental investigations demonstrate that the flow around an abutment in two-stage channels is complex, consisting of a spiral flow, an upflow and a downflow. The turbulence in the spiral flow and the upflow is strong and may be dangerous to navigation. The downflow is mainly responsible for bed scouring. The velocity profile around the abutment obeys the logarithmic law but the boundary layer thickness increases as the scouring process progresses.

The results show that the increase of the bed shear stress near the abutment location depends on the approach discharge. In the present test range, the maximum value of the bed shear stress amplification (t_{max}/τ_{mc}) before the scouring commences is 3.8 times near the nose of the abutment, and this corresponds approximately to the location in which the maximum scour depth was recorded. After the scouring reaches the equilibrium state, the dimensionless bed shear stress at the deepest position is equal to the critical Shields value for sediment motion, while at other places in the scour hole, the bed shear stress is smaller than the Shields value, probably due the effect of the sloping ground in these locations.

REFERENCES

Ahmad, F. and Rajaratnam N. (2000). "Observations on flow around bridge abutment." J. Engrg. Mech., ASCE , 126(1): 51-59.

Cardoso, A.H., and Bettess, R. (1999). "Effect of time channel geometry on scour at bridge abutments."*J. Hydr. Engrg*., ASCE, 125(4), 388-399.

Ettema, R.E. (1980). "Scour at bridge piers." Report No. 236. School of Engrg., The Univ. of Auckland, New Zealand.

Dongol, D.M.S. (1994). "Local scour at bridge abutments." Rep. No. 544, School of Engineering, University of Auckland, New Zealand.

Gill, M.A. (1972). "Erosion of sand beds around spur dikes." *J. Hyd. Div., ASCE,* 98(9), 1587-1602.

Kothyari, U.C., Garde, R.J. and Ranga Raju, K.G., (1992). "Temporal variation of scour around circular bridge piers." J. Hydr. Engrg. ASCE, 118(8), 1091-1106.

Kouchakzadeh, S., and Townsend, D.R. (1997). "Maximum scour depth at bridge abutments terminating in the floodplain zone." *Can. J. Civ. Eng*. 24: 996-1006.

Laursen, E.M. (1963). "An analysis of relief bridge scour." *J. Hydr. Div. ASCE,* 89(3), 93-118.

Lim, S.Y. (1997). "Equilibrium clear-water scour around an abutment." *J. Hydr. Engrg*., ASCE, 123(3), 237-243.

Lim, S.Y. and Yu, G, (2001). "Study on abutment scour in two-stage channel." Proceedings of XXIX IAHR Congress - 21st Century: The New Era for Hydraulics Research and its Applications, Beijing, China, Vol. II, Theme D, 16-21 Sept. 2001, pp. 8-13.

Melville, B.W. (1992). "Local scour at bridge abutments." *J. Hydr. Engrg*., ASCE, 118(4), 615-631.

Melville, B.W. (1995). "Bridge abutment scour in two-stage channels." *J. Hydr. Engrg*., ASCE, 121(12), 863-868.

Niehus, C.A., (1996), "Scour assessments and sediment-transport simulation for selected bridge sites in South Dakota." USGS, Water-Resources Investigations Report 96-4075.

Rajaratnam, N. and Nwachukwu, B.A. (1983). "Flow near groyne-like structure." J. Hydr. Engrg., ASCE, 109 (3), 463-480.

Richardson J.R. and Richardson E.V. (1993). "Discussion of local scour at bridge abutments." By B.W. Melville." *J. Hydr. Engrg*., ASCE, 119(9), 1069-1071.

Sturm, T.W., and Janjua, N.S. (1994). "Clear-water scour around abutments in floodplains." *J. Hydr. Engrg*., ASCE, 120(8), 956-972.

3-D Numerical Modeling of Flow and Scour Around a Pile

By

A. Roulund[1], B.M. Sumer[2], J. Fredsøe[3], J. Michelsen[4]

ABSTRACT

A 3-D flow code, EllipSys3D, tested and validated, has been implemented along with a morphologic model to simulate the scour process around a vertical circular pile in a steady current in the case of non-cohesive sediment. The k-ω turbulence model has been used for closure. The morphologic model includes (1) a two-dimensional bed load sediment transport description, and (2) a description of surface-layer sand slides for bed slopes exceeding the angle of repose. The simulation captured all the bed features, i.e. the scour hole and the formation of a downstream dune at the initial stage, and the truncated cone-shaped scour hole in the equilibrium stage. The maximum equilibrium scour depth obtained from the simulation compares fairly well with the measurements.

INTRODUCTION

During the last 30 years, more than 1000 of about 600.000 bridges in the United States have failed, and 60% of those failures are due to scour, Briaud et al. (1999). More than 85.000 bridges in the U.S. are vulnerable to scour (about 80.000 being scour-susceptible and about 7.000 scour-critical) (Lagasse et al., 1995). Two excellent accounts of scour at bridge piers have recently appeared in the literature. One is a compendium of papers presented in the ASCE Water Resources Engineering Conferences from 1991 to 1998 with 371 abstracts and 75 papers (Richardson and Lagasse, 1999). The other is a book by Melville and Coleman (2000), which, along with the recent knowledge, draws on the experiences on scour in New Zealand, and illustrates a great many examples of case studies.

The present paper deals with scour around a vertical circular pile in steady currents. The key element in the scour process is the so-called horseshoe vortex (Fig. 1). This vortex, combined with the effect of the contraction of streamlines at the side edges of the pile (Fig. 1), can erode a significant amount of sediment away from the neighbourhood of the pile, leading to a truncated-cone-shaped scour hole around the pile.

[1] Technical University of Denmark, Department of Mechanical Engineering, Coastal and River Engineering Section, Building 115, 2800 Lyngby, Denmark. Present address: NIRAS Sortemosevej 2, 3450 Allerød, Denmark
[2] Technical University of Denmark, Department of Mechanical Engineering, Coastal and River Engineering Section, Building 115, 2800 Lyngby, Denmark, (sumer@isva.dtu.dk)
[3] The same as above.
[4] Technical University of Denmark, Department of Mechanical Engineering, Fluid Mechanics Section, Building 403, 2800 Lyngby, Denmark.

Scour around piles in steady currents has been investigated quite extensively (particularly in the context of scour at bridge piers). Reviews of the subject can be found in the books of Breusers and Raudkivi (1991), Hoffmans and Verheij (1997), Whitehouse (1998), Raudkivi (1998), Melville and Coleman (2000) and Sumer and Fredsøe (2002).

While much has been written on the subject of scour around piles in steady currents, comparatively few studies have been presented of the 3-D numerical modeling of scour. Table 1 gives a list of studies on the 3-D modeling of flow and scour around piles in steady currents. As seen from the table, Olsen and his co-workers (1993, 1998) were the only researchers to undertake the 3-D modeling of the actual scour process.

The purpose of the present study is (1) to implement a hydrodynamic model, EllipSys3D, for the 3-D flow around a pile, both with a rigid plane bed and with a sediment bed undergoing scour; and (2) to conduct a 3-D numerical simulation of the actual scour process itself, using the former hydrodynamic model. A major paper, which summarizes the results of the study, is under preparation, Roulund et al. (2002). The present paper reports some of the results obtained for the numerical simulation of the scour process in the case of steady current.

HYDRODYNAMIC MODEL

A three-dimensional general-purpose flow solver, EllipSys3D, has been used to calculate the flow. EllipSys3D is a finite volume numerical model that solves the incompressible Reynolds-averaged Navier-Stokes equations

$$\frac{\partial \rho U_i}{\partial t} + \frac{\partial \rho U_i U_j}{\partial x_j} = -\frac{\partial p}{\partial x_i} + \frac{\partial}{\partial x_j}\left[(\mu + \mu_T)(\frac{\partial U_i}{\partial x_j} + \frac{\partial U_j}{\partial x_i})\right] \tag{1}$$

in which U_i is the i-th component of velocity; t is the time; x_i is the Cartesian coordinates; ρ is the fluid density; p is the dynamic pressure; μ is the viscosity; and μ_T is the eddy viscosity, calculated by a two-equation eddy-viscosity type turbulence model, as detailed in the following paragraphs.

EllipSys3D has been developed at the Risø National Laboratory, Denmark and at the Technical University of Denmark. It is an incompressible general purpose Navier-Stokes solver. It is basically a multiblock finite volume discretisation of the Reynolds Averaged Navier-Stokes equations. A Variety of turbulence models are available. The model is under constant development. It has been implemented successfully in various engineering problems such as those in wind engineering and aeronautical engineering. The basic principles of the model have been described in Sørensen, 1995 and Michelsen, 1992. The following web address can be consulted for further information:
http://www.risoe.dk/vea-aed/numwind/ellipsys.htm

We have also implemented the model to simulate the flow around and forces on a sphere placed near a bed. A paper summarizing the results of this latter study is under preparation.

For steady-state flow calculations, the SIMPLE algorithm (Patankar, 1980) is used. In this algorithm, the pressure field is calculated and the velocity field is corrected so that the continuity equation

$$\frac{\partial \rho}{\partial t} + \frac{\partial \rho U_j}{\partial x_j} = 0 \tag{2}$$

is satisfied in an iterative manner. By underrelaxation of the correction to the velocity field, the transient components of the flow are suppressed. Although the majority of the present study involved steady-state flow calculations, some transient flow calculations have also been performed.

Table 1. A list of studies on 3-D modeling of flow and scour around a pile in a current.

Author	Turbulence model	Steady current: Steady solution; or Transient solution	Bed: Rigid bed; or Sediment bed	Scour	Remarks
Olsen and Melaaen (1993)	k-ε	Steady solution	Sediment bed	Initial stage of scour is simulated. Clear-water scour	Horseshoe vortex is resolved
Olsen and Kjellesvig (1998)	,,	,,	,,	Entire scour process is simulated. Clear-water scour	,,
Richardson and Panchang (1998)	Turbulent closure through a number of advanced schemes	Steady solution, and Transient solution (?)	Three kinds of "frozen" rigid beds, ranging from a plane bed to equilibrium scour hole	Scour process is not simulated	,,
Tseng, Yen and Song (2000)	Large Eddy Simulation	Transient solution	Rigid plane bed	Scour process is not simulated	Horseshoe vortex and vortex shedding are resolved
Present	k-ω	Steady solution, and Transient solution	Both rigid and sediment beds	Entire scour process is simulated. Live-bed scour	Horseshoe vortex is resolved. Vortex shedding is resolved in some rigid-bed simulations

The k-ω model (Wilcox, 1993) has been selected as the turbulence model because of its better performance in the case of boundary-layer flows with strong adverse pressure gradients (Wilcox, 1993; Menter, 1992). The details of (1) the algorithms used in both the steady-state flow calculations and the transient calculations and (2) the turbulence model adopted in the study will be given in Roulund et al. (2002).

The boundaries of the computational domain are (1) Inlet, (2) Outlet, (3) Symmetry Boundaries and (4) Walls.

At the inlet boundary, zero transverse, v, and vertical, w, velocities were specified. The inlet profiles for u, k and ω were based on the equilibrium profiles obtained from uniform-channel flow calculations with similar flow settings. At the outlet boundary, zero-gradient (Neumann) conditions were applied for all quantities. At the symmetry boundaries (i.e., at the sides and top surface of the computational domain), Neumann conditions were applied for k and ω, while no-flux conditions were applied for the three components of the velocity, u, v and w (in which u is the streamwise component of the velocity). At the walls (i.e., at the bed, and at the surface of the pile) zero velocity was specified for u, v and w; zero turbulent energy was specified for k when the wall was smooth, while the Neumann condition was applied when the wall was rough and transitional. Regarding the latter condition, experiments do reveal that the Neumann condition (i.e., $\partial k/\partial n = 0$) is satisfied at the wall, n being the direction normal to the wall; see Nezu, 1977; Sumer et al., 2001 and 2002). The Dirichlet condition was applied for ω,

$$\omega = S_r \frac{U_f^{\,2}}{\upsilon} \tag{3}$$

in which $U_f = (\tau_0 / \rho)^{1/2}$ is the friction velocity based on the wall shear stress τ_0. The quantity S_r is a tuning parameter, and it is used to account for the bed roughness:

$$S_r = \left(\frac{40}{k_s^{\,+}}\right)^3, \quad k_s^{\,+} < 20.2 \tag{4}$$

$$S_r = \frac{100}{(k_s^{\,+})^{0.85}}, \quad k_s^{\,+} > 20.2 \tag{5}$$

in which $k_s^{\,+} = k_s U_f / \nu$ is the wall roughness in wall units, ν is the kinematic viscosity and k_s is Nikuradse's equivalent sand roughness. Wilcox (1993) was the first to introduce the previous boundary condition. The tuning parameter S_r was given by Wilcox (1993) in a form slightly different from that in the preceding equations.

The momentum, continuity and turbulence-model equations are transformed into curvilinear coordinates, linearised and decoupled. The latter has been described in detail in Sørensen (1995), following the principles given in Patankar (1980).

The computational mesh is based on a multi-block structure with each block containing N^3 computational cells where N is the number of cells in each spatial direction. $N = 16$ was used for the scour and transient-flow simulations. The total number of cells in these cases was 197.000. The number of cells across the depth was 32, and the number of cells around the pile perimeter was 64. The length, width and depth of the computational domain were 15D, 18D and 2D, respectively. In the case of steady (not transient) rigid-bed simulations, N was 32; the total number of cells was 786.000; the number of cells across the depth was 64, while the number of cells around the pile perimeter was 128; the length, width and depth of the computational domain were 20D, 20D and 2D,

respectively. (It may be noted that N = 32 required prohibitively large computational times for the scour and transient flow simulations). Fig. 2 shows a detailed picture of the mesh used for the steady-current rigid-bed calculations.

MORPHOLOGIC MODEL

The morphologic model couples the flow solution with a sediment transport description, and routines for updating the computational mesh based on the mass balance of sediment.

There are three elements in the morphologic model: (1) the bed load; (2) the sand slide; and (3) the equation of continuity for sediment.

Each element is now considered individually.

Bed load. A two-dimensional bed load description has been developed. This description is actually an extension of the bed-load equation of Engelund and Fredsøe (1976) to a 2-D vectorial representation. The bed load occurs on a slope (Fig. 3). $\overrightarrow{U_b}$ is the mean transport velocity of a particle moving as bedload. The fluid velocity at the particle position is $\vec{U}$, different from $\overrightarrow{U_b}$ (Fig. 3). Following Engelund and Fredsøe (1976), the latter velocity may be taken as $\vec{U} = a\overrightarrow{U_f}$ in which $\overrightarrow{U_f}$ is the friction velocity, and a is an empirical constant, taken as a = 10.

The rate of bedload transport in volume per unit time and per unit width, $\overrightarrow{q_b}$, is related to $\overrightarrow{U_b}$ by the following equation (Engelund and Fredsøe, 1976)

$$\overrightarrow{q_b} = \frac{\pi}{6} d^3 \frac{p_{EF}}{d^2} \overrightarrow{U_b} \tag{6}$$

in which d is the grain size, and p_{EF} is the percentage of particles in motion in the surface layer of the bed. The above equation implies that the bedload transport is determined by two quantities: p_{EF} and $\overrightarrow{U_b}$.

In the case where the sediment transport takes place on a horizontal bed, Engelund and Fredsøe (1976) obtained the following semi-empirical expression for p_{EF}

$$p_{EF} = \left[1 + \left(\frac{\frac{\pi}{6}\mu_d}{\theta - \theta_c} \right)^4 \right]^{-1/4} \tag{7}$$

in which μ_d is the dynamic friction coefficient, taken as 0.51 (Fredsøe and Deigaard, 1992, p. 218), θ is the Shields parameter and θ_c is the critical value of θ for the initiation of sediment motion at the bed.

We have adopted in the present study the same expression as in Eq. 7 to calculate the quantity p_{EF}. In the case of the sloping bed, p_{EF} may undergo a slight change, in the order of magnitude of (1/cos β) where β is the slope of the bed (Fig. 3). However, this has not been incorporated in the calculations on grounds that such a refinement in the model may be inconsistent with several other assumptions inherent in the formulation of the sediment transport.

The Shields parameter in Eq. 7 is

$$\theta = \frac{U_f{}^2}{g(s-1)d} \tag{8}$$

in which s is the specific gravity of the sediment grains, and g is the acceleration due to gravity. U_f in Eq. 8 is taken as the magnitude of the friction-velocity vector associated with the skin friction.

The critical Shields parameter in Eq. 7, on the other hand, is

$$\theta_c = \theta_{c0}(\cos\beta\sqrt{1-\frac{\sin^2\alpha\tan^2\beta}{\mu_s{}^2}} - \frac{\cos\alpha\sin\beta}{\mu_s}) \tag{9}$$

in which θ_{c0} is the critical Shields parameter for a horizontal bed, taken as 0.05, μ_s is the static friction coefficient, taken as $\mu_s = 0.63$ for the sand used in the present simulation (Lambe and Whitman, 1969, p.149), and α is the angle between the flow velocity vector and the direction of the steepest bed slope (Fig. 3).

The particle velocity is obtained from the two components of the equation of particle motion. The equation of motion in the direction of particle motion, considering that the particle is, on average, moving with a constant velocity:

$$F_D\cos\psi_1 + W\sin\beta\cos(\alpha-\psi) - (W\cos\beta)\mu_d = 0 \tag{10}$$

in which W (= $(\pi/6)\rho g(s\text{-}1)d^3$) is the submerged weight of the particle, F_D is the drag force

$$F_D = \frac{1}{2}\rho C_D\frac{\pi}{4}d^2U_r{}^2 \tag{11}$$

in which C_D is the drag coefficient, and U_r is the velocity of the fluid (at the particle position) relative to the particle (Fig. 3), $\overrightarrow{U_r} = a\overrightarrow{U_f} - \overrightarrow{U_b}$. Luque (1974) (see also Fredsøe and Deigaard, 1992, p. 211) found from his experiments:

$$C_D = \frac{4\mu_s}{3a^2(\frac{1}{2}\theta_{0c})} \tag{12}$$

The equation of motion in the direction perpendicular to $\overrightarrow{U_b}$, on the other hand, reads:

$$F_D \sin\psi_1 - W \sin\beta \sin(\alpha - \psi) = 0 \tag{13}$$

There are also the following geometric relations from Fig. 3

$$U_r \sin\psi_1 - aU_f \sin\psi = 0 \tag{14}$$

and

$$U_r \cos\psi_1 - aU_f \cos\psi + U_b = 0 \tag{15}$$

Eqs. 10, 13, 14 and 15 are to be solved for the four unknown quantities, namely U_b, U_r, ψ and ψ_1. Once U_b and ψ_1 are determined (and therefore $\overrightarrow{U_b}$ is obtained), then inserting $\overrightarrow{U_b}$ and p_{EF} in Eq. 6 will give the bed load transport $\overrightarrow{q_b}$.

Sand slide. Observations show that, during the development of the scour process, there are areas at the upstream side of the scour hole where the local bed slope exceeds the angle of repose, and, as a result, shear failures occur at these locations. Two "ingredients" of this latter process are that, first of all, the backward flow at the base of the pile erodes the foot of the upstream slope of the scour hole (A in Fig. 4), and secondly there is a continuous sediment supply into the scour hole from upstream (B in Fig. 4).

Our visual observations have indicated that, in the upstream part of the scour hole, the bed "avalanched" when the slope β exceeded approximately the angle of repose, $\beta_r = 32^0$, by a few degrees. They have also shown that this shear failure of the soil occurred just below the bed surface, and sand slided down towards the centre of the scour hole, and, after each sand slide, the bed slope was a few degrees lower than the angle of repose.

Based on these observations, a sand slide procedure was developed to calculate the new slope of the bed, and it was incorporated in the morphologic model. The adopted procedure is as follows: (1) Calculate a new sediment transport rate when the local bed slope is exceeded $\beta_r + 2^0$. (2) Do this, based on a new particle velocity U_b, obtained from the following equation:

$$W \sin\beta - \mu_d W \cos\beta - \frac{1}{2}\rho C_D \frac{\pi}{4} d U_b^{\,2} = 0 \tag{16}$$

(This is basically the equation of motion for a sediment particle (undergoing the sand slide) in the direction of the particle motion, considering that the particle is, on average, moving with a constant velocity in an otherwise still water). (3) Update the bed with the ordinary morphology scheme (described in the following paragraphs). (4) Repeat this procedure until the local bed slope was reduced to β_r - 2^0. In this procedure, a pseudo time step was used since it was assumed that the sand slide takes place instantaneously.

Continuity equation for sediment. The mass balance for sediment at each grid point on the bed is

$$\frac{\partial h}{\partial t} = \frac{-1}{1-n}\frac{1}{A}\sum_{i=1}^{4}(\overrightarrow{q_{b,i}} \bullet \overrightarrow{n_i})|l_i| \tag{17}$$

in which h is the bed elevation, n is the porosity (taken as n = 0.4 in the present calculations); A is the projected area (on the x,y plane) of a small bed element; i indicates the number assigned to each side of the projected area (i=1,..4); $\overrightarrow{n_i}$ are the normal vector at the i–th side of the projected area, $\overrightarrow{q_{b,i}}$ is the sediment transport vector at the i–th side of the projected area; and $|l_i|$ is the length of the i–th side of the bed element.

The procedure in the computations was as follows: (1) Generate the mesh; (2) Calculate the flow; (3) Calculate the sediment transport due to bed load; (4) Update the bed; (5) Check the sand slide; and (6) Return Step 1. The morphological time step in the calculations was 0.02 s initially, and gradually raised to 0.1 s. The computational time was 2.5 months on an Alpha 21264 workstation, equivalent to a 1500 MHz Pentium IV.

Finally, it may be noted that, in the present model, the sediment transport is taken as the bed load alone (no suspended-load sediment transport is considered). To the authors' knowledge, no study is yet available, investigating the effect of the suspended load on scour in a systematic manner. However, the data reported in Baker (1986) (where the velocity is increased gradually so as to cover the flow regimes from the clear-water scour to the live-bed scour with the bed-load, the bed-load and suspended load and finally the suspended-load mode sheet-flow regimes; see Melville and Sutherland, 2000, p. 493, or Sumer and Fredsøe, 2002, p. 179) suggests that this effect is not radically significant.

RESULTS AND DISCUSSION

A detailed validation exercise has been undertaken for the hydrodynamic model for the case where the bed was plane and rigid. Three kinds of quantities have been tested, namely the velocity, the pressure and the bed shear stress. The velocities calculated by the model have been compared with our own data, obtained with the Laser Doppler Anemometry technique. (This has been achieved for both smooth and rough bed cases). The pressures have been calculated for the same test conditions as in the experiments of Dargahi (1989) and compared with the measured pressures of the latter author. The bed shear stresses, calculated from the model, have been compared with our own hot-film measurements, and also with the experimental data of Hjorth (1975) where the bed shear stress was measured, again, using the hot-film technique. A detailed description of the entire validation exercise including the description of the experiments will be given in Roulund et al. (2002).

From the latter, it has been concluded that the model captures fairly well the mean features of the 3-D flow, including the horseshoe vortex (one of the key elements in the scour process), meaning that it can be used for the calculation of the scour process around a pile placed in a sediment bed. The following paragraphs will present the results of this numerical experiment where the scour process is simulated using the previously described hydrodynamic and morphologic model.

In the numerical simulation of scour, vortex shedding was not resolved (the steady-state flow simulation was adopted). This was because of the prohibitively large computational

times required for the transient flow solution (where the vortex shedding is resolved) combined with the time-resolved morphologic calculations. We shall return to this point later in the section.

The water depth in the simulation was taken as δ =20 cm, corresponding to the boundary layer thickness. The pile diameter was D = 10 cm. The mean flow velocity was V = 46 cm/s. Based on the mean grain size d_{50} = 0.26 mm, Nikuradse's equivalent sand roughness for the bed was estimated to be k_s = 0.7 mm from the relation $k_s = 2.5\ d_{50}$. The Shields parameter was θ = 0.11, i.e., the scour was in the live bed regime. The ratio between the approach velocity and the critical velocity for the initiation of sediment motion was V/V_c = 1.6.

In the simulation, the bed ripples were resolved. To trigger the development of ripples a perturbation was applied to the prescribed bed roughness in the first 20 seconds of the simulation. The sediment transport description in the present model is based on uniform-size sand, i.e., the sediment gradation was $\sigma_g = d_{85}/d_{50} = 1$.

Fig. 5 shows a sequence of pictures, illustrating the time evolution of the scour hole obtained in the present simulation. As seen from the figure, all the topographic bed features observed in a typical scour process (in the laboratory, or in the field, see for example, Melville and Coleman, 2000 and Sumer and Fredsøe, 2002) are captured. These features are: (1) The semi-circular shape of the upstream part of the scour hole with a slope equal to the angle of repose; (2) The formation of a "bar" downstream of the pile (the deposited sand), and its downstream migration; (3) The formation of a gentler slope of the downstream side of the scour hole; and (4) The formation and migration of ripples outside the scour hole.

Baker (1986) (see also Melville and Coleman, 2000, p. 493) reports experimental data for the equilibrium scour depth as a function of the sediment gradation σ_g and the velocity ratio V/V_c. For V/V_c = 1.25 (the value of the velocity ratio used in the simulation), the experimental data for the equilibrium scour depth can be worked out from the data reported in the latter publications. Table 2 (Row 2) presents the results of this exercise.

Table 2. Equilibrium scour depths for V/V_c = 1.25. Comparison. The experimental values in the second row in the table are worked out from the experimental data of Baker (1986) (see also Melville and Coleman, 2000, p. 493 for Baker's data).

Sediment gradation, σ_g	1.0	1.3	2.3	2.9	4.4	5.2
Equilibrium scour depth, S/D Experiments, δ/D = 3.8-6, Baker (1986)	-	1.9	1.7	0.9	0.4	0.16
Equilibrium scour depth, S/D Numerical result, δ/D = 2, Present	1.5	-	-	-	-	-

Table 2 shows that the normalized equilibrium scour depth S/D for a sediment with a size distribution close to uniform, namely σ_g = 1.3, is S/D =1.9. The present simulation (for sediment with a uniform size distribution) predicts this value as S/D = 1.5 (21% smaller

than the measurements for σ_g = 1.3). It may be noted, however, that part of this discrepancy may be accounted for the relatively small value of the boundary-layer-to-pile-diameter ratio in the simulation, namely $\delta/D = 2$ (see Melville and Sutherland, 1988, for the influence of the boundary-layer thickness on the scour depth; see also Sumer and Fredsøe, 2002, p. 180).

Fig. 6 shows the bed shear stress amplifications for the initial plane bed and for the equilibrium scoured bed in the simulation. The bed shear stress amplification for the scoured bed is reduced considerably. However, the bed shear stress in the scour hole is still larger than outside the scour hole. This is linked to the relatively higher transport rates inside the scour hole (the higher transport rates dictated by the sediment continuity).

As discussed earlier, the vortex shedding is not resolved in the present scour calculations. To observe the influence of the vortex shedding on the flow, some transient flow calculations with a rigid plane bed have been undertaken. These calculations have shown the following. (1) The transient behaviour of the wake was evident from the numerical simulation with the shear layers emanating from the side edges of the pile, rolling up to form the lee-wake vortices sketched in Fig. 1, which eventually lead to vortex shedding; (2) The horseshoe vortex was also evident in the transient calculations (not surprisingly); and (3) The transient component of the flow regarding the horseshoe vortex was practically nonexistent; the present simulation did not resolve the secondary, time-dependent vortices within the horseshoe vortex reported in Baker (1979) and Dargahi (1989).

In the previously described steady-state solutions of the present flow model, the transient component of the flow is suppressed in the iteration procedure of the numerical simulations (see the discussion under Hydrodynamic Model above). In this connection, an interesting question may be: how does the steady solution compare with that obtained by *time averaging of the transient solution* (the time averaging taken over one vortex-shedding period). Fig. 7a shows the contour plot of the bed shear stress obtained from the steady solution, while Figure 7b shows that of the time-averaged bed shear stress from a transient simulation. As seen, the two plots are almost identical. It is only in the wake region where a slight difference is observed. This would enable the large computational times for transient simulations to be reduced tremendously (by as much as an order of magnitude) by adopting steady simulations of the flow, and obviously the latter would be a great advantage when such computations are implemented for scour calculations.

CONCLUSIONS

1. A 3-D hydrodynamic model, EllipSys3D, incorporated with the k-ω turbulence model has been adopted to simulate the flow around a vertical circular pile exposed to a steady current.
2. The model has been coupled with a morphologic model. The latter has been used to calculate scour around a vertical circular pile exposed to a steady current.
3. The present numerical simulation captures all the main features of the scour process.

4. The equilibrium scour depth obtained from the simulation agrees fairly well with the measurements.
5. The calculations show that the amplification in the bed shear stress around the pile is reduced considerably with respect to that experienced at the initial stage where the bed is plane.
6. The calculations also show that the bed shear stress in the scour hole can still be larger than the undisturbed value. This is linked to the contraction of the streamlines in the scour hole towards the pile.
7. Computations with a rigid plane bed reveal that the steady flow calculations give practically the same bed shear stress as the time-averaged bed shear stress obtained from the transient flow calculation.

ACKNOWLEDGEMENTS

This study has been partially funded by the Commission of the European Communities, Directorate-General XII for Science, Research and Development Program Marine Science and Technology (MAST III) Contract No. MAS3-CT97-0097, Scour Around Coastal Structures (SCARCOST), and by the five-year (1999-2004) Framework Programme "Computational Hydrodynamics" of the Danish Technical Research Academy, STVF.

REFERENCES

1. Baker, C. J. (1979). “The laminar horseshoe vortex”. J. Fluid Mechanics, vol. 95, part 2, 347-367.
2. Baker, R. A. (1986). Local Scour at Bridge Piers in Non-Uniform Sediment. Thesis presented to the University of Auckland, New Zealand, in partial fulfillment of the requirements for the degree of Master of Philosophy.
3. Breusers, H.N.C. and Raudkivi, A.J. (1991). Scouring. A.A. Balkema, Rotterdam, viii + 143 p.
4. Briaud, J.-L., Ting, F.C.K., Chen, H.C., Gudavalli, R., Perugu, S. and Wei, G. (1999). “SRICOS: Prediction of scour rate in cohesive soils at bridge piers”. *J. Geotechnical and Geoenvironmental Engineering*, ASCE, vol. 125, No. 4, 237-246.
5. Dargahi, B. (1989). “The turbulent flow around a circular cylinder”. *Exp. in Fluids*, vol. 8, 1-12.
6. Engelund, F. and Fredsøe, J. (1976). “A sediment transport model for straight alluvial channels”. *Nordic Hydrology*, vol. 7, 293—306.
7. Fredsøe, J. and Deigaard, R. (1992). Mechanics of Coastal Sediment Transport, World Scientific, xx + 369 p.
8. Hjorth, P. (1975). Studies on the nature of local scour. Bull. Series A, No. 46, viii + 191 p., Department of Water Resources Engineering, Lund Institute of Technology/University of Lund, Lund, Sweden.
9. Hoffmans, G.J.C.M. and Verheij (1997). Scour Manual. A.A. Balkema/ Rotterdam.
10. Lagasse, P.F., Thompson, P.L. and Sabol, S.A. (1995). “Guarding against scour”. *Civil Engineering*, June issue, 56-59.
11. Lambe T.W. and Whitman, R.V. (1969). Soil Mechanics. John Wiley and Sons, Inc.
12. Luque R.F. (1974). Erosion and Transport of Bed Sediment, Dissertation, Jrips Repro B.V.-Meppel.
13. Melville, B.W. and Coleman, S.E. (2000). Bridge Scour. Water Resources Publications, LLC, CO, USA, xxii + 550 p.
14. Melville, B.W. and Sutherland, A.J. (1988). “Design methods for local scour at bridge piers”. *J. Hydraulic Engineering, ASCE*, vol. 114, No. 10, 1210-1226.
15. Menter, F.R. (1993). “Zonal two equation k-ω turbulence models for aerodynamic flows”. AIAA-paper-93-2906, *AIAA 24th Fluid Dynamic Conference*, July 6-9, 1993, Orlanda, Florida.

16. Michelsen, J.A. (1992). Basis3D - a platform for development of multiblock PDE solvers. Technical report, Dept. of Fluid Mechanics, Technical University of Denmark, AFM 92-05, ISSN 0590-8809.
17. Nezu, I. (1977). Turbulent Structure in Open Channel Flows. Ph.D. thesis, Kyoto University, Japan.
18. Olsen, N.R.B. and Kjellesvig, H.M.(1998). "Three-dimensional numerical flow modelling for estimation of maximum local scour", *J. Hydr. Res*., 36(4), 579-590.
19. Olsen, N.R.B. and Melaaen, M.C. (1993). "Three-dimensional calculation of scour around cylinders". *J. Hydraulic Engineering, ASCE*, vol. 119, No. 9, 1048-1054.
20. Patankar, S.V. (1980). Numerical Heat Transfer and Fluid Flow. Series in computational methods in mechanics and thermal sciences, Taylor and Francis.
21. Raudkivi, A.J. (1998). Loose Boundary Hydraulics. A.A. Balkema / Rotterdam.
22. Richardson, E.V. and Lagasse, P.F. (1999). Stream Stability and Scour at Highway Bridges. Compendium of Papers ASCE Water Resources Engineering Conferences 1991 to 1998. Richardson and Lagasse (eds.). ASCE, 1801 Alexander Bell Drive, Reston, Virginia 20191-4400. xxxi + 1040 p.
23. Richardson J.E. and Panchang V.G. (1998). "Three-dimensional simulation of scour-inducing flow at bridge piers", *J. Hydraulic Engineering, ASCE*, vol.124, No. 5, 530-540.
24. Roulund, A., Sumer, B.M. and Fredsøe, J. (2002). "Numerical and Experimental investigation of flow and scour around a circular pile". Manuscript in preparation.
25. Sumer, B.M. and Fredsøe, J. (2002). Mechanics of Scour in the Marine Environment. World Scientific, xiv + 536 p.
26. Sumer, B.M., Cokgor, S. and Fredsøe, J. (2001). "'Suction removal of sediment from between armour blocks". *J. Hydraulic Engineering, ASCE*, vol. 127, No. 4, pp. 293-306.
27. Sumer, B.M., Chua, L.H.C., Cheng, N.-S. and Fredsøe, J. (2002). "The influence of turbulence on bedload sediment transport". Manuscript submitted.
28. Sørensen, N.N. (1995). General purpose flow solver applied to flow over hills. Ph.D. thesis, Risø National Laboratory, Roskilde, Denmark, Risø-R-827(EN).
29. Tseng, M.-H., Yen, C.-L. and Song, C.C.S. (2000). "Computation of three-dimensional flow around square and circular piers". *International J. for Numerical Methods in Fluids*, vol. 34, 207-227.
30. Whitehouse, R. (1998): Scour at Marine Structures. Thomas Telford, xix + 198 p.
31. Wilcox, D.C. (1993). Turbulence modeling for CFD. DCW Industries, Inc, La Canada, California, USA, 2nd edition.

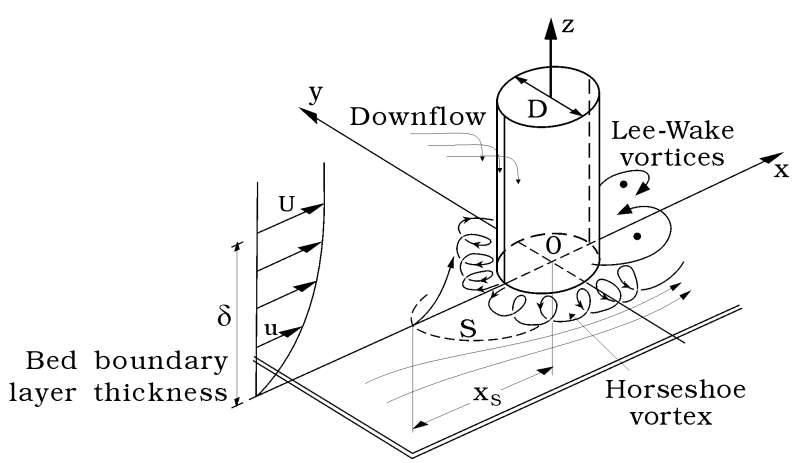

Fig. 1. Definition sketch.

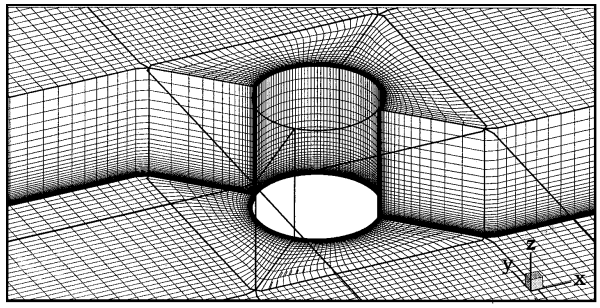

Fig. 2. Detail of mesh and block structure.

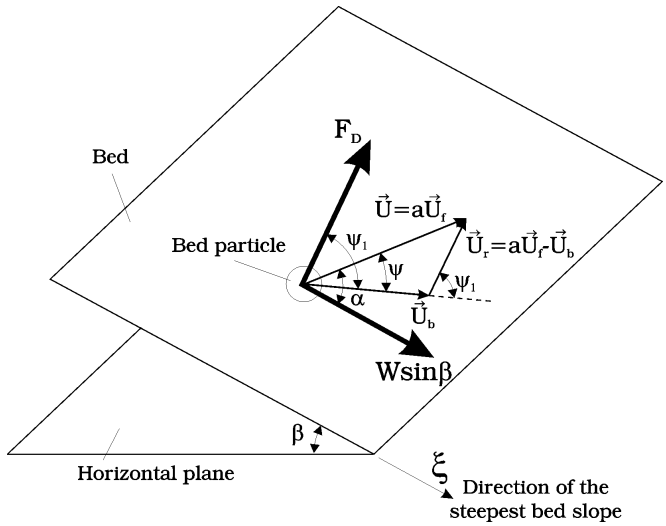

Fig. 3. Force balance on a single bed-load particle on a sloping bed.

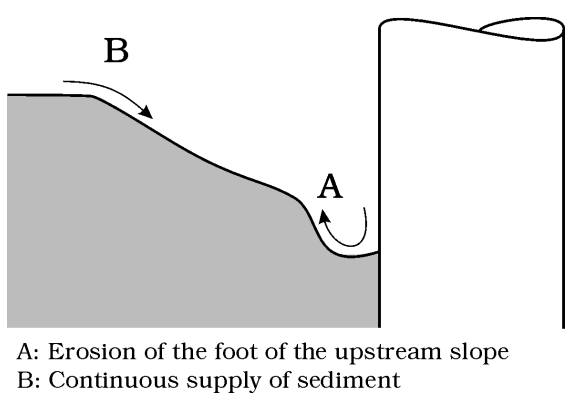

Fig. 4. Sand slide.

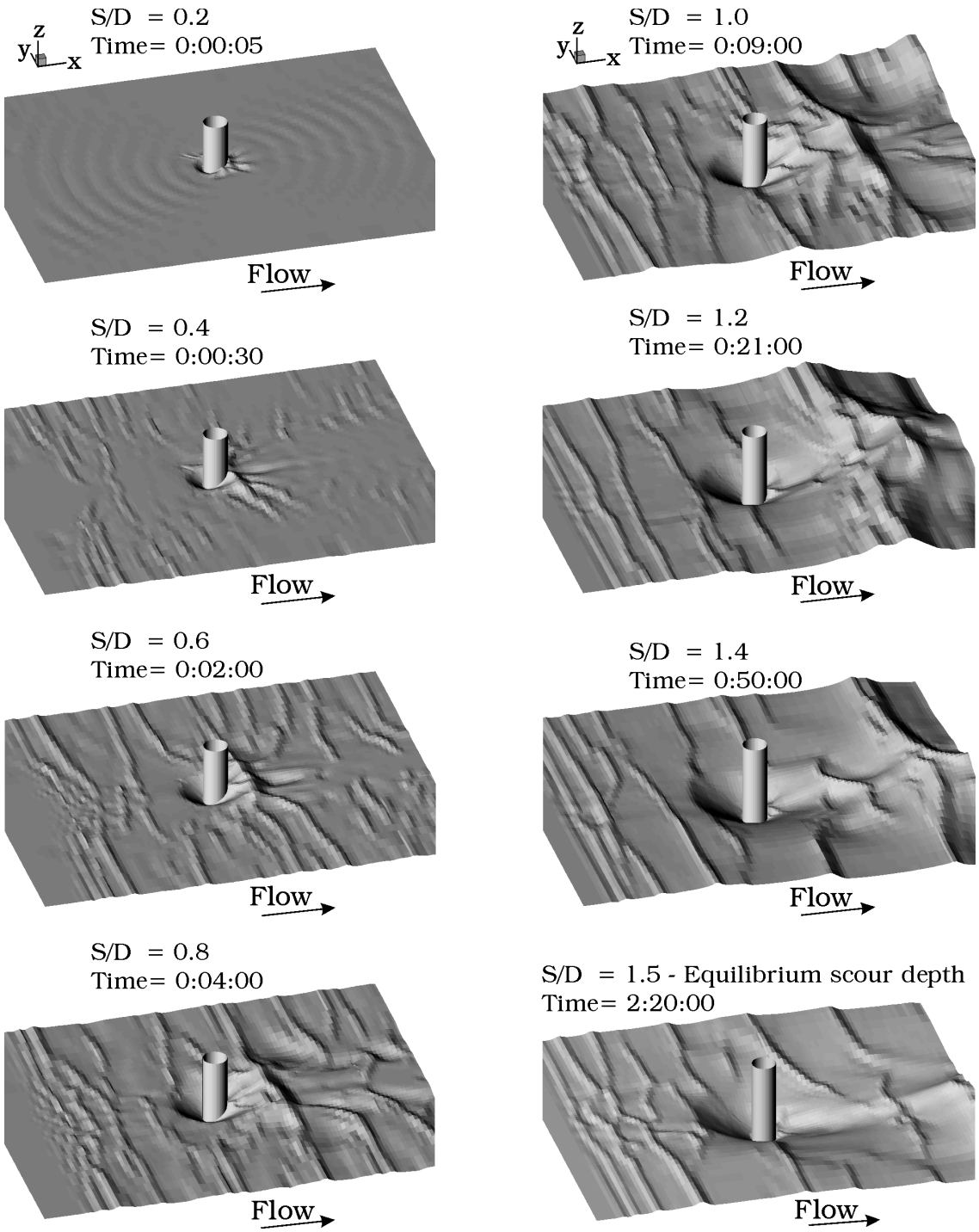

Fig. 5. A sequence of the bed morphology calculated from the present model.

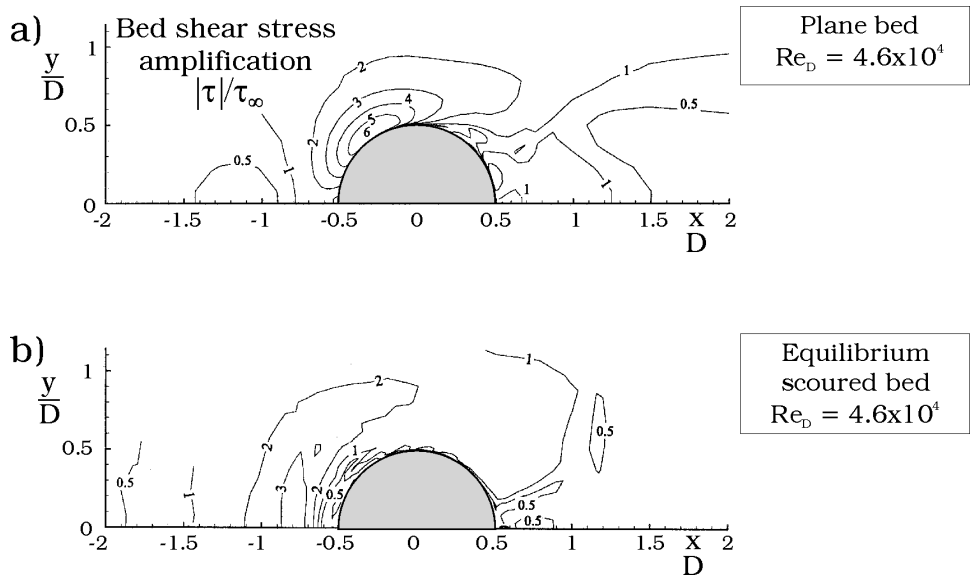

Fig. 6. Amplification in the bed shear stress.

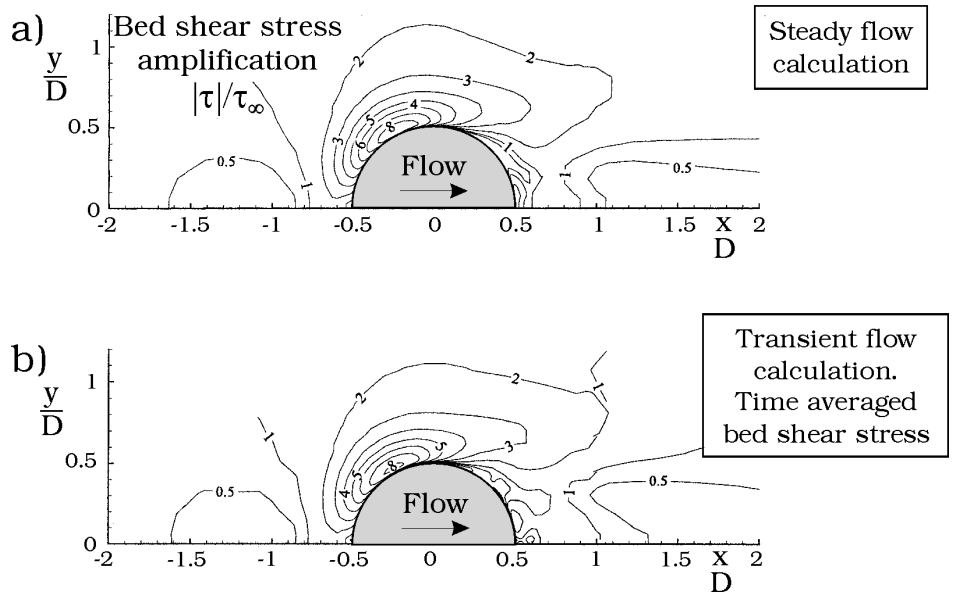

Fig. 7. Amplification in the bed shear stress. Plane bed. Comparison between the steady flow calculation and the transient flow calculation. $Re_D = 4.6\times10^4$, $\delta/D = 2$, $D/k_S = 140$ and $k_S^+ = 15$.

New Approach to Scour Evaluation of Complex Bridge Piers

by
Everett V. Richardson,[1] J. Sterling Jones,[2] and D. Max Sheppard[3]

ABSTRACT

Complex bridge piers are those that have two or three substructural elements subjected to the flow. These substructural elements are the pier stem, pile cap or footing, and piles. Two or more of the substructural elements may be subjected to the flow by design or by long term degradation and/or contraction scour. Ongoing research has determined that the total scour depth can best be determined by separating the complex pier into each of its substructural elements, determine the scour depth for each element and adding them. This paper presents equations and procedures to determine scour depths for the design of new bridges and evaluation of existing bridges with complex pier foundations. However, physical model studies are recommended for complex piers to reduce uncertainly, increase the safety of the design, and reduce cost.

INTRODUCTION

The U.S. Department of Transportation, Federal Highway Administration (FHWA) in 1988 issued a Technical Advisory requiring the States to evaluate the scour vulnerability of all highway bridges over water. A publication titled "Interim Procedures for Evaluating Scour at Bridges" was issues as an attachment. In 1991 the attachment was modified and issued as Hydraulic Engineering Circular 18 (HEC 18) titled "Evaluation Scour at Bridges". In 1993 an updated second edition was issued. Followed in 1995 by a third edition and in 2001 by a fourth edition (Richardson et al, 2001). In addition, in 1991 HEC 20 titled "Stream Stability at Highway Structures" was issued. Followed by the second edition in 1995, and a third edition in 2001 (Lagasse et al, 2001). In 1997 HEC 23 titled "Bridge Scour and Stream Instability Countermeasures" was issued with a second edition in 2001 (Lagasse et al, 2001).

These three publications (HEC 18, 20 and 23) comprise a set of three publications for the use by the States in the design and evaluation of their bridges for scour and stream instability. In the Fourth Edition of HEC 18 a new and improved approach was added for the scour evaluation of complex piers. A complex pier is one where two or more of the foundation components (piles, pile cap or footing and pier shaft) are or may be exposed to the flow. This paper will describe and illustrate this new approach which was developed at the Turner-Fairbank and Florida University research laboratories. In using these method engineering judgment must be used. Engineering judgment should take into consideration the volume of traffic, type of traffic (school bus, ambulance, fire trucks, local road, interstate, etc.), the importance of the highway, cost of a failure (potential loss of life and dollars) and the increase in cost that would occur if the most conservative scour depth is used.

[1] Senior Associate, Ayres Associates, P. O. Box 270460 and Professor Emeritus of Civil Engineering, Colorado State University, Fort Collins, Co
[2] Research Hydraulic Engineer, Federal Highway Administration, Turner-Fairbank Highway Research Center, 6300 Georgetown Pile, McLean, VA
[3] Professor of Coastal and Oceanographic Engineering, University of Florida, Gainesville, FL

TOTAL SCOUR

Total scour at a highway bridge is composed of the following elements

- Long term degradation of the stream bed
- General scour (contraction scour is the main component)
- Local scour at the piers and abutments
- Stream instability

LOCAL SCOUR AT BRIDGE PIERS

Using a study by Jones (1983) of the many equations for the determination of local scour at piers an equation based on the CSU equation (Richardson et al, 1975) was recommended for both live-bed and clear-water pier scour in the Interim Procedures for Evaluating Scour at Bridges. With modifications the CSU equation is the base equation for editions of HEC 18. Mueller (1996), using 384 field scour measurements at 56 bridges to compare 22 equations, concluded that the HEC 18 equation was good for design. The equation predicts maximum pier scour depths. The HEC 18 equation is:

$$\frac{y_s}{y_1} = 2.0\ K_1\ K_2\ K_3\ K_4\ K_w \left(\frac{a}{y_1}\right)^{0.65} Fr_1^{0.43} \qquad (1)$$

where:

y_s	=	Scour depth, m (ft)
y_1	=	Flow depth directly upstream of the pier, m (ft)
K_1	=	Correction factor for pier nose shape from table 1
K_2	=	Correction factor for angle of attack of flow from equation 3
K_3	=	Correction factor for bed condition from table 3
K_4	=	Correction factor for armoring by bed material size, see HEC 18
K_w	=	Correction factor for wide piers, equations 4 and 5
a	=	Pier width, m (ft)
L	=	Length of pier, m (ft)
Fr_1	=	Froude Number directly upstream of the pier = $V_1/(gy_1)^{1/2}$
V_1	=	Mean velocity of flow directly upstream of the pier, m/s (ft/s)
g	=	Acceleration of gravity (9.81 m/s^2) (32.2 ft/s^2)

$$K_2 = (\text{Cos}\ \theta + L / a\ \text{Sin}\ \theta)^{0.65} \qquad (2)$$

If L/a is larger than 12, use L/a = 12 as a maximum in Equation 2.

Table 2 illustrates the magnitude of the effect of the angle of attack on local pier scour.

Table 1. Correction Factor, K_1, for Pier Nose Shape.	
Shape of Pier Nose	K_1
(a) Square nose	1.1
(b) Round nose	1.0
(c) Circular cylinder	1.0
(d) Group of cylinders	1.0
(e) Sharp nose	0.9

Table 2. Correction Factor, K_2, for Angle of Attack of the Flow.			
Angle	L/a=4	L/a=8	L/a=12
0	1.0	1.0	1.0
15	1.5	2.0	2.5
30	2.0	2.75	3.5
45	2.3	3.3	4.3
90	2.5	3.9	5.0
Angle = skew angle of flow L = length of pier, a = pier width			

Table 3. Increase in Equilibrium Pier Scour Depths, K_3, for Bed Condition.		
Bed Condition	Dune Height ft	K_3
Clear-Water Scour	N/A	1.1
Plane bed and Antidune flow	N/A	1.1
Small Dunes	3> H > 0.6	1.1
Medium Dunes	9> H > 3	1.2 to 1.1
Large Dunes	H > 9	1.3

Notes:

1. The values of the correction factor K_2 should be determined using the length of the pier actually subjected to the angle of attack of the flow. Also, Piers set close to abutments must be carefully evaluated for the angle of attack and velocity of the flow coming around the abutment.
2. The correction factor K_3 results from the fact that in sand bed streams a plane-bed or antidunes will exist at most bridge sites for the flood frequencies employed in scour design. When large dunes exists during flood flow, the maximum pier scour may be 30 percent greater than the predicted equation value. This may occur on very large rivers, such as the Mississippi. For smaller streams with a dune bed configuration at flood flow, the dunes will be smaller and the maximum scour may be only 10 to 20 percent larger.
3. The correction factor K_4 decreases scour depths for armoring of the scour hole for coarse bed materials (Mueller & Jones, 1999). Equations to compute K_4 are given in the third and forth editions of HEC 18. However, research is continuing to improve methods to determine K_4
4. The correction factor, K_w (Johnson and Torrico, 1994) is applied when the ratio of depth of flow (y) to pier width (a) is less than 0.8 ($y/a < 0.8$); the ratio of pier width (a) to the median diameter of the bed material (D_{50}) is greater than 50 ($a/D_{50} > 50$); and the Froude Number of the flow is subcritical. Engineering judgment is needed in applying K_w because it is based on limited flume data.

The equations for K_w are:

$$K_w = 2.58\left(\frac{y}{a}\right)^{0.34} Fr_1^{0.65} \quad \text{for } V / V_c < 1 \tag{3}$$

$$K_w = 1.0\left(\frac{y}{a}\right)^{0.13} Fr_1^{0.25} \quad \text{for } V / V_c \geq 1 \tag{4}$$

where:

V_c = Critical velocity of the D_{50} bed material size (see HEC 18). The other variables as previously defined.

SCOUR FOR COMPLEX PIER FOUNDATIONS

Introduction

Most pier scour research has focused on solid piers with limited attention to determining scour depths when (1) pile groups, (2) pile groups and pile caps, or (3) pile groups, pile caps and solid piers are exposed to the flow (Salim and Jones, 1995, 1996, and 1999). The three types of exposure to the flow may be by design or long-term degradation, general (contraction) scour, and local scour, in addition to stream migration. In the general case, the flow could be obstructed by three substructural elements.(the pier stem, the pile cap or footing, and the pile group). Ongoing research (Jones and Sheppard, 2000, Sheppard, 2001) has determined methods and equations to determine scour depths for complex pier foundations. The results of this research are given in HEC 18 and the following sections. The following steps are recommended for determining the depth of scour for any combination of the three substructural elements exposed to the flow.

- The scour depths should be determined for the 100-year flood or smaller discharge if it causes deeper scour and a superflood. A 500-year flood, is recommended in HEC 18.
- If needed, use computer programs to compute the hydraulic variables.
- Analyze the complex pile configuration to determine the components of the pier that are exposed or will be exposed to the flow.
- Determine the scour depths for each component exposed to the flow using the equations and methods presented in the following sections.
- Add the components to determine the total scour depths.
- Plot the scour depths and analyze the results using an interdisciplinary team to determine their reliability and adequacy for the bridge, flow and site conditions, safety and costs.
- Conduct a physical model study if engineering judgment determines it will reduce uncertainly, increase the safety of the design, and/or reduce cost.

Superposition of Scour Components Method of Analysis

The components of a complex pier are illustrated in Figure 1. Note that the pile cap can be above the water surface, at the water surface, in the water or on the bed. The location of the pile cap may result from design or from long-term degradation and/or contraction scour. The pile group, as illustrated, is in uniform (lined up) rows and columns. This may not always be the case. The support for the bridge in many flow fields and designs may require a more complex arrangement of the pile group. In more complex pile group arrangements, the methods of analysis given in this manual may give smaller or larger scour depths.

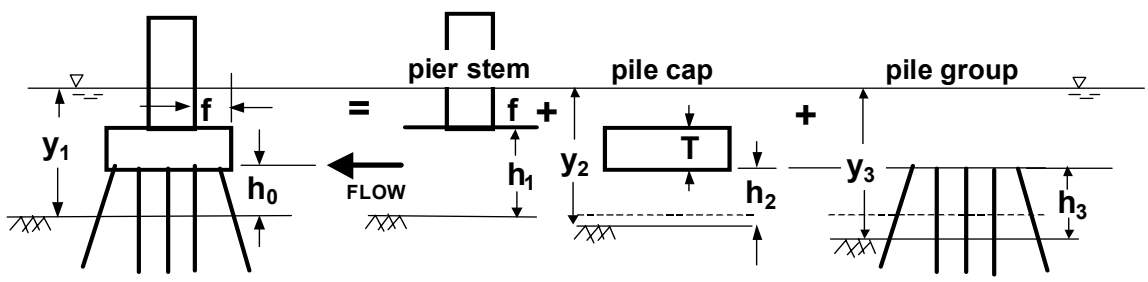

$$y_s = y_{s\ pier} + y_{s\ pc} + y_{s\ pg}$$

Figure 1. Scour components for a complex pier (Jones and Sheppard (2000).

The variables illustrated in Figure 1 and others used in computations are as follows:

- f = Distance between front edge of pile cap or footing and pier, m (ft)
- h_o = Height of the pile cap above bed at beginning of computation, m (ft)
- h_1 = $h_o + T$ = height of the pier stem above the bed before scour, m (ft)
- h_2 = $h_o + y_{s\ pier}/2$ = height of pile cap after pier stem scour component has been computed, m (ft)
- h_3 = $h_o + y_{s\ pier}/2 + y_{s\ pc}/2$ = height of pile group after the pier stem and pile cap scour components have been computed, m (ft)
- S = Spacing between columns of piles, pile center to pile center, m (ft)
- T = Thickness of pile cap or footing, m (ft)
- y_1 = Approach flow depth at the beginning of computations, m (ft)
- y_2 = $y_1 + y_{s\ pier}/2$ = adjusted flow depth for pile cap computations m (ft)
- y_3 = $y_1 + y_{s\ pier}/2 + y_{s\ pc}/2$ = adjusted flow depth for pile group computations, m (ft)
- V_1 = Approach velocity used at the beginning of computations, m/sec (ft/sec)
- V_2 = $V_1(y_1/y_2)$ =adjusted velocity for pile cap computations, m/sec (ft/sec)
- V_3 = $V_1(y_1/y_3)$ =adjusted velocity for pile group computations, m/sec (ft/sec)

Total scour from superposition of components is given by:

$$y_s = y_{s\,pier} + y_{s\,pc} + y_{s\,pg} \tag{5}$$

where:

y_s = Total scour depth, m (ft)
$y_{s\,pier}$ = Scour component for the pier stem in the flow, m (ft)
$y_{s\,pc}$ = Scour component for the pier cap or footing in the flow, m (ft)
$y_{s\,pg}$ = Scour component for the piles exposed to the flow, m (ft)

Each of the scour components is computed from the basic pier scour Equation 1 using an equivalent sized pier to represent the irregular pier components, adjusted flow depths and velocities as described in the list of variables for Figure 2, and height adjustments for the pier stem and pile group. The height adjustment is included in the equivalent pier size for the pile cap.

Determination of the Pier Stem Scour Depth Component

The need to compute the pier stem scour depth component occurs when the pier cap or the footing is in the flow and the pier stem is subjected to sufficient flow depth and velocity as to cause scour. The first computation is the scour estimate, $y_{s\,pier}$, for a full depth pier that has the width and length of the pier stem using Equation 1. In Equation 1, a_{pier} is the pier width and other variables in the equation are as defined previously. This base scour estimate is multiplied by $K_{h\,pier}$, given in Figure 2 as a function of h_1/a_{pier} and f/a_{pier}, to yield the pier stem scour component as follows:

$$\frac{y_{s\,pier}}{y_1} = K_{h\,pier}\left[2.0\,K_1K_2K_3K_4\;K_w\left(\frac{a_{pier}}{y_1}\right)^{0.65}\left(\frac{V_1}{\sqrt{g\,y_1}}\right)^{0.43}\right] \tag{6}$$

where:

$K_{h\,pier}$ = Coefficient to account for the height of the pier stem above the bed and the shielding effect by the pile cap overhang distance "f" in front of the pier stem (from Figure 2)

The quantity in the square brackets in Equation 6 is the basic pier scour ratio as if the pier stem were full depth and extended below the scour.

Determination of the Pile Cap (Footing) Scour Depth Component

The pile cap or footing scour depth component is calculated when the pile cap is in the flow by design, or as the result of long-term degradation, contraction scour, and/or by local scour attributed to the pier stem above it. As described below, there are two cases to consider in estimating the scour caused by the pile cap (or footing). Equation 1 is used to estimate the scour component in both cases, but the conceptual strategy for determining the variables to be used in the equation is different (partly due to limitations in the research that has been done to date

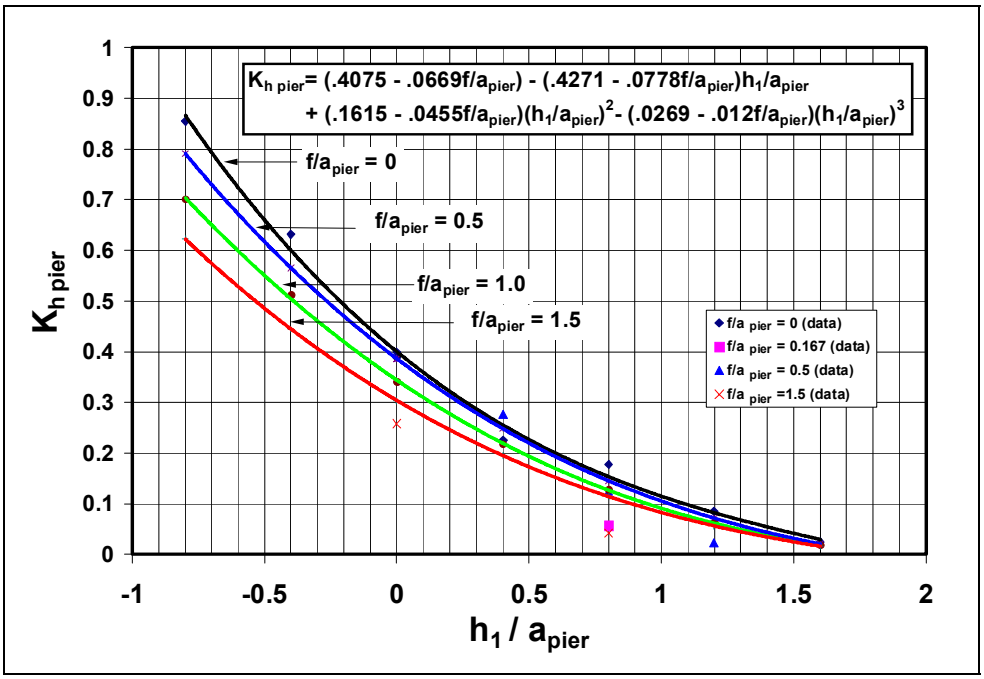

Figure 2. Suspended pier scour ratio (Jones and Sheppard (2000).

Case 1: The bottom of the pile cap is above the bed and in the flow either by design or after the bed has been lowered by scour caused by the pier stem component. The strategy is to reduce the pile cap width, a_{pc}, to an equivalent full depth solid pier width, a^*_{pc}, using Figure 3. The equivalent pier width, an adjusted flow depth, y_2, and an adjusted flow velocity, V_2, are then used in Equation 1 to estimate the scour component.

Case 2: The bottom of the pile cap or footing is on or below the bed. The strategy is to treat the pile cap or exposed footing like a short pier in a shallow stream of depth equal to the height to the top of the footing above bed. The portion of the flow that goes over the top of the pile cap or footing is ignored. Then, the full pile cap width, a_{pc}, is used in the computations, but the exposed footing height, y_f, (in lieu of the flow depth), and the average velocity, V_f, in the portion of the profile approaching the footing are used in Equation 1 to estimate the scour component.

An inherent assumption in this second case is that the footing is deeper than the scour depth so it is not necessary to add the pile group scour as a third component in this case. If the bottom of the pile cap happens to be right on the bed, either the case 1 or case 2 method could be applied, but they won't necessarily give the same answers. If both methods are tried, then engineering judgment should dictate which one to accept.

Details for determining the pile cap or footing scour component for these two cases are described in the following paragraphs.

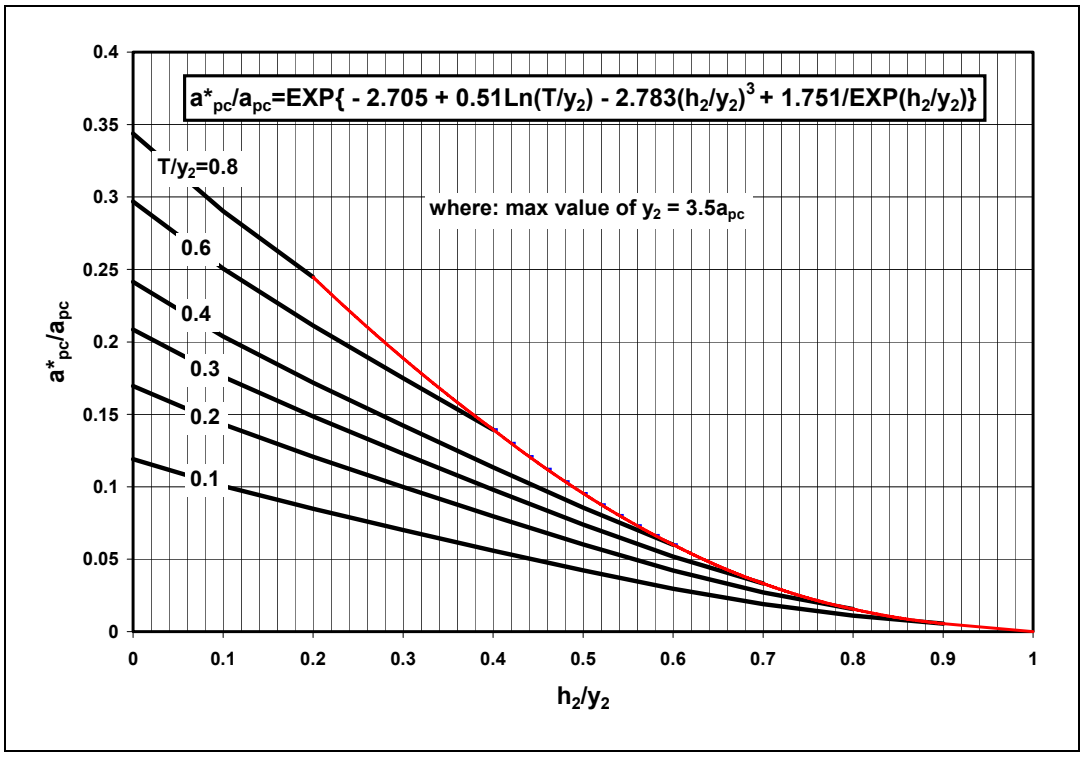

Figure 3. Pile cap (footing) equivalent width (Jones and Sheppard (2000).

<u>Case 1. Bottom of the Pile Cap (Footing) in the Flow above the Bed</u>

T	=	Thickness of the pile cap exposed to the flow, m (ft)
h_2	=	$h_o + y_{s\ pier}/2$, m (ft)
y_2	=	$y_1 + y_{s\ pier}/2$, = adjusted flow depth, m (ft)
V_2	=	$V_1(y_1/y_2)$ = adjusted flow velocity, m/s (ft/s)

where:

h_o	=	Original height of the pile cap above the bed, m (ft)
y_1	=	Original flow depth at the beginning of the computations before scour, m (ft)
$y_{s\ pier}$	=	Pier stem scour depth component, m (ft)
V_1	=	Original approach velocity at the beginning of the computations, m/s (ft/s)

Determine a^*_{pc}/a_{pc} from Figure 3 as a function of h_2/y_2 and T/y_2 (note that the maximum value of $y_2 = 3.5\ a_{pc}$).

Compute $a^*_{pc} = (a^*_{pc}/a_{pc})\ a_{pc}$; where a^*_{pc} is the width of the equivalent pier to be used in Equation 1 and a_{pc} is the width of the original pile cap. Compute the pile cap scour component, $y_{s\ pc}$ from Equation 1 using a^*_{pc}, y_2, and V_2 as the pier width, flow depth, and velocity parameters, respectively. The rationale for using the adjusted velocity for this computation is that the near bottom velocities are the primary currents that

produce scour and they tend to be reduced in the local scour hole from the overlying component. **For skewed flow use the L/a for the original pile cap as the L/a for the equivalent pier to determine K_2**. Apply the wide pier correction factor, K_w, if (1) the total depth, $y_2 < 0.8\ a^*_{pc}$, (2) the Froude Number $V_2/(g\ y_2)^{1/2} < 1$, and (3) $a^*_{pc} > 50\ D_{50}$. The scour component equation for the case 1 pile cap can then be written:

$$\frac{y_{spc}}{y_2} = 2.0 K_1 K_2 K_3 K_4 K_w \left(\frac{a^*_{pc}}{y_2}\right)^{0.65} \left(\frac{V_2}{\sqrt{g y_2}}\right)^{0.43} \tag{7}$$

Next, the pile group scour component should be computed.

<u>Case 2. Bottom of the Pile Cap (Footing) Located On or Below the Bed.</u>

One limitation of the procedure described above is that the design chart in Figure 3 has not been developed for the case of the bottom of the pile cap or footing being below the bed (i.e., negative values of h_2). In this case, use a modification of the exposed footing procedure that has been described in previous editions of HEC-18. The previous procedure was developed from experiments in which the footing was never undermined by scour and tended to be an over predictor if the footing is undermined.

As for case 1:

y_2 = $y_1 + y_{s\ pier}/2$, m (ft)
V_2 = $V_1(y_1/y_2)$, m/s (ft/s)

The average velocity of flow at the exposed footing (V_f) is determined using the following equation:

$$\frac{V_f}{V_2} = \frac{\ln\left(10.93\frac{y_f}{k_s}+1\right)}{\ln\left(10.93\frac{y_2}{k_s}+1\right)} \tag{8}$$

where:

- V_f = Average velocity in the flow zone below the top of the footing, m/s (ft/s)
- V_2 = Average adjusted velocity in the vertical of flow approaching the pier, m/s (ft/s)
- ln = Natural log to the base e
- y_f = $h_1 + y_{s\ pier}/2$ = distance from the bed (after degradation, contraction scour, and pier stem scour) to the top of the footing, m (ft)
- k_s = Grain roughness of the bed (normally taken as the D_{84} for sand size bed material and 3.5 D_{84} for gravel and coarser bed material), m (ft)
- y_2 = Adjusted depth of flow upstream of the pier, including degradation, contraction scour and half the pier stem scour, m (ft)

See Figure 4 for an illustration of variables.

Compute the pile cap scour depth component, $y_{s\,pc}$ from Equation 1 using the full pile cap width, a_{pc}, y_f, V_f as the width, flow depth, and velocity parameters, respectively. The wide pier factor K_w should be used in this computation if (1) the total depth $y_2 < 0.8\ a_{pc}$, (2) the Froude Number $V_2/(gy_2)^{1/2} < 1$, and (3) $a_{pc} > 50\ D_{50}$. Use y_2/a_{pc} to compute the K_w factor if it is applicable. The scour component equation for the case 2 pile cap or footing can then be written:

$$\frac{y_{s\,pc}}{y_f} = 2.0 K_1 K_2 K_3 K_4 K_w \left(\frac{a_{pc}}{y_f}\right)^{0.65} \left(\frac{V_f}{\sqrt{g y_f}}\right)^{0.43} \tag{9}$$

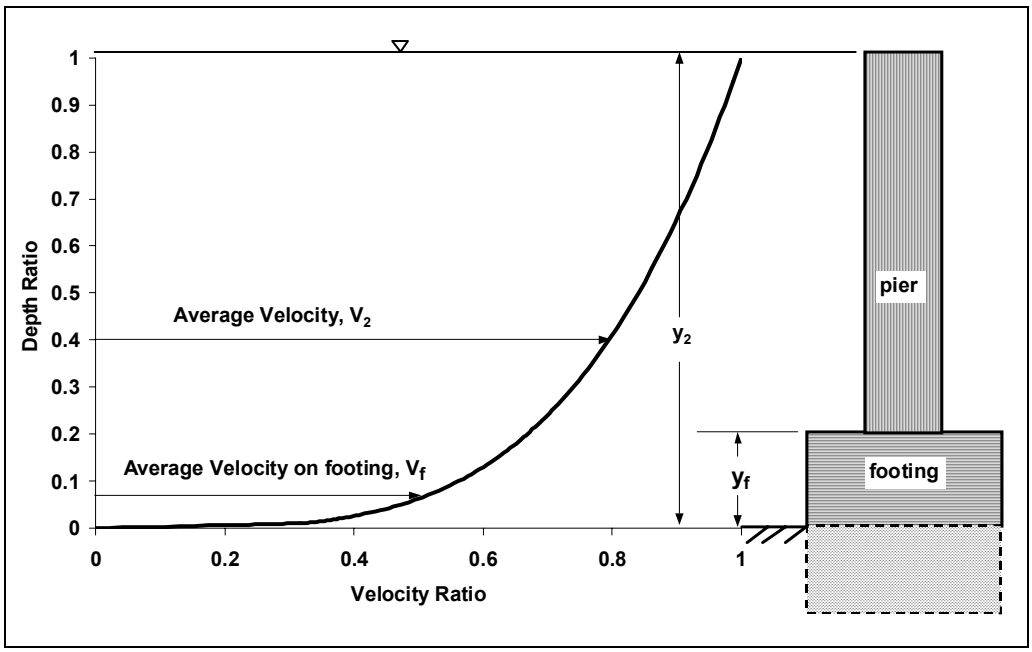

Figure 4. Definition sketch for velocity and depth on exposed footing.

In this case assume the pile cap scour component includes the pile group scour and compute the total scour depth as:

$$y_s = y_{s\,pier} + y_{s\,pc} \quad \text{(For case 2 only)} \tag{10}$$

Determination of the Pile Group Scour Depth Component

Research by Salim and Jones (1995, 1996, and 1999) and Jones 1989 and by Smith (1999) has provided a basis for determining pile group scour depth by taking into consideration the spacing between piles, piles aligned or staggered, angle of attack, the number of pile rows and a height factor to account for the pile length exposed to the flow. Procedures are given for analyzing the following typical cases:

- Special case of piles aligned with each other and with the flow. No angle of attack.
- General case of the pile group skewed to the flow, with an angle of attack, or pile groups with staggered rows of piles.

The strategy for estimating the pile group scour component is the same for both cases, but the technique for determining the projected width of piles is simpler for the special case of aligned piles. The strategy is as follows:

- Project the width of the piles onto a plane normal to the flow.
- Determine the effective width of an equivalent pier that would produce the same scour if the pile group penetrated the water surface.
- Adjust the flow depth, velocity and exposed height of the pile group to account for the pier stem and pile cap scour components previously calculated.
- Determine the pile group height factor based on the exposed height of the pile group above the bed.
- Compute the pile group scour component using a modified version of Equation 1.

For the special case of aligned piles, the projected width, a_{proj}, onto a plane normal to the flow is simply the width of the collapsed pile group as illustrated in Figure 5.

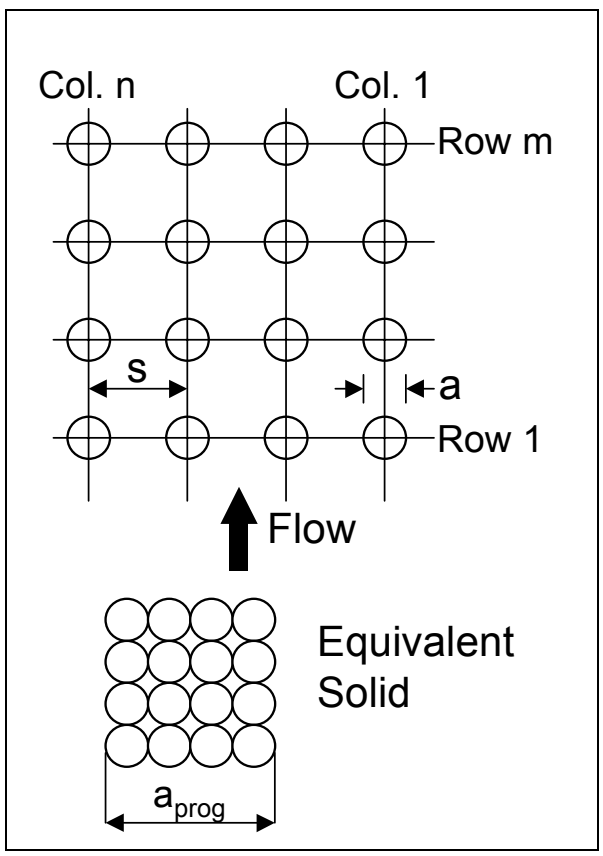

Figure 5. Projected width of piles for the special case of aligned flow.

For the general case, Smith (1999) determined that a pile group could be represented by an equivalent solid pier that has an effective width, a^*_{pg}, equal to a spacing factor multiplied by the sum of the non-overlapping projected widths of the piles onto a plane normal to the flow direction (Figure 6). The procedure for the general case is the same as the procedure for the aligned pile groups except for the determination of the width of the equivalent solid which is a more tedious process for the general case. The sum of the projected widths can be determined by sketching the pile group to scale and projecting the outside edges of each pile onto the projection plane as illustrated in Figure 6 or by systematically calculating coordinates of the edges of each pile along the projection plane. The coordinates are sorted in ascending order to facilitate inspection to eliminate double counting of overlapping areas. Additional experiments are being conducted at the FHWA hydraulics laboratory to test simpler techniques for estimating the effective width, but currently Smith's summation technique is a logical choice.

Smith attempted to derive weighting factors to adjust the impact of piles according to their distance from the projection plane, but concluded that there was not enough data and the procedure would become very cumbersome with weighting factors. A reasonable alternative to using weighting factors is to exclude piles other than the two rows and one column closest to the plane of projection as illustrated by the bold outlines in Figure 6.

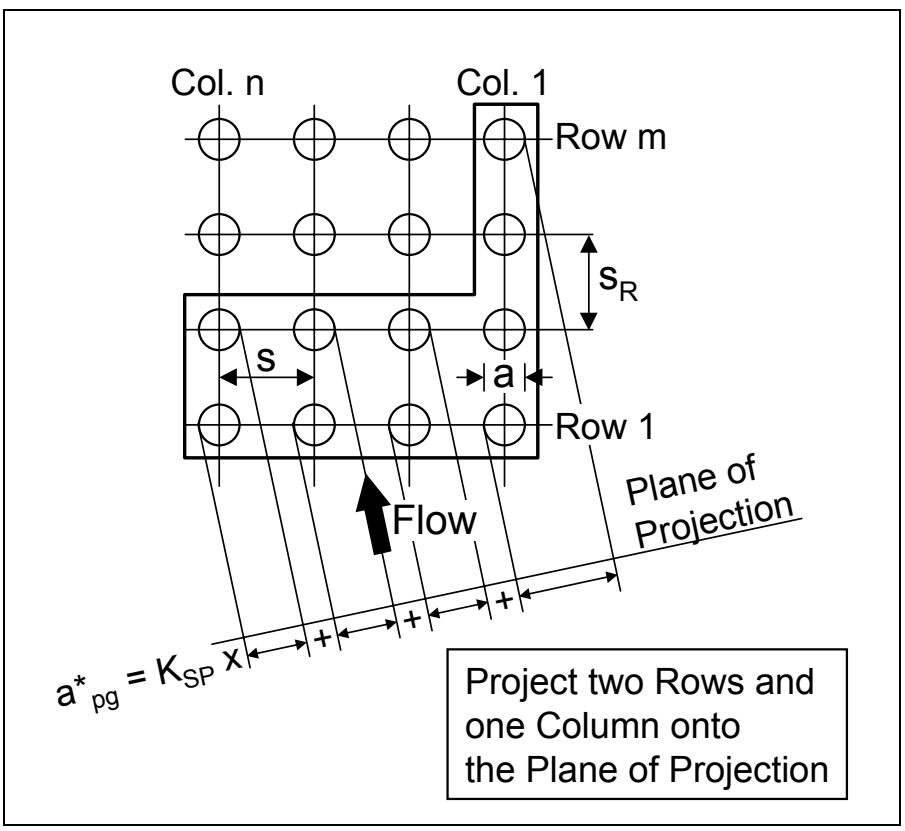

Figure 6. Projected width of piles for the general case of skewed flow.

Effective width of an equivalent full depth pier

The effective width of an equivalent full depth pier is the product of the projected width of piles multiplied by a spacing factor and a number of aligned rows factor (used for the special case of aligned piles only).

$$a^*_{pg} = a_{proj} K_{sp} K_m \tag{11}$$

where:

- a_{proj} = Sum of non-overlapping projected widths of piles (see Figures 5 and 6)
- K_{sp} = Coefficient for pile spacing (Figure 7)
- K_m = Coefficient for number of aligned rows, m, (Figure 8). K_m is constant for all S/a values when there are more than 6 rows of piles.
- K_m = 1.0 for skewed or staggered pile groups

The number of rows factor, K_m, is 1.0 for the general case of skewed or staggered rows of piles because the projection technique for skewed flow accounts for the number of rows and is already conservative for staggered rows.

The adjusted flow depth and velocity to be used in the pier scour equation are as follows:

$$y_3 = y_1 + y_{s\ pier}/2 + y_{s\ pc}/2, \text{ m (ft)} \tag{12}$$

$$V_3 = V_1 (y_1/y_3), \text{ m/s (ft/s)} \tag{13}$$

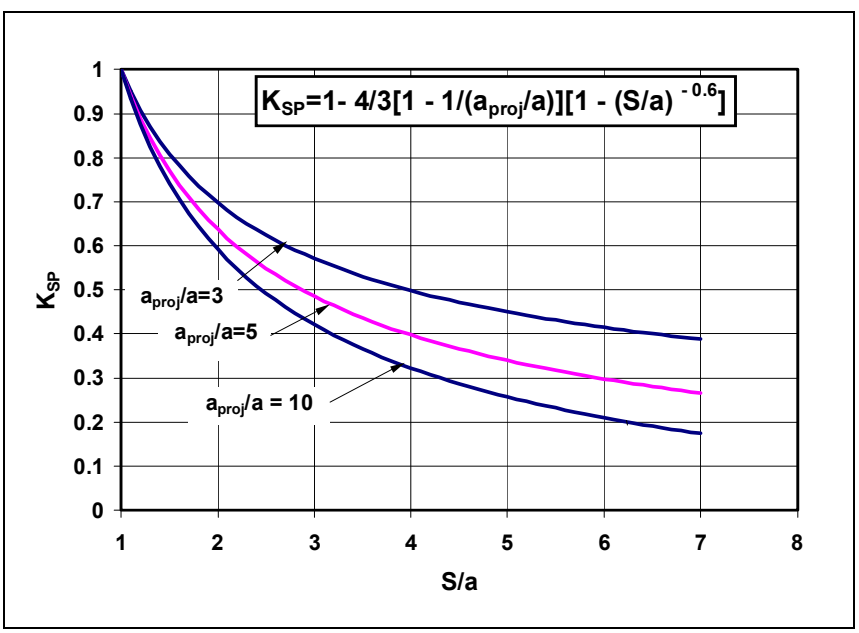

Figure 7 Pile spacing factor (Sheppard, 2001)

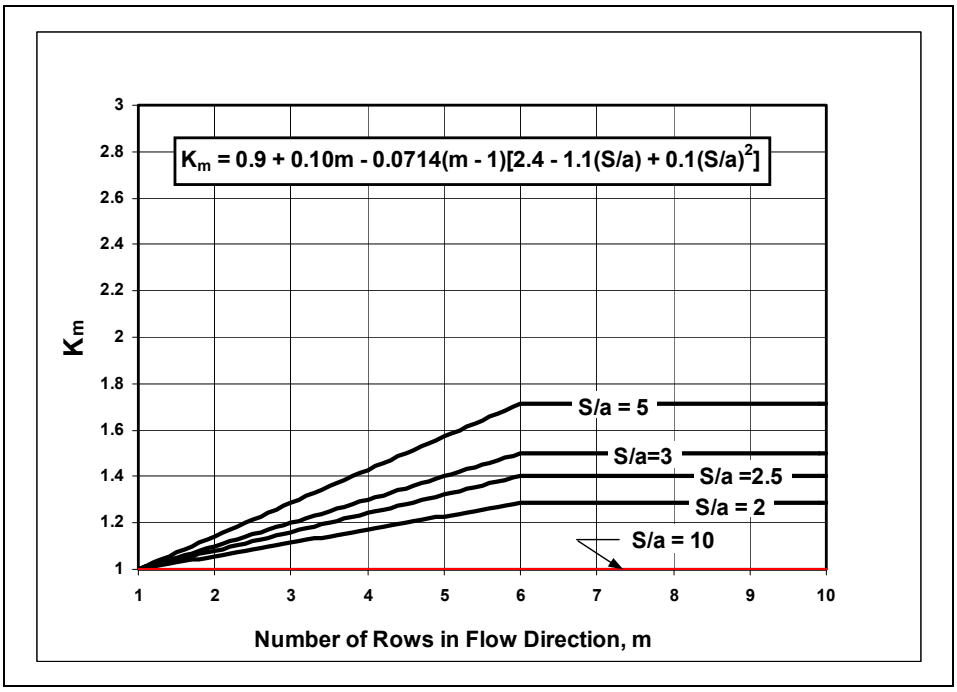

Figure 8. Adjustment factor for number of aligned rows of piles (Sheppard, 2001).

The scour equation for a pile group can then be written as follows:

$$\frac{y_{spg}}{y_3} = K_{hpg}\left[2.0K_1K_3K_4\left(\frac{a^*_{pg}}{y_3}\right)^{0.65}\left(\frac{V_3}{\sqrt{gy_3}}\right)^{0.43}\right] \tag{14}$$

where:

k_{hpg} = Pile group height factor given in Figure 9 as function of h_3/y_3 (note that the maximum value of $y_3 = 3.5\ a^*_{pg}$)

h_3 = $h_0 + y_{s\ pier}/2 + y_{s\ pc}/2$ = height of pile group above the lowered stream bed after pier and pile cap scour components have been computed, m, (ft)

K_2 from Equation 1 has been omitted because pile widths are projected onto a plane that is normal to the flow. The quantity in the square brackets is the scour ratio for a solid pier of width, a^*_{pg}, if it extended to the water surface. This is the scour ratio for a full depth pile group.

Determination of Total Scour Depth for the Complex Pier

The total scour for the complex pier from Equation (5) is:

$y_s = y_{s\ pier} + y_{s\ pc} + y_{s\ pg}$

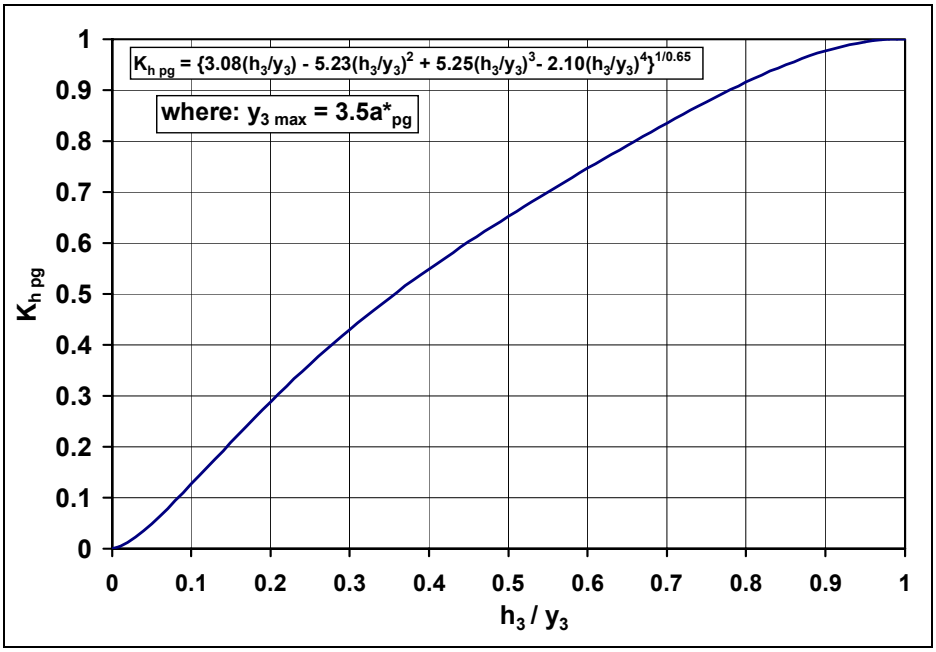

Figure 9. Pile group height adjustment factor (Sheppard, 2001).

The guidelines described in this section can be used to compute scour for a simple full depth pile group in which case the first two components will be zero and the pile group height factor will be 1.0. Engineering judgment must be used if debris is considered a factor in which case it would be logical to treat the pile group and debris as a vertical extension of the pile cap and to compute scour using the case 2 pile cap procedure described previously.

In cases of complex pile configurations where costs are a major concern, where significant savings are anticipated, and/or for major bridge crossings, physical model studies are still the best guide. Nevertheless, the guidelines described in this section provide a first estimate and a good indication of what can be anticipated from a physical model study.

In many complex piers, the pile groups have a different number of piles in a row or column, the spacing between piles is not uniform, and the widths of the piles may not all be the same. An estimate of the scour depth can be obtained using the methods and equations in this section. However, a physical model study should be conducted to determine scour depths for the final design. For guidance in the use of physical modeling see HEC-23 (Lagasse et al, 2001) and River Engineering for Highway Encroachments (Richardson et al, 2001).

CONCLUSION

1. Equations and methods are given for the calculation of local scour for complex piers. Complex piers are piers where scour could be caused by two or three substructural elements. These elements are the pier stem, the pile cap or footing, and the pile group.

2. A physical model study of complex piers, generally, will reduce uncertainly, increase the safety of the design, and reduce cost.

LITERATURE CITED

Johnson, P.A. and E.F. Torrico, 1994, "Scour Around Wide Piers in Shallow Water," Transportation Research Board Record 1471, Transportation Research Board, Washington, D.C.

Jones, J.S., 1983, "Comparison of Prediction Equations for Bridge Pier and Abutment Scour," Transportation Research Record 950, Second Bridge Engineering Conference, Vol. 2, Transportation Research Board, Washington, D.C.

Jones, J.S., 1989, "Laboratory Studies of the Effects of Footings and Pile Groups on Bridge Pier Scour," U.S. Interagency Sedimentation Committee Bridge Scour Symposium, U.S. Department of Transportation, Washington, D.C.

Jones, J.S. and D. M. Sheppard, 2000, "Local Scour at Complex Pier Geometries," Proc. of the ASCE 2000 Joint Conference on Water Resources Engineering and Water Resources Planning and Management, July 30 - August 2, Minneapolis, MN.

Lagasse, P.F., J. D. Schall, and E.V. Richardson, 2001, "Stream Stability at Highway Structures," Hydraulic Engineering Circular No. 20, Third Edition, FHWA NHI 01-002, Federal Highway Administration, Washington, D.C.

Lagasse, P.F., L.W. Zevenbergen, J. D. Schall, and P.E. Clopper, 2001, "Bridge Scour and Stream Instability Countermeasures," Hydraulic Engineering Circular No. 23, Second Edition, FHWA NHI 01-003, Federal Highway Administration, Washington, D.C.

Mueller, D.S., 1996, "Local Scour at Bridge Piers in Nonuniform Sediment Under Dynamic Conditions," Ph.D Dissertation, Colorado State University, Fort Collins, CO.

Mueller, D.S. and J.S. Jones, 1999, "Evaluation of Recent Field and Laboratory Research on Scour at Bridge Piers in Coarse Bed Materials, ASCE 1999 Compendium, Stream Stability and Scour at Highway Bridges, Richardson and Lagasse (eds.), Reston, VA.

Richardson, E.V., Karaki, S., Mahmoud, K., Simons, D.B., and Stevens, M.A., 1975, "Highways in the River Environment." Federal Highway Administration, U. S. Department of Transportation, reprinted July, 1983, Washington, D.C..

Richardson, E.V. and P.F. Lagasse (eds.), 1999, "Stream Stability and Scour at Highway Bridge - Compendium of Papers, ASCE Water Resources Engineering Conferences 1991-1998," American Society of Civil Engineers, Reston, VA.

Richardson, E.V., S. R. Davis, and P.F. Lagasse, 2001, "Evaluating Scour at Bridges," Hydraulic Engineering Circular No. 18 (HEC 18), Fourth Edition, FHWA NHI 01-001, Federal Highway Administration, Washington, D.C.

Richardson, E.V., D. B. Simons, and P.F. Lagasse, 2001, "River Engineering for Highway in Encroachments," FHWA NHI 01-004, Federal Highway Administration, Hydraulic Series No. 6, Washington, D.C.

Salim, M. and J. S. Jones, 1995, "Effects of Exposed Pile Foundations on Local Pier Scour,"

ASCE Water Resources Engineering, Reston, VA

Salim, M. and J. S. Jones, 1996, "Scour Around Exposed Pile Foundations," ASCE North American and Water and Environment Congress, Reston, VA

Salim, M and J. S. Jones, 1999, Scour Around Exposed Pile Foundations," ASCE 1999 Compendium, Stream Stability and Scour at Highway Bridges, Richardson and Lagasse (eds.), Reston, VA.

Smith, W.L., 1999, "Local Structure-Induced Sediment Scour at Pile Groups," M.S. Thesis, University of Florida, Gainesville, FL.

Sheppard, D. M., 2001, "A Methodology for Predicting Local Scour Depths Near Bridge Piers with Complex Geometry's," C. E. Paper, University of Florida, Gainesville, FL.

U.S. Department of Transportation, Federal Highway Administration, 1988, "Scour at Bridges," Technical Advisory T5140.20, updated by Technical Advisory T5140.23, October 28, 1991, "Evaluating Scour at Bridges," Washington, D.C.

U.S. Department of Transportation, 1988, "Interim Procedures for Evaluating Scour at Bridges," Federal Highway Administration, Washington, D.C.

Time Rate of Local Scour at a Circular Pile

by

William Miller Jr.[1] and D. Max Sheppard[2]

ABSTRACT

A mathematical model for the time variation of local scour depth at a singular circular pile has been developed. The scour hole shape is assumed to be that of an inverted frustum of a right circular cone with an angle equal to the angle of repose of the submerged sediment. It is assumed that the area being eroded is confined to a narrow band adjacent to the pile and that the surrounding sediment avalanches into this region so as to maintain the slope of the scour hole equal to the angle of repose. The area of erosion is further limited to an arc roughly extending from the stagnation point to the point of flow separation (~ $\pm 90^{\circ}$ from the leading edge). Sediment transport in the area of erosion is assumed to be due to the effective shear stress in this area created by the mean and secondary flows (horseshoe vortex). The variation of effective shear stress with normalized scour depth has been established based on accurate time history scour data and a flat bed sediment transport function. The form of the sediment transport function is based on those for transport on a flat bed. As might be expected, the shape of the normalized shear stress versus normalized scour depth plots was found to depend on the same sediment, flow and structure dimensionless parameters that govern the equilibrium scour depth. This model requires the use of predictive equations for computing equilibrium scour depths for the conditions encountered in the analysis. The model was developed for clearwater conditions but can be extended to include live bed scour when sufficient data is available for model validation.

INTRODUCTION

Current practice in bridge foundation design requires that design scour depths be estimated as the ultimate (or equilibrium) scour depth for steady flow under design flow conditions. However, for many situations the duration of the peak velocity is insufficient for the scour hole to reach an equilibrium state. This is especially true in the coastal environment where the design flow conditions are usually unsteady, episodic events of relatively short duration (e.g. hurricane generated storm surge). Another factor affecting the percentage of equilibrium scour depth achieved during a design flow event is the magnitude of the design flow velocity. In the tidal plains of many coastal areas, where the terrain is very flat, design flow velocities can be relatively low and thus the rate of scour is small. In order to predict scour depths under these conditions a time dependent model that is capable of handling unsteady flows is needed.

[1] Graduate Research Assistant, Civil and Coastal Engineering Department, University of Florida, Gainesville, FL 32611, wmiller@ufl.edu.
[2] Professor of Civil and Coastal Engineering, University of Florida, Gainesville, FL 32611, sheppard@ufl.edu

MODEL DERIVATION

The model developed in this paper assumes that the geometry of the scour hole can be approximated as an inverted frustum of a right circular cone. Also, as observed by Melville (1975), Ettema (1980) and Nakagawa and Suzuki (1975), it is assumed that sediment is removed only from within a region immediately adjacent to the pier and that this area (the erosion zone) is fed by sediment avalanching down the sides of the scour hole. Following Nakagawa and Suzuki (1975), the width of the erosion zone is assumed to be constant with time and only a function of the diameter of the cylinder. Figure 1 defines the erosion zone and Figure 2 defines the volumes used in the model development and calculation.

The following relationships can be developed using the variables defined in Figures 1 and 2:

$$r_1 = \frac{D}{2} + nD\,, \quad r_2 = \frac{d_s}{\tan\phi}\,, \text{ and } \quad \Delta r = \frac{\Delta d_s}{\tan\phi}\,.$$

The volume of the annulus at the base of the scour hole (ΔV_1) can be calculated from

$$\Delta V_1 = \pi \Delta d_s r_1^2 - \pi \Delta d_s \left(\frac{D}{2}\right)^2 = \pi \Delta d_s n D^2 (1+n)\,. \tag{1}$$

The volume of avalanche material ($\Delta \forall_2$) is calculated as follows

$$\Delta V_{A1} = \int_0^{d_s} \Delta A dy = \int_0^{d_s} \left[\pi (r+\Delta r)^2 - \pi r^2\right] dy = \int_0^{d_s} \left\{ 2\pi \left[\tfrac{1}{2} D(2n+1) + \frac{d_s}{\tan\phi} \right] \frac{\Delta d_s}{\tan\phi} + \pi \left(\frac{\Delta d_s}{\tan\phi} \right)^2 \right\} dy$$

$$\Delta V_2 = \Delta V_{A1} + \Delta V_{A2} = \pi \Delta d_s \left[D(2n+1)\frac{d_s}{\tan\phi} + \left(\frac{d_s}{\tan\phi}\right)^2 \right] + \pi \left(\frac{\Delta d_s}{\tan\phi}\right)^2 d_s + \Delta V_{A2}\,. \tag{2}$$

It can be shown that the small wedge shaped volume (ΔV_{A2}) beside the erosion zone annulus is a function of Δd_s^2 and Δd_s^3 and in the limit goes to zero, so that it is neglected in this calculation.

Adding Equations (1) and (2) gives the total change in volume for a given time increment, Δt. Therefore, the rate of change of volume of the scour hole is

$$\frac{\Delta \forall}{\Delta t} = \pi \frac{\Delta d_s}{\Delta t} \left[nD^2(1+n) + D(2n+1)\frac{d_s}{\tan\phi} + \left(\frac{d_s}{\tan\phi}\right)^2 \right].$$

Or in the limit as $\Delta t \to 0$

$$\frac{d\forall}{dt} = \pi \frac{d(d_s)}{dt} \left[nD^2(1+n) + D(2n+1)\frac{d_s}{\tan\phi} + \left(\frac{d_s}{\tan\phi}\right)^2 \right]. \tag{3}$$

Next, relate this rate of change in volume to the transport of material out of the scour hole. Defining porosity (p) as

$$p = \frac{\forall_w}{\forall_s + \forall_w} = \frac{\forall_w}{\forall}\,,$$

the volume of sediment ($\forall_s$) removed can be related to the volume of the scour hole ($\forall$) by

$$\forall = \frac{\forall_s}{(1-p)} . \tag{4}$$

The volume rate of transport of sediment can be described by

$$\frac{d\forall_s}{dt} = Q = qw , \tag{5}$$

where Q is the rate of transport of material by volume (m^3/s), q is the rate of transport of material by volume per unit width (m^2/s) and w is the width of the area over which the sediment transport function acts. Combining Equations (4) and (5) gives

$$\frac{d\forall}{dt} = \frac{d(\forall_s/(1-p))}{dt} = \frac{d\forall_s}{dt}\frac{1}{1-p} = \frac{qw}{1-p} . \tag{6}$$

If it is assumed that the sediment is transported out of the erosion area perpendicular to the pile as shown in Figure 3, than the width in Equation (6) can be estimated by

$$w = \beta_m 2r = \beta_m 2\left(\frac{D}{2} + nD\right) = \beta_m D(2n+1),$$

where β_m is half of the perimeter of the erosion zone in radians (see Figure 1), D is the diameter of the cylinder and nD is the width of the erosion zone. Equation (6) then becomes

$$\frac{d\forall}{dt} = \frac{qD(2n+1)\beta_m}{1-p} . \tag{7}$$

Combining Equations (3) and (6) gives the relationship between the rate of change of depth of the scour hole and the sediment transport

$$\frac{qD(2n+1)\beta_m}{1-p} = \pi\frac{d(d_s)}{dt}\left[nD^2(1+n) + D(2n+1)\frac{d_s}{\tan\phi} + \left(\frac{d_s}{\tan\phi}\right)^2\right]. \tag{8}$$

Equation (8) can be non-dimesionalized with respect to length and the non-dimensional scour depth can be defined as $y = d_s/d_{se}$. Solving for dy/dt gives

$$\frac{dy}{dt} = qD(2n+1)\beta_m \Bigg/ \left\{\pi(1-p)d_{se}\left[nD^2(1+n) + D(2n+1)\frac{d_{se}y}{\tan\phi} + \left(\frac{d_{se}y}{\tan\phi}\right)^2\right]\right\}. \tag{9}$$

Note that dy/dt has dimensions of $time^{-1}$. To reduce the algebra, introduce the variable K, defined as follows:

$$K = \frac{\pi(1-p)d_{se}}{\beta_m D(2n+1)}\left[nD^2(1+n) + D(2n+1)\frac{d_{se}y}{\tan\phi} + \left(\frac{d_{se}y}{\tan\phi}\right)^2\right] . \tag{10}$$

This reduces the rate equation to the following form:

$$\frac{dy}{dt} = \frac{q}{K} . \tag{11}$$

The next step is to decide on an appropriate sediment transport relationship. Many formulas exist in the literature and it should be kept in mind that the shear stress in the erosion zone within the scour hole is highly episodic, due to the unsteady nature of the horseshoe vortex, and the flow has a strong downward component. Therefore, any formula developed for flow over a flat bed can only approximate a time mean transport in the scour hole. Though somewhat arbitrary, the choice made here was that of Engelund and Hansen (1972), who based their sediment

transport formula on an energy balance. This choice was based on both the simplicity of the formula and the use of an energy balance concept where an excess shear stress serves to mobilize the sediment which is then carried away by the near bed flow. It is hoped that such a scheme will smooth out the effects of the episodic flow. Thus, q in Equation (11) becomes

$$q = C\sqrt{\theta}\left(\theta - \theta_c\right) , \tag{12}$$

where $\theta \equiv u_*^2 / \left(sg - 1\right) gD_{50}$ is the non-dimensional bed shear stress (also known as the sediment number) and θ_c is the critical non-dimensional bed shear stress for the given sediment. The coefficient, C, is assumed to be constant with time and depth for a given set of flow conditions. This is not the constant based on depth and sediment size in the Engelund and Hansen formulation. Thus, equation (12) is not the actual bedload formula of Engelund and Hansen. The bed shear stress is actually an "effective" bed shear stress and may be thought of as the time averaged bed shear stress produced by the mean and secondary flows in the erosion area.

Combining Equations (11) and (12) results in an equation for the time rate of change of the scour depth in terms of effective bed shear stress in the erosion area and the geometry of the scour hole,

$$\frac{dy}{dt} = \frac{C\sqrt{\theta}\left(\theta - \theta_c\right)}{K} . \tag{13}$$

EFFECTIVE SHEAR STRESS BEHAVIOR

The initial value of the non-dimensional bed shear stress in the erosion zone near the pile, θ_0, can be related to the value on the flat bed upstream of the pile using the following reasoning. For scour to be initiated at the structure, the local bed shear stress must exceed the critical shear stress for the sediment. For circular piles, experiments show that the scour does not occur for values of upstream depth averaged velocity below approximately $0.45V_c$. In other words, the upstream depth averaged velocity must be approximately $0.45V_c$ in order for the velocity near the pile to be V_c and scour initiated. Assuming that the bed shear stress (τ) is proportional to the depth averaged velocity squared, we find that

$$\frac{\tau_0}{\tau_u} = \frac{U_c^2}{\left(0.45U_c^2\right)} = \frac{1}{0.45^2} \approx 4.9 ,$$

where τ_0 is the bed shear stress at the pile prior to local scour and τ_u is the upstream bed shear stress. In non-dimensional terms, $\theta_0 = 4.9\theta_u$.

The value for the constant, C, in Equation (12) can now be estimated from experimental data by applying initial conditions to Equation (13). Knowing the time history of the scour depth, dy/dt at t = 0 and K at t = 0 and y = 0 can be determined. The value for C becomes

$$C = \left.\frac{dy}{dt}\right|_0 \frac{K_0}{\sqrt{\theta_0}\left(\theta_0 - \theta_c\right)} . \tag{14}$$

Substituting this value into Equation (13) and calculating dy/dt from a known time history plot, an "effective shear stress" in the erosion area can be back calculated for each data set.

Many researchers (e.g. Sheppard et al., 1995; Ontowirjo, 1994; Melville and Sutherland, 1989) have found that equilibrium scour depths at circular piles can be adequately expressed in terms of the dimensionless quantities V/V_c, y_0/D and D/D_{50}. It is reasonable to assume that the functional dependence of the effective shear stress on scour depth will depend on these same quantities. In order to determine this functional dependence, time history scour depth data is needed from experiments where these quantities are varied; preferably, experiments where two of these groups are held constant while varying the third. The data set used in this study provides the minimal data needed for this analysis. More data is needed and is currently being acquired.

EXPERIMENTAL DATA USED IN THIS ANALYSIS

All of the experimental data used in this investigation is from a study by Sheppard et al. (2002). A number of clearwater scour experiments were conducted in a large 6.1 m wide, 6.4 m deep, 38.4 m long, flow-through type flume located in the USGS Laboratory in Turners Falls, Massachusetts. Three different circular piles (with diameters 0.915 m, 0.305 m, and 0.114 m), three different sediment grain sizes (D_{50} = 0.22 mm, 0.80 mm and 2.9 mm) and a range of water depths were investigated.

The flow parameters monitored were flow discharge (indirectly), velocity, and water depth and temperature. The scour depth was monitored with video cameras inside the piles and with arrays of acoustic transponders attached to the exterior of the piles, just below the water surface. This system provided scour depth measurements at 12 locations along three radial lines throughout the experiments. The tests lasted from 41 hours to 650 hours and were such that near equilibrium scour depth conditions were achieved. Equilibrium scour depths were estimated by extrapolating the curve fit Equation (15), first used by Bertoldi and Jones (1998) and found by Sheppard et al. (2002) to adequately fit their data.

$$d_s(t) = a\left[1 - \frac{1}{(1+abt)}\right] + c\left[1 - \frac{1}{(1+cdt)}\right], \tag{15}$$

where a, b, c, d are constant coefficients determined from the data and t is time. Table 1 summarizes the results.

Experiment numbers 7, 8, 9 and 10 (with D_{50} = 2.9 mm sediment and D = 0.914 m diameter pile) give the best information about the effects of the aspect ratio, y_0/D, on the shear stress versus scour depth relationship. D/D_{50} is the same and V/V_c is nearly constant (0.78 – 0.89) for these experiments. Normalized excess shear stress [shear stress in excess of the critical value, $(\theta-\theta_c)$] versus normalized scour depth plots for Experiments 7-10 are presented in Figure 4. The excess shear stress is normalized by the maximum excess shear stress, $(\theta_p-\theta_c)$, where θ_p is the peak shear stress, and the scour depth is normalized by the equilibrium scour depth, d_{se}.

Figure 5 compares the results from Experiments 1 and 6 and illustrates the case where the aspect and velocity ratios are nearly constant and the normalized sediment size varies. There were no tests in this data set with both D/D_{50} and y_0/D constant and variable V/V_c. The closest approximation of constant D/D_{50} and y_0/D and variable V/V_c is between Experiments 7 and 11

(Figure 4, plot 1 and Figure 6, plot 1, respectively). Though an effect from the aspect ratio difference is expected, since the shear decreases from Experiment 7 to Experiment 11 while the aspect ratio increases (an effect opposite to the trend of Figure 4), it can be assumed that this is the result of the reduction in V/V_c. Also included in Figure 6 is a plot of Experiment 14 which illustrates the effect of large values of D/D_{50} and V/V_c, with an average value for the aspect ratio.

Table 1, Summary of Experiments

exp	D (m)	D_{50} mm)	y_0 (m)	V (m/s)	V/V_c	y_0/D	D/D_{50}	d_{se}/D
1	0.114	0.22	1.19	0.29	0.89	10.44	518	1.38
2	0.305	0.22	1.19	0.31	0.96	3.90	1386	1.34
3	0.915	0.80	1.27	0.40	0.85	1.39	1143	1.20
4	0.915	0.80	0.87	0.39	0.84	0.95	1143	1.04
5	0.305	0.80	1.27	0.39	0.82	4.16	381	1.41
6	0.114	0.80	1.27	0.41	0.87	11.14	143	1.58
7	0.915	2.90	1.22	0.76	0.89	1.33	315	1.51
8	0.915	2.90	0.56	0.65	0.85	0.61	315	1.20
9	0.915	2.90	0.29	0.57	0.83	0.32	315	1.05
10	0.915	2.90	0.17	0.50	0.78	0.19	315	0.79
11	0.915	2.90	1.90	0.70	0.75	2.08	315	1.28
12	0.305	0.22	1.22	0.40	1.23	4.00	1386	1.28
13	0.305	0.22	0.18	0.30	1.10	0.59	1386	0.95
14	0.915	0.22	1.81	0.30	0.95	1.98	4155	1.06

The general behavior of the shear stress with scour depth obtained by this method is consistent with descriptions of local scour processes published in the literature and observed by the authors of this paper. Melville (1975) and Ettema (1980) described three phases of scour as an "initial phase" where the scour hole forms from the flat-bed condition, followed by the "principle erosion phase" where the horseshoe vortex grows rapidly in size and strength and settles into the scour hole. Finally, the "equilibrium phase" occurs where the flow is no longer able to remove sediment. Nakagawa and Suzuki (1975) gave a similar description with four stages: "1) scour near the side of the pier caused by tractive force of the main flow, 2) scour near the leading edge generated by a horseshoe vortex, 3) scour developed by the stable vortex flowing along the pier, and 4) reduction in scour rate due to decrease in transport capacity in the hole."

The observed size and intensity of the horseshoe vortex prior to local scour is, in general, less than it is once the scour hole is formed. Flow separation at the edge of the scour hole feeds energy to the vortex and increases both its size and strength. It is logical that the shear stress will increase initially with scour depth and then at some depth start to decrease. Ultimately, it must reach a value near the critical shear stress where the removal of sediment stops. It also appears that the maximum obtainable size and strength of the horseshoe vortex is primarily a function of the pile diameter and the mean flow velocity. The dependence on pile diameter is believed to diminish with increased pile diameter (Sheppard et al., 2002). The rather abrupt change in the slope of the shear stress versus scour depth when the depth reaches about half the equilibrium value is thought to be the point when the horseshoe vortex is submerged in the scour hole. The rate of shear stress decrease with scour depth is much less from this point to the equilibrium depth.

The combined effects of the aspect ratio (normalized water depth, y_0/D) and normalized velocity (V/V_c) on these processes can be seen in the sequence of plots in Figure 4. As the water depth decreases, for a given pile size, the interference between the surface vortex (surface roller) and the horseshoe vortex increases. This attenuates the strength of the horseshoe vortex and retards its ability to increase the shear stress as the scour hole initially progresses. This also causes the shear stress to be reduced to near the critical value at about half of the equilibrium depth. In the limiting cases of shallow water the rate of scour is very slow for the latter half of the depth. An additional effect reducing the shear stress is the reduction in normalized velocity in this sequence of plots. More data is needed to separate the effects of aspect ratio and velocity.

The effects of normalized sediment size, D/D_{50} can be seen in the plots in Figure 5 and the first plot of Figure 4 (Experiment 7). As the diameter of the pile is decreased (or the sediment size increased) the shear stress remains above the initial value for a greater portion of the scour hole development and the flatter portion of the curve becomes almost non existent. Possible explanations for this behavior are given from the standpoint of changing pile size while keeping the sediment size constant and vice versa. If the sediment diameter is fixed and the pile diameter allowed to decrease (thus decreasing the values for D/D_{50}), as in going from Experiment 14 to 1 to 7 to 6, the size of the horseshoe vortex in comparison with the pile diameter increases. Thus a greater proportion of the scour hole is achieved before the vortex is submerged. If the pile diameter is held constant and the sediment size is allowed to increase (thus decreasing the values for D/D_{50}), the velocity must increase in order for V/V_c to remain constant. With the increased velocity there is more energy available in the mean flow to feed the vortex and thus the shear stress remains above the initial value for a greater proportion on the scour hole.

The data set used in this study is much less suitable for analyzing the effects of normalized velocity, V/V_c on the shear stress versus scour depth relationship. There are no two experiments where both y_0/D and D/D_{50} are held constant while varying the values of V/V_c. There are, however, experiments with different values of V/V_c in which information for the V/V_c dependency can be extracted if the above described effects of y_0/D and D/D_{50} are taken into consideration. In some cases, the effects of y_0/D and D/D_{50} can even be assumed to have reached a limit (i.e. conditions are such that the dependency on y_0/D and D/D50 is minimal). More data is being obtained to improve and verify the relationships developed and presented in this paper.

In order to solve Equation (13) for a given situation the above described relationships must be expressed analytically. The shear stress – scour depth relationship was divided into three segments. The initial segment can be approximated by a parabola with its vertex at the peak of the curve and its y = 0 intersection at $\theta = \theta_0$. The second segment (from the peak to the point of sharp change in slope) can likewise be represented by a second parabola with its vertex also at the peak and going through the point where the slope of the curve changes abruptly (called the peak point with $y = y_b$ and $\theta = \theta_b$). Finally, a straight line can be used to approximate the third segment. The general equations for these segments are as follows:

$$0 \le y \le y_p, \quad \theta = \theta_p - a_1\left(y - y_p\right), \text{ where } a_1 = \frac{\theta_p - \theta_0}{y_p^2}, \tag{16}$$

and y_p is the location of the peak. The second parabola can be expressed as

$$y_p \le y \le y_b, \quad \theta = \theta_p - a_2(y - y_p), \text{ where } a_2 = \frac{\theta_p - \theta_b}{(y_b - y_p)^2}. \tag{17}$$

The final straight line segment can be expressed by the following equation:

$$y_b \le y \le 1, \quad \theta = \theta_c + m_2(y - 1). \tag{18}$$

Empirical relationships for $\left.\frac{dy}{dt}\right|_{t=0}$, θ_p, y_p, y_b, and m_2 were obtained from the data set and are given in the following equations:

$$\left.\frac{dy}{dt}\right|_0 = 0.11\left(\frac{V}{y_0}\right)\tanh\left(1.5\frac{y_0}{D}\right)\left(2.8\frac{V}{V_c} - 1\right)\left[1 + 14\exp\left(-\frac{D/D_{50}}{1200}\right)\right], \tag{19}$$

where V is in m/s and D in m,

$$\frac{\theta_p}{\theta_c} = 6.5\left(\frac{y_0}{D}\right)^{0.07}\left(\frac{V}{V_c}\right)^2\left(\frac{D}{D_{50}}\right)^{-0.03}, \tag{20}$$

$$y_p = 0.4 - 0.15\left(\frac{y_0}{D}\right)^{-0.15}\left(\frac{V}{V_c}\right)^{-0.1}\left(\frac{D}{D_{50}}\right)^{0.1}. \tag{21}$$

If the quantity $\left(\frac{y_0}{D}\right)\left(\frac{V}{V_c}\right)^2\left(\frac{D}{D_{50}}\right)^{-1.5}$ is less than 3 x 10^{-5}, then $y_p = 0$, and $\frac{\theta_p}{\theta_0} = 1$.

$$y_b = 2y_p + 0.35(1 - 2y_p), \tag{22}$$

and

$$m_2 = -0.045\left(\frac{y_0}{D}\right)^{0.7}\left(\frac{V}{V_c}\right)^{7.1}\left(\frac{D}{D_{50}}\right)^{0.11}. \tag{23}$$

Note that Equation (19) has dimensions of time^{-1} (specifically, hours^{-1}) while Equations (20) through (23) are non-dimensional. Figure 7 shows three shear stress curves calculated with Equations (16) through (18) and (20) through (23) plotted against the back-calculated shear stress curves. The results are reasonable considering the extent of the data and the approximate nature of the curve fits.

Using these relationships, Equation (13) was solved for the conditions of the experimental data using a simple fourth order Runga-Kutta technique. Predicted, measured and curve fit of the measured scour depth time history plots for four of the experiments are given in Figures 8 and 9. The first plot in Figure 8 is the prediction with the least error and the second is the prediction with the greatest error. The plots in Figure 9 are for experimental data sets with average error. Once again reasonable accuracy was achieved.

Next a hypothetical prototype scale situation was examined. A 10 m diameter circular dolphin located in cohesionless, uniform diameter sand (D_{50}= 0.3 mm) in a water depth of 10 m is subjected to a steady, depth averaged flow velocity of 0.4 m/s (V/V_c = 1). Sheppard's Equation (Sheppard et al., 2002) was used to compute an equilibrium scour depth of 4.2 m. The computed

scour depth as a function of time is shown in Figure 10. The time required to reach 50% and 90% of the equilibrium scour depth is approximately 13 days and 124 days, respectively. This is only a hypothetical problem for which there is no measured data but the results appear to be reasonable based on the authors' experience with prototype structures.

CONCLUSIONS

A method for estimating the rate at which local scour depths occur is badly needed by both researchers and practicing engineers. Attempts to produce either an empirical or computational model for this purpose have been hampered by the complexity and unsteady nature of the flow and sediment transport processes involved. Any practical attempt to analyze the time dependency of scour depths must, by necessity, work with time averaged and "effective" quantities such as shear stress. The mathematical model developed as part of the work reported here is for the local scour at a single circular pile under clearwater scour flow conditions. The model utilizes experimental data from a study by Sheppard et al. (2002) where time histories of scour depths were measured for a range of pile and sediment sizes and water depths and flow velocities.

The resulting model does a reasonable job of predicting the time histories of the experiments on which it is based, as would be expected. This does, however, show that the relationships developed for the dependency of the effective shear stress versus scour depth on the structure, sediment and flow parameters are close to those displayed by this data set. In addition, the results of the hypothetical prototype scale example seem reasonable and are consistent with what the authors have observed in their field studies. As more laboratory data is available the model can be fine tuned and improved.

The next step is to extend the model to live bed scour conditions. Good time history data for live bed scour tests is difficult to obtain and to interpret. Adding the influx of sediment to the scour hole in the model will be easy. The more difficult part will be in obtaining accurate effective shear stress versus scour depth information.

ACKNOWLEDGEMENTS

The research reported here was conducted under the sponsorship of the Florida Department of Transportation.

NOTATION

a_1	directrix (x 4) for the initial shear stress curve parabolic approximation
a_2	directrix (x 4) for the second shear stress curve parabolic approximation
D	pile/cylinder diameter
C	transport function coefficient
D_{50}	median sediment diameter
d_s	instantaneous scour depth
d_{se}	equilibrium scour depth
Δd_s	change in depth of scour in time Δt

m_2	slope for the final shear stress curve linear approximation
n	width of the entrainment zone as a fraction of the pier diameter
p	sediment porosity
Q	the rate of transport of material by volume (m^3/s)
q	the rate of transport of material by volume per unit width
sg	Sediment specific gravity (ρ_s/ρ)
V	depth averaged upstream flow velocity
V_0	initial depth averaged flow velocity at the pile required to initiate scouring
V_c	depth averaged critical velocity
$\forall$	scour hole volume
$\forall_s$	volume of sediment solids
$\forall_w$	volume of water
w	the width of the area over which the sediment transport function acts
y	non-dimensional instantaneous scour depth ($y = d_s/d_{se}$)
y_0	upstream water depth
y_p	non-dimensional instantaneous scour depth at which the shear stress peak occurs
y_b	scour depth at which the slope of the shear stress curve changes abruptly ("break")
dy/dt	time rate of scour in units of $hours^{-1}$
$dy/dt|_0$	initial time rate of scour in units of $hours^{-1}$
β_m	half of the perimeter of the erosion zone in radians
ϕ	sediment angle of repose
θ	non-dimensional bed shear stress or sediment number, $\theta = u_*^2/(sg-1)gd_{50}$
θ_0	initial non-dimensional shear stress at the pile required to initiate scouring
θ_c	critical non-dimensional shear stress
θ_p	peak non-dimensional shear stress
θ_b	shear stress value at which the slope of the shear stress curve changes abruptly
θ_u	upstream non-dimensional shear stress
ρ	density of water
ρ_s	density of sediment particle
τ	bed shear stress, $\tau = \rho u_*^2$
τ_0	initial bed shear stress at the pile required to initiate scouring
τ_c	critical bed shear stress
τ_u	upstream non-dimensional shear stress

REFERENCES

1. Bertoldi, D.A. and Jones, J.S., 1998, " Time to Scour Experiments as an Indirect Measure of Stream Power around Bridge Piers, Proc. International Water Resources Engineering Conf, Memphis, Tenn, Aug 1998, pp. 264-269.
2. Engelund, F. and Hansen, E., 1972, "A Monograph on Sediment Transport in Alluvial Streams," Technical Press, Copenhagen.
3. Ettema, R., 1980, “Scour at Bridge Piers.” University of Auckland, School of Engineering, Auckland, New Zealand, Rep. No. 216.

4. Melville, B.W., 1975, “Local Scour at Bridge Sites.” University of Auckland, School of Engineering, Auckland, New Zealand, Rep. No. 117.
5. Melville, B.W. and Sutherland, A.J., 1989, “Design Method for Local Scour at Bridge Piers.” Journal of Hydraulic Engineering, Vol. 114, No. 10, 1210-1226, American Society of Civil Engineers, Reston, Virginia, USA.
6. Melville, B.W. and Chiew, Yee-Meng, 1999, "Time Scale for Local Scour at Bridge Piers", Journal of Hydraulic Engineering, Vol. 125, No. 1, pp. 59-65, American Society of Civil Engineers, Reston, Virginia, USA.
7. Nakagawa, H. and Suzuki, K., 1975, “An Application of Stochastic Model of Sediment Motion to Local Scour Around a Bridge Pier.” Proc. 16th IAHR Congress, Sao Paulo, Brazil, Vol. 2, pp 228-235.
8. Ontowirjo, B. 1994. "Prediction of Scour Near Single Piles in Steady Currents." Master's Thesis, UFL/COEL-94/001, Coastal and Oceanographic Engineering Department, University of Florida, Gainesville, FL.
9. Sheppard, D.M., Zhao, G., and Ontowirjo, B. 1995. “Local scour near single piles in steady currents.” ASCE Conference Proceedings: The First International Conference on Water Resources Engineering, San Antonio, TX.
10. Sheppard, D. M., 2002, “Equilibrium Local Scour Depth Prediction Under Clearwater Scour Conditions”, In Preparation, to be submitted to ASCE, J. Hydraulic Engineering,.

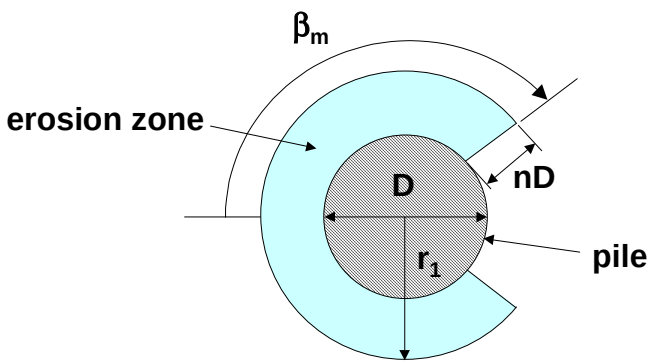

Figure 1. Definition sketch of erosion zone..

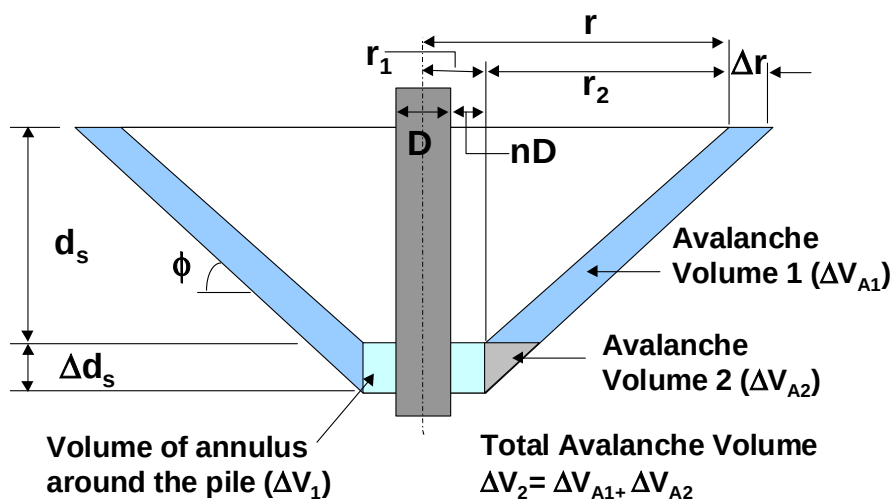

Figure 2. Definition sketch of scour hole..

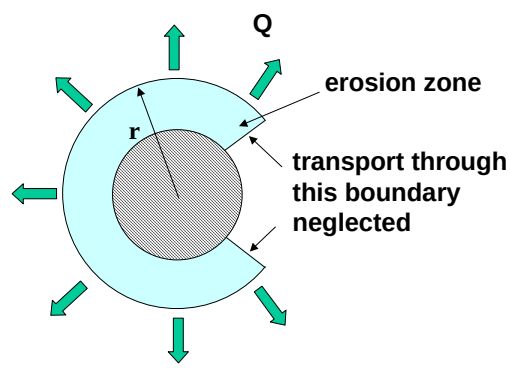

Figure 3. Diagram showing sediment transport out of the erosion zone.

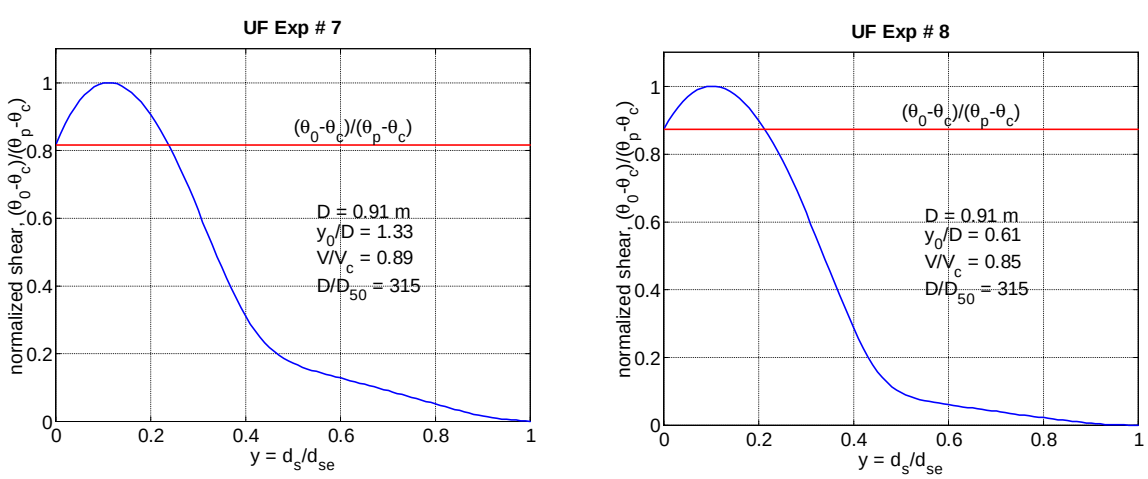

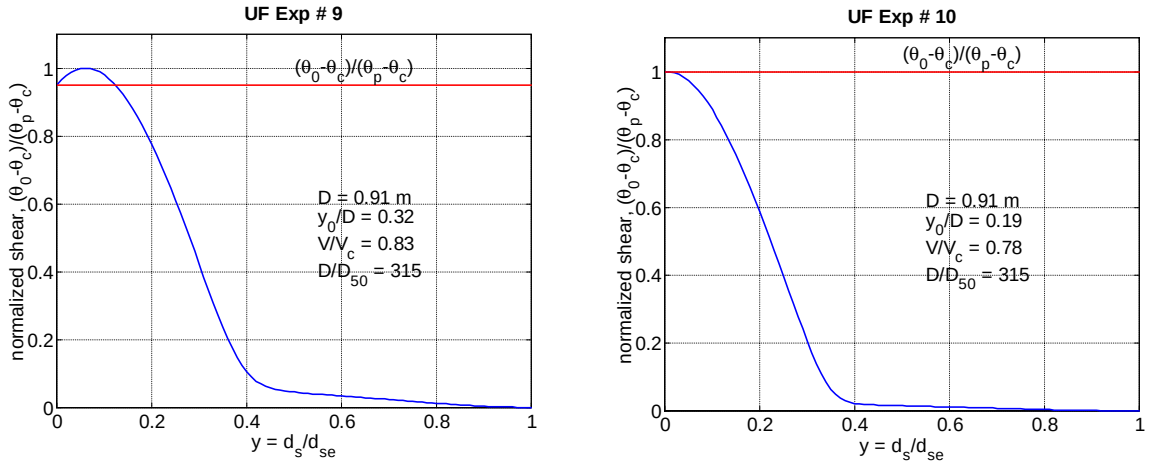

Figure 4. Effects of aspect ratio and velocity ratio on effective (back-calculated) shear stress vs. scour depth.

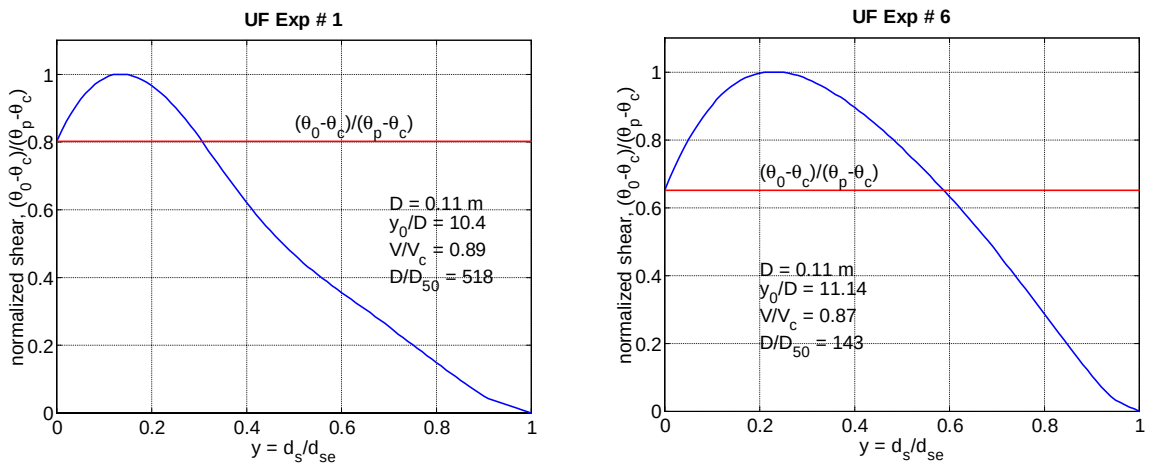

Figure 5. Effective (back-calculated) shear stress vs. scour depth for experiments 1 and 6.

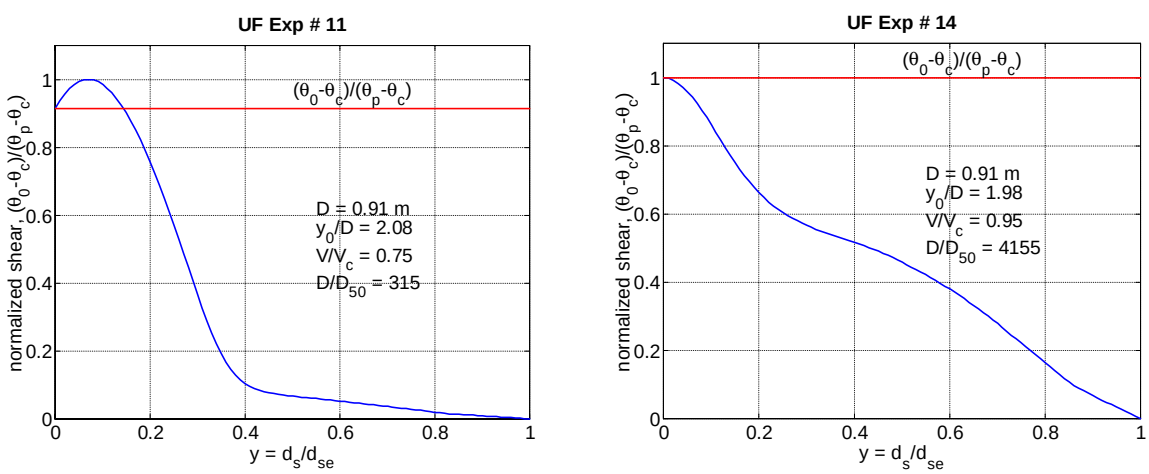

Figure 6. Effective (back-calculated) shear stress vs. scour depth for experiments 11 and 14.

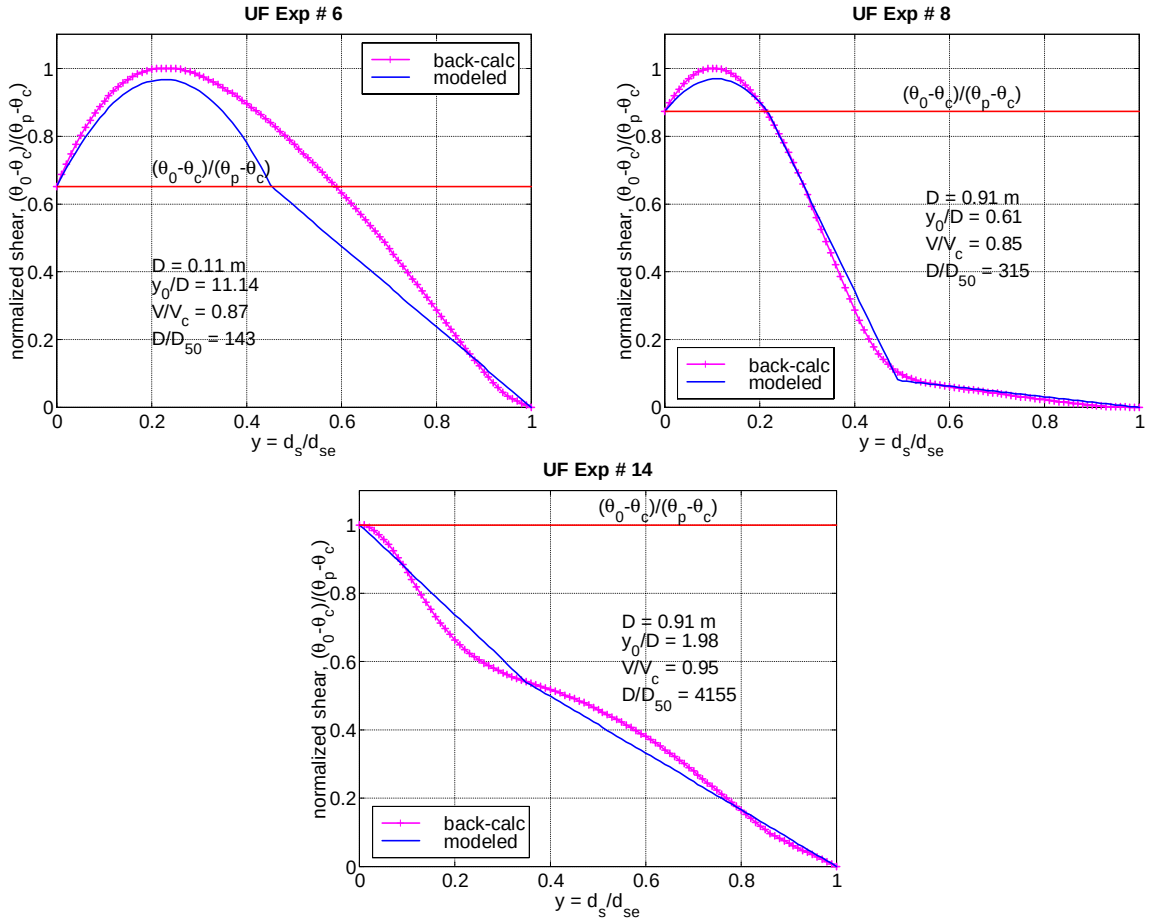

Figure 7. Modeled and back-calculated normalized shear stress, $(\theta-\theta_c)/(\theta_p-\theta_c)$ vs. Scour Depth.

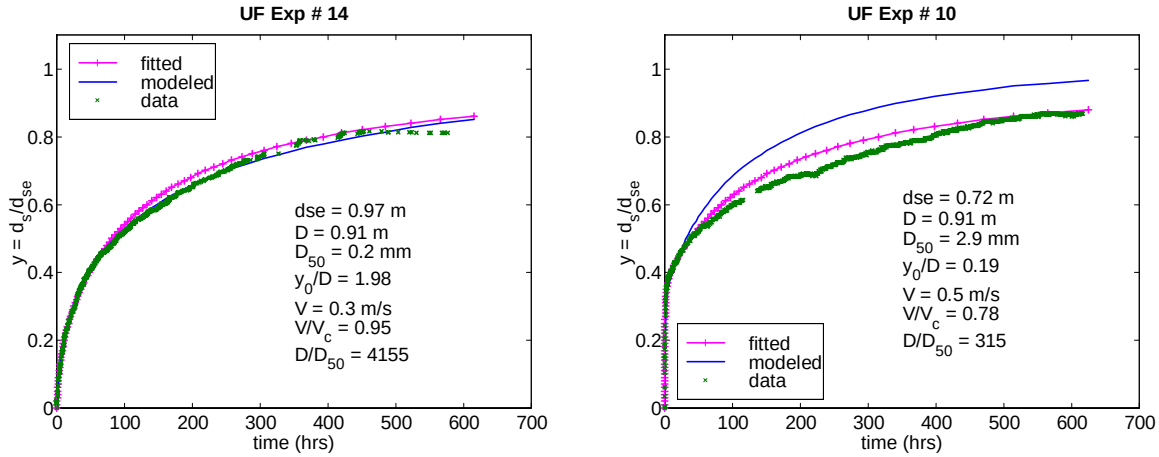

Figure 8. Fitted, modeled and measured normalized scour depth versus time for experiments 14 (least error) and 10 (greatest error).

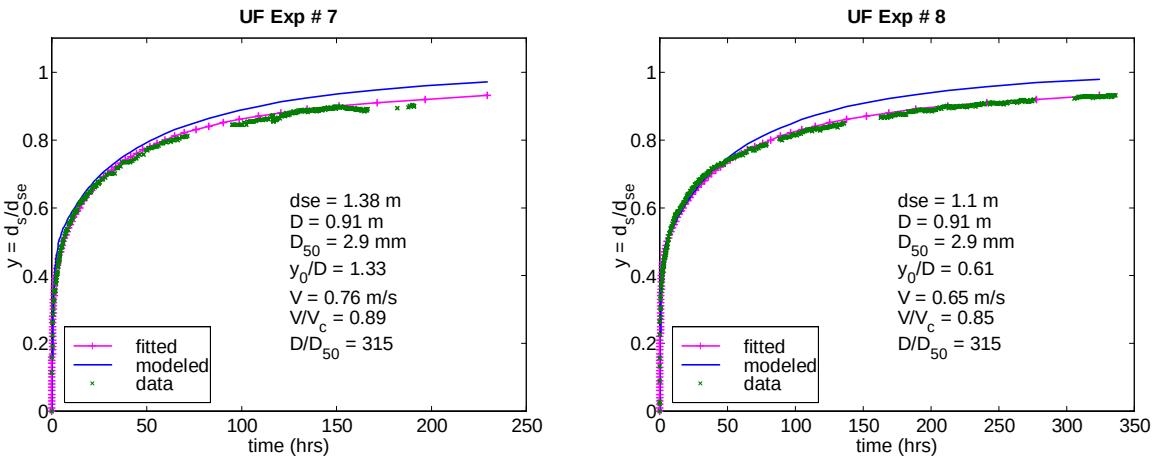

Figure 9. Fitted, modeled and measured normalized scour depth versus time for experiments 7 and 8 (average error).

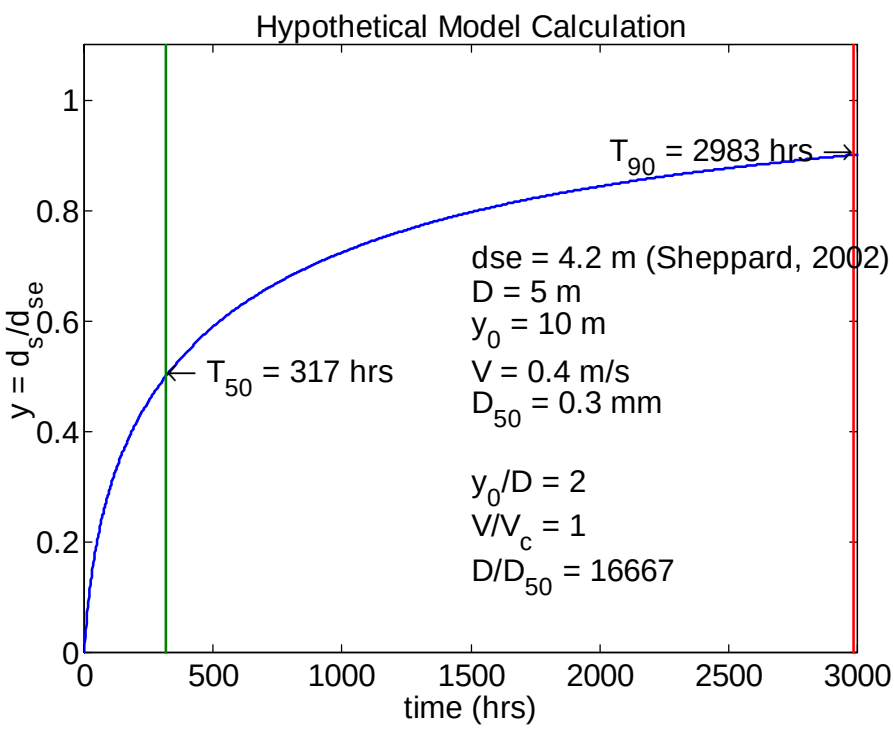

Figure 10. Computed scour depth versus time for a hypothetical prototype structure.

A Case Study of the Possible Effects of Long-Term Climate Change on Bridge Scour

By

Paul Kirshen[1], Lewis Edgers[2], Jennifer Edelmann[3], Marc Percher[3], Brian Bettencourt[3], Emily Lewandowski[3]

Conference on Scour of Foundations
Nov 17-20, 2002
Texas A&M University

Abstract

Long-term climate change due to global warming is expected to produce increased frequency of storms and precipitation in the northeastern United States. Consequently, there may be an increase in peak streamflows and thus an increase in the scour of bridge foundations. A case study of possible impacts was performed in eastern Massachusetts for an important highway bridge with two concrete piers on reinforced concrete spread footings. The bridge selected for this study was classified as close to scour critical by Federal Highway Administration(FHWA)/Massachusetts Highway Department(MHD) criteria under present climate conditions. We evaluated the possible effects due to 10 to 30 percent increases in the 100 year flood discharge caused by climate change and then possible footing remediation and bridge replacement strategies. We found that riprap was the most cost effective footing protection method. If the superstructure of the bridge was in poor condition, a single span superstructure was found to be preferred because it was least expensive compared to multiple span alternatives and scour protection was needed only at the abutments.

Introduction

In the future, climate change is expected to occur because of global warming. In the New England region of the United States, extreme values of storm precipitation may increase leading to higher flood discharges and velocities in rivers and channels (New England Regional Assessment Team, 2001). Bridge scour is directly associated with flooding conditions. Scour will start at the rising stage of the stream when the stream velocities approach the critical range and mobilize the streambed material. This process will continue as long as the flooding continues. Scour will reverse as the flood recedes by depositing sediment on the scoured bed. Once, however, the scour depth drops below the

[1] Research Professor, Civil and Environmental Engineering Department, Tufts University, Medford MA 02155 (paul.kirshen@tufts.edu).
[2] Professor, Civil and Environmental Engineering Department, Tufts University, Medford MA 02155.
[3] Student, Civil and Environmental Engineering Department, Tufts University, Medford MA 02155

bottom of the bridge foundation, the foundation will become unstable and unsafe for travel.

The tragedy at Schoharie Creek in April 1987 when ten people died during the catastrophic failure of the bridge on the New York State Thruway during a near-record flood highlighted the national problem of bridge scour. Stream instability, long-term streambed aggradation or degradation, general scour, local scour, and lateral scour cause 60 percent of all U.S. highway bridge failures (Lagasse, 1995). In addition to their human toll, such failures cost millions of dollars each year in direct costs for replacement and restoration as well as in indirect costs related to disruption of transportation facilities.

Here we examine the possible effects of climate change on bridge scour through a bridge case study. First, the relationship between flow and scour depth was determined. Next, we investigated the effects of increased scour depths on the safety of the case study bridge. Finally, after an in-depth scour analysis, possible solutions were suggested to remedy any potential damage due to scour. This work was conducted as part of a senior capstone design project at Tufts University. Details of the analyses are in Bettencourt et al. (2001).

Case Study Description

The bridge chosen for analysis carries Interstate Route 95 (I-95) over the Neponset River in eastern Massachusetts as shown in Figure 1. The criteria for selection of the case study included location of the bridge within metropolitan Boston , an FHWA/MHD scour rating of 4 or higher (acceptable scour), the availability of recent flood and inspection reports, and a bridge that has already been analyzed with the Hydrologic Engineering Center River Analysis System (HEC-RAS, HEC, 2002) hydraulic modeling software. The availability of the HEC-RAS data set resulted in much of the hydrologic and hydraulic data being already collected, allowing more time for the actual scour analysis.

The Neponset River has its headwaters in Foxboro, Massachusetts and flows northeast into Dorchester Bay. In the Canton, Massachusetts area, which is where our bridge is located, the river is characterized by extensive swamplands and extremely sluggish flow. The bridge that we selected is of major importance because the roadway serves as a critical artery for the City of Boston and all of northern New England. Interstate 95 is classified as an Urban Interstate road and the conveyed daily traffic was reported in May 2000 to be 151,000 vehicles per day, 11% of which is estimated to be truck traffic (MHD,2000).

The bridge actually is two different structures. MHD Bridge C02026 carries I-95 northbound traffic, while Bridge C02027 carries I-95 southbound traffic. The existing structures were constructed in 1955. The northbound roadway was expanded in 1964 to make room for an on-ramp, but the expansion is currently not in use.

Each bridge is a three span, simply supported steel stringer bridge with an 8-inch reinforced concrete deck and a bituminous concrete wearing surface. The center spans are 57 feet long, and the two end spans are 35 feet long center to center of bearings. The bridge piers have a 20-degree skew to the roadway. The existing substructure consists of two reinforced concrete stub abutments with U-back wing-walls, and two reinforced concrete bent type piers on reinforced concrete spread footings. The piers are not protected against scour. The abutments are dry at normal flow conditions, and are armored with 2-foot diameter granite block riprap. The spread footings are bearing on medium dense fine to coarse sand, with traces of inorganic silt. The riverbed material consists of a thin layer of sand and gravel overlying a thick layer of medium dense fine to coarse sand, and a deeper layer of clayey silt. The existing riverbed surface is at elevation 33 feet above sea level (see Figure 2). The bottom of the footing is at elevation 26 feet; thus 7 feet deep is the critical scour depth.

An August 1998 inspection report describes the condition of the superstructure as poor to satisfactory. The reinforced cast-in-place concrete deck is in poor condition. A local deck failure on the bridge that occurred in January 2001 produced a three-foot by four-foot hole breaking completely through the deck (Raphael, 2001). There is heavy map cracking with efflorescence and water staining under the entire bridge and many minor to moderate spalls in the deck with some exposed rebar and rust stains. Some of the minor spalls have been covered by gunite. The existing structural steel stringers have up to 40% section loss due to corrosion, including holes in the web, and there is heavy rusting including lamination at several bearings.

The substructure is rated satisfactory with minor deterioration, but the existing bridge piers do not meet current seismic criteria. The bridge foundations were inspected in February 1999 and were determined to be stable for calculated scour conditions.

Methodology

Three types of scour affect bridges: progressive degradation, general scour, and local scour (Meadowcroft, 1993). Progressive degradation is the general removal of sediment from the river bottom by the flow of the river. This sediment removal and resultant lowering of the river bottom is a natural process, but may remove large amounts of sediment over time. Because progressive degradation may be independent of the presence of the bridge, this type of scour is not classified as bridge scour and was not considered here.

General scour, also called contraction scour, is the removal of sediment from the bottom and sides of the river due to an obstruction in the river channel. General scour is caused by an increase in the speed of the water as it moves through a bridge opening that is narrower than the natural river channel. Because flow velocities increase in the constricted reach, erosion in the river channel is increased.

Local scour is the removal of sediment from around bridge piers or abutments. Local scour is due to the complex, turbulent flow patterns which arise at an obstruction. These flow patterns cause scour holes to form adjacent to the structures.

The case study bridge has abutments which are dry for most storm flows and are already protected by riprap. Therefore the scour at the abutments was ignored in the analysis and only scour in the middle of the channel was analyzed.

Velocities, water surface and energy grade line elevations, and Froude Number conditions for the scour analysis under the present climate were taken from the existing HEC-RAS data and analysis done for the bridge (HNTB, 1999). HEC-RAS was re-run with modified discharge and boundary conditions data to determine hydraulic conditions under climate change.

HEC-RAS solves the equations that describe one-dimensional, steady state, non uniform flow in open channels. The data required for HEC-RAS includes the connectivity of the river system, cross section data, reach lengths, Manning's coefficients, energy loss coefficients, stream junction information, flow regime, boundary conditions, and peak discharge. For the climate change analysis, only two variables were modified: the flow and boundary conditions. The present 10, 50, 100 and 500 year discharges were increased by 10, 20, and 30 percent to simulate a climate change with increased precipitation. New boundary conditions corresponding to the new flows were based on a relationship between upstream flows and downstream boundary conditions from an exponential fitting of the relationship between present 10, 50, 100 and 500 year discharges and their downstream boundary conditions. The R-squared of the fit was 0.9948.

The scour calculations also require a value for the D_{50} grain size diameter. Based upon sieve analysis of bottom sediments, a value of 3 millimeters was estimated.

The following procedures from Hydrologic Engineering Center (HEC, 1993) were then used to determine the scour depth for each of the present and climate change discharge conditions. First, it was determined if the river demonstrated "live-bed flow" or "clear-water flow" conditions. Clear–water scour occurs when there is no transport of bed material upstream of the bridgecrossing . Live-bed scour, on the other hand, occurs when there is transport of bed material from the upstream reach into the crossing. This was done using Neill's Equation, given below.

$$Vc := 11.52(y_1)^{\frac{1}{6}}(D_{50})^{\frac{1}{3}}$$

V_c = critical velocity, ft/second
y_1 = depth of upstream flow, ft

D_{50} = median diameter of bed material, ft

When V_c is less than the upstream velocity, live-bed scour occurs. If V_c is greater than this, clear-water scour occurs. After determining whether the scour was live-bed or clear-water, contraction and local scour were calculated using the below equations.

Live-Bed Contraction Scour (Modified version of Laursen from HEC, 1993):

$$y_2 = y_1 \left[\frac{Q_2}{Q_1} \right]^{\frac{6}{7}} \cdot \left(\frac{W_1}{W_2} \right)^{K_1}$$

Y_1 = depth of upstream flow, ft
Y_2 = depth in contracted section, ft
W_1 = top width upstream, ft
W_2 = top width in contracted section (minus piers), ft
Q_1 = upstream flow, cubic feet per second (cfs)
Q_2 = flow in contracted section, cfs
k_1 = exponent from HEC(1993)

y_S = depth of average scour = y_2-y_1

Clear-Water Contraction Scour (Laursen Equation from HEC, 1993):

$$Y_2 := \left(\frac{Q_2^{\,2}}{120\, D_m^{\frac{2}{3}}\, W_2^{\,2}} \right)^{\frac{3}{7}}$$

Y_1 = depth of upstream flow, ft
Y_2 = depth in contracted section, ft.
W_2 = top width in contracted section (minus piers), ft
Q_2 = flow in contracted section, cfs
Dm = effective mean diameter of bed material ($D_m = 1.25D_{50}$), ft
y_S = depth of average scour = y_2-y_1

Local Scour at Piers (CSU equation from HEC, 1993):

$$y_s = y_1 \cdot 2.0 \cdot K_1 \cdot K_2 \cdot K_3 \cdot \left(\frac{a}{y_1}\right)^{0.65} \cdot (Fr_1)^{0.43}$$

y_1 = depth of upstream flow, ft
K_1 = correction factor for pier nose shape, from HEC(1993)
K_2 = correction factor for angle of attack flow, from HEC(1993)
K_3 = correction factor for bed condition, from HEC(1993)
a = pier width, ft
Fr_1 = Froude Number
y_s = depth of average scour= y_2-y_1

Results

Since the 100 year flood discharge is the design value, results are only reported for this discharge in Table 1. Based upon possible errors in measuring grain size and estimating the downstream boundary point elevation, the scour depths in Table 1 may vary by +/- 0.3 feet.

Table 1 shows that the bridge is in danger of becoming scour critical at the present 100-year flood. We calculated a present scour depth of 6.8 ft, which leaves only 0.2 ft. of soil above the base of the footing. This is not viewed as a "stable" structure and thus some type of rehabilitation or reconstruction is necessary. The table also shows that, as expected, the scour depth increased as the flow increased and that a 10 % increase in discharge will result in the critical scour depth of 7 feet or greater. A computed critical scour condition for this bridge would elevate it from an FHWA/MHD scour rating of 5 (stable) to an FHWA/MHD scour rating of 3 (scour critical) rating. Note also that these results must be considered within the context of a possible error of 0.3 ft as mentioned earlier.

Footing Protection

Once the scour analysis was complete the next step was to determine the costs of: 1) just protecting the footings from scour; and 2) total bridge reconstruction with improved scour protection. For footing protection, channel countermeasures and geotechnical rehabilitation techniques were evaluated to protect against scour. The channel countermeasures included riprap systems and modification of channel hydraulics. The geotechnical rehabilitation techniques included steel sheeting and micropiles. Economic analysis indicated that riprap was the most cost effective method for footing protection from scour.

Riprap has some distinct advantages over other scour prevention techniques including availability, economy, ease of installation, and flexibility. Rock riprap in sufficient size and quantity is readily available in eastern Massachusetts. It can be placed easily around a pier during new construction and with reasonable care during low water flows around

existing structures. Once installed, riprap provides good scour protection as long as it remains in place. However, because riprap is generally obscured by flowing water, inspection and maintenance may be difficult.

According to the HEC (1993):

$$D_{50}=0.692(KV)^2 / (S_s-1)*(2g)$$

D_{50}= median stone diameter for riprap, ft
K= coefficient for pier shape (1.5 for round-nose pier, 1.7 for rectangular pier)
V= velocity on pier, ft/sec
S_s= specific gravity of riprap (normally taken as 2.65)
g= 32.2 ft^2/sec

Using an upstream velocities corresponding to the 100-year flow and K=1.7 for rectangular piers, the median stone diameter was computed to be 0.259 ft (3.1 inches) for the original flow, 0.263 ft (3.2 inches) for the 10% increased flow, 0.287 ft (3.4 inches) for the 20% increased flow, and 0.307 ft (3.7 inches) for the 30% increased flow.

After designing the riprap size, the following design guidelines were considered (Ruff, 1999):

-*Gradation*. A well-graded mixture of rock sizes should be used instead of one uniform size. The maximum size rock should be no greater than twice the D_{50} size.
-*Quality of stone*. Riprap must be durable so that freeze/thaw cycles do not decompose it in a short time – most igneous stones such as granite have suitable durability.
-*Riprap thickness*. The thickness of riprap layers should be 3 times the maximum stone diameter. The top of the riprap mat should be placed at the same elevation as the streambed. The deeper the riprap is placed into the streambed, the less likely it will be moved. Placing the bottom of the riprap mat on top of the streambed is discouraged.
-*Riprap mat width*. The width of the riprap mat should extend horizontally at least two times the pier width, measured from the pier face.
-*Filter material.* In some conditions, filter material is required between riprap and the underlying soil surface to prevent soil from moving through the riprap – a filter cloth material or a layer of gravel is usually used for the filter.

The total cost for riprap installation at our site came to approximately $12,000 for protection around two piers including stone, mobilization costs, and machinery to place the stone. The riprap at the site would have to be annually monitored and reinstalled as needed during the bridge's lifetime. It would also have to be inspected after each high flow event. If riprap was damaged, repairs would have to be made promptly to prevent a potential bridge failure. If repairs were needed repeatedly at one location, the site should be reevaluated to determine if the original design conditions have changed. Channel obstructions such as trees and sediment bars can change flow patterns and cause erosive forces that may damage riprap

Reconstruction

In addition to the scour problems of our selected bridge, the inspection report described in **Case Study Description** noted many structural problems. Load analysis indicated that the existing superstructure was substandard.

Various superstructure alternatives were considered using the MHD type study. The replacement bridge would have to meet statutory loading requirements of the American Association of State Highway and Transportation Officials. The superstructure alternatives included both three-span and single-span continuous and simply supported designs.

The reconstruction analysis also considered the cost of new foundations to allow the loads to be carried into deeper soil strata in order to avoid present and future scour problems. The deep foundation alternatives included drilled piers and pre-cast concrete and steel cast-in-place piles. Construction problems including site access, river construction issues, demolition of existing foundations, and environmental impacts.

The final reconstruction recommendation is a single span concrete bridge. The analyses showed that the single span alternative had a more expensive superstructure than the three-span alternatives. However, the savings in foundation cost of the single span alternative, regardless of which type of deep foundation was used, produced a more economical overall design. It also had the best protection against scour since the only scour concern would be the abutments, which are already protected.

Conclusion

It was found that even a 10 percent increase in the 100 year peak discharge under climate change could make the case study bridge susceptible to scour failure. If the existing superstructure of the bridge was in satisfactory condition, then riprap would be the most cost effective protection method for the existing footings. If the superstructure of the bridge was in poor condition and total reconstruction must be considered, then a single span superstructure was found to be the least expensive. It would have the added advantage that scour protection would only be needed at the abutments.

Acknowledgements

The authors acknowledge the support of Richard Murphy and Paul Nardone of the MHD. The views expressed in this paper are those of the authors and not necessarily those of the MHD. The first two authors also received support from the Climate's Long-Term Impacts on Metro Boston (CLIMB) Project under EPA Agreement Number R.827450-01. It has not been subjected to the agency's required peer and policy review and does not necessarily reflect the views of the agency. No endorsement by the US EPA should be inferred.

References

Bettencourt, B., J. Edelmann, E. Lewandowski, and M. Percher, 2001, The Effects of Climate Change on Bridge Scour, Civil and Environmental Engineering Capstone Project, Tufts University, Medford MA.

HNTB, 1999, Bridge Scour Coding Compliance Program, Summary Report, for MHD, Boston, MA.

Hydrologic Engineering Center,1993, Evaluating Scour at Bridges, HEC 18, Second Edition, February.

Hydrologic Engineering Center, 2002, HEC-RAS User's Manual, http://www.hec.usace.army.mil/software/software_distrib/hec-ras/hecrasprogram.html

Lagasse, P.F., 1995, "Guarding Against Scour", ASCE Civil Engineering, June.

Massachusetts Highway Department, 2000, Hydraulic Study Report, Boston MA.

Meadowcroft, I.C., 1993, "Assessment and Monitoring of Bridges for Scour," in Bridge Management: Inspection, Maintenance Assessment, and Repair, Thomas Telford Limited.

New England Regional Assessment Team, Preparing for a Changing Climate, New England Regional Overview, US Global Change Research Program, University of New Hampshire.

Raphael, L., 2001, "Pothole Bores through Bridge", Boston Globe, January 17.

Ruff, J., 1999, "Riprap Coverage Around Bridge Piers" in Stream Stability and Scour at Highway Bridges, ASCE.

Table 1. Scour Results for 100-Year Flood

100-Year Flood	Scour Depth (ft)
Present	6.8
10%	7.0
20%	7.2
30%	7.5

Figure 1. Bridge Site (from Bettencourt et al., 2001)

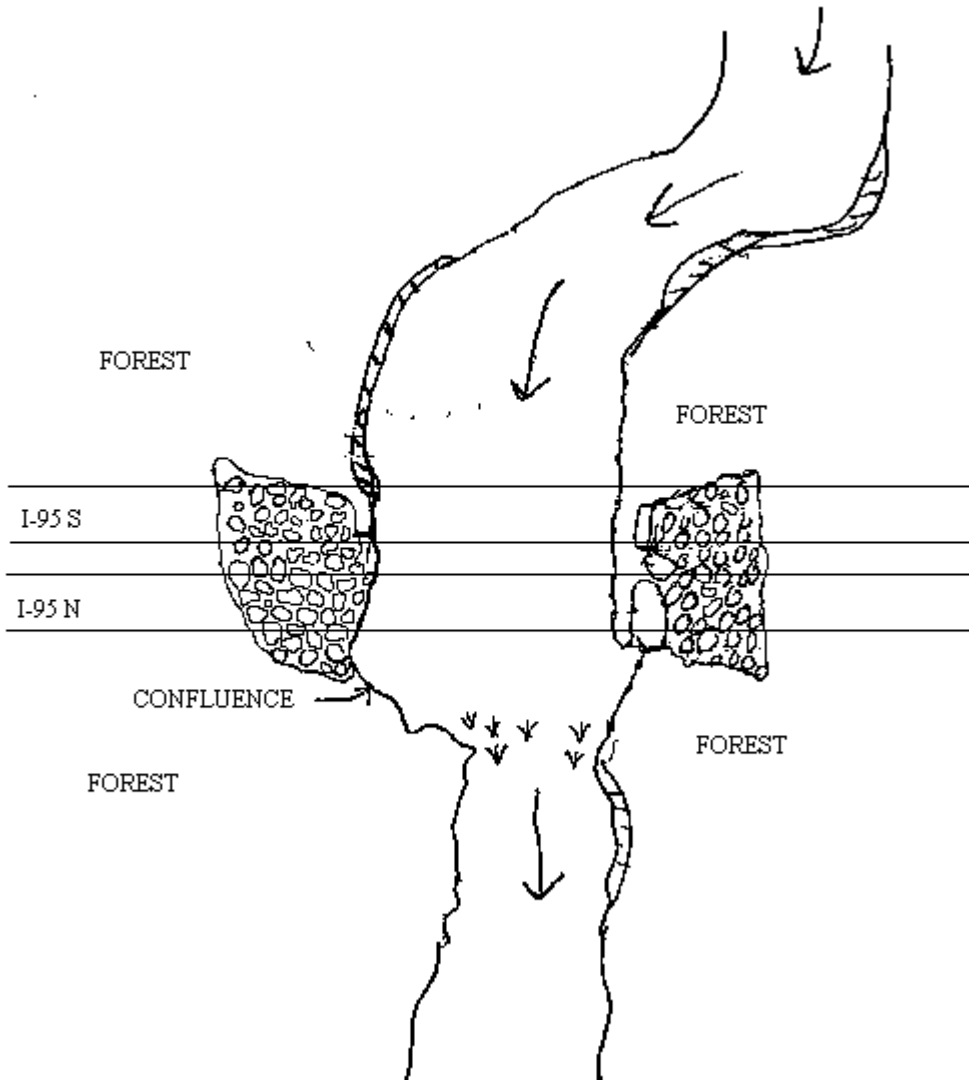

Figure 2. Bridge Footing and Calculated Scour Depths (from Bettencourt et al. 2001)

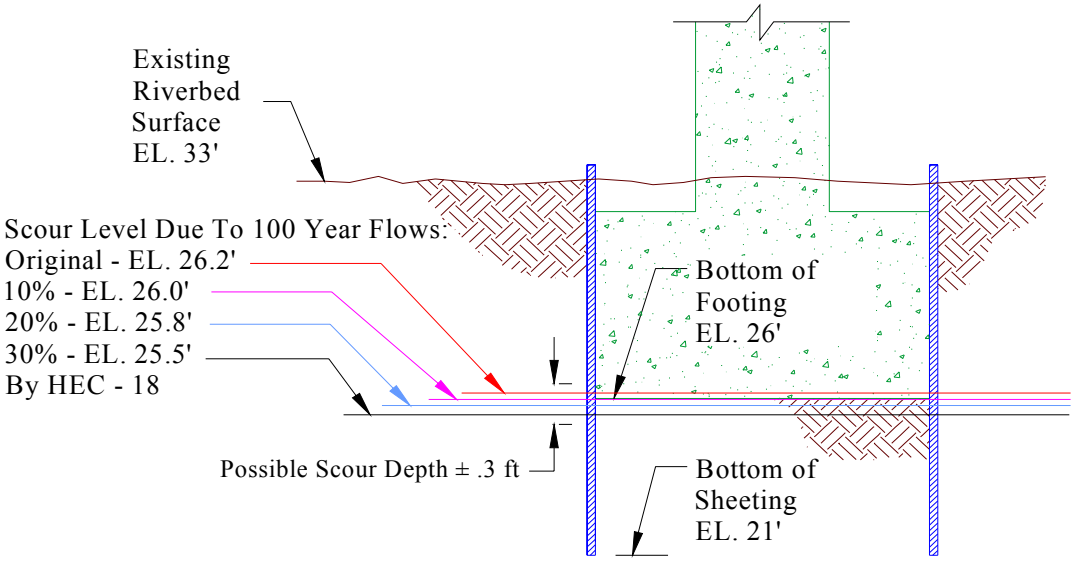

Analysis of Pile Groups Considering Riverbed Scouring

By

Sangseom Jeong[1], Jinoh Won[2], Jungju Suh[2]

[1]Associate Professor, Dept. of Civil Engineering, Yonsei University, 134 Shinchon-dong, Seodaemun-gu, Seoul, 120-749, Korea. (soj9081@yonsei.ac.kr)

[2]Ph.D. student, Dept. of Civil Engineering, Yonsei University, 134 Shinchon-dong, Seodaemun-gu, Seoul, 120-749, Korea. (wjo20@yonsei.ac.kr) , (winaler@yonsei.ac.kr)

ABSTRACT

This paper describes a simplified numerical procedure for analyzing the response of bridge pier foundations due to riverbed scouring. A computationally efficient algorithm to analyze the behavior of a pile group is proposed by considering soil-pile, pile-cap, and pile-fluid interactions. The complex phenomenon of the pile-soil interaction is modeled by discrete nonlinear soil springs (p-y, t-z and q-z curves). The pile-cap interaction is considered by geometric configuration of the piles in a group and connectivity conditions between piles and the cap. The pile-fluid interaction is incorporated into the procedure by reducing the stiffness of the soil-pile reactions as a result of nonlinearity and degradation of the soil stiffness with river bridge scouring. Through the numerical study, it is shown that the maximum bending moment is increased with increasing scour depth. Thus it is desirable to check the stability of pile groups based on soil-pile and pile-cap interactions by considering scouring depth in the riverbed.

INTRODUCTION

Pile groups are the most common type used for bridge foundations because they can transfer applied axial and lateral loads on superstructure to bearing ground efficiently and safely. Pile group foundation consists of several single piles and one pile cap. Total bearing capacity of a pile group is the sum of each bearing capacity of single piles and that of a pile cap which is in direct contact with the soil.

A pile group is not collapsed immediately under sudden attack of flood flows which cause scouring along the pile, because bearing capacity that comes from the interaction between individual pile in a group and a pile cap resists scouring. Therefore, the analysis by considering the scour depth of bridge foundation is required to evaluate the stability of a pile group under applied load.

In this study, a three-dimensional analysis of pile groups is performed by considering soil-pile, pile-cap interactions based on riverbed scouring. The complex phenomenon of the soil-pile interaction is modeled by discrete nonlinear soil springs (p-y, t-z, and q-z curves) and the effect of riverbed scouring is considered by elimination or degradation of the soil stiffness. The pile-cap interaction is analyzed by stiffness method which can be considered by geometric configuration of the piles in a group and connectivity conditions between piles and a cap. Through the three-dimensional analysis program (YS-3DPILE) of pile groups developed in this study, the displacement and rotation of a cap and member forces of individual pile in a group such as bending moment and shear force were estimated with varying scour depth of riverbed.

METHOD OF ANALYSIS CONSIDERING BRIDGE SCOUR

If the scour depth affects below the pile cap, pile groups are not failed at once but has some hazardous effects. For example, excessive horizontal displacement of a pile cap resulting from riverbed scouring may lead to structural damage (Fig. 1). Analysis only based on the estimated scour depth is not sufficient to consider the failure mode of pile groups caused by scouring under flood. So, it is a three-dimensional pile group analysis method that is recommended to think over the effect of scouring and the interaction between each one of piles and a pile cap.

The analytical method considering pile-cap interaction was firstly suggested by Hrennikoff (1949) using the stiffness method. Reese (1970) developed a 3D analytical method of pile groups, using the modified Hrennikoff's method. This method was extended to incorporate the pile-soil-pile interaction by O'Neill et al. (1977) and Chow et al. (1986). In this study, a similar approach suggested by O'Neill et al. (1977) is used and implemented as

(1) Calculation of a pile head stiffness of each pile in a group

: Calculate a pile head stiffness of an individual pile on each loading step in different cases such as different pile properties (embedded length, diameter, and elastic modulus) and different soil layer properties (scour depth, depths of each soil layer and its properties).

(2) Pile-cap analysis considering individual pile head stiffness (k_{ij})

: Using all the individual pile head stiffnesses that are initially estimated in the first loading step, formulate the full stiffness matrix. Calculate pile cap displacement and individual pile head forces (P_{ix}, P_{iy}, P_{iz}) and moments (M_{iz}, $M_{iy,}$ and M_{iz}) for all the piles in the group.

(3) Iteration to convergence

: Compare the computed individual pile head forces and moments with the applied distributed load components used in step (2) for all the individual piles if the difference between them meets the user-specified closure tolerance level. If the convergence criterion is not satisfied, using the new computed pile head forces and moments, calculate a new individual pile head stiffness matrix for each pile again and repeat this iteration process. If it is satisfied, go to next step.

(4) Evaluate response of all individual piles

: Finally, evaluate responses of all the individual piles in a group, using the final individual pile head forces and moments.

The flowchart that shows all the steps described above is also given in Fig. 2. Based on the proposed algorithm, a new computer program YS-3DPILE has been developed to analyze the behavior pile groups by considering both soil-pile and pile-cap interactions. (Jeong, 1999)

LOAD TRANSFER CURVES

For axially loaded piles, the load-transfer curves were modeled by t-z and q-z curves. The type of t-z and q-z curves supported by the program is a linear elastic-plastic curve as shown in Fig. 3. According to soil types such as soil and rock, a maximum unit skin friction, t_{max} was estimated as follows:

In the soil, t_{max} was estimated by β method (Burland, 1973):

$$t_{max} = \beta\sigma'_z \tag{1}$$

where, β is approximately 0.3 and t_{max} is linearly increased to a critical depth (15D, D : diameter), beyond which it remains as a constant to failure.

For the rock, t_{max} was estimated using the method proposed by Reese and O'Neill (1987):

$$t_{max} = 0.15q_u \tag{2}$$

where, q_u is the unconfined shear strength, and limited to 100kN/m^2 (weathered rock), 150kN/m^2 (soft rock), and 200kN/m^2 (hard rock).

In Fig. 3, z_c is a critical displacement of the pile segment at which t_{max} is mobilized. Vijayvergiya recommended 0.2 to 0.3inch for z_c, so in this study 0.2inch (0.5mm) of z_c is adopted.

For laterally loaded piles, the load-transfer curves were modeled by p-y curves. A hyperbolic function was used to describe the relationship of the p-y curve (Fig. 4) which has an ultimate resistance (p_u) and an initial tangent stiffness (E_s). The initial tangent stiffness used in this study was assumed to vary linearly with depth as recommended by Reese et al. (1974).

To analyze the change of group pile behavior, especially in the presence of bridge scouring, load transfer curves (p-y, t-z, and q-z curves) within the scour depth are assumed to be eliminated, beyond which they are reconstructed along the embedded pile length by reducing the ultimate resistance (p_u).

ANALYSIS AND RESULTS

To examine the pile group behavior with riverbed scouring, a series of idealized cases were examined based on the major influencing parameters such as cap rigidity and the spacing between piles. Fig. 5 shows a group pile configuration to be analyzed considering scouring. The material properties for pile groups are shown in table 1. Four piles, arranged by 2 rows and 2 columns and fixed and hinged head conditions are considered between piles and a pile cap. The piles are made of pre-cast concrete and the elastic modulus is 4,000,000 kN/m^2. Each pile is 0.5 m in diameter and 10 m in embedded length. The soil is uniform sand and the friction angle, the cohesion, and the unit weight are 30 degree, 0 kN/m^2, and 17.0 kN/m^3, respectively. The applied axial and lateral loads are 200 kN and 100 kN, respectively. The scour depth (H_s) is increased from 0 to 5 m by increment of 1 m. In each scour depth a three-dimensional analysis was performed.

(1) Effect of Cap Rigidity

Fig. 6 and 7 show the displacement and rotation of a cap with varying scour depths in both fixed and hinged pile head conditions. As shown in these figures, the displacement of the pile cap is increased as the scour depth increases and the magnitude is seem to be significantly larger for the hinged head case than for the fixed head case. The rotation of a pile cap for the fixed head case is also increased with increasing the scour, but its absolute value is not significant. For the hinged head case the rotation of a pile cap is always seem to be zero.

Fig. 8, 9, and 10 show lateral pile displacement, bending moment, and shear force profiles along the embedded pile length of no. ① pile as shown in Fig. 5. Fig. 8 shows that the lateral displacement of pile is increased as the scour depth increases. The distribution of bending moment along the pile and its change with scouring are represented in Fig. 9. For the fixed head case, the maximum bending moment is occurred at the pile head. When scour depth is increased from 0 to 5m, the maximum bending moment at the pile head is increased approximately up to 340%. For the hinged head, the position where the maximum bending moment occurs moves down and its magnitude

increases approximately up to 600% as the scour depth is increased. Fig. 10 is the distribution of shear forces along the pile. For the fixed head case the shear force has a maximum value at the scoured bed level, but for the hinged head case it has a maximum value below the scoured bed level and the magnitude is also increased as the scour depth increases.

(2) Effect of Spacing (s/d)

In the analysis, the pile groups with different pile center-to-center spacing were assumed to have the same initial scour depth. Pile spacings (s/d) selected in this study were 2.0, 4.0, and 8.0. Scour depth used changes from 0 to 5m. Fig. 11 and 12 show the effect of pile spacing with varying scour depths on the lateral displacement and rotation of pile cap. The lateral displacement and rotation of pile cap increase as scour depth is increased. On the other hand, the effect of s/d was more sensitive to the rotation than to the lateral displacement.

Fig 13 shows the magnitude of maximum bending moment as a function of the pile spacing and scour depth. The maximum bending moment developed at the pile head and varies linearly as scour depth increased. However, for the three spacings studied, there is little difference in maximum bending moment.

(3) Difference in Bearing Capacity

The variation of ultimate bearing capacity of vertically loaded pile groups due to riverbed scouring was examined. The ultimate pile capacity was calculated by using the proposed method of US Army Corps of Engineers (1991). Table 2 shows the variation of bearing capacity of pile groups with varying scour depths. The skin friction of single pile is significantly decreased as scour depth is increased, whereas endbearing resistance remains constant because the pile point was located below the critical depth. The ultimate bearing capacity of pile groups, calculated by multiplying number of piles with each single pile capacity, is decreased to about 57% as scour depth is increased from 0 to 5m.

CONCLUSIONS

In this study, a computationally efficient algorithm to analyze a group pile behavior is proposed in consideration of soil-pile, pile-cap, and pile-fluid interactions. A limited parametric study of the response of pile groups was performed to examine the scouring effect. The following conclusions are drawn from the present study:

1. Under the same loading applied before and after scouring, the displacement along the pile length is increased with increasing scour depth.

2. The maximum bending moment along the pile increases as the scour depth increases. This is particularly more significant for hinged head condition than for fixed head condition.
3. The pile spacing effect is significant for the rotation of pile. However the lateral pile cap deflection and maximum bending moment are more influenced by scour depth than pile spacing.
4. To check the stability of bridge piers in the riverbed, it is recommended to perform a group pile analysis considering soil-pile and pile-cap interactions based on scouring effect.

ACKNOWLEDGEMENTS

This paper was supported by grant No. 1999-1-311-02-3 from the interdisciplinary Research program of the KOSEF in Korea.

REFERENCES

1. Burland, J. B. 1973, “Shaft friction Piles in Clay – A Simple Fundamental Approach.” Ground Engineering, Vol. 6, No. 3, pp.30-42.
2. Chow, Y. K. 1987, “Three-dimensional analysis of pile groups.” Journal of Geotechnical Engineering, Vol. 113, No. 6, pp637-651, ASCE, USA.
3. Hrennikoff, A. 1949, “Analysis of pile foundation with batter piles.” Trans., Vol. 79, pp351-374, ASCE, USA.
4. Jeong, S. S., Chung, S. H., and Won, J. O. 2001, “Analysis of group pile-cap interaction by load transfer approach.” Journal of the Korean Goetechnical Society, Vol. 17, No. 3, pp95-102, Korea.
5. O’Neill, M. W., Ghazzaly, O. I., and Ha, H. B. 1977, “Analysis of three-dimensional pile groups with nonlinear soil response and pile-soil-pile interaction.” Proc. 9th Offshore Technology Conf. 2, pp245-256.
6. Reese, L. C., O’Neill, M. W., and Smith, R. E. 1970, “Generalized analysis of pile foundation.” Journal of Soil Mech. Found. Div., Vol. 96, No. 1, pp235-250, ASCE, USA.

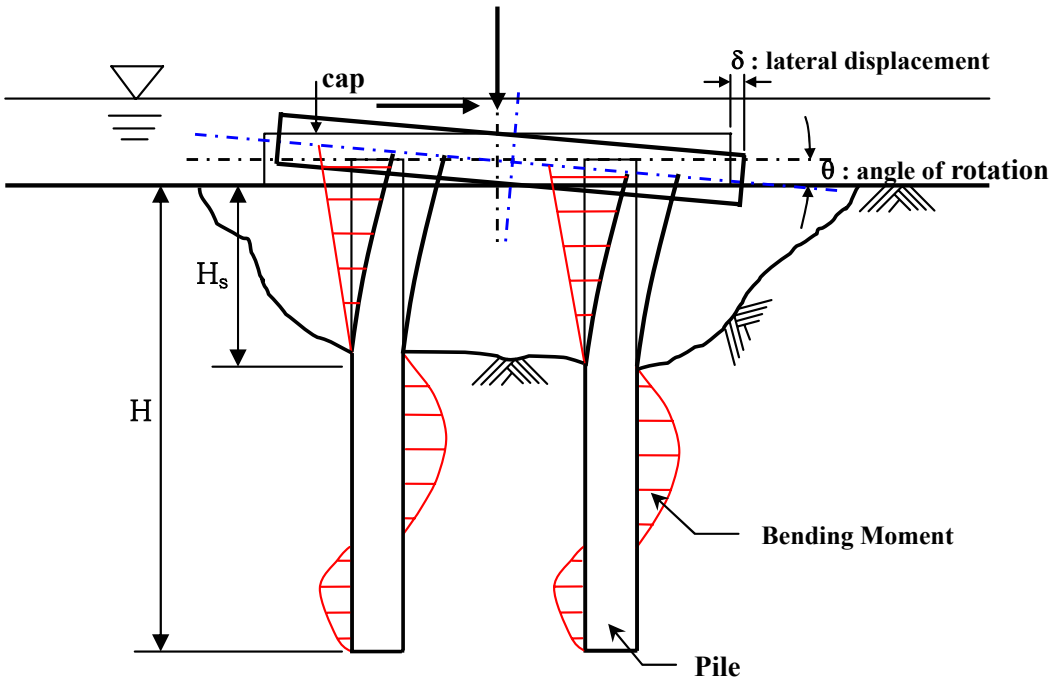

Fig. 1 – Pile groups with riverbed scouring

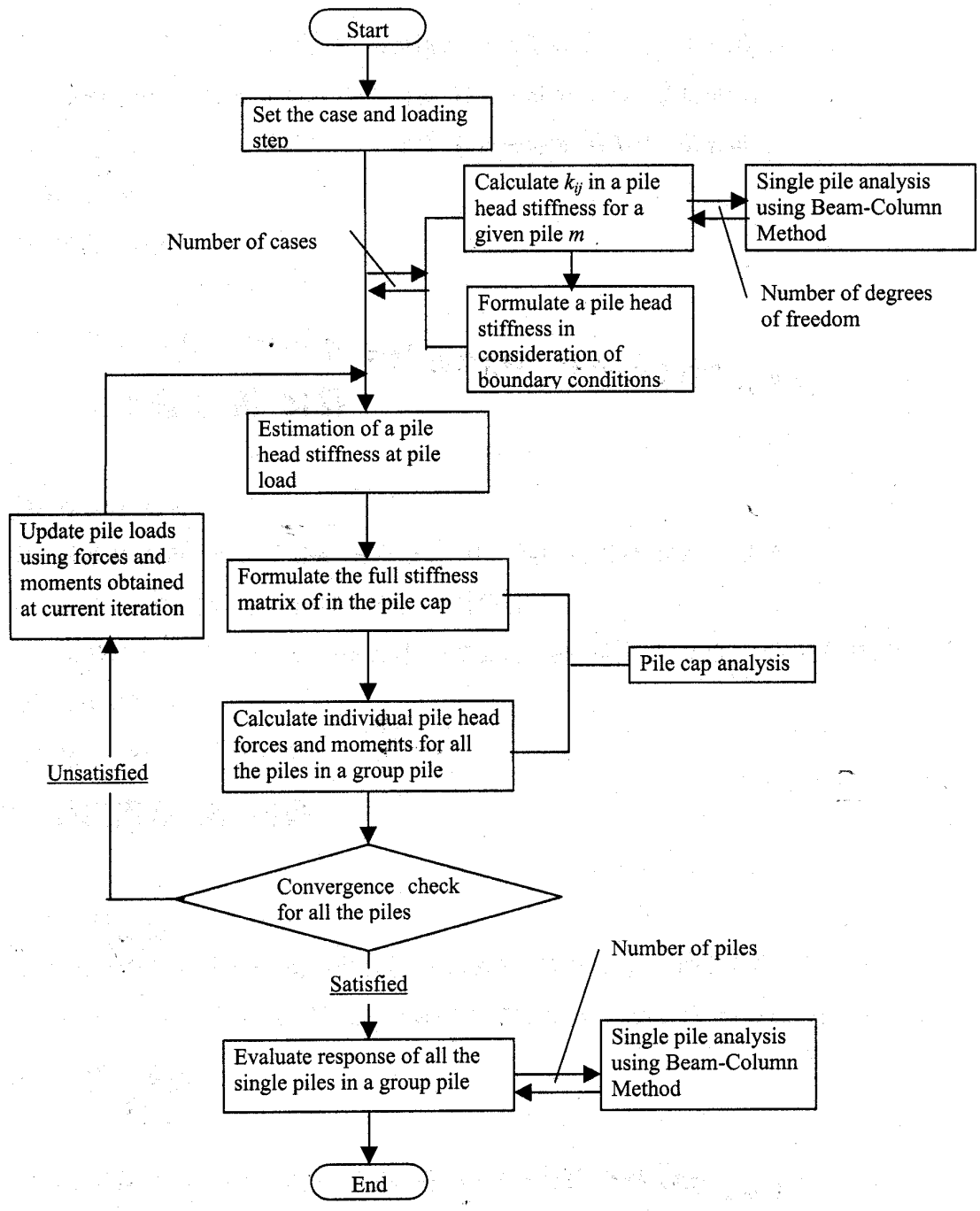

Fig. 2 - Algorithm of three-dimensional group pile analysis

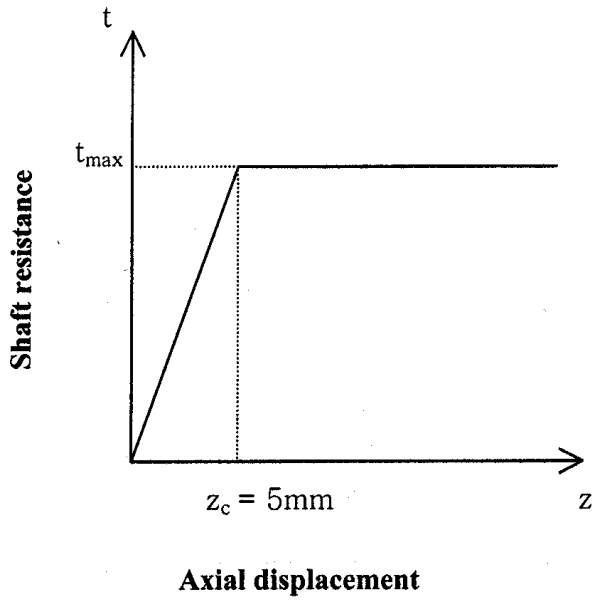

(a)

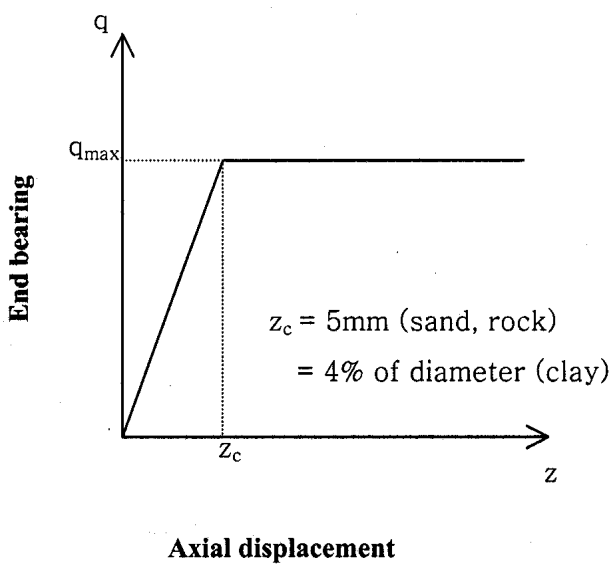

(b)

Fig. 3 - Load transfer curves of axially loaded pile; a) t-z curve, b) q-z curve

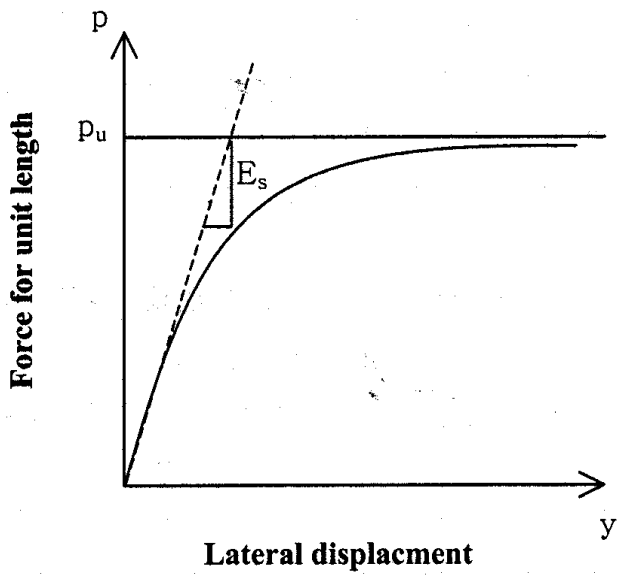

Fig. 4 - Load transfer curves of laterally loaded pile (p-y curve)

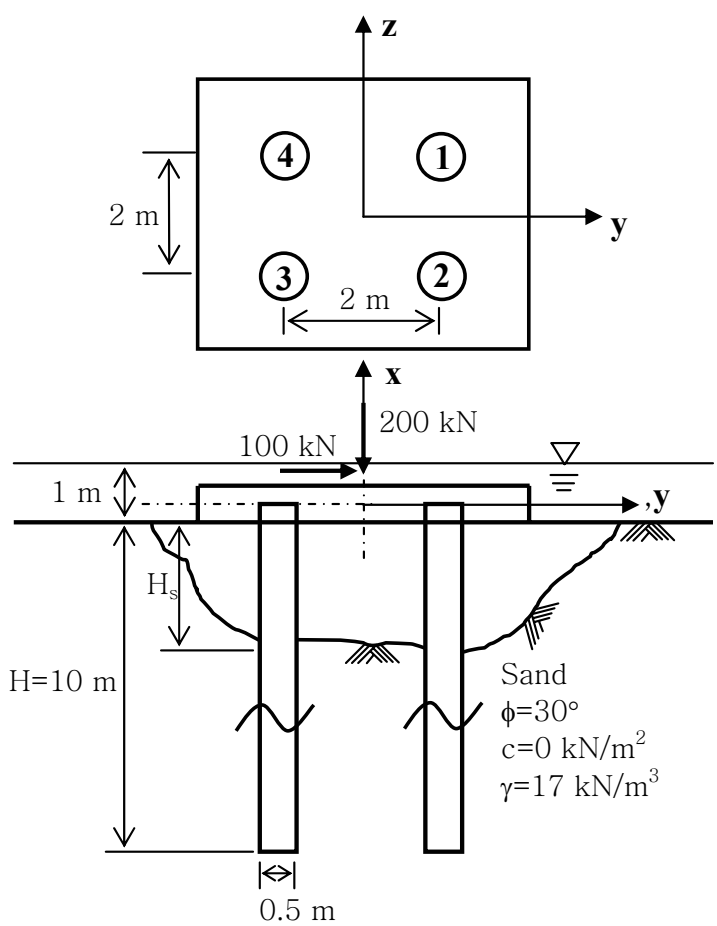

Fig. 5 - A group pile configuration with scouring

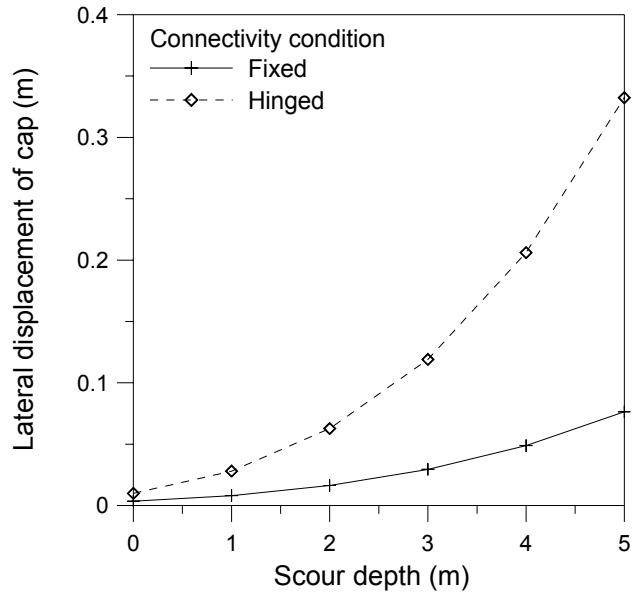

Fig. 6 – Lateral pile cap displacement vs. scour depth

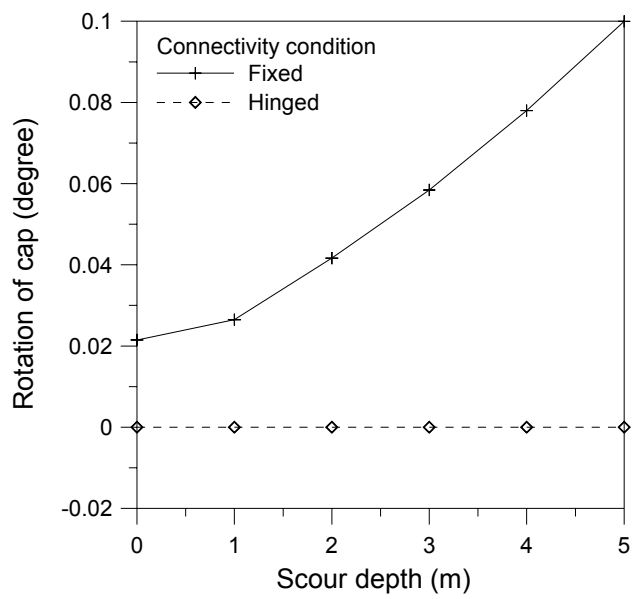

Fig. 7 – Rotation of pile cap vs. scour depth

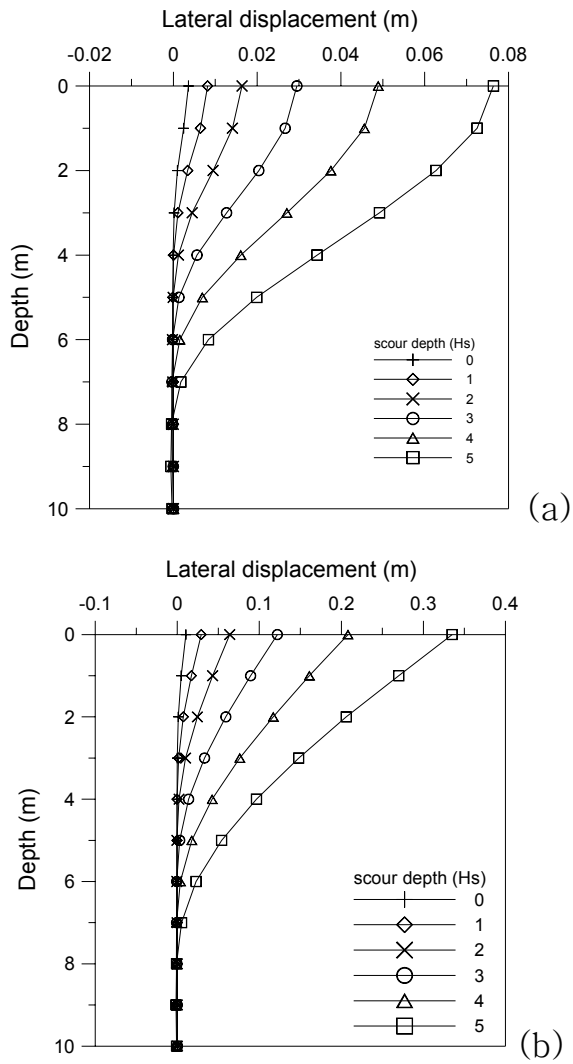

Fig. 8 – Displacement profiles for different scour depths (no. ① pile); a) fixed head condition, b) hinged head condition

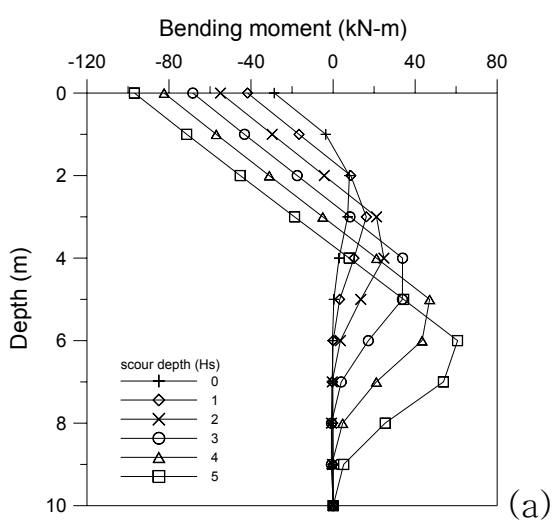

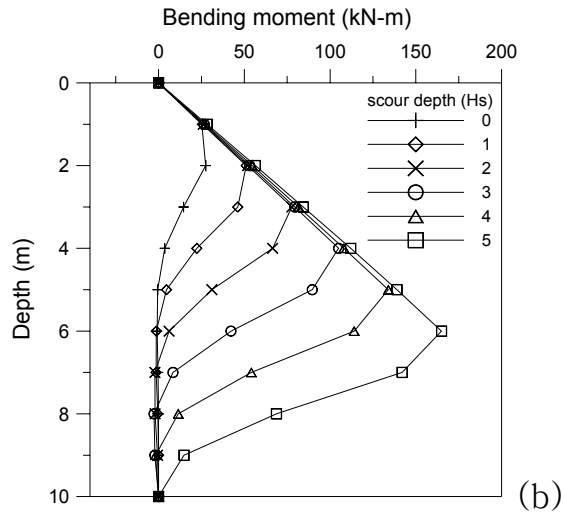

Fig. 9 – Bending moment profiles for different scour depths (no. ① pile); a) fixed head condition, b) hinged head condition

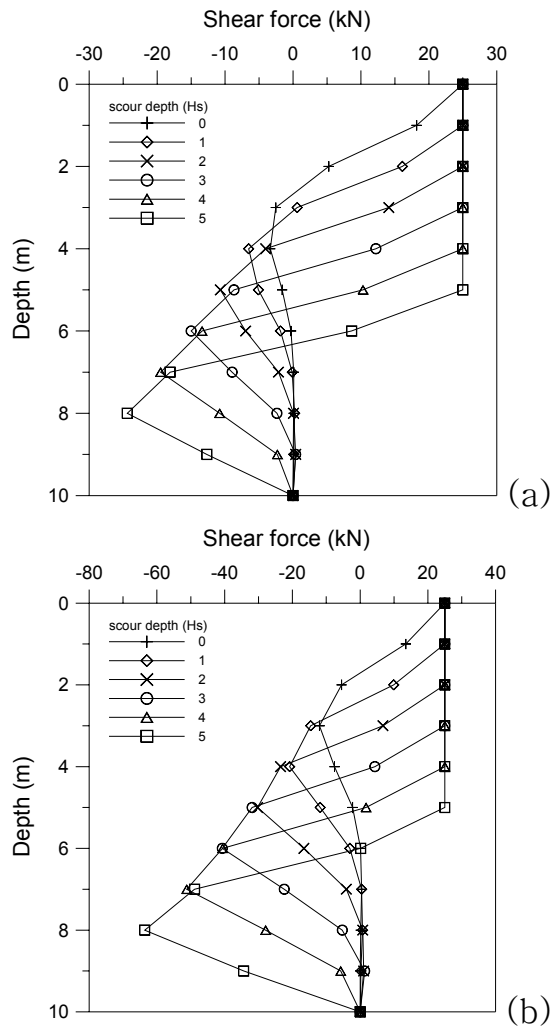

Fig. 10 – Shear force profiles for different scour depths (no. ① pile); a) fixed head condition, b) hinged head condition

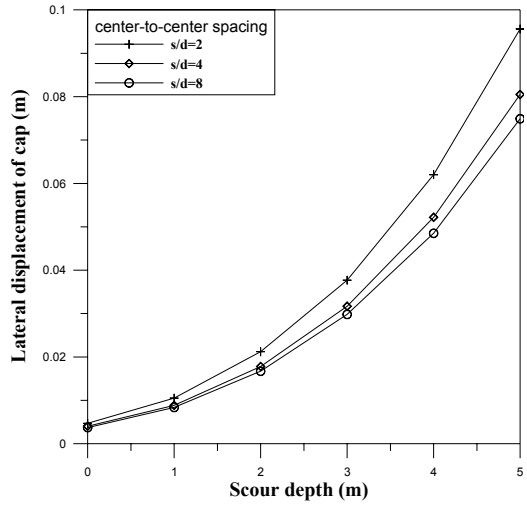

Fig. 11. Effect of pile spacing on pile cap deflection (fixed head condition)

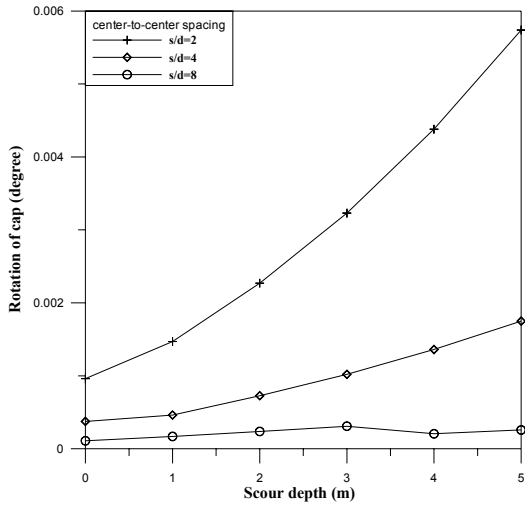

Fig. 12. Effect of pile spacing on pile cap rotation (fixed head condition)

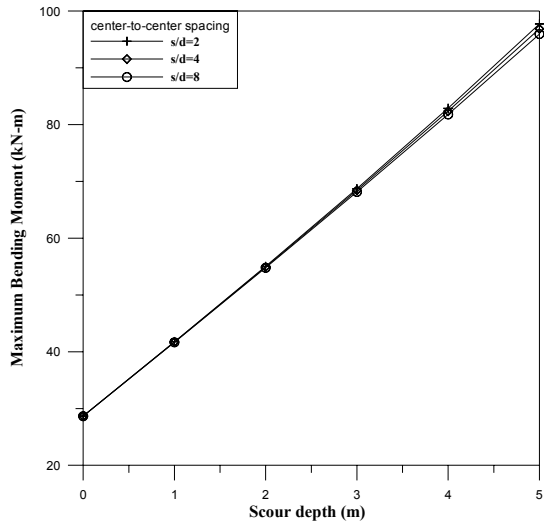

Fig. 13. Effect of pile spacing on maximum bending moment (fixed head)

Table 1. Material properties for pile groups

Pile	Diameter	0.5 m
	Length	10 m
	Elastic modulus	4,000,000 kN/ m^2
Soil	Friction angle	30 degree
	Cohesion	0 kN/m^2
	Unit weight	17.0 kN/m^3
Connectivity condition	Fixed, Hinged	
Loading	Axial	200 kN
	Lateral	100 kN
Scour depth	0, 1, 2, 3, 4, 5 m	

Table 2. Ultimate bearing capacity of pile groups (2×2 arrangement)

	Single pile			Group pile
Scour depth (m)	Skin friction (kN)	Point resistance (kN)	Ultimate bearing capacity (kN)	Ultimate bearing capacity (kN)
0	315.14	171.81	486.95	1947.80
1	273.13	171.81	444.94	1779.76
2	231.11	171.81	402.92	1611.68
3	189.09	171.81	360.90	1443.60
4	147.07	171.81	318.88	1275.52
5	105.05	171.81	276.86	1107.44

Study on the Disasters of Bridge and Bed Protection Works During the Passage of Typhoon Herb

Chang Lin[1], Tsung-Chun Ho[2], Peng-Hao Chiu[3], Kuang-An Chang[4]

Abstract

During July 31 to August 1, 1996, Typhoon Herb swept across Taiwan island, bringing heavy rain and triggering floods that left widespread damages. The disasters of bridge and bed protection works caused by the scour of torrential flood during the passage of Typhoon Herb are investigated in the present study. The purposes of this study are to make clear the scour mechanism causing various damages of these structures, to classify the failure modes of different works, and to propose some countermeasures or ideas for design use. The present study is expected to promote exchange of experiences and techniques concerning disaster prevention or mitigation for bridge foundation and bed protection works.

Keywords: bed protection works; general scour; constriction scour; local scour; lateral (transverse) river bank erosion; head-cutting

Introduction

The level of river bed in the main channels of most rivers in the western area of Taiwan declined apparently during the last decade. The key factors were : (1) the construction of many (sabo) dams and weirs at upstream watersheds (sediment supply to downstream reach was thus largely reduced); (2) long-term over mining of sand and stone along the middle and downstream basins; and (3) the general scour of torrential flood induced by heavy rain or typhoon. One of the typical examples is shown in Fig. 1, in which the large-scale descent of river bed occurring in the reach (between 31 to 50 km measured from estuary) of Kao-Ping River could be seen clearly. During two decades, the maximum lowering of river bed at each section was estimated to be 4 to 17 m, with a mean value of 12 m. Most of infrastructures constructed across rivers were severely endangered by the lowering of river bed. For examples, two extreme cases of bridge substructures with caisson or group pile foundations are presented in Fig. 2 and Fig. 3, respectively. The figures show that serious exposure of

[1, 2, 3] Department of Civil Engineering, National Chung-Hsing University, Taichung, Taiwan 402, Republic of China

[4] Department of Civil Engineering, Texas A&M University, 3136 TAMU College Station, TX 77843-3136, USA

bridge foundations of Ta-Shi Bridge (across Ta-Han River in northern area of Taiwan) and Tzu-Chiang Bridge (across Cho-Shui River in central Taiwan area) reached to an extent of about 9.0 - 11.5 m deep, which may result in serious failure during high flood period or by strong earthquake. To ensure the safety of bridge foundation and control the elevation of river bed, many bed protection works had been built in the neighborhood of bridge piers. Recently, some strict lawful measures have been also adopted by the government agency to control the mining of sand and stone from most main rivers in the western area of the island.

The bed protection works could be roughly divided into several types, for examples, (1) T1 : placing riprap around pier; (2) T2 : installing multilayer gabions (frequently placed over riprap layer) along bridge axis; (3) T3 : concrete or pile jacketing around pier; (4) T4 : setting concrete blocks (such as cube, tetra-pod, ...etc) around pier or along bridge axis; (5) T5 : constructing rigid or deformable (sabo) weir with/without energy dissipaters at downstream side of bridge in the cross-river direction; (6) T6 : laying concrete armor layer from upstream to downstream side along bridge axis; (7) T7 : use of compound works consisting of two or three types as mentioned above.

During July 31 to August 1, 1996, Typhoon Herb swept across Taiwan Island, bringing torrential rain and triggering floods that left widespread damages. The typhoon has been credited for bringing record-high levels of precipitation, dispelling most fears about lingering droughts, with totals of 1094.5 and 1986.5 mm of rain falling in the Alishan area within 24 and 48 hours, respectively.

Severe disasters during the passage of this typhoon could be roughly classified into four categories listed in the following:

1. damage of cross-river structures, such as bridge, bed protection work, pipeline, ... etc., caused by the flow scour of high speed flood.
2. ruin of embankments for river bank and sea-coast, arising from the undermining of high speed curving flow or wave motion as well as from the impingement of high waves or over flooding of high tides.
3. inundation of a number of areas by from waist-high to one-floor-high water, such as Taipei City's Shetze and Panchiao and Chungho in Taipei County due to flood, Hsinhsi and Fangyuan in Changhua County due to high tides.
4. damage to structures and traffic routes by large-scale landslides or debris flows (which were triggered by very heavy rain) occurred within mountainous Nantou County in the central area of Taiwan.

Field survey and laboratory experiment

This study was based both upon the detailed observations and surveys at over 22 bridge

sites and upon some movable-bed hydraulic model tests performed in a laboratory water channel. In the case of field investigation, special attention was paid to the geological state of the river-bed material and the boundary flow conditions. Moreover, slaking durability tests were performed to study the erosion-resistant potential of bed materials that consist of soft mudstone or shale.

The circulating channel was 9.4 m long, 0.5 m wide, and 0.5 m deep with both sides glass-walled. Different model scales for bed protection works and bridge foundations as well as sands of nearly uniform size were considered in the tests. The flow characteristics were considered to be dominated mainly by Froude-number similarity criterion. Some experimental results are used to elucidate the damage behaviors during the scouring process.

The purposes of this study are to make clear the scour mechanism causing various damages of these structures, to classify the failure modes of different works, and to propose some countermeasures or ideas for design use. The present study is expected to promote exchange of experiences and techniques concerning disaster prevention or mitigation for bridge foundation and bed protection works.

Illustration of case study

One of the typical cases explored experimentally in the present study is addressed herein. Li-Ling Bridge across Kao-Ping River was first constructed in October 1989. Its full length is 2380 m, with sixty-eight 35 m clear spans. The bridge piers of P1-P29 are supported by caisson type foundations of 5.0 m in diameter and of 14.0 m in depth. Due to large increase of traffic flow through this bridge, public road agency started constructing a new bridge parallel close to the old bridge at upstream side in early 1993. The new bridge was completely constructed in November 1994. The new caisson foundations of P1-P29 have a diameter of 5.6 m and a length of 14.0 m. The elevation of the top surfaces of these foundations is kept at 23.3 m, which is 2.0 m lower than that of the old bridge. Because the tremendous descent of river-bed in this reach, as shown in Fig. 1, endangered the safety of both bridges, the public road agency was forced to take some countermeasures to control the stability of river bed and to protect the substructures of the bridges. The construction period of the bed protection works was between April 1994 and March 30 1995.

Fig. 4 shows the layout of bed protection works (combining the placing of ripraps, concrete blocks with cavities, and rigid concrete weir) along the downstream side of Li-Ling Bridge. The concrete blocks were joined together by longitudinal and transverse steel bars. The original bed material at bridge site comprised a deep layer of cobble and gravel mixing with sand. Note that the level difference between concrete blocks at upstream and downstream sides of rigid weir was 1.3 m; and many RC pipes (30 cm in diameter) were

installed inside concrete weir to drain infiltration flow, existing in the cobble layer beneath the upstream concrete blocks. It should be also mentioned that fine natural filtering material was backfilled around the base of the concrete weir. Fig. 5 shows the bed protection works (over which very shallow water flow runs smoothly) were completely constructed on March 30 1995 (i.e. during drought season).

Hereafter, the first heavy rain triggered by outer current which was entrained by weak Typhoon Deanna brought small flood in the watershed of Kao-Ping River during June 8-10 1995. The histories of water level and discharge during this flood period, recorded by Taiwan Provincial Water Conservancy Bureau, are shown in Fig. 6. The maximum water level and discharge, occurred on June 9 1995, were 25.44 m and 1600 CMS, respectively. Fig. 7 shows the free surface pattern of the flood peak flowing over the works. Note that the maximum water level was only 1.44 m higher than the top surface of the upstream concrete blocks and the 1600 CMS discharge was relatively small. Unfortunately, these bed protection works suffered considerable damage. The damage state of these structures (which were constructed for protecting the bridge foundations and for preventing the lowering of river-bed) is shown in Fig. 8. It could be clearly seen that many concrete blocks (weighing from 19.2 to around 108.6 tons) subsided seriously due to flow scour, likely caused by hydraulic jump just at downstream side of weir. Also note that the descent of local bed level was larger than the case before the construction of these works. Fig. 9 shows the collapse of the rigid weir and destruction of these concrete blocks after the passage of Typhoon Herb. The maximum water level and peak discharge corresponding to the high flood were 30.8 m and 19700 CMS, respectively.

The failure mechanism caused by flow scour was made clear by performing a 2-D hydraulic model test with a 1/50 scale as shown in Fig. 10. The schematic diagram for the damage process is depicted in Fig. 11, which is corresponding to the following steps:

(1) The flood flow running over the upstream concrete blocks and weir formed the hydraulic jump just at the downstream side of weir, leading to flow impingement on the cavities inside the blocks and on the 0.5 m wide gaps between adjacent blocks. The backfilled bed material consisting of cobble, gravel, and find sand in these cavities and gaps were then picked up and washed away, causing apparent deflection between the first and second rows of concrete blocks (hence, the connecting steel bars in the flow direction were apt to be broken by tension force). As the flood flow proceeded, the deflection became more considerable, resulting in the subsidence of most blocks located at downstream side of weir.

(2) As the first row of blocks (downstream of weir) sank to a level slightly lower than the

RC pipe opening (30 cm in diameter, as shown in Fig. 4), the fine bed material and some part of the natural filtering substance at upstream side of the weir were sucked into the pipes and then issued toward downstream, due to the presence of pressure difference between both ends of the pipes. This fact causes continuous loss of these material, thus leading to the consecutive sinking of the concrete blocks (just at close upstream of weir). A corner flow arising from flow separation between the sinking blocks and the rigid weir existed and the vortex motion made the local scour inside the corner more apparent, also causing more lowering of the blocks.

(3) When the concrete blocks downstream of weir further subsided down to a level approximately at the base of the weir and the suction flow through the pipes toward downstream went on, large amount of the bed and filtering materials were carried rapidly toward downstream through the base of weir. The result forced most of these blocks (at upstream side of weir) to sink more seriously and endangered the stability of group (frictional) piles supporting the rigid weir.

(4) Most of the oncoming flood flowed toward downstream via the bottom of the weir and the drainage pipes, forming large-scale vortex motion at upstream of the weir and triggering more violent scour in the neighborhood of weir base. More bed material was washed away and the blocks subsided more severely.

(5) The discharge flowing via the base and pipes of the weir became larger and flow induced vibration might occur. Only tiny part of the frictional piles (10 m net depth) was still surrounded by original bed material. The stability of the rigid weir was questionable. Note that the damage feature of these works shown in Fig. 8 is quite agreement with that demonstrated by the present hydraulic model test, as shown in Fig. 10 and Fig. 11.

Summary of causes for the damages of bridge and bed protection work

Regarding the disasters of bridge and bed protection work during the passage of Typhoon Herb on July 31 - August 1 1996, at least six important bridges collapsed, subsided, or tilted seriously; and many bed protection works were ruined completely in the western area of Taiwan. Before summarizing the causes for these damages, some typical examples with distinct forms of pier foundation and different types of bed protection work are briefly illustrated in order to promote understanding of the summarized table mentioned below. Fig. 12~15 show the failures of Tou-Chien-Shi Bridge, Chu-Tung Railway Bridge, Li-Kang Bridge, and Kao-Ping Bridge, respectively. Moreover, Fig. 16~20 also show the damages of bed protection works which were constructed at sites of Chung-Cheng Bridge, Shi-Luo Bridge, Shi-Jou Bridge, Ta-Chia-Shi Freeway Bridge, and Wu-Feng Bridge, respectively.

Note that different types of bed protection works could be seen in Fig. 12~20. Summary of causes for the damages of bridge and bed protection woks is shown in Table 1.

Conclusion

The disasters of bridge and bed protection works caused by the scour of torrential flood during the passage of Typhoon Herb have been investigated in the present study. This study is based both upon the detailed observations and surveys at over 22 bridge sites and upon some movable-bed hydraulic model tests carried out in a laboratory channel. One of the typical cases, Li-Ling Bridge, has been depicted in detail. The causes of damages to bridge and bed protection works are summarized in a table. The present study is expected to promote exchange of experiences and techniques in connection with disaster prevention or mitigation for bridge foundation and bed protection works.

Acknowledgments

The authors are grateful to the Ministry of Transportation and Communication (MOTC), the Executive Yuan, R.O.C., for providing the grant-in-aid for this research.

References

1. Lin, C., 1997, "Analysis of bridge pier disasters in the western area of Taiwan and establishment of data base system for pier protection works", *midterm report for MOTC*, pp. 1-525 (in Chinese).
2. University of Toronto Press, 1975, "Guide to bridge hydraulics", Project Committee on Bridge Hydraulics, Roads and Transportation Association of Canada.
3. Zwamborn, J. A., 1981, "Umfolozi road bridge hydraulic model investigation", *Journal of the Hydraulics Division, Proceedings of the American Society of Civil Engineers*, Vol. 107, No. HY11, pp. 1317-1333.

Appendix

The following symbols are used in this paper:

B1: Ta-Shi Bridge	B12: Ta-Chia-Shi Railway Bridge
B2: Ta-Han-Shi Freeway Bridge	B13: Ta-Chia-Shi Dual Railway Bridge
B3: Kan-Yuan Bridge	B14: Ta-Chia-Shi Freeway Bridge
B4: Heng-Shan Railway Bridge	B15: Wu-Shi Freeway Bridge
B5: Chu-Tung Railway Bridge	B16: Chung-Chang Bridge
B6: Chu-Lin Bridge	B17: Chung-Sha Freeway Bridge
B7: Chung-Cheng Bridge	B18: Tzu-Chiang Bridge
B8: Tou-Chien-Shi Freeway Bridge	B19: Wu-Hu-Liao Bridge
B9: Tou-Chien-Shi Railway Bridge	B20: Wu-Feng Bridge
B10: Tou-Chien-Shi Bridge	B21: Li-Kang Bridge
B11: Ta-An-Shi Freeway Bridge	B22: Li-Ling Bridge

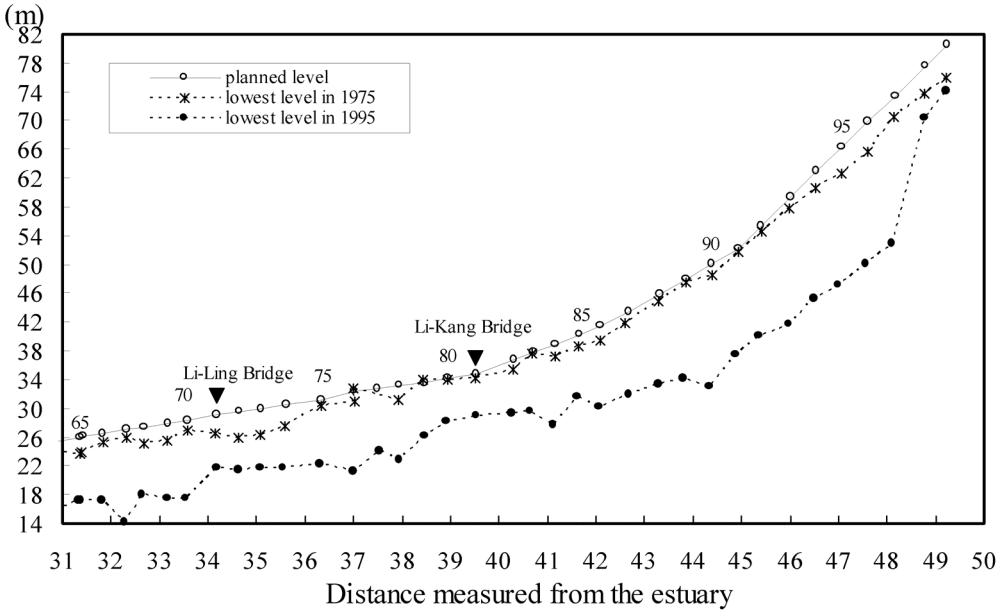

Fig. 1 - Variation of the river-bed level in a reach of Kao-Ping River

Fig. 2 - Serious exposure of the caissons of Ta-Shi Bridge

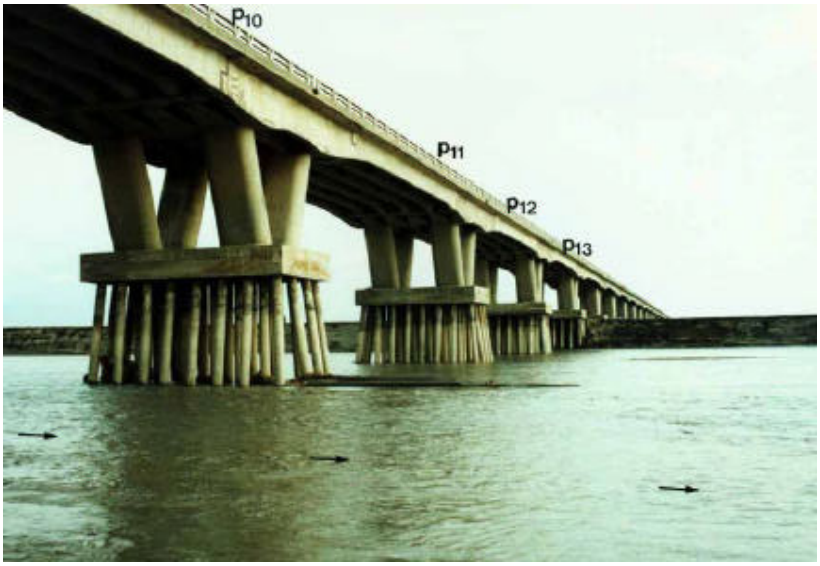

Fig. 3 - Serious exposure of the group piles of Tzu-Chiang Bridge

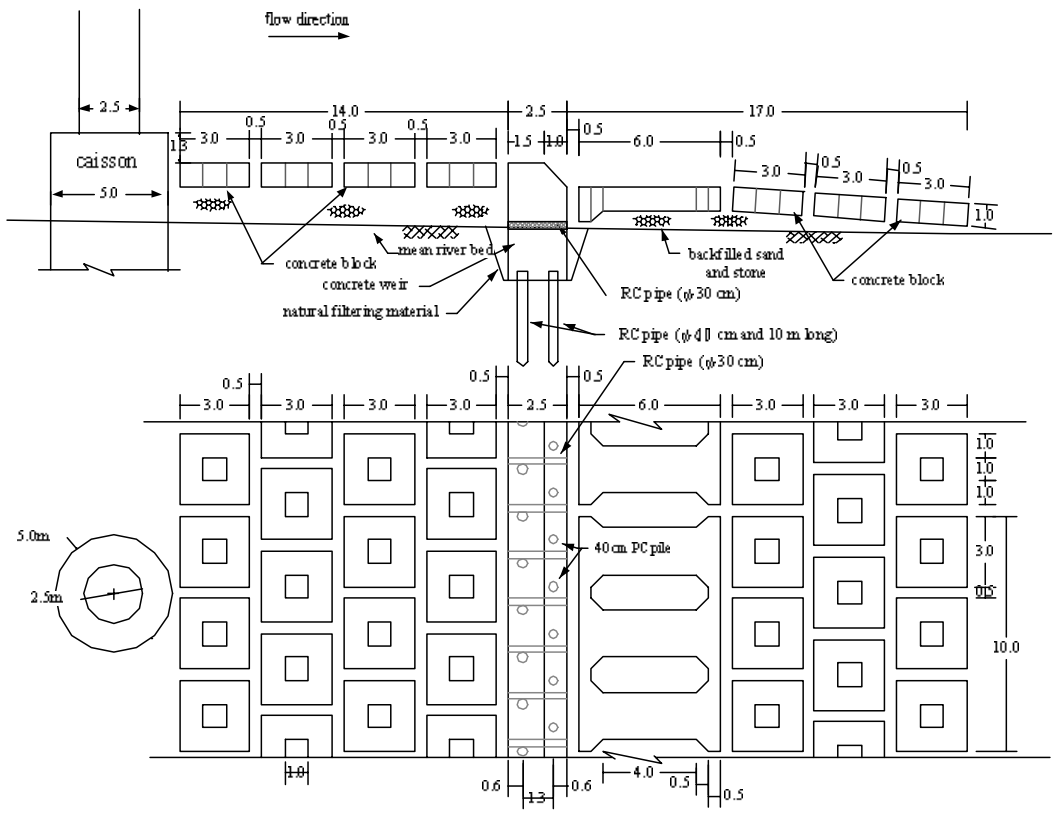

Fig. 4 - Layout of the bed protection works at downstream of Li-Ling Bridge

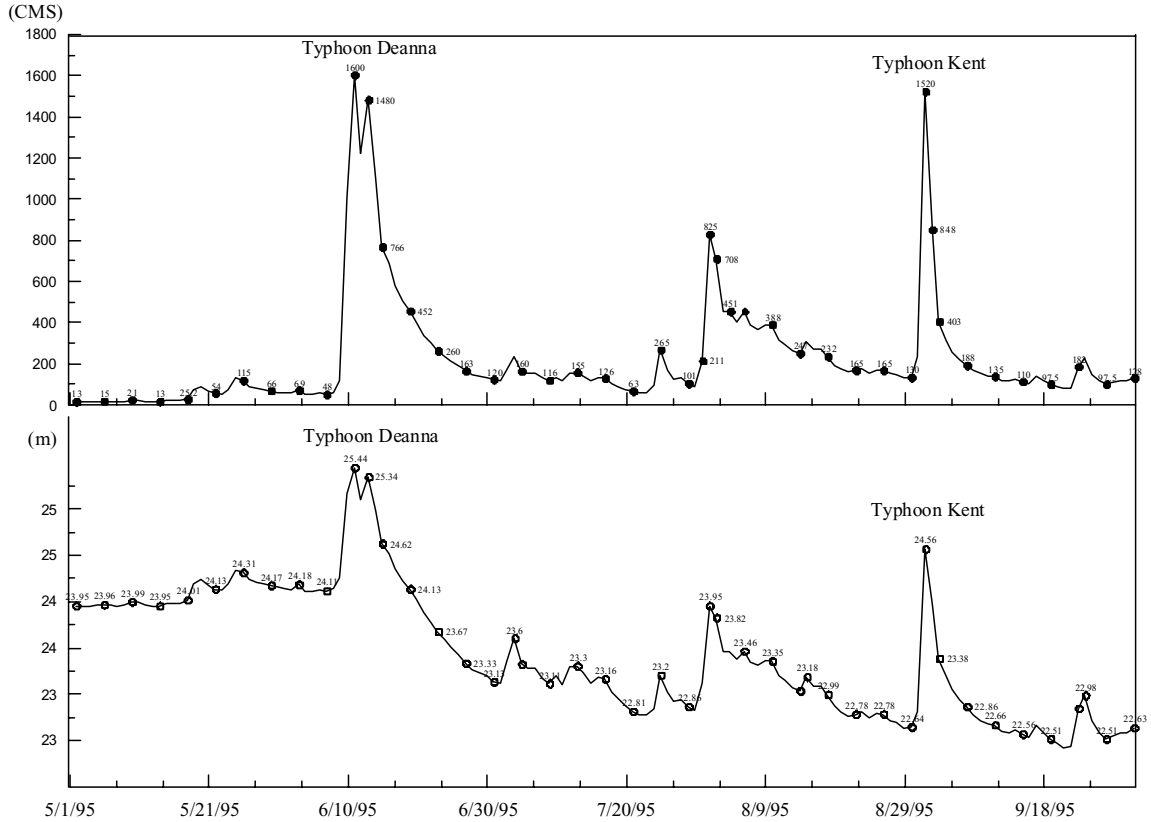

Fig. 6 - Histories of water level and discharge recorded at Li-Ling Bridge

Fig. 5 - Bed protection works were completely constructed.

Fig. 8 - Damage state of bed protection works after the first flood

Fig. 7 - The first flood flowing over bed protection works

Fig. 9 - Damage state of bed protection works after the passage of Typhoon Herb

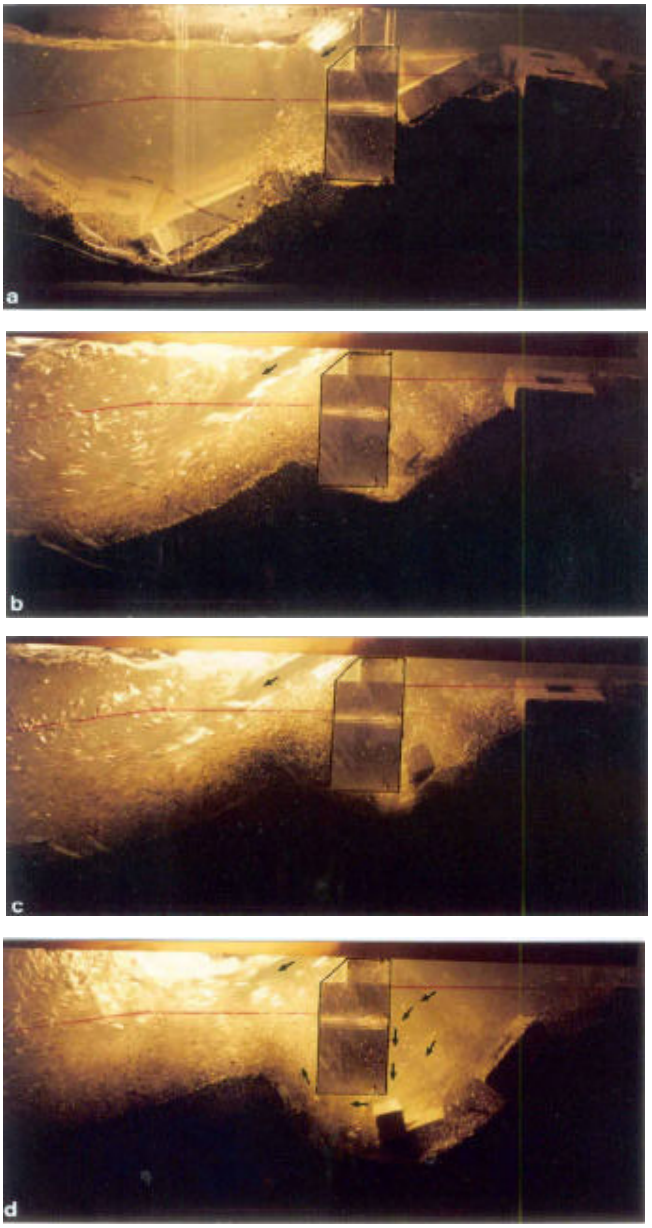

Fig. 10 - Scouring process visualized by hydraulic model experiment

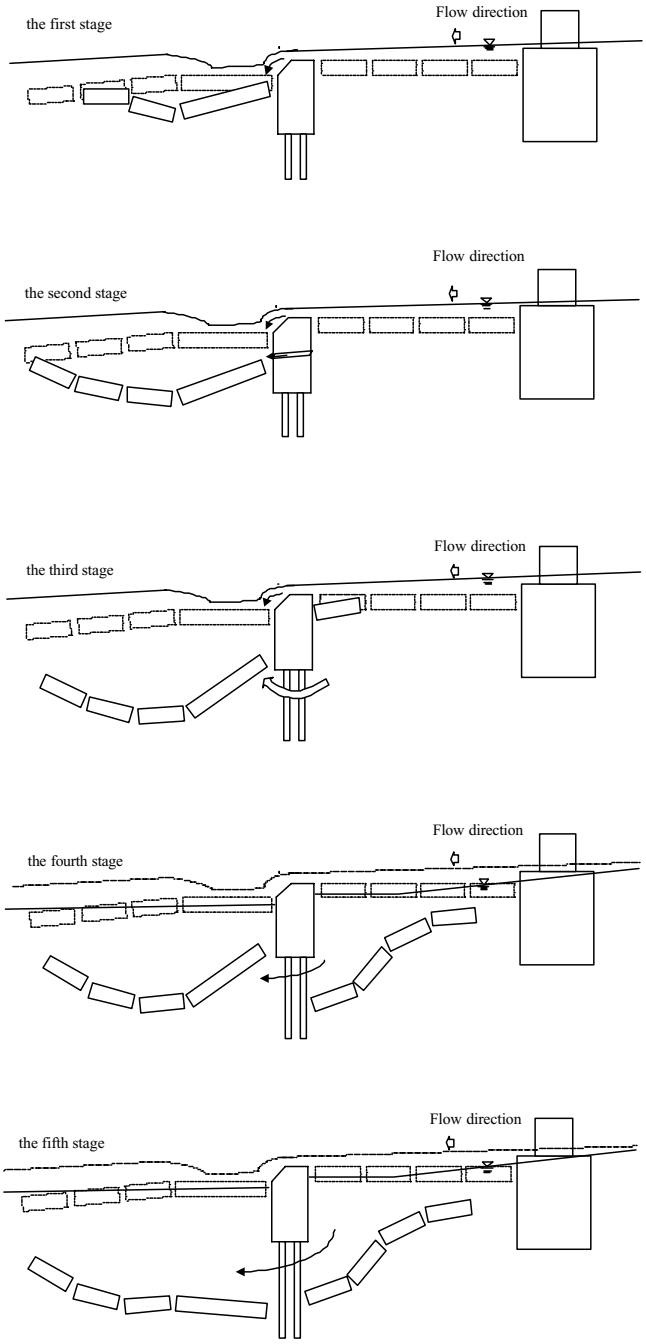

Fig. 11 - Damage process of bed protection works

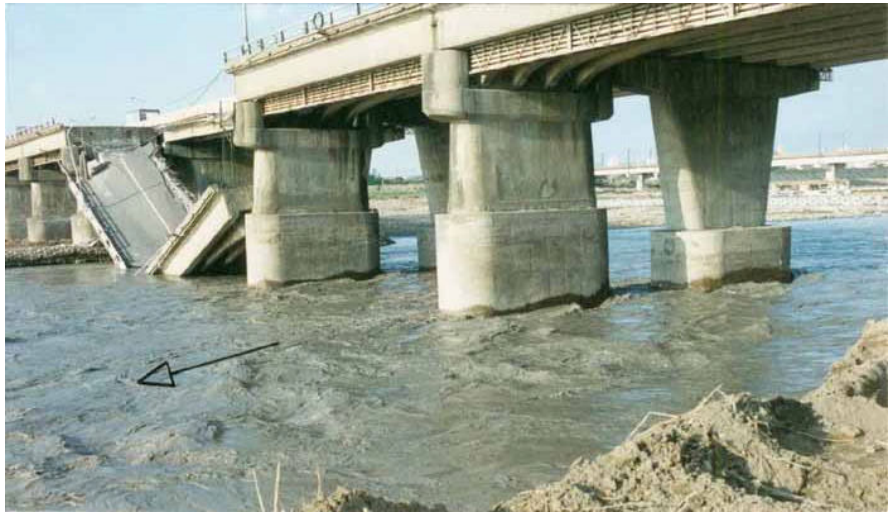

Fig. 12 - Failure of Tou-Chien-Shi Bridge

Fig. 14 - Failure of Li-Kang Bridge

Fig. 13 - Failure of Chu-Tung Railway Bridge

Fig. 15 - Failure of Kao-Ping Bridge

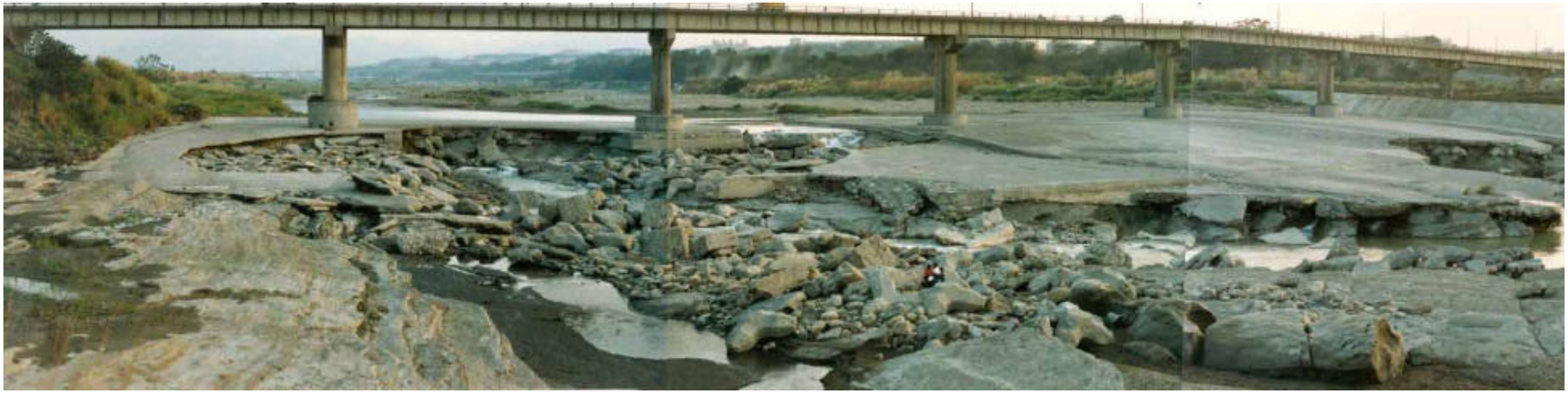

Fig. 16 - Damage of bed protection work at site of Chung-Cheng Bridge

Fig. 17 - Damage of bed protection work at downstream site of Shi-Luo Bridge

Fig. 18 - Damage of bed protection work at site of Shi-Jou Bridge

Fig. 19 - Damage of bed protection work at site of Ta-Chia-Shi Freeway Bridge

Fig. 20 - Damage of bed protection work at site of Wu-Feng Bridge

Table 1. Summary of causes for the damages of bridge and bed protection works

environmental condition	causes of damage	name of bridges										
		B1	B2	B3	B4	B5	B6	B7	B8	B9	B10	B11
bridge foundation	form (caisson or pile)	c	c	c	c	c	c	c	c,p	c	c	c,p
	size (m)				4.2	4.2	5.0	5.5	c:4.0	6.5	4.0	c:5.5
	local scour				○					○		
	insufficient penetration depth				○	○						
river (stream) characteristics	effect of mining of sand and stone on the lowering of river bed	●			○	●	●	●	○	○	○	●
	river meandering or flow curving			●			●					
	river bed material consisting of soft mudstone, shale, or sandstone	○						●				
	constriction at bridge site	○										
	construction of dam or weir at upstream reach	●	●	○								
	flow concentration or local deepening of channel	○		●	○	●	●	●	●	○	○	●
	channel shift or excavation of channel for guiding water flow during construction		○							●	●	
	steep slope of river bed at upstream and downstream of bridge site	○				●	●	●	●			●
	confluence of tributaries			○	○		●					○
	insufficient flow width	○		●	●	○	○					
bed protection works	type		T4	T2	T3	T4	T7	T6	T4	T4	T7	T4
	large elevation difference between top surface of works and river bed		●			●			●		●	●
	torrential flow attacks weak point or boundary		●	○	●	●				●	●	
	constriction scour					●						
	local scour							○				
	scour by free overfall		●			○		●	●	○		●
	head cutting		○					●	○			○
	insufficient flow width due to concrete or pile jacketing around pier				●							
	lateral (bank) erosion by secondary flow due to the existence of works		○		○			○		○	●	

Note: ●major cause ; ○minor cause

Table 1. Summary of causes for the damages of bridge and bed protection works (continued)

environmental condition	causes of damage	name of bridges										
		B12	B13	B14	B15	B16	B17	B18	B19	B20	B21	B22
bridge foundation	form (caisson or pile)	c	c	c,p	c,p	p	p	p	c	c	c,p	c
	size (m)		7.5	c:5.5	c:6.0	0.6	0.6	0.6			c:5.0	5.0
	local scour						○				●	○
	insufficient penetration depth										○	
river (stream) characteristics	effect of mining of sand and stone on the lowering of river bed			○	○	●	○	○			●	●
	river meandering or flow curving											
	river bed material consisting of soft mudstone, shale, or sandstone	○	○						●	●		
	constriction at bridge site											
	construction of dam or weir at upstream reach	●	○									
	flow concentration or local deepening of channel	●	●	●			●	●	●	●	●	
	channel shift or excavation of channel for guiding water flow during construction										○	○
	steep slope of river bed at upstream and downstream of bridge site	●	●	●			●		●	●	○	
	confluence of tributaries											
	insufficient flow width		○						○	○		
bed protection works	type	T3		T4	T4		T7	T5	T5	T5	T2	T7
	large elevation difference between top surface of works and river bed			○					●	●	●	
	torrential flow attacks weak point or boundary			○	○		○	○			○	○
	constriction scour			●			●	●				●
	local scour						●				○	○
	scour by free overfall			○			●	○	●	●	○	●
	head cutting			○			○		●	●		●
	insufficient flow width due to concrete or pile jacketing around pier											
	lateral (bank) erosion by secondary flow due to the existence of works						●	○			●	●

Note: ● major cause ; ○ minor cause

Damages of the Roads-Bridges by Erosion and Remedial Measures in Albania

Bozo, L, Geotechnics Section, Civil Faculty, Polytechnics University of Tirana, Albania

Muceku,Y., Department of Engineering Geology, Center of Tirana Civil Geology, Albania

Abstract

In this paper are shortly described the results of the geotechnics studies carried out last years concerning damages of roads-bridges by river erosion in Albania. The river erosion phenomenon nowadays in our country is become very dangerous, according to:

- The destroying of many engineering objects (roads, bridges) constructed on river banks.
- The loss of many square kilometers of agriculture area.
- The environment damage.

Here we have presented some particular cases of 2 roads and 3 bridges destroyed by above mentioned phenomenon, their remedial measures and causes of this phenomenon, as well.

1. **Introduction**

Albania is mountainous-hilly terrain, where 75% of whole area covered by mountains - hills and 25% by fields. There are many rivers and streams, which are very vehement about on 3/4 of their lengths. The erosion phenomenon by rivers water, currently in Albania is present. It's much favored by high amounts o precipitations, which are 2000-3000 mm/year (in some regions they are 100 mm/hour and 300 mm/24 hour) and by man-made activity, especially in plain area, as well as from climatic, seismic and geologic factors. The study of this phenomenon and the hazard evaluation for the protection and rational, as well as complex exploitation of the environment , is an important direction of geotecnics-engineering geology. It could also help for solving the problems of design and construction of different objects and their protections. On the basis of the study, some theoretical and practical remarks are obtained.

2. **Result and Discussion**

2.1 ***Peshkatari bridge***

Site characteristics

The bridge is located along Tirana-Elbasani national highway, over Erzeni River linking together capital Tirana with southern Albania (Elbasan-Librazhd- Korca-Pogradec towns), as well as corridor Nr-8 connecting Albania with Macedonia and Greece.

The site where the bridge was built comprises Quaternary loose deposits and Tortonian molasses. The Quaternary loose deposits makes up the first terrace of Erzeni River, as well as its bed. They are represented by middle to coarse grain gravels, 1/2 re-worked out made up mainly limestone and less sandstone filled by sands, silts and brown clays. They are not completely compressed and are water saturated. The thickness varies from 1.0m to 2.0m in the first terrace up to 6.0 – 7.0m in the river bed. The above rocks overlay Tortonian sandstone's of molasses, which built up also the Erzeni River's banks. The sandstone's rocks are massive, constituted mainly by quartz with scarce siltstone and argillite thin layers intercalations. The sandstone rocks are coarse grains with a thickness up to 1000m.

According to geomorphology the area is almost flat (first terrace) with westwards very gentle slopes bounded to the north with Mulleti's hills with an altitude 280m to 290m above sea level, and southwards of Petrela hills 500-600m above sea level.

The hills are undulated with (watersheds and valleys), which go downward towards the lowlands. The field is crossed by Erzeni River which have created an U-shaped valley 40-100m wide and 7.0 - 10m deep (Fig. NR. 1, Photo NR. 1), as well as, a lot of meanders along its East-West stream.

Bridge structure

The scheme of bridge comprises continuous beams with piers and massive shoulders, with shallow foundations supported on gravels (Fig. NR. 1, Photo NR. 1) up to 3,5m downdip. The bridge was built during 1935-1937 (c. 65 years old) and it is a two ways highway.

Rivers activity

The approximate surface of drainage basin, where is located the bridge is 292 km^2. During the most rainfall season (October-May) the average discharge is about 118m^3 /sec and maximal one, up to 170 m^3/sec, whereas the mean discharge/year is 8.6 m^3/sec.The suspended load is 68.4 kg/sec and 2150 $\cdot$ 10^3ton/year , as well as, the bed loads 430 $\cdot 10^3$ ton/year.

Table 1.

Grain size m/m	0,01	0,05	0,1	0,2	0,5	1,0	2,0	5,0	10	20	50	100
Suspended load (%)	65	89	97	99	99,5	100	-	-	-	-	-	-
Bed load (%)	17,5	39	60	78,5	82,5	85	88	90	92	96,5	99,5	100

Suspended and bed loads (%) moved by river waters is indicated at the Table Nr. 1. Both the velocity of the river's flowing, which is generally around 0.7m/sec and suspended and bed loads (gravel filled by sands, silts and clays with a relative density from 50% up to 70%) has caused an average erosion of its bed about 1m, it does mean that the river erodes its bed about 1,5 cm/year. The bridge foundation basement consist of gravels with a bearing capacity from 350 KPa up to 400 KPa, that means it stands very good the loads, that comes from construction and river water pressure.

Man-made activity

After 1990 year, when the country has passed from a centralized economy (totalitarian regime) to free and open economy, nobody has taken care from the environment protection for a long time. In these conditions, when the due legislation lacked, Albania has suffered so much from ill treatment of environment, giving rise hazard besides the natural ones.

So, in constructions field especially for capital of Tirana, the great needs for the first inert materials as sands and gravels led to intensive exploitation along of Erzeni river bed . In some parts of river bed, even near by bridge foundation, the bedrock is outcropping lowering 3m up to 5m the base level of the river bed. In this case is artificially increased erosions activity of rivers water from 1,5 cm/year (normal condition) up to 8-10 cm/year.

Damages and causes

From a period of 60 year old of erosions activity, on 1990 year the foundation depth was 2,5m downdip. Whereas, the last ten years the erosion caused by man-made activity discover about 1.0 m of bridge foundation. So, during a rainfall storm (1999 year) the river water discharges (great flowing) was very much increased and in consequence a intensive erosion on river bed occurred, which caused a sinking from 1,98m one of bridge pier (foundation) (Fig. NR. 1, Photo NR. 1, 2,). Also from above phenomenon, is break down the central part of bridge and it is bent, as well as along of it are created many cracks enabled the destruction of it and put out of use (Fig. NR. 1, Photo NR. 1).

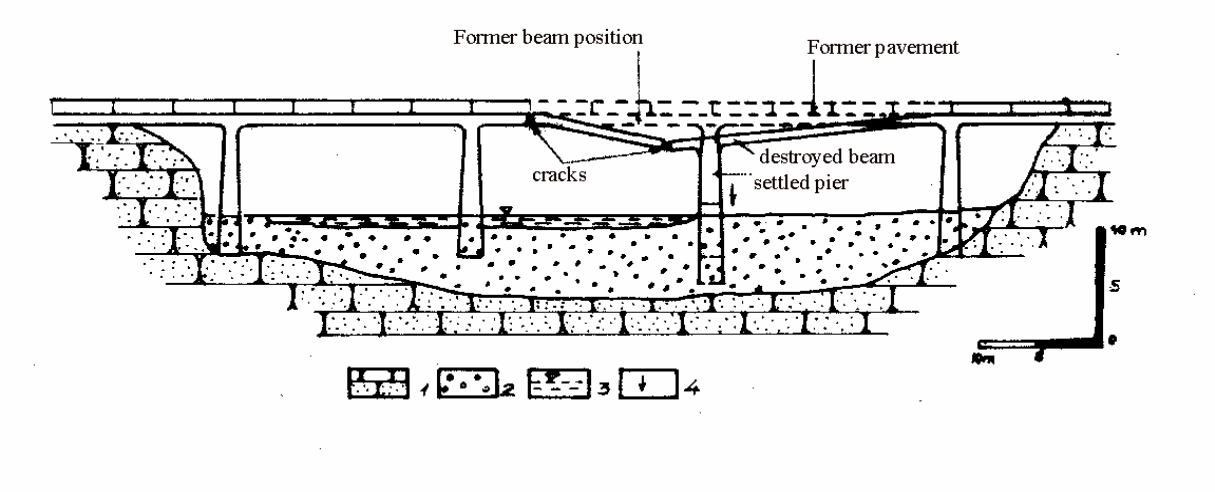

Fig. 1 Cross section of Peshkatari bridge
1. Sandstones, 2. Alluvial deposits, gravels, sands, silts and clays, 3. River water level, 4. Sinking direction

Photo nr. 1. Peshkatari bridge. It's looking to east, and shows, cracks, destroyed beam and a sinking of pier.

Photo nr. 2. Peshkatari bridge. It's looking to south, and shows, the new bridge and the destroyed bridge (right side) which is sunken 1.98 m compared with the new bridge.

Fast remedial measures for provisional use

For a quick connection of this very important highway for Albanian economy, were taken as following engineering measures:

- Grouting with pile against other movements.
- Covering with concrete for reinforcement of damage foundation.
- Covering with stores blacks (gabion).
- Stopping of exploitation of raw material on river bed.
- Construction of provisional metallic bridge over existent one.

Remedial works for highways normal function

- Construction a new bridge with three ways highway.
- Static scheme -system beam column.
- Foundation with molded piles with 1m diameter and support on sandstone's rocks.
- Piers with concrete column.

2.2 ***Mifoli bridge***

Site characteristics

The bridge (older one) links capital of Tirana and several towns of northern and central parts with south-western part of Albania (Vlora, Saranda and Gjirokastra towns). It's constructed over Vjosa River very close its delta. The studied area is built up by alluvium Quaternary loose deposits as silts with thin fine sands layer intercalation (40m thick) and gravels, which are covered by first one.

Bridge structure

It has a combined structure, concrete arch with metallic beams. The foundations are made by metallic piles in tubular shape (Photo NR 3).

River activity

The drainage basin surface of Vjosa River, over which is constructed Mifoli bridge is 6680 Km^2 and its mean altitude above sea level is 858m. The suspended and bed load of this river is 190kg/sec and $5.99 \cdot 10^6$ /year.

Damages and causes

The interaction of seismic vibrations (sands liquefaction) and rivers erosion activity phenomena enabled discovering of bridge foundation (earthquakes of 1967 and 1969

Photo nr. 3. Mifoli bridge. It's looking to north-east, and shows, its structure

Photo nr. 4. Mifoli bridge. It's looking to north, and shows, the sinking of its pier

years), from which a bridge sinking occurred (Photo NR. 4), and simultaneously a horizontal movement on one of its shoulder is done.

Consequences : It is out of use.

Remedial works for highways normal function

Construction of new bridge for the highway and railway purpose with molded pile foundation (38-42m length and 0,8-2m diameter) supported on gravel deposits.

2.3 ***Kallmeti's bridge***

Site characteristics

It's located on Lezha-Shkodra road (old), over one of Drini river branch (Gjon Zefi Stream).

Concerning the geology in the studied area are recognized two major groups of rocks (Fig. NR. 2):

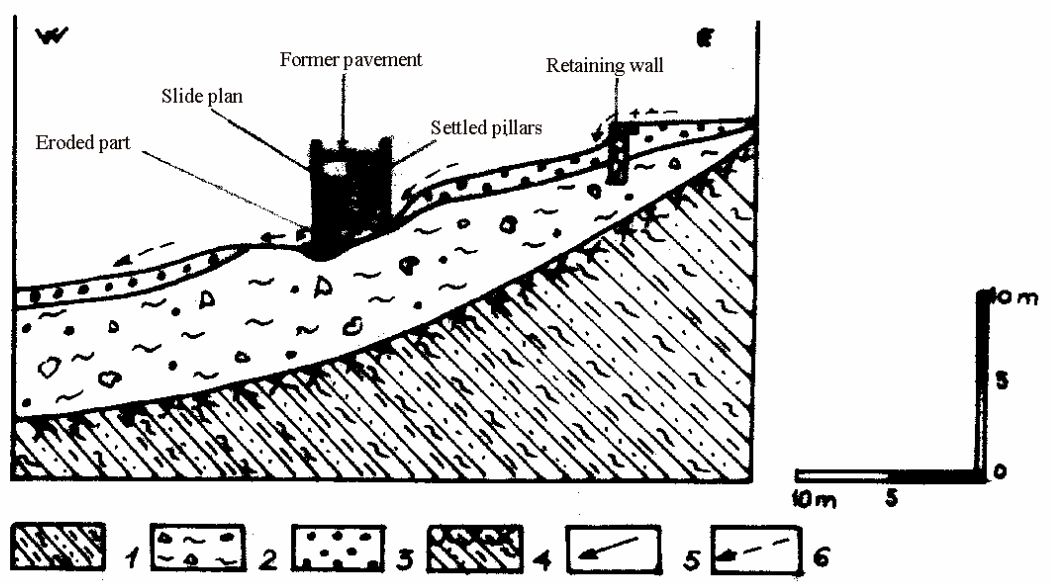

Fig. 2 Cross section of Kallmeti bridge
1. Flysch, 2. Alluvial deposits, clays, sands, gravels, and cobbles, 3. Alluvial deposits, gravels and cobbles, 4. Weathering crust of flysch rocks, 5. eroded soil movement direction, 6. Stream water flow direction

- Quaternary loose deposits comprises proluvium-first terrace and beds deposits of Gjon Zefi stream. The first one consist of silts with 30-35% with the limestones and

sandstones rubble-stones content, that have dimension ranging from 0,05m up to 0,5m. On west bridge they have e fan shape (10-15m thick), whereas on east they lying along stream valley (1-2 m thick). The beds deposits consist of gravels and less stones filled by sands, silts and clays. They have a thickness varies from 0,5 up to 1,5m .

- Oligocene flysch deposits comprises by thin intercalated layers of claystones, siltstones and sandstones, which have a dip angle 40-45^0 on east direction. They overlain by proluvium deposits.

According to morphology the Gjon Zefi stream valley have a 'V' Shape, with steep banks slope and 4-12m wide and 5-6m deep.

Bridge structure

It's a bridge with cement stone masonry pillars (length L=8m) and concrete armored beam. This bridge is about 70 year old (Fig. NR. 2, Photo NR. 5, 6).

Damages and causes

Several factors took part in damaged of bridge, which are as following:

- During 1992,1994,1996 and 1998 year, as results of high quantities of precipitation and without protective measures getting in due time, on stream bed occurred a intensive erosion like a gully, which was extremely rapid. The stream bed erosion from 1992 year up to nowadays is about 1.8m, and below of bridge foundations was created a cavity with 1.4 diameter, as result of it, the bridge foundations has moved downwards (Fig. NR. 2, Photo NR.5, 6).

- The dynamic loads actions induced by motor-car traffic, when in the bridge were appeared a lot of cracks.

Photo nr. 5. Kallmeti bridge. It's looking to north, and shows, the sinking of its pillars and pavement

Photo nr. 6. Kallmeti bridge. It shows cracks of pillars from erosion phenomenon

Consequences

The bridge foundation moved 1,4m (Fig. NR. 2, photo NR. 7, 8) downward and simultaneously it is associated a horizontal movement, where several failures occurred on bridge pillars walls.

Recommendation for remedial measures

- Construction of weirs and groynes.
- Reinforcement of bridge foundation by its grouting.
- Filling of cavity by durable and less deformation materials.
- Construction a new bridge.

2.4 ***Bogova landslide***

It is located on eastern part of Albania along Berati-Corovoda road, on right side of Osumi River valley. On this landslide is constructed above mentioned road, which is affected by this phenomenon. The river valley slope, where the landslide occurred (photo NR. 9), built up by flysch rocks (much weathered) with dip angle 50-60^0 in the same direction with the valley slope inclination, favoring it. Also on bottom of valley slope, flow the Osumi River waters, which continuously contribute to the erosion process, that is one of main factor of landslides creation. The landslide is moving slowly downwards through the valley slope to river bed (Photo 7), together with 200 m of road constructed over its body.

Photo nr. 7. Bogova landslide. It's looking to east, and shows, a destroyed retaining wall (deformed) by mass movement

A lot of factors influenced to mass movement on the studied area, are as following:

- The velocity of river water flow, which is from 0.4m/sec (summer) up to 1.29 m/sec (winter) and its discharge 49.7m^3 /sec together with its suspends and bed loads that are 17.4 kg/sec, operate on the outer bank, causing erosion of it.

- The river banks are built up by flysch rocks are much weathered.

- There is poorly drained. One drained ditch (constructed 20 year ago) for collected of surface water coming from rainfall or other sources was buried. So, much water running throughout, along and cross of the road, as well as down the bank slope of Osumi River. The other water quantities infiltrate and seep in small cracks of weathered flysch rocks. From high value of hydraulic gradient are created many new cracks. The natural gradient value exceed the critic gradient value. Therefore, in this case we have the mechanics suffusion development, where small cracks are become wider and deeper, which have helped landslide development.

- The cutting of many trees on this are during last 10 years is an other factor.

- In the studied area, there are many water springs, and high rain falls, that favored degradation of bank slope of Osumi

Remedial works

For improving of general stability conditions of Bogova landslide have to make engineering measures :

- Construction of weir and groynes.

- Improving of general stability condition by installing a drainage system (2 ditches) to collect surface runoff, which reduce seepage and infiltration in the soil and this exert a positive influence on the main factor of slope stability.

- The stability of landslide by molded piles.

- Planting of trees.

- Construction of retaining wall with drainage system.

- The slope protection by using of gabions or geotextile against surface erosion.

- Protection interior erosion (systematize of two streams close of landslide.

2.5 ***Shkopeti landslide***

Site characteristics

It's located on north-eastern part of Albania along national road linking the Miloti and Burreli towns. This road is constructed on banks of Mati River valley and it is affected by landslide phenomenon. The studied area represents a narrow and deep valley (Mati

River) formed a “V” shape have a slope inclination from 25-35^0 up to 60-80^0 and it is built up by loose Quaternary deposits (deluvium and alluvium) and by melange deposits(Fig. NR. 3, photo NR. 8),. Deluvium consist of rubbles up to stones filled by silts. They have a thickness from 1-2m (upper parts of valley slope) up to 10-12m (down valley slopes). These deposits are situated unconformity over melange deposits. Alluvium deposits are situated along Mati River bed and consist of sands ands gravels, whereas the melange deposits are compassed bay rubbles-stones and pebbles cemented by argillaceous material. They on surface are weathered 0,5m up to 2-3m.

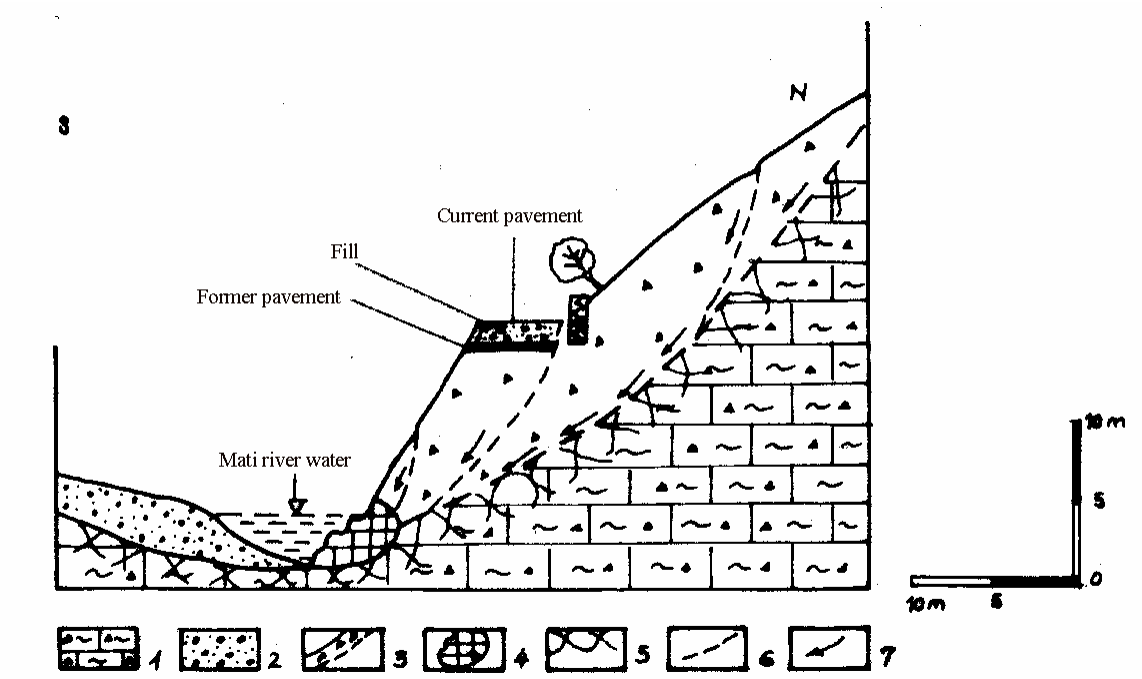

Fig. 3 Cross section of Shkopeti landslide
1. Melange deposits, 2. Alluvial deposits, sands, gravels, 3. Landslide body, 4. Erosional part, 5.Weathering crust of mélange deposits, 6. Slide plain, 7. Slide direction

Photo nr. 8. Shkopeti landslide. It’s looking to north-east, and shows, the movement of Miloti-Burreli road filled by gravels and landslide body

Analysis of phenomenom.

As result of lateral erosion on right side of lower part of Mati River bank slope on which is constructed the road Milot-Burreli, a landslide has occurred. It is 250-300 long, 300-350 wide and 5-10m deep.

One of main factors in the active of landslides is the impact of changing ground water conditions as result of rainfall. By investigation carried out in the area, results that, during high rainfall periods, the river water discharge are much increased, which associated with intensive of bank erosion where the landslide re-initiating going downwards (after 1990 it's moved downward 2.0m).

Landslide has occurred on the boundary between of the loose Quaternary deposits (deluvions) and the melange deposits. As indicated in Fig. the landslide is developed on a steep slope and it is moving on steep slide plain. For that reason favored and from high quantities of rainfall, which infiltrate in slide plain and from bank toe erosion of river water, it begin slowly moving downwards up to reaching of a stationary equilibrium but with possibility to be reactivated from the changing of the environment conditions.

Remedial Measures

The stability of landslide can be done in 2 ways:

a. Construction of concrete wall, which have to support on melange rocks.

b. If the first one is impossible to done, then for stability of landslide needs to construct:

- Two ditches for collect surface runoff, just there where seep and infiltrate in slide plain.
- Construction a new retaining wall with drainage system on upper part of road.
- The protection of the road lower part of the bank slope by using of gabion or geotextile against surface erosion.

3. **Conclusion**

- The damages of the roads and bridges due to rivers erosion activity is a present and continual phenomenon in Albania.
- Analysis of erosion phenomenon is complex, because of in damages of engineering objects from erosion of rivers waters have taken place a lot of factors.
- Engineering measures for stability of situation, created by the above phenomenon are complex, as well. Generally, the solution of this problem, can be done from a specialists team.

4. **References**

Bozo, L., Technics of foundation (part I) 1987, Faculty of Civil Engineering, Polytechnic University of Tirana, 413 pp., (in Albanian).

Bozo, L., Technics of foundation (part II) 1987, Faculty of Civil Engineering, Polytechnic University of Tirana, 172 pp., (in Albanian).

Bozo, L., Geotechnics, 1995, Faculty of Civil Engineering, Polytechnic University of Tirana (Pp. 261) (in Albanian).

Bozo, L., Behaviour of basement and foundation under seismic actions, 1988 Thesis of Ph. D., Polytechnic University of Tirana, 226 pp., (in Albanian).

Muceku, Y., Slope movement and road risk avaluation in Shkopeti valley, Albania. 8th Congress of Albanian Geosciences 2000, abstracts book, p.213.

Muceku, Y., Engineering geological mapping for urban planning and regional development in Tirana region. Geological Survey of Albania, 2001, 38 pp. (in Albanian).

Saraçi, R., Rrjedhja e ngurtë e lumenjve të Shqipërisë dhe problemet e erozionit ujor, 1990. Water as a national asset. The research and management of water resources of Albania. National Scientific Conference, Tirana 1 – 2 October.

Bridge Pier Scour in Bouldery Bed – Indian Scenario

Raman Singh, VSM, KK Razdan & RK Dhiman

Synopsis

Bouldery bed basically consists of bed material of heterogeneous size and shape and does not form a uniform bed stratification. Infact the scour around bridge pier is governed by the bed material around its vicinity. Extreme care should be exercised to establish foundation at sufficient depth to prevent undermining at its foundation. Stability and economy of bridge pier is assessed based on the degree of certainty with which scour is assessed. Estimation of scour on bridge pier located in bouldery bed had been a challenge for bridge engineers. Construction of these foundations led to a time and cost overrun. Since there is no empirical/rational formula available in literature efforts have been made to collect the data of bridges already made on bouldery bed and their behaviour has been observed for longer period. Based on data collection, statistical approach has been applied after duly considering the factor of safety. In the proposed formula efforts have been made to co-relate the scour with velocity in the cross section of the river. Infact velocity when taken after calculation with "manning formula" takes into account all the characteristic of the X-section. Bouldery bed pier scour pattern based on the observation, present practice being followed and proposed formula have been discussed in this paper.

1. INTRODUCTION

A major factor, which governed the stability of bridge foundation, is scouring of river bed at its vicinity. Extreme care should be exercised to establish foundations at sufficient depths to prevent its undermining. Stability and economy of bridge foundations depend upon the degree of certainty with which the scour level is assessed. Estimation of scour level and foundation depth in rivers having bouldery beds poses a real challenge to the bridge engineers as no method presently appears to be available for prediction of scour in such cases. Such uncertainty often leads, to, not only uneconomical bridge designs but also to uneconomical river training works and counter measures. In India, we have large number of bridges across rivers having bouldery bed. In the absence of a rational formula, the present tendency is to apply the same formula as applicable for alluvial bed with a judicious choice of values for the silt factor and unit discharge. The result so obtained is compared with past experience before fixing up a value. This is not a very satisfactory solution especially for situations where bridges are to be built on new alignments. For working out the scour depth, consideration has to be given to general scour, local scour, lateral channel, migration and degradation. Proper method for soil investigation of bouldery strata is also an important factor for finalisation of foundation level. Final approval of foundation level in such strata generally led to delayed completion. Efforts have been made a efforts to derive a reliable and practicable formula for finalising the maximum scour based on expertise gained by the team of engineers after having executed number of bridges on bouldery bed.

*Chief Engineer (Bridges), ** Superintending Engineer (Brs) & *** Executive Engineer (Brs)
SEEMA SADAK BHAWAN, Ring Road, Delhi Cantt, New Delhi-110010
Email : d_himan12@yzhoo.com

2. WHAT IS SCOUR

Scour is the hole left behind when sediment is carried away from the bottom of a river. Although scour may occur at any time, scour action is especially strong during floods. Swiftly flowing water has more energy than calm water to lift and carry sediment to down stream.

Three types of scour affect bridges :-

(a) Local scour is removal of sediment from around bridge piers or abutments. (Piers are the pillars supporting a bridge. Abutments are the supports at each end of a bridge). Water flowing past a pier or abutment may form holes in the sediment; these holes are known as scour holes.

(b) Contraction scour is the removal of sediment from the bottom and sides of the river. Contraction scour is caused by an increase in speed of the water as it moves through a bridge opening that is narrower than the natural river channel.

(c) Degradational scour is the general removal of sediment from the river bottom by the flow of the river. This sediment removal and resultant lowering of the river bottom is a natural process, but may remove large amounts of sediment over time.

3. SCOUR AN OVERVIEW

The design and construction of foundation of bridges is linked to realistic assessment of scour depth, both global and local. The foundations are generally designed to withstand the loads and moments transmitted by the other components of the bridge. They are also designed to have a minimum grip length below the deepest scour level, which is usually calculated based on various parameters. The surest way of assessing the depth of scour in a river is to observe the same during the highest flood period. Unfortunately with the methods available in the country it has not been possible to approach the intended pier location during high floods and observe the deepest scour. Thus the Design Engineer generally relies on the use of formulae for calculation of scour depth. While the various available formulae have been known to give reasonable results in respect of sandy strata, the results have been erratic in other cases. Moreover the various formulae have been originally evolved based on the study and observation of particular types of strata, soil classification and water flow regime.

Over the years there has been a increasing tendency to apply the same formulae for other types of harder strata including conglomerates, large boulders and soft rock. This has resulted in skewing of results and totally unrealistic scour value in extreme cases. While fortunately in India there has not been many cases of failure of foundations due to scour, a large number of bridges are required to have their foundations taken deeper than necessary due to the above referred approach. The consequences to this, the time overruns in many cases have been more than double with corresponding cost overruns. In a number of well foundations, steinings have been damaged due to extensive blasting necessitating extensive repairs. In a few cases the wells had to be rejected because of extensive damages. The situation is acute while dealing with conglomerate strata, particularly encountered in the rivers flowing through the foothills of Himalayas. The substrata of interest to foundation engineering may consist of boulders, shingle, gravel etc. either in loose form or cemented by a matrix, which may be calcareous in nature. Such heterogeneous combination of materials with individual particle size upto two or three meters does not easily lend itself to any logical

assessment or interpretation of scour using available tools. Substantial reliance needs to be placed on observation of behavior of structures built in the past coupled with reasoned judgement of the decision makers in each individual case. Similar situations may also arise in other parts of the country as well. Conglomerate strata are know to have been encountered in the plains in various locations leading to dilemma in the matter of proper assessment of scour.

At the outfall end of the river, the tidal effect needs to be considered. Here fine suspended sediment deposits are common. The deposition process as well as scour if any is also affected by changes in the density of water due to salinity. If these aspects are not considered, scour depth is generally assessed on conservative basis, resulting in wasteful design. Some of the rivers flowing through arid regions e.g. in Rajasthan at the down stream end just disappear, losing the water by percolation and evaporation. In such cases, the assessment of scour needs entirely different perspective. The South Indian peninsula is geologically more stable. The bed and banks of the river are generally highly resistant to erosion. The tendency for a gradation or degradation is insignificant.With such a diverse scenario concerning the characteristics of rivers flowing through the different parts of the country, it is no wonder that diverse problems are being faced by the Engineers. This is further compounded by the use of single formulae (Lacey) for almost all situations.

4. BRIDGE PIER SCOUR

Scour is the erosive action of water in excavation and carrying away material from the channel bed. An obstruction such as a bridge pier causes interference in the flow of stream, which changes the flow pattern at obstruction. These results in deepening the scour hole around the bridge pier beyond the level that would naturally occur from degradation and general scour. This is commonly termed as local scour. The flow around the bridge pier is complex. As the stream flow approaches the pier, adverse gradient caused by the pier, drives a portion of the approach flow downwards the just ahead of the pier. **A change in the downward flow, velocity has a direct effect on the rate of scour and thus on the depth of scour hole**.

4.1 **Local Scour** : Local scour is the local lowering of the bed in the near vicinity of a hydraulic structure such as bridge pier, spur, guide bund etc. Bridge pier locally distorts the flow pattern by increasing local velocities or by inducing whirls, eddies and vortices etc. which results in increased sediment transporting capacity of the channel. The bed particles are lifted up and carried away with the current. This process continues till the normal transporting capacity of the channel is restored. This stage of dynamic equilibrium may also be achieved when the armouring of the bed reaches a limit. Where upper particles of the bed can no more be dislodged by the stream action, further development of scour ceases. The finally attained scour depth is known as maximum or limiting scour. The phenomena of local scour is very complex due to large variations in the field conditions, besides numerous variables describing the flow, fluid and sediment characteristics, the channel and the pier geometry etc., which have their own effects on this phenomena. The efforts made by designers and research scholars in this regard are broadly classified as below :-

(a) Use of empirical formulae for estimation of scour depth.

(b) Laboratory investigations by research scholars to gain insight into the mechanism of scour around a bridge pier, the various parameters entering into the problem and their effects and estimate scour depth in terms of known variables such as depth of flow, velocity, grain size, geometry of the pier and other variables.

(c) Prototype observations of scour with a view to investigate model prototype conformity and place the conclusions from laboratory studies on scour basis.

5. INDIAN PRACTICE FOR DETERMINATION OF MAXIMUM SCOUR AROUND PIERS

(a) The theoretical method recommended is to estimate maximum scour depth as per Indian Road Congress: 78:2000.

below H.F.L. as '2_{dsm}'
Where 'dsm' is normal scour depth below the HFL
$dsm = 1.34 (Db^2 /f)^?$

Where Db= intensity of discharge in cumecs per metre width and shall be the maximum of the following:-

(i) The total discharge divided by the effective linear waterway between abutments or guide bunds:

(ii) The value obtained taking into account any concentration of flow through a portion of the waterway assessed from the study of the cross section of the river.

(iii) Actual observation, if any.

Silt factor given by the expression
$f = 1.76v\ m$

Where 'm' is the weighted diameter of the bed material in millimeter's.

Further IRC recommended that if a river is flashy in nature and the bed does not lend itself readily to the scouring effect of floods, the method given above for calculating maximum depth of scour shall be assessed from actual observations. However for bouldery bed there is no rational or empirical formulae available for use.

6 BED MATERIAL CHARACTERISTIC OF BOULDERY BED AND INTER RELATED FACTOR FOR SCOUR

The size of the channel material is important at low velocity, the scour depth is less for a bigger size boulder since it is difficult for slow moving water to pick up and carry the larger size. Equally important is the uniform sediments, the smaller size materials are carried away and large size remains. This may eventually result in an armoured bed within the scour hole, slowing or stopping of erosion process until higher velocity scores the armored layer. Soil strata generally available in bouldery bed is indicated in Fig. (1).

Various interrelated important parameters, which affect the type and depth of foundation are type of strata, design discharge, silt factor and formulae for scour depth calculations are discussed are as under:-

(a) **Type of Strata** : Erodible/nonerodable beds leads to adopting foundation based on scour/non scour criteria and also an entirely different philosophy in planning

and designing of bridge foundation. The aspects of weathered/fissured rocks further add to the uncertainty in branching out to the two approaches described above. In addition to the type of strata encountered during the actual execution of bridge during the actual execution of bridge foundation is invariably at variance from the one catered during the planning process. Thus owing to partially/entirely different strata at the execution stage at time necessitates in redoing the entire SSI, and/or also adopting an entirely different type of foundation on the other extreme besides causing exceptional delay in order to ensure safety of structure. On the moderate site it tantamounts to raising/lowering the foundations, the effect of which however becomes quite substantial incase there is a significant raising/lowering of the founding levels.

(b) **Design Discharge** : The design discharge for the foundation design is done based on various empirical/rational formulae evolved quite some time back. The applicability of these formulae is best suited for rivers flowing in the plains. It is seen from experience that these empirical relations are not entirely dependable/reliable in estimation of discharge for hilly regions of the Himalayas and NorthEastern Region. Invariably this leads to an enigma regarding this vital parameter leading to a doubt regarding the safety of foundation at a later date.

(c) **Silt Factor** : Silt factor plays a significant role in finalising the scour depth and also the founding levels for the foundation of the bridge structures. Due to lack of adequate borehole data and also various uncertainties associated, the bridge engineers are confronted with a difficult job of choosing an appropriate value of silt factor. This has importance because IRC Code caters for a maximum silt factor of upto 2.42 (Applicable for heavy sand) only. Though IS 7784(Pt-I) gives a increase beyond the range of 2.42 is in discrete jumps of 4.75, 9, 12, 15 & 24 rather than a continuous spectra. Since the silt factor has a significant role to play in finalising foundation depths. However in absence/identification of correct silt factor for boulderly bed there is a problem where in the selection of this important parameter is left to the judgement, discretion and experience of the designer. Also result obtained by the above formulae for bouldery bed are erratic and impracticable.

(d) **Formulae for scour depth**: In addition to the various unknown parameters and uncertainties mentioned above the problem assumes a bigger dimension because of lack of appropriate formulae for finalising the scour depths. Various reasons connected with it are enumerated as under :-

(i) The type of strata/bed ie erodiblity or nonerodibility has a direct impact on deciding whether to finalise a foundation based on scour/non scour criteria, and also to decide whether an open foundation would suffice, or a deep foundation would have to be catered for. It would be in order to state that this significant difference/in adopting different philosophies and depth of two types of foundations have direct impact on the economic of the structure.

(ii) Scour depth calculation significantly depends on the design discharge to be adopted for foundation design. Since the formulae for design discharge are by themselves not applicable, the reliability of scour depth calculations is thus questionable.

(iii) The applicability of these formulae for rivers in hilly region with bouldery beds is debatable and quite often disputed since they have an origin

from alluvial/quasi alluvial streams. This aspect has also been highlighted in clause 703.2.5 IRC 78: 2000.

(iv) IRC 78 : 2000 also clearly states that these formulae are not applicable to rivers with flashy nature.

(v) A close scrutiny of the formulae indicates that the uncertainties associated with the selection of strata, design discharge and silt factor as pointed out above gets further substantiated for various anomalies in the adoption of these formulae for various reasons stated in para ibid.

(vi) Structures designed for scour consideration on the basis of above formulae had led to unnecessary time and cost over the particular job.

(e) In addition to above there are other factor such as whether the flow is clear on it carriers sediments, depth of flow angle of indication of pier, opening ratio on scour depth.

7. PRESENT PRACTICE FOR BOULDERY BED SCOUR

A scour depth in channel is not following regime condition as in the case of sandy soil. Now keeping in view the size of bed material and bank conditions the scour of even each pier can be different in case of longer span on a same x-section of river having defined flow pattern for years together. Accordingly, based on the observation, different foundation has been placed at different RLs in same bridge based on the cross section features. Necessary review of the final foundation level should be made based on the construction problems, toughness of strata and revision of soil parameters subsequent to re-examination of the same. However the sound Engineering practice should be the main aim while reconsideration for review of level if any. Less scourable strata has been considered as engineering friendly and revision has been carried out keeping in view the safety requirement. Bouldery bed generally consists of soil strata comprises of bed material of predominantly of size 300 mm above and remaining material is soil-sand-gravel-matrix. This material is basically in quite disorderly placed in natural bed available for siting the bridge. Normally in case of such bed, the site data is investigated before construction in the form of bore log data. Also the strata actually encountered is generally compared to know engineering properties of the material for finalising the foundation level and review can be done wherever required considering engineering requirements.

8. ASSUMPTIONS FOR BOULDERY BED SCOUR

Data of existing bridges where there had been flash floods in past during the service life of bridges was taken into consideration. It has been observed that bridges have behaved well. In case of bridges there has been lateral cutting of bed instead of vertical cutting indicating that there is less scour around pier than the lateral cutting. In fact this is due to armoured bed around the pier. Also the results of model study of various bridge structures were also studied which have been constructed on bouldery bed. There is also a relationship between velocity and maximum scour anticipated before construction of bridges was reviewed (Fig. 2)

Based on the data collected a basic assumption has been made as per following:-

(i) Flow pattern in bouldery bed is turbulent unsteady and nonuniform.

(ii) Scour observation is site specific.

(iii) Scour depth is a function of area of cross section (A), bed slope (S), rugosity cofficient (N) which in turn depend upon the total discharge per meter length of the X-section.

(iv) Flow pattern in bouldery bed takes a sudden turn and rapid. There is frequent gain and dissipation of specific energy. Scour depth at a particular section is not a continuous function of time.

(v) A soil stratum in the riverbed is predominantly boulders of size 300 m dia and above.

(vi) Siltation at particular X-section while siting the bridge be examined and same shall be taken care while using this formula.

(vii) Scour depth is to be measured below the lowest bed level in a X-Section.

9. SCOUR OBSERVATION AND INTERPRETATION OF DATA

Data collection was done with a systematic approach to correlate maximum scour with a other important parameter. In fact the data of scour observed and existing hydraulic data was critically examined keeping in view the difficulties faced to finalise the foundation level in absence of bouldery bed formula. There are number of bridges constructed on bouldery bed in the country, where the foundation level for these bridges were finalised based on the basis of existing formulae, engineering judgement and nature of the strata. These bridges had behaved reasonably well barring few bridges where excessive scour has been reported. Since this practice had been followed in various bridges in the country an effort was made to collect the design data of these bridges as these bridge sites act as a live model for observation and having faced number of flash flood without any damage and abnormal scour around the pier. Based on this, data of bridges, collected results were examined with reference to velocity and maximum scour below the lowest bed level taken into consideration subsequent to various reviews of foundation level. It is further mentioned that whenever the velocity is calculated based on the Manning formulae it takes into consideration all the properties of the x-section i.e. area, bed slope, rugosity coefficient and wetted perimeter. Only one fact which effect the scour in addition to above is the shape of pier in the mid stream. Based on above basic concept the assumption as per Para 7 are made for our data collection and analysis approach. Data of bridges was examined as per Table (1) and it is found that maximum scour level can be taken as proportional velocity from the lowest level. Also it has been further observed that scour observed within the limit. Direction of flow and other parameter at particular time of flow play important role. As per the above observation, scour depth be desired as follows in case of bouldery bed

D is proportional to V

D max = KV

D max = maximum scour depth from lowest bed level

V = maximum calculated velocity on the basis of manning formulae taken for calculation of discharge taken in m/sec.

K depends upon shape of the pier, bed material and bed slope.

For circular pier K= 1.2and for rectangular pier K= 1.3

Value of 'K' has been initially taken while considering the worse case of scour observed as in case of a bridge in Arunachal Pradesh (India). However the factor can be further modified for adding the affect of shape of the pier. The results obtained with this formulae are more reasonable to result based on silt theory. Now while planning bridge foundation in bouldery bed if the soil strata are predominantly bouldery, this formula can be adopted and accordingly scour depth can be worked out. Photographic record of scour pattern indicated on Page 12 to 15.

10. CONCLUSION

Scour depth in bouldery bed can be thoroughly analysed based on the systematic and scientific approach of the various parameters related to the scour pattern. Based on the study carried out subsequent to data of bridges considered as live model it is emerged that results are quite satisfactory and further study on this are being undertaken to ensure wide applicability of this formula.

****

References

1) Special issue on scour for bridge foundation 1993 - IIBE – Mumbai.
2) IRC:78-2000.
3) Scour Estimation by BS Sadharao Ex-Addl Dir General BRO.
4) SP:13 – Guideline for small bridges and culvert.
5) IRC:5-2000
6) Well and caisson – By Vijay Singh
7) River Scour Proceeding – Central Board of Irrigation and Power Vol-I and II.
8) Model Study Report of Passighat Bridge (India).

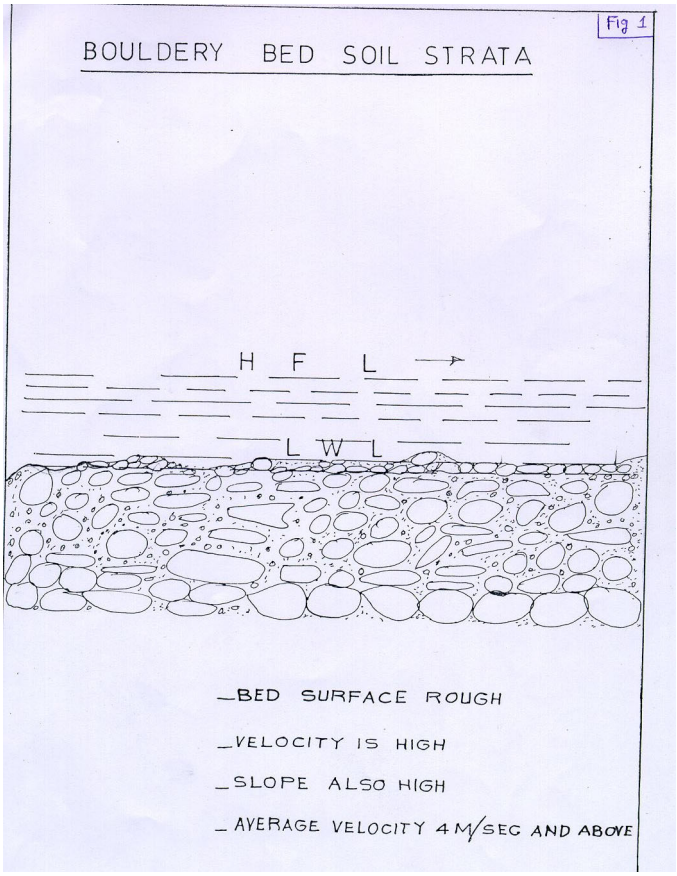
Fig 1
BOULDERY BED SOIL STRATA
H F L
L W L
_BED SURFACE ROUGH
_VELOCITY IS HIGH
_SLOPE ALSO HIGH
_ AVERAGE VELOCITY 4 M/SEC AND ABOVE

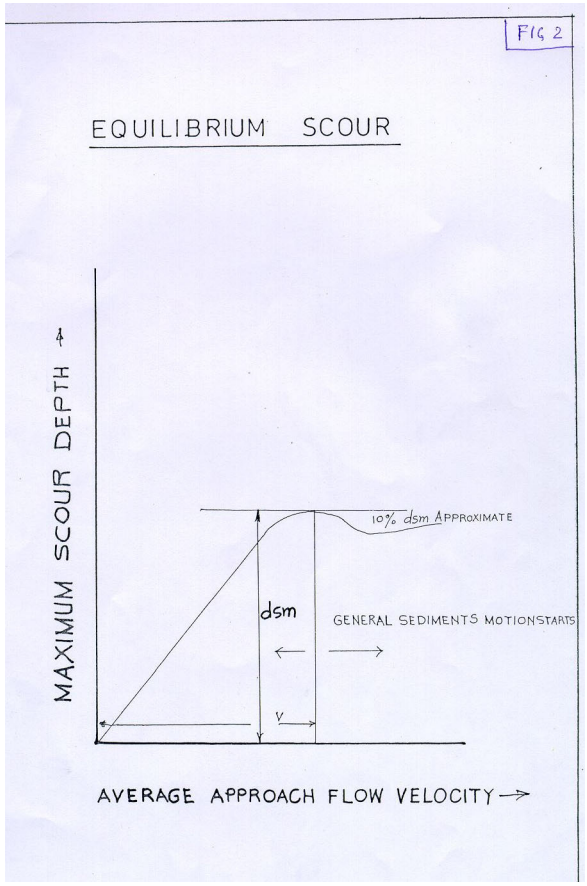
FIG 2
EQUILIBRIUM SCOUR
MAXIMUM SCOUR DEPTH
10% dsm APPROXIMATE
dsm
GENERAL SEDIMENTS MOTION STARTS
V
AVERAGE APPROACH FLOW VELOCITY

BOULDERY BED

SCOUR PATTERN AROUND PIER (1950)

RANGA-II BRIDGE SCOUR OBSERVATION (1968)

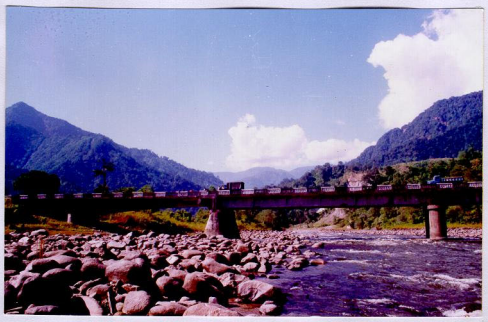

JAMOLA BRIDGE (1970)

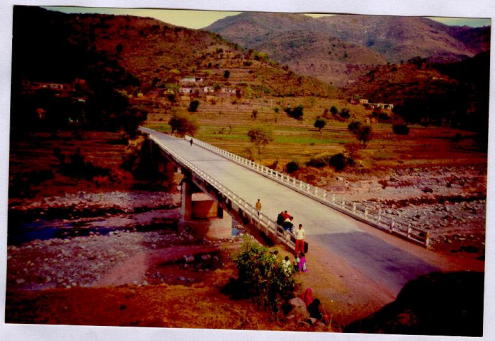

DEDOZA BRIDGE (NO SCOUR OBSERVED SINCE 1969)

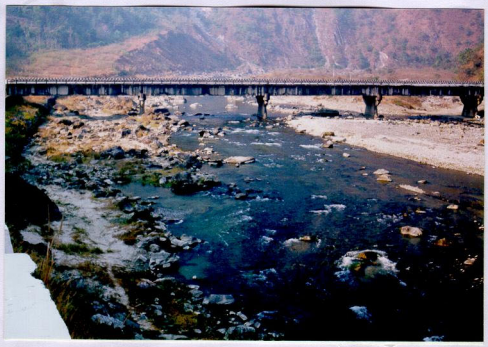

RANGA-I BRIDGE SCOUR OBSERVATION (1968)

SCOUR DATA TABLE OF BRIDGES IN BOULDERY BED (INDIA)

S/ No	Name of Bridge	Span/ Length (M)	Year of constr	Velocity (M/Sec)	Design Scour from lowest bed level (M)	Observed Scour from lowest bed level till about 1997 (M)	Dia of well in Mtr	Bed Slope	Distance between wells	Bed material details	Remarks
1	Ranga-I (AP)	98.00	1968	6.00	4.95	3.30	9.14	1 in 400	52+46	SMB	
2	Ranga-II (AP)	185.00	1968	6.00	6.10	1.10	9.14	1 in 270	39.30+39.30+39.30	SMB	
3	Siji-I (AP)	66.40	1978	4.80	5.20	0.90	6.10	1 in 300	30.50+30.50	SMB	
4	Ego Nallah (AP)	54.80	1978	7.20	6.20	1.20	6.10	1 in 275	27.40+27.40	SMB	
5	Teesta (Sikkim)	185.00	1996	8.00	9.10	1.50	12.00	1 in 385	47.50+90+47.50	SMB & ROCK BELOW	
6	Dalai (AP)	129.00	2000	8.83	8.22	0.50	12.00	1 in 150	65+45+15	SMB	
7	Chander baga (UA)	118.00	1996	3.20	3.10	0.10	Open	1 in 400	5 span/each 22 m length T4 Nos gap slab 2m each		
8	Shivpuri (UA)	140.00	2000	4.20	4.30	0.30	Open	1 in 149	60+60+20	SMB	
9	Dimwe (AP)	87.00	1996	5.10	4.30	0.10	9.14	1 in 300	65+22	SMB	
10	Akkar (Sikkim)	152.00	1988	8.60	8.50	2.00	12.00	1 in 300	79.79	SMB	Cable stayed
11	Beas (HP)	326.00	1974	8.50	9.40	2.10	9.14	1in 400	47x7	SMB	
12	Rorathang (Sikkim)	158.49	1972	5.60	5.80	2.00	10.36	1 in 300	45.72	SMB/Rock	
13	Deoza (AP)	128.00	1969	4.90	5.00	1.00	6.10	1 in 250	25.60x4	SMB	
14	Tippi (AP)	76.25	1969	6.50	6.70	1.10	6.10	1 in 240	18.50x4	SMB	
15	Kud (AP)	99.08	1968	3.20	4.20	0.80	Open	1 in 260	32+32+32	SMB	
16	Ans (J&K)	166.00	1992	4.50	4.10	0.90	8.00	1 in 300	15.94+45*3+12.94	SMB	
17	Sibokorong (AP)	110.00	2000	3.12	3.00	0.20	Open	1 in 300	55+55	SMB	
18	Gular (UA)	83.00	1999	3.85	4.00	0.85	Open	1 in 400	41.50+41.50	SMB/Rock	

- ***SMB = Soil Mixed with Boulder***
- ***HP = Himachal Pradesh***
- ***AP = Arunachal Pradesh***
- ***J&K = Jammu & Kashmir***
- ***UA = Uttaranchal***

Scour Monitoring of Railway Bridge Piers via Inclination Detection

Noritoshi Kobayashi[1], Shintaro Kitsunai[2], Makoto Shimamura[3]

ABSTRACT

Protection of bridge piers against scour is a crucial requisite for safe train locomotion. It is necessary to issue an alert to block the bridge when its piers are endangered by scour. As it is difficult for a human inspector to observe the bridge pier scouring during a flood directly by naked eyes, authors developed the clinometric type of scour monitoring device. These devices have installed since 2000 in East Japan Railway Company area. This device gives the alarm to the train operation room and train operation is suspended, when the inclination of the bridge pier exceeds the threshold value. Moreover, authors developed numeric models for inclination forecast to detect the inclination of a pier before it is in a critical condition due to scour.

THE RULE TO AVOID TRAIN ACCIDENTS CAUSED BY SCOUR HAZARD

East Japan Railway Company (JR East) has a network of 7,538km of track in eastern Honshu in Japan(Fig.1). There are approximately 800 bridges that are prone to of scour damage among about 2,500 bridges over water in JR East and several of them have suffered severe scour damage during the last decade.

Major characteristics of rivers in Japan are their short and steep riverbed. In a flume, stream becomes super-critical flow and water level hardly rises during a flood. Moreover lowering of riverbed progresses at many rivers at present, due to dam construction in the upper and middle reach of rivers

[1] Researcher, Research and Development Center, East Japan Railway Company, n-kobayashi@jreast.co.jp

[2] Assistant manager, Track facilities division of facilities department, East Japan Railway Company, shin-kitsunai@jreast.co.jp

[3] Senior Chief Researcher, Research and Development Center, East Japan Railway Company, m-shimamura@jreast.co.jp

JR East takes two types of measures for this purpose; first, constructing protective facilities around the bridge pier to prevent scour; second, setting a train suspension rule to suspend a train operation before scour develops. In this rule, a scour depth around a bridge pier is estimated by the empirical relationship between a scour depth, water level and width of the bridge pier because it has been difficult to measure the depth of scour directly. When water level grows up and reaches the threshold value during flood, train operation is ordered to suspend. This rule has two major drawbacks, however. The first is that this rule causes many unnecessary train cancellations, and the second is that this rule cannot suspend a train operation before a scour hazard occurs.

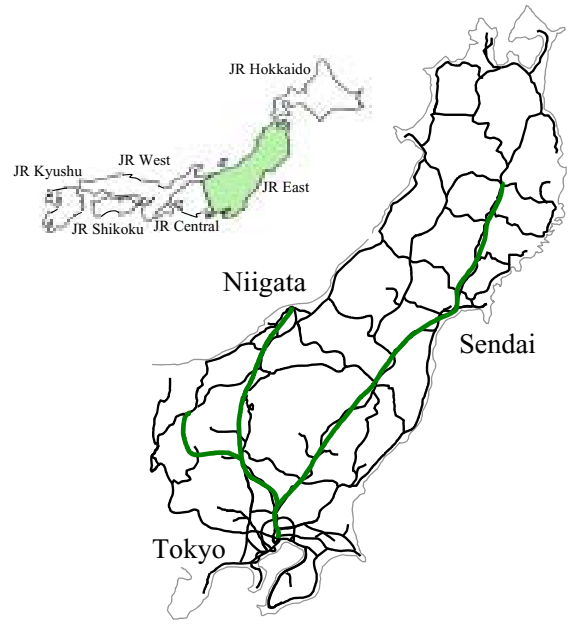

Fig.1 The networks of JR East

To cope with these problems, it is necessary to measure a depth of a scour or a stability of the bridge pier directly. Authors developed four scour monitoring devices that can monitor the riverbed level or stability of the bridge pier[1)], The first is floating switch type, the second electrode type, the third accelerometer type, and the fourth clinometric type. JR East currently installs the clinometric type of scour monitoring device to monitor stability of bridge piers among these devices.

THE RULE FOR REGULATION OF TRAIN OPERATION USING THE WATER LEVEL GAGE

Water level gages have been used to give alarms in case of the threat by scour at bridge piers. JR East has approximately 600 on-line water level gages on bridge piers and water level is measured individually on real time. Scour depth is estimated by means of the empirical relationship among scour depth, water level and bridge pier width. When the estimated scour depth at the spread-footing base of the bridge pier of interest reaches to certain threshold value,

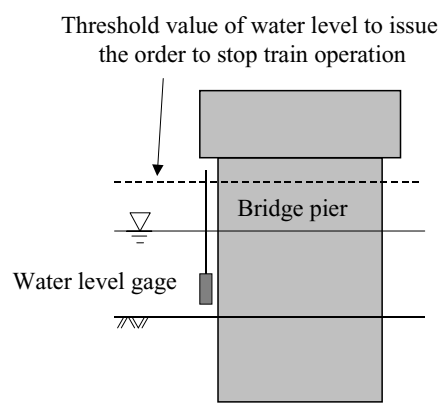

Fig.2 Outline of regulation of train operation during high water

orders to suspend train operation are to be transmitted to the train operators. Fig.2 shows outline of regulation of train operation during high water.

However, this rule causes many unnecessary train cancellations because the estimation is determined considering worst-case scenarios and the threshold value is added unclear safety margin.

Furthermore, this rule dose not ensure to suspend train operation before scour develops in some kind of site-situation, such as in a flume with steep riverbed, where stream becomes super-critical flow and water level hardly rises during flood. Thus, in this kind of site-situation, it is difficult to find the occurrence of a scour with measurement of a water level.

THE PRINCIPLE OF THE CLINOMETERIC TYPE SCOUR MONITORING DEVICE

The clinometric type scour monitoring device is fixed on the top of bridge pier, and monitors the inclination of bridge pier caused by scouring the foundation of bridge

i) The device on the top of the pier　　ii) Inside of the device

Fig.3　The clinometric type of scour monitoring device

pier(Fig.3). This device can measures inclination of the pier in the same principle of a bubble tube type level. Inclination can be measured with the accuracy of 0.001° in the range of ±0.5°per with a frequency more than once per second.

Fig.4 shows time series of the inclination of a certain bridge pier. This figure shows that the bridge

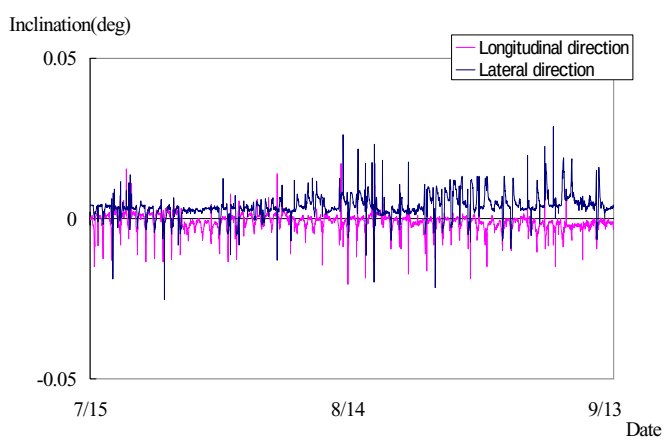

Fig.4　Time series of the inclinations of a certain bridge pier

pier inclination fluctuates within a small range in a day cycle, and it is considered the influence of the movement of the bridge caused by the cycle of a temperature. In Fig.4, a jump of the data shows that a train passed over the bridge. Fig.5 shows scattered diagram of the daily inclination of same bridge and the plotted inclination was observed every thirty minutes during a half year.

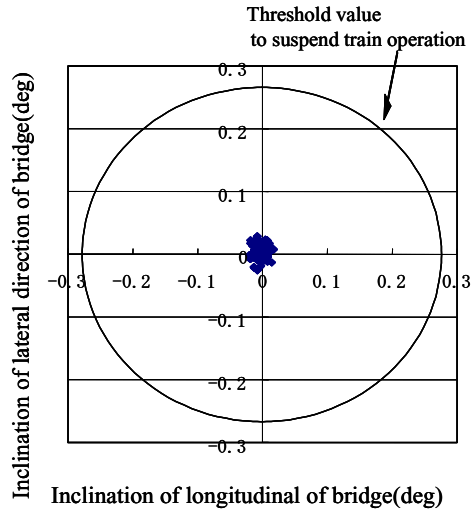

Fig.5 Scattered diagram of the inclinations of a certain bridge pier

THE THRESHOLD VALUE OF THE CLINOMETERIC TYPE SCOUR MONITORING DEVICE

The clinometric type scour monitoring device gives alarms when inclination of the bridge pier exceeds certain threshold values. There threshold values are based on the existent maintenance limits of track irregularity(Table 1).

The relationships between the inclination of a bridge pier and the vertical and horizontal transition is follows(Fig.6):

Vertical gap $\theta_1=4\cdot10^{-4}(La\cdot Lb/(La+Lb))B_1/D$

Horizontal gap $\theta_2=4\cdot10^{-4}(La\cdot Lb/(La+Lb))B_2/H$

where

θ_1 : Inclination angle of the bridge pier for vertical gap(radian)

θ_2 : Inclination angle of the bridge pier for horizontal gap(radian)

Table 1 Maintenance limits of track irregularity(mm)

	Line over 120km/h	Line over 95km/h	Line over 85km/h	Line over 45km/h	Line below 45km/h
Longitudinal level(B_1)	15	17	19	22	24
Line(B_2)	15	17	19	22	24

La : Span of bridge girder of one side(m)

Lb : Span of bridge girder of another side (m)

B_1 : Instruction value for track irregularity of longitudinal level (mm)

B_2 : Instruction value for track irregularity of line (mm)

D : Horizontal distance between the edge of foundation and the rail(m)

H : Vertical distance between the edge of foundation and the rail(m)

The smaller of θ_1 and θ_2 is chosen to be the threshold value of train suspension. The maintenance limits of track irregularity are constant anywhere but the threshold value of the device changes by each bridge due to be the threshold variance of bridge

heights. Generally the threshold values are set between 0.2° and 0.5° in this rule. The inclination that is observed at all the bridges is much smaller than threshold values(Fig.4 and 5).

When the inclination of the bridge pier exceeds the threshold value, the device gives the alarm to the train operation room through the wired network along the track for transmitting the data of the various sensors; such as rain gauges, seismometers, anemometers, and so on, and train operation is suspended. However in order to get rid of the influence of the passing train(Fig.4), the clinometric type scour monitoring device does not issue an alarm without 2 minutes excess of inclination over the threshold value.

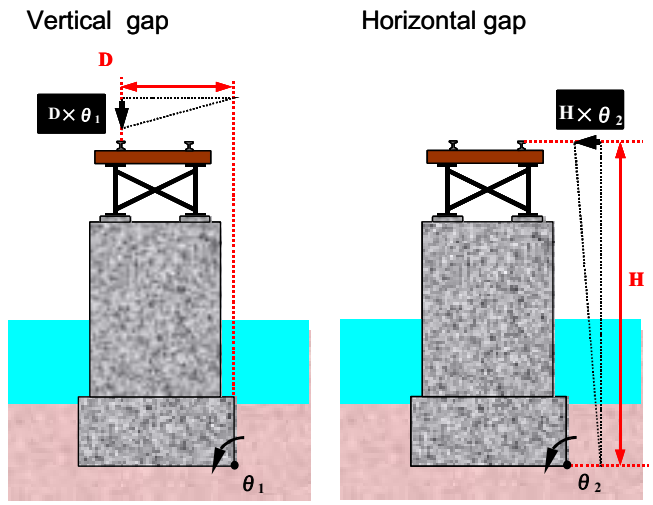

Fig.6 Relationship between the inclination of bridge pier and the gap of it

The cost of the clinometric type scour monitoring device is about ¥300,000 per device. The initial cost per bridge is approximately ¥4,000,000 including three monitoring devices and establishment of devices, power supply and wired network. This device have installed since 2000 in East Japan Railway Company area. It installed 6 bridges in 2000, 70 bridges in 2001, and will install 69 bridges in 2002.

IMPROVEMENT OF THE CLINOMETRIC TYPE OF SCOUR MONITORING DEVICE

The clinometric type scour monitoring device issues an alarm when the inclination of bridge pier exceeds the preset threshold value. There is room for improvement in this device as follow:

(1) Though a bridge pier is scoured and begin to incline, train operation cannot be suspended until an inclination exceeds the threshold value.

(2) The risk of scour depend on whether a pier inclines quickly or slowly, but the device cannot measure a speed of inclination.

In order to improve these points, it could be considered a way to forecast a future inclination and apply it to the rule.

We examined some methods to forecast a future inclination statistically by using time series of the inclination of the bridge pier. In this examination we have tried to find a suitable model to represent a time series of inclination and to forecast a future inclination by using this model. For this purpose, we carried out experiments first using

a reduced scale pier to take data of time series of inclination.

A process of the examination are shown below:

(1) An experiment is carried out with a reduced scale pier as an actual bridge pier inclines by scouring the foundation. This experiment takes data of time series of inclination.

(2) We examine how to forecast a future inclination with the past time series by using the data above.

THE EXPERIMENTS IN INCLINATION WITH REDUCED SCALE PIER

The experiment was carried out with approximately 1/20-scaled stone rectangular solid imitated bridge pier. In the experiment, a reduced scale model standing on the ground was made to incline, and the progress of the inclination of the model was measured every second with the clinometric type scour monitoring device on the top of the model. In order to make the model pier incline without a thrust by outer force, columns of frozen sand were set under the model by digging the ground and supported a half of the weight of the model shown in Fig.7. These columns of frozen sand melted gradually with the heat of the natural environment, and then the model pier lost support and began to incline slowly. The experiment was repeated by changing the length of overhang and the height of earth burying the model. An example of the time series of the inclination data taken by the experiment is shown in Fig.8. It shows that the time series has long-term patterns of growth of the inclination (a sign denotes the direction of inclination) and the other series also have a same trend.

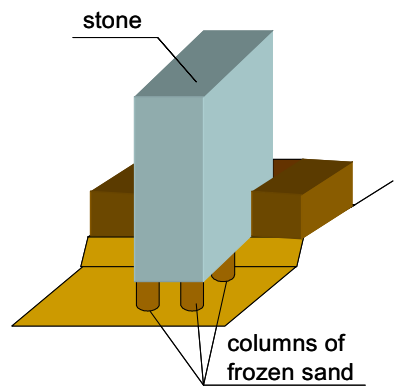

Fig. 7 Experiment in inclination

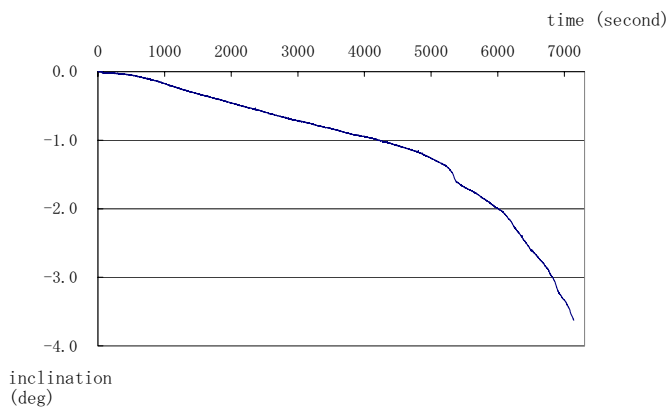

Fig8 Time series of inclination

METHOD OF FORECASTING THE INCLINATION

A method of forecasting the inclination was examined by using the data explained in the preceding chapter. In order to put this method to practical use, the ability of the scour-monitoring device already set at bridge must be considered for the examination of the method. In short, a suitable model for representing the time series of the inclination must be as simple as possible to be computed by the device.

As already mentioned in the preceding chapter, the time series of the inclination obviously has the movement called trend, which is long term and only in one direction. This trend is not linear but curvilinear, and there are several mathematical models to represent curvilinear trend. Since the time series seemed to grow at a constant percentage, two models with this characteristic are useful for the forecast. They are expressed as follows.

Quadratic Trend Model

$$y_t = \beta_0 + \beta_1 t + \beta_2 t^2 + \varepsilon_t$$

Simple Exponential Growth Model

$$y_t = \beta_0 \cdot \beta_1{}^t \cdot \varepsilon_t$$

The coefficients are updated to fit the time series by using most recent data. For example, at time *t* the coefficients are calculated by using the most recent k-steps-data, and then 3k-steps-ahead inclination is calculated by using the model with this coefficients.

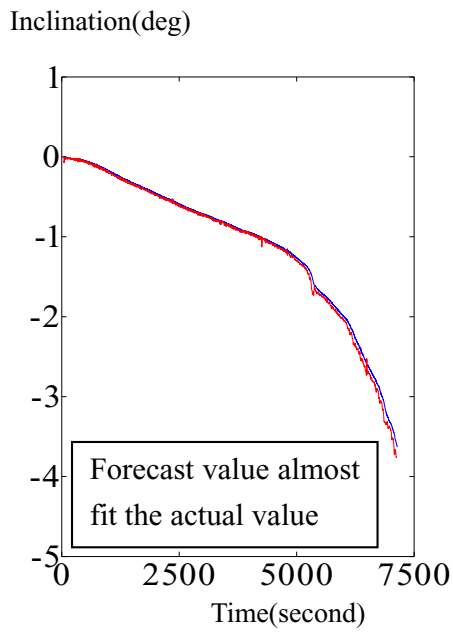

Fig.9 Result of forecast with *simple exponential growth model*

As a result of the examination by stepwise forecast error evaluation, *simple exponential growth model* probed to fit the time series better than *quadratic trend model*. A future inclination forecasted by *quadratic trend model* is sometimes unstable under the influence of data noise.

In order to examine the influence of noise realistically, noise that moves within the same range as measured at the actual bridge was added to the data obtained from the model pier experiment. As a result of forecast model fitting, the forecast by *simple exponential growth model* proved to fit well irrespectively whether the data contain noise or not. On the other hand, the forecast by *quadratic trend model* is often much more seriously discrepant with the sample time series than the case without noise.

These results show that the time series of the inclination can be fitted and extrapolated by *simple exponential growth model* better than by *quadratic trend model.* The former model is robust against the influence of noise and there is less possibility of giving false alarms.

REGULATION RULES BASED ON INCLINATION FORECAST

As already mentioned in preceding section, the result of the examination shows that there is a possibility that the progress of inclination of bridge pier is forecasted with a simple numerical model. The threshold value of inclination does not change by using method of forecast, but this method brings the advantage as follows:

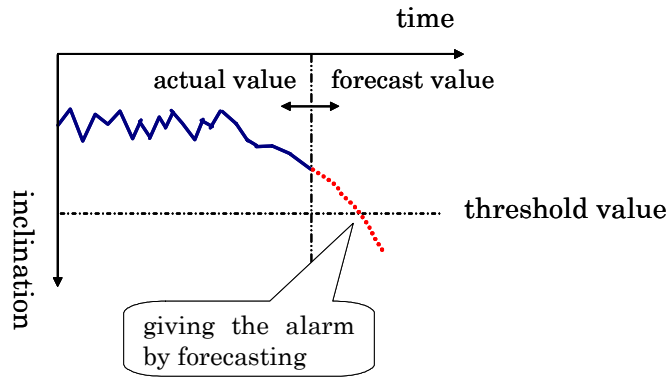

Fig.11 The basic idea of regulation rules based on forecast method

(1) An alarm can be issued before a bridge pier is in a dangerous condition, and foundation of the pier can be inspected and identified.

(2) The time when the inclination of the bridge exceeds the threshold value can be forecasted. As a result, it is clear how fast foundation of bridge pier is scoured and the danger of train passing over the bridge can be judged.

From the practical point of view, the forecast may not be necessarily very accurate, but it is necessary that the accuracy of the forecast is quantitatively evaluated prior to the application of the forecast.

CONCLUSIONS

The development of the clinometric type scour monitoring device was described in this article. JR East is currently monitoring the inclination of the piers of its 76 scour prone bridges with the device and planning to install the device on additional 71 bridges by the end of 2002. It is expected that sufficient amount of statistical data which is necessary to establish an accurate and reliable method to detect bridge pier scouring via inclination data can be obtained from daily measurement records by these operating devices.

REFFERENCE

1) O. Suzuki, M. Shimamura: Development of New Scour Monitoring Devices for Railway Bridges, Scour and Foundation, pp.331~336, Melbourne, 2000.6

Non-Destructive Testing to Determine Unknown Pile Lengths Under Existing Bridges

By

Frank Rausche[1], Mohamad Hussein[2], and Marty Bixler[3]

ABSTRACT

The Pulse Echo Method is commonly used to evaluate the quality of concrete pile foundations. Also called Low Strain Testing Method, this Non-Destructive test utilizes the impact of a hand-held hammer to produce a low intensity stress wave in the pile material. The major component of the impact induced motion is a compressive wave, which propagates axially along the pile and reflects at points where changes occur in the properties of the pile material or soil resistance. An accelerometer affixed to the pile near its top, registers the impact motion and wave reflection effects.

This non-destructive testing method is typically used for evaluation of the structural integrity of drilled shafts, cast-in-place, and driven concrete or timber piles. The method has also been successfully employed for an assessment of unknown pile lengths under existing structures and particularly for bridges susceptible to scour. However, occasional complications such as interaction of the pile with the structure, deterioration of the piles, and other effects require that the standard interpretation method is expanded. The analysis tools available to improve the accuracy of the results include the frequency domain analysis, two-point measurements, and wave-up calculation. This paper presents discussions on the testing method with emphasis on the special aspects associated with evaluation of unknown pile lengths under existing structures. Data from three case histories are presented and discussed.

INTRODUCTION

Deep foundations of bridges over moving water must have enough bearing capacity even after scouring has occurred. When reviewing the adequacy of such a foundation it is therefore necessary to estimate the depth of maximum scour and then assess the remaining pile shaft resistance and end bearing. For existing bridge structures on pile foundations, it is often difficult to obtain accurate information of in-place pile lengths.

[1]President, GRL Engineers, Inc., Cleveland, Ohio, frank@pile.com
[2]Partner, Pile Dynamics, Inc., Cleveland, Ohio, www.pile.com
[3]Project Engineer, GRL Engineers, Inc., Orlando, Florida, MBGRLFL@aol.com

Even if pile driving records exist, the structural integrity of the piles may be in question. Concrete piles particularly are subject to damage during and after installation. Dynamic low-strain integrity testing has been used for many years, on concrete cast-in-place shafts and driven piles, for both structural integrity evaluation and unknown pile length determination (Hussein et al., 1992). The technology is not always without challenge. The method is limited by the length that can be detected depending on the size of pile and the strength of the substrata.

LOW-STRAIN INTEGRITY TESTING

Based on one-dimensional wave propagation, low-strain integrity testing is probably the simplest, quickest and most economical way to non-destructively test for unknown pile length. The principle is that a compressive stress wave will travel through a long slender rod of uniform material at a constant speed, c, which is a function of the material elastic modulus, E, and mass density, ρ, (i.e., $c^2 = E/\rho$). For concrete, this stress wave speed is between 3,000 and 4,500 m/s. To satisfy equilibrium and continuity requirements, the stress wave is reflected at points of soil resistance and changes in pile impedance (impedance is EA/c where A is the pile cross-sectional area). The magnitude of the stress wave dampens out with time.

The stress wave is produced by a small hand-held hammer impact. A heavier hammer, e.g., of 2.5 kg weight, produces lower frequency pulses than a 1 kg hammer. The lower frequency signals travel further, however, their reflections are less clearly defined and therefore more difficult to read than higher frequency signals. The stress (and corresponding strain) is very small and the wave is observed by measuring the induced particle accelerations using a relatively sensitive accelerometer (Note: The term “low-strain” is used to differentiate this testing from the also common “high-strain” testing of piles, which requires that an impact is applied with a heavy ram such that the pile experiences at least a small permanent set. Obviously, the “high strain” method is not applicable to piles under an existing structure). The acceleration signal, recorded as a function of time, can be integrated to display velocity versus time or, after multiplication with the wave speed, velocity on a distance scale.

The Pulse Echo Method is the term given to low-strain testing with the evaluation of the velocity with time (or distance) records. A simple example of wave propagation and pile top reflections is shown in Figure 1 for a pile of length L and with a cross sectional reduction at distance x. The hammer impact produces a downward (positive) velocity at the pile top and thus a positive input “pulse” at the beginning of the velocity record. The impact wave travels down the length of the pile at a speed c. When the compressive wave reaches the pile bottom, it is reflected as a tension wave, which travels back to the pile top. Arriving at the top, the upward traveling wave arrives at a time 2L/c (twice the pile length divided by the wave speed) and causes a sudden pile top velocity increase, often

referred to as the “toe reflection” or “echo”. Normally, the reflection wave causes a pile top velocity similar in shape to the impact signal. The magnitude of the reflection could theoretically be twice that of the impact pulse for a uniform pile. For a pile with non-uniformities or soil resistance, the toe signal is significantly smaller. To make the toe reflection more clearly apparent without unduly increasing the magnitude of reflections from locations closer to the pile top, an exponential amplification is normally applied to the record and it is identified in the velocity plot as an increasing curve under the time/length scale

A reduction in pile impedance, $EA/c = A(E\ \ )^{1/2}$, (i.e., cross sectional area times the square root of elastic modulus and mass density of the concrete; this quantity reflects the shaft quality and size) will also cause a tensile reflection. The time of arrival of the reflection from the impedance reduction at depth x, relative to the time of impact, is 2x/c.

It is also useful to consider the velocities that would be observed at some depth z along the pile length. (Figure 1) Measuring at that location, we would first see the effect of the downward traveling wave produce a velocity equal to the impact pulse at the top (at time z/c). Next we observe the upward reflected traveling wave from the impedance reduction and then later its reflection from the pile top. Eventually, we would see the toe-reflected impact pulse and somewhat later its reflection as a downward wave. The velocity magnitudes of the waves observed somewhere along the pile are generally only one half of the velocities measured at the pile top. This is because the reflection at a free pile end causes a doubling in the velocity magnitude.

A few more observations are important:

- An increase in impedance or a sudden increase in soil resistance will cause a compressive wave reflection and therefore a negative or upward directed velocity.
- The time at which an upward traveling wave arrives at the pile top is a direct measure of the distance of the cause of the reflection from the sensor location.
- The magnitude of a motion is directly related to the severity of the disturbance that causes the upward traveling wave. However, in complex situations with several impedance variations multiple reflections occur which make the interpretation very complex.
- If the pile top is restrained by a structure then it is not truly free and reflections at the pile top may be either positive or negative.
- Applying the hammer impact on a pile cap above the pile head may cause immediate reflections at the cap bottom and therefore an impact wave that is not necessarily a simple sine half wave.
- At the free pile top, motions occurring after impact are a direct indication of “the upward traveling waves” which in turn allow for a simple interpretation of the origin and cause of the upward traveling wave. However,

measuring somewhere along the pile, it is not a simple matter to decide if the measured motion is due to an upward or a downward traveling wave.

APPLICATION TO EXISTING BRIDGE FOUNDATIONS

The pile top surface is normally not accessible for accelerometer measurements. It is therefore necessary to measure the pile motion by attaching the accelerometer with bolt and anchor to the side of the pile. Alternatively, the sensor may be attached on top of the pile cap. The impact may be applied to the bridge deck or to the pile cap. Figure 2 shows one possible scenario. Where the piles extend to a bent directly under the deck, the free pile length is often long enough to allow for two accelerometer attachments. This has the advantage that it is then possible to identify the upward traveling wave (Johnson and Rausche, 1996).

The following examples demonstrate what can be done and what must be expected.

EXAMPLE 1

The tests were performed on the foundation of a 65 year old, five-span bridge, which had suffered excessive differential and total settlements. At the four pier locations, the bridge deck was directly supported by a pile cap and 6 pile–columns. The piles were 406 mm octagonal concrete sections. Only little information was known about the subsurface conditions except that the original records suggested that the piles should be a total of 13.7 m long and extend into sand with silt and clay.

All 24 piles of the four piers were tested by striking the bridge deck with a 2.5 kg hammer and attaching the accelerometer to the side of the piles. The six records for one of the center piers are shown in Figure 3. The velocity records were exponentially amplified as indicated in the graph under each velocity trace with maximum amplification values of 10 for the longer piles and 4 for the shorter piles. The strongest and clearest reflection was then interpreted as the pile toe reflection. One of the six records of Figure 3 was unclear, possibly due to some cracks in the pile. The other piles indicated pile lengths between 5.8 and 9.1 m. Adding the 2.1 m between accelerometer and pile cap would yield total lengths between 7.9 and 11.2 m. The records clearly showed that the piles on the side of the bridge with greater settlements were shorter than the other piles. Piles of the other three piers yielded similar results. Of course, the low strain method does not provide information about pile bearing capacity.

EXAMPLE 2

Several 455 mm square prestressed concrete piles were driven into a sandy soil and tested with the Pulse Echo Method. The structure is a bridge with three

spans. It is 20 years old and no pile driving records could be obtained. Both the 2.5 and 5.5 kg hammers were used in anticipation of possibly very long piles. An often cited general rule of thumb states that 30 pile diameters are a practical limit of depth determination for this method; however, because this limitation depends on soil properties and other factors, it doesn't always hold true. In the present case (Figure 4(a)), a clear toe reflection was apparent for an L/D ratio of 24.

It is sometimes advantageous to transform the records into the frequency domain, particularly if spurious vibrations from a variety of sources tend to mask the pile toe reflection. As a demonstration, a Fourier transform was done on the records in the present example as shown in Figure 4(b). The peaks of the transformed velocity occur at frequencies which are characteristic for the measured record. In this case, it is obvious that the time record is much clearer than the frequency transform. The latter indicates not only the frequency corresponding to the pile length, but also those of other reflections caused by structure and/or soil.

It should also be mentioned that the so-called transient response method, which additionally requires the measurement of the hammer force and which also requires the data interpretation in the frequency domain, is usually of no help when pile length of bridge foundations must be determined. The main reason is frequency components in the records, which originate from the superstructure and are therefore nearly impossible to separate from the frequency response of the pile. However, in the time domain, which identifies the phase shift between these record components, it is a much simpler task to identify the pile length. This method may be of some help in the determination of the dynamic stiffness of a pile, however, it requires that the pile top is free and not attached to a structure.

EXAMPLE 3

This example is one where it was possible to attach two accelerometers to the sides of the test pile at a distance of 2.1 m apart. The piles were 455 mm square prestressed concrete piles with design length of 15.2 m. This 40 year old bridge was experiencing differential settlements near the river channel.

Figure 5 shows the velocities recorded at gage locations g1 and g2. Obviously the two velocities are somewhat complex, i.e. they do not only show an impact pulse and a toe reflection but also other characteristics. Helpful is the time shift between the onsets of the two velocity records, which indicates a wave speed of approximately 4,100 m/s. In order to more confidently interpret the record, the wave up curve for the gage location g1 was calculated, using the algorithm developed by Johnson and Rausche, 1996.

This wave-up record shows very clearly a damage (or crack) reflection at a distance of 4.6 m below the gage 1 location and possibly a pile length below gage 1 of roughly 13.7 m (if the largest wave-up reflection is interpreted as the

toe reflection). The calculated wave up record also shows several additional reflections between damage and toe reflection, which may have been caused by additional cracks or some other dynamic effects. Of course, it is also possible that the wave-up calculation method introduces errors because it requires that differences of the two records are taken, which introduces roughness and uncertainty in the resulting curve.

SUMMARY AND CONCLUSIONS

Low-strain dynamic testing can be effectively used to assess the length of piles under existing bridge structures. The method is generally applicable if the pile penetration is not much greater than 30 pile diameters. Although, successful tests may also be possible for deeper pile embedment depending on the strength of the soil and the quality and the uniformity of the pile. Several data interpretation tools exist, among them frequency analysis and wave up determination from two acceleration records. The most powerful tool is, however, the exponential amplification of the time record.

The low-strain method is also frequently used for the quality and length assessments of deep foundations, buildings, telecommunication tower foundations, masts, antennas and other structures. These applications are often simpler than bridge foundations since they allow for an attachment of the sensor at the top of the shaft or pile.

REFERENCES

Hussein, M., Likins, G., and Goble, G., “Determination of Pile Lengths Under Existing Structures”, 1992 , Deep Foundation Institute 17th Annual Conference, New Orleans, Louisiana.

Johnson, M. and Rausche, F., “Low Strain Testing of Piles Utilizing Two Acceleration Signals”, 1996, Fifth International Conference on the Application of Stress Wave Theory to Piles, Orlando, Florida.

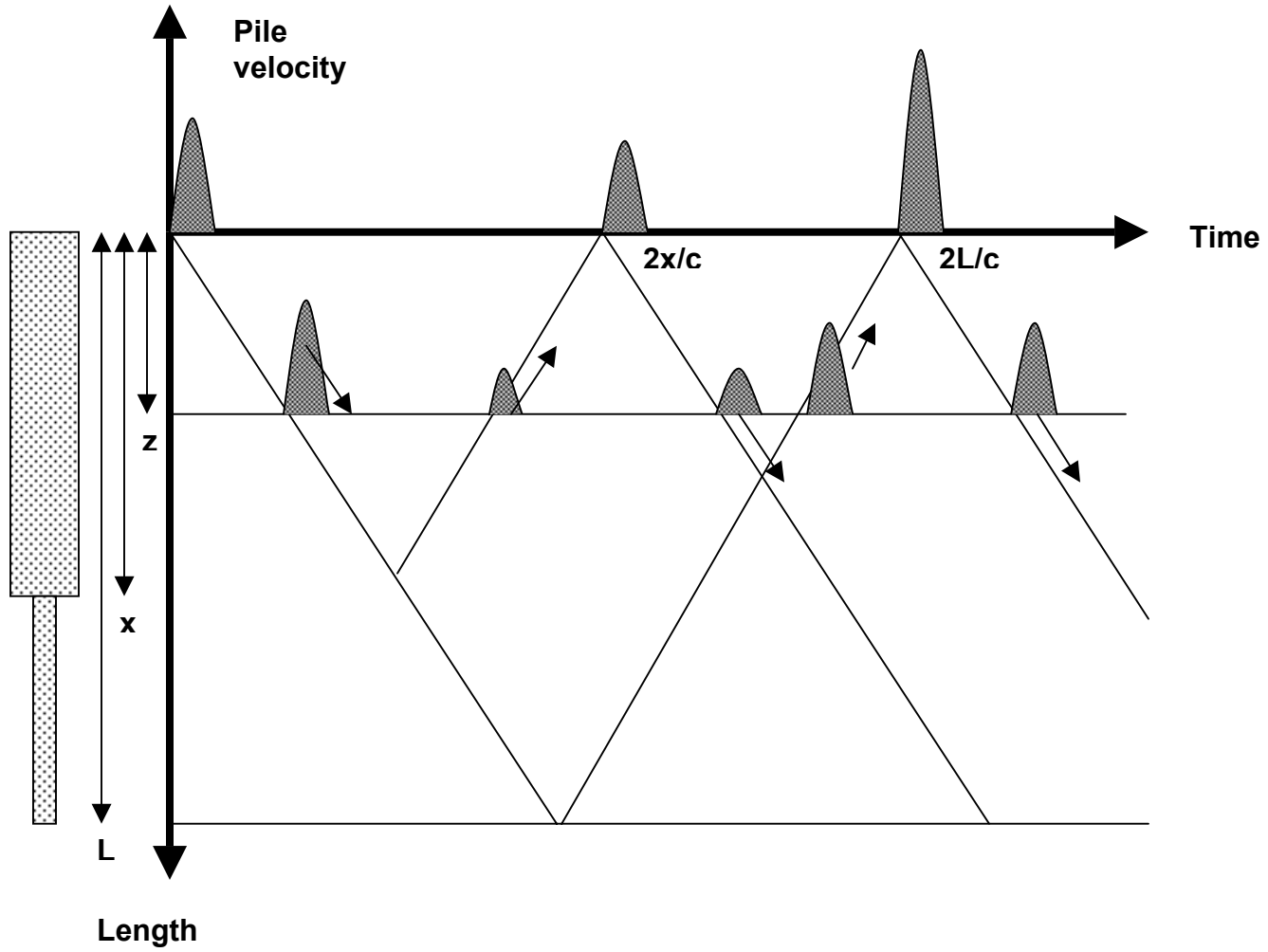

Fig. 1 – Length-Time Plot of Wave Travel Paths and Velocities at Pile Top and in Pile.

(a)

(b)

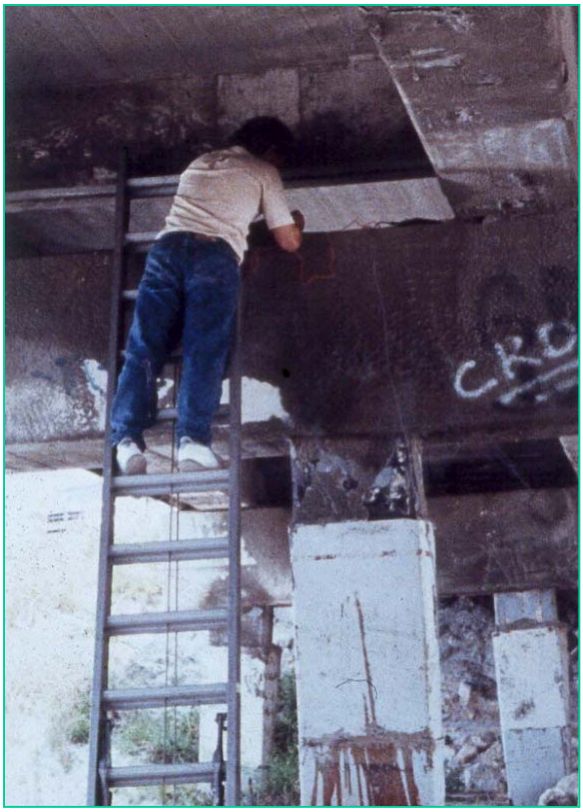

Fig. 2 – Photographs of (a) Bridge Foundation Tested and (b) Application of Impact

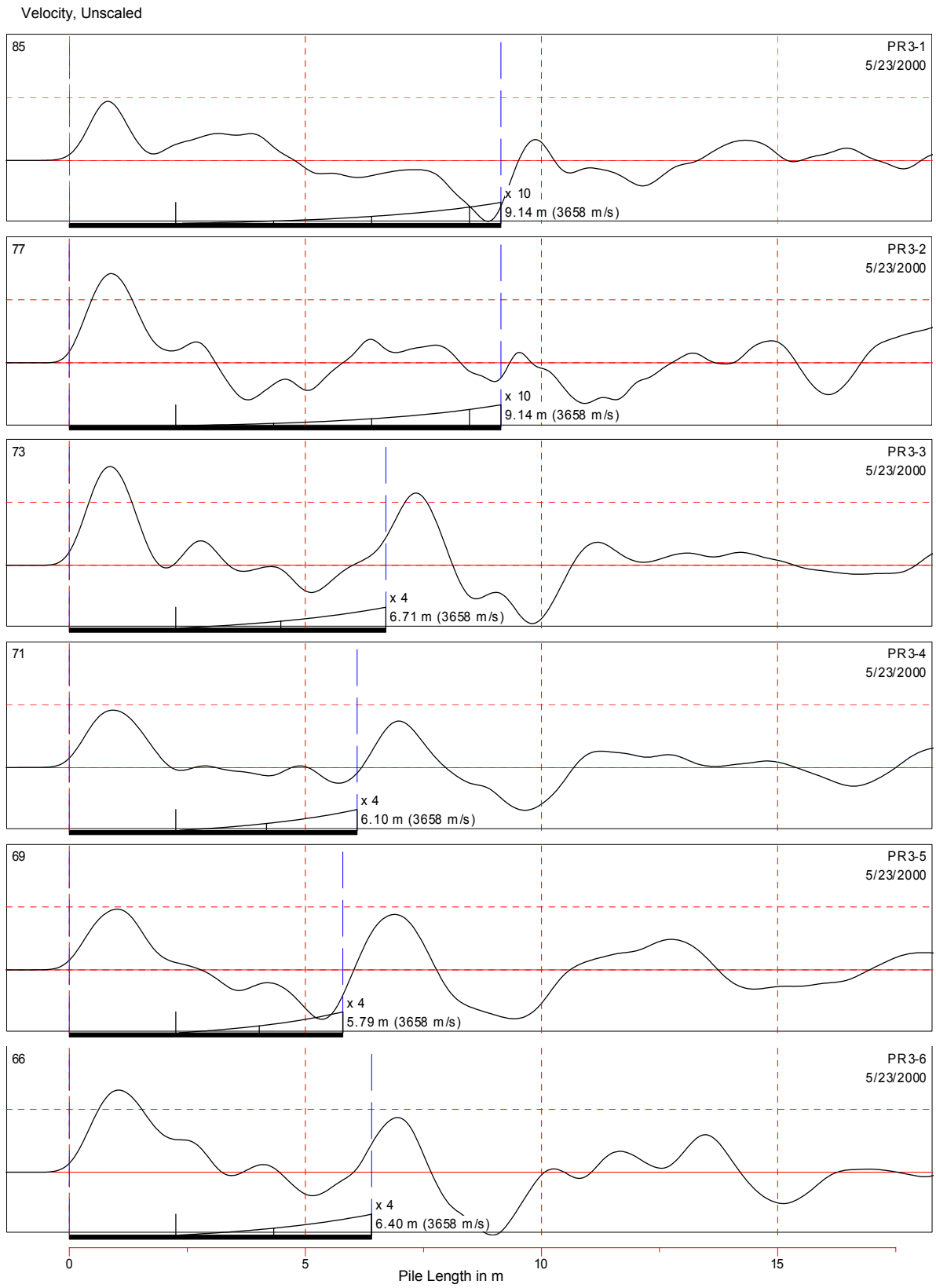

Fig. 3 – Example 1, Pile Velocity Records from 6 Piles Located in the same Bent

(a)

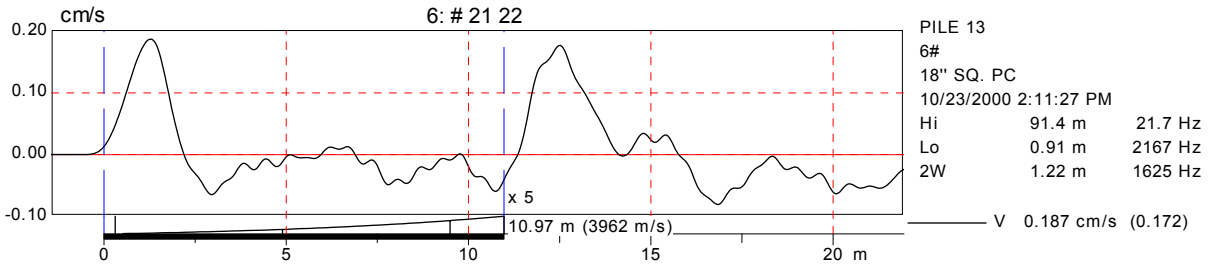

(b)

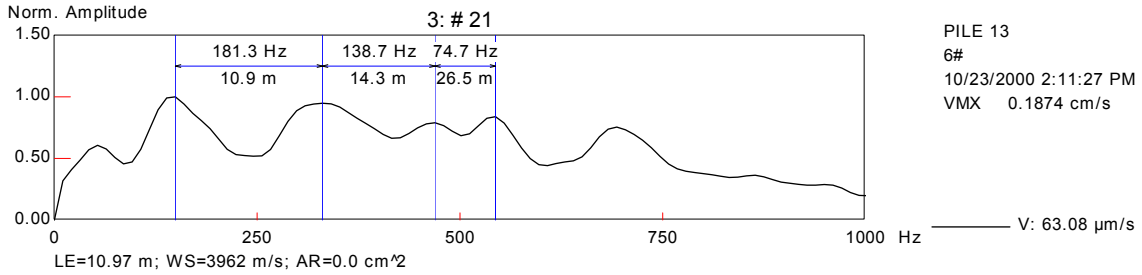

Fig. – 4: Example 2 (a) Pile Integrity Tester (PIT) Velocity Record of a 455 mm Square Concrete Pile and (b) the Associated Frequency Plot

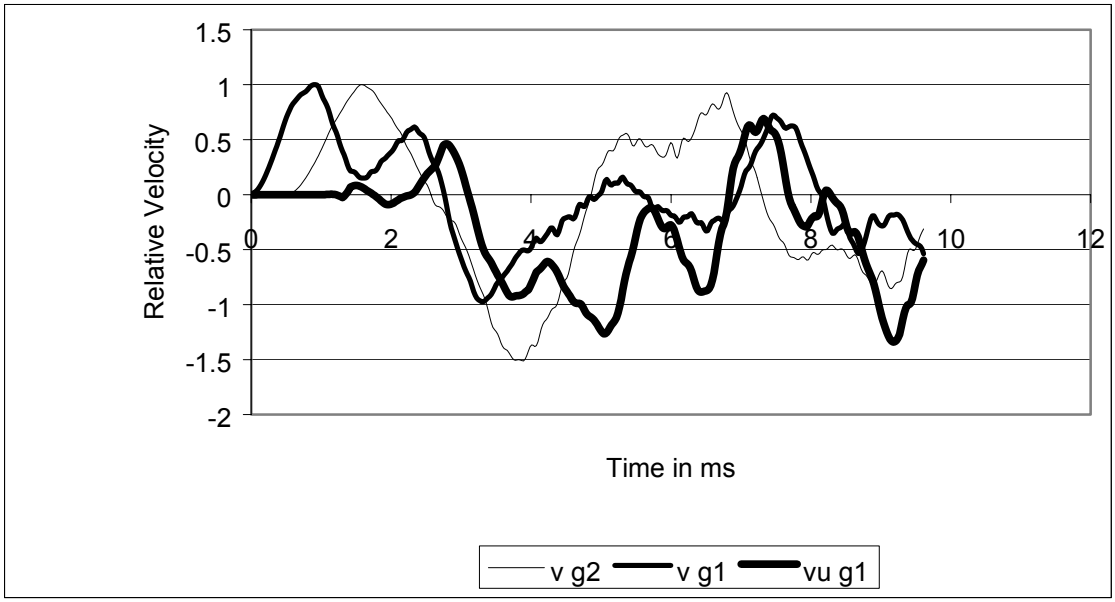

Fig. 5 – Example 3 Velocity Records Taken at Two Locations on Pile and Calculated Upward Traveling Velocity (vu g1) at Upper Location

Determination of Unknown Bridge Foundation Depths with NDE Methods

Larry D. Olson, P.E.

Olson Engineering
5191 Ward Road, Suite 1
Wheat Ridge, CO 80033
Ph - 303-423-1212
Fx - 303-423-6071
ldolson@olsonengineering.com

Abstract
This paper discusses the results of NCHRP 21-5 and 21-5(2) sponsored research on nondestructive evaluation (NDE) methods for determination of unknown bridge foundation depths. Surface and borehole NDE methods are reviewed below along with a discussion of the limitations and accuracy of the NDE techniques. The NDE methods found to be applicable to unknown foundation depth determination were the borehole methods of Parallel Seismic, Induction Field, and Ground Penetrating Radar, and the surface methods of Ultraseismic, Sonic Echo/Impulse Response, Spectral Analysis of Surface Waves and Bending Waves methods. The research further found that the Parallel Seismic and Ultraseismic were the most accurate and broadly applicable borehole and surface methods and these are discussed in detail herein.

INTRODUCTION

There are approximately 481,000 highway bridges in the National Bridge Inventory. The best estimate of the population of bridges over water with unknown foundations, as of April 15, 2000, is about 91,094 from FHWA data. These unknown bridge foundations pose a significant problem to the state DOTs because of scour vulnerability concerns. The foundation depth information in particular is needed to perform an accurate scour evaluation at each bridge site, along with as much other information on foundation type, geometry, materials, and subsurface conditions as can be obtained. This guideline document was prepared to aid state departments of transportation in the specification and performance of engineering investigations to determine unknown bridge foundation depths for bridge scour safety evaluations.

The National Cooperative Highway Research Program (NCHRP) 21-5 project "Determination of Unknown Subsurface Bridge Foundations" (final report dated August, 1995) and the NCHRP 21-5(2) project "Unknown Subsurface Bridge Foundation Testing" (final report dated December, 2000) were performed by the author and his firm to evaluate and develop existing and new technologies that can determine unknown subsurface bridge foundation depths. The NCHRP 21-5 Phase I research focused on the identification of potential NDE methods for determining depths of unknown bridge foundations at 7 bridges in Colorado, Texas and Alabama. The NCHRP 21-5 (2) Phase II research focused on evaluating the validity and accuracy of the identified NDE methods for determining depths of unknown bridge foundations. In this phase, 21 bridge sites were studied in North Carolina, Minnesota, New Jersey, Michigan, Oregon, Massachusetts and Colorado. Phase II research also involved the development of hardware and software needed to perform the NDE testing.

This paper is focused on the use and specification of the borehole Parallel Seismic and surface Ultraseismic methods. These two nondestructive evaluation (NDE) methods were found to be the most applicable methods for determination of unknown foundation depths in this research. A number of other NDE methods were also investigated in the research and found to have more limited applications. These more limited NDE methods are also discussed herein and include the Sonic Echo/Impulse Response, Bending Waves, Spectral Analysis of Surface Waves surface methods and the Induction Field and Ground Penetrating Radar borehole methods.

REVIEW OF SURFACE NDE METHODS

Brief discussions of the surface-based Sonic Echo/Impulse Response, Bending Wave, Ultraseismic, and Spectral Analysis of Surface Waves NDE methods for determination of unknown bridge foundation depths are presented below. Schematics of these four surface NDE methods are shown in Fig. 1.

Sonic Echo/Impulse Response Test

In the Sonic Echo/Impulse Response test, the source and receiver are placed on the top and/or sides of the exposed pile or columnar shaped substructure as shown in Fig. 1a. The depth of the reflector, e.g., a pile bottom, is calculated using the identified sound (compression) wave echo time(s) for SE tests, or resonant peaks for IR tests due to the applied source impact.

Bending Wave Test

The Bending Wave (BW) test is based on the dispersion characteristics and echoes of bending waves traveling along very slender members like piles. The method was first developed for timber piles. The method involves mounting two horizontal receivers a few feet apart on one side of an exposed pile, and then impacting the pile horizontally on the opposite side of the pile a few feet above the topmost receiver in an attempt to identify an echo of bending wave energy from the pile tip as shown in Fig. 1b. Analyses may be performed on BW data by the Short Kernel Method in the time domain (similar to filtering in an SE test), or from modal analysis in the frequency response domain (like the Impulse Response method). The BW method was found to be limited to comparatively short pile foundations in soft soil conditions.

Ultraseismic Test

The Ultraseismic test involves impacting exposed substructure to generate and record the travel of compression or flexural waves down and up the substructure at multiple receiver locations on the substructure as shown in Fig. 1c. This test combines the capabilities of the SE/IR and BW measurements with geophysical processing to separate reflections of wave energy coming from foundation elements versus reflections from the top of exposed substructure. The US method was found to be more accurate and applicable than the SE/IR or BW tests.

Spectral Analysis of Surface Waves Test

The Spectral Analysis of Surface Waves (SASW) test involves determining the variation of surface wave velocity vs. depth in layered systems as shown in Fig. 1d. The bottom depths of wall shaped pier and abutment substructures or footings can be determined if they have suitable flat, horizontal and exposed surfaces for testing. The foundation element bottoms are indicated by slower velocities of surface wave travel in underlying soils. This test was found to be very applicable for these types of foundations where the foundation depths were less than or equal to 2/3 the width of the accessible flat test surface.

REVIEW OF BOREHOLE NDE METHODS

Brief discussions are presented below of the borehole-based Parallel Seismic, Induction Field and Borehole Radar NDE methods for determination of unknown bridge foundation depths. Schematics of these three borehole NDE methods are shown in Fig. 2.

Parallel Seismic Test

The Parallel Seismic (PS) test consists of impacting exposed foundation substructure either vertically or horizontally with an impulse hammer to generate compression or flexural waves which travel down the foundation and are transmitted into the surrounding soil as shown in Fig. 2a. The refracted compression (or shear) wave arrival is tracked at regular intervals by a hydrophone receiver suspended in a water-filled cased borehole (original PS procedure) or by a clamped three-component geophone receiver (new procedure-better for shear wave arrivals) in a cased or uncased borehole (if it stands open without caving). The depth of a foundation is

typically indicated by a weaker and slower signal arrival below the tip of the foundation. Diffraction of wave energy from the foundation bottom was also found to be indicative of its depth in PS tests as well. The PS test was found to the most accurate and widely applicable NDE method for determination of unknown bridge foundation depths of all tested NDE methods.

Induction Field Test

The Induction Field (IF) method is similar in its application to the Parallel Seismic method, but employs the use of electromagnetic waves instead of stress (sound) waves as shown in Fig. 2b. An electromagnetic field is set up in the ground between a steel pile (or electrically continuous reinforced concrete foundation) and a steel electrode (or other electrically isolated steel containing foundation). A triaxial magnetic field search coil is used to measure the field strength in a PVC cased boring drilled within 1 m (3 ft) or less of the foundation that extends about 3 m (10 ft) below the foundation bottom. When the coil goes below the foundation the field amplitude decreases to a minimum thereby indicating the depth of a steel pile or reinforced foundation. Interpretation of the data from the Induction Field method is complicated by the existence of ferrous or other conductive materials in the bridge structure, and the presence of conductors (such as cables or pipes) in the ground around the pile. The IF test is only applicable to reinforced concrete foundations or steel piles that have accessible, electrically connected rebar/steel.

Borehole Radar

The Borehole Radar (BHR) test uses a transmitter/receiver radar antenna to measure the reflection of radar echoes from the side of the bridge substructure foundation as shown in Fig. 2c. The BHR test is most sensitive to foundations of steel or with steel, as the electromagnetic wave energy reflects strongly from steel. The BHR method is limited in its application by wet, conductive clays and salt water as the wave energy is severely attenuated by these subsurface conditions with high dielectric constants.

SELECTION OF NDE METHODS FOR UNKNOWN BRIDGE FOUNDATION DEPTHS

The research showed that the borehole-based Parallel Seismic method was both the most accurate and most applicable NDE method for the determination of the depth of unknown bridge foundations for bridge scour safety evaluation purposes. For this reason, the author suggests that at least initially, one Parallel Seismic test should be performed for each bridge to check the accuracy of depth predictions from any less costly surface methods that may also be applicable for a given foundation type. Ultraseismic or other surface methods that are proven to be accurate based on a comparison with the Parallel Seismic results may then be used with confidence to evaluate unknown foundation depths of other abutments and/or piers on a bridge.

It should be noted that as local experience is gained with the use of any of the borehole or surface NDE methods for various bridge substructure types and subsurface conditions, the accuracy and applicability of the methods will become much better known to DOT engineers. This local knowledge can then be used to further optimize the selection of NDE methods from technical and cost perspectives. Knowledge of unknown foundation bridge substructure will

range from knowing only what is visible to having design drawings and subsurface geology information without as-built plans.

PARALLEL SEISMIC NDE METHOD

Of all the NDE methods investigated during this research, the borehole Parallel Seismic (PS) method shown in Figure 2A was found to be the most applicable to all bridge foundation types. The PS method requires impacting the exposed portion of the substructure and monitoring the response of the foundation and surrounding soil with a receiver in a cased borehole drilled next to the foundation. As the wave energy is monitored by the receiver at depths parallel to and below the bottom of the foundation, it becomes typically weaker and slower below the foundation bottom. This change in the received signals with depth indicates the foundation depth.

Borehole Considerations

The location of the borehole to be drilled should be selected based on minimizing the impact to vehicular traffic. However, when the choice is between some traffic disruption during drilling and testing versus drilling from a barge when over water, it may be best to core and drill through the bridge deck if reinforcement can be avoided or cut with structural engineer approval. The PS method requires that a borehole be drilled next to the foundation to be tested, preferably satisfying the following conditions:

1. The borehole needs to be drilled as close as possible, preferably within 0.9 to 1.5 m (3 to 5 ft) or less from the edge of the foundation to be tested. This requirement is to reduce the effect of the surrounding soil, particularly at sites with unsaturated soil conditions. Where saturated soil conditions exist, PS tests have been successfully performed with larger horizontal offsets from foundation edges.

2. The borehole should extend at least 4.5 m (15 ft) below the minimum required foundation depth (from a capacity/scour perspective considering the subsurface geology) or suspected foundation depth, whichever is greater. This requirement is to ensure that data is collected to the depth of interest. If the borehole is not at least somewhat deeper than the foundation bottom, one can only determine that the foundation is at least as deep as the borehole.

3. The borehole should be cased with a plastic PVC casing of sufficient diameter to insert the NDE tools that will be used (typically 50 to 100 mm, i.e., 2 to 4 inch ID casing). Steel casing is not recommended for use since the steel has faster stress wave velocities than concrete and wood foundation materials, and it prevents the use of the Induction Field and Borehole Radar methods. For all foundation construction materials, the wave velocities through the material are higher than the velocity in the PVC casing. If steel casing is used, the wave traveling through the casing can be faster than the waves traveling through the foundation, thereby making the PS NDE results difficult to interpret.

4. A hydrophone receiver is used in the most commonly performed PS tests due to its omni-directional sensing capabilities and associated sensitivity to compression waves. The

hydrophone receiver must be surrounded by water inside and outside the casing in order to respond to the arrival of the wave energy. A hydrophone in air (without water coupling) will not detect energy traveling through the soil that has been emitted from the foundation element. Water coupling of hydrophones in a boring is easy to achieve where the ground water level is high or the foundation is in water, since then boreholes can be drilled using slurry or just water methods. A PVC casing must be inserted and clean water added to the casing if it is solid. If comparatively clean ground water (minimal fines) is present in a boring, then water can also be allowed to flow in through small sawcuts in a casing. In dry soils with sufficient clay and silt fines so that the boring drains slowly, clean water can be added to the casing and into the boring annulus. However, in dry, free-draining sands and gravels it may be difficult to maintain enough water in the boring to permit testing with a hydrophone. Consequently, in dry soils the borehole annulus around the PVC casing may need to be grouted to ensure good coupling between the borehole casing and the surrounding material. The grouting material should be bentonite based or a lean bentonite-cement mix to avoid having a material that has a similar fast velocity to the foundation material. In a grouted casing, it can be filled with water for hydrophone PS tests (fastest), or left dry and sealed for tests with a triaxial geophone to permit both compression wave and shear wave measurements in the PS test. If a triaxial geophone is used, one can also impact the ground above and measure the compression and shear wave velocities in the soils with a Downhole Seismic test. This information is useful if theoretical modeling of the PS test is to be done and it also provides data on the stiffness of the soils.

5. The casing should be water tight, capped at the bottom, water-filled and free of debris. The water tight casing is required if hydrophones are used as the receivers in the PS tests. Slots may be cut in the casing to permit easier filling provided there is no risk of sediments coming into the casing. Water pressure from the wave energy is measured by the hydrophones in the casing.

6. The internal diameter (ID) of the casing should be at least 50 mm (2 inches) to allow for the use of single hydrophones, multi-channel hydrophones and geophones, and may need to be larger depending on the actual equipment used.

Required Parallel Seismic Test Equipment

When a PS test is performed, it is required to record the impact force and the responses of the receivers. The equipment needed to perform the data collection includes:

1. Digital signal analyzer or PC based data acquisition system with a sampling rate of at least 100 kiloHertz (10 microseconds/12 bit digital data point) on at least 2 channels (4 channels needed for triaxial geophone) with at least 4096 data points per channel,

2. Signal differential amplifier(s) for hydrophone and geophone,

3. Instrumented impulse hammers weighing 1.4 to 5.5 kg (3 to 12 lb) to measure impact force and trigger data acquisition upon impact with power supply,

4. Hydrophone and/or triaxial geophone receivers with necessary cables, connectors, and

power supply (battery, inverter or generator).

Parallel Seismic Data Interpretation

The main objective of Parallel Seismic tests is to determine the depth of the unknown foundations. Based on the NCHRP 21-5 and 21-5(2) research results, several criteria were established for determining the foundation depths based on Parallel Seismic data as follows:

1. Breaks in the slope of the lines in a plot of depth versus recorded time (see Fig. 3),
2. Drop in energy amplitude below the bottom of the foundation (see Fig. 4), and
3. Diffraction of wave energy at the bottom of the foundation (see Fig. 5).

The vertical axes in Figs. 3-5 represent depth below the top of the casing. The horizontal axes represents recorded time in milliseconds (1 mSec = 0.001 seconds).

Examination of Figure 3 shows the case where subsurface conditions are uniform with depth (this usually means saturated soil conditions where the compression wave velocity is that of water, i.e. about 1500 m/s or 4900 ft/s). This allows one to determine the velocity of the foundation element, and to clearly see the foundation bottom as the point where the wave velocity is slower and the amplitude is weaker. The foundation bottom is then taken as the intersection of the foundation velocity line with the soil velocity line as shown in Fig. 3.

The break in the velocity slope is not as clear in the PS results shown in Fig. 4. However, there is a distinct drop in amplitude of the wave energy and a break in the data later in the record at 24 ft that indicates the foundation bottom. In Fig. 5, the arrival of the weaker and fastest compression wave energy is not visible at shallow depths as the data is dominated by tube waves traveling in the PVC cased boring. The tube waves were generated by the pilecap footing which acted as a "speaker" to emit wave energy into the soils that coupled into the cased borehole to generate the tube waves. However, some of the weaker compression wave energy did indeed reach the bottom of the steel H-piles whereby it diffracted into the surrounding soils and generated upward and downward going tube waves in the borehole as well. This arrowhead feature in Fig. 5 accurately indicated the depths of the steel H-piles. Steel H-piles have comparatively high attenuation of wave energy properties due to their comparatively large surface area to cross-sectional area ratio versus solid, round piles and other foundation shapes.

US METHOD FOR UNKNOWN BRIDGE FOUNDATION DEPTHS

The surface Ultraseismic (US) method was researched and developed during the NCHRP 21-5 research for determination of the unknown depths of bridge foundations. The Ultraseismic method is a sonic reflection technique that uses geophysical digital data processing techniques. With the US method, one analyzes the propagation of induced compression and flexural waves as they reflect from foundation substructure boundaries (impedance changes, i.e. changes in the multiple of wave velocity x density x cross-sectional area). This is the same principle that the Sonic Echo/Impulse Response and Bending Wave methods rely on as well. However, the data acquisition and processing for the US method involves recording and display of multiple channels of data to better track the reflections from foundation element interfaces and bottoms as discussed below. The Ultraseismic Vertical Profiling method is shown above in Fig. 1C.

The Ultraseismic method was researched and developed by Olson Engineering to overcome the difficulties encountered by the Sonic Echo/Impulse Response method and the Bending Wave method tests on non-columnar and complex columnar bridge substructures. The Ultraseismic method is a broad application of geophysical processing to both the Sonic Echo/Impulse Response and Bending Wave tests in that the initial arrivals of both compression and bending waves and their subsequent reflections can be analyzed to predict unknown foundation depths.

Two types of Ultraseismic test geometries have been specifically introduced for this problem: US Vertical Profiling and US Horizontal Profiling. For a one dimensional imaging of the foundation depth and tracking the upgoing and downgoing events, the term Vertical Profiling (VP) test method is used as shown in Figure 3 below. In this method, the bridge column or abutment is hit from the top or bottom (both vertically and horizontally) and the resulting wave motion is recorded at regular intervals down the bridge substructure element. Typically, three-component recording of the wavefield is taken in order to analyze all types of ensuing wave motion. A VP line can be run in both a columnar (a bridge pier or pile foundation) and a tabular (a bridge abutment) structure.

For two-dimensional imaging of the foundation depth, the term Horizontal Profiling (HP) test geometry is used where there is flat, horizontal access for testing such as the top of an accessible pier or abutment. In this less commonly applicable US method, the reflection echoes from the bottom are analyzed to compute the depth of the foundation. The source and receiver(s) are located horizontally along the top of accessible substructure, or any accessible face along the side of the substructure element, and a full survey is taken along the top of the element.

The main objective of Ultraseismic tests is to determine the unknown depth of the foundation. Example US results from the NCHRP research are presented herein to illustrate the use of the method and the interpretation of the results. The source/receiver layout for Ultraseismic Vertical Profiling tests on one of the pier columns of Bridge No. 5188, Minnesota Highway 58 in Zumbrota is shown in Fig. 6. The source point was able to be located vertically on top of the concrete beam. Thus, impacts were applied with downward vertical impacts to the top of the beam over the column using a 1.4 kg (3 lb) impulse hammer with a hard plastic tip. A 3-component accelerometer was mounted on the side of the exposed portion of the column at intervals of 0.15 m (0.5 ft) from 1.5 m (5 ft) below the top of the beam to near the ground surface.

Field data for a Vertical Profiling test done to measure flexural waves is shown in Fig. 7. The depth shown in Fig. 7 represents the depth below the top of the concrete beam. All data were debiased to remove any DC shift and f-k filtered to enhance upgoing waves. After this processing, two clear reflection events are apparent in the data. The first reflector corresponds to a depth of 2 m (6.5 ft) below Receiver 24 at a depth of 5 m (16.5 ft) below the top of the concrete beam as shown in Fig. 7. The flexural wave velocity of 1,770 m/sec (5,800 ft/sec) was determined from the slope of the initial downgoing and reflected upgoing waves. This reflection corresponds to a depth of 7 m (23 ft) from the top of the concrete beam. The actual depth of the foundation was equal to 9.4 m (31 ft).

Further examination of Fig. 7 shows there is a second reflector at a depth of 4.3 m (14 ft) below Receiver 24 at a depth of 5 m (16.5 ft) below top of concrete beam. This reflection corresponds to a depth of 9.3 m (30.5 ft) from the top of the concrete beam. The actual depth of the foundation was equal to 9.4 m (31 ft). The shallower reflection is most likely due to a change in the subsurface material properties at this depth which is below water. The most important thing to note in Fig. 7 is that the flexural wave energy is first tracked down the bridge substructure, and that upgoing events correspond to reflectors whose depth can be predicted with geometry as shown. Downgoing events from the bridge structure above the impact point can be eliminated in the US data with the use of f-k filtering.

CONCLUSIONS

The NCHRP 21-5 and 21-5(2) research resulted in greatly improved understanding of the applicability and accuracy of such NDE methods using sonic, ultrasonic, seismic, magnetic and electromagnetic techniques. Of all of the methods researched, the borehole Parallel Seismic Method was found to be the most accurate and versatile method for determining unknown foundation depths for the broadest range of foundation types. The surface Ultraseismic Method was found to be the most accurate method for determining single substructure element depths such as piles, piers, abutments, etc. However, the Ultraseismic method does not provide data on the elements below the first major change in cross-section, such as a pier with a pilecap on piles, where the piles will not be detected.

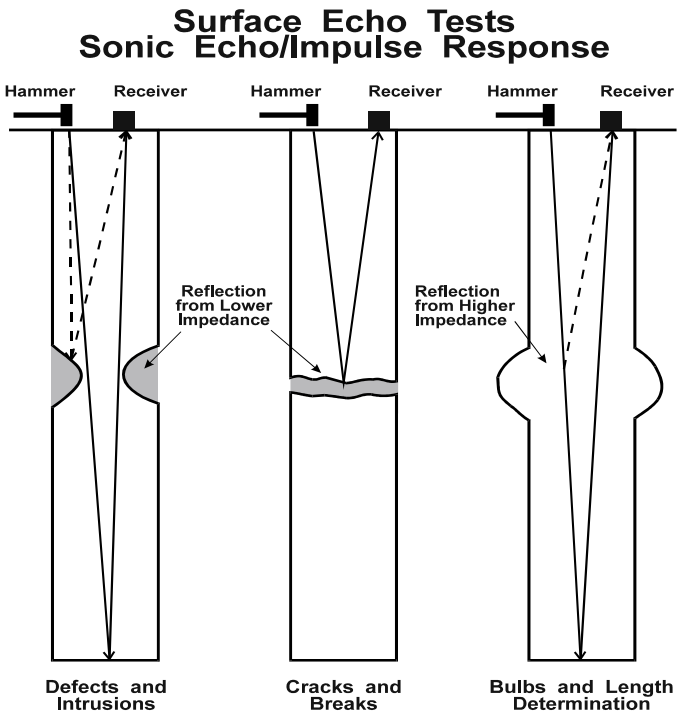

Figure1a - Sonic Echo/Impulse Response Method

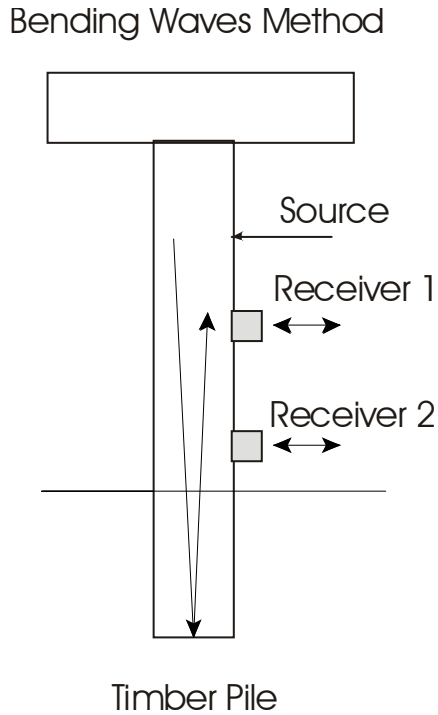

Figure 1b - Bending Waves Method

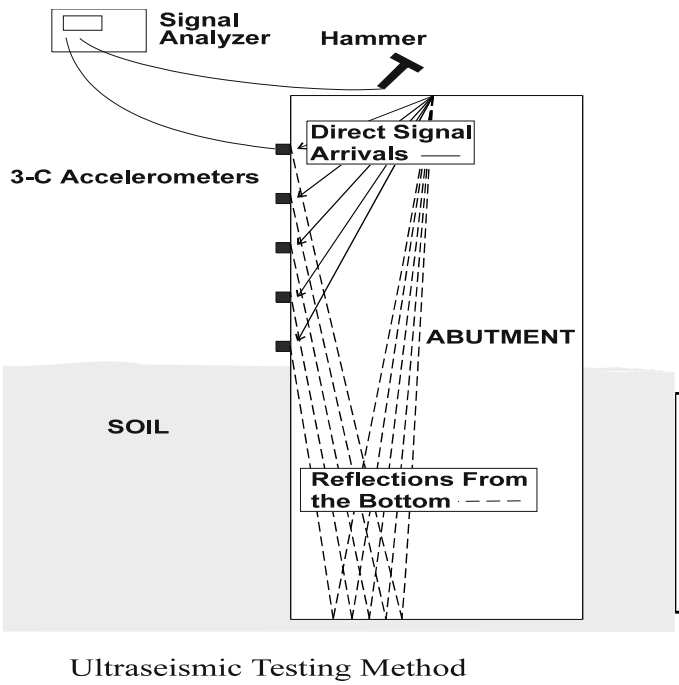

Figure 1c - Ultraseismic Method – Vertical Profiling

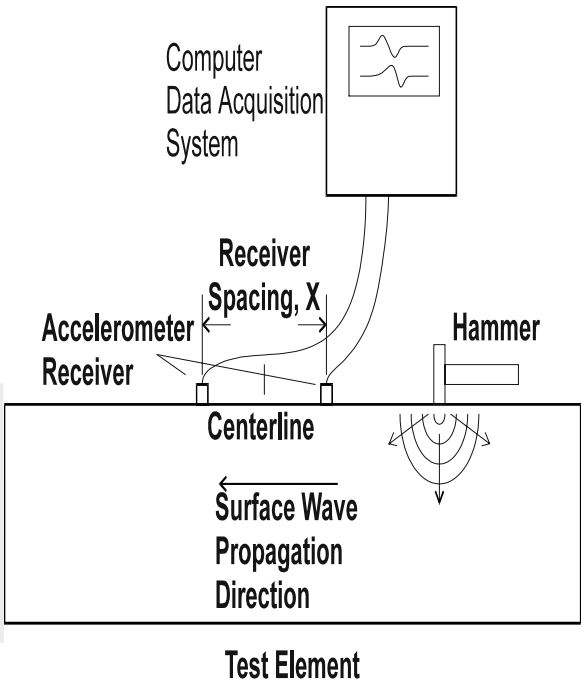

Figure 1d - Spectral Analysis of Surface Waves

Figure 1 – Surface-Based NDE Methods

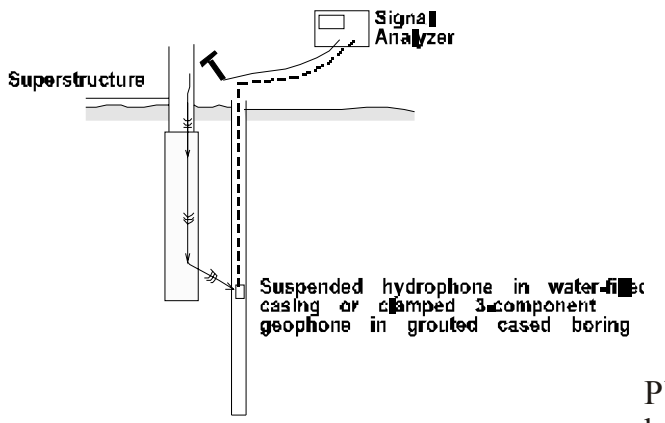

Figure 2a - Parallel Seismic Method

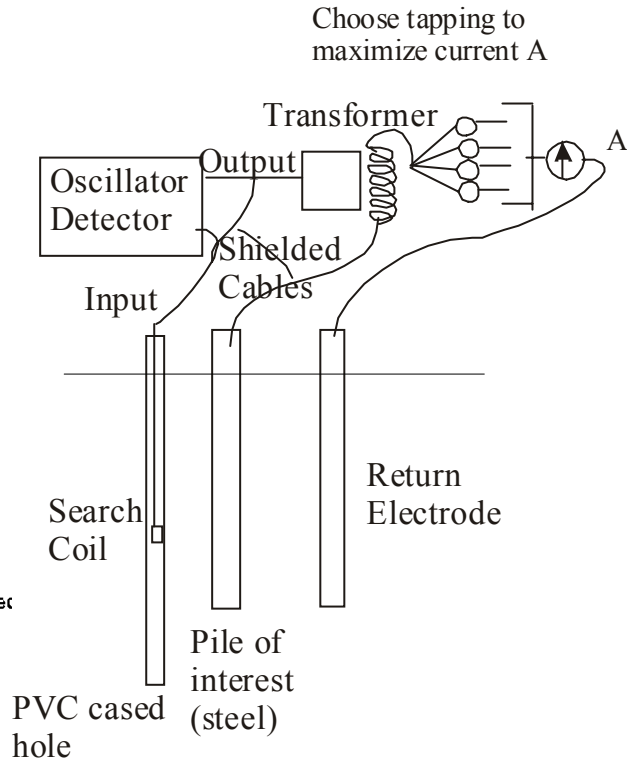

Figure 2b - Induction Field Method

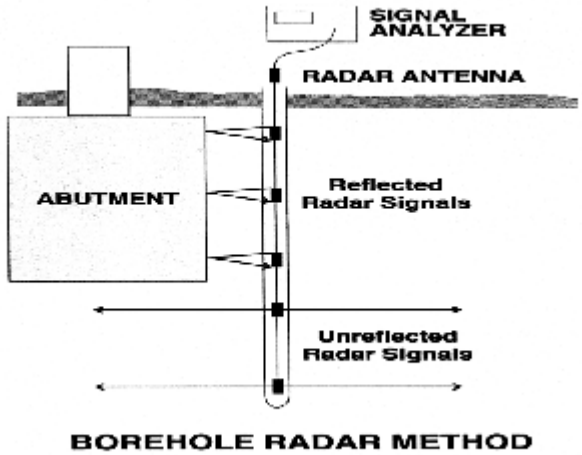

Figure 2 - Schematics of Borehole-Based NDE Methods

Figure 2c - Borehole Radar Method

Compression Wave Velocity in timber pile = 13,500 ft/sec

Pile tip at a depth of 22 ft

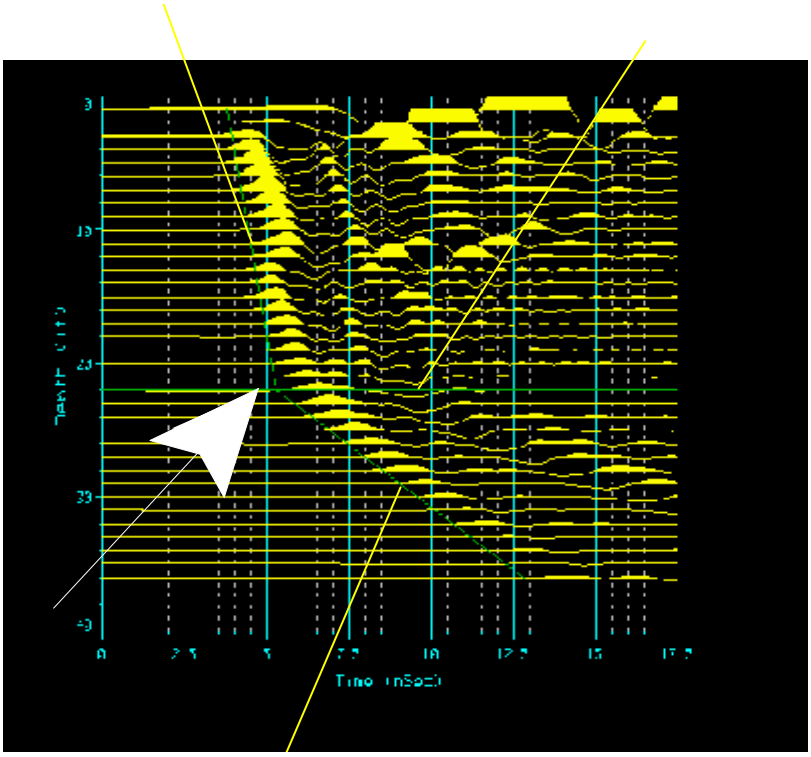

Figure 3 - Parallel Seismic Result for Bridge Timber Pile Foundation Data from a 12-lb Horizontal Hammer Hit and Vertical Geophone Component, Wake County Bridge # 251, North Carolina

Comments:

Depth shown in figure is depth below top of borehole
Drop in amplitude below a depth of 24 ft
Bottom depth = 24 ft (reference is top of borehole)
Top of borehole is 2.6 ft below top of pile
Pile length = 24+2.6 = 26.6 ft (reference is top of pile)

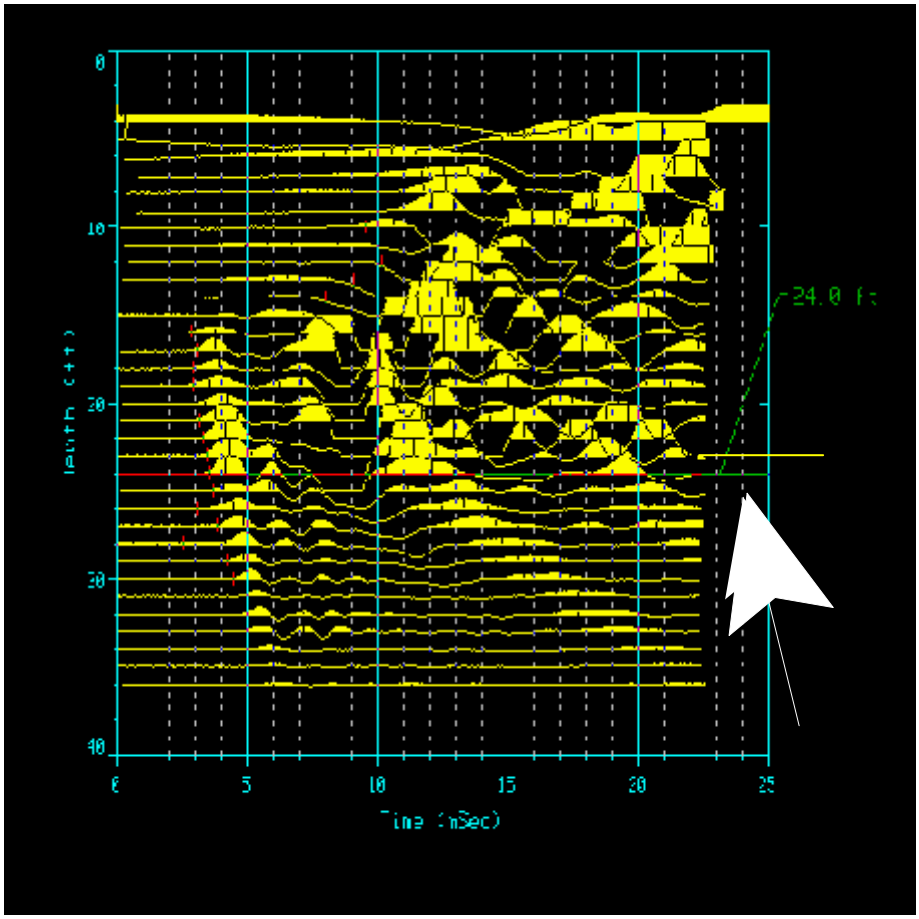

Drop in amplitude below bottom of foundation

Figure 4- Parallel Seismic Data from a 12-lb Vertical Hammer Hit
and Vertical Component Recording of Geophone
Wilson County Bridge # 5, Bent 1, East Pile, North Carolina
Example of Drop in Amplitude below Bottom of Foundation.

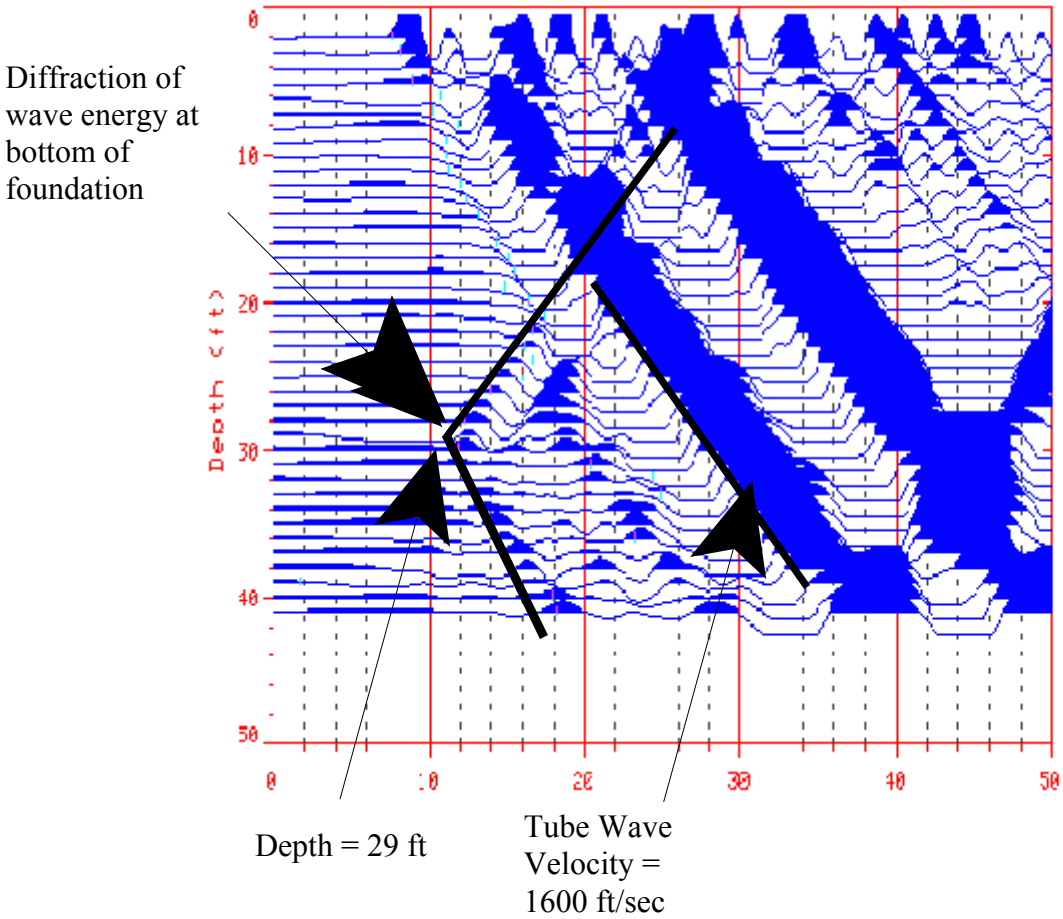

Figure 5- Parallel Seismic Data from a 12-lb Hammer Horizontal Hit and Single Hydrophone Recording,
Steel H-Pile Foundation with Concrete Pilecap on Top
Coors Bridge, Golden, Colorado
Example of Diffraction of Wave Energy at Bottom of Foundation.

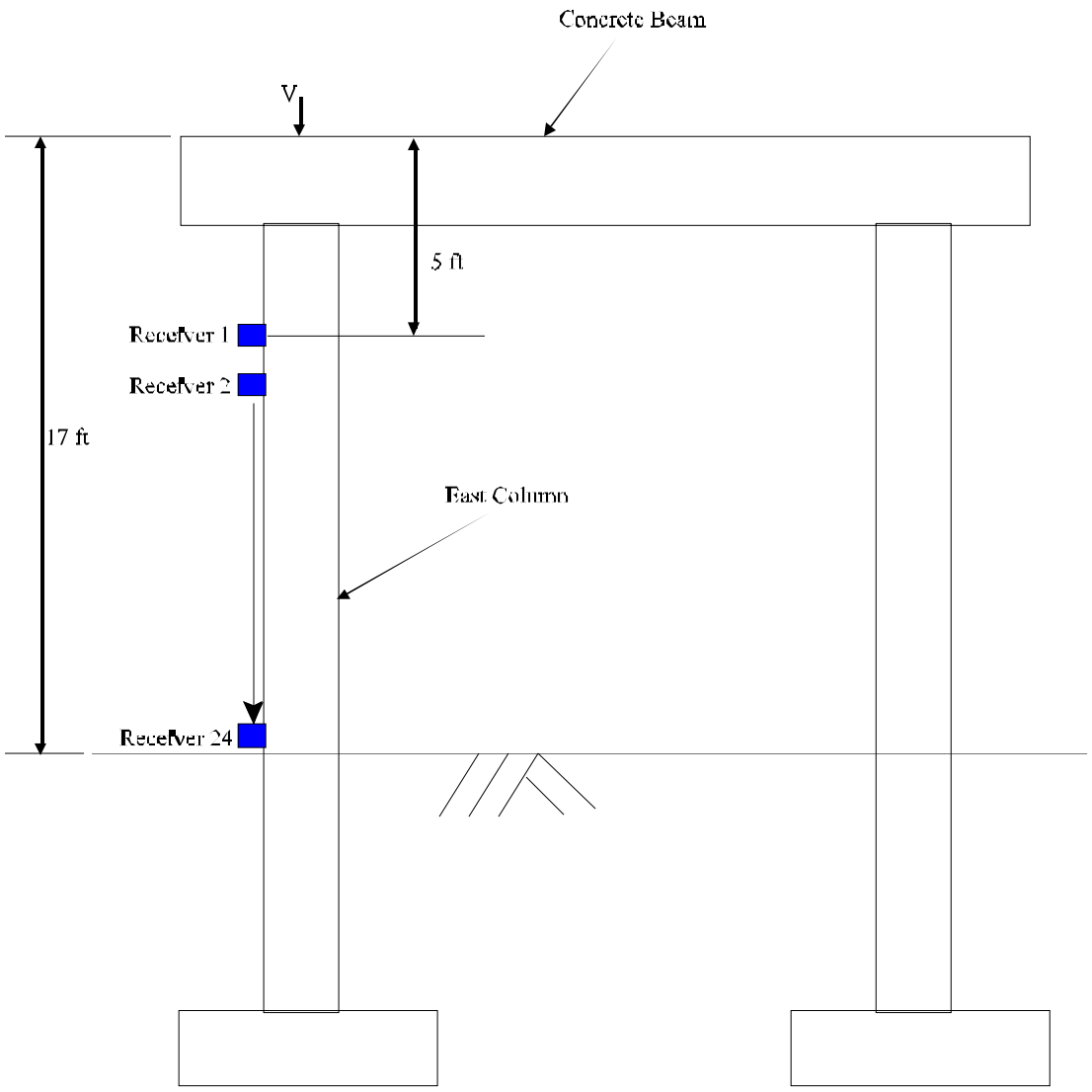

V = Vertical Hammer Hit Location
24 Accelerometer Receiver Locations at Intervals of 0.5 ft

Figure 6 - Source/Receiver Layout for Ultraseismic Tests Performed at Bridge No. 5188
Minnesota Hwy 58, Zumbrota, Minnesota

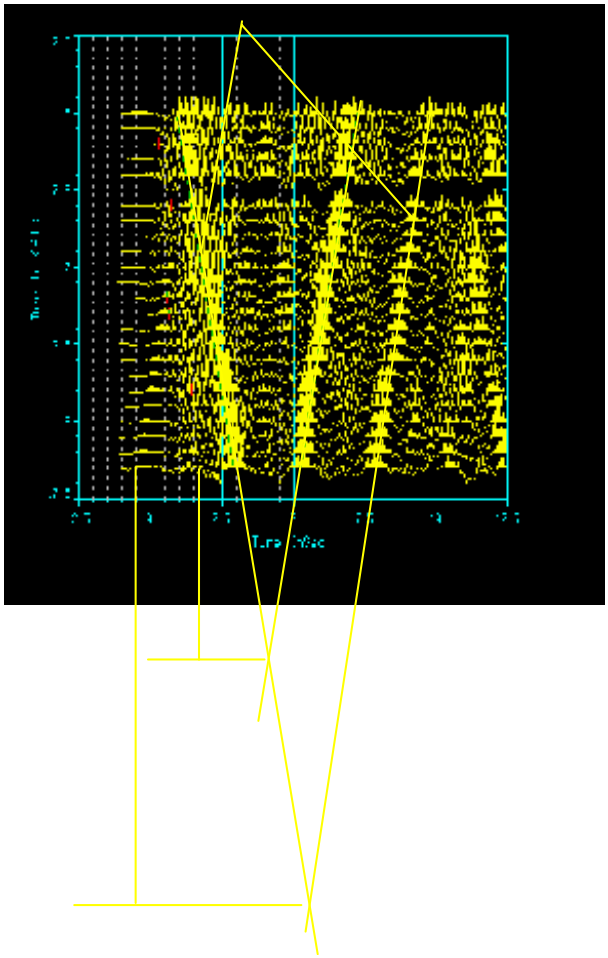

Flexural Velocity at top arrows equals 5,800 ft/sec
Depth shown in Figure is depth below top of pier
Depth of first reflector = 16.5 + 6.5 = 23 ft (reference is top of pier)
Depth of second reflector = 16.5 + 14 = 30.5 ft (reference is top of pier)

Figure 7 - Ultraseismic Data from a 3-lb Vertical Hammer Hit
and Radial Component Recording f-k Filtered to Enhance Upgoing Waves
Bridge No. 5188, Minnesota Highway 58, Zumbrota, Minnesota

Scour of Railway Embankment Foundation Located on Sea-Cliff in Japan

By

Hiroto Suzuki [1], Makoto Shimmura[2]

ABSTRACT

This article depicts a scour damage case of a railway embankment located on sea-cliff and discusses the estimated causes and mechanism of the damage process. The wave protection work with 21.7 m width and 6.5 m height of the railway embankment, which was located on the cliff front of the Sea of Japan between the stations Murakami and Mazima of Uetsu Line, fell down, and the embankment collapsed in December 2000. The main cause of the collapse is presumed to be scour of the wave protection work foundation. The scour seems to be reduced by the high waves attack on the occasion of the seashore retreating at the collapse site judging from the meteorological data analysis and aerial photograph decipher.

INTRODUCTION

It is often the case in Japan that railway tracks located on cliff front have been constructed on embankments protected by retaining walls against the harms of high waves. Score damages of wave protection works are of grave concerns of engineers who take charge of the maintenance of those structures.

Only three cases have been identified that scour by high waves brought about wave protection works of the railway track to fall down in recent two decades. Occurrence dates, sites and high waves causes of three cases are as follows (Figure 1), The first is at Hokuriku Line by winter monsoon on November 2, 1989[1)], the second at Nemuro Line by typhoon on September 16, 1998[2)], and the third at Uetsu Line by low on December 19, 2000.

It is important to investigate the cause of the rare and large-scale damage event

[1] Assistant chief of section, Research and Development Center, East Japan Railway Company, h-suzuki@jreast.co.jp

[2] Senior Chief Researcher, Research and Development Center, East Japan Railway Company, m-shimamura@jreast.co.jp

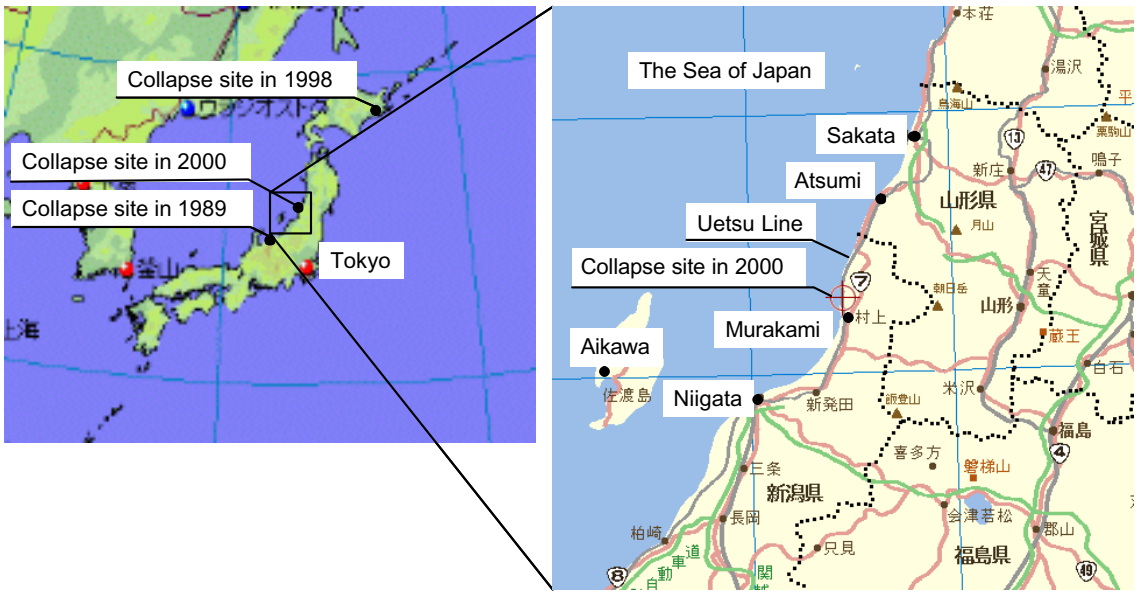

Figure 1　Locations of the collapse site

and to make it known to engineers to reduce the risk of the railway accident. This paper describes the last one among the above three cases and discusses scour problems of the wave protection work located on the cliff front in Japan referring to the weather condition prior to the occurrence of the event and the topography change in and around of the site.

OUTLINE OF THE COLLAPSE

The wave protection work, which was located on the cliff front of the Sea of Japan between the stations Murakami and Mazima of Uetsu Line in Niigata Prefecture, was scoured, and it and the embankment collapsed presumably at 19:26 on December 19, 2000. Figure 1 shows the location of the collapse site of the wave protection work and the embankment. Uetsu Line links between the stations Niigata and Akita along the Sea of Japan. At the collapse site outbound line and inbound line are about 600 m apart.

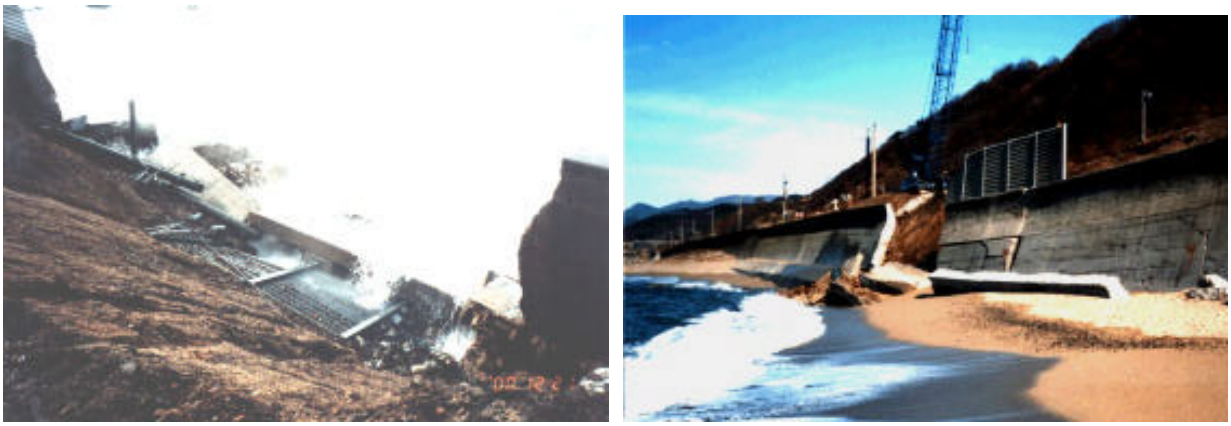

Photo 1　The collapse site of the wave protection work and the embankment

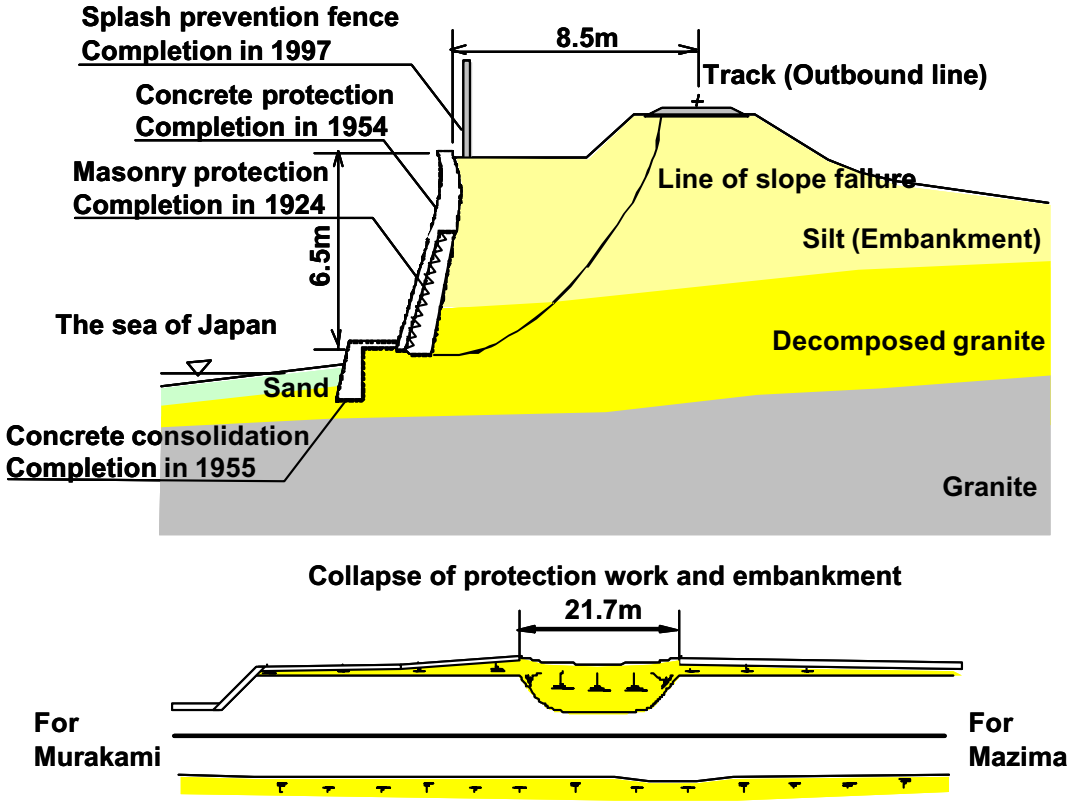

Figure 2 The section and plane diagram of the collapse site

Outbound line, at which the collapse occurred, is laid on the cliff front of the Sea of Japan, and inbound line passes by tunnel in mountain.

Photo 1 is photographs of the collapse site. Figure 2 shows the section and plane diagram of the collapse site of outbound line. The basement rock in and around the collapse site is granite formed from the latter term of Cretaceous period to Paleogene period. Upper layer of it is decomposed granite. The embankment made of silt was constructed on it. This site has 137 m long and from 5 m to 7 m high wave protection work of the railway embankment. The masonry protection work was constructed in 1924, when the present outbound line was laid. In 1954 the front of the masonry protection work was reinforced by concrete and the concrete parapet was constructed, and moreover in 1955 the concrete consolidation of foundation was constructed at the foundation of the wave protection work. In 1997 the splash protection fence was built at the top of the wave protection work, because splash can easily go over the top of the wave protection work, when it was high waves.

The wave protection work and the embankment with 21.7 m width and 6.5 m height collapsed due to scour of the wave protection work foundation. The slope failure reached up to the track ballast layer. The volume of the soil collapsed was about 450 m^2. Moreover about 30 m section each of both sides of the wave protection work collapse was out of the perpendicular.

Train operation was suspended immediate after the collapse occurred. Train operation could be recommenced by single track operation using inbound line on December 20, the day after the collapse day, because outbound line and inbound line are

apart, Thereafter urgent repair work of the collapse site was completed on February 5, 2001, train operation to use outbound line and inbound line was recommenced. In the present repair work is under construction, and it will be completed on December 2003.

WEATHER CONDITION OF THE DAY OF THE COLLAPSE

Photo 2 shows the waves condition of the collapse site before 2 hours of the collapse occurrence, at about 17o'clock on December 19. The sea was rough and splash covered on the railway track. These high waves seem to be the immediate cause of the wave protection work collapse.

Photo 2 The waves condition of the collapse site before 2 hours of the collapse occurrence

Figure 3 is weather maps at 15 o'clock and 21 o'clock of the collapse day, on December

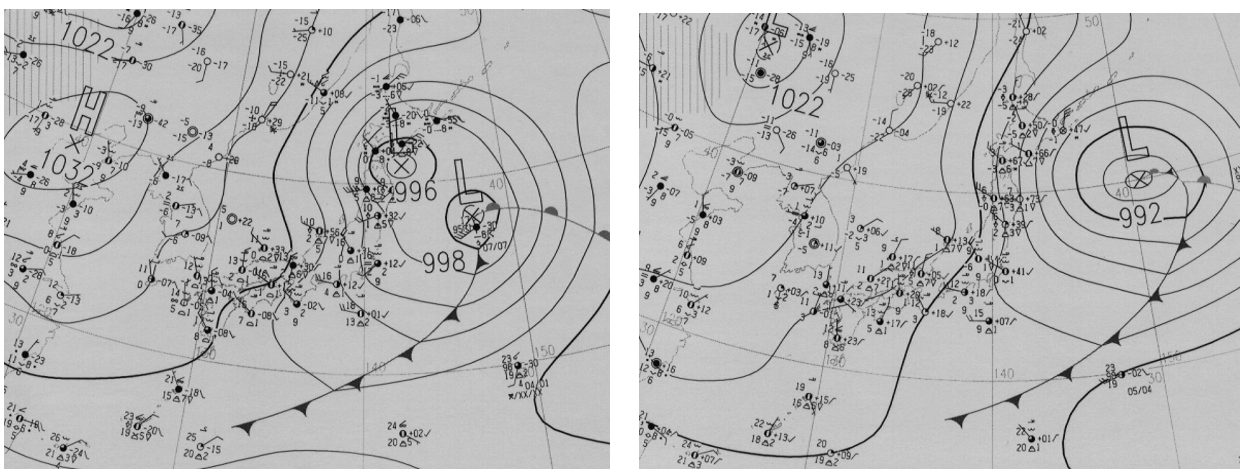

Figure 3 Weather maps at 15 o'clock(left) and 21 o'clock (right) on December 19, 2000

19, 2000. At 15 o'clock there were two deepening lows in the Pacific Ocean which traveled toward the northeast. At 21 o'clock two lows became one and the pressure of low was lower. In the Eastern and Northern Japan it blew strong wind under influence of these lows.

Figure 4 shows time history of wind velocity, precipitation, and temperature at Murakami(Figure 1), where is the nearest meteorological observation site of Japan Meteorological Agency(JMA) from the collapse site. The wind direction changed from east-north-east to south-west, and temperature rose at about 9 o'clock. At that time the low passed over near Murakami. After this the wind velocity grew gradually strong, and

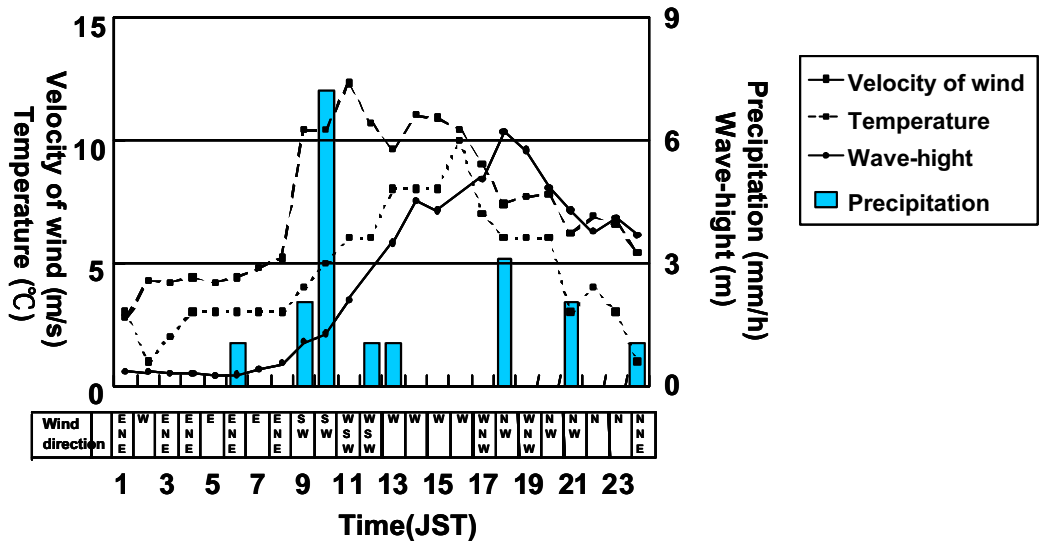

Figure 4 Time history of wind velocity, precipitation, and temperature at Murakami, and significant wave height at Atsumi on December 19, 2000

Table 1 The maximum instantaneous wind velocity of the day of the collapse at Niigata, Aikawa, and Sakata on December 19, 2000 and the return period of it

Observation site	Maximum instantaneous wind velocity (m/s)	Wind direction	Time	Return period (year)
Niigata	30.3	WSW	15:50	Below 2
Aikawa	35.7	W	11:20	7
Sakata	32.1	W	14:05	Below 2

Table 2 The maximum wind velocity of the day of the collapse at Niigata, Aikawa, and Sakata on December 19, 2000 and the return period of it

Observation site	Maximum wind velocity (m/s)	Wind direction	Time	Return period (year)
Murakami	10	W	16:00	5
Niigata	16.4	WSW	11:10	Below 2
Aikawa	21.6	WNW	13:10	3
Sakata	19.1	WNW	15:10	3

the maximum wind velocity which is 10 m/s was recorded at 16 o'clock. 0 to 12 mm hourly rainfall was observed, but it was not a heavy rain to cause of the wave protection work collapse.

Table 1 shows the maximum instantaneous wind velocity of the collapse day at Niigata, Aikawa, and Sakata(Figure 1), where are near meteorological stations of JMA from the collapse site. Table 2 shows the maximum wind velocity at Murakami, Niigata, Aikawa, and Sakata. In the east area of the Sea of Japan the strong wind, the maximum

instantaneous wind velocity is over 30m/s and the maximum wind velocity is over 10m/s. Table 1 and 2 also show return periods of the maximum instantaneous wind velocity and the maximum wind velocity, return periods of them are between below 2 years and 7 years. These high waves like photo 2 were induced by the strong wind in the east area of the Sea of Japan.

Figure 5 is wave maps at 9 o'clock on December 19 and 20, 2000. In the eastern area of the Sea of Japan waves were high.Figure 3 also shows time history of significant wave height at Atsumi(Figure 1), where is the nearest wave observation site of JMA from the collapse site. The significant wave height grew gradually high from 9 o'clock. The maximum significant wave height and wave height, which were 6.19 m and 11.8 m, were recorded at 18 o'clock when almost accords with the time of the wave protection work collapse. Table 3 shows returns period of them, it is below 2 years.

The wind of the collapse day was strong and waves were high, but they were not extremely rough as far as judging from the meteorological data. Though the immediate cause of the wave protection work scour seems to high waves, topography change in and around of the collapse site is presumed to affect the scour.

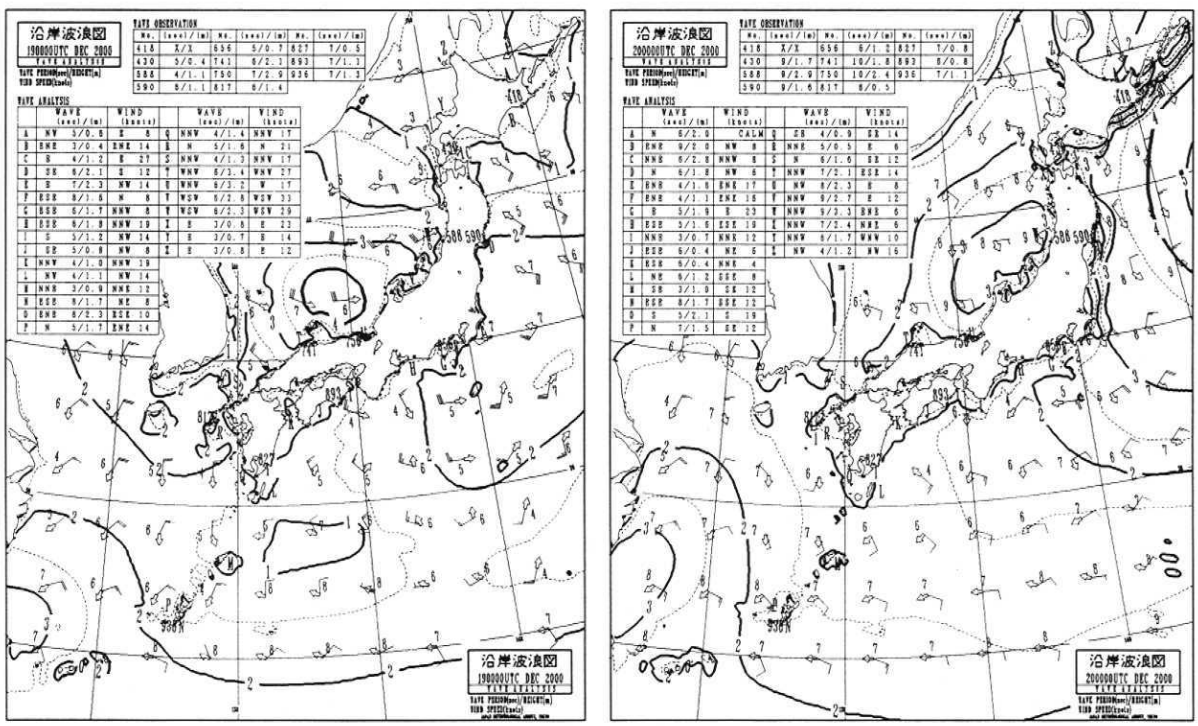

Figure 5 Wave maps at 9 on December 19 and 20, 2000

Table 3 The maximum wave height and the maximum significant wave height at Atsumi, and the return period of it

	Wave height (m)	Time	Return period (year)
Wave height	11.8	18:00	Below 2
Significant wave height	6.19	18:00	Below 2

TOPOGRAPHY CHANGE IN AND AROUND OF THE COLLAPSE SITE

In Japan, coastal erosion progresses at many places in the present. Though Japan has about 34,000 km coastal line, eroding coast was 32% of the full length of the coastal line in 1965. Moreover it gradually increased, 47% in 1985 and 59% in 1995. The cause of the coastal erosion is decrease in sand supply from rivers, because dams and soil saving dams were constructed in the upper and middle reach of rivers.

Figure 6 is aerial photographs and plane diagram in and around the collapse site. In some place of seashore there are outcrops of granite. But there is no outcrop in front of the collapse site. The length of sandy beach of no outcrop site is shorter than one of outcrop sites. According to photograph decipher, the length from the wave protection work to beach line was 40 m in 1959. However, it gradually decreased, in 1976 it was 20 m, and in 1988 it was 18 m, and in 1996 it became 13 m.

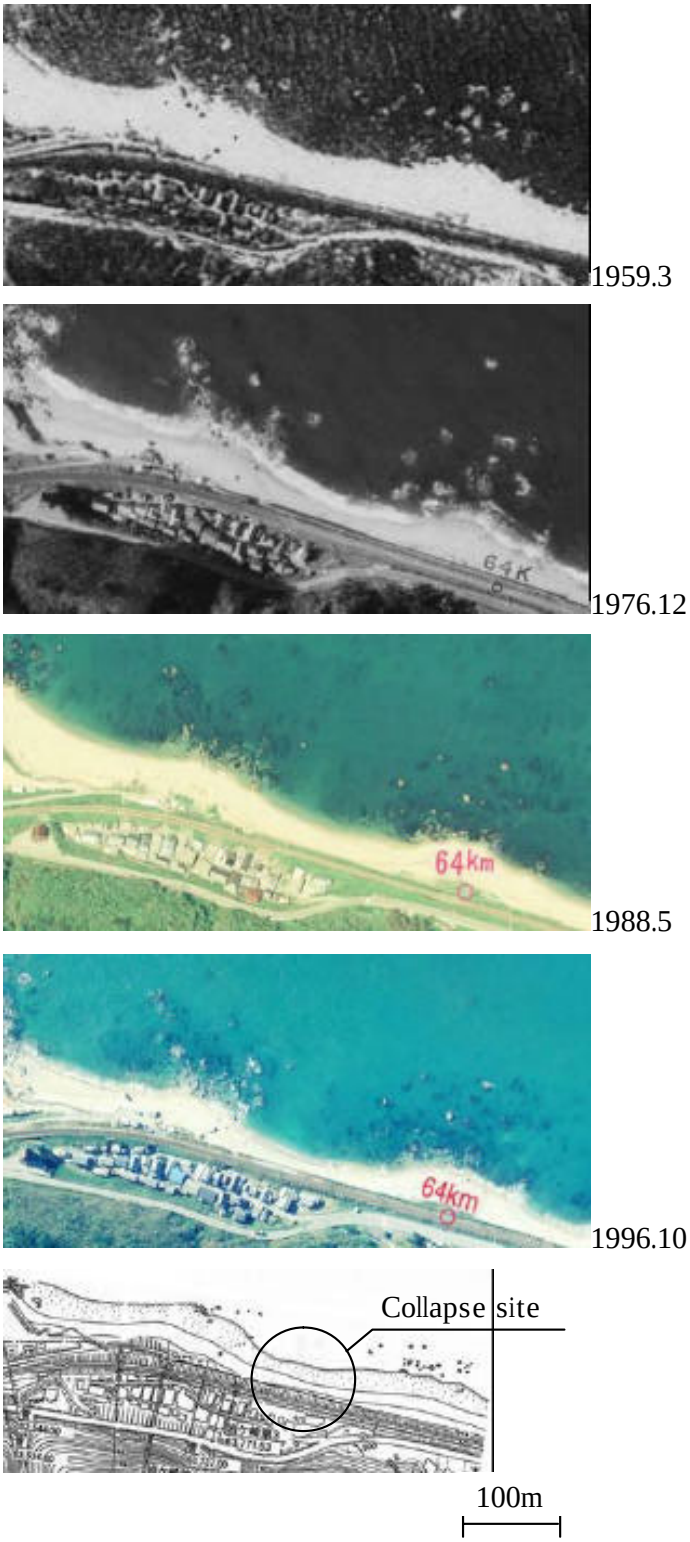

Figure 6 The aerial photographs and plane diagram in and around the collapse site.

The cause of the seashore retreat seems to be the decrease in sand supply from Miomote river. There is the mouth of this river at a distance of 1 km from the collapse site. At the upper reach of this river, Miomote dam and Saruta dam were built in 1953 and 1957. It is most probable that the decreases in supply of sand from rivers were caused by the influences of by the construction of these dams. There are no major rivers which can supply a large amount of sand to the seashore in an about 40 km long section

in southbound from the site, and in about 80 km long section in northbound. This could accelerate the seashore retreat.

Wave energy hitting the wave protection work gradually increased with the progress of the seashore retreat. From about 1996 splash became to easily go over the top of the wave protection works, when it was high waves, as a result, in 1997 the splash prevention fence was built at the top of the wave protection work. Therefore the seashore retreat seems to work as the indirect cause of the scour and collapse of the wave protection work.

CAUSE OF THE COLLAPSE

According to the meteorological data analysis and aerial photograph decipher, the immediate cause of the collapse is the attack of high waves reduced by strong wind, and the indirect cause is the seashore retreat at the collapse site. The presumption mechanism of the damage process is as follows (Figure 7):

1. The seashore in the front of the collapse site gradually retreated by decrease in sand supply.
2. Wave energy hitting the wave protection work increased by the seashore retreat. Moreover splash became to easily go over the top of the wave protection work.
3. The foundation of the wave protection work was gradually scoured by high waves. Moreover soil relaxation progressed with sea water by splash.
4. The wave protection work and embankment collapsed by the scour of the wave protection work foundation reduced by high waves attack on December 19, 2000. Moreover the increase of hydraulic pressure in embankment with sea water supplied by high waves is presumed to affect the slope failure.

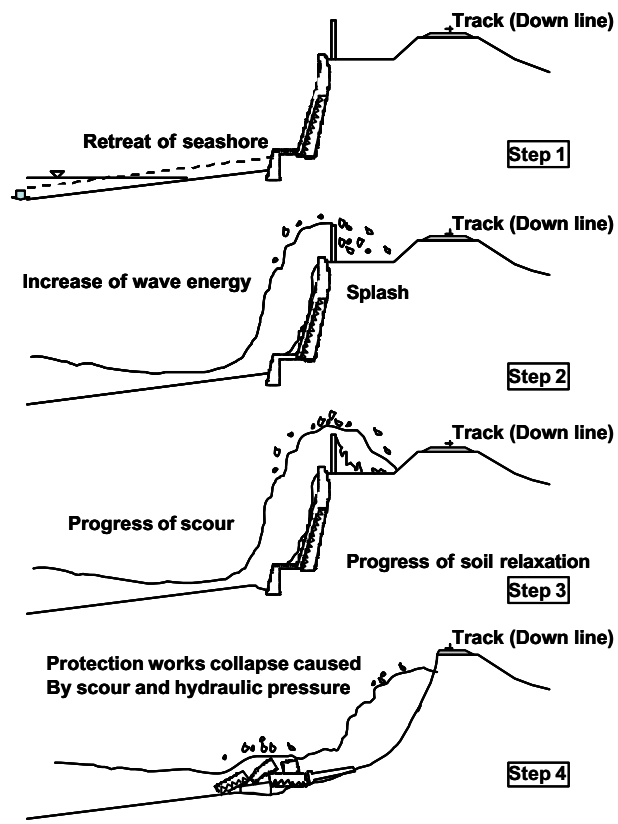

Figure 7 The process of the wave protection work collapse

CONLUSION

1. The foundation of the wave protection work of the railway embankment, which was located on the cliff front of the Sea of Japan, was scoured, and the wave protection work and the embankment collapsed on December 19, 2000. According to the meteorological data analysis and aerial photograph decipher, this scour is estimated to be reduced by high waves caused by the low on the occasion of the seashore retreating in front of collapse site. Moreover the increase of hydraulic pressure in embankment with sea water supplied by high waves is presumed to affect the slope failure.
2. This scour occurred by high waves of which return period is below 2 years. On the other hand, in the present, coastal erosion progresses all over Japan. Therefore judging from this study, at the region of seashore retreating, there is a possibility that a wave protection work is scoured by same process of this scour.
3. We investigated all wave protection works of railway tracks in East Japan Railway company area. As a result of the investigation seashore retreating is progress at three sites. We make plan to reinforce foundations of there wave protection works.

ACKNOWLEDGMENTS

We thank Mr. Hisashi Muraishi of Railway Technical Research Institute for his useful advice and a great help especially in the presumption of the mechanism of the collapse. In this study, we used the weather and wave maps drawn by Japan Meteorological Agency(JMA), and used the meteorological data observed by JMA.

REFERENCES

1) Murakami A. And Noguchi T. 1998: Maintenance of railway structures, Japan railway facilities association, p505-509. (in Japanese)
2) Shimamura S., 1999: Protection work collapse and repair work between the stations Monshizu and Akkeshi of Nemuro Line, Journal of Japan railway facilities association, 37-6, p15-17. (in Japanese)
3) Committee of Coastal Engineering, Japan society of civil engineers, 1998; Creation of littoral drift environment, Maruzen, p1. (in Japanese)

Design and Construction of Scour Foundations for Electric Power Transmission Line Structures

by

Peter M. Kandaris[1], Robert E. Kondziolka[2], James P. Adams[3]

ABSTRACT

Electric power transmission lines can extend over great distances encountering variable geologic and geotechnical conditions that include both active and ephemeral waterways. This paper will discuss the analysis, design and construction of transmission line foundations within flood plains of the desert Southwest.

Determination of foundation dimensions typically requires a knowledge of subsurface strata properties and structural loading. More comprehensive knowledge typically results in more efficient, reliable and economical foundation systems. Waterways introduce added variables of hydraulic force, general bed degradation and transient pier scour. For such foundation systems, additional hydrological information such as stream geometry and flow characteristics must be ascertained in order to optimize design. Furthermore, a probabilistic approach for ephemeral channels should be used to evaluate the chance occurrence of maximum structural loading due to simultaneous wind and water events.

Construction of scour-resistant foundations in the desert Southwest is generally performed during times of low or no-flow conditions, when access is possible in the dry. Scour-resistant foundations for electric transmission line structures are typically drilled piers of greater diameter and depth than normally required. These increases in depth and diameter may create significant challenges for construction that include unstable soils and transient groundwater conditions. Occasional unanticipated flooding is always a concern and must be considered in scheduling construction.

INTRODUCTION

Stream channels in the desert Southwest are normally dry. Flows occur during infrequent periods of runoff and from flash flooding or by subsurface flow from water in-filled fractures beneath mountains. Quantitative information on the frequency, volume and duration of these ephemeral stream flows is often difficult to obtain. Substantive quantitative information becomes even more difficult to obtain since most major waterways in this region include flood control and water diversion features that further limit flow events.

[1] Principal Civil Engineer, Electric System Engineering, Salt River Project, Phoenix, Arizona 85072-2025, USA (pmkandar@srpnet.com)
[2] Manager, Transmission Planning, Salt River Project, Phoenix, Arizona 85072-2025, USA (rekondzi@srpnet.com)
[3] Senior Civil Engineer, Electric System Engineering, Salt River Project, Phoenix, Arizona 85072-2025, USA (jpadams@srpnet.com)

Nonetheless, foundations in these ephemeral waterways must be designed with anticipation of scour from storm events. Embedment analysis includes data from both geotechnical and hydrologic studies. Investigations must take into account not only the anticipated foundation embedment required for support of the structure, but must also evaluate the potential loss of soil support resulting from embankment wash-out, general bed degradation and local scour around the pier. Studies need to be sufficiently deep (in some cases, up to 100 feet below bed surface) to account for substantial scour-induced ground loss.

Foundations for electric transmission line structures typically extend above high water flow elevations (Figure 1). This extension, together with allowance for bank wash-out, bed degradation and local scour loss results in substantial unsupported foundation lengths, sometimes as high as 60 feet. The unsupported foundation length extending above this point is considered reveal (or stick-up). The reveal provides no lateral support and resistance to lateral forces must come from soils below this section.

Geotechnical properties of stream bed deposits need to be determined to sufficient depths for analysis of scour conditions. Particle size analyses or estimates of gradations are essential in determining the depths of general bed degradation.

Figure 1
Electric Transmission Structures
Foundations Designed for
Scour Conditions
(Phoenix, Arizona)

SCOUR AND LOAD ANALYSIS

Drilled pier foundations within stream channels impede normal water flow patterns. This impedance results in increased flow velocities adjacent to the foundation and the development of eddy currents both in front of and behind the foundations causing local scour. In addition, general stream degradation from variable flow events can reduce the nominal bed elevation. Foundations must be designed to not only compensate for ground

loss due to degradation and local scour, but to withstand additional lateral forces due to water flow against the foundation.

Numerous investigators have developed methods from both empirical and experimental studies for analyzing scour loss in the desert Southwest, specifically around pier foundations (Simons, Li & Associates, 1985). The basic elements of the analysis include flow depth and direction, pier shape and dimensions, and flow velocity.

One generally accepted analysis method utilized in the region is an adaptation of the Colorado State University equation for determining local pier scour (Richardson, et al., 1991):

$$y_a = 2.0 \cdot y_1 \cdot k_1 \cdot k_2 \cdot k_3 \cdot k_4 \cdot \left(\frac{a}{y_1}\right)^{0.65} \cdot Fr^{0.43}$$

where:

y_a = scour depth (ft)
y_1 = flow depth just upstream of pier (hydraulic depth) (ft)
k_1 = correction for pier shape
k_2 = correction for angle of attack of flow
k_3 = correction for bed condition
k_4 = correction for armoring by bed material size
a = pier width (ft)
Fr = Froude number = $\frac{v_1}{\sqrt{g \cdot y_1}}$
v_1 = mean flow velocity (ft/sec)
g = gravity constant = 32.2 ft/sec^2

For analysis of ephemeral streams within semi-arid regions, the local practice has been to set k_3 and k_4 equal to 1.0. Traditional electric transmission line pole foundations are round to accommodate pole shaft geometry, so k_1 is also set equal to 1.0.

General bed degradation, or long-term stream degradation is computed as follows (Pemberton and Lara, 1984):

$$y_d = y_b \cdot \left(\frac{1}{\Delta_p} - 1\right)$$

where:

y_d = depth from original streambed to top of the armoring layer, or depth of general bed degradation (ft)
y_b = thickness of armoring layer: 3 armoring particle diameters (D_c), or 0.5 feet, whichever is smaller (ft)
Δ_p = Decimal percentage of original bed material coarser than the armoring size (D_c)
D_c = $1.88 \cdot (v_1)^2$ = diameter of armoring material (mm)

Lateral forces are the primary loads induced with single shaft transmission line structures. These forces introduce high moments with moderate shear forces upon the tops of support foundations. Piers within stream channels are subject to additional lateral load in due to moving water. As previously discussed, foundations are generally placed above a specified flood level, elevated above the channel bed (see Figure 2).

Figure 2
Foundation Reveal (Stick-up)
Above Stream Bed Flood Elevation

Hydraulic loading from moving water can be converted to an equivalent single shear force at the top of the foundation. The load model in Figure 3 utilizes an incompressible flow drag equation for the analysis to determine forces on piers below the water surface (Daugherty and Franzini, 1977).

$$P_H = \frac{C_d \cdot a \cdot \rho \cdot v_1^2}{2}$$

where:

P_H = unit force on pier (lb_f/ ft)
C_d = shape constant (also a function of velocity)
a = pier width (ft)
ρ = fluid density = 1.94 $lb_f \cdot sec^2 / ft^4$
v_1 = mean channel velocity, fps

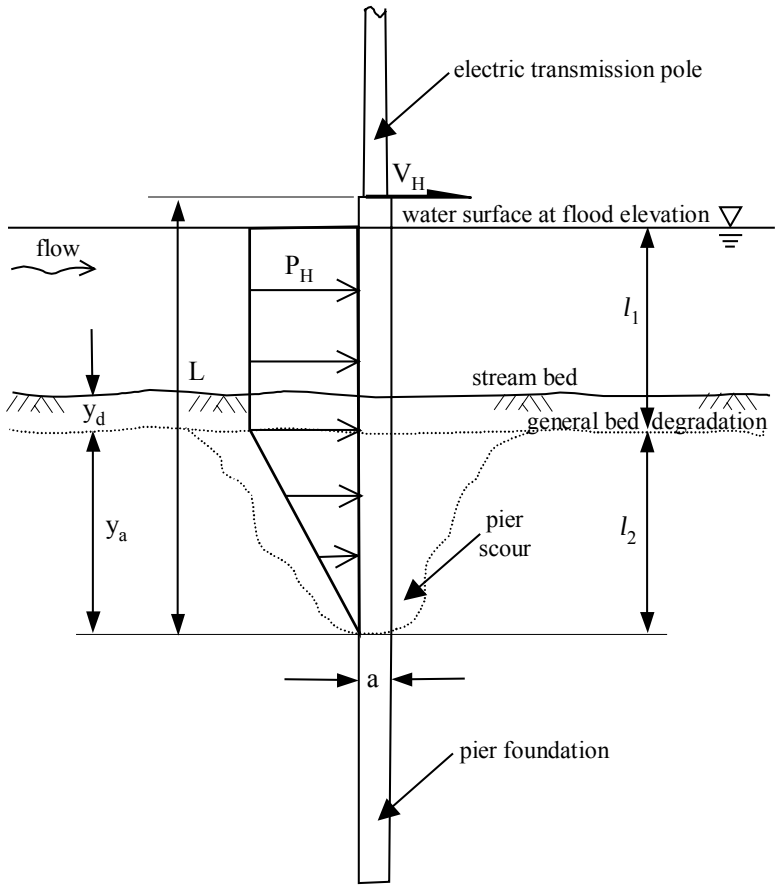

Figure 3.0
Idealized Hydraulic
Load Model

The scour hole width at the top of the stream bed is approximated by $2.7y_a$ (slope is about equal to the angle of repose). Scour is typified by a spiral roller with the cutting shape of a truncated cone. For these reasons, hydraulic loads below grade are approximated by a triangular pressure distribution. Full drag forces are applied above the bottom of the stream bed at the level of general bed degradation. This force linearly drops to zero at the bottom of local pier scour. Determining the resultant shear at the top of foundation then becomes a static equilibrium analysis:

$$V_H = \frac{M}{L}$$

where:

V_H = equivalent single shear force at the top of the foundation (lb_f)

M = moment from hydraulic loads to pier scour depth (ft- lb_f)

$$= \frac{P_H \cdot l_2^2}{3} + P_H \cdot l_1 \cdot \left[l_2 + \frac{l_1}{2} \right]$$

L = length of the pier above bottom of local pier scour (ft)

l_1 = length of the pier above the bottom of the stream bed at the level of general bed degradation (ft)

l_2 = length of the pier above the bottom of local pier scour to the stream bed at the level of general bed degradation (ft)

The combination of loads induced on the foundation from wind on conductors/pole and line tension on the conductors is included with the loads on the submerged foundation section from water flow events. Both environmental factors of wind and water can be evaluated in terms of their frequency for peak events. The goal is to match appropriate maximum events based upon time of year to provide a more reliable estimate of loads.

In the desert Southwest, maximum wind events occur principally during the months of June through October, relating to seasonal monsoon storms that build in the summer heat. Conversely, peak water flows generally occur during the months of November through April, relating to rainfall on snow-packed mountains that feed stream and river channels. During monsoon storms, there is the potential for flash flooding of these normally dry stream channels, but with flows that are generally lower than peak events related to snow runoff. Peak wind forces typically proceed rainfall. In fact, streams may surge from a flash flood storm event located a significant distance from the source. The evaluation of load frequency indicates that foundation load analysis should not include simultaneous peak events, but the maximum probable event in terms of time of year.

Load cases can be developed based on seasonal conditions that combine the peak loads from the most probable events. In general, load cases are developed for peak wind forces combined with lesser flood events, and peak flood events are combined with lower wind conditions.

REGIONAL GEOLOGY

General geology of the desert Southwest is characterized by a series of structural and topographic basins typical of the Basin and Range Physiographic Province of the western United States. Uplift structural block mountain ranges and intervening valley basins are encountered during construction of transmission lines. Mostly internally drained during formation, these basins are infilled with younger and softer materials than the surrounding mountain blocks which can become cemented and consolidated or indurated with age. Unconsolidated alluvial and colluvial deposits are usually confined to modern floodplain washes and waterways, where the erosion process has dominated since the formation of the present drainage system.

Flood plains and channels within the region are a result of this regional geology. Cleaner and more fine-grained sands and gravels occur near surface, and are underlain by more dense, cemented and massive deposits. Particle size distribution of aggregation deposits are mostly a result of waterway flow volume and gradient. For example, the steep-gradient Salt River and its flood plain through central Arizona consists predominantly of dense to very dense, poorly graded sandy gravel and cobbles with some boulders, with deposits ranging from 100 to 250 feet in thickness overlying old alluvial sediments (Beckwith and Hirany, 1991). Conversely, the Big Sandy River in northwestern Arizona typically consists of loose to dense non-plastic sand and gravel grading locally to silty sand and gravel containing some cobbles. This deposit overlies soft sedimentary deposits and/or indurated mud flows from earlier infills. Alluvium in and near ephemeral stream channels can be saturated as shallow as 10 feet below the surface.

CONSTRUCTION CONSIDERATIONS

Within the depths of static groundwater, most construction in alluvial channel deposits will experience instability and sloughing problems, requiring some form of stabilization. Stabilization is also common, but not as prevalent within upper low to no cohesion dry bed soils. Type of and need for stabilization is highly dependent upon particle size distribution, lithology, groundwater condition, and degree of calcareous cementation. In some conditions casing has been placed only to the contact of older sand-gravel-cobble deposits and the remainder of the excavation advanced as an open hole (Beckwith and Hirany, 1991). Stabilization techniques for reinforced concrete drilled shaft foundations vary from thick-walled steel casing to slurry assisted methods. Some of the subsurface soil varieties are shown in Figure 4.

Figure 4. Typical Alluvial Deposits in Ephemeral Stream Channels

Along with subsurface conditions, pier diameter and embedment depth can dictate foundation installation equipment requirements. Scour resistant foundations tend to be larger in both diameter and depth than foundations outside of channels. Pier diameters can range from 5 to 13 feet with lengths of 30 to 90 feet. Open flight augers and bucket augers are typically used for advancing foundation holes within these deposits. In more fine-grained sand and gravel deposits, truck-mounted drill rigs capable of generating 50,000 to 100,000 ft-lbs of torque are generally adequate for both excavation and casing installation. Where very dense sand-gravel-cobble deposits dominate, crane-mounted drill rigs and specialty truck mounted rigs with torque capacities ranging up to 400,000 ft-lbs are required for successful installation (Figure 5).

Concrete placement with the presence of groundwater is performed through a tremie pipe in a continuous operation in such a manner that the concrete always flows upward within the hole. The tremie pipe must be equipped with a bottom valve, or other device which prevents mixing of the water with the concrete inside the pipe and prevent the intrusion of water into the concrete in the event that the tremie pipe is removed and replaced. The tremie pipe is slowly withdrawn as the elevation of the concrete in the hole rises, with the discharge end of the pipe maintained at least five feet below the surface of the concrete.

Figure 5. Crane Rig, Steel Casing and Open Flight Auger

Concrete is usually placed continuously such that no cold joints will form. However, a construction joint may be made in dry conditions if located below the bottom of the anchor bolt assembly and where internal moment is low. With larger diameter scour-resistant foundations, inner permanent corrugated steel pipes may be used within the temporary casing to provide the opportunity for dry placement in wet holes. The interface must be thoroughly cleaned of all laitance and foreign matter. Hardened concrete is roughened to expose aggregate and the rebar wire brushed to ensure proper bonding (Figure 6).

When above the water table, concrete is placed through a hopper or other device so it is channeled in a manner to free fall (clearing the walls of the excavation and reinforcing steel) until striking the bottom. Adequate compaction is achieved by free fall on the concrete below the top 5 feet. The remainder of the concrete is mechanically consolidated by vibration to achieve proper consolidation.

Figure 6. Cold Joint
Within Permanent Inner
Corrugated Steel Liner

When installing foundations within groundwater or where soils are susceptible to caving conditions, evaluation of subsurface concrete integrity can be tested with large diameter foundations via the use of full-length ports. 2-inch diameter schedule 40 polyvinyl

chloride (PVC) pipes can be installed within reinforcement cages to allow for testing by both nuclear and seismic down-hole and cross-hole methods. A PVC port is shown in the photograph on Figure 6. Typically six to eight tubes are installed with closed ends within about one foot of the bottom of the foundation and open ports above the top of concrete.

Typical costs for reinforced concrete transmission line foundations in ephemeral channels from 1990 to 2000 show a range of $350 to $500 per in-place cubic yard of concrete. This cost includes all reinforcement and the structure anchor bolt cage.

CASE HISTORY

An approximate 31 mile long 230 kilovolt electric transmission line was installed from the Salt River Project's Papago Buttes to Pinnacle Peak Substations in the late 1980's in the Phoenix, Arizona Metropolitan area. Part of the construction included 102 tubular steel poles installed on reinforced concrete drilled shaft foundations. Of those, 41 were constructed within the channel and flood plain of the normally dry Salt River. A typical profile of one foundation location is presented in Figure 7.

The geotechnical investigation performed for this work identified the near-surface channel soils as nonplastic medium dense to very dense gravelly sand and sand deposits with a trace to some silt ranging from 4 to 35 feet below grade. Underlying this strata was a very dense sand, gravel and cobble mixture (referred to regionally as SGC) with small amounts of silt and clay present. The lower strata extends to depths of several hundred feet along the Salt River channel. SGC strata commonly contains cobble particle sizes up to about 12-inches in diameter, with occasional 18-inch diameter boulders. The upper 20 or 30 feet of the SGC materials were uncemented or very weakly cemented and very clean (Sergent, Hauskins and Beckwith, 1985). Representative geotechnical design properties of each strata are noted in Figure 7 (γ_{sat} = saturated unit weight, φ' = effective friction angle, c' = effective cohesion, E_p = lateral modulus of deformation).

Because of planned future freeway construction adjacent to the transmission line route, extensive hydrologic information was available for scour analysis (Simons, Li & Associates, 1989, 1990).

Due to the cohesionless nature of near-surface soils, 14.5 feet of bank wash-out at the pole location was assumed to the full depth of the channel. From the hydrologic information, the estimated channel velocity at the 100-year flood elevation was 8.3 feet per second for a flow depth of 20.3 feet. Upon bank wash-out, the angle of attack would become parallel to the foundation, therefore k_2 was estimated as 1.0.

From the mid-strata gradation chart, 11 percent (by weight) of the material was coarser than D_c (the minimum diameter of armoring material). The thickness of the armoring material was determined as the smaller of $3D_c$ or 0.5 foot. A summary of all calculation results is presented in Table 1.

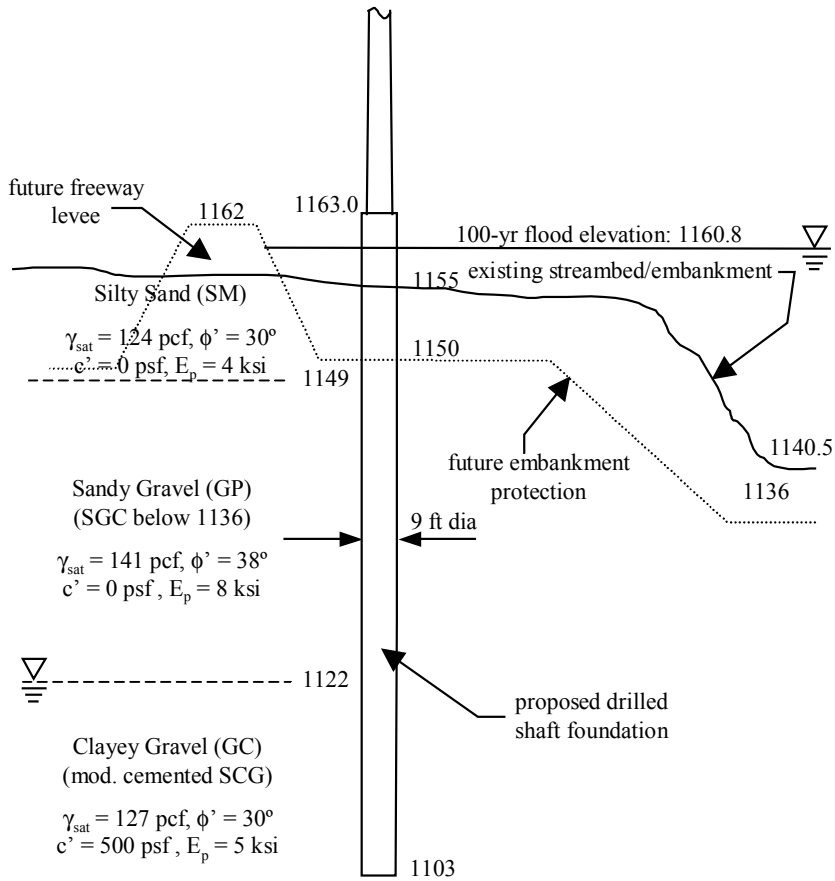

Figure 7. Pier 61R: Pinnacle Peak-Papago Buttes 230kV Transmission Line

Table 1. Scour Calculation Summary for Pier 61R

v_1 (ft/sec)	y_1 (ft)	a (ft)	Fr	k_2	D_c (in)	Δ_p	y_a (ft)	y_d (ft)
8.3	20.3	9.0	0.325	1.0	5.1	0.11	14.8	4.0

The calculation results suggest that, for the 100-year flood event, general bed degradation will cause a loss of natural material to elevation 1136.5 and pier scour down to elevation 1121.7. It should be noted that the soils investigation identified considerable cobble at elevation 1136, in close proximity to the general bed degradation depth.

Evaluation of flood and wind events was then performed. It was decided that two load cases would be evaluated for final determination of pier embedment:

Case (a): 100-yr flood event with working load winds on conductor/pole (≈ 50 mph)

8-ft pier extension above top of existing embankment
+14.5-ft bank wash-out of existing embankment
+ 4.0 ft general bed degradation
+ 14.8-ft pier scour = 41.3-ft reveal

Case (b): 100-yr wind event with 1/2 scour values and flood elevation at 1156.4

8-ft pier extension above top of existing embankment
+14.5-ft bank wash-out of existing embankment
+ 2.0 ft general bed degradation
+ 7.4-ft pier scour = 31.9-ft reveal

Loading upon the foundation must include the forces due to water flow acting upon the revealed portion of the foundation. Shape factor coefficient, C_d, calculated for these piers typically ranged from 0.35 to 0.90. However, to account for sediments and debris in the water, a higher factor of 1.0 was selected. This value also compensated for low values of Reynolds number and the high pier length to diameter ratio. The hydraulic load unit force was then calculated:

$$P_H = \frac{1.0 \cdot 9 \cdot 1.94 \cdot 8.3^2}{2} = 601 \text{ lb}_f/\text{ ft}$$

For load case (a), the increased shear force at the top of the foundation was 10.6 kips with a resisting surface at elevation 1121.7, and for load case (b) the increased shear force at the top of the foundation was 5.9 kips with a soil resisting surface at elevation 1131.1. Previously calculated loads were working values and needed to be increased by appropriate overload (safety) factors (per National Electric Safety Code for electric transmission line structures) to be used in conjunction with pole wind and conductor load cases. With electric transmission line design, an overload factor of 1.65 was applied to working loads for ultimate load design (factored loads). Table 2 presents the combined load cases for both wind and water events.

Table 2. Load Case Summary for Wind and Water Events

Load Case (a) 100-yr flood event					Load Case (b) 100-yr wind event				
Pole loads on foundation			Shear from water (kips)	Total Shear (kips)	Pole loads on foundation			Shear from water (kips)	Total Shear (kips)
P (kips)	M (k-ft)	V (kips)			P (kips)	M (k-ft)	V (kips)		
56.9	5375	69.3	17.5	86.8	114.4	8704	93.9	9.7	103.6

Foundation embedment depths for laterally loaded drilled pier reinforced concrete foundations were determined based on the Electric Power Research Institute TLWorkstation Foundation Analysis & Design (FAD) methodology (Davidson, 1982). Straight-shaft drilled piers without base moment and friction were assumed for this analysis. It was also assumed that drilled piers utilized a minimum 3000 psi (f'_c =28 days) compressive strength concrete. Maximum movement at top of foundation were limited to 5% of foundation diameter for lateral deflection and 1 degree of rotation. The results for each case are presented in Table 3. Minimum foundation diameter was dictated by support pole geometry and the pole anchor bolt arrangement.

Table 3. Pier 61R Lateral Load Embedment Analysis (9-ft diameter)

Load Case	Reveal (ft)	Embedment (ft)	Total Pier Length (ft)	Bottom Elevation (ft)
a. 100-yr flood	41.3	18.5	59.8	1103.2
b. 100-yr wind	31.9	24.0	55.9	1107.1

Based on the analysis, load case (a) controlled the embedment depth of the foundation, with a total pier length of about 60 feet. Of this length, 8 feet would extend above existing grade and 52 feet was to be installed below grade.

A crane-mounted auger drill rig was utilized to place casing and perform excavation work for construction of Pier 61R. The drill hole was advanced with telescoping 12-ft and 11-ft diameter thick-walled steel casing section to a depth of 34.5 feet below grade (elev. 1120.5). Groundwater was encountered near the bottom of casing. The hole was completed to full depth within the moderately cemented SGC strata without need for additional casing (Figure 8a). A 9-ft diameter corrugated metal pipe inner liner was then installed to a depth of 40 feet, with an additional 8 feet extending out of ground (the upper 14 feet was smooth lined). After placement of the reinforcing cage, concrete was tremie pumped to fill the foundation to 35 feet below grade. After cleaning and preparing the cold joint, the remainder of concrete and anchor bolt cage (Figure 8b) was placed in dry conditions. A cementitious sand slurry was pumped into the annulus space between the temporary casing and permanent liner during removal of the temporary casing (a 5-ft head maintained within the temporary liner at all times). The portion of the inner liner above grade and about 5 feet below grade was stripped upon completion of the work to leave a smooth concrete surface.

(a) SGC Material

(b) Anchor Bolt Cage

Figure 8. Drilled Shaft Foundation Installation

Heavy rains during late 1992 and early 1993 resulted in major flows within the Salt River channel. During the second week of January 1993, a number of the scour-resistant foundations on the Papago Buttes to Pinnacle Peak 230kV transmission line experienced a 50-year flow event (about 129,000 cubic feet per second) for about one week. Predicted bank wash-out was observed in some locations along the transmission line route. Extreme wind forces did not occur simultaneously during peak flows. Water forces and scour within the channel destroyed formwork for a new road bridge crossing directly downstream of pole P61R. Foundations were monitored during flooding and checked

after floodwaters receded. Although substantial damage resulted from this flooding to adjacent facilities, electric transmission line foundations were found to have performed as expected. No deficiencies, cracking nor permanent deflections were noted.

CONCLUSIONS

1. The desert southwest includes unique and unusual challenges with respect to major drainage ways. This paper demonstrates that a design approach with loading analysis, derivative theory, empirical values derived from experience, and construction techniques can be developed to deal with large diameter drilled piers in ephemeral conditions.

2. Scour conditions are shown to consist of more than just loss of soil support due to hydraulic conditions against the pier. In the desert Southwest, general riverbed degradation during flow conditions and loss of embankment in which the drilled pier is embedded must also be included. All of the elements combined magnify the loading due to increased exposed length of the drilled pier.

3. A rational approach and methodology for wind and hydraulic loads showed that simply combining the extreme conditions simultaneously is conservative and uneconomical. The results of using a probabilistic approach of combined events results in a more efficient design and lower cost.

4. Construction technique is vital to the success of drilled piers. Specific techniques to deal with local conditions (such as groundwater) and deep large diameter piers in sand, gravel and cobble conditions are shown to provide consistent results. The construction technique discussed include equipment size, permanent and temporary liners, multiple reinforcement/anchor bolt cages and pier integrity monitoring.

5. Implementation of case history provides safe, reliable, inspectable, cost effective and durable drilled piers in difficult ephemeral conditions of the southwest.

REFERENCES

1. Beckwith, G. H. and Hirany, A. (1991) Design and Construction of Drilled Shafts in Coarse Gravel and Cobble Deposits, Proceedings of the 4th International Conference on Piling and Deep Foundations, A. A. Balkema, Rotterdam, pp. 33-40.

2. Daugherty, R. L. and Franzini, J. B. (1977) Fluid Mechanics with Engineering Applications, McGraw-Hill, New York, 564 p.

3. Davidson, H. L. (1982) Laterally Loaded Drilled Pier Research - Volume 1: Design Methodology, EL-2197, Volume 1, RP 1280-1, Electric Power Research Institute, Palo Alto. 87 p.

4. Pemberton, E. L. and Lara, J. M. (1984) Computing degradation and local scour: U.S. Bureau of Reclamation, Technical Guideline, January, 48 p.

5. Richardson, E.V., Harrison, L.J. and Davis, S.R. (1991) Evaluating Scour at Bridges, Hydraulic Engineering Circular No. 18, FHWA-IP-90-017 HEC-18, Federal Highway Administration, Washington, D.C., February (http://www.fhwa.dot.gov/bridge/hec18SI.pdf)

6. Sergent, Hauskins and Beckwith Consulting Geotechnical Engineers (1985) Pinnacle Peak – Papago Buttes 230kV Transmission Line, SHB job number E85-200.

7. Simons, Li & Associates, Inc. (1985) Design Manual for Engineering Analysis of Fluvial Systems, prepared for Arizona Department of Water Resources, Tucson, Arizona.

8. Simons, Li & Associates (1989) Preliminary Hydraulic Analysis of the East Papago Freeway and Red Mountain Freeway Interchange.

9. Simons, Li & Associates (1990) Addendum No. 4 to Preliminary Hydraulic Analysis of the East Papago Freeway and Red Mountain Freeway Interchange.

Propeller Induced Scour

By

Chen Onn Chin[1], Wei Li[2]

ABSTRACT

This study examines the mechanics of propeller jet scour experimentally and identifies the key parameters for the scour process. Densimetric Froude Number, F_0 and relative propeller distance from the bed surface, z_p/D are the two parameters investigated, which have significant effects on the scour. The scour regions can be divided into tangential scour hole, axial scour hole and deposition ridge. The scour hole is slightly skew to the left side of the jet axis if the propeller is rotated anticlockwise when view in the jetwise direction because of the tangential component of the jet flow. Equations of equilibrium scour dimensions are presented. A propeller jet scour is generally less than that of a corresponding circular jet. An upper bound estimate of a propeller jet scour is obtained.

INTRODUCTION

In recent time, the increasing demand of global sea trade and ever greater efficiency mean that larger ships with more powerful engines and self –propelled berthing capability are widely engaged in order to achieve a faster turn-round. Jet velocity of large-diameter propellers or side thrusters can reach 6 to 8 m/s, and the effect of the jet on seabed lasts for some distance of several propeller diameters from the jet exit (Prosser, 1986). When the jet velocity exceeds certain threshold, erosion of the seabed occurs. Severe erosion on the bed or bank of navigation channels and port structures may occur which can lead to navigation hazards and port structure failures. The impact of propeller jets is more serious in a harbor where water is shallow and the propeller is closer to the seabed.

Scour induced by a propeller or thruster jet has become one of the important issues for maintenance and design of navigation channels and harbor structures. Bergh and Cederwall (1981) reported that the damage induced by propellers was quite severe in 25 quay structures of Swedish harbors. Chait (1987) reported that there were many ports in South Africa Suffered from propeller scour damage. A comprehensive understanding of the jet scour is necessary before any effective measure can be taken. Verhey (1983) put forward a method to determine the efflux velocities behind a propeller. Hamill and Johnston (1993) investigated velocity character of propeller jet flow. It was found that the maximum velocity in the zone of flow establishment depends on efflux velocity and propeller properties.

[1] Associate Professor, School of Civil and Environmental Engineering, Nanyang Technological University, 639798, Singapore, (CCOCHIN@ntu.edu.sg)

[2] Research Fellow, School of Civil and Environmental Engineering, Nanyang Technological University, 639798, Singapore, (CWLI@ntu.edu.sg)

The parameters involved in propeller jet scour are many and complex, especially the geometry of the propeller itself, but there are relatively few investigations on the propeller scour process in comparison with scour of circular jets. This study examines the mechanics of the propeller scour and identifies the associated significant parameters. The study shows that two parameters Densimetric Froude Number, F_0 and relative propeller clearance, z_p/D have significant effects on scour. Based on analysis of scour profiles, the expressions of depth, length and width of equilibrium scour hole, and height of deposit ridge are presented. Compared with equilibrium scour profiles of a circular jet, a propeller jet produces a lesser scour depth on the bed for the same F_0. Hence, the circular jet may be considered as an upper limiting case of a propeller jet.

EXPERIMENT

The experiments were conducted in a laboratory tank with water depth H, of 45 cm (Fig. 1). Three-bladed stainless steel propeller of diameter, D of 210 mm, and sand bed with median diameter, d_{50} of 0.25mm was used to simulate a ship propeller and a seabed, respectively. The speed of the propeller was operated from 100 to 400 rpm.

A Micro Acoustic Doppler Velocimeter (MADV) was used to measure the velocities distribution of jet flow in the axial, tangential and radial directions at the distance of x = 0.5D and 3D, where x is the jetwise distance from the propeller. This enabled the discharge and hence the efflux velocities of the propeller jet to be calculated. The temporal development of the scour was recorded from 0.5 hour to 64 hours.

RESULTS AND DISCUSSION

TIME DEVELOPMENT OF SCOUR

Immediately after the propeller was turned on, the sand close to the surface was eroded quickly. The flow was very turbulent and the scour at this stage was vigorous. Most of the eroded particles were transported as suspended load. After a short time, a definite shape of the eroded bed could be seen and further erosion occurred as time progresses. At the crest of the ridge, sand was impelled into suspension and settled down some distance away. After a few hours, the rate of erosion decreased considerably. The scour reached an equilibrium stage asymptotically when the change in maximum depth over time is less than 0.05cm/h.

Developments of scour are plotted from Fig. 2 to Fig. 5. The maximum scour depth and ridge height increases with time steadily. Comparing Fig. 2 with Fig. 3 and Fig 4 with Fig. 5, it can be drawn that rotation speed of propeller plays a significant role in scour profile. Increased speed of propeller can induce to distinct rise of scour depth and ridge height, which mean jet strength of propeller is the key factor for the formation of scour. z_p is another important factor for scour process. In velocity distribution of propeller jet, the velocities weaken fast at the edge of jet in radial. If the propeller axis is relative far away from the seabed, impact of propeller jet will decrease greatly. For example, the maximum scour depth for z_p /D= 1 nearly halves compared with the run of z_p /D= 0.5. It is found for small z_p, axial distance of maximum scour and deposit increases with time, both move in the direction of jet flow. While for large z_p, the site of scour hole and ridge is seldom changed. As z_p increases, the scour hole under propeller becomes relatively small.

SCOUR AT EQUILIBRIUM STAGE

Scour induced by propeller jet can be divided into three zones at equilibrium stage, namely tangential scour hole, axial scour hole and deposition ridge. Formation of three zones depends on many factors, especially the jet strength and the clearance of a propeller to the seabed. The small scour hole under the propeller is tangential scour hole, which is produced by tangential flow of propeller. The most significant factor for the formation of tangential scour hole is the clearance of propeller from seabed. The main scour hole names as axial scour hole will be formed downstream of the flow. The strong axial jet washes on sand bed directly and induces to the largest axial hole. Following scour area stays the deposit area, where sand carried from scour hole form the deposition ridge. Increasing speed of propeller will enlarge the length, width and depth of scour hole and height of ridge.

The equilibrium scour profiles are shown in Fig. 6 and Fig. 7. The scour profiles are not symmetrical about the centerline of the propeller. The location of scour holes is off-centered and tends to fall on the left side of the centerline and the ridge is higher on the right side of the centerline. This phenomenon can be explained by the direction of propeller rotation and the low jet exit velocity. The propeller turned anticlockwise in the experiment when view in the jetwise direction. Following anticlockwise direction, the tangential flow scooped and dumped the sediment to the right side of propeller. As a result, the scour hole tended to be skew towards the left side. Beside, the off-centered scour hole geometry could be attributed to the weak axial velocity component. There is a tendency that larger jet strength result in lesser offset. It can be concluded that for the range of rotation speed adopted, the effect of tangential velocity component is prominent. It is also found that the maximum scour and deposit tends to offset more initially, but as time increases they move towards the centerline.

DIMENSIONAL ANALYSIS

Formation of propeller scour is related to various parameters, such as diameter of propeller, density of fluid, sediment properties, average jet velocity, etc. In view of the many factors that may affect the geometry of the scour, a few variables were summarized. In this study, the properties of fluid, propeller and sand, water depth and attack angle were held constant. As the flow pattern was turbulent, Reynold number could be ignored either. Hence the scour profiles could be expressed mathematically as:

$$d_s, L_s, W_s, z_s = f(D, U_o, z_p, d_{50}, \rho_s, \rho, g, t) \quad (1)$$

Where, d_s = depth of scour hole at time t; L_s = length of scour hole at time t; W_s = width of scour hole at time t; z_s = height of ridge at time t; D = diameter of propeller; U_0 = average jet exit velocity; z_p = clearance from propeller axis to seabed; d_{50} = median diameter of sand; ρ_s = density of sand; ρ = density of fluid; g = acceleration due to gravity; and t = duration of the experiment. The maximum equilibrium scour parameters are denoted by an additional subscript "e".

Equation (1) can be described in dimensionless form:

$$\frac{d_s}{D}, \frac{L_s}{D}, \frac{W_s}{D}, \frac{z_s}{D} = f\left(F_0, \frac{z_p}{D}, \frac{U_0 t}{D}\right) \quad (2)$$

Where, F_0 is Densimetric Froude Number and can be expressed as:

$$F_0 = \frac{U_0}{\sqrt{(\frac{\rho_s}{\rho} - 1) g d_{50}}} \tag{3}$$

At equilibrium, the scour hole and ridge become invariant with time and the dimensionless expression becomes:

$$\frac{d_{se}}{D}, \frac{L_{se}}{D}, \frac{W_{se}}{D}, \frac{z_{se}}{D} = f\,(F_0, \frac{z_p}{D}) \tag{4}$$

From equation (4), multiple regression models are established as:

$$\frac{d_{se}}{D} = k(F_o)^{\beta_1}(\frac{z_p}{D})^{\beta_2} \tag{5}$$

$$\frac{L_{se}}{D} = k(F_o)^{\beta_1}(\frac{z_p}{D})^{\beta_2} \tag{6}$$

$$\frac{W_{se}}{D} = k(F_o)^{\beta_1}(\frac{z_p}{D})^{\beta_2} \tag{7}$$

$$\frac{z_{se}}{D} = k(F_o)^{\beta_1}(\frac{z_p}{D})^{\beta_2} \tag{8}$$

Similarly from equation (2),

$$\frac{d_s}{D} = k(F_o)^{\beta_1}(\frac{z_p}{D})^{\beta_2}(\frac{U_o t}{D})^{\beta_3} \tag{9}$$

Where, k, β_1, β_2 and β_3 are constants in different equations.

In order to get the analytic solution of above equations, linearization are adopted. For example, equation (9) can be written as:

$$y = \beta_o + \beta_1 x_1 + \beta_2 x_2 + \beta_3 x_3 \tag{10}$$

Where, $y = \ln\frac{d_s}{D}$, $\beta_o = \ln k$, $x_1 = \ln F_o$, $x_2 = \ln\frac{z_p}{D}$, $x_3 = \ln\frac{U_o t}{D}$

The coefficients β_0, β_1, β_2 and β_3 can be solved with four equations derived as:

$$n\beta_o + \beta_1\sum_{i=1}^{n} x_{1i} + \beta_2\sum_{i=1}^{n} x_{2i} + \beta_3\sum_{i=1}^{n} x_{3i} = \sum_{i=1}^{n} y_i$$

$$\beta_o\sum_{i=1}^{n} x_{1i} + \beta_1\sum_{i=1}^{n} x^2{}_{1i} + \beta_2\sum_{i=1}^{n} x_{1i}\sum_{i=1}^{n} x_{2i} + \beta_3\sum_{i=1}^{n} x_{1i}\sum_{i=1}^{n} x_{3i} = \sum_{i=1}^{n} x_{1i}\sum_{i=1}^{n} y_i$$

$$\beta_o\sum_{i=1}^{n} x_{2i} + \beta_1\sum_{i=1}^{n} x_{1i}\sum_{i=1}^{n} x_{2i} + \beta_2\sum_{i=1}^{n} x^2{}_{2i} + \beta_3\sum_{i=1}^{n} x_{2i}\sum_{i=1}^{n} x_{3i} = \sum_{i=1}^{n} x_{2i}\sum_{i=1}^{n} y_i$$

$$\beta_o \sum_{i=1}^{n} x_{3i} + \beta_1 \sum_{i=1}^{n} x_{1i} \sum_{i=1}^{n} x_{3i} + \beta_2 \sum_{i=1}^{n} x_{2i} \sum_{i=1}^{n} x_{3i} + \beta_3 \sum_{i=1}^{n} x^2_{3i} = \sum_{i=1}^{n} x_{3i} \sum_{i=1}^{n} y_i \quad (11)$$

These equations are solved in SPSS Data Editor program, and the solution of equation (9) is:

$$\frac{d_s}{D} = 0.04(F_o)^{1.14}(\frac{z_p}{D})^{0.20}(\frac{U_o t}{D})^{-1.18} \quad (12)$$

Equation (5) to (8) can be solved in the same way, and following results can be obtained:

$$\frac{d_{se}}{D} = 0.12(F_o)^{1.00}(\frac{z_p}{D})^{-0.87} \quad (13)$$

$$\frac{L_{se}}{D} = 0.72(F_o)^{1.13}(\frac{z_p}{D})^{0.19} \quad (14)$$

$$\frac{W_{se}}{D} = 0.95(F_o)^{0.85}(\frac{z_p}{D})^{-0.37} \quad (15)$$

$$\frac{z_{se}}{D} = 0.11(F_o)^{0.89}(\frac{z_p}{D})^{-0.88} \quad (16)$$

From above equations, it is found that F_0, namely index of propeller jet strength, always has a positive effect on jet scour profiles, while effect of z_p/D is complicated. Based on the equations obtained, a comparison was taken between the measured maximum equilibrium scour depth with previous study of circular jet scour (Chin et al., 1996) in Fig. 8. It is found that the propeller jet has a lesser impact on the bed than circular jet for the same F_o. This has to do with a more rapid decay of propeller jet in the jetwise direction.

CONCLUSIONS

The scour process induced by a propeller jet is examined. The study shows that two parameters F_o, and z_P/D have significant effects on the scour. During the scouring process, more than 50% of the equilibrium scouring depth, length and width were reached within the first hour and scour hole approached equilibrium stage asymptotically in 64 hours. All the dimensions d_{se}, z_{se}, L_{se} and W_{se} increases with F_o, but increasing z_p/D causes d_{se}, W_{se} and z_{se} to decrease.

Propeller jet scour comprise of tangential scour hole, axial scour hole and deposition ridge. As the most important factors controlling scour process, F_o, and z_p/D affects the formation of three zones in different way. Because of the regular rotation direction of propeller and low jet velocity, the equilibrium scour profiles are not symmetrical about the centerline of the propeller. It is likely that higher propeller speed results in lesser offset, and the offset will decreases in the process of scour.

Equilibrium scour depth, length, width and deposit ridge height is expressed mathematically. Compared with the equilibrium scour profiles induced by circular jet, the propeller jet has less impact, an upper bound estimate of a propeller jet scour is obtained consequently. Relationships between scour profiles and environment parameters presented in this paper are available for estimating scour hole and deposit in engineering practice.

REFERENCES:

1. Bergh, H., Cederwall, K., 1981, "Propeller Erosion in Harbors", Bulletin No. TRITA-VBI-107, Hydraulics Laboratory, Royal Institute of Technology, Stockholm, Sweden.
2. Chait, S., 1987, "Undermining of Quay Walls at South African Ports Due to the Use of Bow Thrusters and Other Propeller Units", P.I.A.N.C., Bulletin No 58, 1987, pp 107-110.
3. Chin C.O., Chiew Y.M., Lim S.Y. and Lim F.H., 1996, "Jet Scour around Vertical Pile", Journal of Waterway, Port, Coastal, and Ocean Engineering, ASCE, Vol. 122, No 2, pp 59-67.
4. Hamill, G.A. and Johnston, H.T., 1993, "The Decay of Maximum Velocity within the Initial Stages of a Propeller Wash", Journal of Hydraulic Research, IAHR, Vol. 31, No 5, pp 605-613
5. Prosser, M.J., 1986, "Propeller Induced Scour", Reports of The British Ports Association, RR 2570, February, 1986, pp1-33
6. Verhey, H. .J., 1983, "The Stability of Bottom and Banks Subject to the Velocities in the Propeller Jet behind Ships", Delft Publication, No 303, Delft Hydraulics Laboratory, Netherlands.

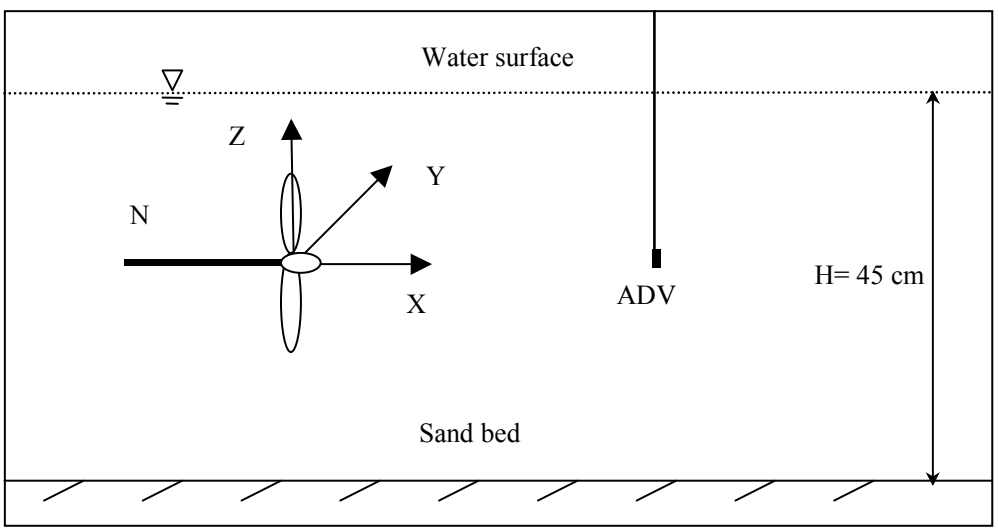

Fig. 1 Experimental Set-up

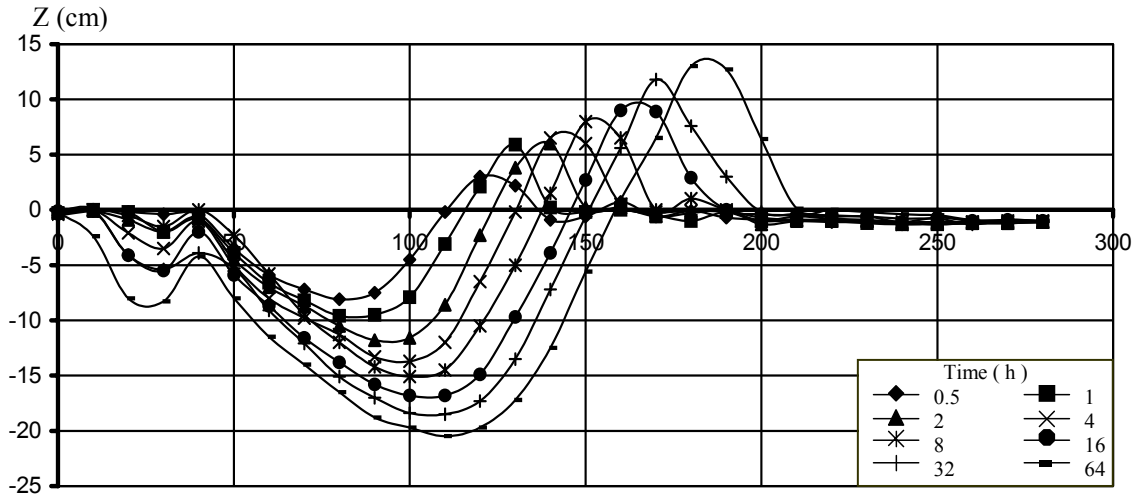

Fig. 2 Centerline Profiles of Scour Development (z_p/D=0.5, N=200rpm)

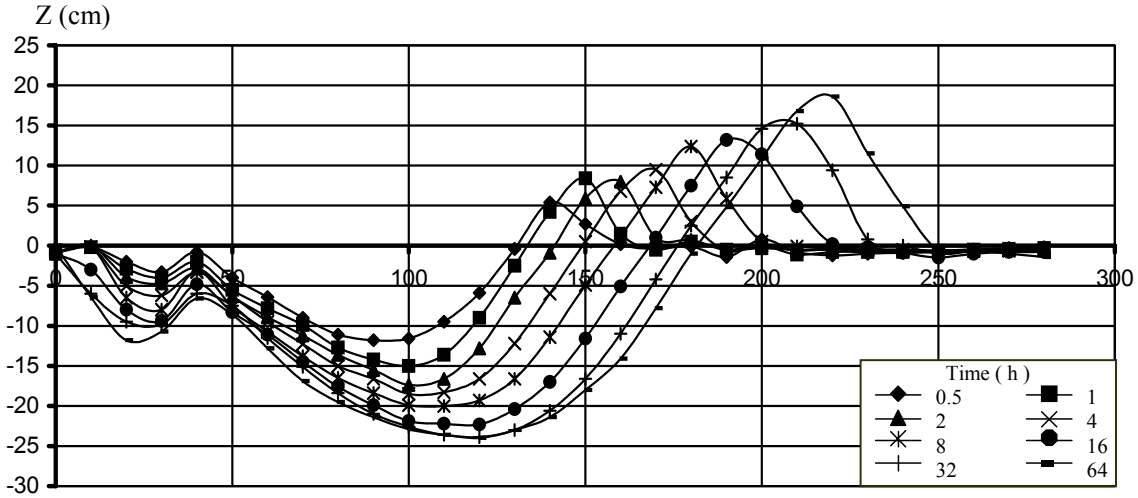

Fig. 3 Centerline Profiles of Scour Development (z_p/D=0.5, N=250rpm)

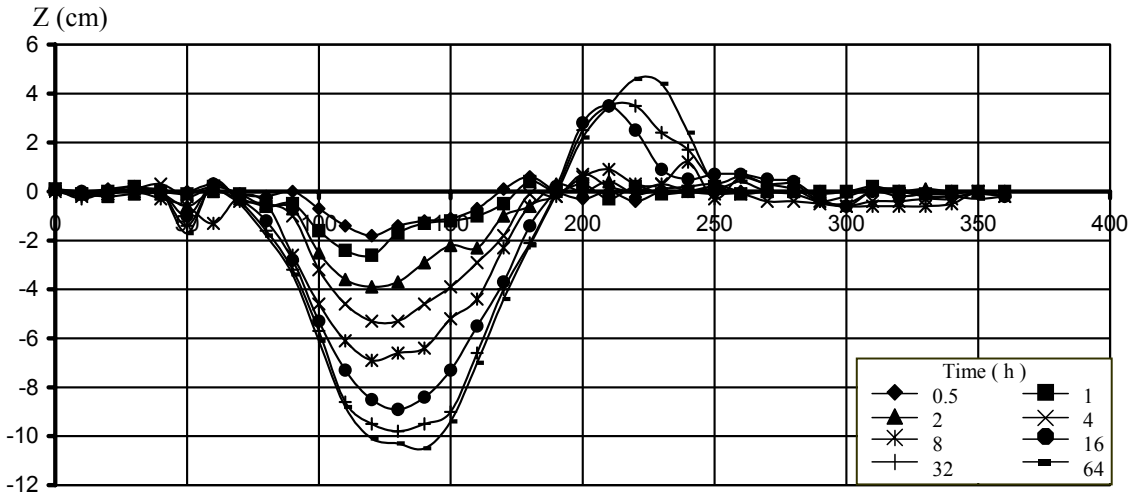

Fig. 4 Centerline Profiles of Scour Development (z_p/D=1, N=200rpm)

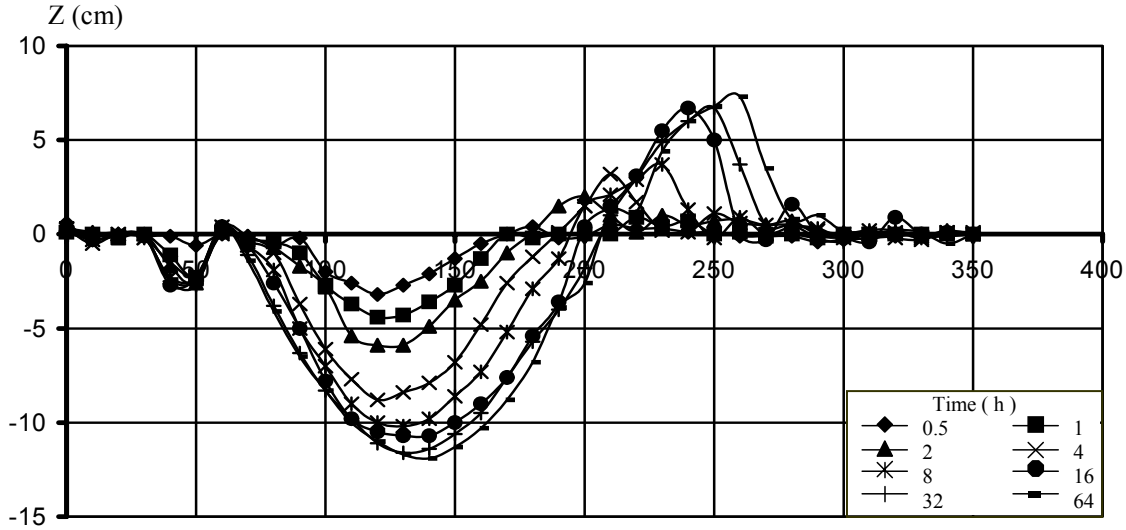

Fig. 5 Centerline Profiles of Scour Development (z_p/D=1, N=250 rpm)

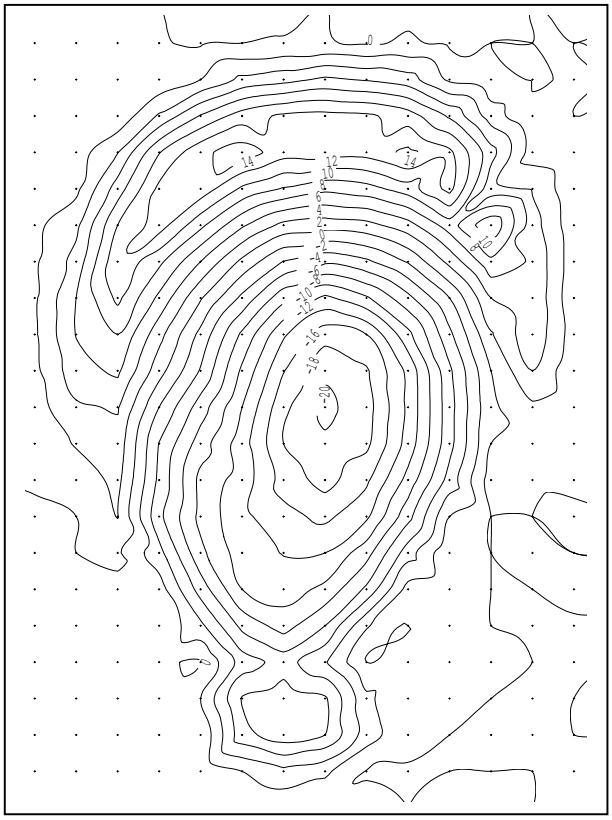

Fig. 6 Equilibrium Scour Profile at $z_p/D=0.5$, N=200rpm

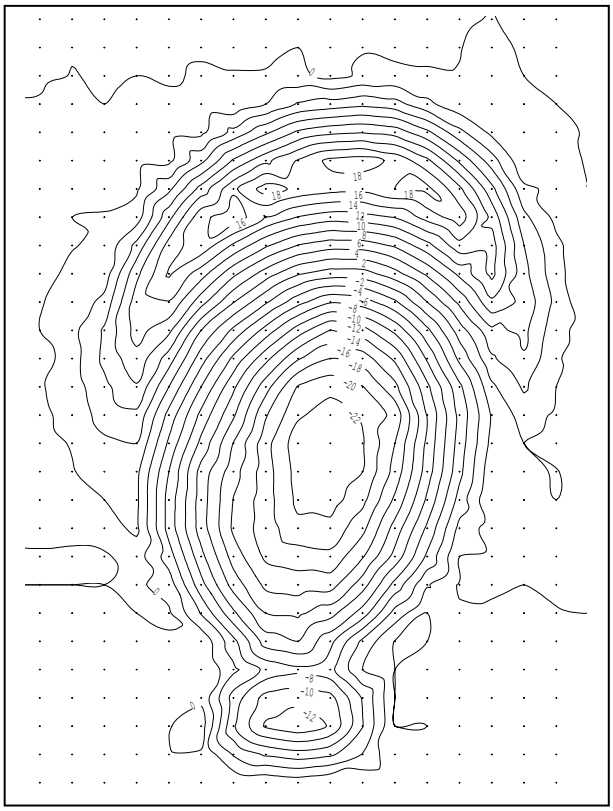

Fig. 7 Equilibrium Scour Profile at $z_p/D=0.5$, N=250rpm

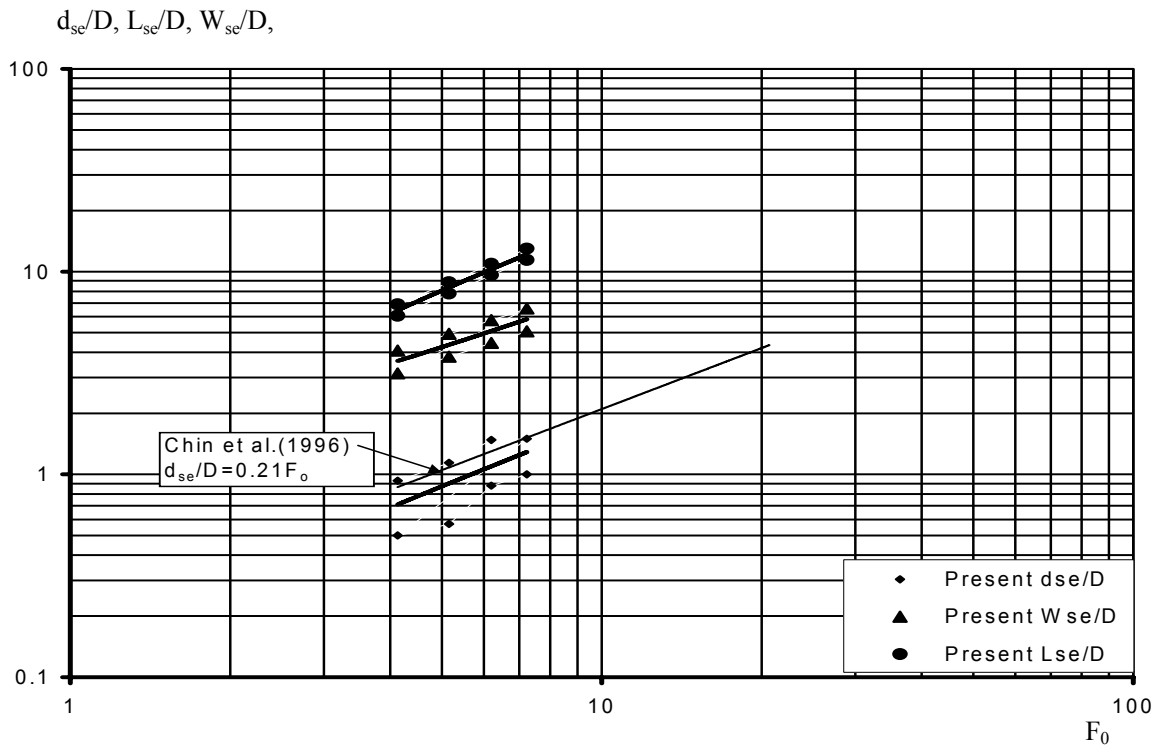

Fig. 8 Comparison of Scour Profiles between Propeller Jet and Circular Jet

Confederation Bridge – New Scour Design Methodology for Complex Materials

R.B. Nairn[1] and C.D. Anglin[2]

ABSTRACT

The $800 million Confederation Bridge, spanning 13 km across the Northumberland Strait in Eastern Canada, presented many engineering challenges, one of which was the assessment of scour potential and protection requirements for the 65 bridge piers. The direct application of standard scour assessment/design techniques was not possible for this project due to the combination of complex flow conditions (waves and currents), complex pier geometries (conical pier bases, with some piers located in dredged pits), and complex seabed conditions (highly weathered and fractured bedrock). A multi-faceted coastal engineering investigation was undertaken by Baird & Associates to assess scour potential, define scour protection requirements and design scour protection. Key activities included geotechnical investigations to define the seabed characteristics, numerical modeling to define the wave, current and water level conditions at the crossing site, physical modeling of wave-current interaction with the bridge piers, the development of a new methodology to estimate the scour potential of the seabed around the bridge piers under extreme wave and current conditions, and post-construction scour monitoring. This paper provides an overview of the investigations completed, including a description of the new scour design methodology and the results of the scour monitoring program over the five year period since the bridge was completed.

INTRODUCTION

The 13 km long, $800 million Confederation Bridge crosses the Northumberland Strait and joins the provinces of New Brunswick and Prince Edward Island in Eastern Canada (refer to Figure 1). The bridge, developed under a finance-design-build-operate agreement between Strait Crossing Bridge Limited (SCBL) and the Canadian Government, was constructed in 1994-97, and opened to traffic on June 1, 1997.

Figure 1 – The Confederation Bridge

[1] Baird & Associates, 200-627 Lyons Lane, Oakville, ON, Canada, L6J 5Z7 (rnairn@baird.com)
[2] Baird & Associates, 500-1145 Hunt Club Road, Ottawa, ON, Canada, K1V 0Y3

One of the engineering challenges associated with this $800 million project was the assessment of scour potential and scour protection requirements for the 65 bridge piers. The direct application of standard scour design techniques (such as those documented in TAC, 1973 and HEC-18/FHWA 1993, available at the time of the original design investigations) was not possible due to the unique combination of complex flow conditions, complex pier base geometries and complex seabed conditions. This paper provides an overview of the multi-faceted coastal engineering investigation undertaken to assess the scour potential and scour protection requirements for the Confederation Bridge, and presents a new methodology to assess the potential for scour around bridge piers.

RELEVANT SITE AND PROJECT CHARACTERISTICS

At the crossing location, the Northumberland Strait is approximately 13 km wide, with water depths ranging from 0 to 30 m (typically in the order of 15 m). Under extreme design conditions, the bridge may be exposed to winds up to 120 km/h, waves of significant height (H_s) up to 4.5 m and peak period (T_p) up to 9 s, and currents up to 2.5 m/s (the latter generated by the combined effects of tides, surges and wave-driven longshore currents). Seabed conditions are highly variable, and consist of highly weathered mudstone, siltstone and sandstone, which are sometimes overlain by glacial till.

The crossing consists of the main bridge (forty four 250 m long spans), the East approach (seven 93 m long spans) and the West approach (fourteen 93 m long spans). The main bridge piers (P1 to P44) consist of an 8 m wide octagonal shaft cast integral with a conical ice shield (20 m base diameter) and supported by a conical pier base (22 m base diameter). The pier base may rest directly on the seabed or in dredged pits up to 14 m deep. Figure 2a provides a schematic illustration of a typical main pier. For the approach piers (E1 to E7 and W1 to W14), which are located in water depths less than 8 m, the conical pier base is also the ice shield, as shown in Figure 2b.

Figure 2a – Schematic of Main Pier

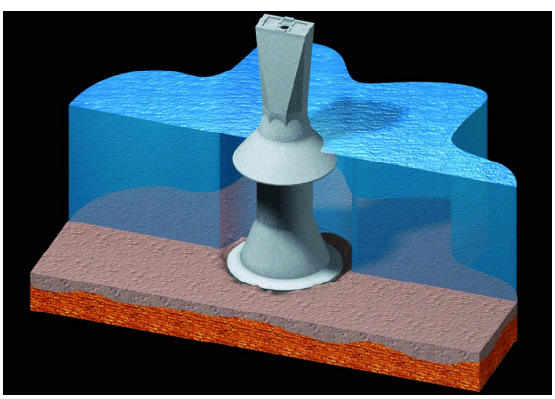

Figure 2b – Model of Approach Pier

The individual bridge components, weighing up to 8,000 t, were pre-cast on land and placed in the Strait using a heavy lift vessel (HLV Svanen) guided by a differential global positioning system (refer to Figure 3).

Figure 3 – HLV Svanen Placing a Main Bridge Span

KEY SCOUR DESIGN ISSUES

An extensive literature review was undertaken in an attempt to identify scour assessment techniques that could be applied to the Confederation Bridge. This included review of numerous technical papers and several design manuals related to scour around bridge piers, as well as numerous papers related to scour around coastal structures. In general, the bridge papers focused on the scour of cohesionless sediments (i.e. sands and gravels) around rectangular or cylindrical piers in unidirectional flows, while the coastal structures papers focused on wave-induced scour of cohesionless sediments along breakwaters, revetments and seawalls (i.e. long, linear structures, without three-dimensional flow effects). In addition, a few papers were reviewed that dealt with erosion/scour of cohesive materials and weak rock by unidirectional flows. However, it was concluded that there were no acceptable techniques to define scour potential for the Confederation Bridge project because of the following unique features and complex conditions:

- combined waves and currents;
- conical pier bases, some located in dredged pits; and
- highly weathered and fractured bedrock seabed.

As such, it was necessary to develop a new methodology to assess scour potential for this project.

DEVELOPMENT OF NEW SCOUR ASSESSMENT METHODOLOGY

Initial laboratory studies (Cornett et al., 1994) were undertaken to characterize and quantify the erosion potential of the various seabed materials at the crossing location. This included flume tests to assess the erodibility of both core and slab samples of till, mudstone, siltstone and sandstone. These test results showed considerable variability, as illustrated in Figure 4 for the weakest (till and mudstone) samples.

Figure 4 – Erodibility Test Results for Till and Mudstone from Northumberland Strait

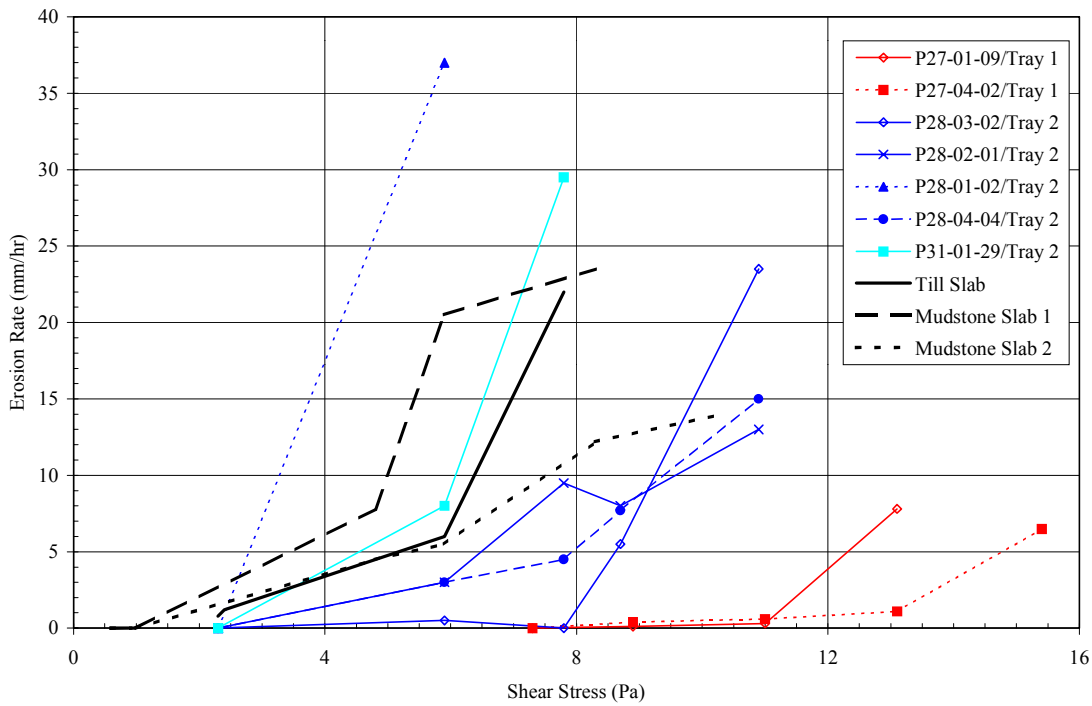

Considering the rock materials (mudstone, siltstone and sandstone), it was noted that the sample sizes were not sufficient to incorporate the highly variable bedding/fracture/joint patterns within the insitu rock mass, clearly an important parameter in the overall erosion process for these materials. Given the complex nature of the erosion process, and the associated variability in the test results, it was not possible to develop a reliable method to quantify the erosion process as a function of either shear stress or near bed velocity.

Subsequently, a promising new approach (Annandale, 1995) to estimate the erosion potential of "complex materials" was identified. In general terms, Annandale's (1995) approach relates the driving force for scour, as defined by the "stream power" parameter, P (which provides a measure of the rate of energy dissipation in the near bed flow), to the resistance to scour, as defined by the "erodibility index", EI (which provides a measure of the in-situ strength of the material). Annandale's (1995) database, and his relationship between stream power and erodibility index (which defines the threshold for scour) is based on observations of erosion (or no erosion) in spillways downstream of dams. A subset of the Annandale database (for "rock and complex earth materials") is presented in Figure 5. This figure shows a log-log plot of stream power versus erodibility index for approximately 150 field observations in materials ranging from cohesive sediments to hard, massive rock. The closed symbols represent events where erosion did occur, while the open symbols represent events where erosion did not occur. The sloping line is the estimated "erosion threshold" relationship between stream power and erodibility index.

Figure 5 - Erodibility of Rock and Complex Earth Materials
(after Annandale, 1995)

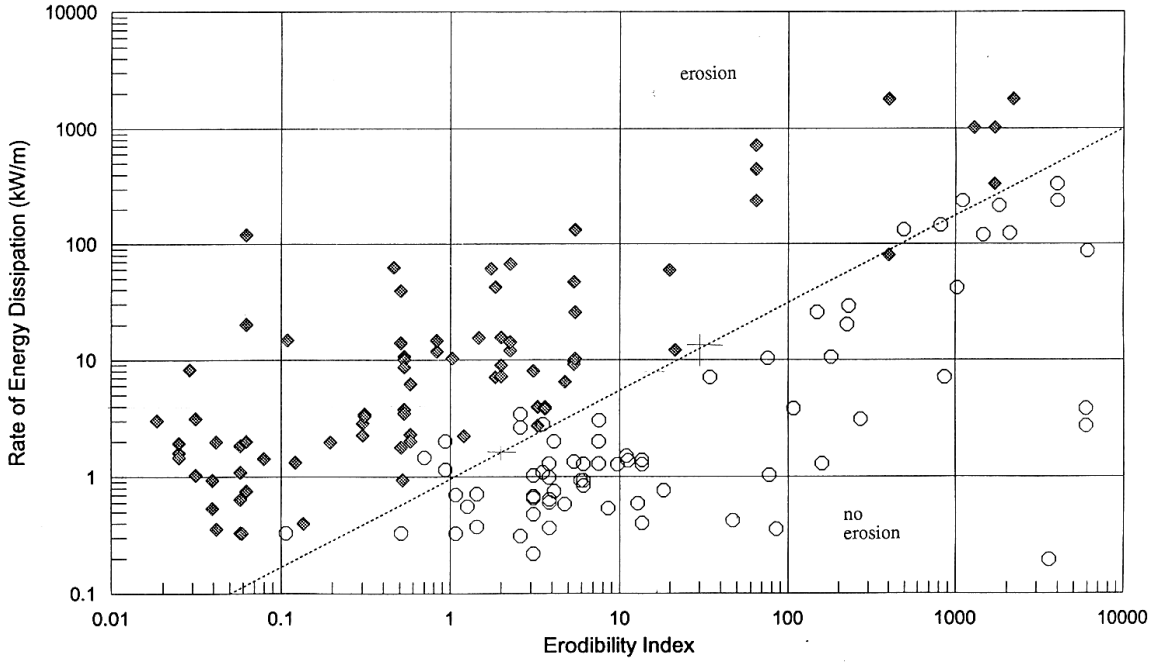

Annandale materials:
[cohesive sediment][weathered shale][sandstone][dolerite][hard rock]

Northumberland Strait seabed materials:
[till][mudstone, siltstone, sandstone]

As shown above, the estimated erodibility indices for the seabed materials encountered along the Confederation Bridge crossing alignment fall within the range of Annandale's database (the available geotechnical data and EI calculations are summarized later in this paper). However, in order to develop and apply this methodology to the Confederation Bridge project, it was necessary not only to evaluate the stream power (driving force for scour) and erodibility index (resistance to scour) for this project, but also to calibrate and verify the methodology for the assessment of scour potential around conical bridge piers exposed to combined waves and currents. These aspects of the investigation are described below.

Driving Force for Scour

Two general issues must be addressed with respect to quantifying the driving force for scour around the Confederation Bridge piers. First, the ambient flow conditions (waves and currents) at the crossing location must be defined, and second, the local influence of the bridge piers on these flow conditions must be defined.

Numerical modeling techniques were utilized to define the ambient flow conditions at the crossing location. Tidal and surge induced currents and water levels in the Strait were

estimated on an hourly basis over a 23 year period (1973-95) using the MIKE21 hydrodynamic model of the Danish Hydraulic Institute. The model was driven by recorded water levels at either end of the Strait and the model predictions were successfully verified against available recorded current data (approximately three months) at the crossing location. The mean and large tidal ranges at the crossing location are approximately 1.5 m and 2.25 m respectively, with peak tidal currents (depth-averaged) in the order of 0.9 m/s (during large tides). Water level fluctuations and currents associated with storm surges can be similar in magnitude to the tidal effects.

A parametric wind-wave hindcast model was used to estimate hourly wave conditions at four locations along the crossing alignment for the same 23 year period. The wave predictions were validated against available recorded wave data (approximately five months) at the crossing location. Extreme wave heights were estimated using a peak over threshold (POT) extreme value model. For example, the 2-year and 100-year significant wave heights (H_s, the average the highest one third of the waves; the maximum wave height, H_{max}, is typically 1.6 to 2 times H_s) near the middle of the crossing are in the order of 3 m and 4 m respectively. Shallow water processes, including refraction, shoaling, breaking and wave-driven longshore currents, were estimated using the COSMOS coastal processes model (Southgate and Nairn, 1993).

The hindcast water level, current and wave data were used to estimate the near bed velocity, shear stress and stream power, considering the combined effect of both waves and currents, on an hourly basis over the 23 year period of the environmental database. The combined shear stress was calculated using the method of Myrhaug and Slaatelid (1990), as presented in Soulsby et al. (1993), while the combined velocity was calculated as the vector sum of the maximum wave orbital velocity and the depth-averaged tidal/surge current. Stream power was calculated as the product of the combined shear stress and the combined velocity. Given the importance of water depth on wave orbital motions, the calculations were repeated for a range in water depths representative of the 65 bridge pier locations.

Severe stream power events were extracted from the time series data base and input to a POT extreme value model to estimate extreme events as a function of return period. The 100-year event was selected as the design condition to evaluate the requirement for, and the design of, scour protection.

The influence of the various pier shapes and dredged pit depths on the local flow conditions around the base of the piers were investigated for a range in water depths using a 1/70 scale model in a 1.2 m wide flume at the Canadian Hydraulics Centre in Ottawa, Canada (Cornett, 1996). Figure 6 presents a schematic diagram of the test configuration in the flume. The flume setup allowed the simulation of unidirectional currents with either “following” or “opposing” irregular wave conditions at a range in water depths.

Figure 6 – Schematic Diagram of Test Configuration in Flume

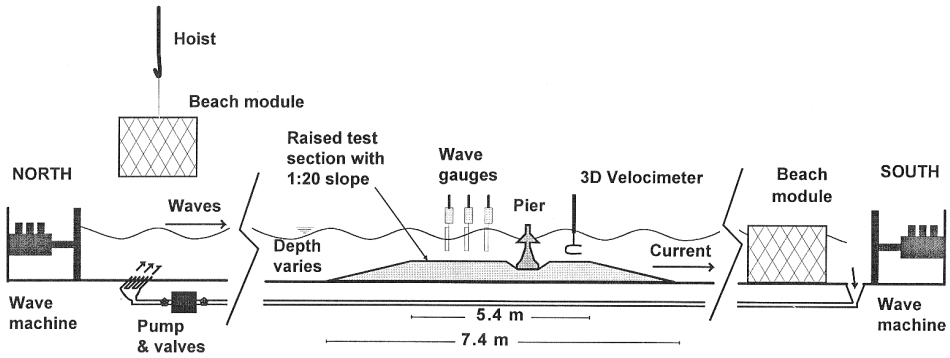

The flow patterns around the base of the piers were defined with the aid of a laser doppler velocimeter, acoustic velocity meters, flow visualization and tracer materials. Stream power magnification factors were developed for the various conditions encountered at the 65 bridge piers through a comparison of the stream power required to initiate the "scour" of tracer materials with and without the pier in place. Well-sorted coarse sands and fine gravels were used for the tracer materials, with median grain sizes (D_{50}) ranging from 1 to 5 mm. The tracer mat was placed to a thickness of two to three grains, and "scour" was defined as the complete removal of grains from any area resulting in an exposed patch on the flume floor. This was found to be a more repeatable "threshold condition" than the "initiation of motion" of individual grains for the irregular wave conditions in these tests.

Figure 7 shows photographs of the tracer mat around a model approach pier before and after a test. In general, scour of the tracer mat initiated on either side of the piers as a result of acceleration of flows in these areas. Flow visualization techniques confirmed that a strong horseshoe vortex did not develop on the upstream/upwave side of the piers, probably as a result of the conical shape of the pier base.

Figure 7 – Tracer Mat Around Model Approach Pier Before and After Test

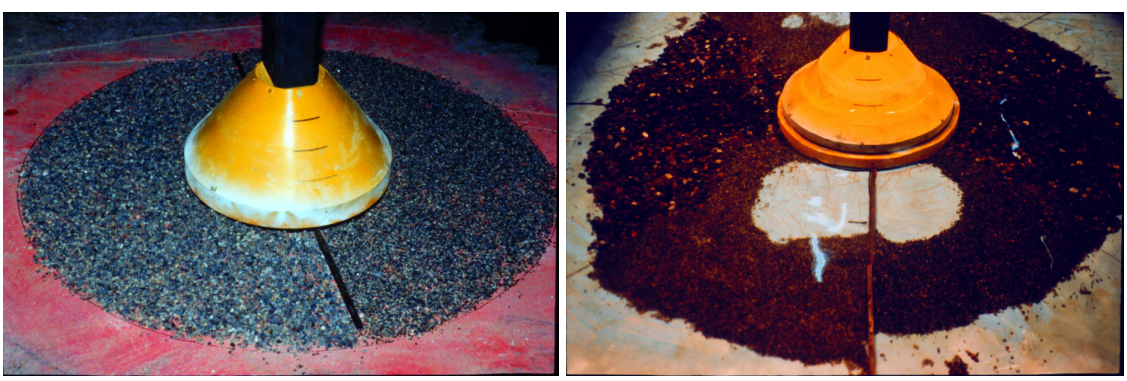

The resulting estimates of the stream power magnification factor (PMF) varied from approximately 1.6 for a deep water main pier placed in a deep pit, to approximately 6 for moderate depth main piers and shallow water approach piers placed directly on the seabed. The tracer test results for the main piers are summarized in Figure 8.

Figure 8 – Main Pier Magnification Factors Estimated from Tracer Test Results

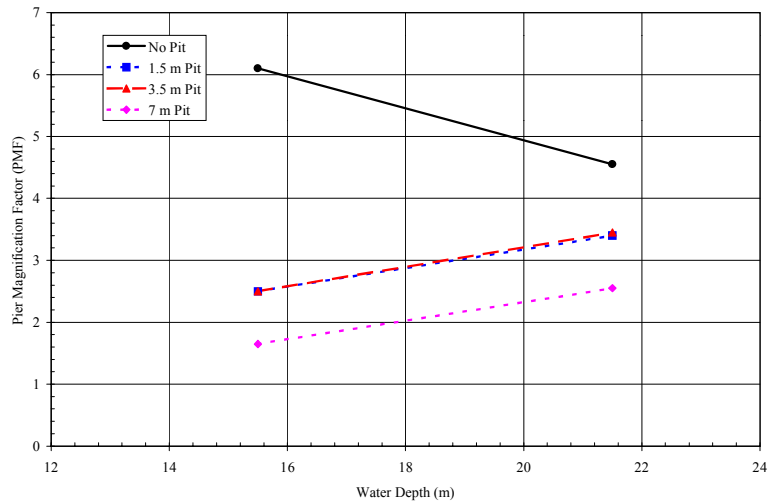

The PMF is proportional to the cube of velocity; hence, PMF's of 1.6 to 6 correspond to velocity magnification factors of approximately 1.2 to 1.8. The upper limit, for a conical pier base placed directly on the seabed, is somewhat larger than the values recommended in HEC-23 (FHWA, 2001c) for the application of the Isbash equation to design scour protection around round nose and rectangular piers (1.5 and 1.7 respectively). The reduction in PMF with deeper pits infers the existence of an "equilibrium" scour depth that could be estimated using such tracer tests (i.e. no further scour when PMF = 1.0).

Seabed Resistance to Scour

Estimating the erodibility of the highly weathered and variable seabed materials was one of the most challenging aspects of the project. As noted earlier, considerable variation was noted in the results of the erodibility flume tests. Further, the size of the test samples (both cores and slabs) was insufficient to incorporate the highly variable bedding/fracture/ joint patterns within the insitu rock mass. As such, it was not possible to describe or quantify the erosion process using only these test results. Ultimately, the empirical erodibility approach developed by Annandale (1995) for scour in spillways was adopted. In this approach, the erosion resistance of the material is quantified by the "erodibility index", EI, which accounts for the mass strength of the material, the typical block size, the interparticle shear stress, and the orientation of the layers of rock. The erodibility index is calculated as the product of four dimensionless variables, all defined from standard borehole records, as summarized below:

$$EI = K_m K_b K_d J_s$$

where EI = erodibility index
K_m = mass strength number
K_b = block size number
K_d = joint roughness number, and
J_s = joint structure number

As part of the geotechnical investigation undertaken to support the design of the bridge piers and foundations, between two and ten boreholes were drilled at each of the 65 bridge pier locations. A total of approximately 300 boreholes were drilled. Erodibility indices were calculated by a geologist/geotechnical engineer for each core run (approximately 0.3 m lengths) for each borehole. The erodibility indices showed considerable variability in both the horizontal and vertical dimensions, reflecting the highly variable nature of the materials on which the bridge piers are founded. This variability was a primary consideration in the incorporation of a factor of safety in the scour design methodology.

Calibration of Methodology

The Confederation Bridge represents the first known application of Annandale's (1995) methodology to bridge piers, waves and currents, or design of any kind. As such, calibration and verification of the methodology was a key component of the investigation.

Fortuitously, observations of actual scour experienced around one of the first piers installed early in the project provided valuable information for calibration of the new methodology. Figure 9 provides an illustration of the measured scour around Pier E7. The scour extended up to 5 m out from the base of the pier, with undermining of up to 1 m in and 1.5 m below the pier base. This scour was caused by a moderate storm event (return period of approximately five years) that occurred in November 1994. No significant scour was noted around several other East approach piers in place at that time.

Figure 9 - Scour in Bedrock Observed at Approach Pier E7 (Nov. 1994)

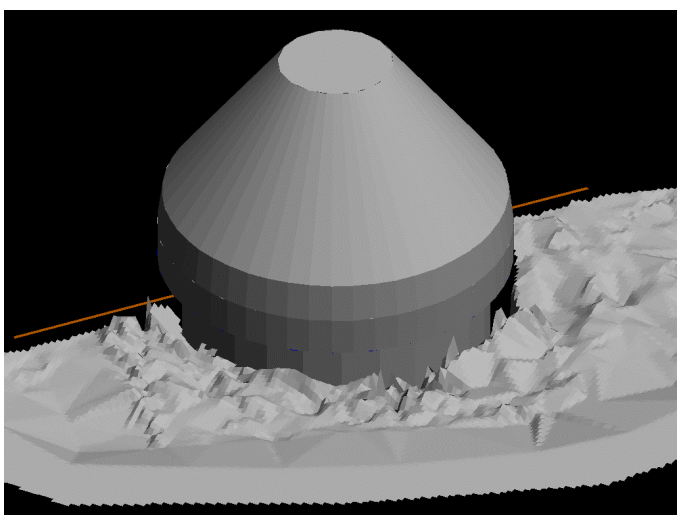

The wave and current conditions during this event were hindcast using the numerical models, and the corresponding flow patterns around the piers were simulated in the physical model. Based on this information, along with the geotechnical data describing the seabed conditions in the vicinity of the East approach piers, comparisons of measured and predicted scour were used to calibrate the methodology. The key calibration parameters were the wave height (ie. H_{avg}, H_s, $H_{1/10}$, H_{max}), the wave period (ie. T_{avg}, T_p,

T_{max}), the combined shear stress (ie. τ_{mean}, τ_{max}) and the bottom roughness (k_s). The best comparison between estimated and observed scour at the single pier was obtained using H_{max}, T_{max}, τ_{max} and a bottom roughness of 0.3 m. The use of the maximum wave height, wave period and shear stress can be qualitatively justified by the hypothesis that the erosion process for the weathered bedrock is a threshold process, and that once a rock fragment has been dislodged and removed from the surrounding matrix, the remaining material will be more susceptible to erosion. The lack of scour at the adjacent piers can be explained by the presence of stronger materials at these locations.

A qualitative confirmation of the methodology was also made through consideration of the morphological development of the seabed across the Strait. Through the application of the erodibility index approach, it was possible to explain the existence of glacial till over the underlying bedrock for areas with depths greater than about 13 m (i.e. in these areas the 100-year stream power event was less than the stream power required to erode the till material according to Annandale's (1995) relationship).

REQUIREMENT FOR SCOUR PROTECTION

A pier by pier assessment was undertaken in order to define the requirement for scour protection at each of the 65 bridge piers. In general, this assessment included the following steps:

- for each borehole at each pier, define the maximum EI value in the "buffer zone" between the seabed (or the mass excavation level for piers placed in a dredged pit) and the pier founding elevation; these "local EI values" represent the strength of the most erosion resistant material above the pier founding elevation (note that scour is allowed in the buffer zone, but not below the pier founding elevation);
- estimate the "design threshold EI value" at each pier based on the local design stream power (100-year ambient stream power value times pier magnification factor) and Annandale's (1995) scour threshold relationship;
- compare the "local EI values" at each pier to the "design threshold EI value", and recommend scour protection if the factor of safety (local EI value/design threshold EI value) is less than two to four (a higher factor of safety was used at piers with greater variability in seabed conditions, and/or where the tolerance for scour was lower).

Based on the results of this assessment, scour protection was recommended at 14 of the 65 bridge piers.

MODELING AND DESIGN OF SCOUR PROTECTION

The design of the scour protection system was developed and optimized using a physical model investigation. These model tests were completed in the same wave flume as the tracer tests described earlier, again at a scale of 1:70. The scour protection tests were used to define the size of armour stone required to remain stable during the 100 year design wave and current conditions. The extent of the scour protection was defined based

on the results of the tracer tests, which defined the "zone of influence" of the piers where ambient flow conditions were significantly affected by the presence of the pier. The recommended protection design consists of one or two layers of armour stone placed in a 10 m wide band around the base of the piers. The size of the armour stone is dependent on the water depth, with larger stones being required in shallower depths. Additional information on the modeling and design of the armour stone scour protection is provided in a companion paper in these proceedings (Anglin et al, 2002).

CONSTRUCTION

SCBL chose to install scour protection at five of the 14 piers where Baird recommended protection. This decision was based on careful consideration of the cost of scour protection (approximately $0.5 million per pier) versus the risk of scour, recognizing the significant uncertainties and (likely) conservative approach to the assessment of scour potential. Armour stone scour pads were installed at three approach piers (refer to Figure 12), while construction logistics led to the design and implementation of tremie concrete scour pads at two other approach piers (refer to companion paper by Anglin et al (2002) in these proceedings for additional information).

Figure 12 – Armour Stone Scour Pad at Shallow Water Approach Pier (photo by Boily)

In response to SCBL's decision, Baird recommended a detailed and systematic scour monitoring program. This recommendation was accepted by SCBL; the resulting monitoring program is discussed further below.

SCOUR MONITORING PROGRAM

An extensive long-term monitoring program was designed and implemented by Baird in order to assist SCBL in identifying any scour that might occur around the base of the bridge piers such that appropriate action can be taken before scour compromises the intregrity of the structure (ie. before scour extends beneath the founding elevation of any pier). The scour monitoring program is a critical component of the overall scour investigation for the following reasons:

- the Confederation Bridge represents the first known application of the new scour assessment methodology to bridge piers, waves and currents, or design of any kind;

- there are significant uncertainties associated with the estimation of the driving forces for scour and the seabed resistance to scour; and
- there is a desire to minimize seabed survey requirements around the pier bases.

In addition, and recognizing the limitations noted above, Baird recommended to SCBL that a systematic reassessment of the scour assessment and design methodologies be undertaken approximately five years after the bridge opened, with the seabed response over this time to be accurately quantified using appropriate survey techniques.

Initially, the 65 bridge piers were broken into priority classes based on the estimated risk of scour, with the highest priority class (nine AA piers) being those at which scour protection was recommended by Baird (FS < 4) but not implemented by SCBL. In addition, Baird developed and installed a near real-time wave and tide prediction system, using numerical models similar to those utilized in the original scour assessment and design study. This software system is installed on the SCBL computer network in the bridge administration/operations building. The system is updated by SCBL staff on a bi-weekly basis (and immediately following severe storms) in order to define any requirement for action by bridge operations and maintenance staff. For example, a pier base inspection is "flagged" at specific piers if an event occurs which is more severe than any prior event, or if the factor of safety against scour is less than four, or if a certain period of time has elapsed since the last survey. Figure 13 presents a sample output report from the system for one half of the piers

Figure 13 – Sample Output Report from Scour Monitoring Database System

Confederation Bridge Scour Monitoring Database

Update Date: 26JAN99 Update Period: 04JAN99 to 17JAN99

Pier	Priority Class or Protect. Type	Max Event Prior to Last Survey	Last Survey Date	Max Event Since Last Survey	Exceeded Time Int.	Prior Event	FS Against Scour	Survey Required
E03	Arm 8	2388.0	10MAR98 15JUN98	2831.0 26NOV98	N	Y	Prot'd	Y
E04	AA	3847.0	10MAR98 23JUL98	4093.0 26NOV98	N	N	< 4	Y
E05	AA	1544.0	26NOV98 21DEC98	551.8 23DEC98	N	N	10 - 20	N
E06	AA	1826.0	26NOV98 21DEC98	624.5 23DEC98	N	N	4 - 10	N
E07	Trm10	1696.0	26NOV98 17DEC98	586.1 23DEC98	N	N	Prot'd	N
P01	B	233.4	10MAR98 17JUL98	298.0 26NOV98	N	N	20 - 100	N
P02	B	151.5	10MAR98 28JUL98	191.4 26NOV98	N	N	20 - 100	N
P03	A	170.4	10MAR98 28JUL98	215.7 26NOV98	N	N	10 - 20	N
P04	A	151.5	10MAR98 07JUL98	191.4 26NOV98	N	N	4 - 10	N
P05	B	135.4	10MAR98 07JUL98	170.8 26NOV98	N	N	10 - 20	N
P06	B	131.2	10MAR98 17JUL98	165.5 26NOV98	N	N	10 - 20	N
P07	A	129.2	10MAR98 10JUL98	163.0 26NOV98	N	N	10 - 20	N
P08	C	118.8	10MAR98 10JUL98	126.1 26NOV98	N	N	20 - 100	N
P09	A	110.7	10MAR98 22JUL98	117.2 26NOV98	N	N	10 - 20	N
P10	D	94.0	10MAR98 06JUL98	98.8 26NOV98	N	N	> 100	N
P11	D	83.5	10MAR98 02SEP98	87.4 26NOV98	N	N	> 100	N
P12	D	73.5	10MAR98 14SEP98	76.5 26NOV98	N	N	> 100	N
P13	D	63.3	10MAR98 06JUL98	65.6 26NOV98	N	N	20 - 100	N
P14	D	59.5	10MAR98 08JUL98	61.5 26NOV98	N	N	> 100	N
P15	C	55.4	10MAR98 09JUL98	57.1 26NOV98	N	N	20 - 100	N
P16	D	46.4	10MAR98 08JUL98	47.4 26NOV98	N	N	> 100	N
P17	C	58.1	10MAR98 24JUL98	60.0 26NOV98	N	N	20 - 100	N
P18	D	69.9	10MAR98 27JUL98	72.7 26NOV98	N	N	10 - 20	N
P19	AA	72.6	10MAR98 21JUL98	75.5 26NOV98	N	N	4 - 10	N
P20	D	54.7	10MAR98 09JUL98	56.4 26NOV98	N	N	> 100	N
P21	D	69.9	10MAR98 09JUL98	72.7 26NOV98	N	N	> 100	N
P22	B	64.0	10MAR98 09JUL98	67.6 26NOV98	N	N	20 - 100	N
P23	C	75.9	10MAR98 09JUL98	80.8 26NOV98	N	N	20 - 100	N
P24	D	68.8	10MAR98 13JUL98	72.9 26NOV98	N	N	> 100	N
P25	C	64.0	10MAR98 13JUL98	67.6 26NOV98	N	N	20 - 100	N
P26	D	50.0	10MAR98 14JUL98	52.2 26NOV98	N	N	> 100	N

* after Last Survey Date indicates accepted survey

Maximum Wave Conditions During Update Period

Pier	Date & Time	Max Hs(m)	Tp(s)	Approx. Return Period (yrs)
E04	16JAN99-02	1.38	5.5	n/a
P01	16JAN99-02	1.67	5.5	< 2
P14	16JAN99-02	1.69	5.6	< 2

The output from the system is digitally archived to provide a historical database for each pier documenting the conditions (stream power) to which each pier has been exposed since the bridge opened in June, 1997.

SCBL has followed this monitoring program since the bridge opened in 1997, and has undertaken at least one diver inspection around every pier, and numerous diver inspections around the high priority AA piers. Scour was detected during a diver inspection around one of the AA piers (P41) in 1998 (despite the fact that the scour hole was partially infilled with loose granular material). The scour reached a maximum depth of 1.6 m below the original seabed (approximately 1 m below the pier base elevation), and extended 12 to 15 m out from the pier base over a +/-100 degree sector. This pier was subsequently protected with an armour stone scour pad.

No significant scour has been observed around any of the other piers during diver inspections, despite the fact that the bridge has been exposed to several moderate storm events (the most severe of which had an estimated return period in the order of five years) for which the original scour assessment predicted scour at some of the AA piers. These results suggest that the original scour assessment may be conservative, as intended.

However, it is noted that diver inspections are qualitative, and can only identify significant changes or specific problems in localized areas (i.e. scour below the pier base). The diver inspections might not identify widespread, ongoing scour around a pier base. Further, it is interesting to note that P41 was not the most critical AA pier, and that scour was predicted to occur at other piers before it actually occurred at P41 (i.e. other AA piers had lower estimated factors of safety against scour). This information highlights the limitations and uncertainties in the original scour assessment methodologies, principally as a result of the large variation in (and limited characterization of) seabed material characteristics, but also the application of a new methodology for scour potential in complex materials subject to complex flow conditions.

In response to these issues, and to SCBL's interest in reducing their monitoring requirements/costs, Baird again recommended that a systematic reassessment of the scour assessment and design methodologies be undertaken. SCBL has initiated this process, with detailed multi-beam sonar (MBS) seabed surveys being undertaken around 14 piers (including all nine AA piers) in the summer of 2001. The remaining piers are to be surveyed using MBS in the summer of 2002. The MBS survey data provide an accurate description of the existing seabed surface, and have be overlain on the pre-construction/ as-built seabed surveys to allow an estimate of changes in the seabed elevation between the two surveys. A sample result, showing the change in seabed elevation around a West approach pier between 1997 (as-built) and 2001 (four years later), is presented in Figure 14.

Figure 14 – Sample Contour Map of Change in Seabed Elevation, 1997-2001

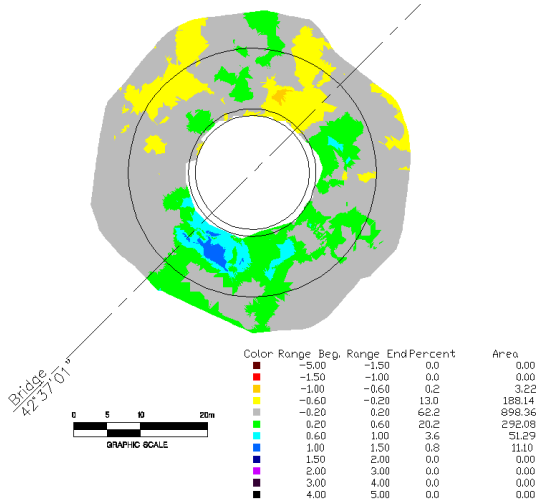

This information, along with the archived wave/current information and the results of diver inspections undertaken between 1997 and 2002, will be used to review/verify/ refine the scour assessment and design methodologies, and, if possible/appropriate, to support a reduction in the scour monitoring requirements.

CONCLUSIONS

A multi-faceted coastal engineering investigation was completed to support the assessment of scour and design of scour protection around the Confederation Bridge piers. This investigation led to the development of a new methodology to assess scour potential around bridge piers which can address complex flow conditions, pier geometries and foundation materials, but can also be applied to less complicated scour design problems. This methodology, derived from the empirical erodibility approach of Annandale (1995), has been calibrated for the Confederation Bridge project on the basis of the seabed response (scour or no scour) measured around four approach piers in place during a moderate storm event which occurred early in the construction period.

An extensive long-term monitoring program has been implemented to quantify the exposure of the bridge piers to potential scour events, to identify and address any scour that does occur, and to provide the information necessary to verify and improve the new scour assessment methodology. Preliminary results of the monitoring program, including diver inspections around all piers and multi-beam sonar seabed surveys around selected piers, suggest that the original scour assessment methodology may be conservative, as intended. A detailed reassessment study has been proposed, but has not yet been undertaken.

It is noted that the Annandale (1995) approach is referenced in the most recent version of HEC-18 (FHWA, 2001) in Appendix M – Scour Competence of Rock. The Confederation Bridge project represents the first known application of this method to bridge scour assessment and design.

ACKNOWLEDGEMENTS

The input and direction provided by SCBL over the course of this project is gratefully acknowledged, as is their permission to publish this paper.

REFERENCES

1. Anglin, C.D, Nairn, R.B., Cornett, A.M., Dunaszegi, L., Turnham, J. and Annandale, G.W. (1996), "Bridge Pier Scour Assessment for the Northumberland Strait Crossing", 25th International Conference on Coastal Engineering, ASCE. Orlando, FL.
2. Anglin, C.D., Nairn, R.B., Cornett, A., Dunaszegi, L. and Turnham, J. (1997), "Bridge Pier Scour Assessment for the Confederation Bridge", Canadian Journal of Civil Engineering, Vol. 24, No. 6, National Research Council of Canada, Ottawa, ON.
3. Anglin, C.D. Itamunoala, F. and Millen, G. (2002), "Riprap as a Permanent Scour Protection Measure", Proceedings of First International Conference on Scour of Foundations, Texas A&M University, College Station, Texas.
4. Annandale, G.W. (1995), "Erodibility", Journal of Hydraulic Research, IAHR 33(4).
5. Cornett, A.M. (1996), "Model Tests in Support of Scour Protection Design for the Northumberland Strait Crossing", National Research Council of Canada, Canadian Hydraulics Centre, Report HYD-CTR-008, Ottawa, ON.
6. Cornett, A.M., Sigouin, N. and Davies, M.H. (1994), "Erosive Response of Northumberland Strait Till and Sedimentary Rock to Fluid Flow",. National Research Council of Canada, Institute of Marine Dynamics, Report TR-1994-22, Ottawa, ON.
7. Federal Highway Administration, National Highway Institute (FHWA, 2001a), "Evaluating Scour at Bridges", Hydraulic Engineering Circular No. 18, Fourth Edition.
8. Federal Highway Administration, National Highway Institute (FHWA, 2001b), "Stream Stability at Highway Structures", Hydraulic Engineering Circular No. 20, Third Edition.
9. Federal Highway Administration, National Highway Institute (FHWA, 2001c), "Bridge Scour and Stream Instability Countermeasures", Hydraulic Engineering Circular No. 23, Second Edition.
10. Myrhaug, D. and Slaatelid, O.H.. (1990), "A Rational Approach to Wave-Current Friction Coefficients for Rough, Smooth and Transitional Turbulent Flow", Coastal Engineering, 14(3): 265-294.
11. Soulsby, R.L., Hamm, L., Klopman, G., Myrhaug, D., Simons, R.R. and Thomas, G.D. (1993), "Wave-Current Interaction Within and Outside the Bottom Boundary Layer", Coastal Engineering, 21(1): 41-69.
12. Southgate, H.N. and Nairn, R.B. (1993), "Deterministic Profile Modelling of Nearshore Processes - Part 1 - Waves and Currents", Coastal Engineering, 19(1): 27-56.
13. Transportation Association of Canada (TAC, 1973), "Guide to Bridge Hydraulics", First Edition.

Instruments to Measure and Monitor Bridge Scour

by
Everett V. Richardson,[1] Ph.D., P.E.

ABSTRACT

Field and laboratory research sponsored by the Federal Highway Administration, State DOT's and the Transportation Research Board has developed a toolbox of fixed and portable instruments for measuring and monitoring scour depths at bridges. Fixed measuring instruments are magnetic sliding collar, Low-cost sonar and float-out cylinders. Portable are physical probing rods and weights on cable, low-cost sonar, and geophysical. A toolbox of instruments is needed in-order-to select the appropriate instrument for the many varied bridge, stream and environmental conditions. These instruments have satisfactory operated in this varied environment. They have significantly improved the scour database, methods of predicting scour depths, bridge scour monitoring and to bridge safety.

INTRODUCTION

In the United States, as of April 2002, there are 26,149 scour critical bridges, 20,353 scour susceptible and 88,912 with unknown foundations These statistics come from an on going screening and evaluation program of the 484,286 bridges over water in the United States. With limited funds available, these bridges cannot all be replaced or repaired. Also, during a flood, scour is generally not visible and on the falling stage of a flood, scour holes generally fill in. Therefore, scour depths of scour critical, and scour susceptible bridges and bridges with unknown foundations must be monitored during high flows. This monitoring with a suitable plan of action (for example close the bridge when scour reaches a given depth) is considered to be an adequate scour countermeasure for these bridges. In addition, every bridge in the U. S must be inspected every two years. If the foundations cannot be inspected during the two-year inspection, an underwater inspection is required every 5 years. These inspections require that a profile of the elevation of the streambed at the bridge be taken. Thirdly, the development and/or improvement of equations to determine bridge scour depths require field measurements of scour depths along with the corresponding hydraulic conditions. For these reasons, two basic categories of instruments, portable or fixed, have been developed in the United States.

Whether to use fixed or portable instruments in a scour monitoring or measurement program depends on many different factors. Unfortunately, there is not one type of instrument that works in every situation encountered in the field. Each instrument has advantages and limitations that influence when and where they should be used. The idea of a toolbox, with various instruments that can be used under specific conditions, best illustrates the strategy to use in selecting instrumentation for a scour-measuring/monitoring program. Specific factors to consider include the frequency of

[1] Senior Associate, Ayres Associates, P.O. Box 270460 and Professor Emeritus of Civil Engineering, Colorado State university, Fort Collins, CO, 80527

data collection, the physical conditions at the bridge and stream channel, and traffic safety issues.

Fixed instrumentation is used when frequent measurements or regular, ongoing measurements (e.g., weekly, daily, or continuous) are required. Portable instruments would be preferred when only occasional measurements are required, such as for the inspection program, or during a major flood. The physical conditions at the bridge, such as height off the water and type of superstructure, can influence the decision to use fixed or portable equipment. For example, bridges that are very high off the water, or that have large deck overhang or projecting geometry's, would complicate portable measurements from the bridge deck. Making portable measurements from a boat assumes that a boat ramp is located near the bridge, there is sufficient clearance under the bridge for safe passage of a boat and the turbulence and velocity of the flow allow the boat to get near the foundations. . Bridges with large spread footings or pile caps or those in very deep water can complicate the installation of some types of fixed instruments. Stream channel characteristics include sediment and debris loading, air entrainment, ice accumulation, or high velocity flow, all of which can adversely influence various measurement sensors used in fixed or portable instruments. Traffic safety issues include the need for traffic control or lane closures when either installing or servicing fixed instruments, or attempting to make a portable measurement from the bridge deck.

Therefore, it is apparent that the selection of the instrument category (fixed or portable) and the specific instrument types to be used in a measurement/monitoring plan is not always straightforward. In some situations there is no clearly definable plan that will be successful, and the plan is developed knowing that the equipment may not always work as well as might be desired. Ultimately, the selection of any type of instrumentation must be based on a clear understanding of its advantages and limitations, in consideration of the conditions that exist at the bridge and in the channel and the objectives of the monitoring/measuring program.

To improve the state-of-practice the National Academy of Science's Transportation Research Board (TRB) under the National Cooperative Highway Research Program (NCHRP) funded research programs to develop fixed and portable instruments to measure scour depths. In addition, to facilitate the technology transfer of instrumentation-related research to the highway industry, the Federal Highway Administration (FHWA)(1998) developed a Demonstration Project (DP97) on scour monitoring and instrumentation. The purpose of the Demonstration Project was to promote the use of new and innovative equipment, both fixed and portable, to measure scour, monitor changes in scour over time, detect the extent of past scour, and serve as countermeasures. This paper provides information on the development and use of portable and fixed instrumentation. The experience of several State Highway Agencies with the use scour depth instrumentation is also included.

FIXED SCOUR MEASURING INSTRUMENTATION

A review of the literature (Lagasse, et al, 1997 and 2001) determined that fixed scour-measuring and -monitoring instruments could be grouped into four broad categories:

1. Sounding rods - manual or mechanical device (rod) to probe streambed

2. Buried or driven rods - device with sensors placed vertically into streambed
3. Fathometers - commercially available sonic depth finder
4. Other Buried Devices - active or inert buried sensor (e.g., buried transmitter)

Sounding Rods

Laboratory and field testing of sounding rod devices, determined that 1) binding of the rod in its supporting enclosure (pipe) could be a factor for large scour depth; 2) in sand bed streams, sand deposited between the rod and its supporting enclosure also would bind it up; and 3) in sand- and noncohesive bed materials the rod would penetration into the bed a significant and indeterminate amount. However, successful installations have been reported on coarse-bed streams by the manufacturer (Cayuga Industries) and USGS (Lagasse, et al, 1997).

Buried or Driven Rods

Buried/Driven rods includes all sensors and instruments supported by a vertical support member such as a pipe, rail or column placed vertically in the bed, at the location where scour would be expected to occur. Installation of the support column is either by driving, jetting, augering, or excavation and burying. Examples of buried/driven rods include Hubbard's electrode-empedence (Laursen and Toch, 1956), New Zealand's "Scubamouse" (Melville, et al, 1989), Wallingford's "Tell-Tail" (Waters, 1994) and Transportation Research Board's (TRB) "Magnetic Sliding Collar" (Lagasse et al, 1997, 1998, 2001) The following discussion will focus on magnetic sliding collar devices.

Magnetic Sliding Collar . Both simple (manually read) and automated readout magnetic sliding collar were developed in the TRB project. Plans are given in NCHRP Report 397 B (Schall, et al 1997)

The instrument consists of a 51-mm (2-inch) diameter stainless steel support pipe in 1.5-m (5-foot) sections, which is buried in the bed of the stream. . A magnetic collar slides on the support pipe, (Figure 1 and 2). To determine the position of the collar, in the manually read device, a sensor consisting of a magnetic switch attached to a battery and buzzer on a long graduated cable is lowered through the annulus of the support pipe. The buzzer is activated when the sensor reaches the magnetic collar. Collar position is determined by using the graduated cable to determine the distance from an established datum near the top of the support pipe to the magnetic collar.

The automated readout magnetic sliding collar consists of string of magnetically actuated reed switches located at pre-selected intervals (152-mm (6-inch), 304.8-mm (1 ft), and etc) along the length of a waterproof flexible tubing, which is inserted in the support pipe. Magnets on the sliding collar actuate the reed switch as it is lowered by scour. A data logger provides excitation voltage for the reed switches and records the elevation of the scour depth. The data logger can be down loaded periodically into a portable computer or accessed by phone (landline or satellite). Power can be provided locally or by solar panels (see Figure 2 and 4).

Thirty-six manually read or automated sliding collar devices have been installed in eleven States. They were successfully installed and operated on tidal estuaries, and ephemeral and perennial rivers (Lagasse, et al, 2001, Price, 2002).

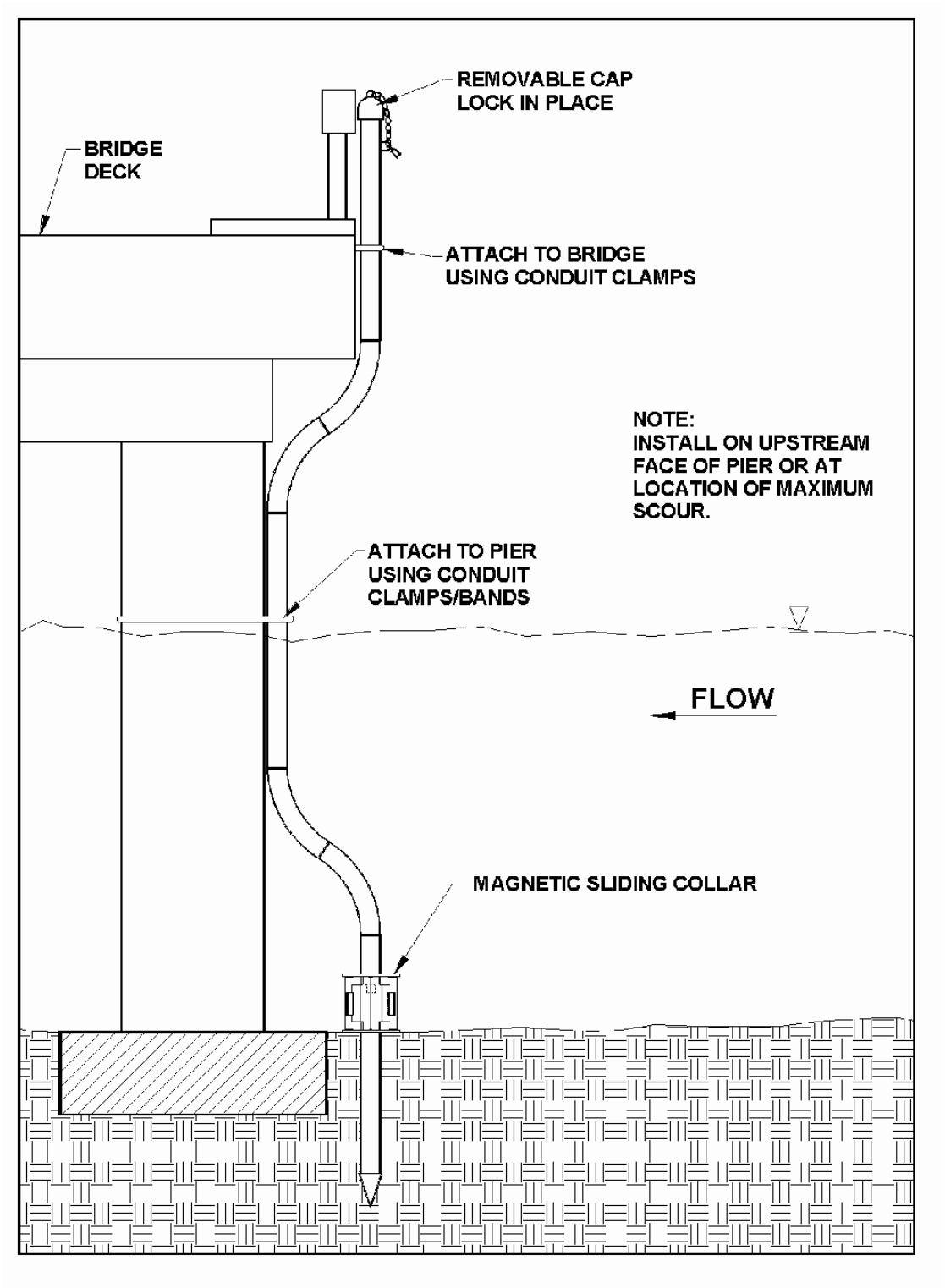

Figure 1. Manual read out magnetic sliding collar device (Schall, et al, 1997B).

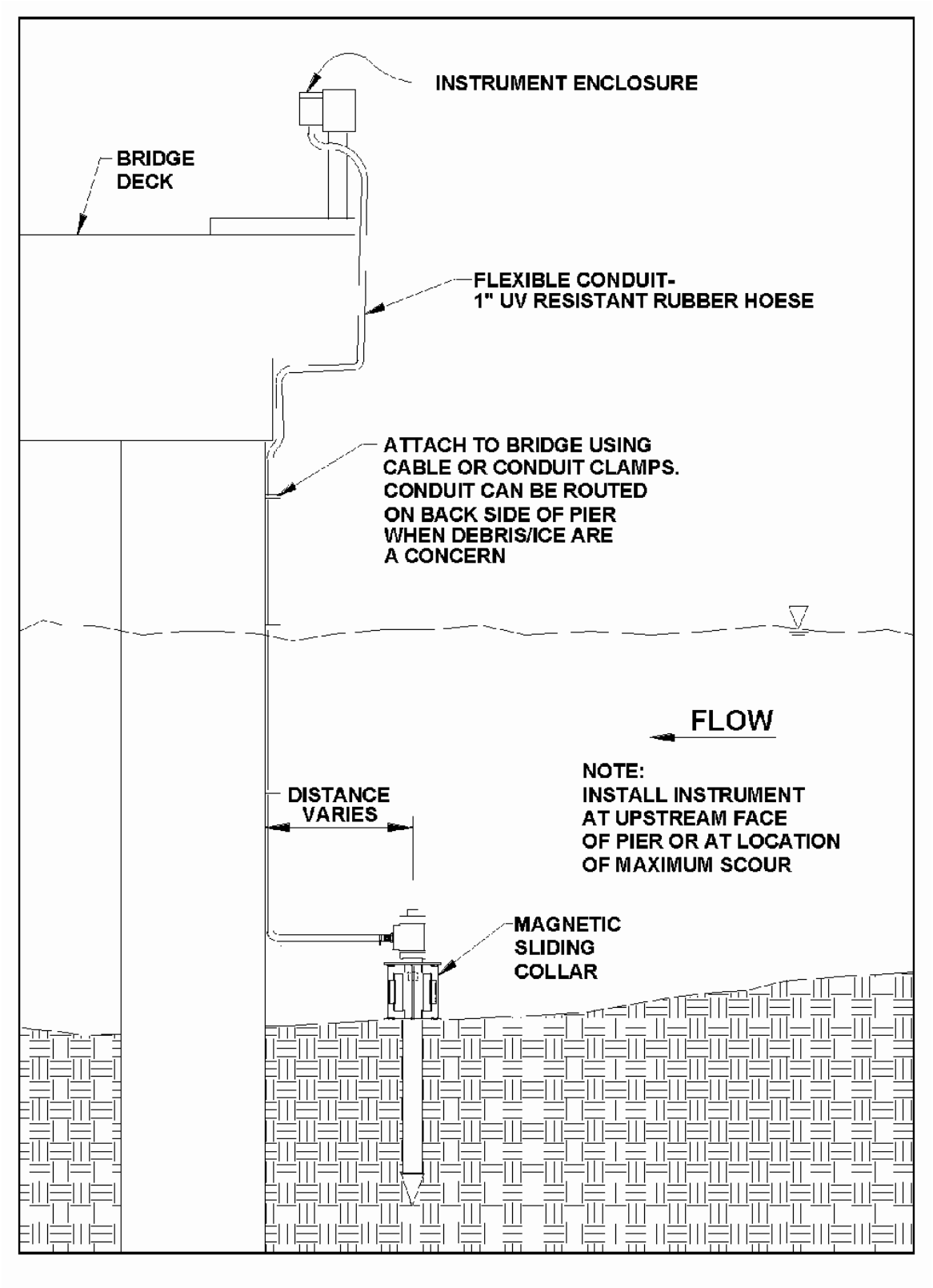

Figure 2. Automated read out magnetic sliding collar system (Schall, et al, 1997B).

Fathometers

Fathometers, a sonar instrument or sonic sounder, which measures distance based on the travel time of a sound wave through water. Fathometers consists of the electronics (black box) for generating and receiving the sound pulse and converting it to distance. And a transducer, which is in the water, transmits and receives the sound wave to and from the bed. Transducer frequency (typically around 200 kHz) and beam width are important considerations in the use of sonar for scour monitoring work. There are several fathometers available commercially, which are relatively expensive instruments for a scour-monitoring-measuring function. Research conducted by the NCHRP project determined that low-cost fathometers (recreational-type sonar fish-finders) could be used for measuring scour (Lagasse, et al, 1997).

The low-cost fathometers would determine the scour depth plus or minus 0.3 m (1 ft), which is acceptable for field scour measurements. Such devices are readily available from several manufacturers. These commercially available fishfinders do not have corrections for temperature and salinity effects on the speed of sound. However, studies found that there should not be a concern for most installations, with the limits of ± 0.3 m [± 1.0 ft] accuracy and for the depth and temperature ranges expected at most riverine and tidal bridge sites. If necessary, the corrections for temperature and salinity can be made as a post-processing step.

Low-cost fathometers scour measuring/monitoring instruments consists of a fishfinder, its transducer, an above water serviceable transducer mounting, data logger, power source and read out device (Schall et al, 1997A, Lagasse et al, 2001). The power source can be solar panel or power line. Read out can be by down loading to a computer or telemetry. Generally telemetry is by phone, either landline or cellar. Transducers need to be cleaned periodically. This is made easy by installing a conduit to the pier and sliding the transducer on a pipe inside the conduit for easy removable and bridge service. The master instrument can be configured to service many transducers (Price, 2002).

Fathometers are mounted so the transducer is aimed at the location where maximum scour will occur. The sonar signal must be unobscured by debris or ice. Loss of signal can occur with air entrainment or very high sediment concentrations. However, normally these are not of major concern for most applications. The fathometers have operated successfully in concentrations of sand as large as 50,000 ppm and silts and clays as large as 100,000 ppm.

Sixty-three low-cost fathometers have been installed in 11 States and the District of Columbia. They were successfully installed and operated on tidal estuaries, and ephemeral and perennial rivers (Lagasse, et al, 2001, Price, 2002). Six transducers are successfully monitoring the scour at six piers on the I-95 (Woodrow Wilson) bridge over the Potomac River estuary downstream from Washington, D. C., (Price, 2002) One master instrument (fish-finder sonar, data logger, solar panel, battery, and landline phone) services the six transducers.

Other Buried Devices

Other Buried Devices includes sensors, which could be buried in the bed of a river at various elevations. When scour exposes these instruments they would float out of the

scour hole. These float-out devices could be either untethered or tethered to the pier or abutment. Obtaining scour data from a tethered device could be as simple as visually inspecting which tethered devices have been removed from the hole by scour. Untethered devices would most likely incorporate a motion-activated transmitter, with a receiver on the bridge or stream bank sensing when a transmitter has been moved and activated (Winter, 1995, Price, 2002).

Float-out Cylinder As a monitoring device, to protect scour susceptible bridges on ephemeral stream, a buried transmitter "float-out" device was developed for application on bridge piers (Price, 2002). This device consists of a 6 x by 11-inch cylinder with a radio transmitter buried in the channel bed at a pre-determined depth. When the scour reaches that depth, the float-out cylinder rises to the surface and begins transmitting a radio signal to a receiver in an instrument shelter on the bridge. The receiver transmits the information to a central location by telemetry. Normally by Landline or cell phone. The battery in the cylinder lasts 8 to 10 years. Installation requires using a conventional drill rig with a hollow stem auger (Figure 3). After the auger reaches the desired depth, the float out transmitter is dropped down the center of the auger. Substrate material refills the hole as the auger is withdrawn. Two cylinders are often placed in the auger hole. The first to alert that scour is approaching a problem and the second at the critical depth where action needs to be taken.

Figure 3. Hollow stem auger and installation of a float-out cylinder. (Lagasse et al, 2001)

The float-out devices can be monitored by the same type of master instrument shelter/data logger currently being used to telemeter low-cost fathometer or automated sliding collar data. A master instrument shelter serves all devices. It contains the data logger, phone telemetry, and a solar panel/gell-cell battery for power, (Figure 4).

One hundred and twenty nine float-out devices have been installed at bridges in Alabama, Arizona, California, and Nevada (Lagasse et al, 2001, Price, 2002). Most devices were installed at various levels below the streambed as described above. However, several devices at bridges in Nevada were buried in riprap at the base of bridge piers to monitor riprap stability, (Figure 5). At several of the bridges sliding-collar or low-cost sonar instruments were installed.

One of the bridges experienced several scour events that triggered threshold warnings during February 1998. In one case the automated sliding collar dropped 1.5 m (5 ft) causing a pager call-out. Portable sonar measurements confirmed the scour recorded by the sliding collar. Several days later, another pager call-out occurred from a float-out device buried about 4 m (13 ft) below the streambed. In both cases, the critical scour depth was about 6 m (20 ft) below the streambed and no emergency action was called for to insure public and/or bridge safety.

PORTABLE SCOUR MEASURING EQUIPMENT

A wide variety of instruments have been used for making portable scour measurements. In general, the methods for making a portable scour measurement can be classified as:

1. Physical probing
2. Fathometers (Sonar)
3. Geophysical

Physical Probes

Sounding poles and sounding weights on a cable are the most common physical probes. Sounding poles are long poles used to probe the bottom, (Figure 6). Sounding weights, sometimes referred to as lead lines, are typically a torpedo shaped weight suspended by a measurement cable, (Figure 7). Sound weights typically range from 3.7 to 75 kg (10 to 200 lbs). The lighter weights can be used with a hand line. Whereas, the heavier weights use a crane and reel. They can be used from the bridge or from a boat. Physical probes collect discrete data and can be limited by large depth and velocity (e.g., during flood flow condition) or debris and/or ice accumulation. Advantages of physical probing include not being affected by air entrainment or high sediment loads, and it can be effective in fast, shallow water.

Fathometers

Fathometers or acoustic depth sounders, as described in the fixed instrument section are widely used for portable scour measurements. Fish finders and precision survey-grade hydrographic survey fathometers are used. However, low-cost fish-finder type sonar instruments have been widely used for bridge scour investigations. When the measurements are made from the bridge, transducers are attached to a pole (Figure 8), hand-line, tethered float, or attached to a boom. Tethered float platforms include kneeboards, (Figure 9) and pontoon-style floats, (Figure 10). The size of the float is important for stability in fast moving, turbulent water.

Figure 4. Typical instrument shelter with data logger, cell-phone telemetry, and a solar panel/gel-cell for power. (Lagasse et al, 2001)

Figure 5. Installation of a float-out device to monitor riprap stability. (Lagasse et al, 2001)

Floating or non-floating systems can be deployed from a bridge inspection truck. This is particularly useful when the bridge is high off the water. For example, bridges that are greater than 15 m (50 ft) off the water are typically not accessible from the bridge deck without using this approach.

An articulated arm to position a sonar transducer was developed under an FHWA research project (Bath, 1999). The system was mounted on a trailer and could be used on bridge decks from 5-15 m (16-50 ft) above the water surface. An onboard computer calculated the position of the transducer, relative to a known position on the bridge deck, based on the angle of the boom and the distance between the boom pivot and transducer. A NCHRP project is developing a truck mounted articulated arm to position a sonar transducer using the same concepts, (Figure 11) (Shall, 2002)

A Sonar Scour Vision system was developed by American Inland Divers, Inc (AIDI) using a rotating, and sweeping 675 Khz high resolution sonar (Barksdale, 1994). The transducer is mounted in a relatively large hydrodynamic submersible, or fish, that creates a downward force adequate to submerge the transducer in velocities exceeding 6 m/s (20 ft/s). Given the forces created, the fish must be suspended from a crane or boom truck on the bridge. From a single point of survey, the system can survey up to 100 m (328 ft) radially. Data collected along the face of the bridge can be merged into a real-time 3-dimensional image with a range of 90 m (295 ft) both upstream and downstream of the bridge.

Manned boats are used as a platform for scour measurements. They generally require adequate clearance under the bridge and nearby launch facilities. This can be a problem at flood conditions when the river stage may approach or submerge the bridge low chord, and/or boat ramps may be underwater. Normally a fathometer is used for depth measurements and GPS systems for location.

The safety, launching and clearance issues have led to the development of a prototype unmanned boat. It uses a small flat bottom jon boat, an 8 hp outboard motor, fathometer and GPS with remote controls. It was successfully tested during six flood events (Mueller and Landers, 1999).

The advantage of GPS over traditional land-based surveying techniques is that line-of-sight between control points is not necessary. GPS also works at night and during inclement weather, which could be a real advantage for scour monitoring during flood conditions. The disadvantage of GPS is the inability to get a measurement in locations where overhead obstructions exist, such as tree canopy or bridge decks. However, GPS measurements up to the bridge face, without venturing under the bridge, have been successful.

Figure 6. Sounding pole measurement.

Figure 7. Lead-line sounding weight with truck mounted crane.

Figure 8. Portable sonar in use. Transducer on tip of rod.

Figure 9. Kneeboard float with transducer.

Figure 10. Pontoon float, note the transducer.

Figure 11. Truck mounted articulated arm with sonic transducer, fathometer, and computer.

Geophysical

Geophysical instruments, based on wave propagation and reflection measurements, determine the interfaces between materials with different physical properties. A primary difference between sonar and geophysical techniques is that geophysical methods provide sub-bottom information, while sonar can only "see" the water-soil interface and is not able to penetrate the sediment layer. The main difference between different geophysical techniques are the types of signals transmitted and the physical property changes that cause reflections. A seismic instrument uses acoustic signals, similar to sonar, but at a lower frequency (typically 2-16 kHz). Like sonar, seismic signals can be scattered by air bubbles and high sediment concentrations. A ground penetrating radar (GPR) instrument uses electromagnetic signals (typically 60-300 mHz), and reflections are caused by interfaces between materials with different electrical properties. In general, GPR will penetrate resistive materials and not conductive materials. Therefore, it does not work well in dense, moist clays, or saltwater conditions.

The best application of geophysical technology is to determine scour depth after a flood during lower flow conditions in areas of infilling. In general, the cost and complexity of the equipment and interpretation of the data are limiting factors for widespread use and application as a portable scour monitoring device. These issues have moderated as newer, lower cost GPR devices with computerized data processing capabilities have been developed. However, GPR may still be limited by cost and complexity, and often the need for bore hole data and accurate bridge plan information to properly calibrate and interpret the results.

SUMMARY

Fixed scour depth measuring/monitoring equipment has been successfully used under many different bridge, stream and climate environmental conditions. Their success has required a toolbox approach. The instruments in the toolbox are magnetic sliding collar, low-cost sonar and float-out cylinders. The have been installed in remote locations with solar panels for power and telemetry for instant access to scour depth information.

Portable scour measuring instruments are physical probing with rod or weights, sonar and geophysical. Physical probing and sonar are useful for real-time measuring scour during a flood and for routine measurements of bridge cross-sections. Geophysical instruments are better used for scour determination after the flood and scour holes have filled in.

The development of these fixed and portable scour measuring instruments, along with GPS, remote controlled boats, instrumented trucks, and awareness of the need to measure and monitor scour at bridges have significantly improved the scour data base, methods of predicting scour depths, monitoring bridges for scour and to bridge safety.

REFERENCES

Barksdale, G. 1994, "Bridge Scour During the 1993 Floods in the Upper Mississippi River Basin," ASCE Compendium on Stream Stability and Scour at Bridges, Richardson, E.V. and Lagasse, P.F. (eds.), Reston, VA. p 551.

Bath, W.R., 1999, "Remote Methods of Underwater Inspection of Bridge Structures," FHWA Report RD-99-100, Turner-Fairbank Highway Research Center, McLean, VA.

Federal Highway Administration, 1998, "Scour Monitoring and Instrumentation," Demonstration Project 97 Participants Workbook, FHWA-SA-96-036, Office of Technology Applications, Washington, D.C.

Lagasse, P.F., E.V. Richardson, J. D. Schall, G.R. Price, 1997, "Instrumentation for Measuring Scour at Bridge Piers and Abutments," NCHRP Report 396, Transportation Research Board, NRC, National Academy Press, Washington, D.C., 110 pp.

Lagasse, P.F., E.V. Richardson, J. D. Schall, J. R. Richardson, and G.R. Price, 1998, "Fixed Instrumentation for Monitoring Scour at Bridges," ASCE Compendium on Stream Stability and Scour at Bridges, Richardson, E.V. and Lagasse, P.F. (eds.), Reston, VA. p 505.

Lagasse, P.F., L.W. Zevenbergen, J.D. Schall, and P. E. Clopper, 2001, "Bridge Scour And Stream Stability Countermeasures," Hydraulic Engineering Circular 23, Second Edition, FHWA NHI 01-003, Federal Highway Administration, Washington, D.C.

Laursen, E. M. and Toch A., 1956, "Scour Around Bridge Piers and Abutments," Bull No. 4, Iowa Highway Research Board, Iowa Institute of Hydr. Research, Iowa City, IA, 60 pp.

Melville B.W., Ettma, R., and Jain, S.C., 1989 “Measurement of Bridge Scour,” Bridge Scour Symposium, Turner-Fairbank Highway Research Center, cosponsored by Federal Highway Administration and Subcommittee of Sedimentation, Interagency Advisory Committee on Water Data, OWDC, USGS, McLean, VA, pp. 183-194.

Mueller, D.S. and M.N. Landers, 1999, "Portable Instrumentation for Real-Time Measurement of Scour at Bridges," Federal Highway Administration Publication No. FHWA-RD-99-085 (FHWA approval pending), Turner-Fairbank Highway Research Center, McLean, VA.

Price, G. R., 2002, "Personnel Communication," Instrument Systems, Inc., 1317 Webster Ave., Ft. Collins, CO, 80524

Schall, J.D., G.R. Price, G.A. Fisher, P.F. Lagasse, and E.V. Richardson, 1997a, "Magnetic Sliding Collar Scour Monitor-Installation, Operation, and Fabrication Manual," NCHRP Report 397B, Transportation Research Board, NRC, National Academy Press, Washington, D.C.

Schall, J.D., G.R. Price, G.A. Fisher, P.F. Lagasse, and E.V. Richardson, 1997b, "Sonar Scour Monitor-Installation, Operation, and Fabrication Manual," NCHRP Report 397A, Transportation Research Board, NRC, National Academy Press, Washington, D.C.

Schall, J.D., 2002, "Personnel Communication," Ayres Associates, P. O. Box 270460, Ft. Collins, CO, 80527

Waters, C.R., 1994, “The HR Wallingford Scour Monitoring System,” 1994 Centenary Year Bridge Conference, Cardiff, United Kingdom pp. 323-328.

`

Development and Implementation of a Scour Monitoring Program for Selected Bridges Crossing the Trukee River

Keith E. Dennett[1], Pat Fritchel[2], Raj Siddharthan[3], and Amir Soltani[4]

PROJECT OVERVIEW

Based on the results of a bridge scour assessment conducted in 1993, hydraulic engineers at the Nevada Department of Transportation (NDOT) concluded that the accepted mathematical methods typically used to predict bridge pier scour (e.g., HEC-18) are likely to substantially overestimate the potential for scouring around bridge piers in the Truckee River. This was evidenced by the fact that most of the bridges classified as "scour critical" by these methods withstood a significant flood (a 100+ year storm event) in 1997 with little or no detectable damage.

A preliminary analysis of the scour equations presented in HEC-18 has indicated limitations in predicting scour depths when the riverbed consists mainly of large diameter particles (+0.4 ft). The bed of the Truckee River consists mainly of coarse gravels, cobbles, and boulders which is consistent with glacial outwash geomorphology.

The long-term objective of the research project is to calibrate the accepted scour equations for conditions in the Truckee River. To accomplish this objective, a bridge scour monitoring program is being implemented. This program will incorporate both fixed and portable scour monitoring devices to quantify bridge scour during significant runoff events. The monitoring data that is collected will enable specific parameters in the HEC-18 equations, such as the factor K_4, which accounts for coarse grain particles, to be adjusted to reflect the local conditions.

BACKGROUND SUMMARY

A bridge scour evaluation program was developed and implemented by NDOT in November 1993 in order to comply with recommendations from the Federal Highway Administration (FHWA) (Soltani *et al.*, 1993). Under this evaluation program, all of the bridges owned by NDOT were evaluated and the vulnerability of these bridges to scour was estimated.

Bridges are classified as either "stable" or "scour critical" according to their vulnerability to scour using a rating system developed by the FHWA (FHWA, 1995). A "scour critical" bridge is

[1] Assistant Professor, Department of Civil Engineering, Mail Stop 258, University of Nevada, Reno, NV 89557, USA, E-mail: dennett@unr.nevada.edu
[2] Graduate Research Assistant, Department of Civil Engineering, Mail Stop 258, University of Nevada, Reno, NV 89557, USA
[3] Professor, Department of Civil Engineering, Mail Stop 258, University of Nevada, Reno, NV 89557, USA
[4] Chief Hydraulic Engineer, Nevada Department of Transportation, 1263 S. Stewart Street, Carson City, NV 89712, USA

one that has abutment or pier foundations that are considered unstable due to (1) observed scour at the bridge site or (2) the potential for scour as determined from a scour evaluation study (FHWA, 1995).

A scour evaluation study may consist of three parts identified as Level 1, Level 2, and Level 3 (Williams *et al.*, 1997). A Level 1 study is a qualitative evaluation of the stability of a streambed at a bridge crossing and an examination of the bridge structure for evidence of scour. A Level 1 study is often used to identify bridges that require more detailed study. A Level 2 study involves the collection of field data, hydraulic modeling, and prediction of the estimated maximum depth of scour for a selected design flood. A Level 3 study typically involves sediment transport modeling.

The development of realistic models for sediment transport is presently limited by the ability to identify, formalize, and parameterize the individual transport and reaction processes that occur (Van Cappellen and Wang, 1995). The rate of erosion or resuspension depends on the erosive forces exerted by the flowing water at the sediment-water interface and the resistance of the sediment to erosion or resuspension (Lagasse *et at.*, 1995).

Determining an expression for the rate of erosion or resuspension remains one of the most challenging aspects of modeling the bed exchange process (Bedford, 1992). The currently accepted expressions for predicting the amount of sediment transport and potential for scour around bridge piers (e.g., HEC-18) have been successfully applied in many locations (Richardson and Davis, 1995). However, when these expressions are applied to channel reaches along the Truckee River, they seldom provide results that are consistent with observed field measurements of sediment transport and potential for scour. This may be due to a combination of geomorphic, hydrologic, and hydraulic conditions in the Truckee River.

This research project will extend earlier studies completed by NDOT. The results of the earlier work indicated that a number of bridges should be classified as scour critical. However, subsequent field inspections conducted by NDOT personnel suggested that there was no evidence of excessive scouring at a number of these locations.

RESEARCH AND ANALYSES

This project focuses on bridge sites located along the Truckee River and involves the installation of devices to monitor bridge scour. Four bridge sites have been selected initially based on the availability of historical information at bridge sites, previous field measurements of scour, site accessibility, and pier construction and configuration. Specific tasks being conducted during this project are described below.

Preliminary Review of Bridge Sites

Four bridges (Keitzke Lane, Kuenzli Street, Keystone Avenue, and Mayberry Drive) were selected for initial evaluation out of several bridges along the Truckee River. A literature review was performed to gather historical information contained in bridge construction reports, periodic bridge inspection reports, and any available reports on field monitoring of pier scour. Bridge sites that have been classified as “scour critical” based on previous Level 1 and/or Level 2 scour

analyses received primary consideration. Boring logs were examined in order to define the geologic strata at each bridge site. However, the geotechnical information was usually too general to obtain a detailed classification of the particle sizes. Therefore, it will be necessary to conduct more a detailed geotechnical investigation at each of the selected bridge sites in order to classify particle sizes and subsurface conditions.

The selected bridges vary in pier construction and orientation in the flow as indicated below and shown in Figures 1 through 4.

- Kietzke Lane: square pier with the corner skewed into the direction of flow
- Kuenzli Street: elongated square pier oriented in direction of flow
- Keystone Avenue: cylindrical pier groups oriented in direction of flow
- Mayberry Drive: elongated square pier with chamfers in direction of flow

Evaluation of Scour Monitoring Devices

Information on a variety of scour monitoring devices (e.g., fixed and portable) has been gathered and evaluated (Lagasse et al., 1997). The selection of appropriate scour monitoring devices for a monitoring program depends on site conditions and operational limitations of particular types of instrumentation. Site conditions that affect monitoring include streambed composition, bridge height, depth of flow, and flow velocity. Operational limitations are related to poor performance during periods of excessive sediment transport and bed load transport, debris flows, and ice flows, as well as specialized training required to operate certain pieces of equipment.

The channel bed in the Truckee River consists mainly of very coarse, large materials that may require pre-drilling or track-hoe excavation for the installation of embedded rod devices (e.g., sliding collar and piezoelectric). The costs associated with installation as well as right-of-way constraints made the use of these devices cost prohibitive for this project. As a result, they were eliminated from further consideration.

The sounding rod device is ideal for the coarse bed materials in the Truckee River. However, because of high velocities associated with seasonal flow variations in the Truckee River, the use of this type of device has been excluded due to problems with the unsupported length.

From the research completed to date, fixed sonar devices and geophysical devices appear to be the most appropriate choices for the proposed long-term monitoring in the Truckee River. Sonar devices should be relatively easy to install and are considered to be one of the more accurate types of scour monitoring devices. They are also capable of providing time-history and aggradation measurements. Installation by equipment on the bridge deck may be possible on some of the lower bridges. A major shortcoming of this device is that debris may inhibit its ability to make accurate streambed measurements during high flow conditions.

The geophysical devices which employ ground-penetrating radar also appear to be a viable option. This device could possibly offer an alternative to sonar devices in case a sizable storm event does not occur in the near future. Instead of monitoring future scour, it may be possible to use geophysical monitoring to correlate previous scour depths to historical runoff events. In

addition to recording historical scour depths, this technique could potentially be useful in determining unknown pier depths. Further research and evaluation is ongoing in these areas.

Scour monitoring programs will typically involve a combination of fixed, portable, and geophysical instrumentation to collect data in the most efficient manner. Portable instrumentation should be used to "ground truth" fixed instruments to ensure accurate results and to evaluate the potential shift of the location of maximum scour. The sonar device appears to be the best alternative for portable instrumentation. Although its functionality during high flows is suspect, it can be used as a secondary device for confirmation of the results from the fixed device during lower flows.

The portable scour monitoring device owned by NDOT has been evaluated in several trials along the Truckee River. The device, which consists of a sonar instrument mounted on a surfboard frame, needed to be modified slightly to deliver consistent results. As shown in Figure 5, these modifications include a PVC frame and balancing weight. After several trials of different measuring techniques and board configurations, it was determined that streambed elevations may be effectively obtained with this device. The board is manually pulled across the river on a steel guide cable attached to posts on opposite sides of the river. As the river rises, the cable may be raised on the posts to maintain the proper cable to river height for the board frame.

Preliminary Scour Equation Evaluation

Two of the bridges (Kuenzli and Keitzke) included in this project were evaluated utilizing the revised pier scour equation from the Fourth Edition of HEC-18 (Richardson and Davis, 2001) and compared to results obtained using the equation from the Third Edition (Richardson and Davis, 1995). As shown in Table 1, the depth of scour obtained with the Fourth Edition equation is significantly less than the value obtained by the Third Edition equation. Furthermore, the scour rating code, Item 113[5] is less severe for these bridges, yielding a rating of 3(C) using the Third Edition equation, which is indicative of a calculated depth of scour below the bottom of the footing.

For the Keitzke Bridge, the Fourth Edition equation predicted a scour depth less than the footing depth and a scour code rating of either 3(C) or 5, depending on the results of a structural analysis of the foundation.

For the Kuenzli Bridge, the Fourth Edition equation yielded a scour depth significantly less than the Third Edition equation. However, the calculated depth of scour was still below the bottom of footing, so the scour rating would still remain critical at 3(C).

From a sensitivity analysis conducted on the Keitzke Bridge, the scour consistently decreased as particle size increased until a particle size of approximately 0.4 feet was reached. As shown in Figure 6, for particle sizes greater than 0.4 feet, the results predicted a constant scour depth of 7.5 feet. Evidently, this is due to limitations associated with the K_4 factor in the equation. The minimum value of K_4 is 0.4.

[5] Recording and Coding Guide for the Structure Inventory and Appraisal of the Nation's Bridges (FHWA, 1995)

Similar results were obtained for the other two bridges, Keystone Avenue and Mayberry Drive. In light of these preliminary results, the scour code for other NDOT bridges may be revised to less severe ratings, pending re-evaluation utilizing the revised equation in the Fourth Edition of HEC-18. Moreover, calibration of the scour equation to the bed conditions of the Truckee River could result in additional bridges being classified as non-scour critical. Mueller and Jones (1999) concluded that the coefficients (e.g., K_4) based on laboratory data do not provide sufficient reductions in computed scour depths to compare favorably with observed depths. Additionally, they recommend further research to improve on scour predictions in nonuniform coarse bed material. Therefore, it is likely that the scour rating for other bridges will be reduced further following additional research and refinement of the scour coefficients.

ACCESS PLAN AND GEOTECHNICAL INVESTIGATION

A major component of the detailed geotechnical investigation will involve the development of a soil profile of the bed material with depth for a few locations along the Truckee River. By classifying the soil profile with depth, the significance of bed armoring for protecting the bed from scour can be determined.

Accessing the Truckee River to obtain large quantities of bed material to quantify particle size distributions is a significant task due to physical and environmental constraints. It was decided to utilize soil profile information for particle size characterization at the riverbank in lieu of adjacent to the pier. This will greatly reduce the impact to the river, simplifies permitting, and reduces the cost and time frame for soil sampling. A pit approximately 10 to 12 feet deep should be sufficient to characterize the soil at a level below the spread footings of the piers.

The bridge sites were evaluated for ease of access and it appeared that all of the riverbanks near the selected bridges are accessible. However, the access routes still need to be evaluated for equipment safety. Additionally, right-of-way (ROW), soil classification techniques, and environmental permitting need to be addressed. The access plan will consist of the following elements.

1. Perform an equipment safety review.
2. Conduct a preliminary environmental impact review.
3. Identify the ROW, access easements, and property owners along the access areas.
4. Determine the techniques and procedures to be used for classifying soil.
5. Conduct a preliminary field review by all affected parties.
6. Assess the bridge site for accessibility and select final bridges for monitoring.
7. Prepare access plans and reports for each selected bridge site including:
    - Base topography, boundaries, existing improvements and vegetation areas
    - Identify on plan areas of disturbance, fill, excavation an best management practices
    - Prepare a traffic control plan
    - Prepare permit applications and supporting reports for the United States Army Corps of Engineers and the City of Reno
8. Process permits through the appropriate agencies
9. Perform the geotechnical investigation and classify the particle size distributions.

LONG-TERM MONITORING PLAN

The long-term scour monitoring plan will consist of measuring pier scour with fixed and portable devices over an extended period of time. The flow in the Truckee River will be monitored using the United States Geological Survey (USGS) gauging stations that are already in place at various sites along the Truckee River. Fixed scour monitoring devices installed at the selected bridge sites will be monitored continuously to monitor changes in scour depth over time.

Detailed measurements of the channel cross sections at the selected bridge sites will be collected. These channel cross sections will be compared to any available historical records of channel cross sections at the same site. Channel cross sections at each of the selected bridge sites will be measured approximately every four months or immediately following significant flow events in order to monitor changes in overall channel geometry with time.

CALIBRATE EXISTING EQUATIONS FOR CONDITIONS IN THE TRUCKEE RIVER

The experimental data collected during this study will be used in an effort to calibrate the existing scour models presented in HEC-18 (Richardson and Davis, 2001) for the conditions that are observed in the Truckee River. Current methods tend to substantially overestimate the depth of scour around bridge piers in the Truckee River. For example, appropriate values for parameters such as the correction factor K_4 used to account for armoring by bed material will be determined using the data collected during this study.

CONCLUSIONS

The proposed research project will help NDOT identify how to improve the existing methods for predicting scour depth at bridge crossings along the Truckee River. Further, the results of this project will provide valuable experimental data that can be incorporated into modeling studies of the resuspension and deposition of sediments in the Truckee River and other rivers having similar characteristics. The erosion and scour of sediments around bridge piers and abutments is important to the fields of hydraulic, geotechnical, and bridge engineering. Improved prediction is needed to ensure the stability of these structures.

REFERENCES

Bedford, K.W. (1992) Sediment exchange process parameterization. *Chemical Dynamics in Freshwater Ecosystems*, edited by F. Gobas and J. McCorquodale, Lewis Publishers, 63.

Federal Highway Administration, 1995, *Recording and Coding Guide for the Structure Inventory and Appraisal of the Nation's Bridges*, Report No. FHWA-PD-96-001, Office of Engineering, Bridge Division.

Lagasse, P.F., Richardson, E.V., Schall, and Price, G. R., 1997, Instrumentation for Measuring Scour at Bridge Piers and Abutments, NCHRP Report 396.

Lagasse, P.F., Schall, J.D., Johnson, F., Richardson, E.V., and Chang, F., 1995, *Stream Stability at Highway Structures*, Second edition, Hydraulic Engineering Circular No. 20, Publication No. FHWA-IP-90-014, Office of Technology Applications, Federal Highway Administration.

Mueller and Jones, 1999, "Evaluation of Recent Field and Laboratory Research on Scour at Bridge Piers in Course Bed Materials", ASCE Compendium, *Stream Stability and Scour at Highway Bridges*, Richardson and Lagasse (eds.), Reston VA.

Richardson, E.V., and Davis, S.R., 1995, *Evaluating Scour at Bridges*, Third edition, Hydraulic Engineering Circular No. 18, Publication No. FHWA-IP-90-014, Office of Technology Applications, Federal Highway Administration.

Soltani, A.M., Grunert, M., Beeston, T., and Miller, C., 1993, *Bridge Scour Evaluation Plan for Existing Structures*, Nevada Department of Transportation.

Van Cappellen, P., and Wang, Y. (1995) Metal cycling in surface sediments: Modeling the interplay of transport and reaction. *Metal Contaminated Aquatic Sediments*, edited by H.E. Allen, Ann Arbor Press, Chelsea, Michigan, 21-64.

Williams, Rhea P., Crompton, E. James, and Hale, Glenn S., 1997, *Summary of Level 1 and Level 2 Analyses of Bridge Scour at Selected Sites in the Carson River Basin, Nevada, 1995-96*, United States Geological Survey, Open-File Report 96-658-A, Carson City, Nevada.

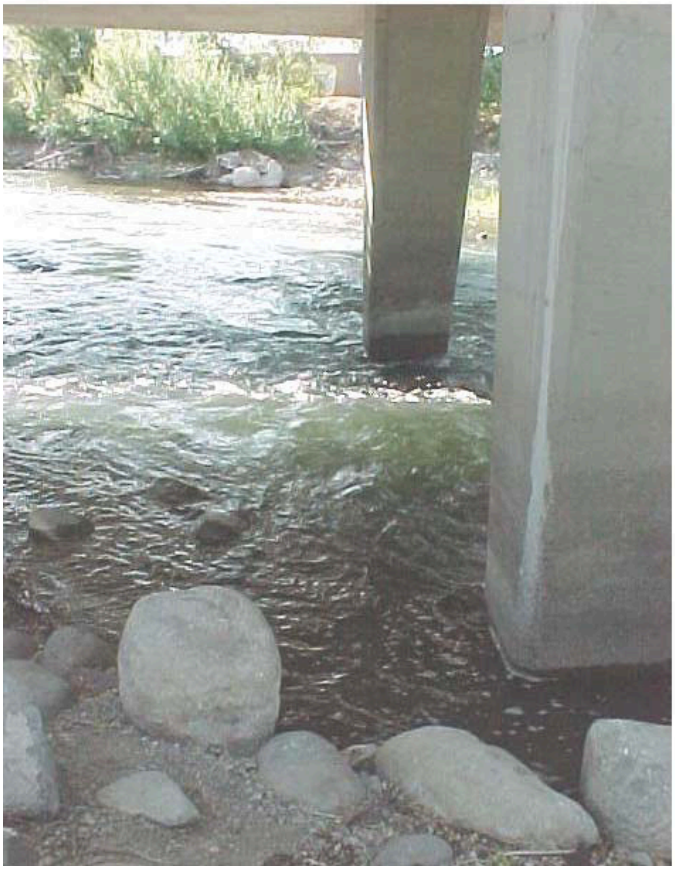

Figure 1. Kietzke Lane Bridge Piers

Figure 2. Kuenzli Street Bridge Pier

Figure 3. Keystone Avenue Bridge

Figure 4. Mayberry Drive Bridge

Table 1. Comparison of Local Pier Scour Equations

Bridge / Equation	K_4	Scour Depth, Y_s (ft)	Footing Depth (ft)	Scour Code Rating *
Keitzke/HEC-18, Third Edition	0.79	14.8	8.5	3(C)
Keitzke/HEC-18, Fourth Edition	0.40	7.5	8.5	5 or 3(B)
Kuenzli/HEC-18 Third Edition	1.00	22.6	9.8	3(C)
Kuenzli/HEC-18 Fourth Edition	0.48	10.5	9.8	3(C)

* 3(B) indicates that the bridge is "scour critical" but scour is within the limits of the footings; 3(C) indicates that the bridge is "scour critical" and scour is below the base of the spread footing; 5 indicates that the bridge foundations are stable.

Figure 5. Sounding Board Testing

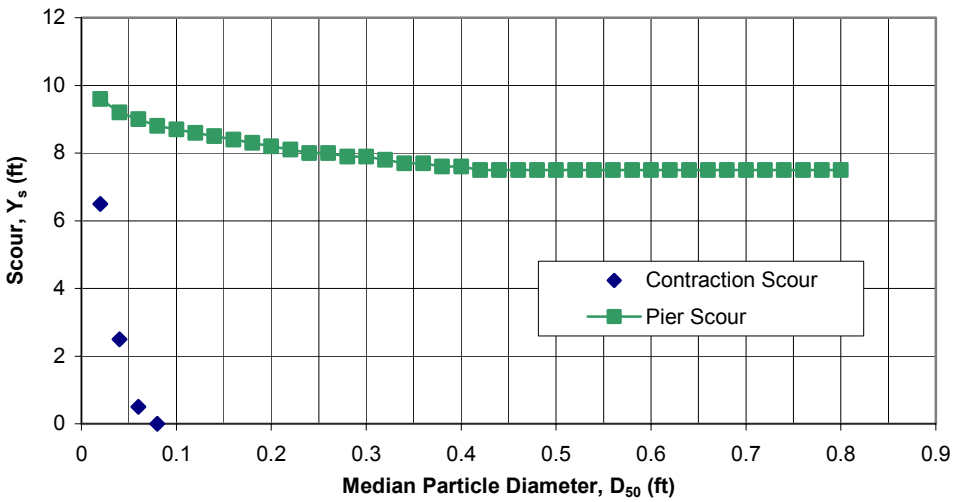

Figure 6. Scour Sensitivity for the Keitzke Bridge

Seismic Methods to Identify Scour Depth Around Deep Bridge Foundations

By

E. J. Mercado[1], E. B. Davies[2], J. A. McDonald[3], M. W. O'Neill[4]

ABSTRACT

Two methods to detect scour around bridge piers that are based on principles of seismology are described. The first method, the parallel seismic survey, requires that a string of hydrophones be placed in a water-filled casing external to the pier being monitored. A seismic event is produced by a hammer blow to the top of the pier. Clear indications of scour were observed in a controlled field experiment. When a multi-component foundation, such as a group of piles, is to be monitored, a reverse parallel seismic survey is suggested in which the seismic events are produced at various depths in the water and the signals recorded at the tops of the piles. While these methods can be applied after a flood has subsided, they are probably not robust enough to withstand the action of a major flood. Therefore, a second method is described in which the sensing elements (hydrophones) are placed in a tube within the foundation to protect them during a flood. With this method the seismic source is an air gun that is placed in the water near the pier being monitored and which can be activated during a flood. The results from this test, the pier-interior scour detection system survey, are not as clear as those from the parallel seismic survey; nonetheless, field experiments indicate that a scour zone can be detected.

INTRODUCTION

In bridge management it is essential that departments of transportation know whether a bridge's foundation has been compromised by scouring of the soil surrounding the foundation. Although scour may sometimes reduce axial pile capacity by a small amount, a relatively small depth of scour can have a large negative impact on the stiffness and capacity of laterally loaded piles or drilled shafts. It is therefore desirable that the bridge owner have knowledge of the amount of scour around both abutments and central piers at all times. This paper describes two seismic techniques for identifying scour

[1] President, North American Geotechnical Co., Seabrook, Texas, 77586, USA (Ejmer@aol.com)
[2] Geophysicist, North American Geotechnical Co., Seabrook, Texas, 77586, USA
[3] Professor, Department of Exploration Geophysics, Curtin University of Technology, Perth 6845, Western Australia, AUSTRALIA
[4] Cullen Dist. Professor of Civil Engineering, University of Houston, Houston, Texas, 77204-4003, USA (oneill@uh.edu)

around bridge piers that may be useful in this effort and summarizes large-scale tests in which these techniques have been used experimentally. At present, depth of scour information is usually obtained using human divers. The techniques described here make it unnecessary for divers to inspect the foundations.

The seismic techniques are (1) the parallel seismic survey (PSS), which has been used successfully to identify depths of foundations (Olson et al., 1998; Mercado and O'Neill, 2000), and (2) the pier-interior scour detection system (PISDS), which has a potential advantage over the PSS because in can be operated in real time under severe flood conditions (Davies et al., 2001). In the former method it is necessary to install a cased borehole through the water and into the soil away from the pier being studied. However, it is likely that a stand-alone casing would be destroyed during a flood, meaning that the PSS should be performed only after the flood has subsided and the casing installed. The PISDS, in contrast, uses a pile or drilled shaft that is part of the foundation as its housing and so will survive for as long as the pier itself survives (Davies et al., 2002). The current paper briefly describes the two systems and gives results of deployment of both at a well-controlled test site.

TEST SITE

A facility to test scour detection systems was constructed at the National Geotechnical Experimentation Site at the University of Houston (Maher and O'Neill, 1983; O'Neill, 2000). The soil formation at the surface and extending to a depth of at least eight meters is the Beaumont formation, consisting of mostly overconsolidated, plastic clay with occasional sand seams and partings. A test pond was excavated within the site. A schematic of this test pond is shown in Fig. 1. The sides of the pond were lined with geotextiles to mitigate sloughing of the walls, which were cut on a 1:1 slope. The depth of water was approximately 1.5 m (5 ft). Two drilled shafts, termed "piers" here, 0.61 m in diameter and 5.2 m long, were constructed in the pond as indicated in Fig. 1. The three locations denoted "BH-1, BH-2, and BH-4" are locations at which PVC casings had been pushed into small-diameter boreholes and grouted to the soil at the bottom of the pond at some distance from the drilled shafts. The location marked "BH-3" consisted of a PVC pipe that had been cast into Pier 2. All PVC pipes extended approximately 7.8 m below the natural ground surface, except for BH-3, where the casing extended only to the toe of the pier. The experiments that are described were performed first with a no-scour condition (flat bottomed pond) and then with a simulated scour condition, in which, after emptying the pond, 1.2 m (4 ft) of soil around each pier and throughout the zone between the piers was hand excavated to simulate a scour event. The sides of this scour excavation were cut vertically. Upon completion of excavation in the scour zone, the pond was re-filled with water. After several days of exposure of the soil to the ponded water the water was removed, at which time it was observed that the sides of the scour excavation had sloughed irregularly into the excavation. This condition was assumed to represent the state of clay soil after a scour event (scour hole backfilled with loose sediments).

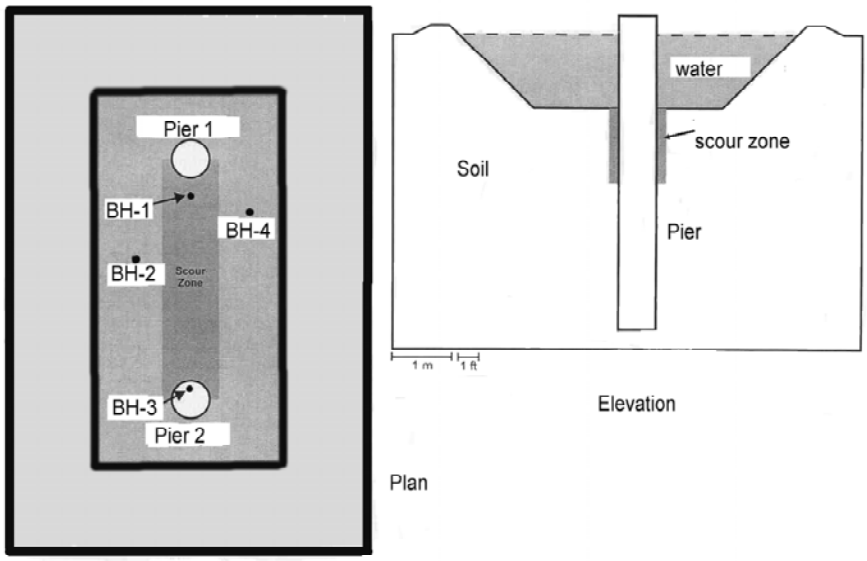

Fig. 1. Schematic of Test Pond

PSS MONITORING

A set of unclamped hydrophones was placed in tubes BH-1, BH-2 and BH-4, which had been filled with water. The hydrophones were Mark Products Model P-44 hydrophones, sensitivity of 14 μvolts per μbar pressure, which were spaced 0.305 m apart vertically. An Oyo Geospace Model DAS-1 digital data acquisition system was used to acquire data from the hydrophones at a digitizing rate of 62.5 μsec per sample. The recorded data were filtered with a broadband filter passing signals between 3 and 4000 Hz. The detection process began with tapping the head of Pier 1 with a steel hammer while the hydrophones were being monitored. Seismic waves in the soil surrounding the test pier were created through refraction. These waves were subsequently picked up by the hydrophones.

Figure 2 shows the results of a PSS test for a scour condition with the array of hydrophones placed in tube BH-1, 0.61 m from the face of Pier 1 and in line with the center of the scour trench, where there was a minimum of sloughed soil. The data in Fig. 2 are unfiltered (other than indicated above) and are typical of PSS data for a drilled shaft embedded completely in soil. The linear first-break pattern occurs down to the depth of the toe of the pier (Line AB). Below the toe of the pier the first-break arrival times exhibit a marked change (Line CD). The intersection of Lines AB and CD define the depth of the toe, which is the usual interpretation of PSS data. No scour zone can be clearly identified.

The detection of a scour zone is predicated on the principle that the soft infilled soil within the scour zone will attenuate the energy of the seismic (P-) waves refracted from the pier. To investigate this effect, the experiment was repeated with the array of hydrophones located in borehole BH-4. The results are shown in Fig. 3b and compared

with a similar test for no-scour conditions in Fig. 3a, where the hydrophones were in BH-1 (equivalent to Fig. 2 but for the no-scour condition). The structural configuration of the scour trench at BH-4 at the time of that test is shown on the left-hand panel of Fig. 3b. It is seen that a considerable amount of sloughed material was located between the hammer source on the pier and BH-4. A marked attenuation in the amplitude of the seismic events can be observed for those hydrophones located adjacent to the scour zone. The depth of the scour zone can be identified clearly by plotting the amplitude of the signal versus depth. Marked changes occur at the elevations of the top and bottom of the scour zone (Mercado and O'Neill, 2001).

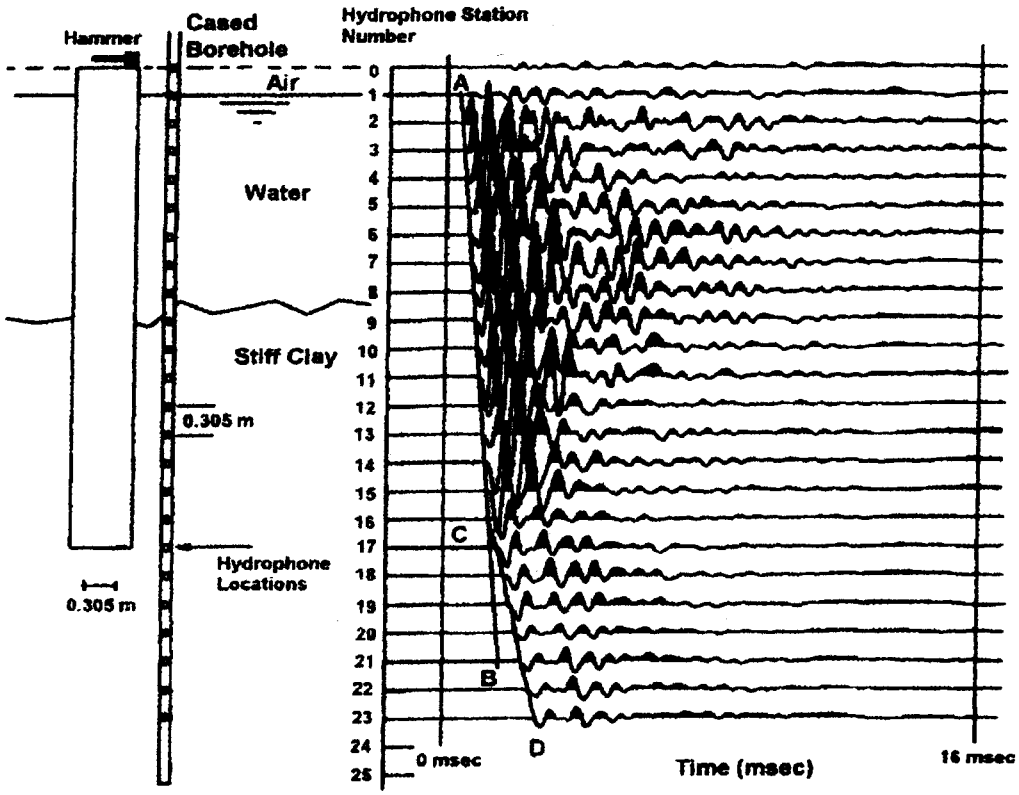

Figure 2. First Wave Arrivals from Pier 1 in BH-1 for the Scour Case, PSS

The data suggest that the PSS is a technique that can take advantage of the reduced seismic wave velocities of infilled soil to detect scour either after a flood event has passed or, possibly, during a flood event if the access tube can be protected from hydraulic forces and debris impact. However, research should continue toward the goal of developing a seismic system as reliable as the PSS but better able to withstand the flood environment.

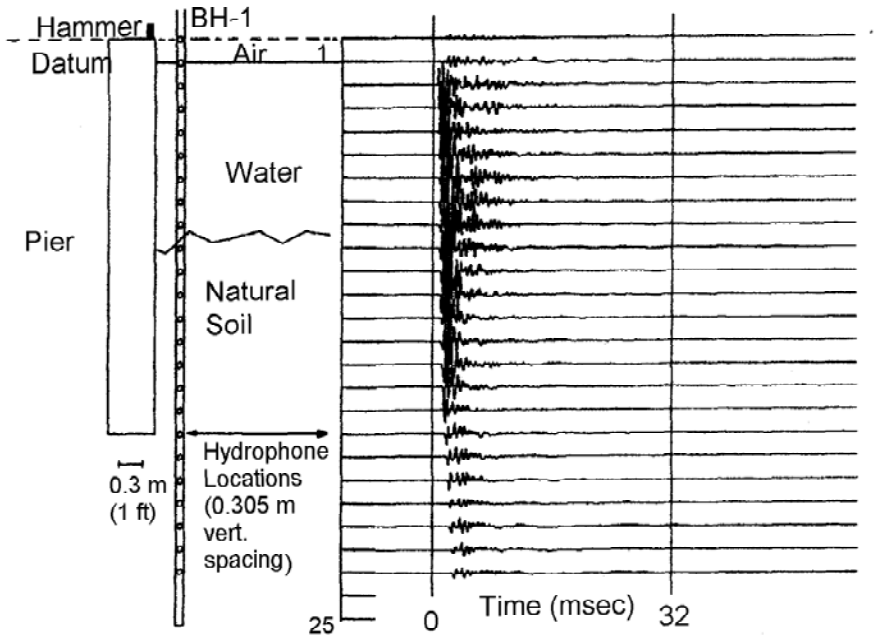

Figure 3a. Plot of PSS Signals in BH-1, No-Scour Condition

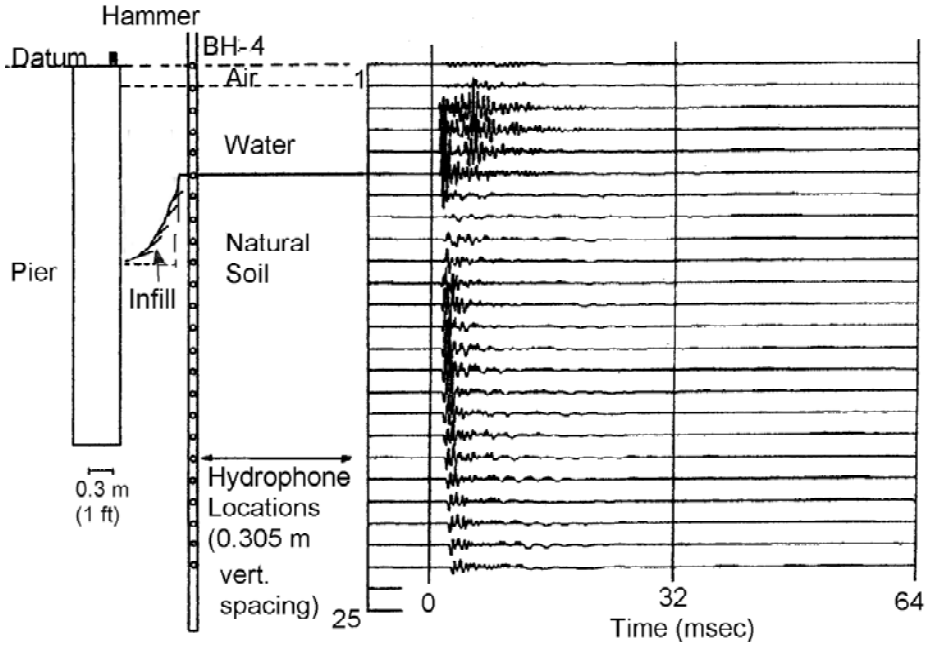

Figure 3b. Plot of PSS Signals in BH-4, Scour Condition

PILE GROUPS: REVERSE PSS TECHNIQUE

The PSS method is valid for single piles or drilled shafts, which constitute the foundation elements for many bridges. However, when the foundation is a group of piles, the method becomes less useful. To address this problem, a variation of the PSS method might be suitable for pile groups (Mercado and McDonald, 2002). Shown schematically in Fig. 4 is an arrangement in which the source (perhaps an air gun) is placed at several positions vertically along a track (perhaps a pipe driven into the sediments like a pile), filled with water, in a post-flooding situation. For the lower locations of the source, the waves created by the source strike the bottoms of the piles and propagate up the piles with the P-wave velocity of the pile material. These waves excite geophones attached to the tops of selected piles in the exterior of the group (Fig. 4). As the source moves closer to the surface the ray paths finally intersect the individual piles at the critical angle to convert to refraction waves, which also travel up the pile to excite the geophones. By reciprocity, the first break pattern recorded at each geophone will duplicate the first break patterns for the case where the source is located at the top of the pile and the receivers (hydrophones) are at various depths exterior to the pile (the standard PSS procedure). While this technique has yet to be field-tested by the authors, it should provide usable information if it is possible to vary the energy of the source to suit the geometry of the pile group and the attenuation characteristics of the soil at the site.

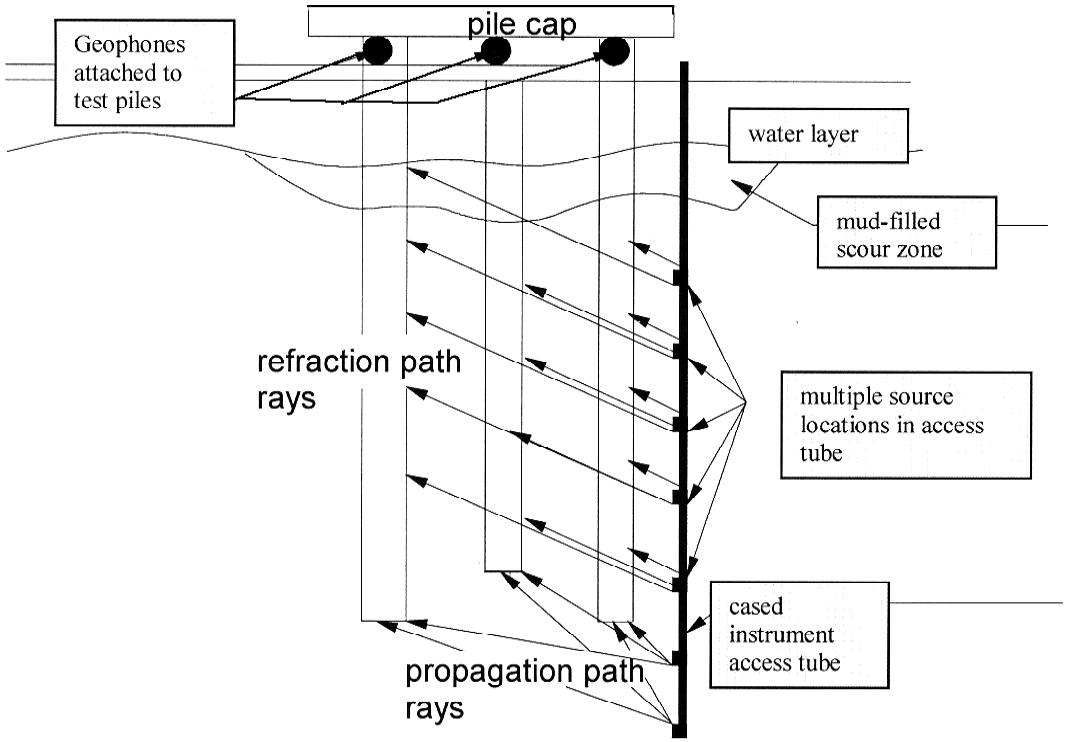

Figure 4. PSS Reverse Source-Detector Geometry for Investigation of Scour Around Pile Groups (Mercado and McDonald, 2002)

PISDS MONITORING

Although the PSS can be useful under certain circumstances in remotely gauging the depth of scour around a foundation within a body of water, a more physically robust detector will usually be needed in order to observe scour development in real time. One way of making a detector more robust would be for it to be located within an active foundation element, such as a pile or drilled shaft, or within a special drilled shaft or pile constructed for the express purpose of protecting the detector. It is possible, however, that the presence of a concrete shaft or steel pipe around a cased receiver hole might reduce the quality of the seismic data recorded within the cased hole. The "pier-interior scour detection system," or PISDS, nonetheless uses a pier-interior cased hole to house hydrophones. The feasibility of this system was investigated at the same site at which the PSS system data in the previous section were acquired.

The PISDS uses unclamped hydrophones within a water-filled casing, in a manner similar to the PSS. The data acquisition system is also the same as that used for the PSS. The seismic sources were a hammer, per the PSS, and an air gun. The air gun was a Bolt Technology Model DHS 500 gun with an 82 cm^3 firing chamber. In most cases it operated at a chamber pressure of 6900 kPa, with air as the gun gas. The hammer source was a 0.7 kg steel hammer.

The air gun was placed in the water at a designated depth and distance from Pier 2 (shot point). The trigger for the air gun also started the digital recording of the hydrophone traces. For the hammer-source tests, the hammer was struck directly atop Pier 2 with the hydrophone detectors housed within BH-3, inside Pier 2.

HAMMER SOURCE EXPERIMENTS. In theory the first wave arrivals in the hydrophones should be the P-waves generated in the pier by the hammer strike. These are then followed by later waves generated by other seismic events, including, perhaps, events associated with the scour zone. Hammer source tests were conducted on Pier 2, and the first arrival times did indeed correlate with direct P-wave propagation in the pier for a wave velocity of 4420 m/s, which was independently verified by Davies et al., 2001. This fact indicated that the pier-interior geophones could be of potential use in detecting P-wave propagation velocity within the pier and thereby in detecting scour zones.

OFFSET TESTS. The next step in investigating the PISDS method was to see if pier interior hydrophones and pier exterior hydrophones could give comparable data, it having been shown in the PSS tests that pier-exterior hydrophones within a borehole can detect scour zones. This step was performed using the air gun as a source and placing the detector system (hydrophone string) in BH-3, a pier-interior cased hole, and in BH-1, a pier-exterior cased hole. The air gun was placed in the water at a depth of 0.3 m and a distance of 1.5 m form BH-3. The experiment was repeated with the air gun at a depth of 0.3 m and 1.5 m away from BH-1 (with the air gun, BH-1 and Pier 1 all in the same vertical plane). The results of these tests are shown in Fig. 5 for the scour condition, where there was a minimum of infill material.

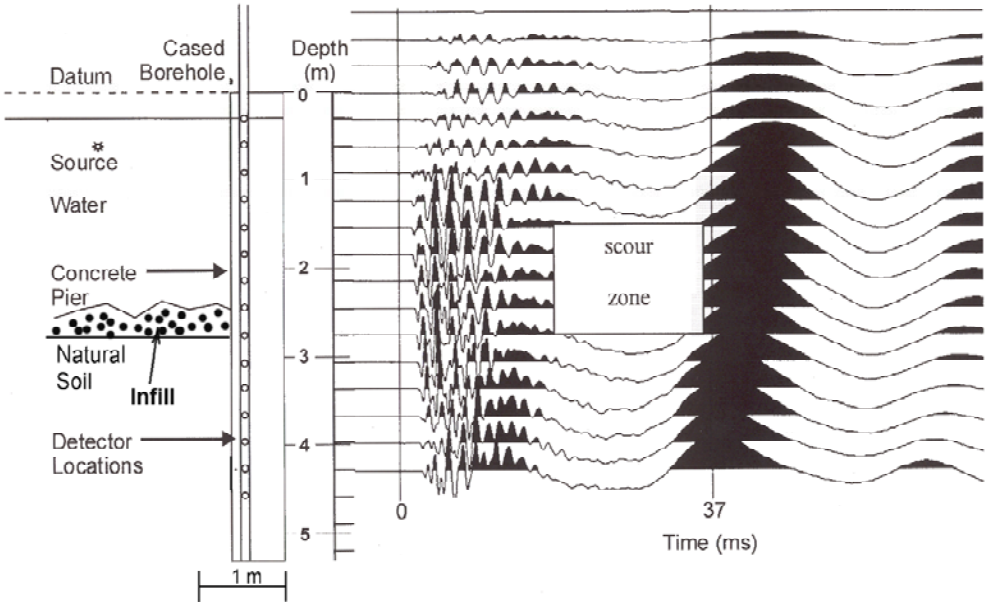

Figure 5a. Results of Offset Test for Pier-Interior Cased Hole (BH-3)

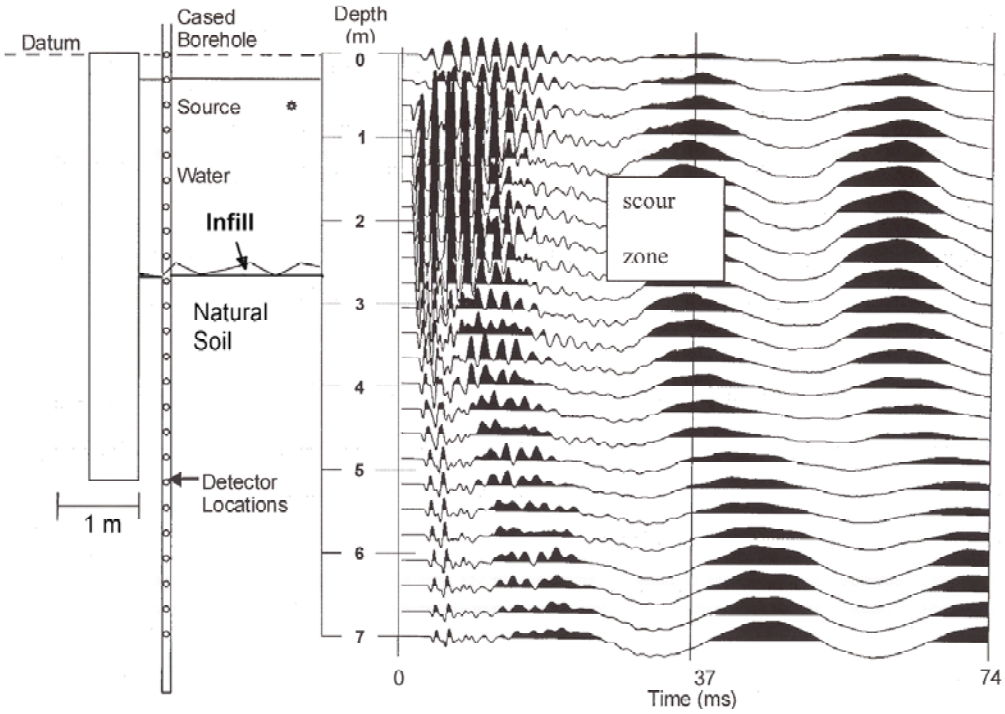

Figure 5b. Results of Offset Test for Pier-Exterior Cased Hole (BH-1)

One way of evaluating the data in Fig. 5 is to compare visually Figs. 5a and 5b. Over the range of detector locations, the data in Fig. 5b are of slightly higher quality than those in Fig. 5a. However, in the depth range of 1.5 to 3.7 m (scour zone and natural soil just below the scour zone), the first breaks are well defined on both data sets. At later times, after the first breaks, the two data sets differ considerably due to the presence of much stronger reflections (up-going waves) from the toe of the pier for the borehole interior case (Fig. 5a). This observation strongly suggests that data from the pier-interior borehole may be useful in scour zone detection if such detection can be performed by observing first breaks in the hydrophone traces.

A method to utilize first break times for the pier-interior borehole is to compare graphs of measured first break times with direct P-wave arrival times from a water source 0.305 m below the water surface and 1.5 m from a string of vertical hydrophones (field test condition) computed from a simple flat-layer, elastic geophysical wave propagation model (Dobrin, 1974; Davies et al., 1996). Analyses were made by considering the conditions shown in Table 1 and then by tracing the wave rays through their fastest path (through water or through water and soil) to the location of a particular hydrophone to obtain the theoretical time of first wave arrival, considering wave refraction at the

Table 1. Parameters used in flat-layer wave propagation model

Condition analyzed	**P-wave velocity (m/s)**		
	Water (0-1.5 m)	**Scour zone (1.5-2.7 m)**	**Natural soil (below either 1.5 or 2.7 m)**
A. Source in water, hydrophones in water	1525 (full depth)	Not modeled	Not modeled
B. Source in water, upper hydrophones in water, lower hydrophones in high velocity soil at a depth of 1.5 m	1525	Not modeled	1675 (below 1.5 m)
C. Source in water, upper hydrophones in water, lower hydrophones in low velocity soil at a depth of 1.5 m	1525	1070	1070 (below 2.7 m)
D. Source in water, upper hydrophones in water, lower hydrophones in high velocity soil below a depth of 2.7 m	1525	1525	1675 (below 2.7 m)

interface between the media using the principles of Snell's Law. The concrete pier itself is not considered since wave travel distance in the concrete is very small compared to wave travel distance in the water or soil. [BH-3 was on the side of Pier 2 closest to the air gun source.]

In Table 1 Condition A is for water only and is relevant only for the upper hydrophones, above the soil; Condition B represents the no-scour condition; Condition C may represent either scour with soft, sloughed sediment (infill) below a depth of 1.5 m or no-scour with a soft natural soil below the water; Condition D represents scour with no infill in the scour zone. The measurements (no-scour and scour conditions) and computed first arrival times for the conditions in Table 1 are shown for the pier-exterior borehole in Fig. 6a and for the pier-interior borehole in Fig. 6b.

INTERPRETATION. One way to interpret Fig. 6 is to consider the arrival time-hydrophone depth plot for "no-scour" conditions to be the baseline. In practice, this could be the set of readings taken shortly after a detection borehole is installed. Scour is evident, then, when the first-arrival-time measurements from a source (such as an air gun) situated at the same location as existed for the baseline readings deviates from this baseline. The depth at which the "scour" data separate from the baseline in both Figs. 6a and 6b is 1.5 (pier interior hydrophones) to 1.7 m (pier exterior hydrophones), which represents the elevation of the bottom of the test pit before simulated scour occurred.

For no-scour conditions, the data from both pier interior and pier exterior boreholes show some agreement below 1.5 m (bottom of water) with the computed values for Condition C, which simulates a low-velocity halfspace (soft soil) below water. For the scour condition from depths of about 3.0 m to 4.3 m the measurements from both pier exterior and pier interior boreholes generally agree with Condition D, in which the low-velocity soil in the scour zone has been replaced with water, or perhaps sloughed soil with very large water-filled voids.

The similarity of the comparisons in the pier interior and pier exterior boreholes is evidence that the pier interior system can be used to monitor scour outside the pier. For the pier-interior method to become practical and reliable further experiments of this type in other types of soil (specifically, cohesionless soil) need to be conducted, and signal filtering rules need to be determined for flood conditions, where water cavitation and similar phenomena can both produce background noise and attenuation of seismic waves from the source.

Finally, it is noted that the PSS and PISDS methods are protected by U. S. Patent Number 5,753,818.

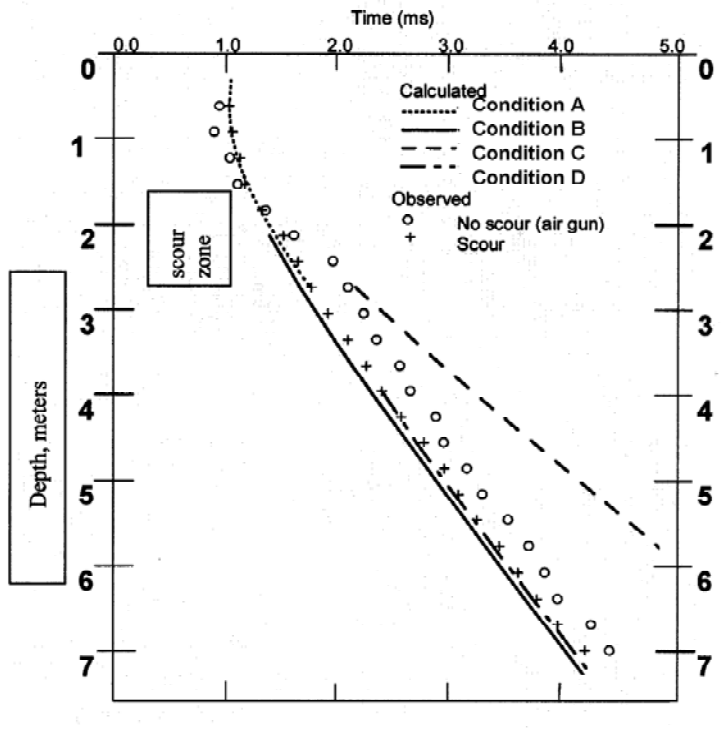

Figure 6a. Measured and Computed First Arrival Times at Hydrophone Locations, Pier-Exterior Borehole

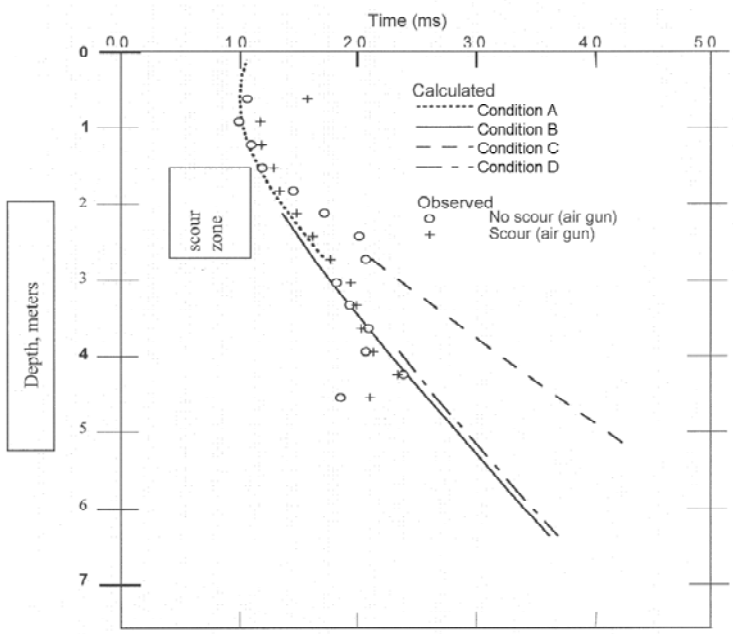

Figure 6b. Measured and Computed First Arrival Times at Hydrophone Locations, Pier-Interior Borehole

CONCLUSIONS

The following conclusions are drawn from this study.

1. The PSS method should be effective in detecting scour around single piles or drilled shafts (piers) after a flood has passed when loose infill soil appears in the scour zone.

2. The reverse-PSS method may be a useful technique in detecting scour around groups of piles after a flooding event.

3. Seismic events within water generated outside a concrete pier were detected in a cased tube cast within the pier.

4. The seismic events recorded within the pier-interior cased hole compare favorably with corresponding events recorded in a pier-exterior borehole. As a consequence, the PISDS method, which uses the pier-interior hole to protect the receiving instruments during a flood, has the potential to be used to indicate scour conditions adjacent to a pile or drilled shaft in real time during a flood.

ACKNOWLEDGMENTS

Funding for this project was provided by the National Science Foundation, Grant Number ISI 9200277. Facilities were provided by the Allied Geophysical Laboratories and the Department of Civil and Environmental Engineering of the University of Houston.

REFERENCES

Davies, E. B., E. J. Mercado, J. A. McDonald, and M. W. O'Neill (1996). "A Real Time Scour Measurement Instrument," *Final Report*, North American Geotechnical Company, Seabrook, Texas, May, 246 pp.

Davies, E. B., E. J. Mercado, M. W. O'Neill, and J. A. McDonald (2001). "Field Experimental Studies of a Riverbed Scour Measurement System," *Journal of Environmental and Engineering Geophysics*, Vol. 6, Issue 2, June, pp. 57 – 70.

Davies, E. B., E. J. Mercado, J. A. McDonald, and M. W. O'Neill (2002). "Studies of a Riverbed Scour Monitor System Using a Pier-Interior Cased Borehole," *Journal of Environmental and Engineering Geophysics* (in review).

Dobrin, M. B. (1974). *Introduction to Geophysical Prospecting*, McGraw-Hill, New York.

Mahar, L. J., and M. W. O'Neill (1983). "Geotechnical Characterization of Desiccated Clay," *Journal of Geotechnical Engineering*, ASCE, January, pp. 56-71.

Mercado, E. J., and M. W. O'Neill (2000). "Geophysical Survey Techniques to Determine Lengths of Piles and Drilled Shafts," *Use of Geophysical Methods in Construction – Geotechnical Special Publication No. 108*, Ed. by W. Nazarian and J. Diehl, ASCE, August, pp. 155-169.

Mercado, E. J., and M. W. O'Neill (2001). "A New Non-Destructive Method to Measure Scour Depth and the Depth of Unknown Foundations," Proceedings, Midwest Hydraulic Engineers Conference, Madison, Wisconsin, Federal Highway Administration, Washington D. C., August, 8 pp.

Mercado, E. J., and J. A. McDonald (2002). "Two New Non-Destructive Methods to Measure Scour Depth and the Depth of Unknown Foundations," *Geophysics*, (under review), 10 pp.

Olson, L. D., F. Jalinoos, and M. F. Auoad (1998). "Determination of Unknown Subsurface Bridge Foundations," *NCHRP Report No. 21-5 (Interim)*, National Cooperative Highway Research Program, National Academy of Sciences, Washington, D. C., August, pp. 36 – 38.

O'Neill, M. W. (2000). "National Geotechnical Experimentation: University of Houston," *National Geotechnical Experimentation Sites – Geotechnical Special Publication No. 93*, Ed. by J. Benoît and A. Lutenegger, ASCE, April, pp. 72 – 101.

Portable Scour Monitoring Research

James D. Schall[1] and Gerald R. Price[2]

[1] Vice President, Ayres Associates, Fort Collins, CO 80527; PH (970) 223-5556
[2] President, ETI Instrument Systems, Fort Collins, CO 80524; PH (970) 484-9393

Abstract

Scour monitoring can be completed by either fixed or portable instruments. Fixed instruments are those that are installed and left at the bridge. During the last ten years, significant research and progress has been made with fixed instrumentation. However, fixed instrumentation is not suitable, practical, or cost effective for all bridges. In many cases portable monitoring may be a better solution, and yet, not much research has been completed to improve this type of technology.

Recognizing this limitation, the National Cooperative Highway Research Program (NCHRP) funded project 21-07, "Development of Portable Scour Monitoring Equipment." The objective of this research was to improve deployment, positioning, and data collection procedures for portable scour monitoring work. These improvements will facilitate data collection under adverse conditions, and will allow more successful monitoring at a wide range of bridges under flood flow conditions. The research was conducted recognizing the need to provide solutions that are easily used and affordable by state and local bridge owners.

The research concentrated on developing a truck mounted articulated crane to quickly and safely position various measurement devices. Collection of position and scour data is automated and a data file is written that allows plotting channel section or scour hole bathymetry.

Introduction

Monitoring and measuring the scour conditions at a bridge can be completed by a variety of instrumentation. Fixed instruments are those that are installed and left at the bridge and typically involve a sensor for making the scour measurement, a power supply and a data logger. More recently, telemetry has become a common component of many fixed instrument systems. During the last ten years, significant research and progress has been made with fixed instrumentation, both through research activity, commercial development and field installations, often completed by state DOT's. However, fixed instrumentation is not suitable, practical, or cost effective for all bridges. In many cases portable monitoring during a flood is a better solution, and yet, not much research has been completed to improve this type of technology.

Physical probing has been used for many years as the primary method for portable scour monitoring by many DOT's. More recently, sonar has seen increased use, in part due to the technology transfer provided through FHWA's Demonstration Project 97, Scour Monitoring and Instrumentation (FHWA, 1998). However, probing and sonar techniques both have limitations during flood events when the flow depth and/or velocity are high. Low flow monitoring during the 2-year inspection cycle with this type of technology has been effective and is used by many DOT's; however, critical decisions on bridge safety during flood flow conditions have been hampered by the limitations of

the existing equipment and its application. As a result, some bridges have been closed unnecessarily, causing traffic delays and increased expenses, while other bridges that should have been closed were not, resulting in increased risk and liability.

Research Objective and Criteria

Recognizing these concerns, the National Cooperative Highway Research Program (NCHRP) funded project 21-07, "Development of Portable Scour Monitoring Equipment." The objective of the research was to develop improvements and/or alternatives to existing portable scour monitoring equipment and techniques for measuring stream bed elevations at bridge foundations during flood conditions. The equipment and techniques developed should be operational under the following conditions:

1. Flow velocities exceeding 3.5 m/s
2. High sediment concentrations
3. Floating debris
4. Ice accumulation
5. Limited clearance
6. Pressure flow
7. Overhanging or projecting bridge geometries
8. Bridges with decks more than 15 m above the water
9. Air entrainment
10. Easily used and affordable by state and local bridge owners
11. Transportable by pickup, van, or similar vehicle
12. Accuracy of 30 cm +/-

Research Tasks

Given these conditions, which represent the real world conditions that bridge inspectors must often work under, it is unlikely that one instrument or device will meet all the desirable criteria. To address the research needs, the project was divided into two Phases. The purpose of Phase I was to complete literature review and identify alternative technologies, allowing development of a detailed work plan for Phase II. Phase II included prototype development, extensive field testing, and documentation of the results.

A significant part of the Phase II research was the development of a truck mounted articulated crane to quickly and safely position various measurement devices. Articulated cranes, also known as knuckle boom or folding cranes, are commonly used in the construction and building materials industry. The following sections summarize the work completed related this research task.

Articulated Arm Crane Research Results

There are various manufacturers of articulated arm cranes, each with a variety of models that differ by their reach and lifting capacity. For purposes of this research, a smaller crane with a long reach, but not much weight lifting capability was desired. The long reach was necessary to be able to work off of higher bridge decks, and the size of the crane was important to improve maneuverability, as well as to minimize lane closure and traffic control issues.

After researching the available models and evaluating reach capabilities and cost, a Palfinger model PK 4501 C crane was selected (Figure 1). This crane has a maximum reach of 36 feet with a lifting capacity at this distance of 600 Lbs. In 2001, the base price for this crane was $14,500, with an installation cost of $1,800. This crane is small enough to be installed on a Ford F-450 truck or equivalent.

The most common location for a crane is immediately behind the cab of the truck. An alternative location is at the back of the truck, behind the rear axle. A rear mount puts more load at the back of the truck, and can cause weight distribution problems if the truck is also carrying substantial weight on the flat bed. The advantage of the rear mount is better clearance around the truck, since the cab is not in the way. For purposes of scour monitoring, with no substantial weight being transported on the truck bed, a rear mount seemed advantageous.

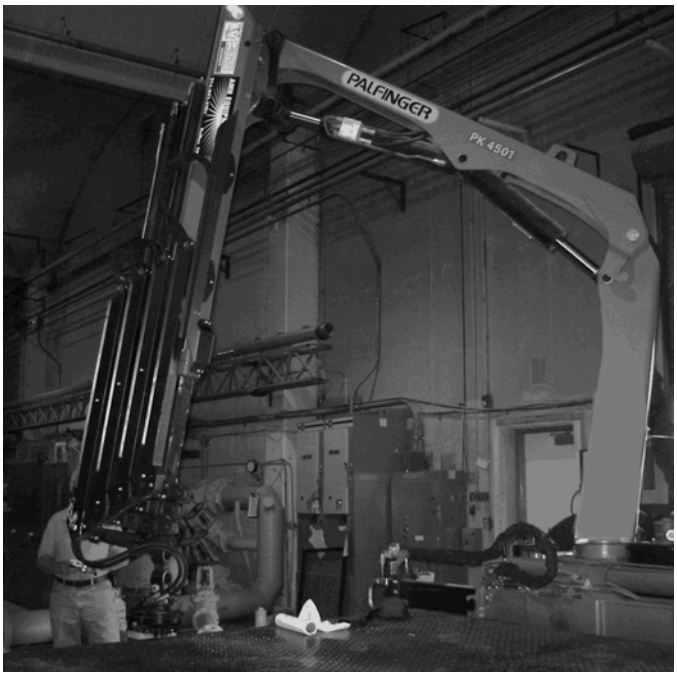

Figure 1. Palfinger PK4501C crane.

Based on the reach of the PK4501C crane, mounted with an offset to the center of the truck, the PK4501C has the capability to reach 6.5 m (21.25 ft) below the bridge deck when the truck is a maximum of 0.3 m (35 in) from the edge of the bridge. A hydraulic rotator was added to the end of the crane to provide better ability to position and control instrumentation. In addition to the rotational ability at the end of the crane, the rotator itself was attached to a custom fabricated mounting bracket that provided an additional articulation at the end of the crane arm. With the rotator mounting bracket the total reach of the crane below the bridge deck was 7.0 m (23.0 ft).

Instrumentation Installed on Crane

A variety of sensors were installed on the truck and crane to allow geometric calculation of the position of the end of the rotator. Tilt meters were used to measure the vertical deflection angle of the crane arm and the rotator arm. A draw wire was used to measure the linear extension of the arm, and a draw wire around the circumference of a circle attached to the base of the crane was used to measure crane rotation. The azimuth of the rotator was measured with a potentiometer through a gear and sprocket mechanism. An acoustic stage sensor was used to measure the distance to the water surface. Tilt data for the crane and rotator, the azimuth of the rotator, and the linear extension of the arm are transmitted by a radio modem from an instrument box at the end of the crane, that also transmits sonar data. The data is pre-processed with a Campbell CR10 data logger prior to transmission to the computer on the truck. A second CR10 is used to process truck data, which includes the azimuth of the crane, distance to the water surface, distance traveled across the bridge deck, and winch data when using cable suspended methods.

Given the desire to operate at flood conditions with high velocities, a streamlined probe was built to position the sonar transducer directly in the water using the articulated arm. The probe was fabricated from a section of helicopter blade, and proved to be very stable when placed in high velocity flow during field trials. The streamlined probe eliminated the vortex shedding problems of a simple cylinder shaped rod exposed to high velocity flow. The fin on the streamlined probe could freely rotate, which allowed the fin to follow the current no matter what horizontal angle the crane was positioned in. The fin was attached to a 2 m (80 in), 125 mm (2 in) schedule 80 stainless steel pipe. Given the distance the crane could reach below the bridge deck (7.0 m or 23.0 ft), the crane could reach nearly 9.1 m (30 ft) below the bridge deck for a sonar measurement.

To provide physical probing capability an extendable rod was fabricated. The rod extensions were built with 125 mm (2 in) stainless steel, Schedule 80 pipe in 1.5 m (5 ft) lengths, allowing a total length up to 4.5 m (15 ft). Threaded unions were machined to allow individual sections to be screwed together to create the longer extensions. Using the articulated crane for physical probing is most appropriate in a gravel/cobble bed, or to evaluate riprap conditions, since the strength of the crane hydraulics makes it difficult to know exactly when the channel bottom is reached.

The truck also includes two winches to allow cable suspended measurements using a sounding weight or a float based deployment of a sonar transducer. Two winches allows more control of the location and placement of cable suspended instruments (Figure 2). The float was built using a kneeboard with a wireless sonar to transmit data to the bridge deck with a modem. The kneeboard can be floated under the bridge deck to get measurements where direct measurement with the arm, or cable suspended weights are not possible.

The position of the truck as it moved across the bridge was monitored with a standard surveying measuring wheel attached to the back of the truck. Pulse counters were added to the wheel and connected to the Campbell CR10 data logger to electronically register the distance traveled. Figure 3 shows the completed articulated arm truck.

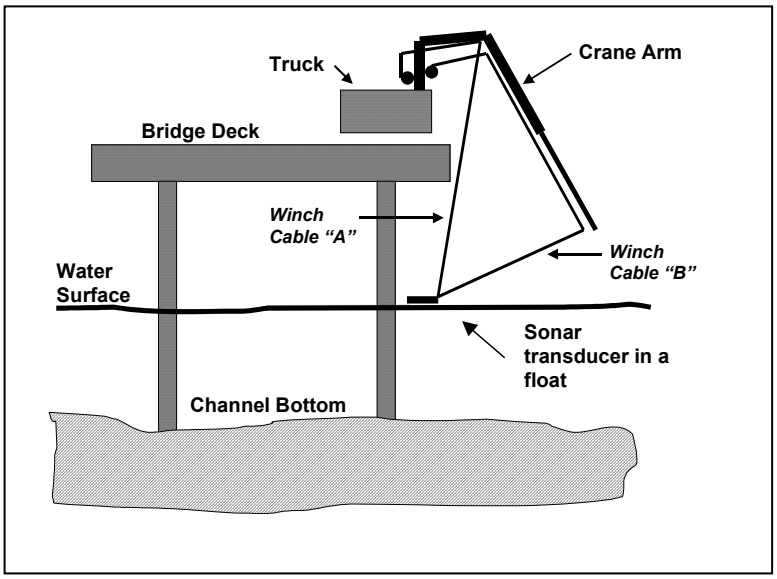

Figure 2. Two winch concept for cable suspended operations.

Figure 3. Completed articulated arm truck.

Data Collection Software

A windows based software package was developed to automate the data collection process. Data collection and processing occurs with a laptop computer equipped with two serial ports, one for the boom data, and one for the truck data, as sent by the two Campbell CR10 data loggers. The program includes a calibration menu that allows calibrating all sensors. Four programs were created: one for direct probing with the end of the crane, one for sonar measurements with a wireless sonar mounted on the articulated arm, one for measurements completed with the kneeboard, and one for cable suspended operations. All programs produce an x,y,z data file that can be read by other programs for contouring and plotting. The coordinate system for the x,y,z file is referenced to the profile line for the bridge, as typically shown on bridge plans, to allow easy comparison with elevation and station data for the bridge. The software for sonar measurements with the crane allows point measurements, or continuous recording as the crane is either driven across the bridge, or with the truck in a stationary position and sweeping the crane in an arc.

Field Testing

The objective of field testing was to evaluate the performance of the articulated arm truck at a variety of sites, representing a range of bridge and site conditions. The purpose of this testing was to validate the performance of the prototype devices and/or procedures under real world conditions, as implemented by highway personnel. Ideally, detailed testing would occur during flood conditions to evaluate the performance of the articulated arm relative the twelve criteria established as part of the research objective. In particular, this included a range of bridge conditions (high bridge decks, limited clearance, etc) and flow conditions (high velocity and sediment concentrations, floating debris, ice, pressure flow and air entrainment). The drought conditions during 2002 throughout much of the United States limited the opportunity to test the truck in flood conditions, but ultimately, ten bridges in seven states were visited. The following paragraphs present the results from two of these test sites.

Colorado I-70

Initial field testing was completed at the I-70 bridge over the Colorado River near DeBeque Canyon in western Colorado. The bridge has three piers on pile caps with 12 H-piles under each pile cap. The bridge was designed for a 50-year discharge of 900 m^3/s (32,000 cfs), and experiences velocities in excess of 3 m/s (10 fps), even at low flow. The channel bed material is primarily gravels and cobbles. The bridge has been rated scour critical based on observed conditions (Item 113, rating 2). The upstream channel bend has migrated, creating a skewed alignment into the bridge opening, and causing a large scour hole at pier 2, that extends through the bridge opening to the downstream side. Prior to extensive riprap placement in mid- march 2002, a 6 m (20 ft) scour hole had developed, exposing about 3 m (10 ft) of pile.

Figure 4 shows the flow conditions between pier 2 and the right abutment. At about mid-span the velocities were about 3.5 m/s (11 fps), and the flow depth was about 2 m (6.5 ft). Data was collected at both the upstream and downstream side of the bridge sweeping multiple arcs with the articulated arm and using a sonar mounted on the end of the crane (Figure 5). Results of the data collection indicated that the recently placed riprap has generally filled the scour hole back to the streambed elevation. As part of a cooperative effort with NCHRP Project 24-07, *Pier Scour Countermeasures*, this bridge will be monitored on a regular basis over the next 2-3 years to evaluate the performance of the riprap.

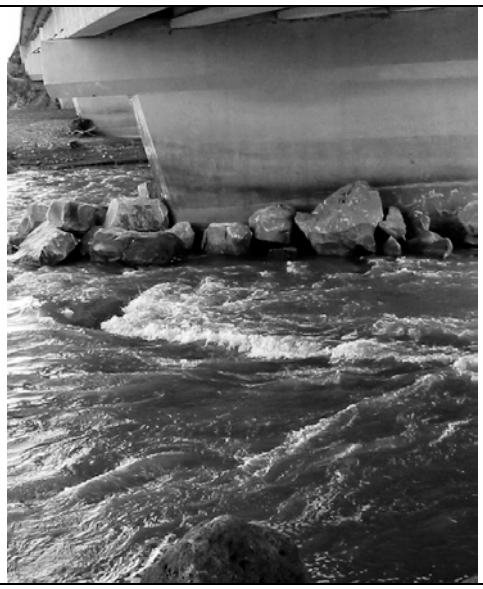

Figure 4. Flow conditions between the right abutment and Pier 2.

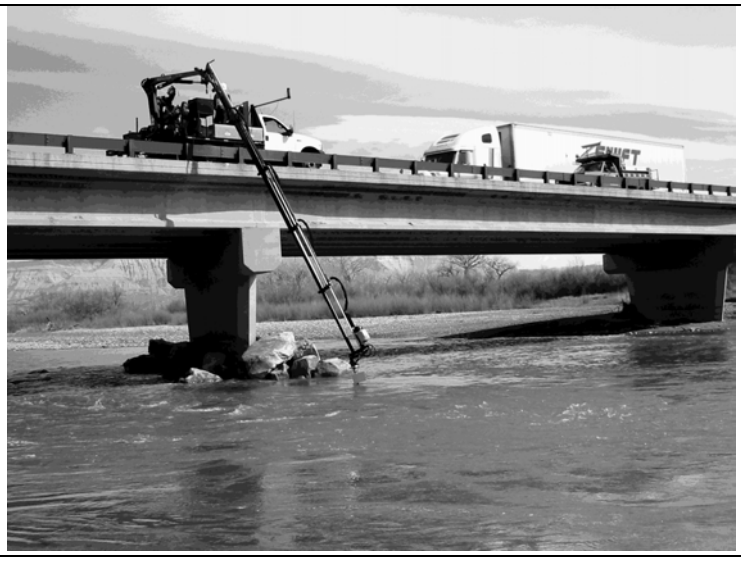

Figure 5. Using the articulated arm to sweep arc's around recently placed riprap.

Indiana State Route 61

Indiana S.R. 61 crosses the White River southeast of Vincennes, Indiana. The bridge has 5 spans on piers with pile caps with steel H piles driven to approximate refusal. At the time of inspection, the river was at flood stage and the southern part of the state was experiencing the wettest May on record. The bridge has not had any major scour problems, but has had a large sand bar in the bridge opening that had been contracted for removal. In addition to potential pier scour during the recent high flows, Indiana DOT was particularly interested to see if the sand bar was still present.

Testing at this bridge provided the opportunity to work at flood stage with relatively high velocities (about 2.1 m/s or 7 fps). The bridge had large grate inlets that required positioning the truck away from the barrier for a cross section measurement. This had not been tried before, but worked fine since the crane could still be articulated into position. Figure 6 shows the truck as it is driving across the bridge collecting cross section data. A wireless sonar in the sounding weight was also tested at this bridge (Figure 7), and was found to track the current and remain in a steady position, which had been a problem with earlier versions of the modified sounding weight.

Figure 8 illustrates typical results available with the articulated arm truck. The x,y,z data collected from these measurements along with bridge plan information were used in Microstation to create the plots shown in Figure 8. The top drawing shows the limits of the cross section data collected, and the arc's that were taken at piers 3 and 4. The middle part of the figure shows the cross section plotted, and at the bottom of the figure are the contour plots developed for each pier.

Conclusions

As a result of this research improved measurement devices and deployment procedures have been developed that will more successfully allow portable scour monitoring at a wide range of bridges under flood flow conditions. The adverse flow conditions that exist during flooding, including high velocities and debris, make these type of measurements difficult and can limit the success rate, even when properly applied, or applied to the best ability of the inspector.

The articulated arm developed under this research, with its automated data collection and multiple sensor capability, provides improved capability to collect data during flood conditions. Given the complexity of flood flow monitoring, including both difficult bridge conditions and difficult flow conditions, more than one measurement procedure is required to address as many situations as possible. The articulated crane should be a valuable addition to the inspectors "tool box" that will facilitate flood based scour monitoring.

References

Federal Highway Administration (FHWA), 1998. *Scour Monitoring and Instrumentation,* Publication No. FHWA-SA-96-036.

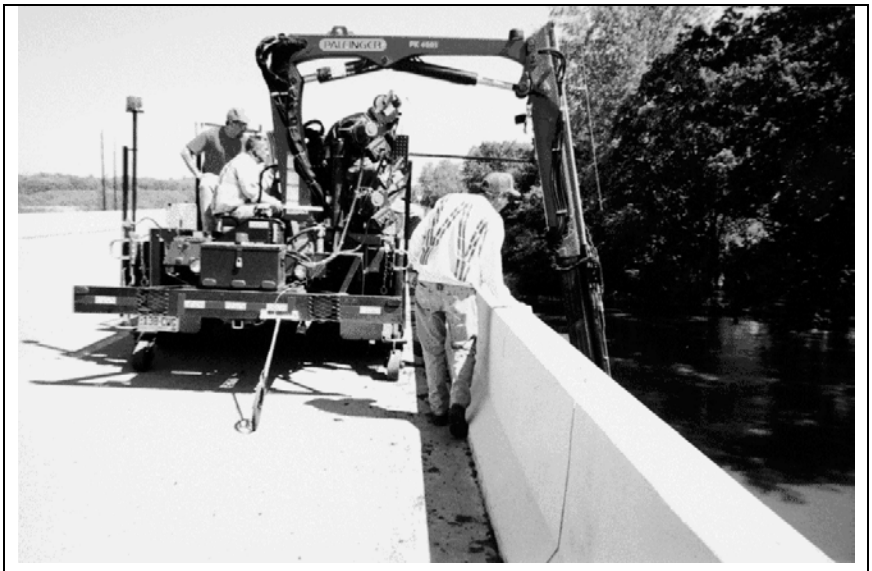

Figure 6. Collecting cross section data while driving the truck across the bridge.

Figure 7. Wireless sonar in a sounding weight.

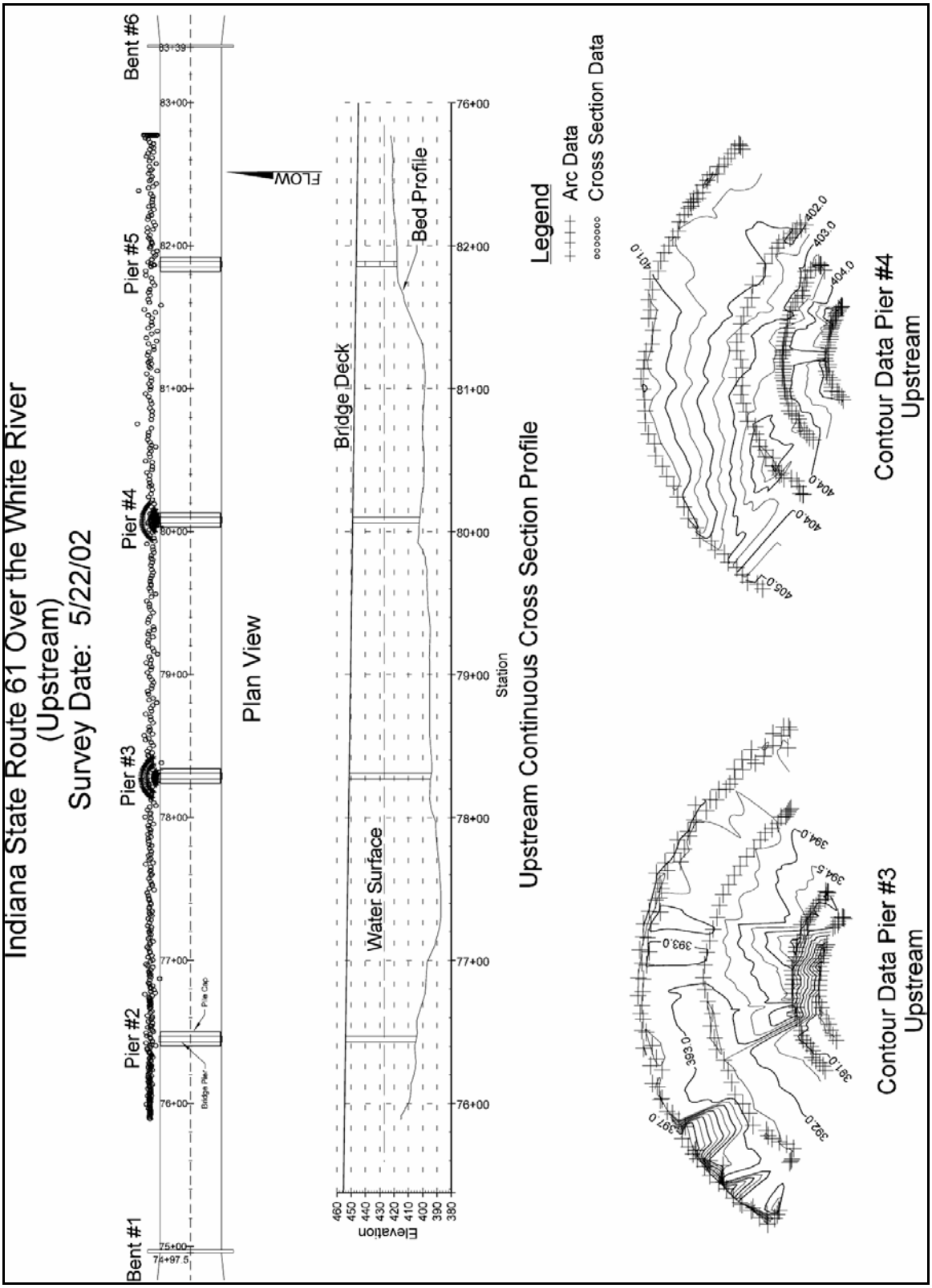

Figure 8. Typical results obtained with the articulated arm.

Active Scour Monitor Instrumentation in the California Transportation System

By
Steve Ng
California Department of Transportation, Branch Chief Engineer

Introduction

The California Department of Transportation – Caltrans, has embarked on a program to eliminate potential scour damage to the vast number of waterway crossings throughout the State of California. Identifying and developing scour mitigation countermeasures for each scour critical structure is the first part of the solution. However, the monies allocation, environmental permit and clearance approvals, and construction of the mitigation plan can take months, if not years, to complete. To minimize the risks to the traveling public once a scour problem has been identified until mitigation completion Caltrans seeks methods to actively monitor the scour conditions at scour critical structures. Although monitoring does nothing to prevent scour from occurring, active monitoring is expected to provide some warning that scour conditions have reached a level requiring immediate attention. Such active monitoring contributes to maintaining safety for the traveling public. This paper reviews what has been implemented, the successes and failures, as well as the possible future of scour monitoring in California.

The Short Course in Scour Monitoring Technology

Caltrans employs scour monitoring only as an interim measure to alert of problems until a permanent fix can be employed. Caltrans will not install Scour monitoring unless the permanent rehabilitation has been determined and is projected to have an excessively long implementation time. Our methods are changing and being developed as we accumulate more performance data. Also, cheaper and newer instrumentation packages are discovered as interest increases. Bridge instrumentation used to require a

hardwired power source and technicians to travel to the site to download data. Some applications use accelerometers to record real time seismic events or frost warnings. Increasingly, we can now power some of these devices with solar panels and download data with cellular communications.

The following are some scour monitoring methods and known performance to date.

Passive Monitoring

Visual inspections by the Area Bridge Maintenance Engineer (ABME) on a biennial schedule (or more often, such as after a significant event.) Inspection of the structural integrity of the bridge, waterway, and any countermeasures needed to be performed. Knowledge of the interactions between man and nature will have to be assessed to determine the demands of the site. Additional investigations can be performed as site conditions warrant. The field site investigation should be considered essential for every bridge site.

The advantage is the involvement of "Engineering Judgement", a first hand inspection is critical to determining the condition of a bridge. An experienced ABME can identify structure and waterway conditions that are markedly different from the previous inspections. The ABME is capable of looking at a number of symptoms and combining them to arrive at the structure condition.

Cons: Involves "Engineering Judgement", experience required, the more, the better.

May not be timely.

Large personnel force required to adequately address the large number of bridges in California.

ABME is looking at many items in one site visit. Their level of expertise is broad, but may be limited in issues regarding the hydraulic aspects of the site.

Web based data sites

Bridges are most susceptible to damage during high velocity flows. High velocity water is directly related to high stream discharge. Discharge release information may be available from some locations in close proximity to our bridge site. Release information from some reservoirs or the Department of Water Resources (DWR), California Data Exchange Center (CDEC) provides near real-time discharge information at selected locations. This information can be used to alert us of conditions warranting additional actions. Monitor information from specific bridge sites is also compiled and available from a Caltrans web site outside of the Caltrans firewall. (Need to expand this portion regarding the Caltrans Scour 2002b software). This provides access to data from offsite locations. This is hoped to improve response time during emergency alerts. (Personnel will not have to travel to the office to review data, if they can just turn to their home PC.) This data supplements information gathered from other sources.

Pros: Almost real-time information available.

Cons: Limited information available.

Stage Gage

Waterway discharges can be directly correlated to the water surface elevation at a known location on the stream. If web based data above is not available a site stage gage may be installed. A stage gage can be located and set to alert of high discharges. Stage gages can be of several types:

Pressure Gages are submerged in the flow and sense how much water is above the sensor. They are subject to clogging from stream silt material. The early model of these devices we installed were found to be very sensitive to temperature. All readings needed to be adjusted for the local ambient temperature.

Acoustic Stage Gages are mounted at the bridge soffit above the water and send sound waves down to the water surface. The reflected sound wave time determines the water surface elevation. These have a limited range of about 10m for a battery powered unit. One site was rendered unusable by local vegetation (a fast growing tree was found directly under the device).

Footed Sliding Rod (a.k.a. Brisco© monitor)

A 3m long rod with a 15cm +/- diameter foot (plate) at one end and the other end attached to a wire wrapped around a measuring reel. The foot sits on the channel bed typically sited at the pier nose. The rod is housed in a pipe (or sleeve) mounted to the pier. As the scour hole develops, the foot slowly falls into the hole lowering the rod and pulling the attached wire. The revolutions on the reel are counted and converted to a depth.

Pros: Simple design.

Cons: The Brisco Monitior name is a proprietary product.
Limited measurement range.
Subject to damage or lockup from debris.

As scour hole develops, the unsupported length of rod increases and is subject to bending. (i.e. the rod may wash out of the pipe sleeve and move downstream dragging the wire with it.)

Unknown availability.

Good "As-builts" required to clear substructure obstructions.

Device reports the lowest scour hole depth to date and is impractical to reset.

Sliding Magnetic Collar

A 3m to 6m pipe is driven into the channel at the location where monitoring is appropriate. A 15cm diameter ring assembly with magnets mounted close to the central pipe. As scour occurs, the ring assembly slides down the pipe to the bottom of the scour hole. Wire leads down the pipe sense the location of the magnets. The magnet depth is recorded at the data logger for storage and download.

Pros: May be best suited for monitoring general scour conditions.

Cons: Debris and large gravel can lock the ring assembly, inhibiting the ring movement.

Limited measurement range.

Mounting bracket securing the top of the pipe may catch debris.

Ground conditions may not be suitable for driving pipe.

Good "As-builts" required to clear substructure obstructions.

Device reports the lowest scour hole depth to date and is impractical to reset.

Scour "sticks"

A rod with some sort of switch system mounted along the length or at intervals along the length. Not beyond concept stage. Original concept was for a pezio-electric film or series of switches mounted along the length of the rod. As scour occurs, the switch(es) would be able to sense the displacement of the bed material. In theory, this should be able to sense the scouring and the infill of the scour hole. The film is subject to damage during installation or bed load movement of heavy bed materials.

Time Domain Reflectometers (TDR)

Need to gather some additional background information regarding the single application we have in place. This device is a sensor wire embedded in a hole backfilled with material similar to the surrounding footing material. As scour occurs, it is sensed in the device. Our current application requires a site visit, connection to the sensor with a PC?, etc. I need to fill in the details here. A manufacturer has contacted me regarding a new variation of this device, but I have not seen nor heard what the device has changed to.

Sonar transmitters – Bridge Mounted

A sonar transducer is mounted on the pier face pointed down to the channel. Reflected sound waves determine the depth of the scour as it is occurring.

Pros: Real-time measurement of the scour hole as it forms and refills.

Cons: Data requires user interpretation of the data. Not always clear where the scour depths are.

Debris and suspended bed material can obscure and invalidate the readings.

Some aesthetic objections.

The device must be submerged to be activate.

Good "As-builts" required "to aim" the device to an unobstructed view of the anticipated scour hole.

Sonar transmitters – Truck Mounted

A demonstration for California is planned for this coming April. I will have more to add to this later.

Ground Radar transmitters

Same as the sonar transmitter in concept, but I do not know of any working model. I do not think this ever has gotten beyond the concept phase. Should have a higher power demand. Likely also subject to a large amount of interpretation of the results, but should in theory be able to read through more types of materials.

Float-outs

Self contained buoyant cylinders are buried in the anticipated scour hole limits. A tilt switch, radio transmitter, and battery are in the float-out. The float-out is installed in the vertical upright position. When the scour hole develops, the device floats to the surface, turns horizontal, and transmits a signal to a receiver station at the bridge. At least two float-outs per location are typically deployed to give us a warning stage and a critical, must take action, stage.

Pros: Positive signal tells us exactly where the scour hole is at what time.

Should provide reliable results.

Cons: Once triggered, the device floats downstream away from the bridge and is lost.

Must be installed in an upright position.

Subject to interference from other radio sources.

Once installed, we do not hear from them until scour occurs. (So we will always wonder in the back of our minds, if they are really there and ready to work).

Limited battery, but not really a problem since the permanent rehabilitation should be installed before the battery fails.

Tilt Meters (a.k.a. Clinometers)

Tilt meters are very precise electronic levels. They are accurate enough to measure the bridge movements from temperature changes alone. In fact, the normal amount of movement due to temperature must be monitored first to determine the normal movement levels, before setting alarm limits for excessive movement. Tilt meters are installed on the bridge at a fix point such as a pier. As the bridge settles due to scour, the alarm value will be reached, triggering an alarm.

Pros: Proven technology.

Cons: Tells us that the bridge is falling down. There may not be sufficient warning to make effective repairs to limit damage to the structure. Hopefully, there will be sufficent time to close the structure to traffic to protect the public.

GPS tracking stations

Monitoring stations are mounted to the bridge. These stations determine the bridge position with data received from Global Positioning Satellites (GPS). Depending upon the site specifics, a single station position could be determined to within 2cm. With the use of another GPS reference station (at a known stationary position), the accuracy of the moving station can be determined to within 1cm (according to the manufacturer under ideal conditions.) Monitoring data is directly uploaded to a web site for processing by the manufacturer prior to being available via a secured web site. California is evaluating this method, but has not determined its suitability.

The future

Working on some concepts. I do not want to divulge any manufacturer's secrets. Looking to make things smaller, easier to install, easy to monitor and still provide us more data with few false readings.

Conclusion

In general, there is no single preferred method of monitoring scour at a bridge site. The best solution for one site will likely not work at the next location. A combination of methods should be considered to complement each other. The Hydraulic Engineer will have to consider all of the information available to him/her to determine the appropriate course of action.

A Methodology for Predicting Channel Migration NCHRP Project No. 24-16

Peter Lagasse[(1)], William Spitz [(2)], and Lyle Zevenbergen[(3)]

[(1)] Senior Vice President, Ayres Associates, Fort Collins, CO 80527; PH (970) 223-5556
[(2)] Geomorphologist, Ayres Associates, Fort Collins, CO 80527; PH (970) 223-5556
[(3)] Project Manager, Ayres Associates, Fort Collins, CO 80527; PH (970) 223-5556

Abstract

Stream channel migration can have a significant impact on the design, maintenance, and inspection of bridges and other highway facilities. Practicing highway hydraulic engineers could benefit from a practical methodology to predict the rate and extent of channel migration in their efforts to reduce the cost of design, repair, rehabilitation, and countermeasures for lateral channel instability. The objective of Research Project 24-16 is to develop a practical methodology to predict the rate and extent of channel migration (i.e., lateral channel shift and down valley migration) near transportation facilities.

The research products will include not only a final report describing the predictive methodology, but also an extensive archived database, published on CD-ROM, that contains detailed morphological data, aerial photos, historical banklines, and maps for more than 1,400 bends on 87 rivers and streams across the United States. In addition, a stand-alone aerial photo/map comparison handbook that provides a complete applications supplement for Project 24-16 will be published. The comparison techniques in the handbook will include GIS measurements and extrapolation routines. The archived database and handbook will be intended for use by FHWA and State DOTs, but should also be of interest to future researchers and practitioners responsible for river channel maintenance and river restoration/rehabilitation projects.

Introduction

Rivers prone to channel migration may be spanned by static structures and paralleled by fixed highway alignments and other appurtenances. Channel migration (alluvial river meander planform deformation) is a major consideration in designing bridge crossings and other transportation facilities in affected areas; it causes the channel alignment and approach conditions present during construction to deteriorate as the upstream channel location changes. Channel migration can result in the following: (a) excess bridge pier and abutment scour, (b) threats to bridge approaches and other highway infrastructure, (c) worsened debris problems, and (d) obstructed conveyance through bridge openings.

Channel migration includes lateral channel shift (expressed in terms of distance moved perpendicular to the channel center line, per year) and downvalley migration (expressed in distance moved along the valley, per year). Engineers are concerned about predicting channel migration as it moves through the bridge elements (piers and abutments) or endangers other highway infrastructure during design life.

Geomorphologists may view channel stability from the perspective of hundreds or thousands of years. For highway engineering purposes, however, a stream channel can be considered unstable if the rate or magnitude of change is such that the planning, location, design, or maintenance considerations for a highway crossing are significantly affected during the life of the facility. The kinds of changes that are of concern are: (1) lateral bank erosion; (2) aggradation or degradation of the streambed; (3) short-term fluctuations in streambed elevation (scour and fill); and (4) avulsion. This research is concerned specifically with only lateral channel instability (including down valley migration) resulting from meander migration.

Project Objective

The objective of Research Project 24-16 is to develop a practical methodology to predict the rate and extent of lateral and down valley channel migration in proximity to transportation facilities. The methodology should enable practicing engineers to locate and design new bridges, highway facilities, or other structures, accommodate for anticipated channel migration, evaluate the risk to existing facilities, and if necessary, determine the need for and design countermeasures against the effects of channel migration. A prediction of channel migration could also be used to alert bridge inspection personnel to the potential for channel change that could affect the safety of a bridge. In addition, this methodology could be applied to channel restoration and stabilization efforts.

Research Approach

The fluvial processes involved in predicting meander migration are very complicated and the variables of importance are difficult to isolate. The major factors affecting alluvial stream channel forms are:

- stream discharge (magnitude and duration), temperature, and viscosity
- sediment load, including types and caliber of sediments
- longitudinal valley slope
- bank and bed resistance to erosion
- vegetation
- geology, including bedrock outcrops, clay plugs, and changes of valley slope
- human activity

In an analysis of flow in alluvial rivers, the flow field is further complicated by constantly changing discharge. Significant variables are, therefore, quite difficult to relate mathematically. It is often necessary to list measurable or computable variables, which effectively describe the processes occurring, and then to reduce the list by making simplifying assumptions and examining relative magnitudes of variables. This means that it is necessary to strive toward an acceptable balance between accuracy and limitations posed by data needs and analytical complexity.

Many laboratory and field studies have been carried out in an attempt to determine the variables controlling river response. To the present time, the problem has been more amenable to an empirical solution than an analytical one. Computer solutions to complex hydraulic problems

have extended the range of fluvial process problems that can be solved analytically, but simplifying assumptions are still required. While the mathematical complexity of the analytical solution may be justified for research purposes, empirical approaches may produce results of greater utility to practicing engineers. After careful review of empirical and deterministic (physical process mathematical modeling) approaches to predicting meander migration, it was concluded that empirical approaches are more likely than deterministic approaches to yield a practical methodology that will be useful to practicing engineers.

The approach consists of the following tasks, many of which have already been completed:

- Conduct a complete and thorough literature review on meander migration.
- Access and evaluate a number of relatively complete existing data sets.
- Enhance existing data sets by acquiring recent aerial photography at selected study sites and obtain data on hydrologic, hydraulic and sediment characteristics.
- Analyze the enhanced data sets with photogrammetric comparisons.
- Develop a screening procedure to identify *stable* meandering reaches.
- Develop a classification system for river/meander types for stratification of the database.
- Develop a stand-alone Handbook for map/aerial photograph comparison techniques for measuring and predicting meander migration supplemented with regression analysis results.
- Compile and archive a database on CD-ROM that contains all acquired meander site data.
- Conduct necessary internal and external testing and evaluation and revise as necessary.
- Develop a detailed plan and recommendations for incorporating the results of this research into ongoing FHWA/National Highway Institute technology transfer programs.

Procedure for Developing the Methodology to Predict Meander Migration

The following six steps are necessary to achieve the goals of NCHRP Project 24-16:

(1) Assemble Final Data Set. In order to develop a methodology for predicting meander migration that can be used by bridge engineers and inspectors as well as other users, it was necessary to obtain data on numerous meandering rivers having a wide range of morphologies throughout the United States. The necessary data typically includes channel cross sections, channel planform, bed and bank material characteristics, vegetation, discharge data, sediment loads, floodplain characteristics, geology, and watershed characteristics. The data for each site was assembled and compiled into Microsoft Excel workbooks containing spreadsheets designated for each bend.

Existing data was collected from a variety of sources and researchers. The primary data set upon which much of this project is based comes from work conducted by Dr. James Brice of the U.S. Geological Survey. The Brice data set consists of morphometric data (Brice, 1982) as well as aerial photos, maps, and historic bankline tracings for 805 bends at 82 sites on 59 rivers. Under a research project at Johns Hopkins University, the data set was inventoried and additional data was derived for 133 of the Brice sites by Cherry et al. (1996). Additional survey and sediment data was collected for the Brice sites by field personnel from WES, the USGS, and the

University of Nottingham, UK in 1999. Eight additional data sets, some with historic banklines or channel position atlases, covering 646 bends at 57 sites on 28 rivers were acquired from other sources.

Attempts were made to acquire appropriate historic aerial photography from various agencies for the data sets that had no historic bankline comparisons. Aerial photography from the 1990s and topographic maps were acquired for all the data sets. Updated discharge data was also obtained for each of the sites used in this project.

(2) Screen and Classify River and Meander Types. According to Brice (1982), it should be easy to identify stable meanders by their width characteristics. A simple stratification of meanders would be of value to the bridge engineer as a screening procedure, allowing identification of meanders that are very stable. Rather than developing regional relationships, a geomorphic classification was developed during this step to lead the user of the methodology to a suitable procedure for a particular river or meander type. A classification scheme modified from the channel pattern classification originally developed by Brice (1975) is presented in **Figure 1** as an approach for both screening and classification. It is likely that the most common river types (or meander modes) encountered by DOTs in the field will be addressed by this classification.

(3) Measure Meander Morphology. In order to relate a meander to rate and type of change and to correlate its behavior with other variables, it is necessary to describe the meander quantitatively. Numerous investigators have done this by measuring amplitude, wavelength, radius of curvature, sinuosity, width and depth of the channel, width-depth ratio, and ratio of centerline radius of curvature to width. Following selection of meanders or sets of meanders for study, the maps and aerial photographs were compared in order to determine the rate of migration or change for each meander or segments of meanders.

(4) Collect Data on Controlling Variables. Each meander will be affected by its location and by the controlling variables that act upon it. This study assembled data on the character of the valley (slope, alluvial variability, bedrock controls), hydrology, and sediment type. Sediment type in the bed and banks of an alluvial river reflects the type of sediment load moved through the channel. Hydrologic data was obtained from nearby gaging stations. Channel dimensions and valley slope were obtained from topographic maps and aerial photographs. These data plus data on bed and bank sediments were obtained from various sources. Schumm (1960) concluded from his studies of Great Plains and Australian streams that width-depth ratio and sinuosity are determined by the type of sediment load moved through a channel. Although sediment loads will not be measured, width-depth ratio can be used as a surrogate for sediment load data.

(5) Develop Methodology. Based upon these steps, a predictive methodology has been developed for the highway engineer. Meander change or lack of change can be determined by comparing maps and aerial photographs of different dates. Because comparative aerial photography or maps are generally available, this may represent the most reliable predictor of meander migration for a specific site. A methodology and guidelines will be provided for comparison techniques ranging from the use of simple overlays to GIS techniques that can be implemented with the hardware and software normally available to a state highway agency. The

predicted meander change is then compared with a frequency distribution of measured rates from the data set to assess the reasonableness of the prediction.

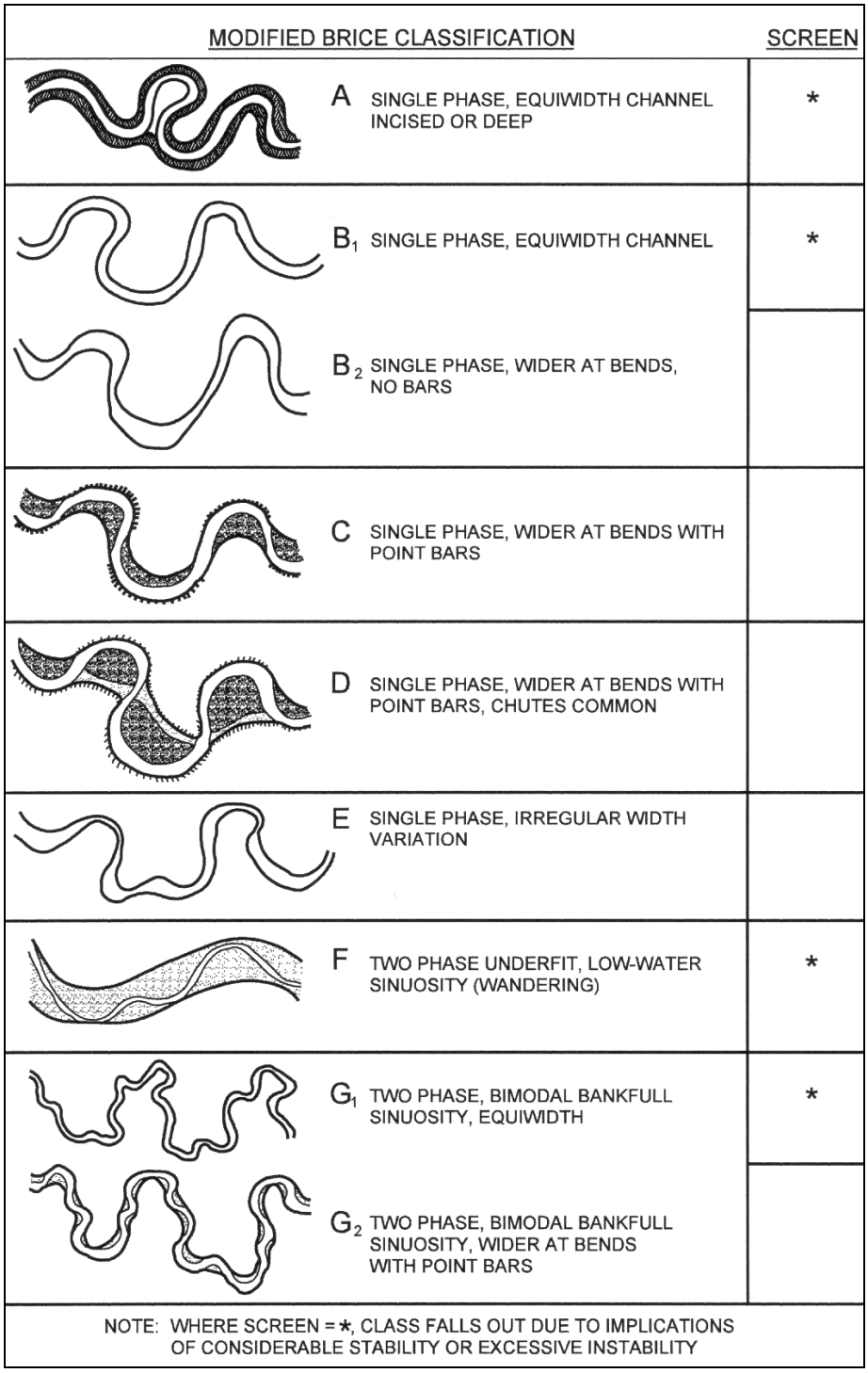

Figure 1. Modified Brice Classification of meandering rivers.

Measuring Meander Migration

Before predictive tools for channel migration can be developed, one must be able to measure and describe channel migration. A standard approach for use in analyzing data sets must be developed and this approach should be adhered to for all subsequent measurements.

Bend migration can be reasonably described by four modes of movement (**Figure 2**). Extension is across-valley migration and is easily measured at the center of the bend radius (R_c). Similarly, translation is down-valley migration and is also measured at the center of the bend radius. Expansion (or contraction) increases (or decreases) bendway radius. Rotation is a change in the orientation of the bendway with respect to the valley alignment.

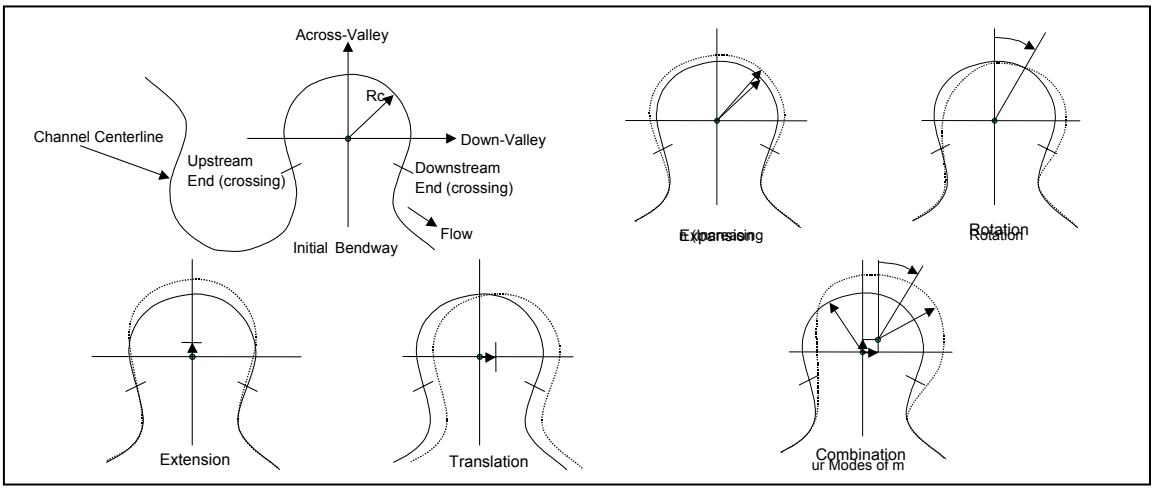

Figure 2. Measuring meander migration.

A change in any of these four modes of movement results in a change in the location of the outer bankline. Combinations of these modes of movement would result in a wide variety of bendway shapes through time. To apply this approach one must identify a valley orientation, locate the radial center of the bend, and measure the bendway radius and the orientation of the bendway with respect to the valley. If this is performed for consecutive aerial photos, rates of change in each of the modes of movement can be computed. This type of geometric information is needed to graphically depict channel migration of individual bends.

Predicting four modes of movement is a significant task for every bend of interest (Figure 2). However, actual bend migration is even more complex. One part of the bend may be expanding faster or translating down-valley faster than another. This would result in changes in bend symmetry. The above approach assumes fairly symmetrical bends. As a concession to practicality one must limit the number of modes of movement to the fewest possible and even four modes may be too complex to be practical. Although eliminating rotation is consistent with the project description, rotation will be accounted for since it is the vector representation of the combination of translation and extension. Expansion (a change in R_c) will be included, if

possible, as it could have a major impact on the location of the outer bank and because rates of migration appear to be correlated to R_c/W (bend radius of curvature/width).

A GIS measurement tool to obtain the necessary data for both photogrammetric and regression analyses was developed for this project. The methodology for prediction of meander migration will concentrate on three modes of migration (extension, translation, and expansion - see Figure 2). If movement in these three modes can be predicted, the primary threats to a bridge or highway facility will be established. The GIS measurement tool has the capability to predict (extrapolate) meander migration at a given bend where the necessary sequential aerial photography or mapping is available.

Aerial Photo and Map Comparison Handbook

The principal product of this research will be an Aerial Photo and Map Comparison Handbook. As a minimum, the Handbook will cover the following topics:

- Screening and classification of meander sites
- Sources of mapping and aerial photographic data
- Basic principles and theory of aerial photograph comparison
- Simple overlay techniques
- GIS or computer supported techniques
- GIS based measurement and extrapolation techniques
- Sources of error and limitations
- Illustrated examples and applications
- Supplementing comparison analysis with regression results

While the final report for NCHRP 24-16 will provide a complete summary of the findings, recommendations, and implementation plan resulting from the project, the Handbook will provide the specific techniques and guidance to apply those results. The Handbook will also cover the screening and classification techniques (as a first step in any meander migration analysis) and the application of the results of the project regression analyses (as a check on the results of the photo/map comparison or as an analysis methodology where time-sequenced photography or mapping is not available). Finally, the Handbook will include a detailed description of the GIS meander migration prediction tool which will be compatible with the most recent version of ArcView.

Anticipated Research Results

A major task of this research is the development of aerial photograph comparison techniques and the GIS meander migration prediction tool that will provide an accurate means of predicting meander migration. As an example, aerial photograph comparison techniques and the GIS meander migration prediction tool were used in a preliminary attempt to predict meander migration on the White River in Indiana. Aerial photographs from 1937 and 1966 were acquired for a reach of the river, the banklines were delineated on each set of photographs, and the banklines were registered for comparison. Using the GIS meander migration prediction tool, the bankline position for 1995 was estimated.

Figure 3 shows the actual 1937 bankline position of seven meander bends and the 1995 bankline positions of the bends predicted by the GIS meander migration prediction tool superposed on the 1966 aerial photograph. The 1995 bankline positions of the bends predicted by the GIS meander migration prediction tool were then overlain on the 1995 photograph obtained for this reach. **Figure 4** shows the predicted 1995 bankline position superposed on the 1995 aerial photograph of the river.

A comparison of the actual bankline locations with the predicted bankline positions reveals that the GIS meander migration prediction tool can predict meander migration with relatively good accuracy. As seen in Figure 4, the 1995 bankline positions of Bends 3 and 4 and the cutoff at Bend 5 were accurately predicted. The unexpected and anomalous bankline positions can be accounted for by a man-made cutoff (Bends 1 and 2), a natural cutoff (Bends 5, 6 and 7), and, possibly, bank protection (Bends 3 and 5) prior to 1995. The man-made cutoff of Bend 1 may have been in response to the major threat posed by meander migration to a levee nearby. The cutoff has also caused Bend 2 to become distorted compared to the predicted shape. The cutoff of Bend 5 has resulted in the distortion of Bend 5 and abandonment of Bends 6 and 7. The migration of the outer bank along the downstream limb of Bend 3 and at the apex of Bend 5 has been partially halted by apparent bank protection. It is quite likely that the bankline positions of Bends 1 and 2 as well as the revetted portions of Bends 3 and 4 would have closely matched the predicted positions if not for man's influence.

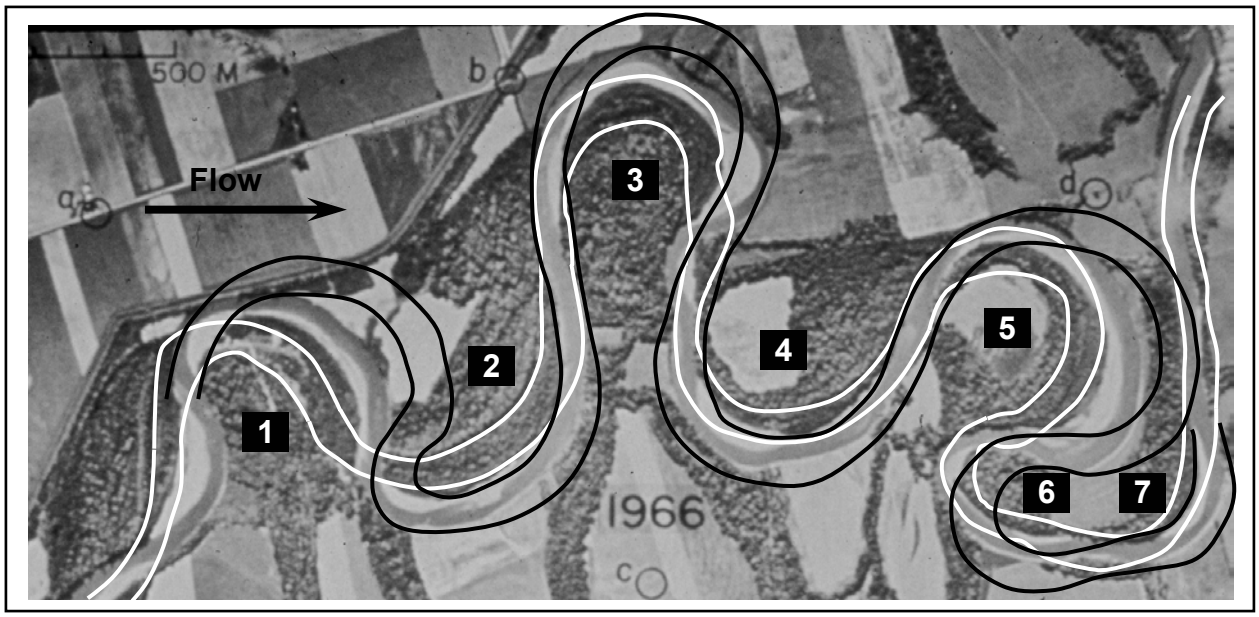

Figure 3. Aerial photo of the White River in 1966 showing the actual 1937 banklines (white) and the 1995 bankline positions (black) predicted by the GIS meander migration prediction tool.

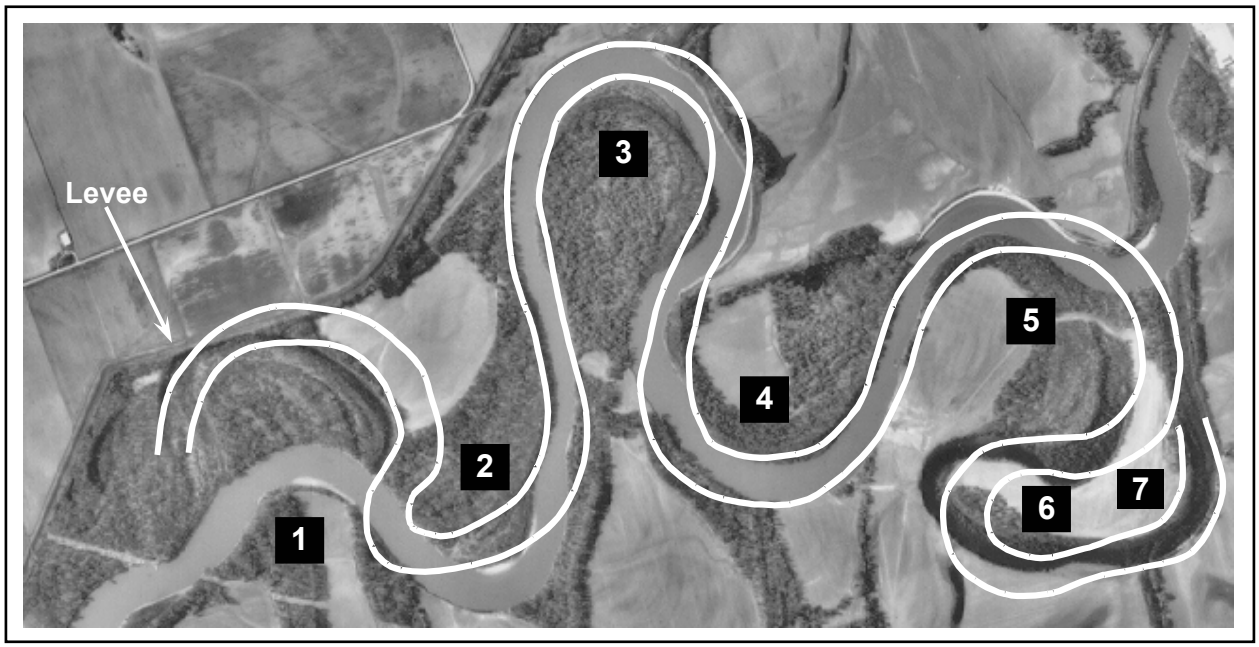

Figure 4. Aerial photograph of the White River in 1995 showing the bankline positions predicted using the GIS meander migration prediction tool.

Summary

A practical methodology to predict the rate and extent of channel migration at highway bridges could help reduce the cost of design, repair, rehabilitation and countermeasures for lateral channel instability. A screening procedure to identify *stable* meandering stream reaches would ensure that engineering and inspection resources are not allocated to locations where there is little probability of a problem developing.

The analytical products of this research, map/aerial photograph comparison techniques, and guidelines to predict channel migration in proximity to transportation facilities, will provide a practical quantitative methodology that will enable informed decision making at all levels. The methodology will be useful in reconnaissance, design, rehabilitation, maintenance and inspection of highway facilities, particularly if it is packaged to facilitate ease of application. The end result will be a more efficient use of highway resources and a reduction in costs associated with the impacts of channel migration on highway facilities.

The archived database will include all meander site data acquired for this study. With the archived data set, future researchers will have a readily accessible database in a very useable format for a variety of studies. These studies could include additional empirical analyses and more complex regressions based on the archived data. Additional data could be added to supplement or complement the database. As deterministic modeling code improves over the next decade, this archived data will facilitate calibration and verification of physical-process models of river meandering, providing additional tools beyond the empirical techniques of this research for the highway hydraulic engineer.

It is anticipated that this project will be completed by mid-2003. Following the completion of the project, a final report detailing the methodology, the Aerial Photo and Map Comparison Handbook, and the archived database will be copyrighted and published.

References

Brice, J.C., 1975. *Air Photo Interpretation of the Form and Behavior of Alluvial Rivers*, Final report to the U.S. Army Research Office, Durham, North Carolina.

Brice, J.C., 1982. *Stream Channel Stability Assessment*, Report No. FHWA/RD/82/021, U.S. Department of Transportation Office of Research and Development, Washington, D.C., 42 p.

Cherry, D.S., Wilcock, P.R., and Wolman, M.G., 1996. *Evaluation of Methods for Forecasting Planform Change and Bankline Migration in Flood-Control Channels*, Johns Hopkins University, Prepared for: U.S. Army Engineer Waterways Experiment Station, Vicksburg, MS.

Schumm, S.A., 1960. *The Shape of Alluvial Channels in Relation to Sediment Type*, USGS Prof. Paper 352-B, pp. 17-30.

Schumm, S.A., 1977. *The Fluvial System*, John Wiley, N.Y., 338 p.

Predicting Meander Migration: Evaluation of Some Existing Techniques

Jean-Louis BRIAUD[1], Hamn-Ching CHEN[2], Siyoung PARK[3]

1. Spencer J. Buchanan Professor, Dpt. of Civil Engineering, Texas A&M University, College Station, Texas, 77843-3136, USA. (briaud@tamu.edu)
2. Professor, Dpt. of Civil Engineering, Texas A&M University, College Station, Texas, 77843-3136, USA.
3. Graduate Student, Dpt. of Civil Engineering, Texas A&M University, College Station, Texas, 77843-3136, USA.

ABSTRACT

River meanders migrate over time; this migration endangers civil engineering structures in general and highways bridges in particular. Predicting and preventing this migration is part of the responsibility of the hydraulic engineer and of the geotechnical engineer working together. This article describes and evaluates two approaches used to predict the migration of meanders: the empirical approach and the time-sequence maps and extrapolation approach. Empirical methods are based on correlations using data bases of observed behavior while the time-sequence method uses previously observed movement of a given meander to predict its future migration. Six case histories on four rivers are used to evaluate the precision and accuracy of these methods by comparing the predicted and measured migration. The results show that some empirical methods are conservative, some are unconservative, none of them are very accurate or precise. The time sequence method gives more information on the meander movement, is relatively precise and accurate to predict the radius of the best-fit circle of the future meander location, but is not precise to predict the migration rate of the center of that circle.

INTRODUCTION

Rivers are dynamic systems. The action of the flowing water can change the elevation and the lateral location of the riverbed and the riverbanks. Meanders are particularly prone to changes in lateral location because of the centrifugal force that increases the shear stress at the interface between the water and the soil. Predicting the movement of a meander is both difficult and necessary. It is difficult because many factors influence the process and necessary because such a movement may create expensive maintenance problems for nearby bridges. A comprehensive survey of existing knowledge was assembled on this topic (Briaud et al., 2001).

After a presentation of the three general approaches available to predict meander migration, this article gives details about two of them. Then, six meander migration case histories related to four rivers are presented including the measured movements. Finally, the measured movements are compared with the movements predicted by the two approaches and conclusions are drawn.

DEFINITIONS

Figure 1 shows the migration of meanders on the Brazos River near Navasota, Texas. At the location labeled “reference line case 1” on the figure, the meander has

moved over 300 meters towards the bridge abutment from 1910 to 1981. At the location labeled "reference line case 2" on the figure, the meander has moved over 200 meters towards the Navasota River over the same period. As in the case of any erosion problem, predicting such movements requires the knowledge of three input parameters: the geometry, the water and the soil. The geometry of the meander and of the river cross-section impacts the hydraulic shear stress generated at the interface between the water and the soil. Figure 2 gives a definition of the factors used to describe a meander geometry. The water, including the flow velocity, also influences the hydraulic shear stress applied to the soil. The soil controls the erosion rate on the resistance side. These simple concepts are fundamental but one must also acknowledge the complexity of some factors. For example, the interface may not be soil; it could be rock or vegetation or a man-made material used as a countermeasure. Also, the shear stress developing at the interface may lead to a slope failure of the bank; the slumped mass of soil is then eroded by the flowing water.

GENERAL APPROACHES

The existing approaches to predict meander migration make use of geometry, water, and soil parameters in various ways. These approaches can be divided in three categories: those using time-sequence maps and extrapolation, those using empirical equations, and those using fundamental modeling.

With the time-sequence maps and extrapolation approach, meander migration is predicted by accumulating topographic maps and aerial photographs of the riverbanks at various dates in the past, measuring the migration rate from those maps and extrapolating into the future. These maps and aerial photographs can be obtained from local libraries, or from web sites such as http://mac.usgs.gov/mac/findmaps.html or http://terraserver.microsoft.com/. The advantages of this approach are that it is relatively simple and that it is based on full-scale observations at the site. The drawbacks are the limited availability of maps and photographs, and the assumption that future flow and soil conditions will be the same as in the past. This method is commonly used by Departments of Transportation.

With the empirical approach, a database of observed meander migrations and associated parameters is assembled, most influential parameters are selected, a regression is performed and an equation is proposed. The advantages of this approach are that it is simple and that it is based on full scale observed data. The drawbacks are that the equation may not include all the essential parameters influencing the process, and that the applicability of the equation is limited by the extent of the database both in terms of quantity of data and geographical area. This approach is also quite common.

The fundamental modeling approach consists of modeling the erosion process at the water-soil interface and projecting it into time by using future hydrographs (water velocity versus time). This approach has the advantage of simulating the real phenomenon on a site-specific basis. It has the drawback of being more complicated because it requires the site-specific measurement of soil properties and the selection of future hydrographs. One such method is in the development stages at Texas A&M University.

TIME-SEQUENCE MAPS AND EXTRAPOLATION METHOD

In this article the time-sequence maps and extrapolation method is described and evaluated against case histories. This method was mentioned by Brice (1982) and is being refined by Lagasse and his colleagues at Ayres Associates in Fort Collins, Colorado (Lagasse, 2001). Figure 3 shows a sketch describing how the method is used and Figures 4 and 5 show real examples. In a first step, a map of the meander is obtained for a first date, t_1 (1958 on the example of Figure 4). A first best-fit circle is drawn to match as much of the t_1 dated meander shape as possible. The location of the center, C_1, and the radius R_1 of that first circle are recorded (Figure 3). Then a map of the meander is obtained for a second date t_2, more recent than the first date t_1 (1969 on the example of Figure 4). Again a second best-fit circle is drawn to match as much of the t_2 dated meander shape as possible. The location of the center, C_2, and the radius R_2 of that second circle are recorded (Figure 3). Now in order to predict the position of the meander at a future date t_3, the following linear extrapolation process is used. The distance C_2C_1 is measured, by using the scale on the map, and divided by the time (t_2-t_1) to obtain the meander migration rate $M_{r\,(1\text{-}2)}$. This rate, which is the mean rate from t_1 to t_2 is assumed to be the same as the rate $M_{r\,(2\text{-}3)}$ from t_2 to t_3. The distance C'_3C_2 between the predicted location C'_3 of the center of the t_3 dated best-fit circle and the measured location C_2 of the center of the t_2 dated best fit circle is predicted by:

$$C'_3\,C_2 = (t_3 - t_2) \times M_{r(1-2)} \tag{1}$$

Furthermore, the direction of vector C'_3C_2 is assumed to be the same as the direction of vector C_1C_2; the location of C'_3 is thereby completely determined. The actual location of the center of the t_3 dated best-fit circle is C_3 (Figure 3) and the measured migration rate of the circle centers is $C_3C_2 / (t_3 - t_2)$. The predicted radius R'_3 of the t_3 dated best-fit circle is obtained by linear extrapolation of radii R_1 and R_2.

$$R'_3 = R_2 + \frac{R_2 - R_1}{t_2 - t_1} \times (t_3 - t_2) \tag{2}$$

Equation (2) expresses the assumption that the meander rate (dR/dt) remains constant. The actual radius of that circle is R_3 (Figure 3). The predicted location of the t_3-dated best-fit circle is thereby completely predicted.

The actual location and size of the t_3-dated circle can be obtained from a meander map corresponding to the date t_3. The difference between the location and size of the predicted t_3-dated circle and the measured t_3-dated circle help evaluate the precision and accuracy of the time-sequence maps and extrapolation method. In this article, four rivers' case histories are used to study a total of six meander sites. For each meander site, maps corresponding to several dates were collected and used to predict the location and size of the t_3-dated best-fit circle as well as to measure the location and size of the t_3-dated best-fit circle. This leads to a total of 10 predicted vs. measured comparisons.

SELECTED EMPIRICAL METHODS

Some of the most commonly used empirical approaches are described and evaluated against case histories. They are the Keady and Priest (1977) approach, the Hooke (1980) approach, the Brice (1982) approach, and the Nanson and Hickin (1983) approach.

Keady and Priest (1977) collected meander migration data from published reports on the Mississippi River in Tennessee, Louisiana, and Mississippi, on the Red River in

Arkansas, on the Pearl River in Louisiana, on the Tombigbee River in Mississippi, on the Buffalo River in Louisiana, and on the Red Deer River in Alberta, Canada. This gave them eight data points from which they obtained their equation. The selected influencing parameters are s, the free surface slope of the river, and a, the amplitude of the meander (Figure 2). The equation is:

$$M_r = 0.315\,(g\,a)^{0.5}\,f(s) \tag{3}$$

where M_r is the meander migration rate (m/yr), g is the acceleration due to gravity (m/s^2), a is the meander amplitude (m) (Figure 2), f(s) is the function of s, the free surface slope of the river, shown in Figure 6.

Hooke (1980) collected meander migration data using field measurements and historical maps for 11 streams in Devon, England. Hooke isolated the catchment area, A, as the main influencing parameter and derived his equation based on those data. The catchment area is the area drained by the river or by the river system. Then, Hooke compared the rates obtained in Devon with rates found in the literature for 43 streams. For this article, both sets of data were merged and a single regression was derived (Figure 7). This is why the equation is called Hooke's modified equation:

$$M_r = 0.0669\,A^{0.46} \tag{4}$$

where M_r is the meander migration rate (m/yr), and A is the catchment area (km^2).

Brice (1982) collected meander migration data for 43 meanders in four different river types (equiwidth, wide bend, braided-point bar, and braided). An equiwidth river is one where the width of the river is approximately constant; these tend to be small rivers. A wide bend river is one where the river width is larger at the meanders. A braided point-bar river is one where the inside of the meanders fills with sand bars and the main channel does not fill the entire width at lower flows. A braided river is one where the main channel develops sinuosity within the larger width of the river; these tend to be very large rivers with high flow fluctuations. Brice selected the channel width, b, as the main influencing parameter and obtained his equation from regression against the 43 data points (Figure 8). Brice equation is:

$$M_r = 0.01\,b \tag{5}$$

where M is the meander migration rate (m/yr), and b is the width of the river channel (m). As can be seen on Figure 8, the meanders of braided rivers tend to migrate less than predicted by equation (5) while those of wide bend rivers tend to migrate more than predicted by equation (5).

Nanson and Hickin (1983) collected meander migration data for 18 river channels in Western Canada including the Beaton River. They selected the radius of curvature normalized with respect to the channel width, r_c / b, as the main influencing parameter. Then they plotted their data (Figure 9) and observed that when the ratio r_c / b was between 2 and 3 the migration rate tended to be maximum. They drew two envelopes on their data. The equations of these two lines were found to be:

$$M_r / b = 0.1\,((r_c / b) - 1) \qquad \text{when } r_c / b \text{ is smaller than 2.3} \tag{6}$$

$$M_r / b = 0.35\,(r_c / b)^{-1} \qquad \text{when } r_c / b \text{ is larger than 2.3} \tag{7}$$

where M_r is the meander migration rate (m/yr), b is the channel width (m), and r_c is the radius of curvature of the meander (m). As can be seen on Figure 9, these are envelopes that should lead to upper bound predictions. The idea that there is an optimum ratio r_c / b leading to a maximum migration rate, much like a resonance phenomenon, can be explained as follows (Figure 10). At large r_c / b ratios, the radius r_c is large compared to

the channel width b and, for a given flow velocity, the centrifugal force which is inversely proportional to the radius of curvature is small; this leads to a small erosion rate. At very small r_c / b ratios, the width of the channel b is large compared to the radius of curvature, the water can actually flow almost straight through the river, and its flow tends to straighten it. When the ratio r_c / b is between 2 and 3, the centrifugal force is significant and the water is forced to follow the outer bank; this leads to the maximum migration rate.

BRAZOS RIVER AT SH 105: CASE HISTORIES 1 AND 2

The location of these two meander case histories is shown on Figure 11. The site of case history 1 is of concern because the river is getting dangerously close to the embankment of State Highway 105 which was built in 1951 (Figure 1) and the site of case history 2 is of concern because the Brazos River is getting very close to the Navasota River. Six topographic maps and aerial photographs were collected covering the period from 1910 to 1999. Figure 1 shows the migration problem at location 1 and location 2 on the Brazos River while Figure 12 gives a close-up view of the migration problem at location 1 on Figure 1. The migration of the meanders was measured along the reference lines that are shown on Figures 1 and 12. These directions were chosen to represent the direction of concern for the DOT. Note that the prediction equations presented earlier do not specify the direction in which the migration takes place. It is understood that these predictions represent the maximum migration rate.

The discharge in the Brazos River over the period of meander migration observation was obtained from the USGS web site (http://www.usgs.gov) for the gage station at the bridge site (Gage no. 08109000). The discharge is usually quoted in m^3/s, it is recorded daily and averages can be obtained over chosen periods. The variation of the monthly mean discharge Q (m^3/s) is shown in Figure 13 for the period from 1910 to 2000. Note that no data was collected from 1910 to 1918. The catchment area at the gage site is 77567 km^2 according to the USGS web site. The free surface slope of the river was obtained by using the elevation of two consecutive gage stations near the meander site (read at http://www.usgs.gov) and dividing the elevation difference by the distance between the two gages read on the topographic map. The value obtained was 0.00018. The discharge history, the catchment area, and the free surface slope are some of the parameters quantifying the water influence on meander migration.

The prediction methods also require parameters quantifying the influence of the geometry of the meander. These parameters include the width of the channel, the radius of curvature of the meander, and the amplitude of the meander (Figure 2). The width of the channel was measured on each one of the topographic maps and aerial photographs. The values obtained are listed in Table 1 and averaged 103 m for case 1. The radius of curvature was considered to be the radius of the circle that best fitted the mid stream shape of the meander. This was done by manual trial and error using a compass for each date (Figure 1). The values obtained are listed in Table 1 and averaged 564 m for case 1. The meander amplitude was obtained by using the meander considered and the adjacent one, and applying the definition of Figure 2. The values obtained are listed in Table 1 and averaged 206 m for case 1. The process followed to determine these geometric factors involves a certain amount of subjectivity; therefore the measurements may vary

somewhat from one person to another. The measurements for these case histories are summarized in Table 1.

As mentioned earlier, it is reasonable to assume that the best prediction methods for meander migration require the knowledge of geometric factors, water factors, and soil factors. Unfortunately in these case histories no detailed soil data was available nor is any soil data required in the prediction equations. Progress in this direction needs to be made.

OTHER CASE HISTORIES

The third case history is the case of the Nueces River near US 90 which was built in 1967. The site was of concern because in 1998 a flood nearly destroyed the right abutment of the bridge. Three topographic maps and aerial photographs could be found covering the period from 1958 to 1995. Figure 4 shows the migration of the meander upstream of the bridge; the migration movements were measured along the reference line shown on Figure 4. The discharge in the Nueces River was obtained from USGS gage station no 08192000 which is xx km from the meander site. The variation of the monthly discharge is shown in Figure 14 from 1958 to 2000. The other parameters for this case history are shown in Table 1.

The fourth meander case history is the case of the Trinity River near FM 787 which was built in 1975 (Figure 15). The site of this meander is of concern because the meander is migrating dangerously close to the FM 787 embankment. Three topographic and aerial photographs were found covering the period 1971 to 1999. Figure 15 shows the migration of the meander upstream of the bridge; the migration movements were measured along the reference line shown on Figure 15. The discharge in the Trinity River was obtained from USGS gage station no. 08066500, which is at the bridge site. The variation of the monthly mean discharge is shown in Figure 16 from 1970 to 1999. The other parameters for this case history are shown in Table 1.

The fifth and sixth meander case histories are located on the Guadalupe River near US 59 which was built in 1967. The site is of concern because the meander upstream from the bridge is attacking the left abutment and the meander downstream from the bridge may lead to a cut-off. Such a cut-off would increase the slope of the river locally and impact the migration rate of the upstream meander. Four topographic maps and aerial photographs were found covering the period 1959–1995. Figure 5 shows the migration of the two meanders; the migration movements were measured along the reference lines shown on Figure 5. The discharge in the Guadalupe River was obtained from USGS gage station no. 08176500 which is xx km from the meander site. The variation of the monthly mean discharge is shown in Figure 17 from 1959-1999. The other parameters for these two case histories are shown in Table 1.

PREDICTED vs. MEASURED MEANDER MIGRATION

In order to evaluate the accuracy and precision of the empirical methods**,** equations 3 through 7 were used together with the data of Table 1 to obtain the predicted migration rates of Table 2. Also shown in Table 2 are the measured migration rates for the case histories. Note that some of the migration rates for the Trinity River are negative, indicating that the meander moved back towards earlier positions. This is due to the fact that countermeasures were installed on the Trinity River during those periods of time and were successful in reversing the migrating process. Such cases were removed from the

comparisons. Migration rate predictions and measurements were made for each period of observation leading to a total of 18 comparisons in Table 2 minus the 4 values of the Trinity River deemed influenced by countermeasures. For each prediction, the parameter value (a, b, r_c) corresponding to the beginning of the period was used in the equation.

The comparisons are presented in Figure 18. As can be seen The Keady and Priest method is reasonably conservative, the Hooke method seems overly conservative, the Brice method is seriously underpredicting the measurements, and the Nanson and Hickin method splits the measured data. On the basis of this data alone, the Keady and Priest method appears to be a reasonably safe method to use keeping in mind that the scatter is significant.

In order to evaluate the accuracy and the precision of the time-sequence and extrapolation method, the following process was used. For a given date t_1, the best-fit circle was found by trial and error, the center location C_1 and the radius R_1 were recorded (Figure 3). For the next available date t_2, the best-fit circle was also found, again the center location C_2 and the radius R_2 were recorded. Using R_1, R_2, t_1 and t_2, the radius R'_3 of the best fit circle for the meander at the next available date t_3 was predicted using equation 2. The predicted value R'_3 could then be compared to the measured value R_3 obtained from the best-fit circle corresponding to the actual meander shape at the date t_3. The migration rate of the center of the best-fit circle $M_{r(1-2)}$ between the dates t_1 and t_2 was calculated. The time sequence maps and extrapolation method consists of assuming that the migration rate $M_{r(2-3)}$ of the center between the dates t_2 and t_3 is the same as $M_{r(1-2)}$; this is stated in equation 2. Therefore comparing the predicted value $M'_{r(2-3)}$ of the measured value $M_{r(2-3)}$ is the same as comparing the measured values of $M_{r(1-2)}$ and $M_{r(2-3)}$. Measured and predicted values of the radius and of the center of migration rates are shown in tables 3 and 4 and in Figure 18. Table 3 and 4 indicate 10 comparisons, however the Trinity River case was not used because it was influenced by countermeasures.

The comparisons are presented in Figure 19. As can be seen the time-sequence maps and extrapolation method gives a reasonably satisfactory prediction of the radius of the meander but not of the center migration rate. Note that in some cases (Brazos River, Table 4, 1981-1988 and 1988-1995) the predicted movement of the center of the circle is in opposite direction to the measured movement. As pointed out earlier this method is much more operator dependent than the empirical methods, however it is superior to the empirical method in that it gives a much more complete position of the meander.

Table 1 shows a column of the values of the ratio r_c / b. Inspection of this column of r_c / b values indicates that if the initial ratio is high, the meander tends to evolve by decreasing its r_c / b ratio towards a value around 2 which corresponds to the highest migration rate shown by Nanson and Hickin on Figure 9. If the initial value of r_c / b is about 2 the value remains about equal to 2 and the meander migrates at its highest migration rate.

CONCLUSIONS

Meander migration can be predicted using one of three types of approaches: time-sequence extrapolation, empirical equations, and fundamental modeling. This article describes the time-sequence and extrapolation approach and four empirical equations used to predict meander migration rates: Keady and Priest (1977), Hooke (1980), Brice

(1982), Nanson and Hickin (1983). Then four case histories of meander migration are presented including maps indicating the movement over long periods of time and the flow history over that same period. Predictions are made according to the methods presented and compared to the measurements from the case histories.

For the empirical methods, the comparisons indicate that the Keady and Priest method is reasonably conservative, that the Hooke method is overly conservative, that the Brice method is seriously underpredicting the measurements, and that the Nanson and Hickin method splits the measured data with significant scatter. On the basis of this data alone, the Keady and Priest method appears to be a reasonably safe method to use keeping in mind that the scatter is significant.

For the time-sequence and extrapolation method, the comparisons indicate that this method gives a reasonably satisfactory prediction of the radius of the meander but not of the center migration rate. In some cases, the predicted movement of the center of the circle is in opposite direction to the measured movement. This method is much more operator dependent than the empirical methods, however it is superior to the empirical method in that it gives a much more complete position of the meander.

ACKNOWLEDGEMENTS

This project was sponsored by the Texas Department of Transportation (TxDOT). At TxDOT, the project director was Tom Dahl and the project coordinator was David Stolpa. They both helped in providing the field data as well as Pat Williams and Terry Paholek of the Bryan District, John Kilgore of the San Antonio District, Robert Balfour of the Beaumont District, and Gerald Freytag of the Yokum District.

REFERENCES

1. Briaud J.-L., Chen H.-C., Edge W., Park S., Shaw A., 2001, " Guidelines for Bridges Over Degrading and Migrating Streams; Part 1: Synthesis of Existing Knowledge", Texas Transportation Institute Report no. 2105-1 for the Texas Dpt. of Transportation, Texas A&M University System, College Station, Texas, USA, pp.174.
2. Brice J.C., 1982, "Stream Channel Stability Assessment," Report No. FHWA/RD-82/021, Federal Highway Administration, Washington, DC, USA, p.41.
3. Hooke J.M., 1980, "Magnitude and Distribution of Rates of River Bank Erosion, Earth Surface Processes, Vol. 5, No. 2, pp.143-157, John Wiley, Chichester, NY.
4. Keady P.D., Priest M.S., 1977, "The Downstream Migration Rate of River Meandering Patterns," Proceedings, 12th Mississippi Water Resources Conference, Jackson, Mississippi, USA, pp.29-34.
5. Lagasse P., 2001, Personal Communication, Ayres Associates, 3665 JFK Parkway, Bldg 2, Ste. 200, Fort Collins, CO, 80527.
6. Nanson G.C., Hickin E.J., 1983, "Channel Migration and Incision on the Beatton River," Journal of Hydraulic Engineering, Vol. 117, No. 7, (Discussion and Closure), ASCE, Reston, Virginia, USA, pp. 942-946.

Table 1 – Summary of Case History Data.

Case History	Year	Channel Width b(m)	Radius of Curvature r_c(m)	Ratio r_c/b	Meander Amplitude a(m)	Free Surface Slope s (mm)	Catchment Area A (km^2)
Brazos at SH105 (Case 1)	1910	109	747	6.9	120	0.00018	77567
	1958	98	600	6.1	187	0.00018	77567
	1981	84	453	5.4	220	0.00018	77567
	1988	89	558	6.3	244	0.00018	77567
	1995	133	460	3.5	258	0.00018	77567
Brazos at SH105 (Case 2)	1910	107	1733	16.2	120	0.00018	77567
	1958	107	1173	11.0	187	0.00018	77567
	1981	120	746	6.2	220	0.00018	77567
Nueces at US90 (Case 3)	1958	134	365	2.7	261	0.0009	4820
	1969	122	300	2.5	248	0.0009	4820
	1995	70	391	5.6	274	0.0009	4820
Trinity at FM787 (Case 4)	1971	125	182	1.5	254	0.00008	44512
	1976	73	182	2.5	259	0.00008	44512
	1983	112	??	1.5	191?	0.00008	44512
	1988	132	201	1.5	207	0.00008	44512
	1999	155	276	1.8	201	0.00008	44512
Guadalupe at US59 (Case 5)	1959	50	88	1.8	187	0.00037	13468
	1981	58	88	1.5	183	0.00037	13468
	1988	54	100	1.9	204	0.00037	13468
	1995	92	125	1.4	204	0.00037	13468
Guadalupe at US59 (Case 6)	1959	42	137	3.3	475	0.00037	13468
	1981	33	125	3.8	475	0.00037	13468
	1988	67	108	1.6	483	0.00037	13468
	1995	75	104	1.4	516	0.00037	13468

Table 2 – Predicted and Measured Meander Migration Rates (Empirical Methods).

Case History	Period	Keady & Priest (1977) **m/yr**	Hooke (1980) **m/yr**	Brice (1982) **m/yr**	Nanson & Hickin (1983) **m/yr**	Measured **m/yr**
Brazos at SH105 (Case 1)	1910 - 1958	5.4	11.9	1.1	5.6	3.4
	1958 - 1981	6.7	11.9	1.0	5.6	5.5
	1981 - 1988	7.3	11.9	0.8	5.4	1.6
	1988 - 1995	7.7	11.9	0.9	5.0	5.6
	1995- 1999	7.9	11.9	1.3	13.4	??
Brazos at SH105 (Case 2)	1910 - 1958	5.4	11.9	1.1	2.3	2.2
	1958 - 1981	6.7	11.9	1.1	3.4	5.2
	1981 - 1988	7.3	11.9	1.2	6.7	??
Nueces at US90 (Case 3)	1958 - 1969	4.8	3.3	1.3	17.2	2.4
	1969 - 1995	4.7	3.3	1.2	17.4	4.5
Trinity at FM787 (Case 4)	1971 - 1976	22.0	9.2	1.2	5.7	-1.3
	1976 - 1983	22.2	9.2	0.7	10.2	8.0
	1983 - 1988	19.1?	9.2	1.1	??	-4.9
	1988 - 1999	19.9	9.2	1.3	6.9	3.6
Guadalupe at US59 (Case 5)	1959 - 1981	4.0	5.3	0.5	3.8	0.95
	1981 - 1988	4.0	5.3	0.6	3.0	7.7
	1988 - 1995	4.2	5.3	0.5	4.6	3.0
Guadalupe at US59 (Case 6)	1959 - 1981	6.4	5.3	0.4	4.5	0.4
	1981 - 1988	6.4	5.3	0.3	3.0	4.8
	1988 - 1995	6.5	5.3	0.7	4.1	8.3

? doubt in the data, ?? no data

Table 3 – Predicted and Measured Radius for the Best Fit Meander Circle (Time Sequence Maps and Extrapolation Method).

Case History	Year	Radius (measured) (m)	Radius (predicted) m)
Brazos at SH105 (Case 1)	1910	747	
	1958	600	
	1981	453	530
	1988	558	408
	1995	460	663
Brazos at SH105 (Case 2)	1910	1733	
	1958	1173	
	1981	746	905
Nueces at US90 (Case 3)	1958	365	
	1969	300	
	1995	391	146
Trinity at FM787 (Case 4)	1971	182	
	1976	182	
	1983	??	182
	1988	201	
	1999	276	
Guadalupe at US59 (Case 5)	1959	88	
	1981	88	
	1988	100	88
	1995	125	119
Guadalupe at US59 (Case 6)	1959	137	
	1981	125	
	1988	108	121
	1995	104	91

Table 4 – Predicted and Measured Movement Rate for the Center of the Best Fit Circle (Time Sequence Maps and Extrapolation Method).

Case History	Period (yr)	Center Migration Rate (measured) (m/yr)	Center Migration Rate (predicted) (m/yr)
Brazos at SH105 (Case 1)	1910 - 1958	6.7	6.7
	1958 - 1981	12.2	12.2
	1981 – 1988	(-)19.0	(-)19.0
	1988 - 1995	19.0	
Brazos at SH105 (Case 2)	1910 - 1958	15	15
	1958 - 1981	22	
Nueces at US90 (Case 3)	1958 - 1969	5	5
	1969 - 1995	2.8	
Trinity at FM787 (Case 4)	1971 – 1988	3.2	3.2
	1988 – 1999	6.7	
Guadalupe at US59 (Case 5)	1959 – 1981	1.0	1
	1981 – 1988	14	14
	1988 – 1995	7.1	
Guadalupe at US59 (Case 6)	1959 – 1981	0.4	0.4
	1981 – 1988	4.8	4.8
	1988 - 1995	4.3	

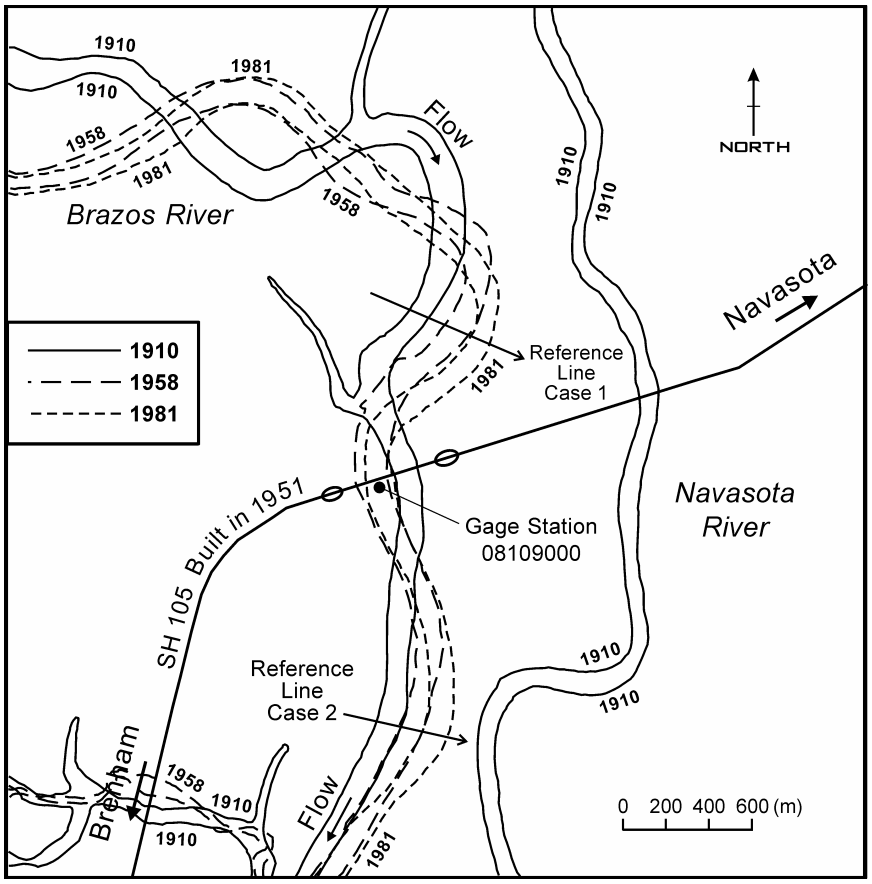

Figure 1 – Meander Migration for the Brazos River at SH 105

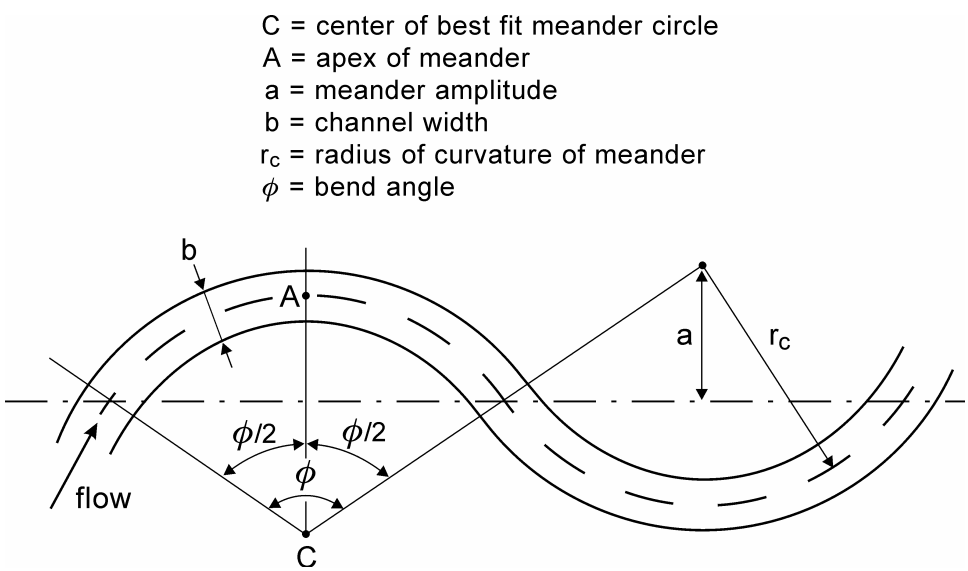

Figure 2 – Geometry Parameters for Meanders

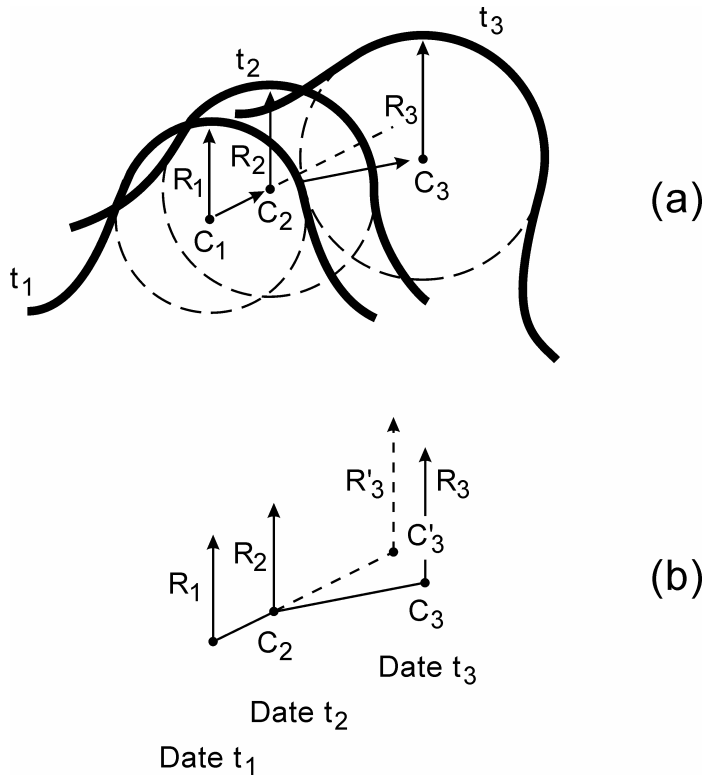

Figure 3 – Definitions for the Time Sequence Maps and Extrapolation Method

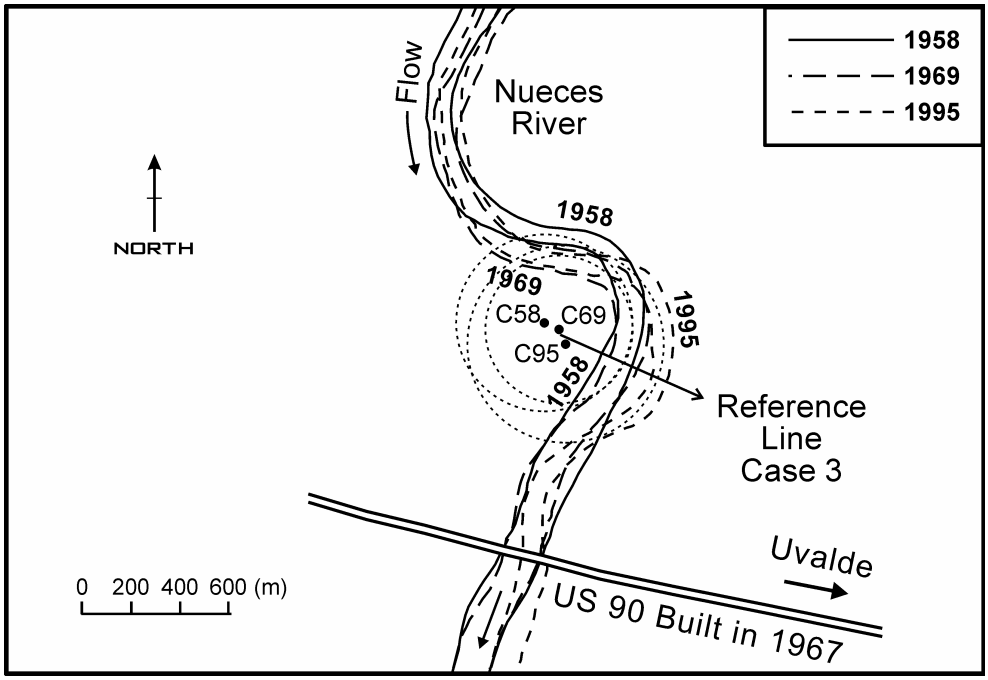

Figure 4 – Meander Migration for the Nueces River at US 90

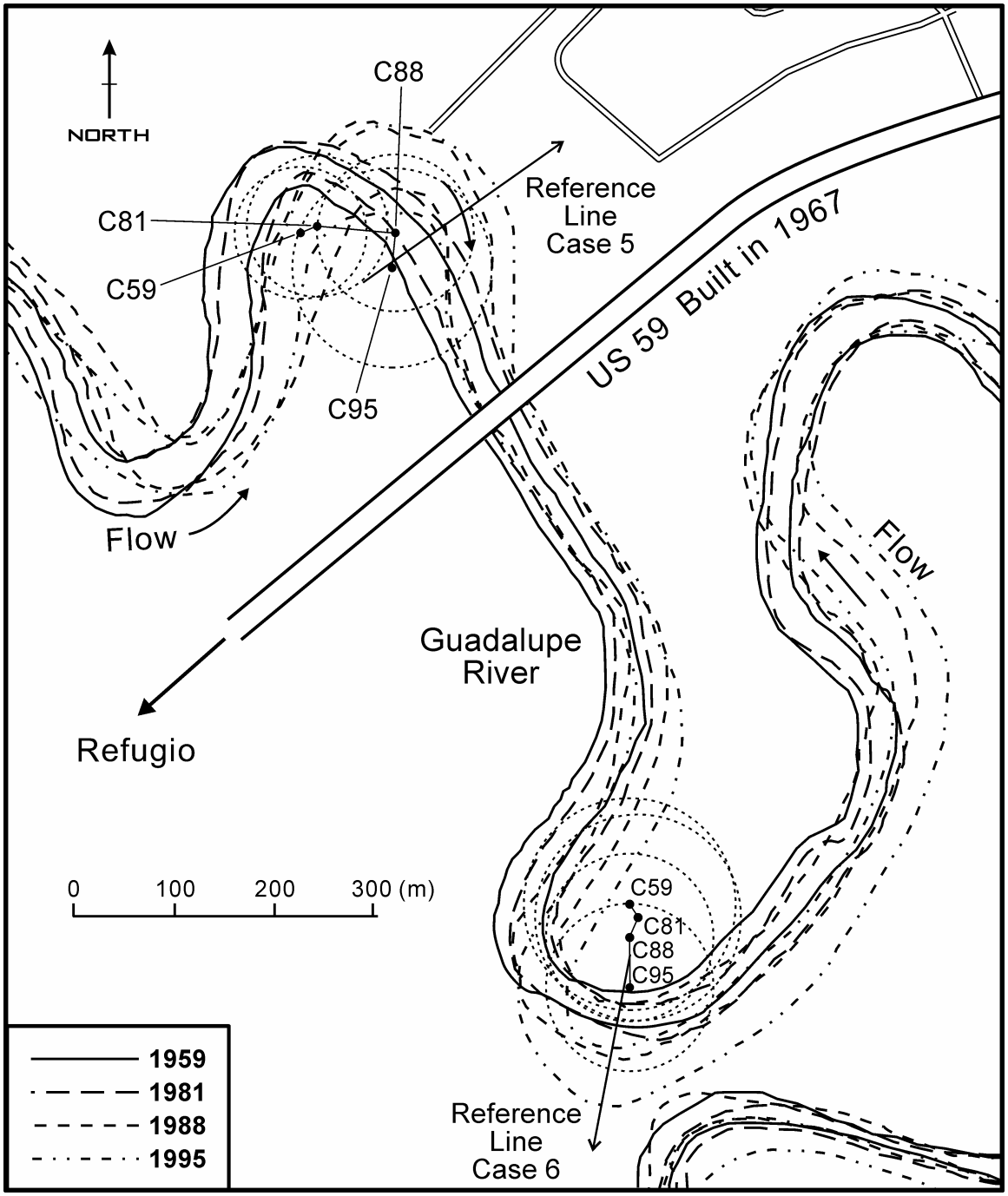

Figure 5 – Meander Migration for the Guadalupe River at US 59

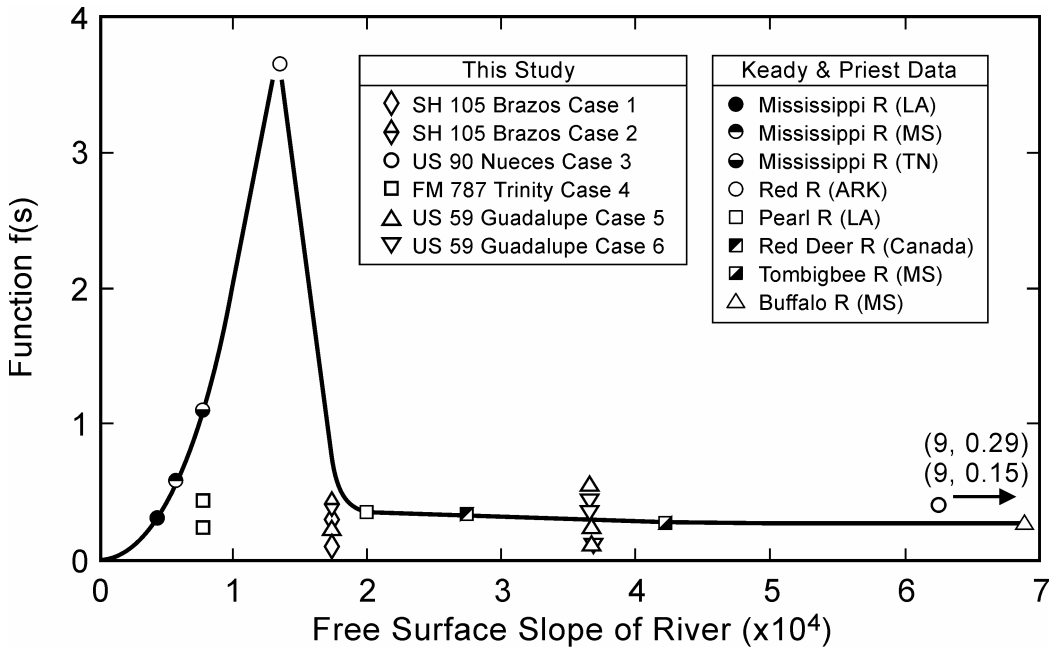

Figure 6 – Function for Keady and Priest (1977) Method

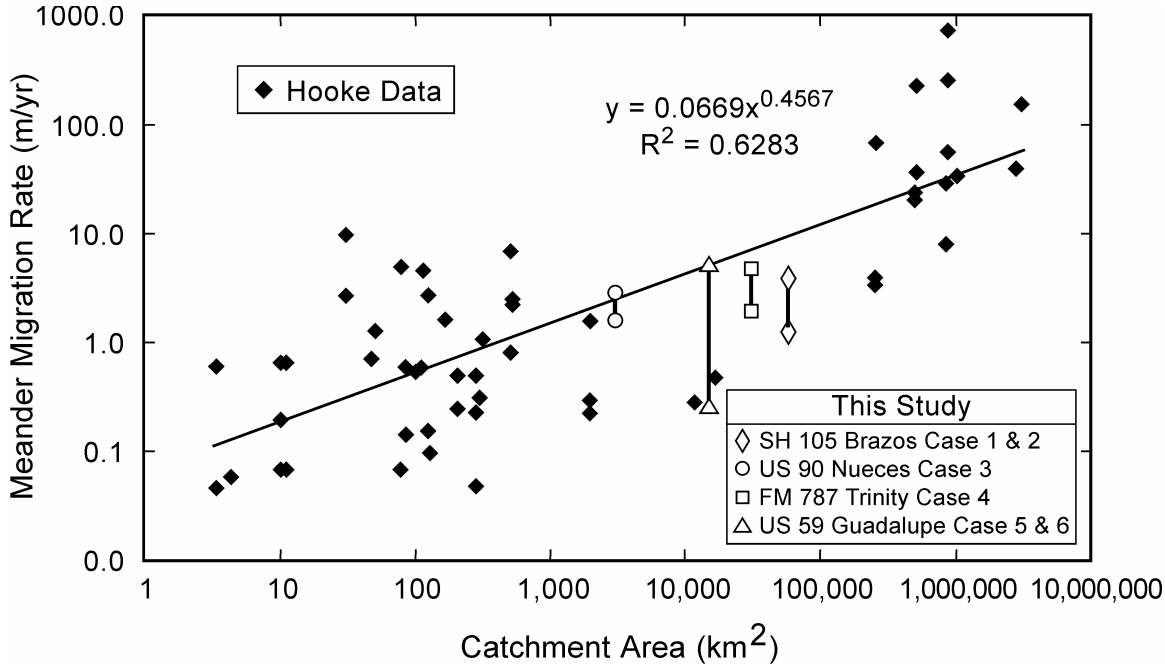

Figure 7 – Data Used by Hooke (1980) to Develop his Method

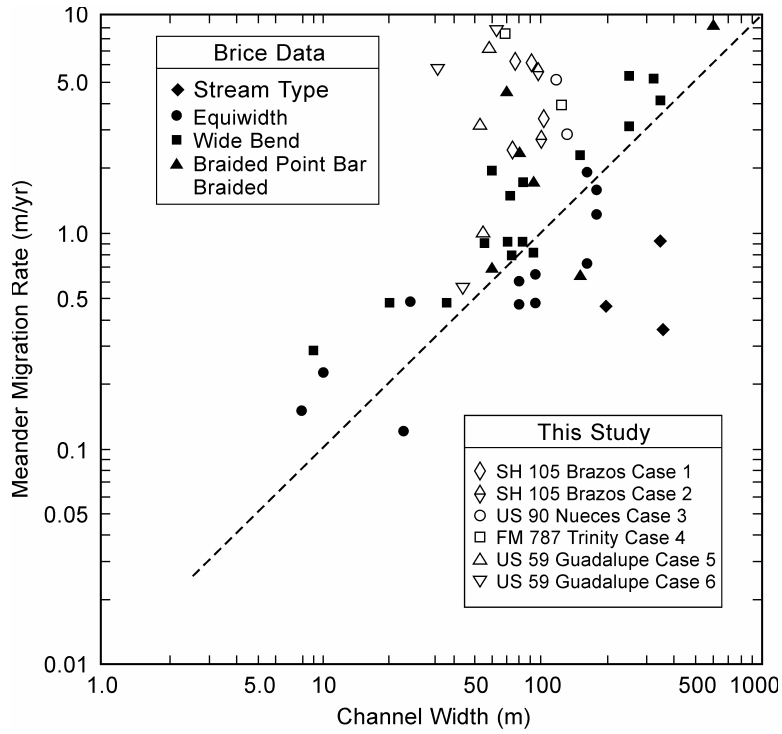

Figure 8 – Data Used by Brice (1982) to Develop his Method

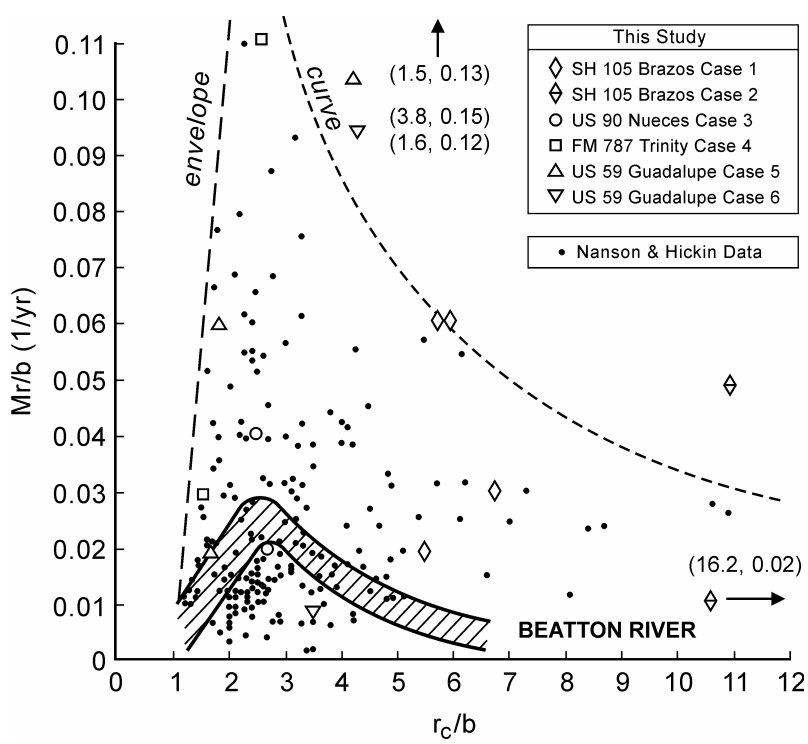

Figure 9 – Data Used by Nanson and Hickin (1983) to Develop Their Method

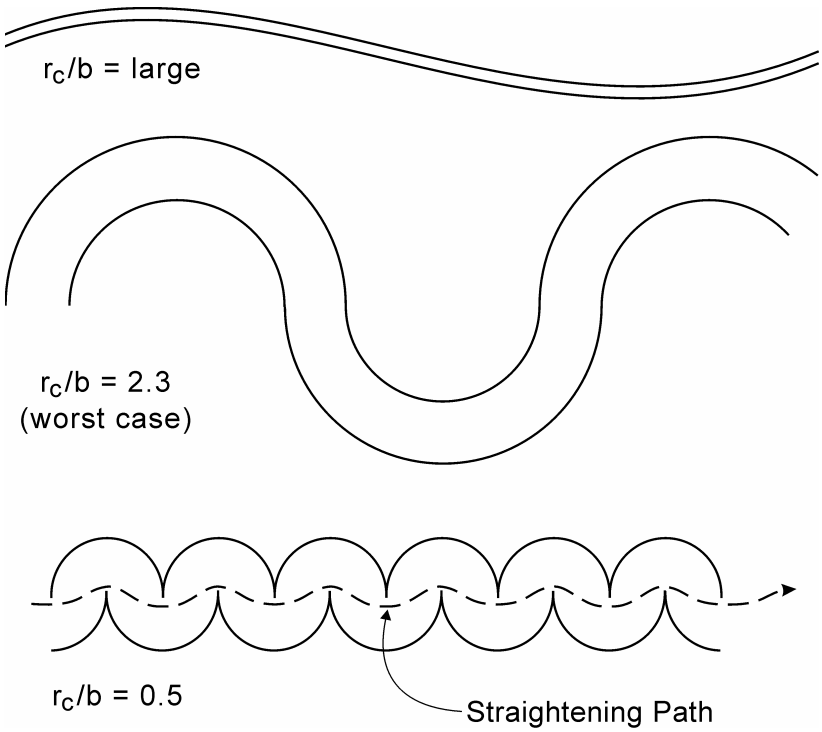

Figure 10 – Rivers with Different Relative Radius of Curvature

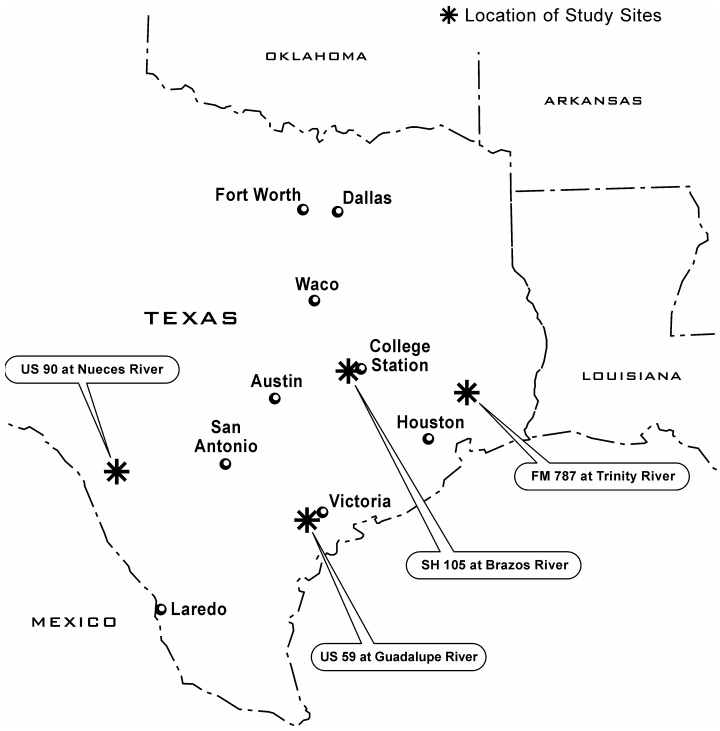

Figure 11 – Map Showing the Location of the Case Histories

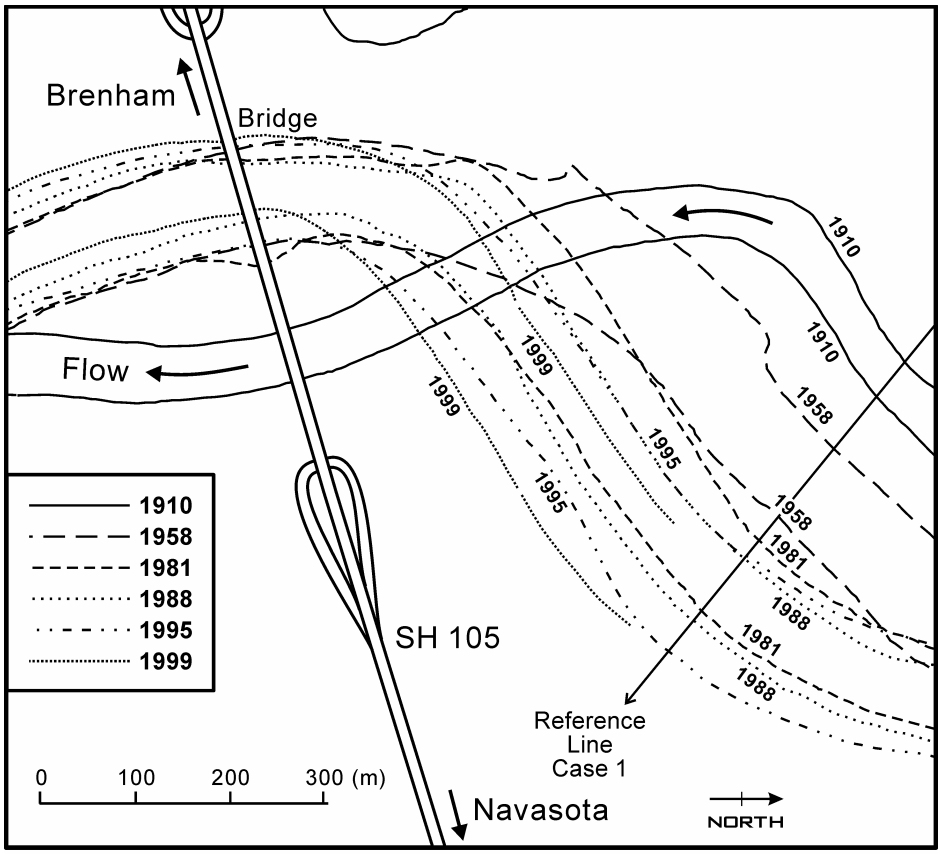

Figure 12 – Close up of the Meander Migration for the Brazos River at SH105

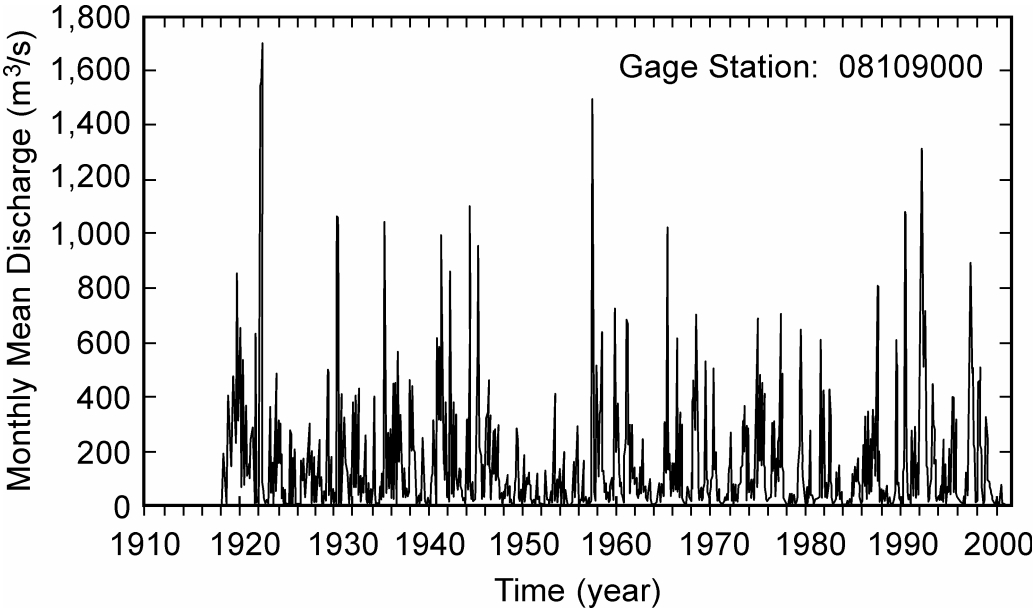

Figure 13 – Mean Monthly Discharge versus Time for the Brazos River at SH 105

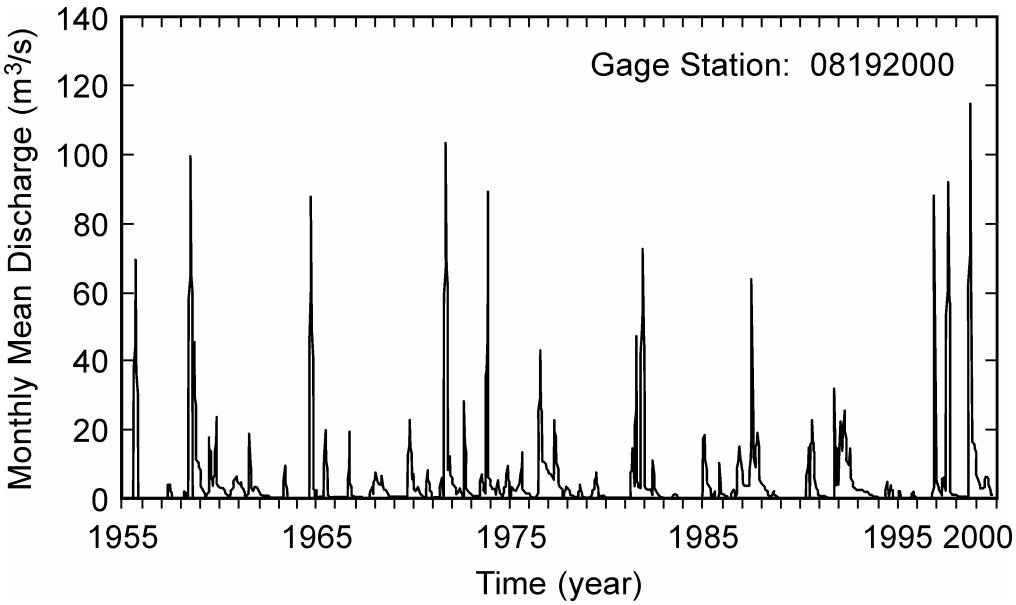

Figure 14 - Mean Monthly Discharge versus Time for the Nueces River at US 90

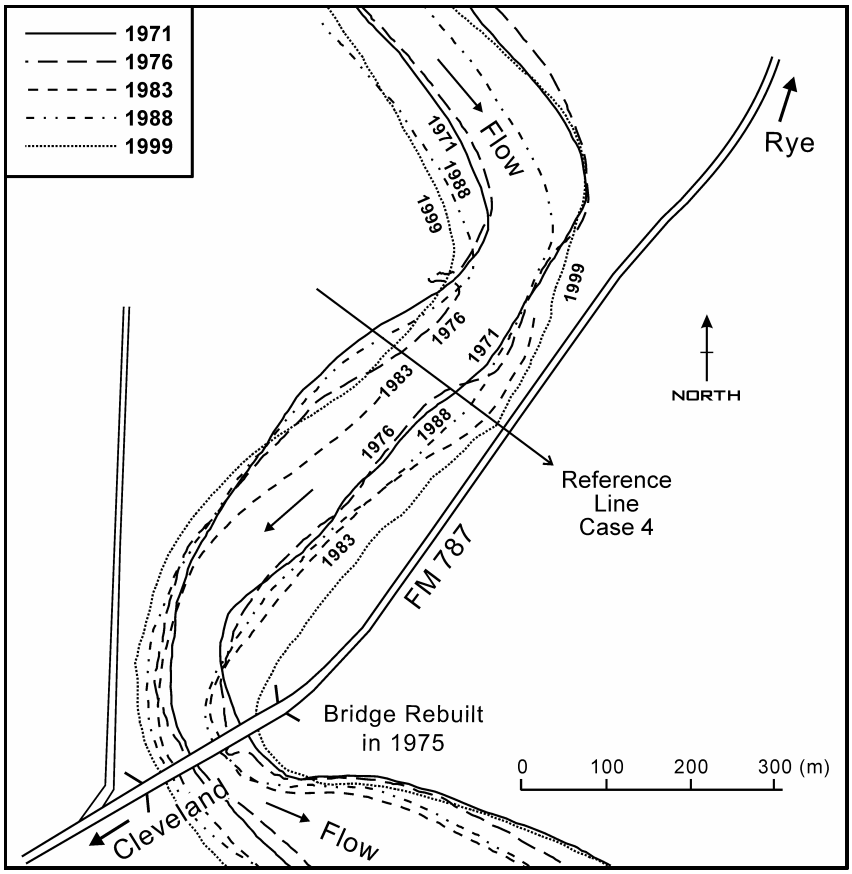

Figure 15 - Meander Migration for the Trinity River at FM 787

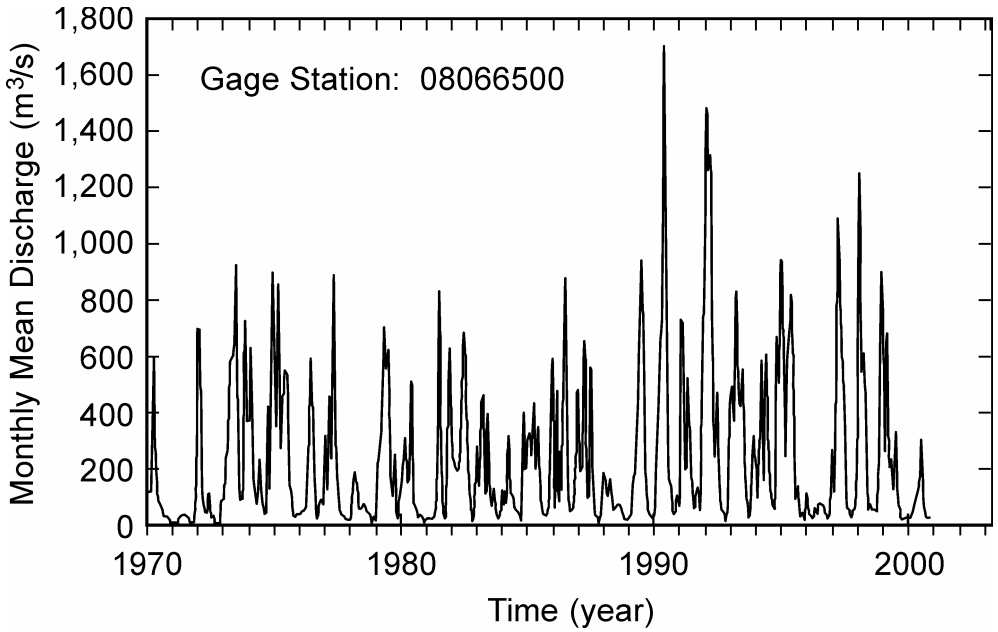

Figure 16 - Mean Monthly Discharge versus Time for the Trinity River at FM 787

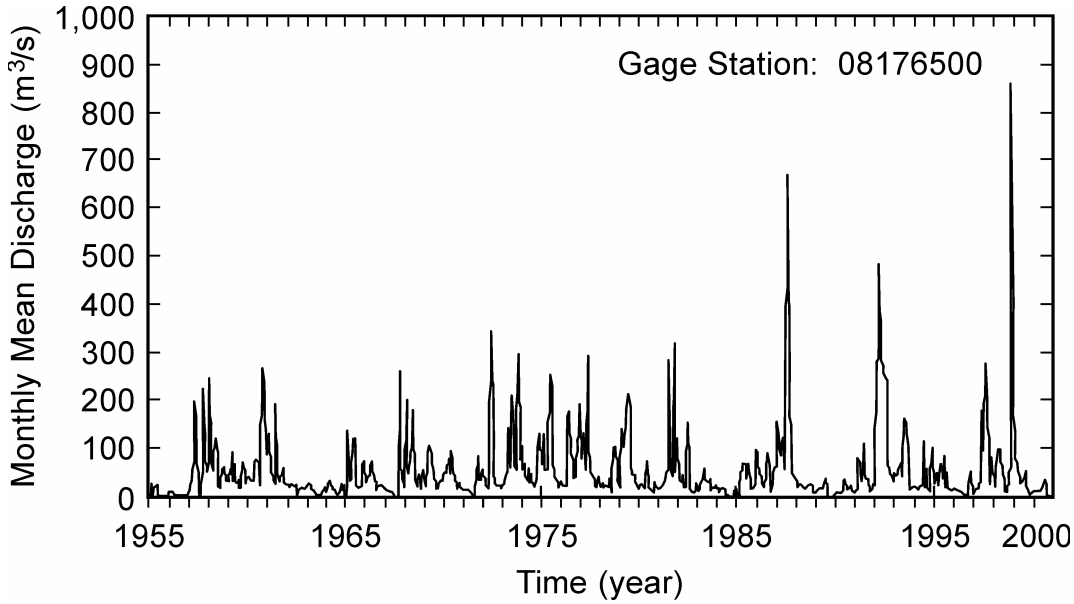

Figure 17 - Mean Monthly Discharge versus Time for the Guadalupe River at US 59

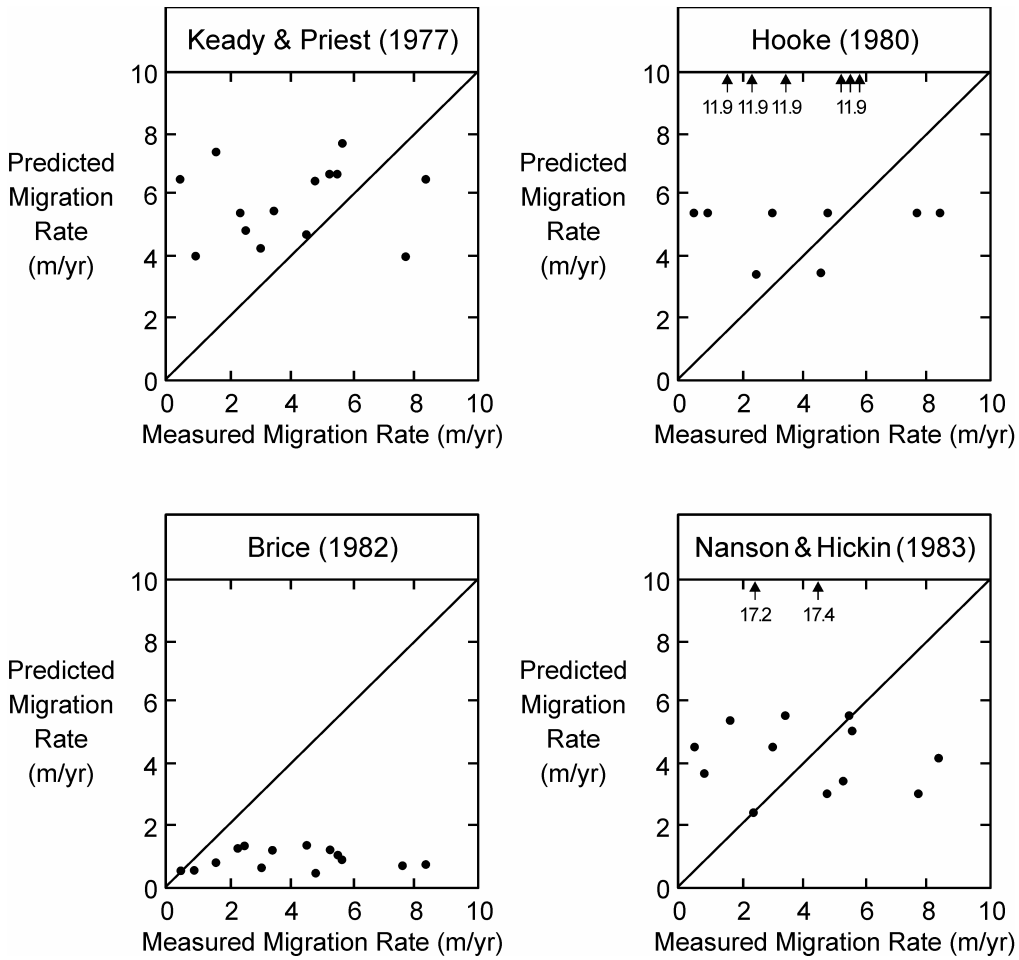

Figure 18 – Predicted versus Measured Migration Parameters for the Time-Sequence Maps and Extrapolation Method

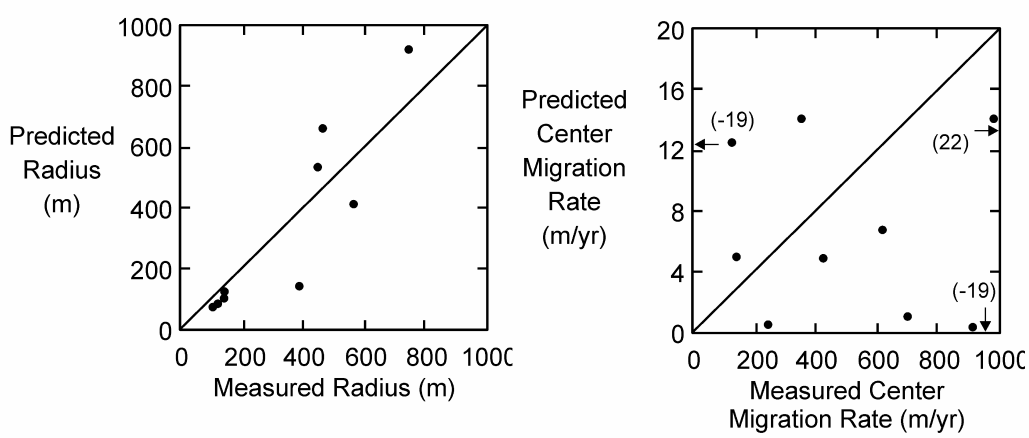

Figure 19 - Predicted versus Measured Migration Rates for the Empirical Methods

Collapse and Erosion of Khon Kaen Loess with Treatment Option

By

P. Punrattanasin[1], A. Subjarassang[2], O. Kusakabe[3], T. Nishimura[4]

ABSTRACT

Khon Kaen loess is one of the problematic soils in the Northeastern region of Thailand. The soil has a potential to collapse, which has been caused by wetting. This study reports the characteristics of Khon Kaen loess under saturated and unsaturated conditions. From laboratory testing results, shear strength of Khon Kaen loess increases linearly with matric suction at low suction pressure and remains constant beyond the residual suction. Its relationship gives ϕ^b parameter of 32 degrees. Since Khon Kaen loess exists in abundance and covers a very large area of the region, this study aims to investigate the suitability of this soil as a material for road construction. A series of trial slope embankments were constructed in order to evaluate the behavior of the loess. The field observations showed that the testing embankment was stable under traffic loading and erosion of soil occurred by water infiltration from ground surface. The trial embankment reinforced with geosynthetic materials was also tested. The results showed the effectiveness of geosynthetic material as one of the remedial measures.

1. INTRODUTION

Loess is known in civil engineering as one of the major problem soils because of its collapse and sudden decrease in volume of voids which has caused severe settlement problems for many structures founded on it. The loess terrain exists in abundance in the Northeastern region of Thailand. The loess deposits can be classified into two, Red Loess and Yellow Loess (Phien-wej et al., 1992). Lithologically and mineralogically, the two units are similar but different in oxidation states causing color difference. The thickness ranges from a few meters to more than 6 m. Thick loess deposits are found in high elevation areas of the region including Khon Kaen, which is the economic center of the upper region (Fig.1). Firstly, the soil was considered as a good bearing layer. Sarujikumjonwattana et al. (1987) found that wetting of the soil by leaking water from drains and sewers caused the severe settlement and damage of the irrigation structures and low-rise buildings.

[1] Lecturer, Dept. of Civil Engineering, Fact. of Engineering, Khon Kaen University, Thailand
[2] Former Graduate Student, Dept. of Civil Engineering, Tokyo Institute of Technology, Tokyo, Japan
[3] Professor, Dept. of Civil Engineering, Tokyo Institute of Technology, Tokyo, Japan
[4] Associate Professor, Dept. of Civil Engineering, Ashikaga Institute of Technology, Tochigi, Japan

In this study, the properties of Khon Kaen loess are presented under saturated and unsaturated conditions. Trial embankments are also tested. The objectives of this test were to provide a case record and to evaluate the potential of the soil as a material for road construction.

2. SOIL PROPERTIES

A series of laboratory tests were carried out on red loess unit. The samples were from outcrop found in Khon Kaen University, where several foundation problems associated with this soil had occurred. Undisturbed samples of the soil were taken by means of block sampling. The samples were carefully trimmed and waxed from the bottom of excavated pits (Fig.2). The tests were initially conducted on the soil under in situ water content, after which the soil was wetted by water infiltration from the ground surface. In the laboratory tests, engineering properties of the loess were investigated through index tests, the direct shear test, the oedometer test and the saturated and unsaturated triaxial compression test.

2.1 Index properties

Index properties of Khon Kaen loess are summarized in Table 1. The soil is silty fine sand (SM). The loess consists of 65% sand, 30% silt and 5% clay (Fig.3). Udomchoke (1991) studied the microstructure of this soil and found that Khon Kaen loess consists of well-sorted fine sand grains but poorly sorted silt and clay particles. Sand grains have smooth, sub-rounded surfaces indicating eolian origin. The skeleton grains are held together by means of cementation of clay matrice in the form of clay bridge bonds. Most of the clay content, which is predominantly kaolinite, is present in the form of a surface coating on coarse grains.

2.2 Direct shear test

The direct shear test is the simplest, the oldest and the most straightforward procedure to measure the short term shear strength of soil in terms of total stresses. To obtain the strength parameters c and ϕ of the soil, the direct shear tests were performed with natural undisturbed samples and pre-wetted samples with various depths of soil layers. In the experiment, the direct shear tests were performed under unconsolidated undrained condition. Figure 4 shows the strength parameters c and ϕ with depth.

2.3 Compressibility of soil

The oedometer test is used for the determination of the consolidation characteristics of soils of low permeability. Analysis of data from tests is presented as a standard conventional procedure to explain the compressibility of soils. However, the loess is naturally unsaturated. In the test, the unsaturated undisturbed and remolded samples were subjected to the axial load in the oedometer box without the swelling process. Figure 5 shows the comparison of the compressibility characteristic between undisturbed and remolded sample. From the curve of undisturbed sample, the compression index is 0.0135 with maximum past pressure of 1334 kPa. The compression index of remolded sample is only half of the undisturbed sample. In the section of unsaturated soil, the results from modified oedometer test with soil suction control will be shown.

2.4 Triaxial compression test

Series of triaxial compression tests were carried out to obtain strength parameters of the loess under various consolidation pressures. Specimens prepared from cylindrical samples 50 mm in diameter were used. The tests conducted in this study were the consolidated-undrained test. Figure 6 shows the triaxial test setup and the strength envelop of the three tests. From the experimental results, the Mohr-Culomb shear failure envelope gives a c' value of approximately zero and ϕ' of 38 degrees.

2.5 Unsaturated soils

A theoretical framework for unsaturated soil mechanics widely accepted in geotechnical engineering is the concept of stress state variables introduced by Fredlund and Morgenstern (1977). Unsaturated soil behaviors could be explained in terms of two independent stress state variables (i.e., net normal stress, $(\sigma - u_a)$ and matric suction, $(u_a - u_w)$). The shear strength equation for unsaturated soils proposed by Fredlund et al. (1978) has been accepted widely in geotechnical engineering and is given as,

$$\tau = c' + (\sigma - u_a)\tan\phi' + (u_a - u_w)\tan\phi^b \qquad (1)$$

where, τ = shear strength, c' = effective cohesion intercept, σ = total normal vertical stress, ϕ' = effective angle of internal friction with respect to net normal stress, u_a = pore-air pressure, u_w = pore-water pressure, ϕ^b = angle of internal friction with respect soil suction.

2.6 Soil-Water Characteristic Curve

The SWCC can be described as a measure of the water –holding capacity (i.e. storage capacity) of the soil, when subjected to various values of suction. Changes in soil, water and air phases take on different forms and influence the engineering behavior of unsaturated soils. The relationship between amount of soil water and soil suction was evaluated using a pressure plate apparatus and vapor equilibrium technique (Fig.7). The soil-water characteristic curve for Khon Kean loess was tested from a saturated condition to a totally dry condition (i.e. for soil suctions ranging from 0 to 1,000,000 kPa) and was shown in Fig.8. The air-entry value can be obtained by extending the constant slope portion of the soil-water characteristic curve to intersect the suction axis at saturated condition. Evaluated air-entry value for the soil is 27 kPa. When matric suction exceeds the air-entry value, desaturation starts in the liquid phase. The soil dries rapidly with increasing suction.

2.7 Triaxial for unsaturated soil

Figure 9 shows the schematic diagram of modified triaxial apparatus for unsaturated soil. A series of unconsolidated-undrained triaxial tests were carried out in order to find the ϕ^b value. The shear strength under constant net normal stress and varying matric suction are summarized in Table 2. Figure 10 (a) shows the relationship between shear strength and matric suction up to 100 kPa. An extended Mohr-Colomb equation (Eq.1) is used to interpret the test results. When matric suction is zero (saturated condition), the

shear strength is calculated as 820 kPa with c' equal to zero, ϕ^b equals to 32 degrees under a constant net normal stress of 200 kPa. The shear strength data of Khon Kaen loess subjected to high suctions are presented in Fig.10 (b). A constant net normal stress of 200 kPa was applied with various total suctions. The suctions applied were always larger than the residual suction of 500 kPa. Figure 10 (b) shows that shear strength of Khon Kaen loess remains constant beyond residual soil suction.

2.8 Modified oedometer test

The relationship between the volume change and loading conditions of unsaturated soil can be illustrated by the modified oedometer test result. The test aims to obtain the volume change characteristic of the soil with different matric suctions compared to the saturated condition. The modified oedometer apparatus is schematically shown in Fig. 11. The specimen is subjected to air pressure through a top cap. The burette connected with high air entry ceramic disk at the bottom base can measure the drained water. The $e - \log p$ curve is shown in Fig. 12. The curves show that the deformation characteristic of the unsaturated soil is flatter than that of the saturated soil. Under the same pressure, the settlement of saturated soil is larger than the unsaturated one.

3. TRIAL TEST EMBANKMENT

Evaluation of slope instability is an inter-disciplinary effort requiring contributions from engineering geology and soil mechanics. The main objectives of the slope analysis of Khon Kaen loess embankment are to assess the stability of slope under given conditions and to assess the potential of the soil as a material for road construction. Natural slopes in soil are of interest to geotechnical engineers. The soil composing any slope has a natural tendency to collapse under the influence of gravitational and other forces. Figure 13 shows agricultural pond in Khon Kean University before and after raining. The collapse and erosion phenomenon of the loess are evident in Fig 13 (b).

3.1 Site conditions and design of trial embankment

The test site is located in Khon Kaen University. The construction area chosen was flat for the most part and near the borrow pits of fill material. The design of the test embankment configuration was based on the typical section from Department of Highway, Thailand. The final layout of the fill and the cross section of the embankment are shown in Figs.14 and 15, respectively. The test area is divided into two parts to simulate the general traffic load of 2 t/m^2 and to simulate the rainy season in the Northeastern region of Thailand as shown in Fig. 16 and Fig. 17. To facilitate monitoring of the construction and to observe the performance of the embankment, field instruments were installed. The instrument layout was selected based on the results of the limit equilibrium analysis and the total number of instruments. The instrumentation of unreinforced slope consists of piezometers, total pressure cells and inclinometer casings. Pneumatic piezometers were installed to monitor the positive and negative pore pressures. The pneumatic-type total pressure cells were installed to measure the total pressure imposed by the fill on the bottom of the embankment. The applied total stresses measured from the monitoring agreed well with those deduced based on the thickness of fill and the measured unit weight of the fill. Horizontal movement of the ground was monitored by measuring the displacement from inclinometer.

3.2 Embankment construction

The Khon Kaen loess was used as a fill material. The fill unit weight, as determined by in situ tests, averaged 20.2 kN/m^3. The natural water content of the fill was 6%. A series of soil layers were constructed with a thickness of 0.5 m. Field density measurements on the layers indicated an average unit weight of 18.5 kN/m^3. After reaching a designed thickness of 2.5 m, the first half of the trial embankment was statically loaded with dead weight of 2 t/m^2. The staged loading is 0.333 t/m^2 in steps. The second half of the embankment was soaked with water to simulate flood after a heavy rainfall.

3.3 Performance of trial embankment and results

A number of instruments were installed to provide warning of any potential failure. These instruments which recorded minute movements were monitored during and post construction. The variations of horizontal displacement with depths obtained from inclinometers are shown in Fig. 18 (a) and 18 (b). At the end of simulation processes, maximum horizontal displacement of about 1 mm and 8 mm were found from loading area and soaked area, respectively.

The embankment was found to stand free at a slope of about 53° . The displacement profile at 2.5 m embankment thickness did not indicate any failure zone. The soils in the soaked area suddenly dropped after being soaked for 20 days as caused by the water infiltration (Fig.19). The erosion continued to occur as more water was added. The variations of excess pore water pressure with time for different pneumatic piezometers placed below the fill were recorded (Fig. 20). The excess pore pressures in all the piezometers were small up to the end of construction. A small increase in the excess pore pressure is observed in response to the infiltration of water from the top surface of the embankment. The excess pore water pressure responses indicated by piezometer 2 and 3 were very similar even though the piezometers were placed at different depths.

3.4 Treatment option

To enable the redesign of failed slope, the planning and design of preventive and remedial measures were necessary. The second phase of trial embankment was constructed. A single layer of geogrid and bi-dimensional geojute were used for the reinforcement. The random structures of the geojute hinder particle migration, interlocks with the grass roots while the geogrid is capable of supporting long term tensile loads. Figure 21 shows the stable reinforced embankment. Details of the instrumentation, construction and performance of the reinforced embankment will be provided in a subsequent paper.

4. CONCLUSIONS

The characteristics of Khon Kaen loess have been investigated by both laboratory and field testing. The results of the laboratory tests on undisturbed and remolded samples described in this paper are reported. Strength of the loess decreases as a result of wetting. The research primarily focused on the strength characteristic of the unsaturated soil over a wide range of soil suctions. Suctions were applied using pressure plate apparatus and vapor equilibrium technique. The compacted loess was desaturated to the residual state of unsaturation through the use of chemical salt solutions. The testing results show that the air-entry value of the soil is about 27 kPa. The SWCC also gives that the residual

water content and residual suction are 5% and 500 kPa, respectively. The unsaturated triaxial results showed that shear strength of soil increases with matric suction at low suction pressure. Its relationship between shear strength and soil suction in the transition stage gives the ϕ^b of 32 degrees. After the suction exceeds the residual soil suction, the shear strength remains constant (i.e., horizontal failure envelope with respect to soil suction). Using Khon Kaen loess as a material for road construction showed that erosion by water infiltration will cause the soil failure of fill embankment. Geosynthetics material used as a reinforcement is one of the alternatives to stabilize the embankment.

ACKNOWLEDGEMENT

The research was developed under the cooperation between Khon Kean University, Thailand, Tokyo Institute of Technology and Asikaga Institute of Technology, Japan. The construction and monitoring of the test embankments were funded by the Department of Civil Engineering, Faculty of Engineering, Khon Kaen University and the Hitachi Foundation, Japan. The authors wish to acknowledge the assistance of Dr.Watcharin Gasaluck, Dr.Warakorn Mai-riang, Dr.Noppadol Phien-wej and Mr.Nattapong Kowittayanant. The geosynthetic materials were supplied by Cofra (Thailand) Ltd.

REFERENCES

1. Fredlund, D.G. and Morgenstern, N.R., 1977. "Stress state variables for unsaturated soils", *ASCE Journal of Geotechnical Engineering*, Vol.103, pp.447-466.
2. Fredlund, D.G., Morgenstern, N.R., and Widger, R.A., 1978. "The shear strength of unsaturated soils", *Canadian Geotechnical Journal*, Vol.15, pp.313-321.
3. Phien-wej, N., Pientong, T., Balasubramaniam, A.S., 1992. "Collapse and strength characteristics of loess in Thailand", *Engineering Geology*, Vol.32, pp.59-72.
4. Sarujikumjonwattana, P., Malapet, M., and Sertwicha, S., 1987. "Settlement of spread footings in Khon Kaen University Campus caused by moisture increase at constant load", Khon Kean Univ.Publ., Thailand.
5. Udomchoke, V., 1991. "Origin and engineering characteristic of problem soils in Khorat Basin, Northeastern Thailand", D.Tech.Diss, Asian Institute of Technology, Bangkok, Thailand.

Table 1 – Index properties of Khon Kaen loess

Property	Khon Kaen Loess
Specific gravity	2.60
Natural dry unit weight (kN/m^3)	15.3
Natural water content during rainy season (%)	8-12
Liquid limit (%)	16.0
Plastic limit (%)	13.0
Plasticity index	3.0
Soil classification (USCS)	SM
Optimum moisture content (%)	9.7
Maximum dry density (kN/m^3)	21.1
Permeability coefficient (cm/s)	2.80 x 10^{-6}

Table 2 – Summary of stress conditions during unsaturated triaxial tests

Net normal stress (kPa)	Soil suction (kPa)	Shear strength (kPa)
200	0	820
200	40	837
200	64	870
200	69	867
200	100	880
200	9,800	1,069
200	83,400	1,349
200	296,000	1,460

Fig.1 – Areas of loess deposits (stippled area) in Thailand (after Phien-wej et al. 1992)

(a) Block sample

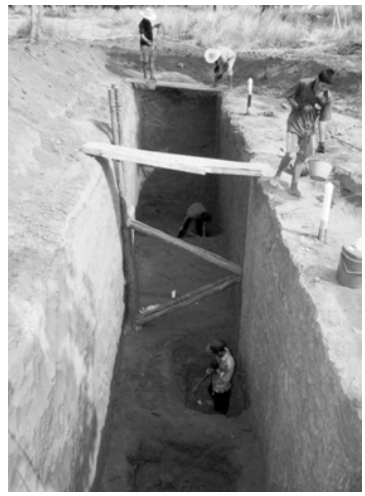

(b) Excavated pit

Fig. 2 – General view of a test pit at Khon Kaen University

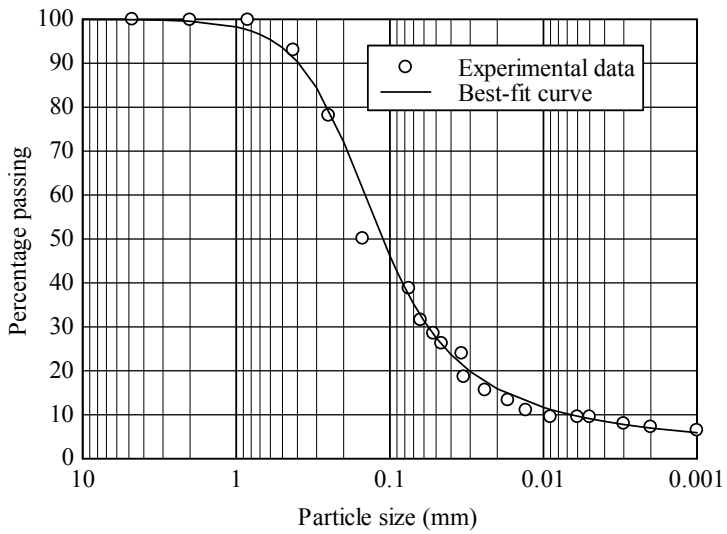

Fig. 3 – Particle size distribution of Khon Kaen loess

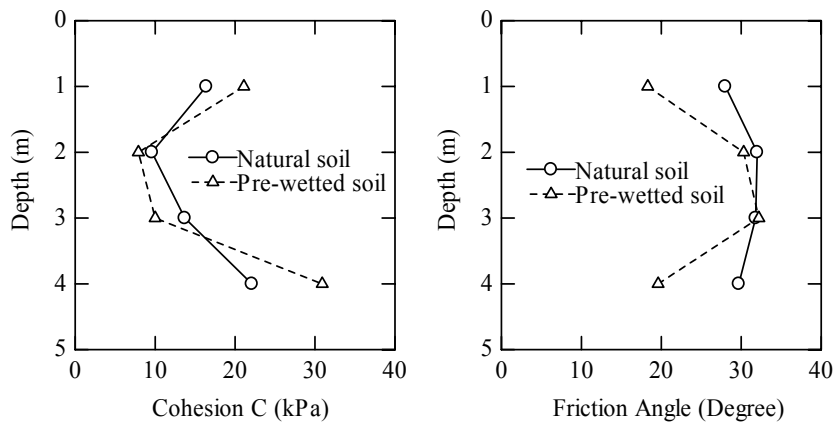

Fig. 4 – Summary of direct shear tests of undisturbed sample

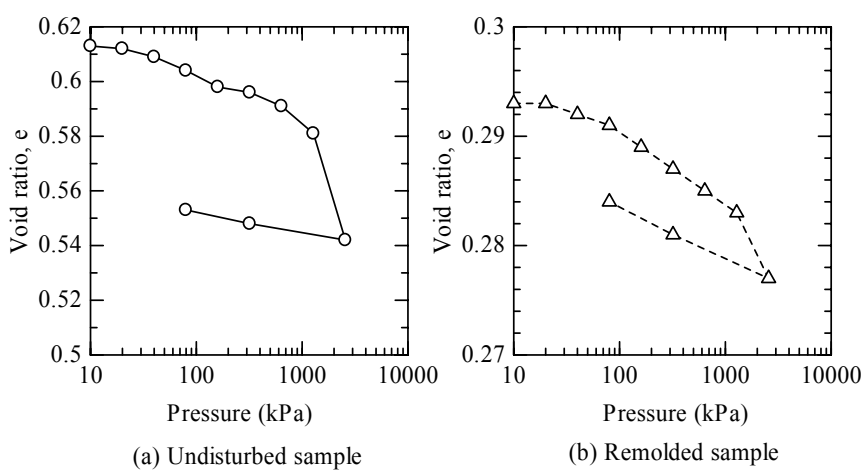

Fig. 5 – Oedometer test results

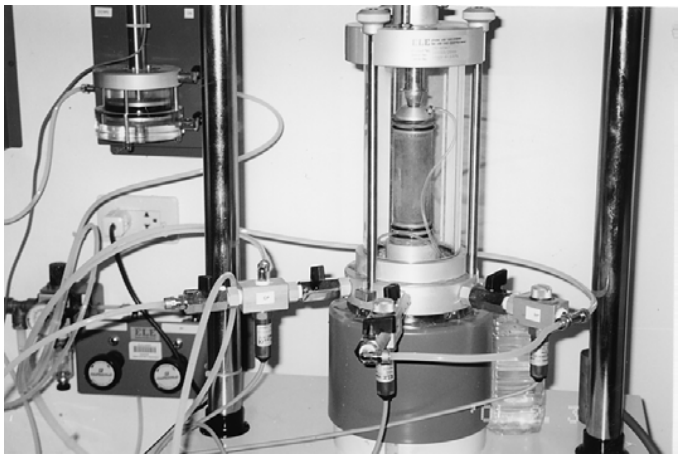

(a) Test setup

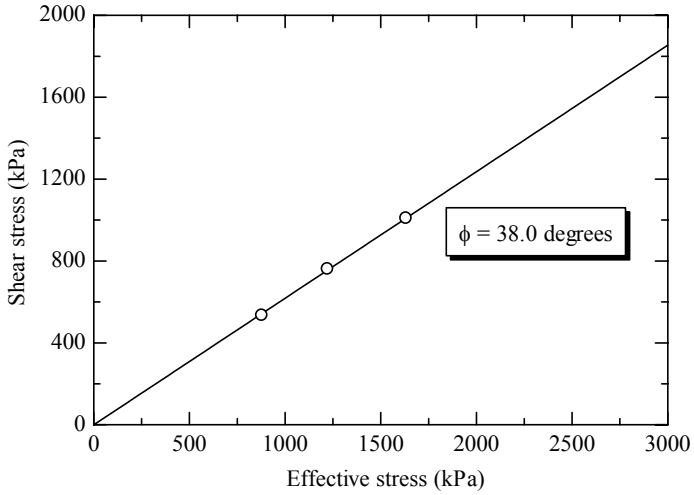

(b) Test result

Fig. 6 – Triaxial compression test results from undisturbed samples

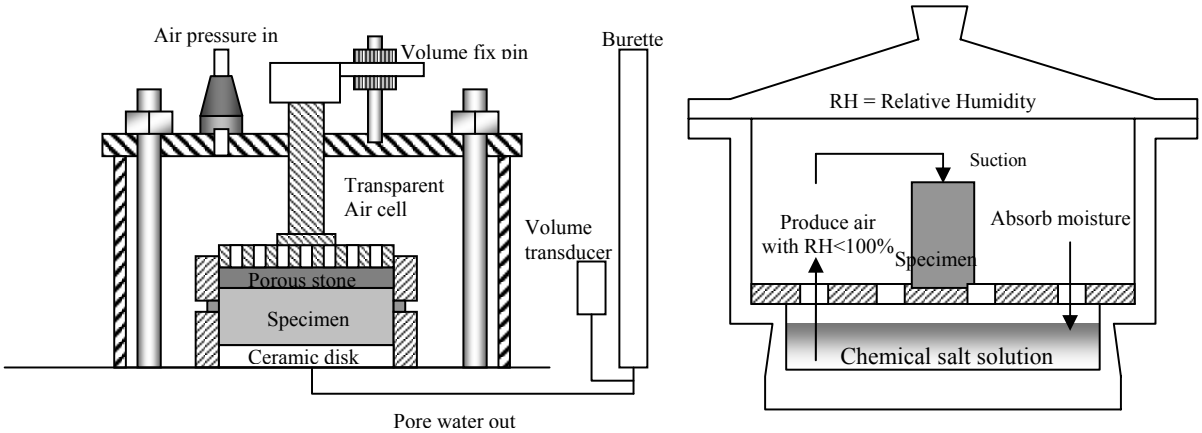

(a) Pressure plate apparatus (b) Vapor equilibrium technnique

Fig. 7 - Apparatus for SWCC test

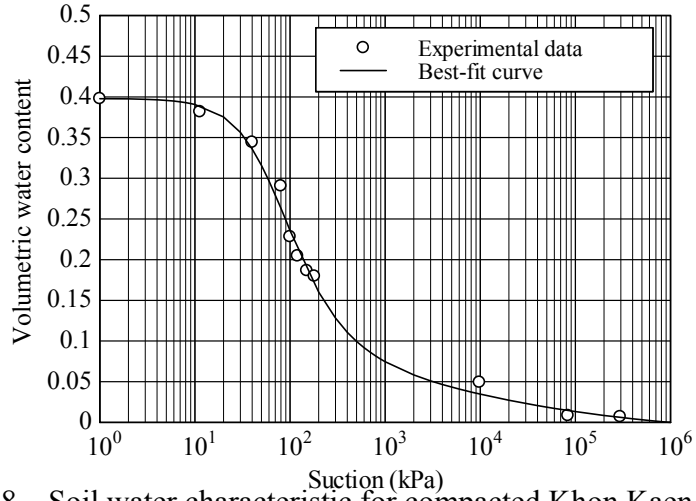

Fig. 8 – Soil water characteristic for compacted Khon Kaen loess

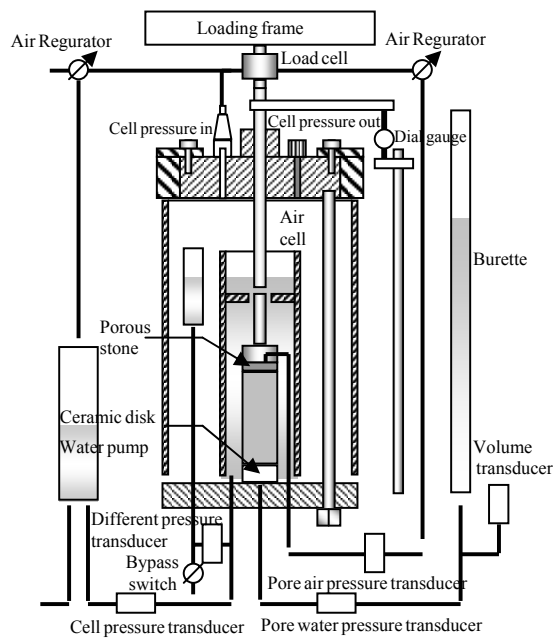

Fig. 9 - Schematic of modified triaxial apparatus for unsaturated soil

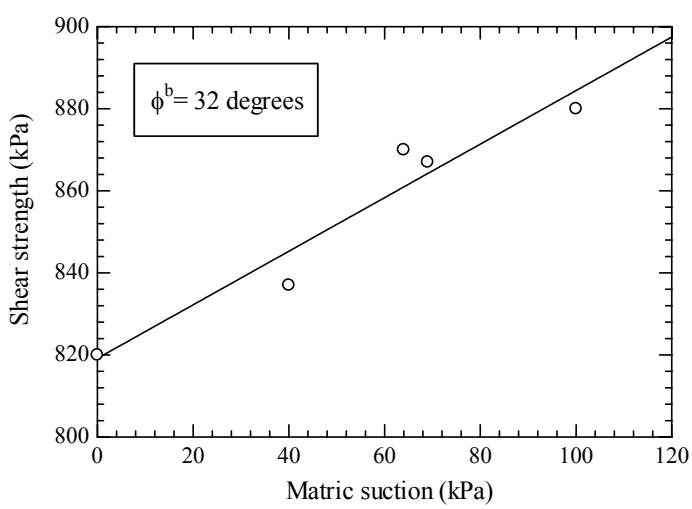

(a) Relationship between shear strength and matric suction at a constant net normal stress of 200 kPa

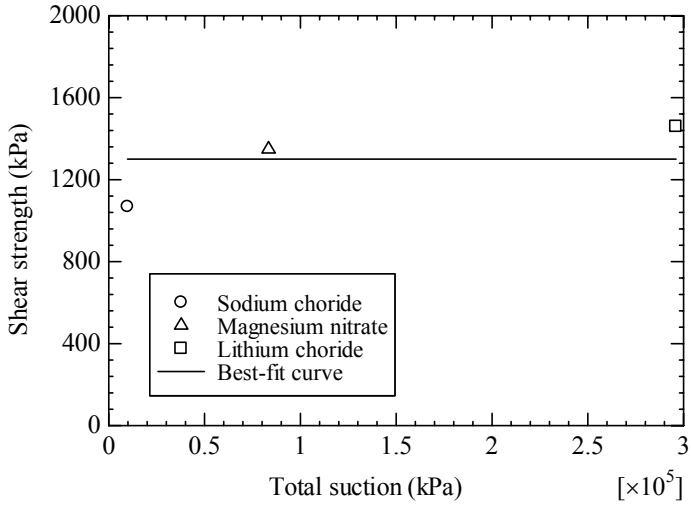

(b) Relationship between shear strength and high suction a net normal stress of 200 kPa

Fig. 10 – Shear strength versus metric suction

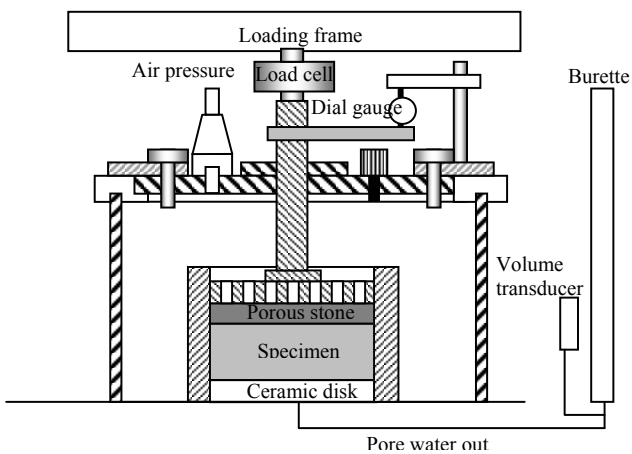

Fig. 11 – Modified oedometer apparatus for unsaturated soil

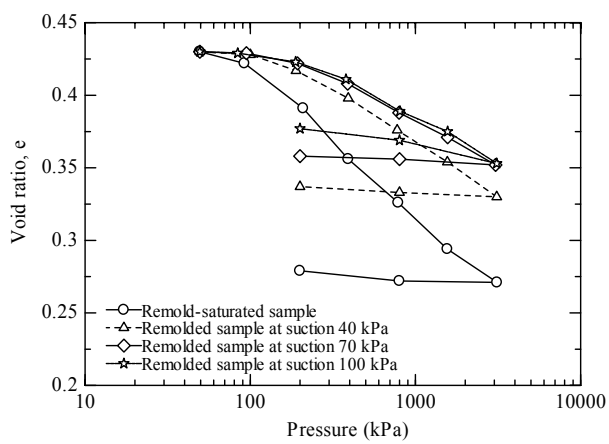

Fig.12 – Oedometer test result from remolded samples

(a) Before (b) After

Fig. 13 – Collapse and erosion of agricultural pond

Fig. 14 – General view of trial embankment

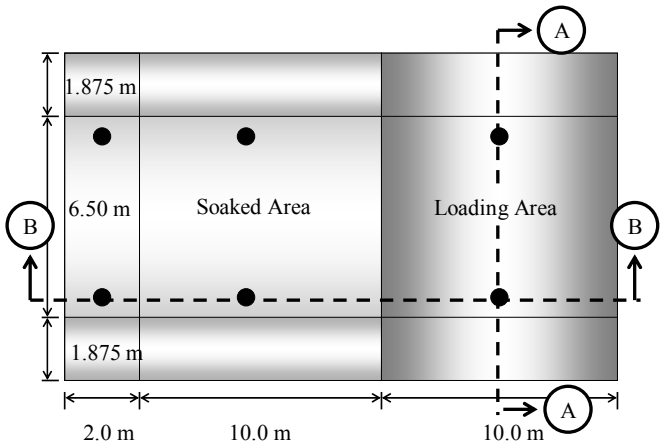

(a) Plan view

Fig. 15 – Cross section of the embankment

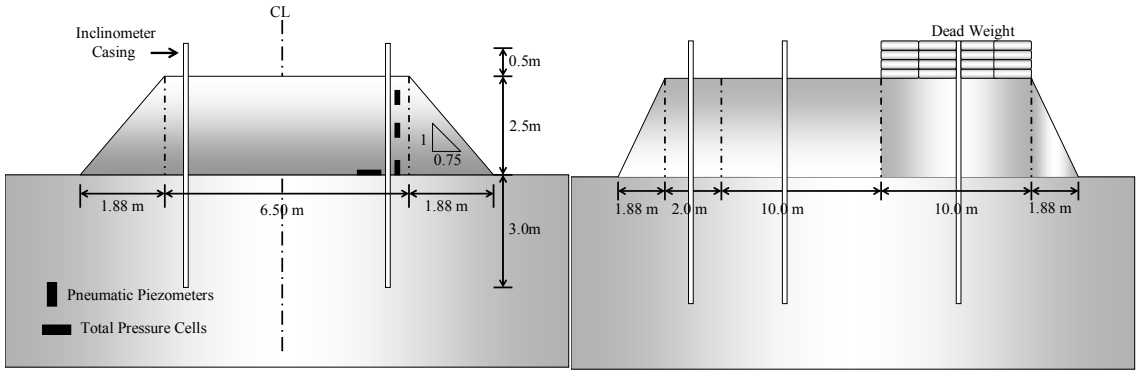

(b) Section A-A (c) Section B-B

Fig. 15 – Cross section of the embankment

Fig. 16 – Simulation of load by dead weight

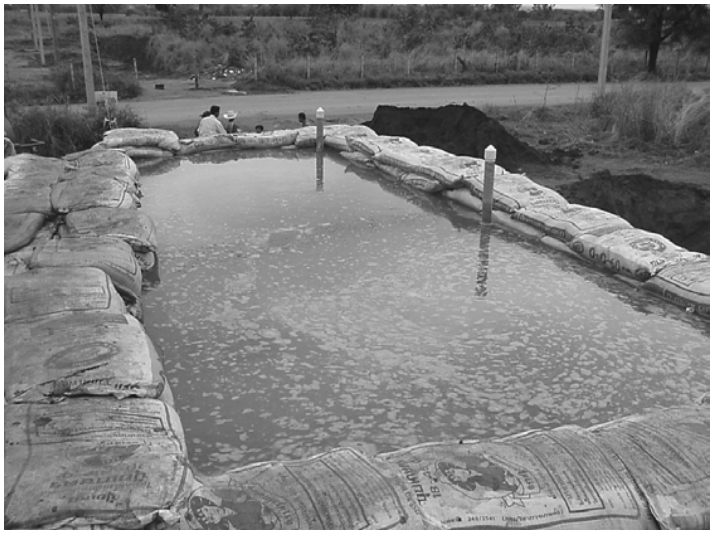

Fig. 17 – Soaking process

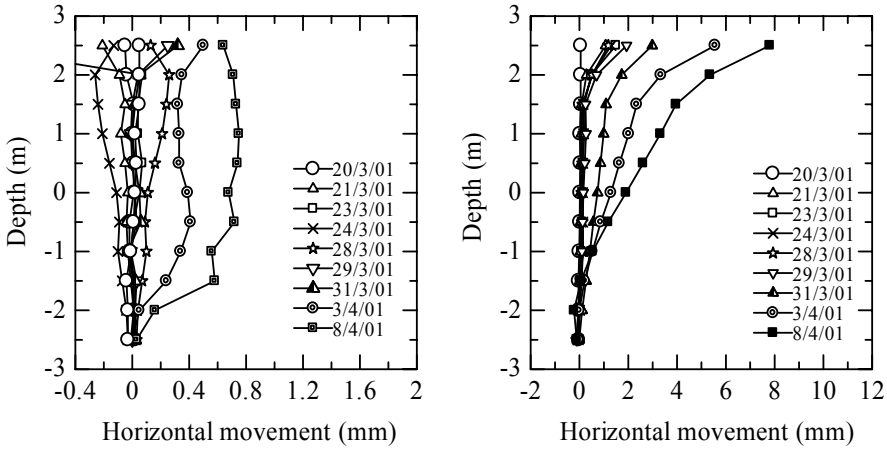

(a) Loading area (b) Soaked area

Fig.18 – Horizontal movement of the embankment

Fig. 19 – Erosion failure of trial embankment

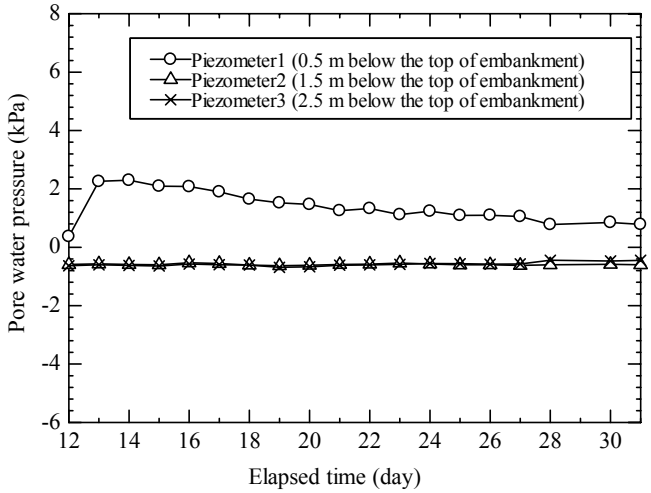

Fig. 20 – Pore pressure distribution in the embankment erosion process

Fig. 21 – Reinforced embankment

Analysis of Contraction and Abutment Scour at Two Sites in Minnesota

Chad R. Wagner and David S. Mueller
9818 Bluegrass Parkway Louisville, KY 40207
502-493-1912

Abstract

The U.S. Geological Survey (USGS) deployed the USGS bridge-scour data collection team to collect real-time scour (contraction and local) measurements at two contracted bridge openings over the Pomme de Terre River in western Minnesota during record flooding in the Minnesota River Basin in April 1997. The compiled field data were used to calibrate a step-backwater model (HEC-RAS) at each site. The total computed scour depths compared very well with total scour depths measured in the field. A much poorer agreement was found when comparing the computed abutment and contraction scour depths with the depths measured in the field. The overall comparison provided insight to the capabilities and limitations of using one-dimensional models and the available abutment and contraction scour equations to predict scour at contracted bridge openings. New methodologies must balance the desire to fully explain complex processes with the need to provide procedures that are time and cost effective to apply.

Introduction

During record flooding in the Minnesota River Basin in April 1997, the U.S. Geological Survey (USGS), in cooperation with the Federal Highway Administration (FHWA), deployed the USGS bridge-scour, data-collection team to collect real-time scour (contraction and local) measurements at contracted bridge openings. An analysis of two surveyed sites during the April 1997 flooding is presented. Both contracted bridges span the Pomme de Terre River, where an estimated 200-year discharge was calculated at the USGS Appleton streamflow-gaging station (05294000) located approximately 19 km downstream of the U.S. Route 12 bridge. The compiled field data (channel and floodplain bathymetry, water discharge, water-surface elevations, roughness, and bridge geometry) were used to calibrate a step-backwater model at each site. Abutment and contraction scour were calculated in HEC-RAS (U.S. Army Corps of Engineers, 1998) using the equations and methods outlined in HEC-18 (Richardson and Davis, 2001). The hydraulics and predicted depth of scour based on the calibrated model were compared with the field measurements.

U.S. Route 12 over the Pomme de Terre River

Site Description

U.S. Route 12 crosses the Pomme de Terre River about 20 km west of Danvers, Minn. The single-span steel-truss structure was constructed in 1933 with a maximum span length of 26.9 meters. The bridge has vertical-wall abutments with wing walls; each abutment and wing wall rests on concrete footings supported on timber piling. Neither abutment was riprapped nor was

there any other scour protection measures. A field investigation conducted by BRW, Inc. (1995) prior to the flood revealed no evidence of significant scour at the abutment face.

During the April 1997, flood both contraction and abutment scour resulted at the bridge. A large scour hole developed at the right abutment, scouring below the abutment cutoff wall resulting in failure of the fill material behind the abutment. Slumping of the embankment slope and some deformation of the approach highway were observed. Although scour measurements showed a scour hole 2 m below the footing of the left abutment, no deformation was observed near the left abutment. These conditions resulted in closure of the bridge. Because of the age and scheduled replacement of the bridge, the bridge was not repaired but was replaced with a new structure after the flood.

Discussion of Field Data

Data were collected during the flood (on 4/5/97 and 4/9/97) at U.S. Route 12 over the Pomme de Terre River. A manned boat was deployed during the initial visit on 4/5/97. The use of the manned boat and an acoustic Doppler current profiler (ADCP) allowed bathymetry and three-dimensional velocities to be measured at the bridge, and in the approach and exit sections extending about 100 m upstream and 70 m downstream. Heavy vegetation and submerged obstructions in the floodplains limited data collection to the main channel. Measurements on 4/9/97 were limited to data collected from the bridge deck. Channel bathymetry was measured along the upstream and downstream faces of the bridge, and at selected locations beneath the bridge using an echo sounder deployed on a knee-board. Velocity magnitudes and water discharge were measured using a vertical axis current meter. Water-surface elevations were measured by taping down from the top-of-curb on the bridge both upstream and downstream, near the left abutment. On 4/5/97, the water-surface elevation was 310.70 m above North American Geodetic Vertical Datum (NGVD) of 1929 at the upstream edge of the bridge, and the total discharge was 141.6 cubic meters per second (m^3/s). By 4/9/97, the water-surface had risen to an elevation of 311.5 m, and the discharge had increased to 162.8 m^3/s.

The direction of flow through the bridge was controlled by the configuration of the upstream floodplains. The channel upstream of the bridge was straight but the left floodplain was much wider and carried considerably more flow than the right floodplain. A sketch of spot streambed elevations and the flow direction on 4/9/97, which shows the severe skew of the flow to the bridge opening is shown in Figure 1.

An elevation of 307.9 m was used as the contraction scour reference surface from analysis of pre-flood cross-sections throughout the study reach. A summary of the contraction-scour data is shown in table 1. The profile of the contracted section on 4/5/97 was measured under the bridge from data collected by an ADCP. The maximum erosion of the streambed was 2.3 m from the defined reference surface; however, when the entire streambed below the bridge was averaged the depth of contraction scour was only 0.9 m. The hydraulic data presented for 4/5/97, also were collected with the ADCP. Measurements made with a sounding weight on 4/9/97, were collected during the discharge measurement along the upstream face of the bridge, and no approach data are available. An echo sounder mounted on a knee-board also was used to make measurements

on 4/9/97. The board was floated from upstream to downstream under the bridge; the measurements reflect the depths at the upstream or downstream face of the bridge.

The reference surface used to determine the depth of abutment scour was the concurrent ambient bed; therefore, the depth of abutment scour reported is additional local scour below the depth of contraction scour (table 2). An ADCP was used for data collection on 4/5/97, using a weighted-average of all four beams as the measured depth. Because a weighted-average was used, it is possible that the local abutment scour was not accurately measured, and no values are reported.

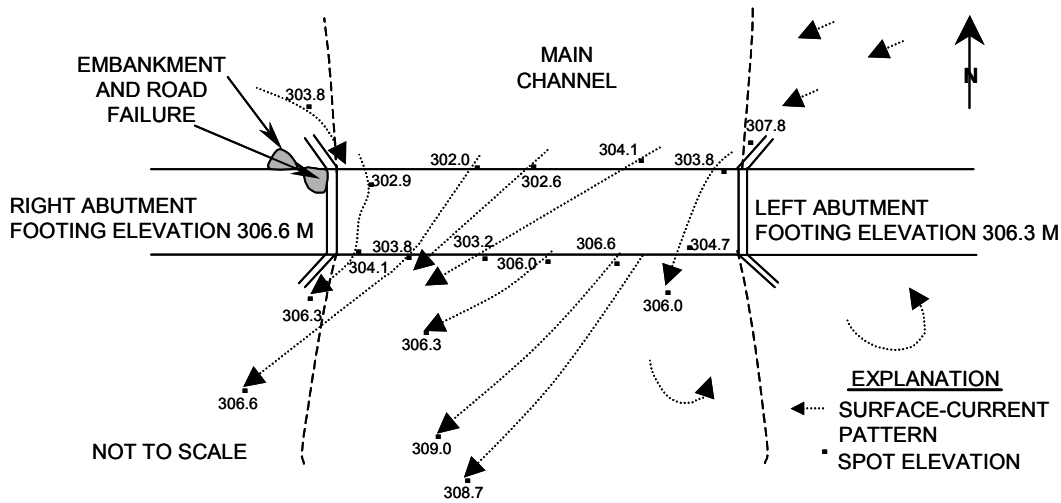

Figure 1. Sketch of U.S. Route 12 over Pomme de Terre River, Minnesota showing spot elevations and surface current patterns on April 9, 1997. (Elevations are in meters referenced to NGVD of 1929.)

Table 1. Summary of contraction scour measurements at U.S. Route 12 over the Pomme de Terre River in Minnesota.

Measurement Number	Date	Location	Equipment	Scour Depth (m)	Accuracy (m)
1	4/5/97	Centerline	ADCP	0.9	0.6
2	4/9/97	Upstream	Sounding weight	3.2	0.6
3	4/9/97	Upstream	Echo sounder	3.8	0.6
4	4/9/97	Downstream	Echo sounder	1.4	0.6

	Contracted Section				Uncontracted Section			
	Width (m)	Depth (m)	Discharge (m^3/s)	Average Velocity (m/s)	Width (m)	Depth (m)	Discharge (m^3/s)	Average Velocity (m/s)
1	26.8	3.7	142	1.5	21.3	2.4	51.0	1.0
2	26.8	7.3	163	0.8	--	--	--	--
3	26.8	7.2	163	0.9	--	--	--	--
4	26.8	5.3	163	1.2	--	--	--	--

The cross sections measured on 4/9/97 all showed a similar pattern with abutment scour holes on each side and a sharp mound in between the scour holes but skewed toward the left abutment (figure 2). It appears that the abutment scour holes may have overlapped. The highest elevation in the center of the cross section was subtracted from the reference surface to obtain the depth of contraction scour. The abutment scour was reported as the depth below the highest elevation in the center of the cross section. All velocities presented in table 2 were from the discharge measurement made along the upstream side of the bridge. Although no abutment scour was observed on 4/5/97, the velocities at the abutments were much higher (left – 1.6 m/s, and right – 1.8 m/s).

Model Calibration

The HEC-RAS model (Hydraulic Engineering Center, 1998), a one-dimensional step-backwater model, was calibrated to represent the field hydraulics as accurately as possible. The bathymetry from the April 1997 flood was used to build the calibration models for the two sets of data (4/5/97 and 4/9/97). Because bathymetry data collected on 4/9/97, was limited to the upstream and downstream edges of the bridge, the cross sections collected on 4/5/97 were used to build the HEC-RAS model for 4/9/97. The majority of the floodplain bathymetry utilized in developing the models was taken from a full valley section found in the original bridge plans and adjusted to be consistent with topographic maps. The water-surface elevation observed at the upstream bridge face rose 0.76 m between 4/5/97 and 4/9/97. The model only showed a 0.3 m change and was unable to accurately reproduce the observed change without unreasonable changes to the model input. This large hydraulic variation may be attributed to the U.S. Route 12 bridge reach being under a backwater condition because of some unidentified downstream condition.

Table 2. Summary of abutment scour data for
U.S. Route 12 over the Pomme de Terre River in Minnesota.

Date	Abutment	Location	Equipment	Scour Depth (m)	Accuracy (m)	Embankment Length (m)	Velocity At Abutment (m/s)	Depth At Abutment (m)
4/9/97	Right	Upstream	Sounding weight	2.4	0.6	307	1.3	9.1
4/9/97	Right	Upstream	Echo sounder	2.1	0.6	307	1.3	9.4
4/9/97	Right	Downstream	Echo sounder	3.4	0.6	307	1.3	8.2
4/9/97	Left	Upstream	Sounding weight	0.9	0.6	121	1.2	7.6
4/9/97	Left	Upstream	Echo sounder	0.5	0.6	121	1.2	7.6
4/9/97	Left	Downstream	Echo sounder	1.8	0.6	121	1.2	6.7

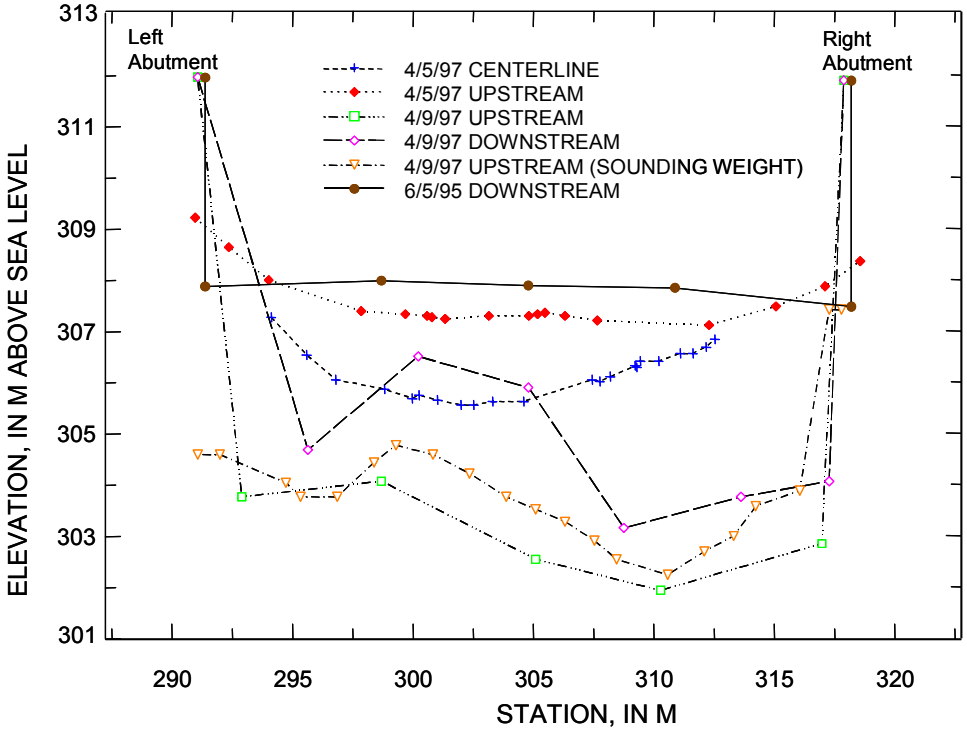

Figure 2. Measured cross sections at U.S. Route 12 over the Pomme de Terre River, Minnesota.

Large ice drifts were observed during both site visits, indicating the potential for the formation of a debris and (or) ice dam downstream of the data-collection area. Analysis of the Appleton gaging-station records was of little assistance since the gage was washed out on 4/6/97 by the failure of a small upstream dam. The water-surface elevation at the upstream side of County Route 22 located about 10 km upstream changed only 0.2 m over the same period; therefore, the model was considered calibrated despite the apparent discrepancy with the water-surface elevation observed on 4/9/97.

One of the most important factors in using one-dimensional models at contracted bridges is the model capablity to accurately represent the velocity distribution laterally across the stream and floodplain. depict how The velocity distributions depicted in figures 3 and 4 show the variation between the model and field measurements, using the geometry from 4/5/97 and 4/9/97. The distribution shown in figure 3 reveals that the measured flow was skewed toward the right abutment. HEC-RAS did not duplicate this skewed flow pattern but rather computed a relatively uniform flow distribution across the cross-section caused by the model assigning flow tubes of equal conveyance through the geometrically uniform bridge section. For the scoured channel bathymetry, HEC-RAS more accurately reproduced the observed velocity distribution (figure 4), although the model does not simulate the region of reverse flow that occurred adjacent to the left abutment. The HEC-RAS computed velocities are greater near the deeply scoured region

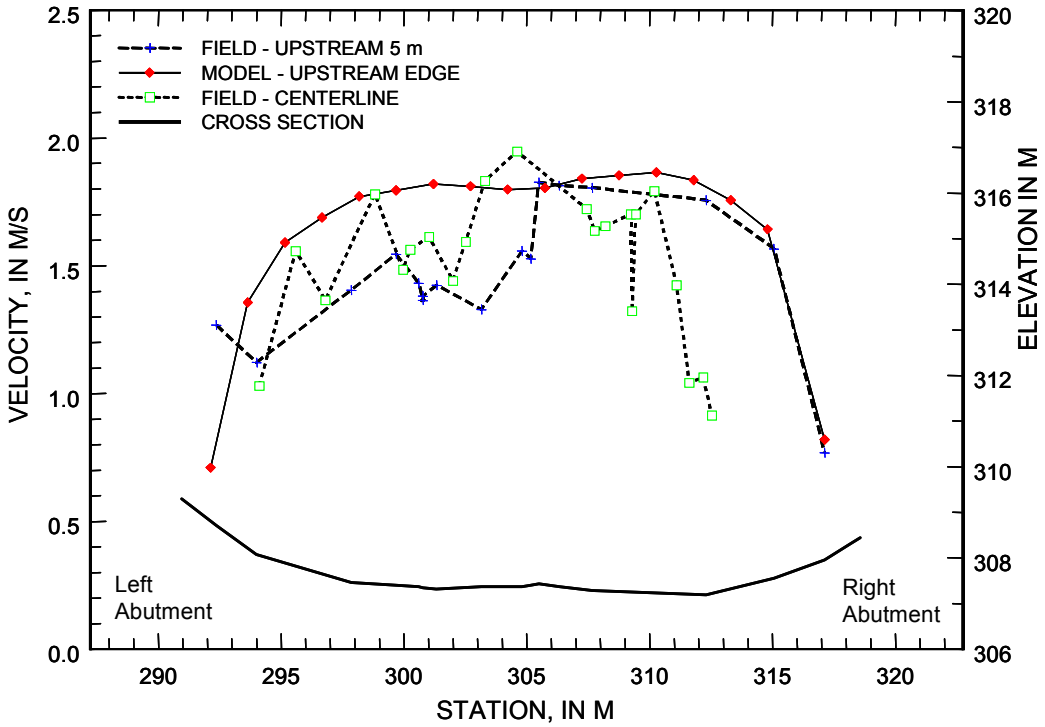

Figure 3. Comparison of observed and model velocity distributions at U.S. Route 12 over the Pomme de Terre River, Minnesota for April 5, 1997.

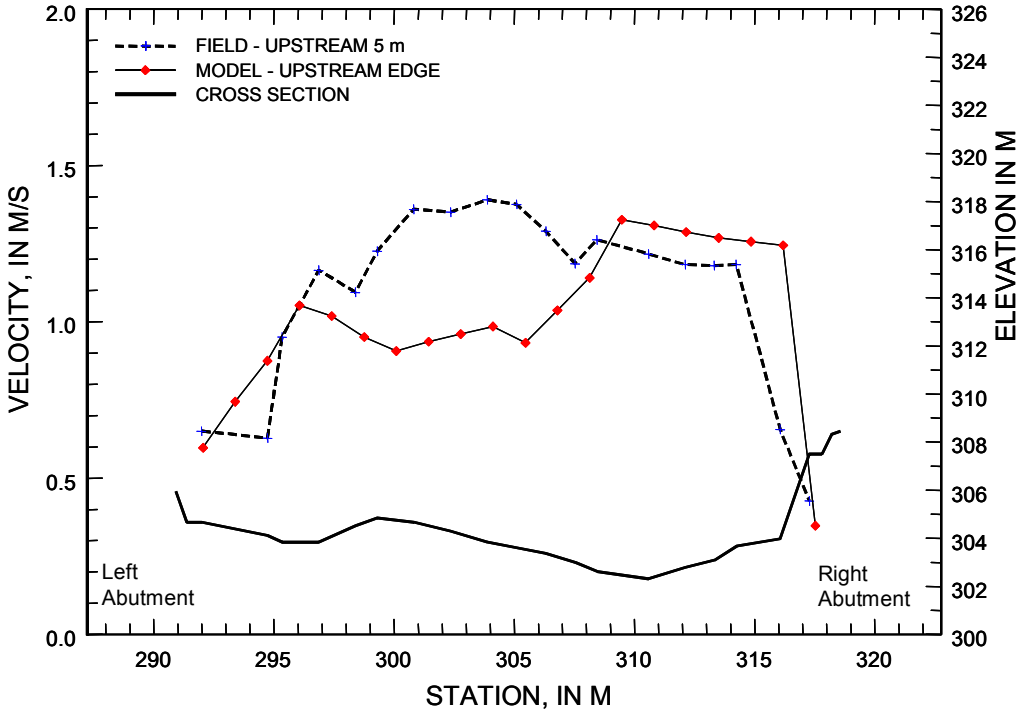

Figure 4. Comparison of observed and model velocity distributions at U.S. Route 12 over the Pomme de Terre River, Minnesota for April 9, 1997.

adjacent to the right abutment because the slope and roughness are constant across the cross section, so the conveyance becomes dependent upon the depth of flow.

Assessment of Scour Computations

The calibrated model was used to assess how accurately the scour for this flood could have been estimated. The bathymetry in the calibrated model was replaced with the original bathymetry extracted from the BRW, Inc. WSPRO model, which represented the pre-flood condition. The discharges from both 4/5/97 and 4/9/97, then were run through the HEC-RAS model with the original bathymetry to determine the hydraulic parameters required to compute bridge scour. The contraction scour was computed in HEC-RAS by allowing the model to use the default equation (live-bed or clear-water) depending upon the hydraulic conditions. A comparison of observed and model-computed contraction scour is shown in table 3.

The computed depth of contraction scour was less than the observed value for all measurements. The contraction scour observed on 4/9/97, may not be typical live-bed contraction scour because depth of contraction scour could be affected by overlapping abutment scour holes. The abutment scour was computed in HEC-RAS using both the Froehlich equation and the HIRE equation. These two equations recommended in HEC-18 (Richardson and Davis, 2001, p. 7.8). The HIRE equation is only applicable (but not required) if the embankment length to flow depth at the abutment (L/a) is greater than 25 (Richardson and Davis, 2001, p. 7.8). In this case the L/a ratio is approximately 33.5. A comparison of the observed and model-computed abutment scour is shown in table 4.
The data summarized in table 4 show the overprediction of scour that is common for abutment scour computations. Although the abutment scour equations overpredicted the local scour and the contraction scour equation underpredicted the contraction scour (table 3), when added together the total scour was estimated with reasonable accuracy and actually underpredicted the scour observed at the upstream edge of the bridge on 4/9/97. These are surprising results that should be viewed with caution because the flow skew through the bridge could not be accounted for in the one-dimensional model, and the individual components were both in error. The agreement may, therefore, be coincidental.

Swift County Route 22 over the Pomme de Terre River

Site Description

Swift County Route 22 crosses the Pomme de Terre River near Artichoke Lake, Minn., and is located 10 km upstream from the U.S. Route 12 bridge. This bridge has two piers in the main channel with the abutments set at the edge of the main channel. The spill-through slopes at the abutments were protected by riprap and formed the banks of the main channel. The bridge is located in a very sinuous reach of the river with two large meanders immediately upstream and downstream of the bridge (figure 5). The floodplains are composed of farmland and forest.

Table 3. Comparison of observed to computed contraction scour at U.S. Route 12 over the Pomme de Terre River in Minnesota.

Date	Location (Edge of Bridge)	Equation	Depth of Scour (m) Computed	Observed
4/5/97	Upstream	Live-bed	0.4	0.9
4/9/97	Upstream	Live-bed	0.6	3.8
4/9/97	Downstream	Live-bed	0.6	1.4

Table 4. Comparison of observed to computed abutment and total scour at U.S. Route12 over the Pomme de Terre River in Minnesota.

				Observed		Based on Froehlich Equation		Based on HIRE Equation	
Date	Abutment	Location (Edge of Bridge)	Equipment	Local Scour Depth (m)	Total Scour Depth (m)	Local Scour Depth (m)	Total Scour Depth (m)	Local Scour Depth (m)	Total Scour Depth (m)
4/9/97	Right	Upstream	Sounding weight	2.4	5.6	4.6	5.2	10.8	11.4
4/9/97	Right	Upstream	Echo sounder	2.1	5.9	4.6	5.2	10.8	11.4
4/9/97	Right	Downstream	Echo sounder	3.4	4.8	4.6	5.2	10.8	11.4
4/9/97	Left	Upstream	Sounding weight	0.9	4.1	4.0	4.6	5.2	5.8
4/9/97	Left	Upstream	Echo sounder	0.5	4.3	4.0	4.6	5.2	5.8
4/9/97	Left	Downstream	Echo sounder	1.8	3.2	4.0	4.6	5.2	5.8

During the flooding in April 1997, the USGS visited this site three times. During all three visits the floodplain flow was concentrated in the right floodplain. This concentration of flow in the right floodplain likely is caused by the channel alignment upstream of the bridge. No defined point of reattachment along the right embankment was found during the flood. Flow was toward the main channel along the entire length of the right embankment. The flow separated from the right embankment, nearly perpendicular to the main channel flow, and joined the main flow just left of the rightmost pier (figure 6). During the measurements made on 4/5/97, the flow from the right floodplain was so intense that a standing wave formed upstream of the bridge where the floodplain and main-channel flow began mixing. The area from the rightmost pier to the right abutment was primarily slack and reverse flow. The depth of flow at the right abutment progressively deepened from 4.5 m on 4/4/97, to 6 m on 4/9/97. On 4/9/97, a portion of the right embankment slumped, forcing Swift County officials to temporarily close the bridge until riprap was placed to protect the bridge.

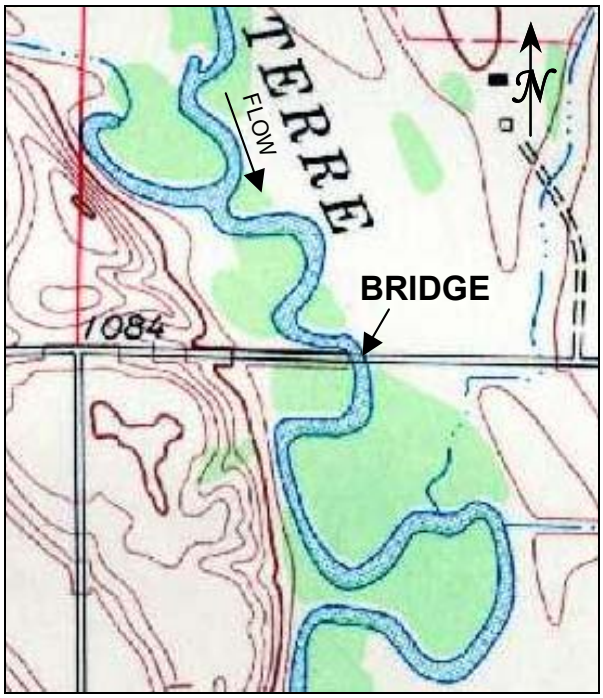

Figure 5. Plan view of Swift County Route 22 over the Pomme de Terre River, Minnesota (no scale).

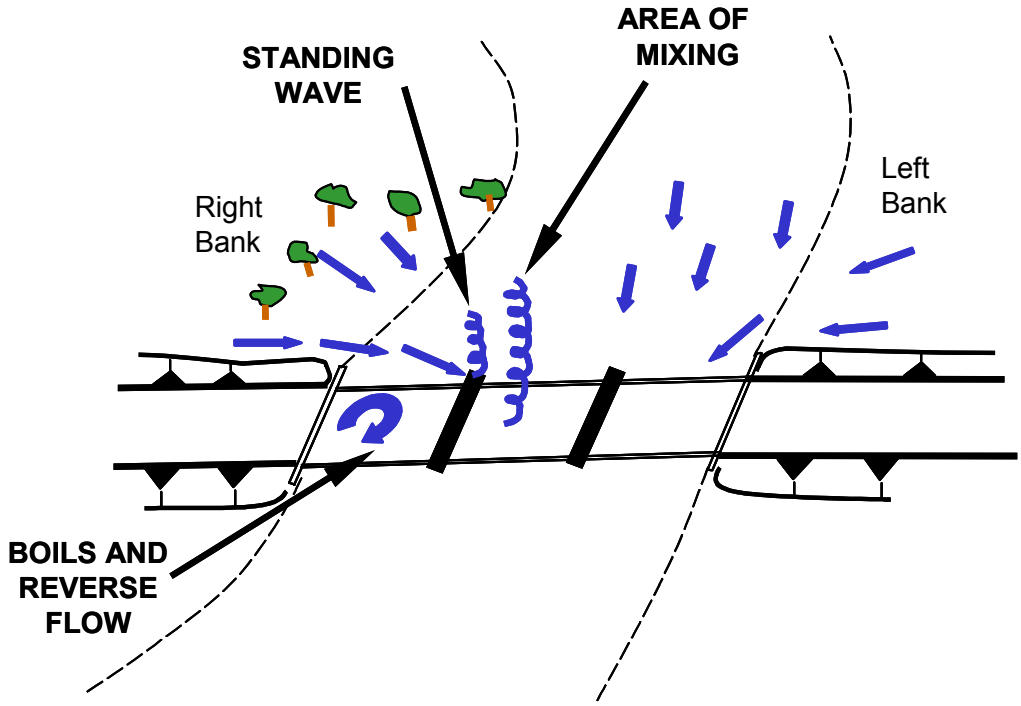

Figure 6. Sketch of flow conditions at Swift County Route 22 over the Pomme de Terre River, Minnesota (not to scale).

Discussion of Field Data

Data-collection efforts were restricted to data that could be collected from the bridge deck for all three site visits during the flood (4/4/97, 4/5/97, and 4/9/97). All bathymetry data were collected by floating an echo sounder attached to a knee-board across the river while being controlled by a hand line from the bridge. The board was allowed to float downstream and streambed elevations were collected as far as 30 m downstream from the bridge. Data collected upstream of the bridge was restricted to the upstream edge of the bridge deck and the area around the upstream end of the right wing wall. Data could not be collected in the floodplains because of heavy vegetation. Velocity magnitudes and water discharge were measured during two of the three site visits using a vertical-axis current meter deployed along the upstream edge of the bridge. Water-surface elevations were measured at the upstream edge of the bridge from the top of the bridge deck between the left most pier and the left abutment. The hydraulic data collected during the flood are summarized in table 5. Additional bathymetry data were collected 21 m upstream from and 30 m downstream from the bridge after the flood during a low-water site visit on July 15, 1997. The elevation and geometry changes experienced by the streambed at the bridge during the period of data collection are shown in figure 7.

The rightmost pier may have had some effect on the depth of scour at the right abutment, yet it is difficult to determine the effect of the pier on the depth of local abutment scour. The effect of the abutment is believed to be the dominant scouring factor; therefore, all scour is credited to the abutment with none reported for the pier. The observed velocity in the area at the right abutment dropped considerably as the scour-hole depth increased. The velocity at the left abutment held steady through the data-collection period, as did the depth and shape of the scour hole. All abutment scour measurements were collected from the upstream edge of the bridge.

Contraction scour typically is computed as the difference in average bed elevation between the uncontracted and contracted sections, adjusted for bed slope. Because of the inability to collect field measurements in the uncontracted section during the flood, a cross section collected in 1991 included in the bridge plans was used as a reference surface. All contraction scour measurements were made along the upstream edge of the bridge. There is less than 0.3 m difference in the bed elevation near the center of the channel (beyond the limits of the abutment scour holes) between the 1991 cross section and those collected during and after the 1997 flood (Figure 7). A value of zero for contraction scour is reported.

The reference surface used to determine the depth of abutment scour was the concurrent ambient bed; therefore, the depth of abutment scour reported is additional local scour below the depth of contraction scour, which for this site was negligible. A reference surface at 313.7 m above NGVD of 1929 was used to measure local abutment scour. A summary of the abutment scour data is presented in table 6.

Table 5. Summary of hydraulic data collected at Swift County Route 22 over the Pomme de Terre River in Minnesota.

Date	Water-Surface Elevation (m, NGVD of 1929)		Discharge (m^3/s)	Velocity (m/s)	
	Upstream	Downstream		Average	Maximum
4/4/97	317.02	316.93	--	--	--
4/5/97	317.15	317.06	132	1.3	2.5
4/9/97	317.34	--	146	1.2	1.8

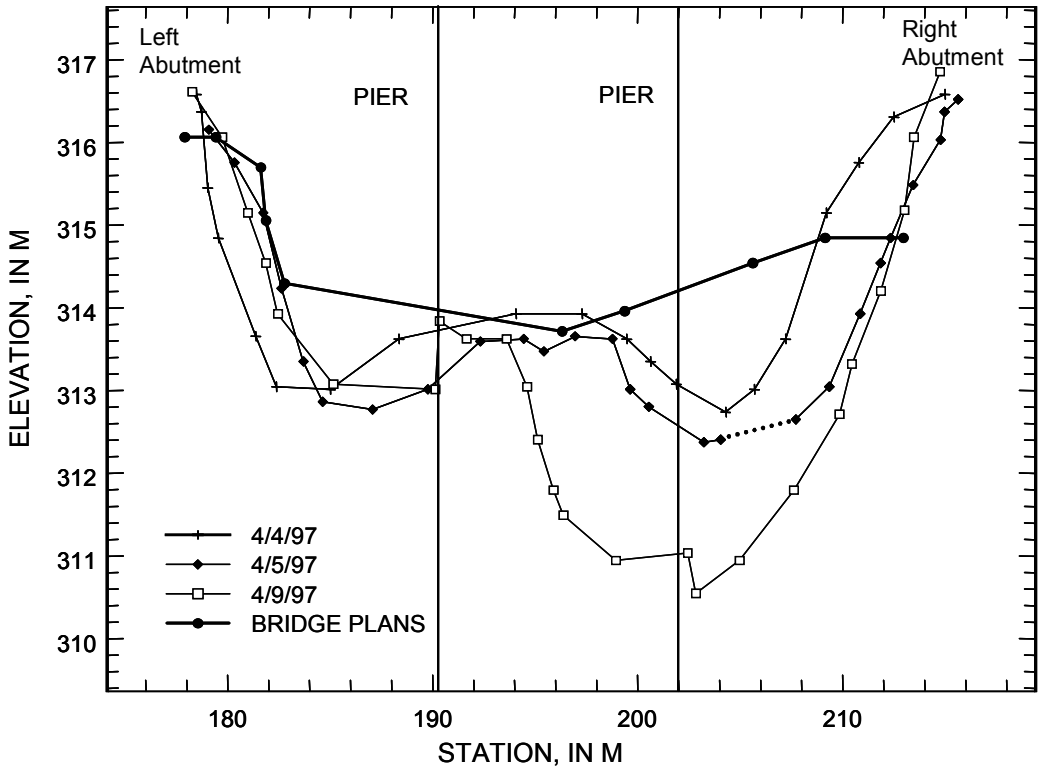

Figure 7. Cross sections collected along the upstream edge of Swift County Route 22 over the Pomme de Terre River, Minnesota.

Table 6. Summary of abutment scour field data for Swift County Route 22 over the Pomme de Terre River in Minnesota.

Date	Abutment	Location	Equipment	Observed Scour Depth (m)	Accuracy (m)	Embankment Length (m)	Velocity At Abutment (m)	Depth At Abutment (m)
4/4/97	Right	Upstream	Echo sounder	1.2	0.3	157	--	4.2
4/5/97	Right	Upstream	Echo sounder	1.2	0.3	162	2.5	4.8
4/9/97	Right	Upstream	Echo sounder	3.0	0.5	166	1.0	6.4
4/4/97	Left	Upstream	Echo sounder	0.9	0.3	44	--	4.0
4/5/97	Left	Upstream	Echo sounder	0.9	0.3	47	1.5	4.4
4/9/97	Left	Upstream	Echo sounder	0.6	0.3	50	1.6	4.3

Model Calibration

The data collected on 4/5/97, 4/9/97, and 7/15/97, were utilized to develop and calibrate the HEC-RAS model. Because no bathymetry data were collected during the flood in either the approach or exit sections, low-flow cross sections measured before and after the flood were used. The bathymetry data collected on 7/15/97, along with geometry taken from the bridge plans, were the basis for the cross sections upstream and downstream of the bridge crossing. Despite the added hydraulic complexities introduced by the meander of the channel near the C.R. 22 bridge, the HEC-RAS model simulated the water surface at the bridge within 0.06 m of field measurements on 4/5/97 and 4/9/97. When an ineffective flow area representing the recirculation zone between the right abutment and the rightmost pier was included, the model simulated the water-surface elevation at the bridge within 0.03 m of the data collected in the field.

The velocity distributions from the model and the field compared favorably, when taking into account that the one-dimensional model is not capable of replicating the two-dimensional features of the flow field. The velocity distributions for the model, using the geometry from 4/5/97 and 4/9/97, and field measurements collected with a vertical-axis current meter along the upstream edge of the bridge are shown in figures 8 and 9. The one-dimensional model results did not accurately compare with the 4/5/97 observations (figure 8). Although model simulated the peak velocity near the rightmost pier reasonably well, the model velocities were too high on near the right bank and in the center of the main channel and too low along the left bank. The model more accurately redistributed the flow after the scour had fully developed. The errors displayed should be expected when using a conveyance method to distribute flow that is complex and dominated by two-dimensional contraction effects. Because data were not available for the approach section, no comparisons could be made upstream from the bridge.

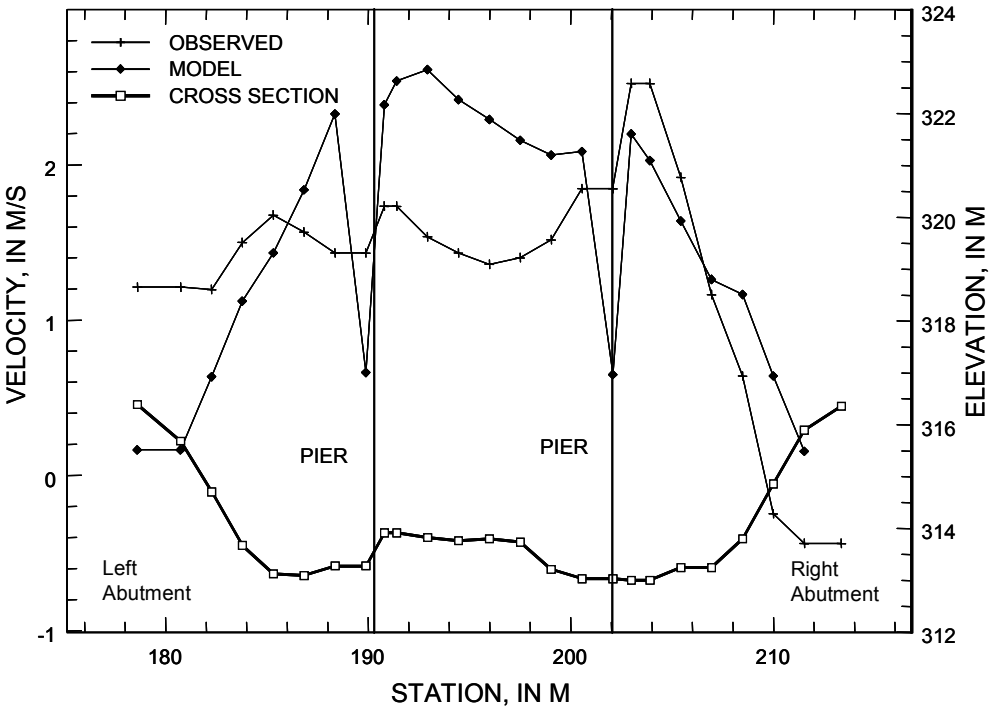

Figure 8. Comparison of observed and model velocity distributions for April 5, 1997, at Swift County Route 22 over Pomme de Terre River, Minnesota.

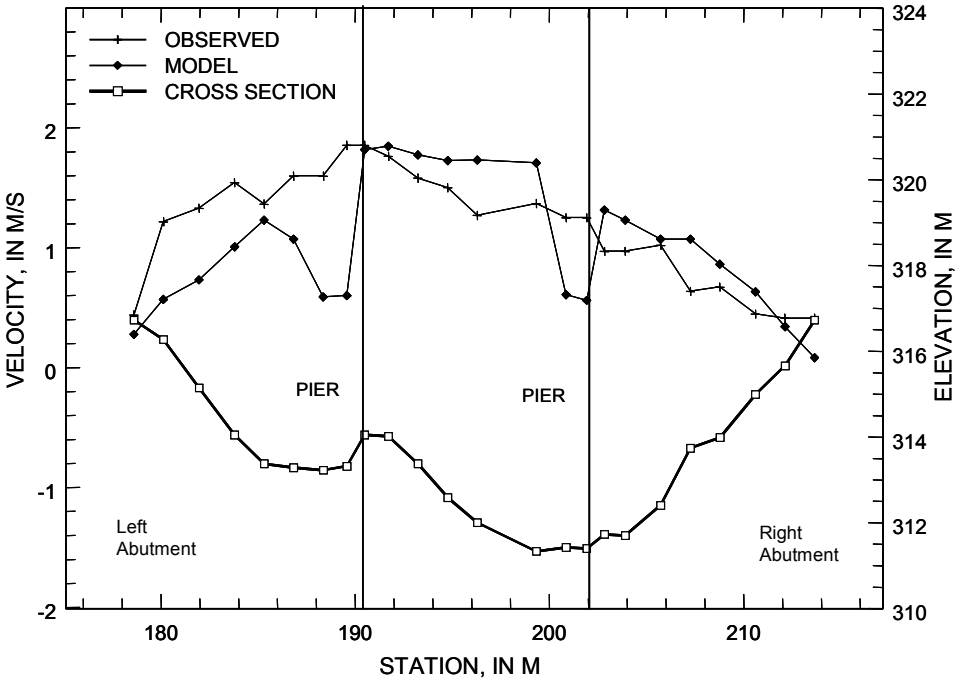

Figure 9. Comparison of observed and model velocity distributions for April 9, 1997, at Swift County Route 22 over Pomme de Terre River, Minnesota.

Assessment of Scour Computations

The calibrated model was used to assess how accurately the scour for this flood could have been predicted. The original geometry of the bridge section was taken from the bridge plans and input into the calibrated HEC-RAS model. The approach and exit cross sections were modified to be consistent with the streambed elevations from the bridge plans. The ineffective flow area between the rightmost pier and the right abutment was assumed to be effective because it is unlikely that it would have been assumed ineffective without field observations. The discharges from both 4/5/97 and 4/9/97, were then modeled with the original bathymetry to determine the hydraulic parameters needed for scour computations. The model analysis did not include the data collected on 4/4/97, because no hydraulic measurements were made during that site visit.

The contraction scour was computed in HEC-RAS by allowing the model to use the default equation (live-bed or clear-water) depending upon the hydraulic conditions computed by the model. The model correctly predicted little or no contraction scour for the prescribed discharges.

Abutment scour was computed in HEC-RAS by both the Froehlich equation and the HIRE equation. The data contained in table 7 show that the Froehlich equation accurately predicted abutment scour, when compared to the fully developed scour holes on 4/9/97. Because the equations predict maximum depth of scour, the Froehlich equation accurately predicted and overpredicted the depth of scour, when compared to the scour holes measured on 4/5/97, which had not fully developed. The HIRE equation overpredicted scour for all hydraulic conditions.

Table 7. Comparison of observed to computed abutment scour at Swift County Route 22 over the Pomme de Terre River in Minnesota.

				Local Scour Depth		
Date	Abutment	Location	Equipment	Observed (m)	Froehlich Equation (m)	HIRE Equation (m)
4/5/97	Right	Upstream	Echo sounder	1.2	2.9	3.8
4/5/97	Left	Upstream	Echo sounder	0.8	0.7	2.8
4/9/97	Right	Upstream	Echo sounder	3.0	3.3	4.1
4/9/97	Left	Upstream	Echo sounder	0.6	0.9	3.1

Summary and Conclusions

In cooperation with the FWHA, the USGS developed a comparison of computed abutment and contraction scour depths with depths measured in the field for U.S. Route 12 and Swift County Route 22 over the Pomme de Terre River in Minnesota provides insight to the capabilities and limitations of using one-dimensional models and the available abutment and contraction scour equations to predict scour at contracted bridge openings. The application of the methods outlined in HEC-18 to these bridges showed a similar variability of results as the comparisons published in the literature. HEC-RAS and the equations recommended in HEC-18 provided reasonable predictions for maximum total scour at the two bridges; however, the magnitudes of the individual scour components (abutment and contraction) did not compare well with the field data. Although field data in the approach sections were inadequate to provide a comprehensive evaluation of the capability of a one-dimensional model to represent a complex two-dimensional flow field, the comparisons that could be made showed the one-dimensional model computed flow distributions that were comparable with the field data for the fully developed scour hole conditions, but were less accurate for initial conditions and in areas of highly curvilinear flow.

The complexity and variability of conditions at bridges make the development of predictive methodology difficult. The equations oversimplify most conditions, but modification of the methodology to account for site complexity and variability is not simple. New methodologies must balance the desire to fully explain complex processes with the need to provide procedures that are time and cost effective to apply. Additional field data and model studies are needed to continue to improve scour prediction methodology.

References

1. Richardson, E.V. and Davis, S.R., 2001, Evaluating scour at bridges (4th ed.): Hydraulic Engineering Circular No. 18, 378 p.

2. Hydrologic Engineering Center (HEC), 1998, HEC-RAS River Analysis User's Manual Version 2.2, Hydrologic Engineering Center, Davis, CA.

3. BRW, I., 1995, Bridge scour investigation, final report for bridge 5359, trunk highway 12 over Pomme de Terre River: Minnesota Department of Transportation.

Factors Affecting Stream and Foundation Stability at Existing Bridges in New Jersey

Salim M. Baig[1] P.E., Joseph J. Zarriello[2] P.E. and Mohiuddin A. Khan[3] Ph.D. P.E.

ABSTRACT

Scour analysis procedures for existing bridges as adopted by FHWA (HEC-18) require extensive data collection both in the field and in the design office. Data collection methods are discussed here to serve as guidelines. For 'unknown foundations,' when no as-built drawings are available, test borings are found necessary, in order to determine any presence of rock, rock elevations and the foundation depth.

The factors, which affect stream stability, include the location of the bridge either close to a river bend or at a skew angle to the direction of flow, aggradation, longitudinal slope and coefficient of roughness. The factors which affect foundation stability include the use of shallow foundations, placing the footing above computed scour depth or deficiencies such as absence of river training measures, lack of foundation armoring.

A methodology for scour study is summarized here. In addition to hydrologic studies applicable to New Jersey rivers (Stankowski method), hydraulic studies (applying HEC-RAS software) and detailed scour analysis (using Excel Spreadsheets for HEC-18 formulae) were performed. The procedures developed represent the current state of art in USA and serve as practical basis for a similar scour study.

Scour studies of two typical bridges show that the S.I. & A. Inventory Codings for Phase I need to be revised. The first bridge can be 'salvaged' by extensive foundation repairs, while the second bridge would need replacement (Figures 1 and 2).

INTRODUCTION

Recently, the New Jersey Department of Transportation completed an in-depth study to evaluate the condition of over 200 bridges, whose foundations are subjected to continued undermining from floods. STV Incorporated were assigned the task of performing the in-depth (Stage II, Phase 3) scour studies for eleven bridges. Two of the bridges (Figures 3 and 4) are selected here as typical cases to represent the eleven 'scour critical' bridges, for the purpose of a unified analytical approach and for countermeasures design. The bridges are located in the same watershed in Hunterdon County.

[1] Chief, Bureau of Structural Evaluation, New Jersey DOT, 1035 Parkway Avenue, Trenton, NJ 08625
[2] Project Manager, STV Inc., 820 Bear Tavern Road, Suite 105, Trenton, NJ 8628-1021
[3] Manager Bridge Design, STV Inc., 820 Bear Tavern Road, Suite 105, Trenton, NJ 8628-1021

Stream stability and bridge scour have been addressed as a design criteria in the AASHTO LRFD Bridge Design Specifications 1998, Section 2.6 (Ref. 1). Section 2.6.4.4.2 requires "the design flood shall be more severe of the 100-year events or from an overtopping flood of lesser recurrence interval. For check flood for scour, the stability of bridge foundation shall be investigated for scour conditions resulting from a designated flood not to exceed the 500-year event." A flow diagram (Figure 5) developed by STV shows the detailed procedure for evaluating scour. Data Collection procedures based on office and field surveys are summarized in Appendix A.

DESCRIPTION OF THE CROSSINGS

Both the bridges are of single span and are located in Tewksbury Township, Hunterdon County. The Guinea Hollow Road Bridge is located in the watershed of the North Branch of the Rockaway Creek (See Figure 3). The bridge is 1360 feet upstream from the confluence with Rockaway Creek. The waterway is oriented at a 20 degree angle to the bridge. There were no available as-built drawings to verify the footing sizes and depths.

The Water Street Bridge is located in the watershed of the Tributary to North Branch of the Rockaway Creek (See Figure 4). It was constructed originally in 1938 and re-constructed in 1948. The bridge is 700 feet upstream from the confluence with the North Branch of Rockaway Creek. The waterway is oriented at 45-degree angle to the bridge.

INVESTIGATING CONDITIONS OF UNKNOWN FOUNDATIONS

FHWA published recommendations to investigate unknown bridge foundations (Ref.6),"About 104,000 bridges in National Bridge Inventory have unknown foundations". In terms of the type and/or depth. These unknown bridge foundations pose a significant problem to state DOT's from a scour safety evaluation perspective. Because of the risk of scour undermining bridge foundations and the threat to public safety … the foundation type and depth information is needed to perform an accurate scour evaluation of each bridge." Foundation details and as-built plans were not available for these existing bridges. HEC 18, Appendix K (Ref. 3) describes detailed procedures. The suitability of alternate methods (Refs. 6 and 7) are discussed here:

1. **Direct methods such as probes, augers or rotary drilling adjacent to footings**: Probes which were carried out underwater to locate the top of existing footings did not give accurate information. Digging test pits was not used due to the danger of undermining existing footings.

2. **Nondestructive tests:** Ground penetrating radar or acoustical emission techniques were considered. Due to the unknown type of soil and stone masonry supported on stone sub-strata, this technique could not determine accurate depth of footings.

3. **Drilling test borings:** Drilling through the heel of abutment footing, obtaining bore hole logs and analyzing them was found to be a reliable method and provided detailed foundation and rock information. The method and cost was approved by NJDOT. The test boring provided information on footing depth, elevation and quality of rock located under the footing.

HYDRAULIC AND GEOMORPHIC FACTORS AFFECTING SCOUR

ASCE Compendium (Ref.2) lists several scour studies based upon a variety of causes. Hydraulic and geomorphic factors appear to be the most important and are discussed.

- **Upstream Features:** Guinea Hollow Road bridge is located downstream of a small dam and a footbridge. The presence of dam has helped to reduce high velocities downstream at the bridge location during flood events. However, the Water Street Bridge is located in a heavily forested area. The flow velocities are average.

- **Direction of River Flow:** Both the bridges are located on a well-developed bend and have sharp skew angles which cause the shifting of thalweg and non-uniform velocity distribution leading to scour of the bed and bank at the outside of the bend, and deposition at the inside of the bend.

- **Existing River Training Measures:** For both bridges, there is no evidence of dyke or spurs constructed along the outer bend to reduce the effects of long term scour. Hence the scour has remained unmitigated throughout the long life of the structure.

- **Longitudinal Slope:** The longitudinal slopes of the channel vary between 3% and 4% upstream for Guinea Hollow Road Bridge and between 2.4% and 3% downstream for Water Street Bridge. The slopes are not steep and as per Manning's equation for normal depth in an open channel, critical or supercritical velocities are not affected.

- **Aggradation:** The channel beds are littered with stones and small size boulders providing partial armoring of the bed against scour holes. Coefficient of roughness is affected. Part of the Water St. Bridge opening is clogged by medium size stones deposited by earlier floods, thereby reducing effective channel area and increasing velocity of flow under the bridge

- **Type of Stream Bed:** Soil samples tested in the laboratory have shown the Guinea Hollow Road bridge stream bed as granular in nature, with some large stones mixed with gravel and a substantial fraction of sand. Median size of aggregate (D_{50}) varies between 1 to 5 mm. Gravel layer has an armoring effect and leads to low degradation.

For Water Street bridge medium sand and traces of fine sand mixed with gravel are found with the median sizes of the aggregate (D_{50}) varying between 1 to 2 mm. The degradation of streambed or banks has been significant.

- **Bridge Skew**
  For Guinea Hollow Bridge the skew of 20 degrees in plan has resulted from a bend. The meander may continue to move laterally outward and downstream, eroding the left bank and increasing scour depth in the future.
  For Water St. Bridge the channel makes an abrupt change in direction upstream of the bridge, creating an increase in water velocity. The bridge skew of 45 degrees has resulted from bend or river meander. The meander may continue to move laterally outward and downstream, eroding the Right Bank and increasing scour in the future.

- **Depth below riverbed to top of Footings:** Test borings have shown the depths of bottom of spread footings as 'shallow' making them scour critical.

SCOUR DEPTH SUMMARY

Contraction, local and total scour depths for check flood500 years are plotted in Figures 6 and 7. Modified Laursen's equation, Froehlich's equation and Hire's equation are summarized in Appendix B.

Flood Discharge Frequency	Long Term Scour ft.	Contraction Scour ft.	Local Scour ft.	Total Scour ft.	Net Scour to bedrock ft.
South Abutment, Guinea Hollow Road Bridge -50 Year	0	4.30	14.95	19.25	7.0
100 Year	0	4.59	15.33	19.92	7.0
500 Year	0	5.49	16.07	21.56	7.0
East Abutment, Water Street Bridge - 50 Year	0	6.99	16.18	23.18	1.2
100 Year	0	7.38	17.67	25.05	1.2
500 Year	0	6.98	12.65	19.62	1.2

Notes:

1. The bottom of footing elevation has been determined by test boring.
2. Elevations referenced to National Geodetic Vertical Datum (NGVD) 1929.
3. Scour below the bedrock (granite) was neglected for 50, 100 and 500 year floods since elevation of igneous rock controls.
4. For Water Street Bridge due to levee at the banks under 500 year flood, the water overbanks. Both the wetted perimeter and roughness coefficient increase. Hence lower velocity and scour depth occurs.

5. For both bridges, the computed potential total scour is substantial for 50 and 100 year floods and scour depth exceeds the depth of footing, making the bridge scour-critical.

CHECKING PHASE I SCOUR CRITICAL DETERMINATION

Preliminary NJDOT (Stage I) study has shown that both the bridges are scour critical. Present STV (Stage II) study based on applicable methods and formulae (Figures 6 and 7) indicate that the bridge is scour critical and confirm the earlier findings:

Guinea Hollow Road Bridge

- Evidence of undermining at both abutment footings
- Evidence of poor quality masonry walls with missing mortar in joints
- Evidence of large size scour holes close to the abutments: Two large scour holes of over 3 feet depth are located in the bridge area is shown in Fig. 3 indicating severe scour. The size of scour hole is likely to increase in the future and undermine the south abutment footing.

Water Street Bridge

- Evidence of undermining at the east abutment footing
- Evidence of large size scour holes close to the abutments

Further, test boring at east abutment has shown that there is good quality rock within 2 feet below bottom of footing, thereby reducing effective scour depth considerably. There appears to be a deficiency in the original design, of placing the footing at a shallow depth. The east abutment footing has become fully exposed; thereby making any remedial measures expensive or ineffective.

RECOMMENDED BRIDGE INVENTORY CODINGS

Codings serve as the indicator of structural health of the bridge. Based upon the in-depth (Stage II) bridge scour evaluation, earlier Stage I, SI&A Codings (Federal Coding Guides, Ref. 5) for this structure may be revised as follows:

Coding Guides	Description	Stage I Coding- Guinea Hollow Road Bridge	Stage II Coding- Guinea Hollow Road Bridge	Stage I Coding- Water St. Bridge	Stage II Coding- Water St. Bridge
Item 61	Channel/Channel Protection (Stream Stability, Channel Condition, Slope Protection)	6	6	7	7
Item 71	Waterway Adequacy (Overtopping Flood frequency	9	9	5	5
Item 113	Scour Critical Bridges (Abutments are rated as unstable due to scour)	4	3*	7	2**

* Stage I SI&A rating is revised to 3 based on scour analysis.
** Stage I SI&A rating is revised to category 2, based on scour analysis.

Computed scour calculations for Stage II, Phase 3 show that the bridges are scour critical and scour depth is below the bottom of spread footing base. The conditions of the bridges are considerably worse than estimated in Stage I and remedial measures need to be implemented on a priority basis.

COUNTERMEASURE EVALUATION

In order to preserve the long term structural integrity of the bridge from damage by scour the following remedial measures, in line with HEC-23 (Ref. 4) countermeasures matrix, need to be implemented:

Structural countermeasures: Cast-in-place concrete apron (Fig. 1) serves as a good example.

Hydraulic (Armoring) countermeasures: Common materials used for revetment are riprap, gabion mattress, concrete bags or toskanes. Timber or Steel sheeting or concrete paving, to armor the exposed faces of the existing footings was investigated to select the most cost-effective method. Due to confined space under the bridge, driving of sheeting would not be practical. Hence, riprap adjacent to abutment footing and level with riverbed elevation was adopted (Eq. 8.1, Page 8.3, Ref. 4). Also, countermeasures directive in HEC-18 (Appendix J, Page J.3, Ref. 3) was followed.
For Water Street Bridge, bottom of east abutment footing is at the same level as the riverbed. Hence any riprap will be washed away during the flood and will not act as an armor. Placing grout bags on geotextile Class C layers, adjacent to East abutment appears to be a cost-effective method (Fig. 2).

Environmental concerns: Stream encroachment permit and a General Permit # 10 from NJDEP are required to install armoring. Hence sizes of revetments need to be controlled and construction method should prevent river pollution.

Monitoring: Visual inspection on a regular two-year cycle and flood watch needs to be carried out. Monitoring efforts need to be increased during high flow events.

Recommendations

For Guinea Hollow Road Bridge, placing of riprap adjacent to the apron on north and south abutments appears to be the most cost-effective method. Conceptual sketches, showing riprap depth and extent of riprap at south abutment, are shown in Figure 1. Cost of countermeasures are estimated at $75,000. Details of work are as follows:

1. Repairs prior to implementing countermeasures, (including filling missing mortar joints, removing debris from channel bed, filling scour holes and gaps between the bottom of footing and top of soil next to south abutment, with concrete)
2. Constructing concrete aprons (including cofferdams and de-watering)
3. Providing riprap at abutments & wingwalls

For Water St. Bridge underpinning the East abutment footing will be expensive and requires bridge closure. Previous repairs, such as reconstructing the apron footing have not worked due to shallow depth of foundation in the original construction.

Replacement of bridge is likely to take several years and during this period interim countermeasures are required (Ref. 4). Riprap placement requires a 3 feet minimum depth below the riverbed (Fig. 2). Cost of interim countermeasures are estimated at $67,000. Details of work are as follows:

1. Repairs prior to implementing countermeasures, (including removing debris from channel bed, and filling scour holes).
2. Building temporary cofferdam and de-watering, filling gap below the bottom of footing at east abutment with concrete for approximately 20 ft. length.
3. Placing grout bags at east abutment (including textile layer).

GUIDELINES AND CONCLUSIONS

The procedures developed here represent the current state of art in USA, as presented in a flow diagram and serve as practical basis of any similar scour study.

1. **Investigation of factors affecting stream and foundation stability:** It was confirmed that both the bridges are scour critical and the bridge footings have become unstable. Abutments are skewed to the direction of flow, and the existing footing elevation is placed above the computed scour depth. There are no existing river training measures or foundation armoring. Upstream features also affect flood velocities and increased scour.
2. **Organizing data collection:** Due to the variety of in-house and field data required for completing scour analysis, an NJDOT memorandum was adopted. A sample of the format is shown in the Appendix A.

3. **Importance of investigating 'unknown foundation' in scour analysis:** Test boreholes were driven to provide important missing data for footing and rock elevations. This leads to a reliable and economical design of countermeasures.

4. **Streamlining HEC-18 procedures by Flow diagram**: H & H, scour analysis and countermeasures design procedures are summarized in Figure 5, and are recommended for application and reference on similar in-depth studies.

5. **Determining SI &A Coding**: Phase I bridge coding was checked and revised based on extensive Phase II studies. This approach warns of any immediate danger of collapse of footing. Accurate determination of Inventory Codings help in future planning and cost allocations for substructure repairs or for replacement of bridge.

6. **Design of Countermeasures:** For Guinea Hollow Road Bridge, strengthening the footing by apron wall and installation of armoring, such as riprap are recommended. For Water Street Bridge, underpinning the east abutment footing and providing countermeasures for both abutments will approach the cost of a replacement

structure. Hence replacing the 63-year-old bridge appears to be a better choice in economic terms. Interim repairs and replacement of bridge are recommended.

7. **Monitoring:** Continued monitoring of the footings and of the main channel, during routine biennial inspections, will be necessary. Monitoring after floods is also required.

REFERENCES

1. AASHTO Load Resistance Factor Design (LRFD) Bridge Design Specifications, 1998
2. ASCE – Stream Stability and Scour at Highway Bridges, Water Resources Eng., 1999
3. FHWA – Evaluating Scour at Bridges Fourth Edition, HEC No. 18, 2001
4. FHWA – Bridge Scour and Stream Instability Countermeasures, HEC No. 23, 1997
5. FHWA – Federal Coding Guide, 1994.
6. FHWA - Determination of Unknown Subsurface Bridge Foundations, NCHRP Report No. 21-5, Geotechnical Guideline No. 16, 1998
7. Melville B.W. and Coleman S.E. –Bridge Scour, Water Resources Publication, 2000
8. NJDOT Bridge Design Manual 1998

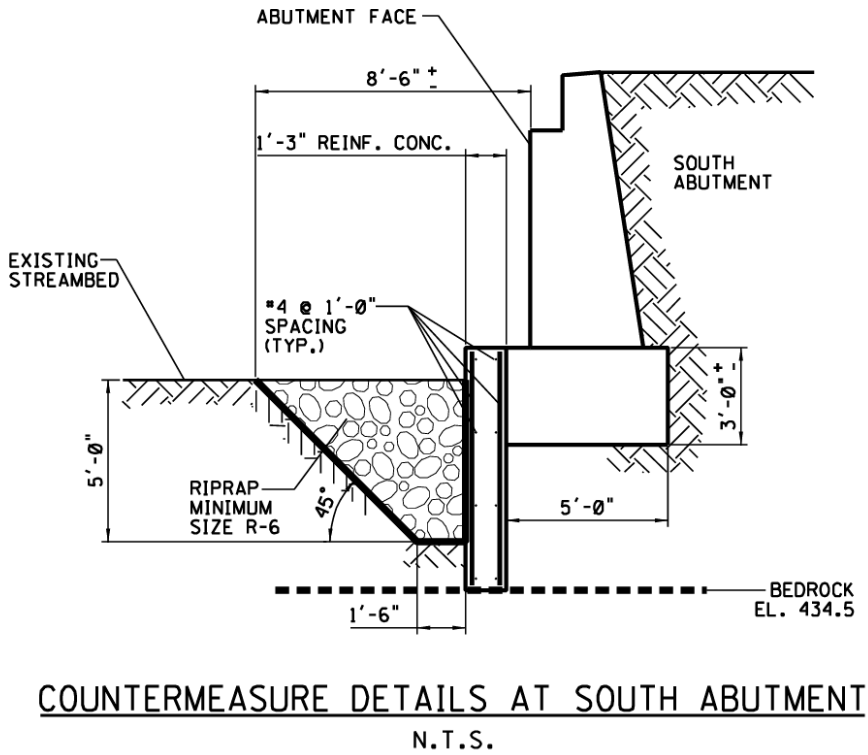

Figure 1. Scour Countermeasures - Structure No. 1000-041
Guinea Hollow Road Over North Branch Rockaway Creek

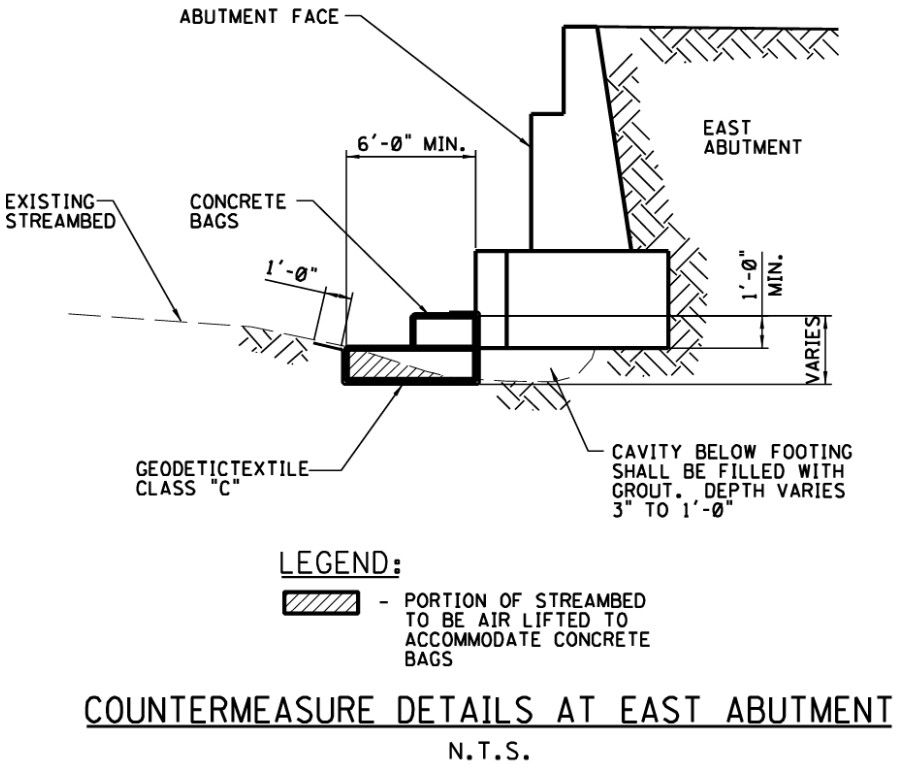

Figure 2. Scour Countermeasures - Structure No. 1000-042
Water Street Over Trib. To North Branch Rockaway Creek

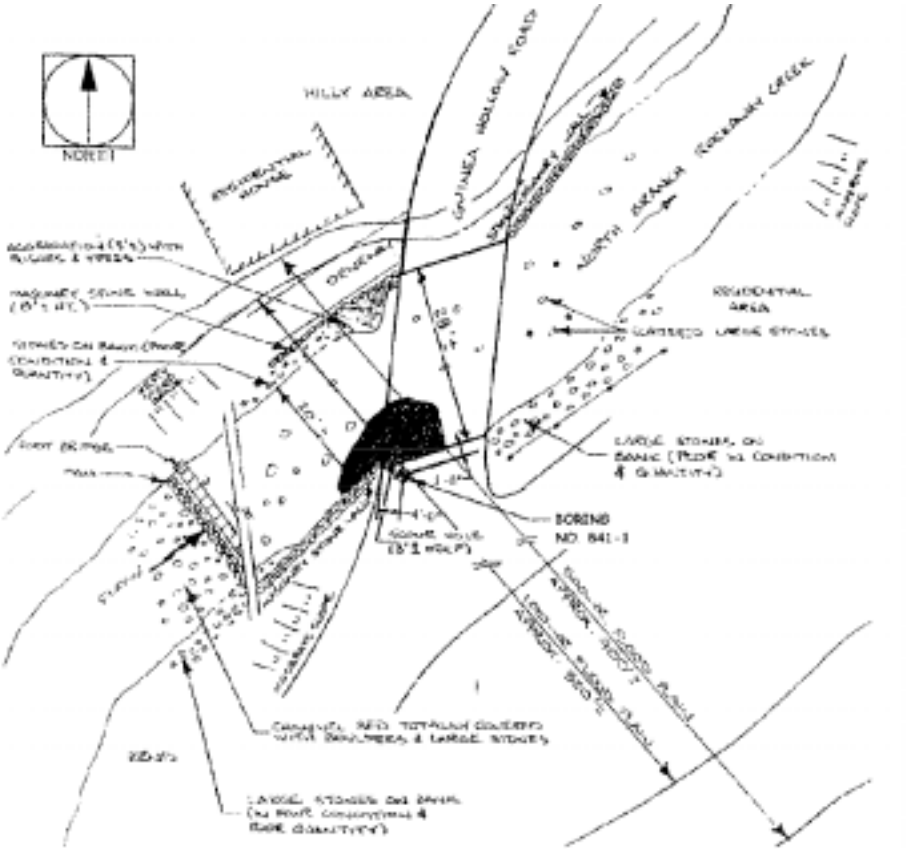

Figure 3. Bridge Plan - Structure No. 1000-041
Guinea Hollow Road Over North Branch Rockaway Creek

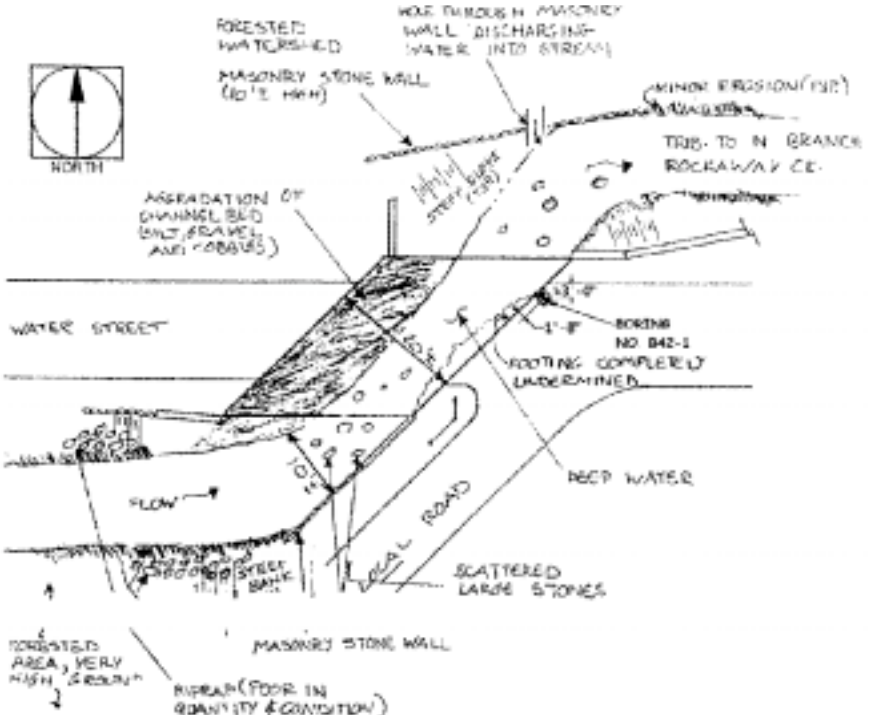

Figure 4. Bridge Plan - Structure No. 1000-042
Water Street Over Trib. To North Branch Rockaway Creek

FIGURE 5 : SCOUR STUDY PROCEDURE FOR EXISTING BRIDGES

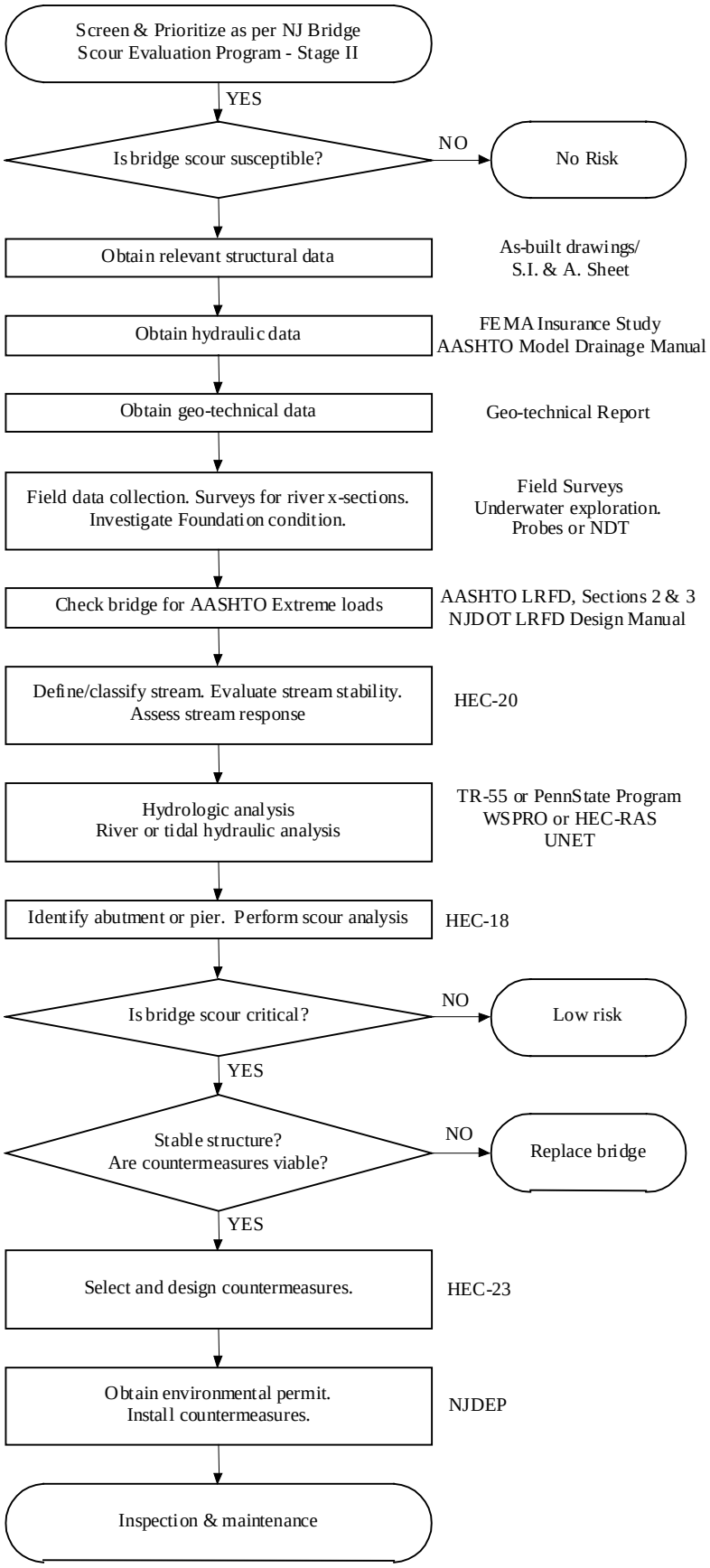

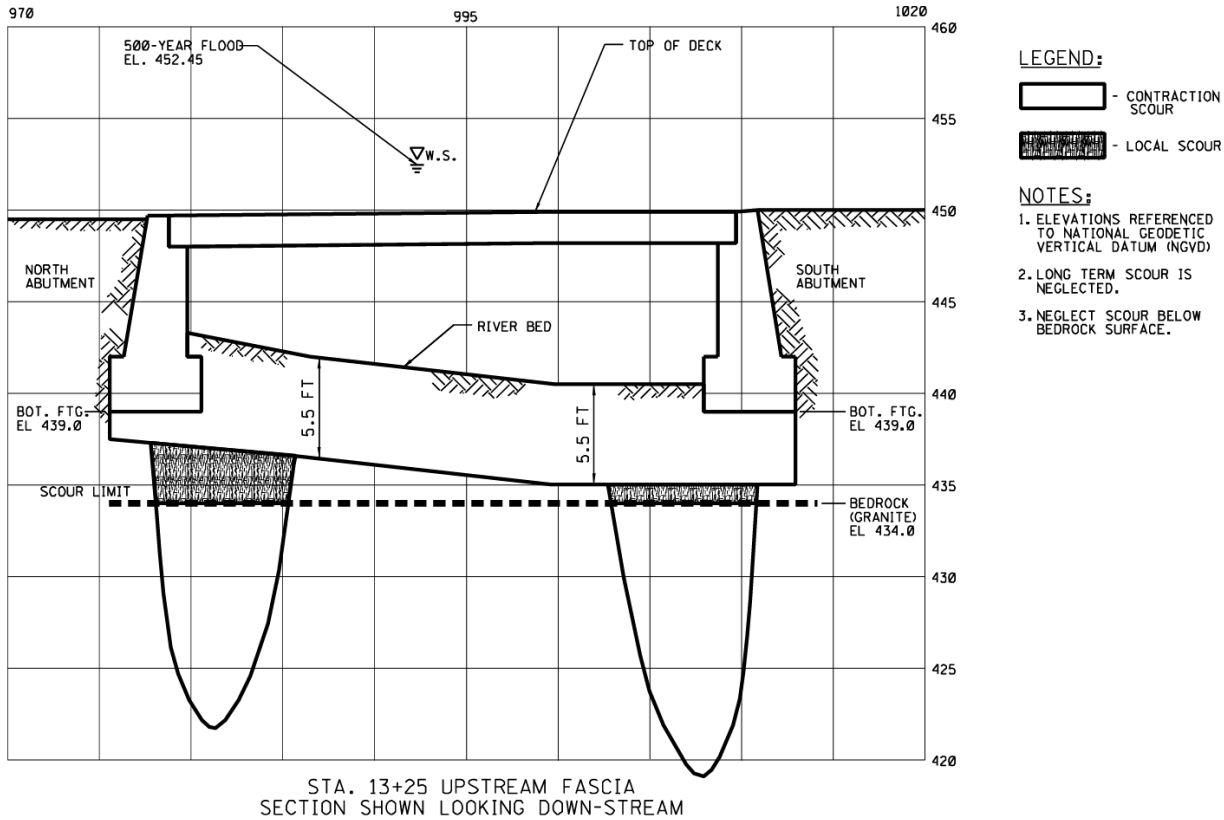

Figure 6. Calculated Scour Depths For 500 Year Flood - Structure No. 1000-041 Guinea Hollow Road Over North Branch Rockaway Creek

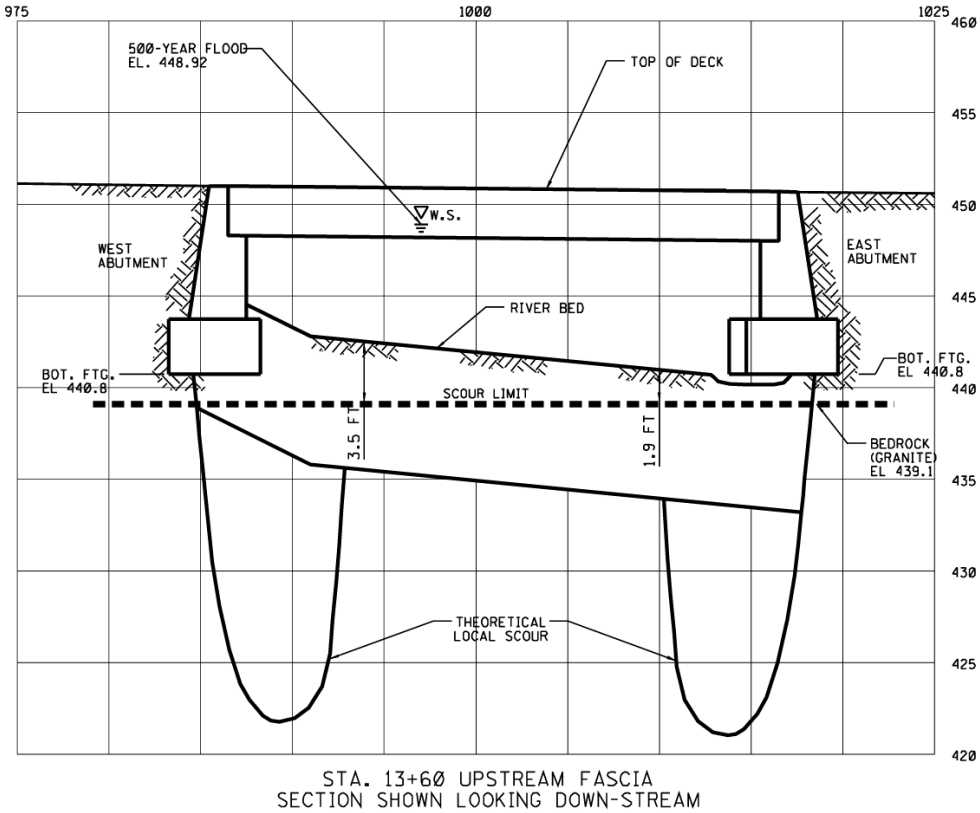

Figure 7. Calculated Scour Depths For 500 Year Flood - Structure No. 1000-042 Water Street Over Trib. To North Branch Rockaway Creek

APPENDIX A - DATA COLLECTION PROCEDURE

- **Design Office Data Survey**

To perform scour analysis, a data collection procedure is required, as follows:

a. Compile an inventory of all reliable field data and data available in the design office.
b. Prepare a list of remaining data, which is necessary to perform scour analysis, and the method, extent and duration of obtaining such data.

- **Field Survey**

Gage Data for peak flood discharges was not available.
A field survey of the two bridges, by a team of licensed structural, hydraulic and geotechnical engineers was carried out during March and April 2001.

The team performed the following tasks:

1. Recorded visual observations for: Scour holes, shift in thalweg of main channel, cracks and open mortar joints in stone masonry abutments, deposit of stones and debris from earlier floods, evidence of river training measures or scour countermeasures in place.
2. Investigated the need to drill test borings to determine depth of rock and the type of bearing material.
3. Prepared photographic documentation
4. Obtained river cross sections.
5. Evaluated stream and waterway characteristics.
6. Evaluated 'n' values (Manning's roughness coefficients).
7. Prepared Data Collection items including purpose and methodology listed below:

Item	**Purpose**	**Data Collection**	**Methodology for Obtaining data**
Field Surveys	Waterway Opening	Yes	Observations and Measurements
Underwater Survey	Scour Holes	Yes	Probing
River Cross-Sections	HEC-RAS Model	Yes	Surveying Instruments
Soil Parameters	Roughness Coefficients/ D50	Inspection & Photos/Grab Samples	Characteristics of banks bed material. Visual & Sieve Analysis
Foundation Details	Size and Scour Damage	Inspection & Photos	Probing and Exposed Footings
Test Boring	Depth of Footing / Rock	Boring Log	Drilling / Coring

APPENDIX B – SCOUR ANALYSIS

Hydrologic & Hydraulic Analyses

Discharges for 50 year, 100 year and 500 year storms were calculated for the watershed based on the Stankowski Regional Equations found in "Magnitude And Frequency of Floods in New Jersey with Effects on Urbanization" (Special Report 38, by Stephen J.

Stankowski, U.S. Geological Survey). This is the preferred method for determining storm flows in New Jersey. The Stankowski Regional Equation is based on a thorough study of relationships between flood data and meteorological characteristics for 103 sites in the state. The parameters for the Stankowski Regional Equation are drainage area, channel slope, surface storage index, and index of manmade impervious cover.

The water surface profile was determined using HEC-RAS version 3.0 software (Ref. 2). FEMA study based on HEC-2 study is available only for Guinea Hollow Road bridges. However, the existing cross sections were determined to be outdated (over 20 years old) and inaccurate as a result of potential sedimentation and erosion over many years. The new input data consisted of eight recently surveyed cross sections, five upstream and three downstream.

SCOUR DEPTHS

Scour analysis was performed in accordance with HEC-18 (Ref. 3) and NJDOT Design Manual, Section 46 (Ref. 8). The intent of HEC-18 is to establish methods for estimating various scour components for use in conjunction with engineering judgement, to evaluate potential depth of total scour. Calculated scour depths are summarized in Tables 1 and 2. Modes of bed transport were Live Bed and Clear Water. Excel Spreadsheets were developed based on applicable methods and formulae (Ref. 3, 7 and 8). Sample results are summarized in Tables 1 and 2 and are plotted in Figures 6 and 7.

- **Long Term Scour**

Field observations and past inspection reports did not reveal evidence of continuing or significant long term aggradation or degradation. Any long term scour was neglected.

- **Contraction Scour**

This occurs mainly from the contraction of flow area, which results in increased velocity and shear stress on channel bed.
The computation of critical velocity was based on Laursen's equation

$$V_C = 10.95\,(y_1)^{1/6} \times (D_{50})^{1/3}$$ (Eq. 5.1, Page 5.2).

A comparison was made with the mean velocity value obtained from HEC-RAS analysis. Modified Laursen's eq. for Live Bed mode determined the depth of contraction scour.
Live Bed Contraction Scour $y_2/y_1 = (Q_2/Q_1)^{6/7} \times (w_1/w_2)^{k1}$ (Eq. 5.2, Page 5.10)
Another modified Laursen's equation for Clear Water mode was used.

$$y_2 = (K_u Q^2/(D_m^{2/3} \times w^2))^{3/7}$$ (Eq. 5.4, Page 5.13)

$$y_s = y_2 - y0$$ (Eq. 5.5, PAGE 5.13)

- **Local Scour**

Froehlich's Equation is given by

$\mathbf{y_s = (2.27 \times K_1 \times K_2 (L'/y_a)^{0.43} \times Fr^{0.61} + 1)y_a}$ (Eq. 7.1, Page 7.8)

This occurs from vortices, which are caused by flow obstructions and are cyclic in nature. Based on the ratio of projected abutment length to flow depth (L/y1)< 25, either Froehlich's equation or Hire's equation for live bed scour was used to estimate potential depth of local scour at each abutment. Resulting scour depths estimated by Froehlich's equation seem excessive. However HEC-18 states that the equation be used to aid in the placement of countermeasures. Therefore calculated depths will be treated as an estimate of potential depth of scour.

HIRE's Equation is given by $\mathbf{y_s = y_1 \times 4 \times Fr^{0.33} \times K_1 K_2 / 0.55}$ (Eq. 7.2, Page 7.9)

Total scour depth = Depths of (Long term scour + Contraction scour + Local scour)

AUTHOR INDEX

Author	Page
Abghari, A.	684
Adams, J. P.	954
Alonso, C.	349, 734
Anglin, C. D.	582, 978
Annandale, G. W.	449
Awad, M. A.	471
Baig, S. M.	1111
Barkdoll, B.	734
Bermudez, H.	719
Bettencourt, B.	842
Bettess, R.	162
Bixler, M.	918
Boehm, D. W.	609
Bollaert, E.	449
Bos, K. J.	567
Bozo, L.	884
Briaud, J-L.	57, 156, 227, 242, 272, 373, 459, 1061, 1188, 1208
Cao, Y.	227, 459
Casado, J. M.	34
Chang, K-A.	869
Chen, H-C.	14, 156, 242, 373, 459, 1061, 1188,1208
Cheng, L.	175
Chiew, Y-M.	70, 707
Chin, C-O.	968
Chiu, P-H.	869
Choi, S-U.	206
Chung, M-K.	227
Cian, C.	1152,1155
Coleman, S.	749
Curry, J. E.	292
D'Odorico, P.	272
Davies, E. B.	1019
Davis, S.	227
Dennett, K. E.	642, 1008
Dhiman, R. K.	560, 896
Di Stasi, J. M.	516
Ding, D.	540
Dumas, C. E.	112
Edelmann, J.	842
Edgers, L.	842
Escarameia, M.	320
Ettema, R.	364, 383, 734
Farrag, K.	283
Ferrando, G.	1152, 1155
Fredsoe, J.	795
Fricthel, P.	642, 1008
Fukui, J.	47, 410
Gardner, R. W.	623
Guven, O.	292
Hager, W. H.	774
Heibaum, M. H.	1
Ho, C. L.	516
Ho, T-C.	869
Hoe, D.	749
Hoffmans, G.	92
Huessin, M.	918
Hunt, B.	227
Islam, M. S.	684
Itamunoala, F.	582
Jeon, E. J.	272
Jeong, S.	854
Jia, Y.	349, 1181
Johnson, P. A.	678
Jones, J. S.	140, 485, 810
Jung, B-S.	437
Kajima, R.	421
Kandaris, P. M.	954
Kanno, Y.	307
Kant, G.	567, 656
Khan, M. A.	1111
Kim, H.	437
Kirshen, P.	842
Kitsunai, S.	910
Kobayashi, N.	910
Kondziolka, R. E.	954
Krolack, J.	112
Kruisbrink, A. C. H.	567
Kuhnle, R.	349, 734
Kumar, A. V.	500
Kusakabe, O.	1081
Kwak, K.	227
Lachhab, A.	364
Lagasse, P.	1051
Lauchlan, C.	184
Lewandowski, E.	842
Li, W.	968

Author	Page
Li, Y.	156, 242, 373, 459, 1188, 1208
Lim, S-Y.	395, 785
Lin, C.	869
Lindo, M. H.	656
Lindsey, W. B.	699
Link, O.	1160
Lopardo, M. C.	34
Lopardo, R. A.	34
Maeno, S.	218
Martinez, E.	364
Masahiko, S.	337
May, R. W. P.	184, 320
McDonald, J. A.	1019
Melville, B.	120, 734, 749
Melville, J. G.	292
Mercado, E. J.	1019
Mia, F.	218
Michelsen, J.	795
Millen, G.	582
Miller, Jr., W.	827
Mishra, S. K.	699
Mohapatra, D. K.	560
Molinas, A.	485
Morvant, M.	283
Muceku, Y.	884
Mueller, D. S.	257, 1096
Muraishi, H.	337
Murakami, S.	307
Nago, H.	218
Nairn, R. B.	978
Nakajima, D.	337
Nakato, T.	528
Neelamani, S.	500
Nevels, Jr., J. B.	764
Ng, S.	1042
Nishimura, T.	1081
Nishitani, M.	47
Nurtjahyo, P.	156, 242, 373, 459
O'Neill, M. W.	1019
Ogihara, K.	337
Oh, B. C.	437
Oliveto, G.	774
Olson, L. D.	929
Otuka, M.	410
Pagan-Ortiz, J. E.	636
Parchure, T.	734
Park, S.	1061
Parola, A.	734
Percher, M.	842
Phillips, R.	719
Piepers , T	1166
Price, G. R.	1032
Punrattanasin, P.	1081
Rao, S. N.	500
Rausche, F.	918
Razdan, K. K.	896
Rees, P.	516
Richards, D. L.	670
Richardson, E. V.	810, 993
Roulund, A.	795
Sainz, J. A.	597
Sakakiyama, T.	421
Salgado, R.	597
Sassa., S.	546
Schaefer, K. J.	623
Schall, J. D.	1032
Schleiss, A.	449
Sheppard, D. M.	198, 810, 827
Shimamura, M.	910, 945
Siddharthan, R.	642, 1008
Singh, R.	896
Soltani, A.	642, 1008
Spaan, G. B. H.	656
Spitz, W.	1051
Subjarassang, A.	1081
Suh, J.	854
Sultan, N.	719
Sumer, B. M.	795
Suzuki, H.	945
Tan, S-K.	785
Unger, J.	774
Verheij, H. J.	92, 567
Wagner, C. R.	257, 1096
Wang , S. Y	1176, 1181
Wang, J.	156, 242, 373, 459, 1188, 1208
Wang, W.	1188, 1208
Won, J.	854
Wu, Z.	307
Wu,W.	1176
Xu, Y.	1181
Yang, W.	206
Yasuhara, K.	307
Youn, S-Z	437
Yu, G.	395, 785
Zanke, U.	1160
Zarriello, J. J.	1111
Zevenbergen, L.	1051
Zha, J.	684
Zhang, L.	540
Zhou, W.	540